

AD-A229 375



SWANEA

(SOUTHWEST ASIA-NORTHEAST AFRICA)

A CLIMATOLOGICAL STUDY

VOLUME I--THE HORN OF AFRICA

by

1st Lt Michael J. Vojtesak
1st Lt Kevin P. Martin
TSgt Gregory Myles

JUNE 1990

DTIC
ELECTE
NOV 13 1990


APPROVED FOR PUBLIC RELEASE;
DISTRIBUTION IS UNLIMITED

USAF
ENVIRONMENTAL TECHNICAL
APPLICATIONS CENTER


Scott Air Force Base, Illinois, 62225-5438

REVIEW AND APPROVAL STATEMENT

USAFETAC/TN-90/004, *SWANEA (Southwest Asia, Northeast Africa), A Climatological Study, Volume I--The Horn of Africa*, June 1990, has been reviewed and is approved for public release. There is no objection to unlimited distribution of this document to the public at large, or by the Defense Technical Information Center (DTIC) to the National Technical Information Service (NTIS).


PATRICK J. BREITLING
Chief Scientist

FOR THE COMMANDER


WALTER S. BURGMANN
Scientific and Technical Information
Program Manager
23 May 1990

REPORT DOCUMENTATION PAGE

2. Report Date: June 1990
3. Report Type: Technical Note
4. Title and Subtitle: SWANEA (Southwest Asia-Northeast Africa), A Climatological Study--Volume I, The Horn of Africa
6. Authors: 1st Lt Michael J. Vojtesak; 1st Lt Kevin P. Martin; TSgt Gregory Myles
7. Performing Organization: USAF Environmental Technical Applications Center (USAFETAC/ECR), Scott AFB, IL 62225-5438
8. Performing Organization Report Number: USAFETAC/TN-90/004
12. Distribution/Availability Statement: Approved for public release; distribution is unlimited.
13. Abstract: The first in a five-volume series that describes the climatology of a region known as "SWANEA," an acronym for "Southwest Asia and Northeast Africa." Volume I describes a subregion of SWANEA known as "the Horn of Africa," an area that, for this study, has been divided into four other subregions of "climatic commonality." After describing the general geography of the Horn of Africa, the report discusses major meteorological features, including semipermanent climatic controls, synoptic disturbances, and mesoscale and local features. Finally, the four so-called "seasons" in each of the Horn's four climatically similar subregions are discussed in detail.
14. Subject Terms: CLIMATOLOGY, METEOROLOGY, WEATHER, GEOGRAPHY, AFRICA, HORN OF AFRICA.
15. Number of Pages: 242
17. Security Classification of Report: Unclassified
18. Security Classification of this Page: Unclassified
19. Security Classification of Abstract: Unclassified
20. Limitation of Abstract: UL

Standard Form 298

PREFACE

This study was prepared by the United States Air Force Environmental Applications Branch, Readiness Support Section (USAFETAC/ECR), in response to a support assistance request (SAR) from the 5th Weather Wing, Langley AFB, VA, under the provisions of Air Weather Service Regulation 105-18. It documents work done under USAFETAC project 807-11, and is the first in a five-volume series that discusses the climatology of the area known as "SWANEA" (Southwest Asia-Northeast Africa). Like its predecessors (studies of the Persian Gulf and Caribbean Basin), this work is complemented by two other SWANEA studies. One describes transmittance climatology in the 3-5 and 8-12 micron bands; the other, refractivity climatology. Publication of these complementary studies parallels or follows the parent work.

The project would not have been possible without the dedicated support of the many people and agencies we have listed below in the sincere hope we've not omitted anyone.

First, our deepest gratitude and appreciation to Mr Walter S. Burgmann, Mr Wayne E. McCullom, Mr Ronald W. Coyle, Mr William Reller, Mr David P. Pigors, Mrs Kay Marshall, Mrs Elizabeth M. Mefford, and Mrs Susan Keller of the Air Weather Service Technical Library.

Thanks also to Mr Henry (Mac) Fountain, Mr Vann Gibbs, Mr Dudley (Lee) Foster, and other members of Operating Location A (OL-A), USAF Environmental Technical Applications Center, Asheville, NC, for providing data, data summaries, and technical support that the authors had previously thought impossible.

To Maj William F. Sjoberg, Maj Charles W. Tuttle III, Mr Kenneth R. Walters Sr, SSgt Gordon K. Hepburn, and TSgt Richard C. Bonam of USAFETAC's Readiness Support Section (ECR), our thanks for their hard work, assistance, guidance, and encouragement.

Thanks to Mr Robert Fett of the United States Naval Environmental Prediction Research Facility and Lt Cmdr Rutsh (Naval Liaison to Air Force Global Weather Central--AFGWC) for their assistance in providing supplemental data for this project.

Thanks to Mr Maurice Crew of the United Kingdom Meteorological Office for providing copies of studies not available elsewhere.

Thanks to Lt Col Frank Globokar, Lt Col John Erickson, Maj Daniel Ridge, Maj Roger Edson, and Capt Patrick Condray, for their cooperation in establishing and providing "peer review" of draft manuscripts.

Finally, all the authors owe sincere gratitude to the Technical Editing Section of the AWS Technical Library (USAFETAC/LDE)--Mr George M. Horn and Sgt Corinne M. Gage. Without their patience and cooperation, this project could not have been completed.

CONTENTS

	Page
Chapter 1 INTRODUCTION.....	1-1
Area of Interest.....	1-2
Geography.....	1-4
Study Content.....	1-4
Climatological Regimes.....	1-4
Conventions.....	1-5
Data Sources.....	1-5
Related References.....	1-5
 Chapter 2 MAJOR METEOROLOGICAL FEATURES OF THE HORN OF AFRICA	
Semipermanent Climatic Controls.....	2-2
Synoptic Disturbances.....	2-52
Mesoscale and Local Features.....	2-70
 Chapter 3 THE INDIAN OCEAN PLAIN	
Situation and Relief.....	3-2
The Southwest Monsoon.....	3-7
The Southwest to Northeast Monsoon Transition.....	3-14
The Northeast Monsoon.....	3-21
The Northeast to Southwest Monsoon Transition.....	3-26
 Chapter 4 THE ETHIOPIAN HIGHLANDS	
Situation and Relief.....	4-4
The Southwest Monsoon.....	4-8
The Southwest to Northeast Monsoon Transition.....	4-17
The Northeast Monsoon.....	4-23
The Northeast to Southwest Monsoon Transition.....	4-33
 Chapter 5 THE ADEN COASTAL FRINGE	
Situation and Relief.....	5-4
The Southwest Monsoon.....	5-5
The Southwest to Northeast Monsoon Transition.....	5-13
The Northeast Monsoon.....	5-18
The Northeast to Southwest Monsoon Transition.....	5-24
 Chapter 6 THE YEMEN HIGHLANDS	
Situation and Relief.....	6-3
The Southwest Monsoon.....	6-5
The Southwest to Northeast Monsoon Transition.....	6-12
The Northeast Monsoon.....	6-18
The Northeast to Southwest Monsoon Transition.....	6-25
 BIBLIOGRAPHY.....	BIB-1

FIGURES

	Page
Figure 1-1 The Southwest Asia-Northeast Africa (SWANEA) Region	1-1
Figure 1-2 The Horn of Africa and its Four "Zones of Climatic Commonality"	1-2
Figure 1-3 The Great (Afro-Arabian) Rift System	1-3
Figure 2-1a Mean January Sea Surface Temperatures ($^{\circ}\text{F}$).....	2-2
Figure 2-1b Mean April Sea Surface Temperatures ($^{\circ}\text{F}$).....	2-2
Figure 2-1c Mean July Sea Surface Temperatures ($^{\circ}\text{F}$)	2-2
Figure 2-1d Mean October Sea Surface Temperatures ($^{\circ}\text{F}$)	2-2
Figure 2-2a Mean January Position of the Azores High.....	2-3
Figure 2-2b Mean April Position of the Azores High.....	2-4
Figure 2-2c Mean July Position of the Azores High	2-5
Figure 2-2d Mean October Position of the Azores High	2-5
Figure 2-3a Mean January Gradient Flow	2-6
Figure 2-3b Mean April Gradient Flow	2-7
Figure 2-3c Mean July Gradient Flow	2-8
Figure 2-3d Mean October Gradient Flow.....	2-9
Figure 2-4 Extent of the Monsoon Climate (shaded area) Across the World.....	2-10
Figure 2-5 Southwest Monsoon Circulation Over Southern Asia and the Indian Ocean (from Hamilton, 1987)	2-11
Figure 2-6a Mean July 200-mb Flow Over the North Indian Ocean and Arabian Sea	2-12
Figure 2-6b Mean May 200-mb Flow Over the North Indian Ocean and Arabian Sea.....	2-12
Figure 2-7 Mean July 200-mb Zonal Flow	2-13
Figure 2-8a Mean April Surface Position of the Mascarene High	2-14
Figure 2-8b Mean July Surface Position of the Mascarene High	2-14
Figure 2-8c Mean August Surface Position of the Mascarene High	2-15
Figure 2-8d Mean October Surface Position of the Mascarene High	2-15

Figure 2-9	Entry Point for Cross-Equatorial Outflow from the Mascarene High into the Indian Ocean Plain and Eastern Ethiopian Highlands.....	2-16
Figure 2-10	Successive Positions of the 20-Knot Isotach at 3,000 Feet (915 meters) AGL Between April and July (from Findlater, 1971).....	2-17
Figure 2-11	Observed Characteristics (Shear Zones/Cloudiness) of the Somali Jet (from Findlater, 1972).....	2-18
Figure 2-12	Movement of the Somali Jet Core, 13-14 August 1966 (from Findlater, 1969).....	2-19
Figure 2-13	Multiple Low-Level Jets on 26 July 1966 (from Findlater, 1969).....	2-20
Figure 2-14	A Southern Hemisphere Frontal Passage Typical of Those That May Produce Air Flow Surges in the Somali Jet	2-21
Figure 2-15a	Composite 3-Hour Wind Speed (m/s) Profiles for Burao, SI	2-22
Figure 2-15b	Composite 3-Hour Wind Speed (m/s) Profile for Obbia, SI	2-22
Figure 2-16	The Pakistani Heat Low in Association with a Large-Scale Thermal Low-Pressure Trough (shaded) Over SWANEA Region During Northern Hemisphere Summer.....	2-23
Figure 2-17	Mean Surface Monsoon Trough Positions: April through November	2-24
Figure 2-18	Vertical Cross Section of the "African Interior" Monsoon Trough and the Intertropical Discontinuity (ITD) (from Omotosho, 1984).....	2-25
Figure 2-19	Mean Surface Monsoon Trough Position and Natural Pathways (Arrows) for Low-Level Inflow	2-26
Figure 2-20a	Mean June Positions of the 3,000-foot Monsoon Trough (NET) and the Southern Equatorial Trough (SET) (from Findlater, 1971)	2-27
Figure 2-20b	Mean July Positions of the 3,000-foot Monsoon Trough (NET) and the Southern Equatorial Trough (SET) (from Findlater, 1971)	2-28
Figure 2-20c	Mean August Positions of the 3,000-foot Monsoon Trough (NET) and the Southern Equatorial Trough (SET) (from Findlater, 1971)	2-29
Figure 2-21a	Mean October Surface Position of the Asiatic High.....	2-30
Figure 2-21b	Mean November Surface Position of the Asiatic High	2-31
Figure 2-21c	Mean January Surface Position of the Asiatic High	2-32
Figure 2-21d	Mean March Surface Position of the Asiatic High	2-33
Figure 2-21e	Mean April Surface Position of the Asiatic High	2-34
Figure 2-22a	Mean January Surface Position of the Saharan High.....	2-35
Figure 2-22b	Mean April Surface Position of the Saharan High.....	2-35

Figure 2-23a	Mean November Gradient Flow and Position of the Saudi Arabian High.....	2-36
Figure 2-23b	Mean January Gradient Flow and Position of the Saudi Arabian High.....	2-37
Figure 2-23c	Mean March Gradient Flow and Position of the Saudi Arabian High.....	2-37
Figure 2-24	Interaction of Saudi Arabian and Saharan High Surface Flow Produces the Red Sea Convergence Zone (RSCZ) (from Fett, 1980)	2-38
Figure 2-25	RSCZ Positions: October--April	2-39
Figure 2-26a-c	Mean January Upper-Air Flow Patterns (850, 700, 500, 300, 200 mb).....	2-40
Figure 2-27a-c	Mean April Upper-Air Flow Patterns (850, 700, 500, 300, 200 mb).....	2-43
Figure 2-28a-c	Mean July Upper-Air Flow Patterns (850, 700, 500, 300, 200 mb).....	2-45
Figure 2-29a-c	Mean October Upper-Air Flow Patterns (850, 700, 500, 300, 200 mb)	2-48
Figure 2-30a	Mean January Position of the Subtropical Ridge	2-51
Figure 2-30b	Mean July Position of the Subtropical Ridge.....	2-51
Figure 2-31a	Mean January Positions of the Polar and Subtropical Jet Streams	2-52
Figure 2-31b	Mean July Positions of the Polar and Subtropical Jet Streams	2-53
Figure 2-32a	Typical Jet Positions During Formation of Genoa Low	2-54
Figure 2-32b	Typical Jet Positions During Formation of Atlas Low	2-54
Figure 2-32c	Typical Jet Positions During Formation of Cyprus Low	2-55
Figure 2-33	Mediterranean Cyclogenesis Regions	2-55
Figure 2-34	Mediterranean-Generated Cyclonic Activity and Trailing Cold Front Entering the Gulf of Aden.....	2-56
Figure 2-35a	Synoptic Surface Chart (16 April 1964, 1200Z/1500 LST) Showing an Eastward-Tracking Atlas Low	2-58
Figure 2-35b	Synoptic Surface Chart (17 April 1964, 1200Z/1500 LST) Showing Secondary Low Formation Along the Active Cold Front.....	2-58
Figure 2-36a	Primary (solid arrow) and Secondary (dashed arrow) Mid-Latitude Storm Tracks, December, January, and February	2-59
Figure 2-36b	Primary (solid arrow) and Secondary (dashed arrow) Mid-Latitude Storm Tracks, March and April.....	2-59
Figure 2-36c	Primary (solid arrow) and Secondary (dashed arrow) Mid-Latitude Storm Tracks, November.....	2-60

Figure 2-37a	11 July 1978 Satellite-Derived Wind Vectors Over the Equatorial Western Indian Ocean (from Cadet and Desbois, 1981)	2-60
Figure 2-37b	12 July 1978 Synoptic Chart (1200Z/1500 LST) for the Southeast African Coast and the Large Island of Madagascar (from Cadet and Desbois, 1981)	2-60
Figure 2-37c	13 July 1978 Synoptic Chart (1200Z/1500 LST) for the Southeast African Coast and Madagascar (from Cadet and Desbois, 1981)	2-61
Figure 2-37d	14 July 1978 Synoptic Chart (1200Z/1500 LST) for the Southeast African Coast and Madagascar (from Cadet and Desbois, 1981)	2-61
Figure 2-37e	14 July 1978 Satellite-Derived Wind Vectors Over the Equatorial Western Indian Ocean (from Cadet and Desbois, 1981)	2-61
Figure 2-37f	15 July 1978 Synoptic Chart (1200Z/1800 LST) for the Southeast African Coast and Madagascar (from Cadet and Desbois, 1981)	2-61
Figure 2-37g	15 July 1978 Satellite-Derived Wind Vectors Over the Equatorial Western Indian Ocean (from Cadet and Desbois, 1981)	2-62
Figure 2-37h	16 July 1978 Synoptic Chart for the Southeast African Coast and Madagascar (from Cadet and Desbois, 1981)	2-62
Figure 2-37i	16 July 1978 Satellite-Derived Wind Vectors Over the Equatorial Western Indian Ocean (from Cadet and Desbois, 1981)	2-62
Figure 2-37j	17 July 1978 Synoptic Chart (1200Z/1500 LST) for the Southeast African Coast and Madagascar (from Cadet and Desbois, 1981)	2-62
Figure 2-37k	17 July 1978 Satellite-Derived Wind Vectors Over the Equatorial Western Indian Ocean (from Cadet and Desbois, 1981)	2-63
Figure 2-38	Schematic Cross-Section Through Squall Line System (from Gamache and Houze, 1982)	2-63
Figure 2-39a	May Tropical Depression and Cyclone Tracks 1891-1960 (from Indian Met Dept, 1964)	2-64
Figure 2-39b	October Tropical Depression and Cyclone Tracks, 1891-1960 (from Indian Met Dept, 1964)	2-65
Figure 2-39c	November Tropical Depression and Cyclone Tracks, 1891-1960 (from Indian Met Dept, 1964)	2-65
Figure 2-40	Large-Scale Thermal Trough Position (shaded area) July	2-66
Figure 2-41	Mean July Position of the Saharan Low	2-67
Figure 2-42a	Mean January Surface Position of the Sudanese Low	2-67
Figure 2-42b	Mean April Surface Position of the Sudanese Low	2-68
Figure 2-42c	Mean July Surface Position of the Sudanese Low	2-68
Figure 2-42d	Mean October Surface Position for the Sudanese Low	2-68

Figure 2-43	Mean July Gradient-Level Flow Showing the Position of the Saudi Arabian Low.....	2-69
Figure 2-44a	Typical Daytime Valley Circulation (After Flohn, 1969).....	2-70
Figure 2-44b	Typical Nighttime Mountain Circulation (After Flohn, 1969)	2-71
Figure 2-45a-h	The Life Cycle of a Typical Mountain-Valley Wind Circulation	2-71
Figure 2-46	Initial Flow Pattern Over Topographic Barrier; Wind Speed Less Than 15 Knots (from Barry, 1981)	2-73
Figure 2-47	Vertical Cross-Section of Mountain Lee Wave (Gravity Wave) Formation (from Barry, 1981) ...	2-73
Figure 2-48	The "Common" Daytime Sea Breeze and Nighttime Land Breeze.....	2-75
Figure 2-49a-f	Typical "Frontal" Land-Sea Breeze Sequence	2-75
Figure 2-50a	Local Topography at Cape Guardafui (Ras Asir) (from Findlater 1971).....	2-76
Figure 2-50b	Synoptic Scale Winds at Cape Guardafui (Ras Asir) (from Findlater, 1971).....	2-77
Figure 2-50c	Mean July Surface Streamline Flow (from Findlater, 1971)	2-77
Figure 2-51	WBGT Heat Stress Index Activity Guidelines	2-78
Figure 2-52a	Average Maximum WBGT--January.....	2-79
Figure 2-52b	Average Maximum WBGT--April.....	2-80
Figure 2-52c	Average Maximum WBGT--July.....	2-81
Figure 2-52d	Average Maximum WBGT--October	2-82
Figure 3-1	The Indian Ocean Plain	3-2
Figure 3-2a	The Coastal Dunes and Lowlands.....	3-3
Figure 3-2b	The Dissected Hills	3-4
Figure 3-2c	The Elevated Western Plateau.....	3-5
Figure 3-3	Mean Southwest Monsoon Cloudiness Frequencies, Indian Ocean Plain.	3-7
Figure 3-4	Southwest Monsoon Frequencies of Ceilings Below 3,000 Feet (915 meters), Indian Ocean Plain.....	3-8
Figure 3-5	Southwest Monsoon Frequencies of Visibilities Below 3 Miles, Indian Ocean Plain.....	3-9
Figure 3-6	Mean July-August Wind Speed (kts) and Prevailing Direction, Indian Ocean Plain	3-10
Figure 3-7	Mean Annual Wind Direction for Mandera, Kenya.....	3-10
Figure 3-8	Mean Southwest Monsoon Monthly/Maximum 24-Hour Precipitation, Indian Ocean Plain.....	3-11

Figure 3-9	Mean July Flow Pattern at 3,000 Feet (915 meters) AGL (from Findlater, 1970)	3-12
Figure 3-10	Mean Southwest Monsoon Daily Maximum/Minimum Temperatures ($^{\circ}$ F), Indian Ocean Plain	3-13
Figure 3-11	Mean October Flow Pattern at 3,000 Feet (915 meters) AGL (from Findlater, 1971)	3-14
Figure 3-12	Mean SW-NE Monsoon Transition Cloudiness Frequencies, Indian Ocean Plain	3-15
Figure 3-13	SW-NE Monsoon Transition Frequencies of Ceilings Below 3,000 Feet (915 meters), Indian Ocean Plain	3-16
Figure 3-14	SW-NE Monsoon Frequencies of Visibilities Below 3 Miles, Indian Ocean Plain	3-17
Figure 3-15	Mean October-November Wind Speed (kts) and Prevailing Direction, Indian Ocean Plain	3-18
Figure 3-16	Mean SW-NE Monsoon Transition Monthly/Maximum 24-Hour Precipitation, Indian Ocean Plain	3-19
Figure 3-17	Mean SW-NE Monsoon Transition Daily Maximum/Minimum Temperatures ($^{\circ}$ F), Indian Ocean Plain	3-20
Figure 3-18	Mean Northeast Monsoon Cloudiness Frequencies, Indian Ocean Plain	3-21
Figure 3-19	Northeast Monsoon Frequencies of Ceilings Below 3,000 Feet (915 meters), Indian Ocean Plain	3-22
Figure 3-20	Northeast Monsoon Frequencies of Visibilities Below 3 Miles, Indian Ocean Plain	3-23
Figure 3-21	Mean Northeast Monsoon Wind Speed (kts) and Prevailing Direction, Indian Ocean Plain	3-23
Figure 3-22	Mean Northeast Monsoon Monthly/Maximum 24-hour Precipitation, Indian Ocean Plain	3-34
Figure 3-23	Mean Northeast Monsoon Daily Maximum/Minimum Temperatures ($^{\circ}$ F), Indian Ocean Plain	3-35
Figure 3-24	Mean NE-SW Monsoon Transition Cloudiness Frequencies, Indian Ocean Plain	3-26
Figure 3-25	NE-SW Monsoon Transition Frequencies of Ceilings Below 3,000 Feet (915 meters), Indian Ocean Plain	3-27
Figure 3-26	NE-SW Monsoon Transition Frequencies of Visibilities Below 3 Miles, Indian Ocean Plain	3-28
Figure 3-27	Mean NE-SW Monsoon Transition Wind Speed (kts) and Prevailing Direction, Indian Ocean Plain	3-29
Figure 3-28	Mean May Flow Pattern at 3,000 Feet (915 meters) AGL (adapted from Findlater, 1971)	3-30
Figure 3-29	Mean NE-SW Monsoon Transition Monthly/Maximum 24-Hour Precipitation, Indian Ocean Plain	3-31
Figure 3-30	Mean NE-SW Monsoon Transition Daily Maximum/Minimum Temperatures ($^{\circ}$ F), Indian Ocean Plain	3-32

Figure 4-1a	The Ethiopian Highlands.....	4-2
Figure 4-1b	Climatological Summaries for Selected Stations in the Ethiopian Highlands.....	4-3
Figure 4-2a	The Western Highlands.....	4-4
Figure 4-2b	The Great Rift Valley.....	4-5
Figure 4-2c	The Eastern Highlands.....	4-6
Figure 4-3	Mean Southwest Monsoon Cloudiness Frequencies, Ethiopian Highlands.....	4-9
Figure 4-4	Southwest Monsoon Frequencies of Ceilings Below 3,000 Feet (915 meters), Ethiopian Highlands.....	4-10
Figure 4-5	Southwest Monsoon Frequencies of Visibilities Below 3 Miles, Ethiopian Highlands.....	4-11
Figure 4-6	Mean Annual Wind Direction, Addis Ababa, Ethiopia.....	4-12
Figure 4-7	Mean Annual Wind Direction, Asmara, Ethiopia.....	4-13
Figure 4-8	Mean Southwest Monsoon Surface Wind Speed (kts) and Prevailing Direction, Ethiopian Highlands.....	4-14
Figure 4-9	Generalized Southwest Monsoon 850-mb Streamline Flow Pattern and Low-Level Moisture Inflow Trajectories.....	4-14
Figure 4-10	Mean Southwest Monsoon Monthly Precipitation, Ethiopian Highlands.....	4-15
Figure 4-11	Mean Southwest Monsoon Daily Maximum/Minimum Temperatures (°F), Ethiopian Highlands.....	4-16
Figure 4-12	Mean SW-NE Monsoon Transition Cloudiness Frequencies, Ethiopian Highlands.....	4-17
Figure 4-13	SW-NE Monsoon Transition Frequencies of Ceilings Below 3,000 Feet (915 meters), Ethiopian Highlands.....	4-18
Figure 4-14	SW-NE Monsoon Transition Frequencies of Visibilities Below 3 Miles, Ethiopian Highlands....	4-19
Figure 4-15	Mean SW-NE Monsoon Transition Wind Speed (kts) and Prevailing Direction, Ethiopian Highlands.....	4-20
Figure 4-16	Mean SW-NE Monsoon Transition Monthly Precipitation, Ethiopian Highlands.....	4-21
Figure 4-17	Mean SW-NE Monsoon Transition Daily Maximum/Minimum Temperatures (°F) Ethiopian Highlands.....	4-22
Figure 4-18	Mean Annual Wind Direction, Addis Ababa, Ethiopia.....	4-23
Figure 4-19	Mean Northeast Monsoon Cloudiness Frequencies, Ethiopian Highlands.....	4-24

Figure 4-20	Northeast Monsoon Frequencies of Ceilings Below 3,000 Feet (915 meters), Ethiopian Highlands	4-25
Figure 4-21	Northeast Monsoon Frequencies of Visibilities Below 3 Miles, Ethiopian Highlands	4-26
Figure 4-22	Mean Northeast Monsoon Wind Speed (kts) and Prevailing Direction, Ethiopian Highlands	4-27
Figure 4-23	Generalized Low-Level Flow Across the Eastern Highlands (shaded) during the Northeast Monsoon	4-27
Figure 4-24	Generalized Low-Level Flow Across the Western Highlands (shaded) during the Northeast Monsoon	4-28
Figure 4-25	Mean Northeast Monsoon Monthly Precipitation, Ethiopian Highlands	4-29
Figure 4-26a	Surface Streamline Analysis, 19 December 1979 (0600Z/0900 LST).....	4-30
Figure 4-26b	700-mb Analysis, 19 December 1979, (0000Z/0300 LST).....	4-31
Figure 4-27	Mean Northeast Monsoon Daily Maximum/Minimum Temperatures (°F), Ethiopian Highlands	4-32
Figure 4-28	Mean NE-SW Monsoon Transition Cloudiness Frequencies, Ethiopian Highlands	4-33
Figure 4-29	NE-SW Monsoon Transition Frequencies of Ceilings Below 3,000 Feet (915 meters), Ethiopian Highlands.....	4-35
Figure 4-30	NE-SW Monsoon Transition Frequencies of Visibilities Below 3 Miles, Ethiopian Highlands....	4-36
Figure 4-31	Mean NE-SW Monsoon Transition Wind Speed (kts) and Prevailing Direction, Ethiopian Highlands.....	4-37
Figure 4-32	Mean NE-SW Monsoon Transition Monthly Precipitation, Ethiopian Highlands	4-38
Figure 4-33	Mean NE-SW Monsoon Transition Daily Maximum/Minimum Temperatures (°F), Ethiopian Highlands.....	4-39
Figure 5-1a	The Aden Coastal Fringe	5-2
Figure 5-1b	Climatological Summaries for Selected Stations in the Aden Coastal Fringe.....	5-3
Figure 5-2	Mean Southwest Monsoon Cloudiness Frequencies, Aden Coastal Fringe.....	5-5
Figure 5-3	Southwest Monsoon Frequencies of Ceilings Below 3,000 Feet (915 meters), Aden Coastal Fringe.....	5-6
Figure 5-4	Southwest Monsoon Frequencies of Visibilities Below 3 Miles, Aden Coastal Fringe	5-7
Figure 5-5a	Complex Surface Circulation on the Southeastern Aden Coastal Fringe	5-8
Figure 5-5b	Closeup View of Individual Vortex Over Cape Guardafui, Somalia (from Findlater, 1971).....	5-9

Figure 5-6	Mean Southwest Monsoon Wind Speed and Prevailing Direction, Aden Coastal Fringe.....	5- 6
Figure 5-7a	Mean Annual Wind Direction, Aden, AD.....	5-10
Figure 5-7b	Mean Annual Wind Direction, Djibouti, DJ	5-10
Figure 5-8	Mean Southwest Monsoon Monthly/Maximum 24-Hour Precipitation, Aden Coastal Fringe	5-11
Figure 5-9	Mean Southwest Monsoon Daily Maximum/Minimum Temperatures (°F), Aden Coastal Fringe.....	5-12
Figure 5-10	Mean SW-NE Monsoon Transition Cloudiness Frequencies, Aden Coastal Fringe	5-13
Figure 5-11	SW-NE Monsoon Transition Frequencies of Ceilings Below 3,000 Feet (915 meters), Aden Coastal Fringe.....	5-14
Figure 5-12	SW-NE Monsoon Transition Frequencies of Visibilities Below 3 Miles, Aden Coastal Fringe....	5-15
Figure 5-13	Mean SW-NE Monsoon Transition Wind Speed (kts) and Prevailing Direction, Aden Coastal Fringe.....	5-16
Figure 5-14	Mean SW-NE Monsoon Transition Monthly/Maximum 24-Hour Precipitation, Aden Coastal Fringe.....	5-16
Figure 5-15	Mean SW-NE Monsoon Transition Daily Maximum/Minimum Temperatures (°F), Aden Coastal Fringe.....	5-16
Figure 5-16	Mean Northeast Monsoon Cloudiness Frequencies, Aden Coastal Fringe.....	5-16
Figure 5-17	Northeast Monsoon Frequencies of Ceilings Below 3,000 Feet (915 meters), Aden Coastal Fringe.....	5-19
Figure 5-18	Northeast Monsoon Frequencies of Visibilities Below 3 Miles, Aden Coastal Fringe	5-20
Figure 5-19	Mean Northeast Monsoon Wind Speed (kts) and Prevailing Direction, Aden Coastal Fringe.....	5-20
Figure 5-20	Mean Northeast Monsoon Monthly/Maximum 24-Hour Precipitation, Aden Coastal Fringe	5-21
Figure 5-21	The Polar Jet (PJS) and Subtropical Jet (STJ) Interact Over the Subtropics.....	5-22
Figure 5-22	Mean Northeast Monsoon Daily Maximum/Minimum Temperatures (°F), Aden Coastal Fringe.....	5-23
Figure 5-23a	Mean April Gradient Flow, Aden Coastal Fringe.....	5-24
Figure 5-23b	Mean May Gradient Flow, Aden Coastal Fringe	5-24
Figure 5-24	Mean NE-SW Monsoon Transition Cloudiness Frequencies, Aden Coastal Fringe	5-25
Figure 5-25	NE-SW Monsoon Transition Frequencies of Ceilings Below 3,000 Feet (915 meters), Aden Coastal Fringe.....	5-26
Figure 5-26	NE-SW Monsoon Transition Frequencies of Visibilities Below 3 Miles, Aden Coastal Fringe....	5-27

Figure 5-27	Mean NE-SW Monsoon Transition Wind Speed and Prevailing Direction, Aden Coastal Fringe.....	5-27
Figure 5-28	Mean NE-SW Monsoon Transition Monthly/Maximum 24-Hour Precipitation, Aden Coastal Fringe.....	5-28
Figure 5-29	Mean NE-SW Monsoon Transition Mean Daily Maximum/Minimum Temperatures (°F), Aden Coastal Fringe.....	5-29
Figure 6-1	The Yemen Highlands.....	6-2
Figure 6-2	Mean Southwest Monsoon Cloudiness (Isolines) and Frequencies of Ceilings Below 3,000 Feet (915 Meters), Yemen Highlands.....	6-6
Figure 6-3	Southwest Monsoon Frequencies of Visibilities Below 3 Miles, Yemen Highlands.....	6-7
Figure 6-4	Mean Southwest Monsoon Wind Speed (kts) and Prevailing Direction, Yemen Highlands.....	6-8
Figure 6-5a	Mean Annual Wind Direction, San'a, YD.....	6-8
Figure 6-5b	Mean Annual Wind Direction, Khamis Mushait, SD.....	6-9
Figure 6-5c	Mean Annual Wind Direction, Ta'iz, YD.....	6-9
Figure 6-6	Mean Southwest Monsoon Monthly/Maximum 24-Hour Precipitation, Yemen Highlands.....	6-10
Figure 6-7	Mean Southwest Monsoon Daily Maximum/Minimum Temperatures (°F), Yemen Highlands.....	6-11
Figure 6-8	Mean SW-NE Monsoon Transition Cloudiness (Isolines) and Frequencies of Ceilings Below 3,000 Feet (915 Meters), Yemen Highlands.....	6-12
Figure 6-9	SW-NE Monsoon Transition Frequencies of Visibilities Below 3 Miles, Yemen Highlands.....	6-13
Figure 6-10	Mean SW-NE Monsoon Transition Wind Speed (kts) and Prevailing Direction, Yemen Highlands.....	6-14
Figure 6-11a	Mean Annual Wind Direction, Khamis Mushait, SD.....	6-14
Figure 6-11b	Mean Annual Wind Direction, San'a, YD.....	6-15
Figure 6-12	Mean SW-NE Monsoon Transition Monthly/Maximum 24-Hour Precipitation, Yemen Highlands.....	6-16
Figure 6-13	Mean SW-NE Monsoon Transition Daily Maximum/Minimum Temperatures (°F), Yemen Highlands.....	6-17
Figure 6-14	Mean Northeast Monsoon Cloudiness (Isolines) and Frequencies of Ceilings Below 3,000 Feet (915 Meters), Yemen Highlands.....	6-18
Figure 6-15	Upper-Level (300-mb) Flow Supporting an Intense Frontal Passage into the Northern Yemen Highlands.....	6-19
Figure 6-16	Northeast Monsoon Frequencies of Visibilities Below 3 Miles, Yemen Highlands.....	6-20

Figure 6-17	Mean Northeast Monsoon Wind Speed (kts) and Prevailing Direction, Yemen Highlands.....	6-21
Figure 6-18a	Mean Annual Wind Direction, Ta'iz, YD.....	6-22
Figure 6-18b	Mean Annual Wind Direction, San'a, YD.....	6-22
Figure 6-19	Mean Northeast Monsoon Monthly/Maximum 24-Hour Precipitation, Yemen Highlands.....	6-23
Figure 6-20	Mean Northeast Monsoon Daily Maximum/Minimum Temperatures ($^{\circ}$ F), Yemen Highlands.	6-24
Figure 6-21	Mean NE-SW Monsoon Transition Cloudiness (Isolines) and Frequencies of Ceilings Below 3,000 Feet (915 Meters), Yemen Highlands.....	6-25
Figure 6-22	NE-SW Monsoon Transition Frequencies of Visibilities Below 3 Miles, Yemen Highlands.....	6-27
Figure 6-23	Mean NE-SW Monsoon Transition Wind Speed (kts) and Prevailing Direction, Yemen Highlands.....	6-27
Figure 6-24	Mean NE-SW Monsoon Transition Monthly/Maximum 24-Hour Precipitation, Yemen Highlands.....	6-28
Figure 6-25	Mean NE-SW Monsoon Transition Daily Maximum/Minimum Temperatures ($^{\circ}$ F), Yemen Highlands.....	6-29

Chapter 1

INTRODUCTION

AREA OF INTEREST. This study--the first of five volumes that cover the entire "SWANEA" (Southwest Asia-Northeast Africa) region shown in Figure 1-1--describes the geography, climatology, and meteorology of the Horn of Africa, an area that is politically divided among seven countries: Somalia (SI), Ethiopia (ET), Djibouti (DJ), Yemen-Sana (YD), and

Yemen-Aden, including Socotra Island (AD) and small portions of Sudan (SU) and Saudi Arabia (SD). For this study, the Horn of Africa has been divided into the four zones of "climatic commonality" (the Indian Ocean Plain, the Ethiopian Highlands, the Aden Coastal Fringe, and the Yemen Highlands), as shown in Figure 1-2, next page.

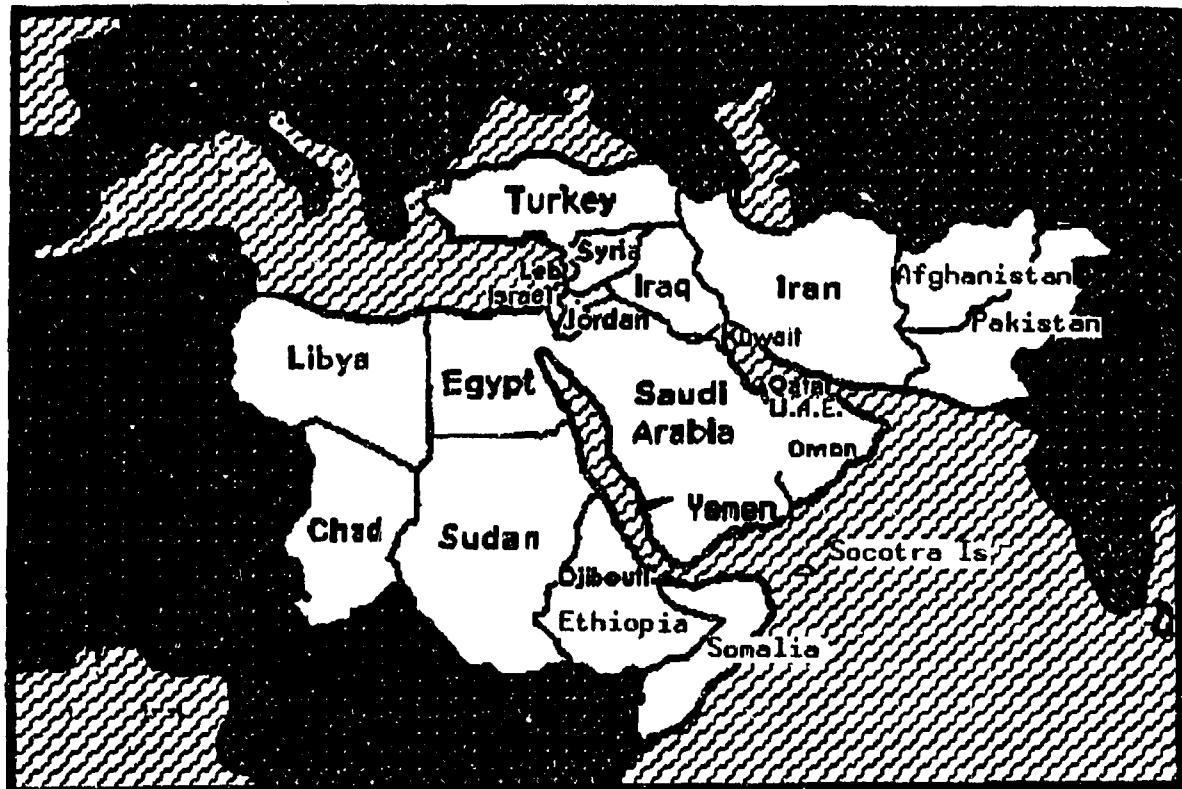


Figure 1-1. The Southwest Asia-Northeast Africa (SWANEA) Region.

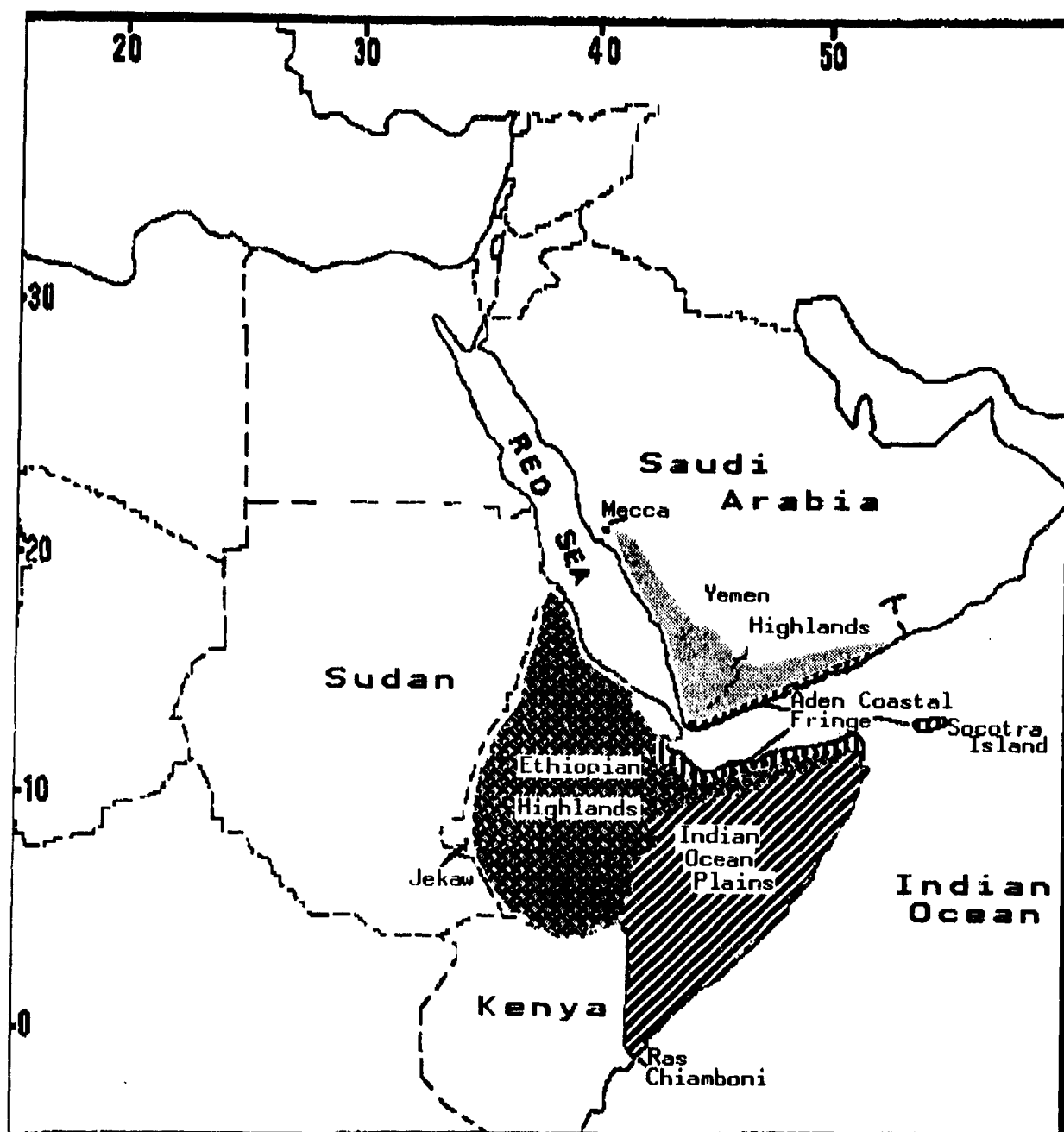


Figure 1-2. The Horn of Africa and its Four "Zones of Climatic Commonality".

GEOGRAPHY. From Jekaw, ET, in the west, to Socotra Island in the east, the region described here as the "Horn of Africa" is 1,360 NM wide. It contains extensive mountain ranges, plateaus, and adjacent coastal lowlands that extend 1,600 NM from the northern Yemen Highlands near Mecca, SD to Ras Chiamboni,

SI. The eastern border is marked by the Indian Ocean and Gulf of Aden coastline. Kenya and Sudan, respectively, are on the southern and western borders. The northern borders from west to east are formed by the Red Sea on the west and the Rub al Khali Desert in south central Saudi Arabia on the east.

The Afro-Arabian Rift System (or Great Rift System) shown in Figure 1-3 dominates topography in the Horn of Africa. This massive feature runs north to south across 53 degrees of latitude from 20° S to 33° N. Numerous north-to-south mountain ranges average 650 NM in length and 400 NM in width. The largest is the Eritrean Mountain system in northwestern Ethiopia (see the Ethiopian Highlands, Figure 4-1a). The Eritrean

Mountains run from 7,000 to 8,000 feet (2,134-2,743 meters). Numerous volcanic peaks rise above 12,000 feet (3,658 meters) on the African mainland and above 10,000 feet (3,050 meters) on the Arabian Peninsula. Mount Dashan, in the Eritrean Mountains, is the highest at 15,158 feet (4,620 meters) MSL. Several hundred fresh water lakes, fed by numerous springs and seasonal runoff, are found in the mountainous interior.

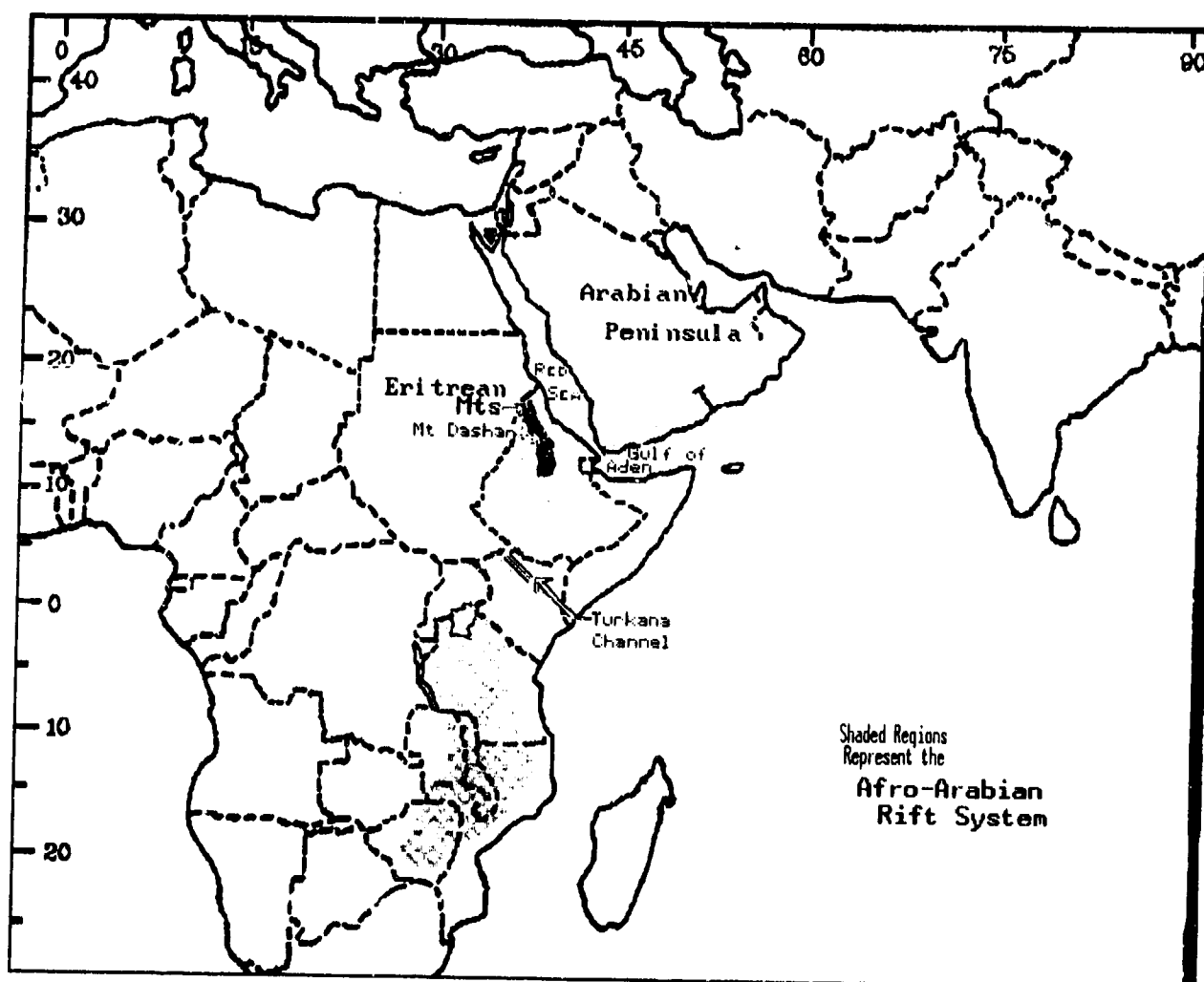


Figure 1-3. The Great (Afro-Arabian) Rift System.

The massive mountain complex formed by the Great Rift System has a significant effect on Horn of Africa climate by presenting a natural barrier between two distinctly different air masses; areas west of the Great Rift System are dominated by maritime tropical and continental tropical air masses, while areas to the east are

influenced exclusively by Indian Ocean maritime tropical air masses. Natural breaks in the Great Rift System, however, allow these air masses to converge below 850 millibars. The Red Sea/Gulf of Aden corridor and northern Kenya's Turkana Channel are the only outlets for low-level air mass convergence.

The rest of the Horn's surface area (about half) is semiarid alluvial plain, all lying below 3,280 feet (1,000 meters). Meteorology, topography, and latitude contribute significantly to aridity. Orographic uplift and large-scale circulation patterns provide scant annual rainfall (2-10 inches/52-254 mm) over these plains north of 6° N. Between 656 and 3,280 feet (200 and 1,000 meters), the plains are eroded plateaus and rolling hills cut up by intermittent stream beds. Lowlands below 656 feet/200 meters border the Gulf of Aden and Indian Ocean. The land surface here is dominated by lava beds, salt deserts, and sand dunes.

STUDY CONTENT. Chapter 2 provides a detailed discussion of the major climatic controls that affect the Horn of Africa. These controls range from the macroscale ("semipermanent climatic controls"), through the synoptic ("synoptic disturbances"), to the mesoscale. The individual treatments of each climatic subregion in subsequent chapters do not include repeated descriptions of these phenomena, but provide specifics unique to the individual subregion by focusing on mean distributions and local anomalies of sky cover, winds, precipitation, temperature, and visibility. Meteorologists using this study should read and consider the general discussion in Chapter 2 before trying to understand or apply the individual climatic zone discussions in Chapters 3-6. This is particularly important because the study was designed with two purposes in mind: first, as a master reference to the entire Horn of Africa, and second, as a modular reference to the several subregions of the Horn of Africa. Chapters 3-6 discuss "situation and relief" and "general weather" for each the four subregions, by season.

The Indian Ocean Plain (Chapter 3) lies between 2° S and 11° N and 41 to 51° E. The weather and climate here are controlled by the circulations of the Southwest and Northeast Monsoons. The land-sea breeze effect and southern hemisphere cold fronts (south of 4° N) are also important mesoscale and synoptic weather features. The Southwest Monsoon is characterized by phenomena such as the surface Monsoon Trough and the Somali Jet. During the Northeast Monsoon, southern hemispheric surges and local effects dominate weather patterns.

The Ethiopian Highlands (Chapter 4) span a large area. This extensive mountain system lies between 3 and 18° N, and between 34 and 50° E. Average elevation is 5,000 feet (1,524 meters). Since the entire subregion is affected by low-, mid-, and upper-level flow from the North African continent and the Indian Ocean throughout the year, Chapter 4 discusses a variety of phenomena

such as the surface Monsoon Trough, cyclonic activity, and monsoonal wind flow. Complex mountain/valley circulations are also important weather features.

The Aden Coastal Fringe (Chapter 5) is a narrow strip that lies along the Gulf of Aden and Red Sea coastlines between 10 and 13° N and between 42 and 53° E. It includes Socotra Island. Since the entire subregion is dominated by monsoonal and coastal weather phenomena, Chapter 5 describes the influences of the Southwest/Northeast Monsoon flow patterns and land/sea breeze effects.

The Yemen Highlands (Chapter 6), the northernmost subregion in the study area, lie along the southeastern edge of the Red Sea basin between 13 and 21° N and between 40 and 46° E. This mountainous subregion is bordered by vast subtropical deserts--the Sahara and the Rub al Khali--to the east, north, and west. Elevations in the Yemen Highlands average 6,000 feet (1,829 meters). From November to May, the northern Yemen Highlands are occasionally affected by Mediterranean weather. As a result, Chapter 6 stresses the Northeast and--to a lesser extent--Southwest Monsoon flow patterns while emphasizing cyclonic activity and mesoscale weather features.

CLIMATOLOGICAL REGIMES. Although the Horn of Africa is dominated by monsoon circulation, weather in each of the "climatically similar" subregions is distinctly different because of its location and orientation to prevailing airflow. The length of each monsoon season varies from subregion to subregion because the study area covers such a wide latitude belt. Typically, the Horn of Africa sees a 1- to 2-month transition period between the Southwest and Northeast Monsoons because the monsoonal flow must travel distances as great as 25-30 degrees. As a result, times and durations of seasons and transition periods vary from year to year and place to place. This study uses local names whenever appropriate to highlight variations in the monsoon seasons, transition periods, and typical conditions in a particular subregion.

Topography has an important influence on climate here; orographic uplift may accentuate the seasons and transitions. Since surface flow across the extensive mountain ridges, depending on orientation, may be moist in one location but dry in another at the same time, the presence of the Southwest Monsoon does not necessarily mean wet weather everywhere in the Horn of Africa. The reverse is also true--the Northeast Monsoon is not "dry" everywhere.

CONVENTIONS. The spellings of place names and geographical features are those used by the United States Defense Mapping and Aerospace Center (DMAAC). Distances are in nautical miles (NM), except for visibilities, which are in statute miles. Ceilings and cloud bases are in feet/meters above ground level (AGL)* but cloud tops are above mean sea level (MSL). Elevations are in feet with a meter or kilometer (km) equivalent immediately following. Temperatures are in Fahrenheit (F) with a Celsius (C) conversion following. Wind speeds are in knots. Precipitation amounts are in inches, with a millimeter (mm) conversion following. Most synoptic chart times are given in Greenwich Mean Time (GMT or Z), with a local standard time (LST) conversion. When synoptic charts are not provided, only LST is used.

**NOTE: The AGL cloud bases given in this study are generalized over large areas. Readers must consider terrain in applying these generalized values. For example, the AGL cloud bases given the Chapter 4 discussions of the Ethiopian Highlands are generally representative of valley reporting stations, but not of locations in surrounding mountains, where ceilings and cloud bases would be lower, and where, in fact, many locations would be obscured.*

DATA SOURCES. Most of the information used in preparing this study came from two sources, both within the United States Air Force Environmental Technical Applications Center (USAFETAC). Studies, books, atlases, and so on, were supplied, with rare exceptions, by the Air Weather Service Technical Library, or AWSTL, which is the only dedicated atmospheric sciences library in the Department of Defense and the largest such library in the United States. Climatological data came direct from the Air Weather Service Climatic Database or through Operating Location A, USAFETAC--the branch of USAFETAC responsible for maintaining and managing this database.

RELATED REFERENCES. This study, while more than ordinarily comprehensive, is not the only source of meteorological and climatological information for the military meteorologist concerned with the Horn of Africa. The United States Navy has published several excellent handbooks on this area and the adjacent coastal waters. USAFETAC/DS-87/034, Station Climatic Summaries--Africa, provides summarized meteorological observational data for several major airports in the study area. Staff weather officers and forecasters are urged to contact the Air Weather Service Technical Library for as much data on the study area as is currently available.

Chapter 2

MAJOR METEOROLOGICAL FEATURES OF THE HORN OF AFRICA

The "major meteorological features" of the Horn of Africa are listed below as they appear and are described in this chapter. These features affect the weather and climate of the Horn of Africa the year-round. The same features may be discussed in more detail in subsequent chapters as they relate to individual subregions of the study area.

Semipermanent Climatic Controls	2-2
Sea Surface Temperatures	2-2
The Azores High	2-3
The Influence of Large-Scale Meteorological Features on Gradient Flow	2-6
The Monsoon Climate	2-10
The Southwest Monsoon	2-10
The Tibetan 2(X)-mb Anticyclone	2-11
The Tropical Easterly Jet (TEJ)	2-13
The Mascarene (South Indian Ocean) High	2-13
The Somali Jet	2-16
The Pakistani Heat Low	2-22
The Monsoon Trough	2-23
The Northeast Monsoon	2-30
The Asiatic High	2-30
The Saharan High	2-34
The Saudi Arabian High	2-36
The Red Sea Convergence Zone	2-38
Mid-and Upper-Level Flow Patterns	2-40
The Subtropical Ridge	2-50
Synoptic Disturbances	2-52
Jet Streams	2-52
Cyclonic Activity	2-55
Storm Tracks	2-60
Southern Hemisphere Polar Surges	2-60
Tropical Disturbances	2-63
Thermal Lows	2-66
Mesoscale and Local Features	2-70
Mountain-Valley Winds	2-70
Mountain Waves	2-72
Duststorms	2-73
Land/Sea Breeze	2-75
Wet Bulb Globe Temperature (WBGT) Heat Stress Index	2-78

SEMIPERMANENT CLIMATIC CONTROLS

SEA SURFACE TEMPERATURES (SSTs). Figures 2-1a-d provide mean SSTs for Horn of Africa coastlines on the western Indian Ocean, the Gulf of Aden, and the Red Sea. Warm surface waters keep immediate coasts mild all year, but the marine boundary layer rarely

extends more than 30 NM inland or above 3,000 feet (915 meters). The diurnal temperature range is only 10-20°F (6-11°C) along the coast, but inland (outside the marine boundary layer's influence), the range is 20-35°F (11-19°C).

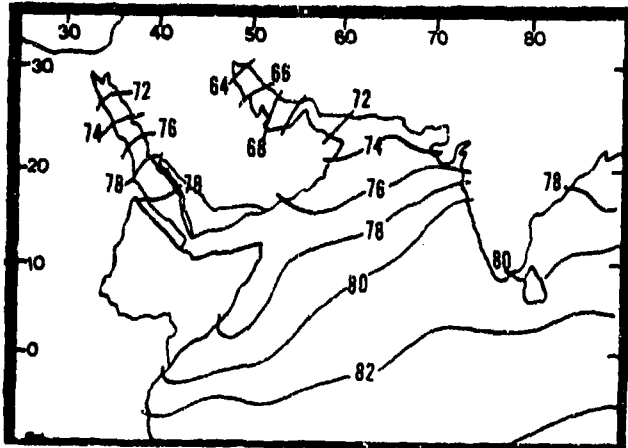


Figure 2-1a. Mean January Sea Surface Temperatures (°F). The largest gradients are in the Red Sea, where SSTs vary between 71 and 78°F (22-26°C). A north to south increase is caused by cooler mid-latitude January air masses. South of 25° N, Red Sea and Gulf of Aden SSTs are 74-78°F (23-26°C). Along the Somalia coast, water temperatures range from 77 to 81°F (25 to 27°C).

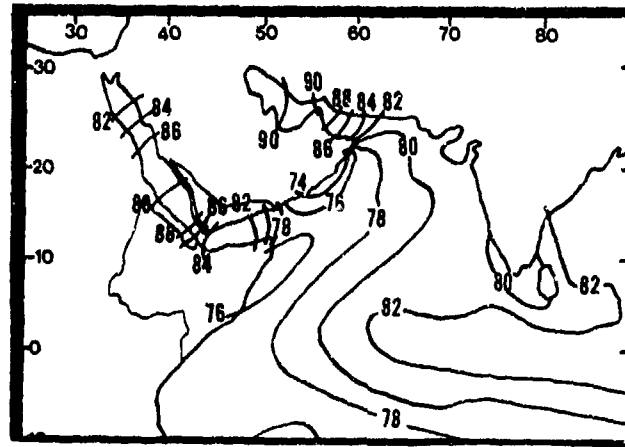


Figure 2-1c. Mean July Sea Surface Temperatures (°F). In the Red Sea and Gulf of Aden, mean July SSTs average 78-88°F (26-31°C). In the northeastern Gulf of Aden (near Ras Fartak) and in Somalia coastal waters, SSTs are lower because of strong upwelling caused by the Somali Jet.

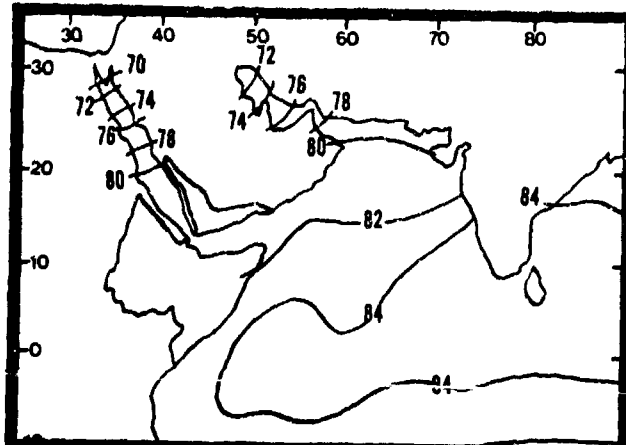


Figure 2-1b. Mean April Sea Surface Temperatures (°F). April SSTs are about the same (78-81°F/26-27°C) in the southern Red Sea, the Gulf of Aden, and the western Indian Ocean. Although Red Sea SSTs are cooler (70-78°F/21-26°C) North of 23° N, they don't influence the Horn of Africa's coastal environment.

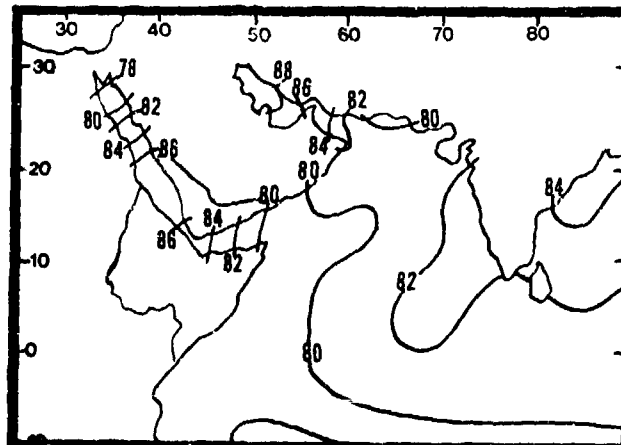


Figure 2-1d. Mean October Sea Surface Temperatures (°F). October SSTs range from 80 to 81°F (27°C) along the Somalia coast and in the extreme northern Red Sea, and from 86 to 87°F (30°C) in the central and southern Red Sea. As already mentioned, the cooler northern Red Sea waters don't affect the Horn of Africa.

THE AZORES HIGH. The position of this semipermanent high varies from 29° N, 29° W in January (Figure 2-2a) to about 37° N, 37° W in July (Figure 2-2c). Mean sea level pressure varies from 1021 mb in January to 1025 mb in July. The high's influence on the Horn of Africa is strongest between November and April, but weakest between May and October, when

northwesterly outflow from the High rarely penetrates south of 15° N. Typically, the Yemen Highlands, the northern Ethiopian Highlands, and the Aden Coastal Fringe are the only subregions affected by northwesterly flow between November and April. Mean northwesterly surface flow into the central and southern Red Sea averages 3-5 kts between December and early April.

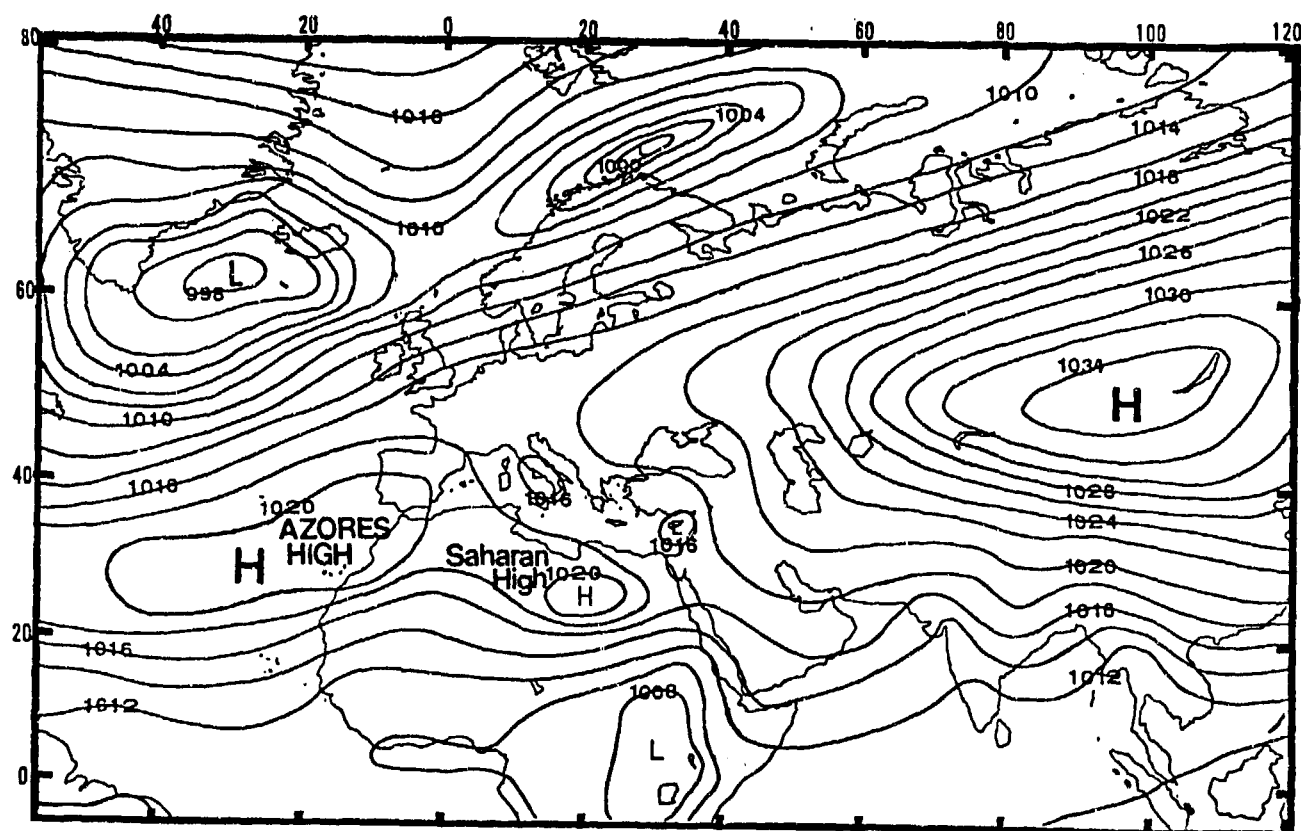


Figure 2-2a. Mean January Position of the Azores High.

Between December and February, the Azores High extends eastward (as shown in Figure 2-2a) over the western Sahara. It joins a secondary high pressure cell (the Saharan High) to form a weak high-pressure ridge over the Sahara Desert. Slight deviations in the High's mean strength and position may temporarily tilt the ridge axis from west-east to northwest-southeast. A very strong Azores High may tilt the ridge's eastern edge northward over the coastal waters of western Europe while the Saharan High remains fixed over the northern Sahara. If the Azores High maintains its surface position along the west coast of Europe for 3 or more consecutive days, a "blocking" pattern may be established to allow the 500-mb Polar Jet (which see) to slide southward into the north central Sahara. This Polar Jet position

produces cold weather outbreaks and severe duststorms over the Sahara Desert, the Red Sea, and the eastern Mediterranean Basin.

Between March and May, the Azores High, with central pressure now 1021 mb, moves slowly west-northwest to near 30° N, 37° W (see Figure 2-2b). Its spring migration to the west and away from the African continent weakens the mean high-pressure ridge over North Africa. Cyclonic activity (see "Synoptic Disturbances") dips southward over the western Mediterranean Sea and Atlas Mountains, reaching the northern fringes of the Horn of Africa most frequently in March. Normally, cold fronts produce severe sandstorms along the western edges of the Ethiopian Highlands.

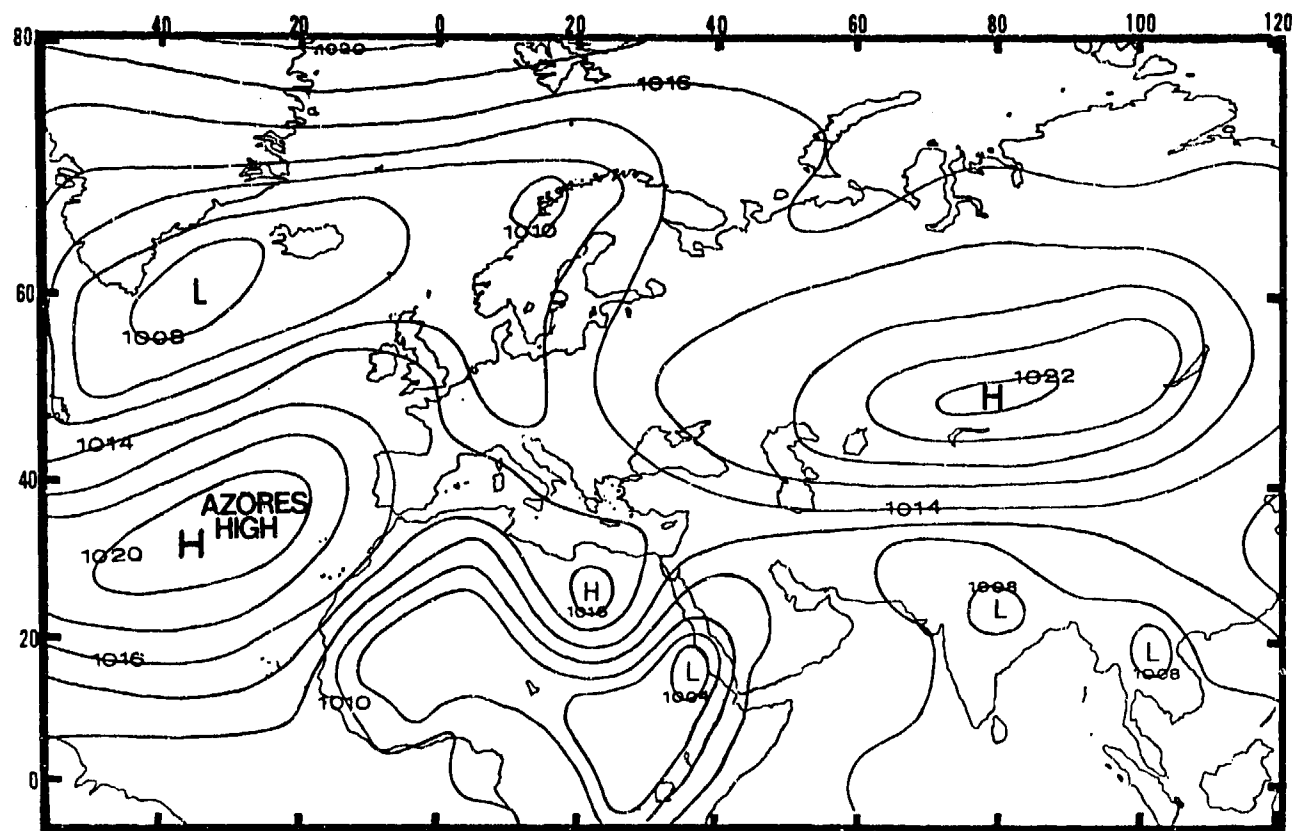
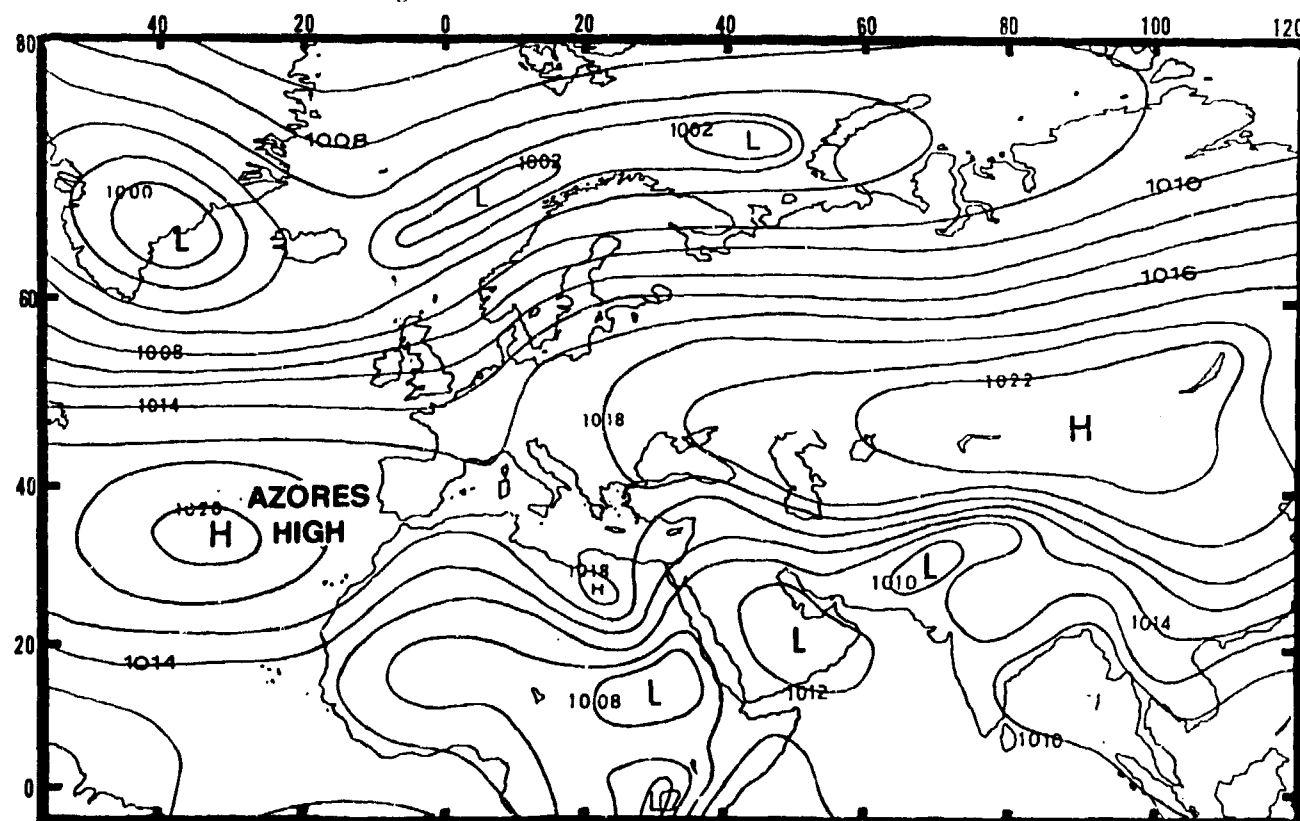
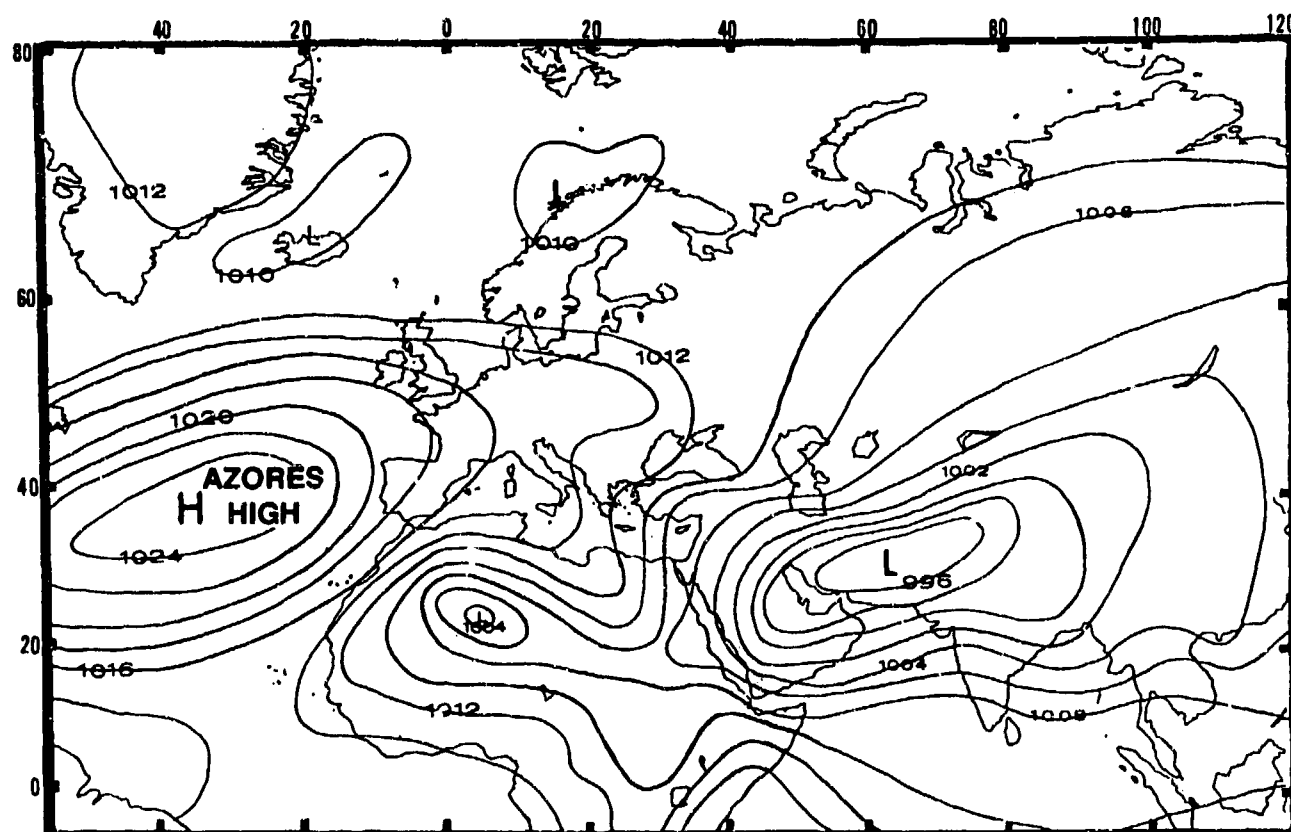


Figure 2-2b. Mean April Position of the Azores High.

Between June and September, the Azores High's central pressure strengthens to 1025 mb. Its mean summer position is near 37° N, 37° W. Figure 2-2c shows the High at its northernmost position, where it effectively blocks any significant cyclonic activity from entering the Sahara Desert and Red Sea. When the ridge is weak and there is strong low pressure off Iceland, however, cyclonic activity can penetrate southward. The prevailing WNW-NW mid-level winds are weak. As a result, surface cold fronts move slowly across the Sahara.

Although the hot and dry desert air modifies the front rapidly, strong mid-and upper-level troughs can cause significant weather in extreme northern sections of the Horn of Africa.

Between October and November, the Azores High moves south to a new mean position at 35° N, 30° W. Figure 2-2d shows the Azores High and the mean high pressure cell developing in the Sahara.



THE INFLUENCE OF LARGE-SCALE METEOROLOGICAL FEATURES ON GRADIENT FLOW.

Gradient-level flow over the Horn of Africa is controlled by the Azores High (see page 2-3), the South Atlantic High (not shown), the Southwest Monsoons (page 2-10), and the Northeast Monsoon (page 2-30). The strengths and locations of these four features determine the low-level flow and resulting positioning of the Monsoon Trough. The annual north-south Monsoon Trough oscillation, in turn, determines the types of air masses

(and the resultant weather) that will affect the Horn of Africa.

Figures 2-3a-d show mean gradient flow over the Horn of Africa in January, April, July, and October. January flow (Figure 2-3a) west of the Great Rift System is controlled by Azores high outflow, but flow east of the Rift System is controlled by the Northeast Monsoon. By April (Figure 2-3b), the Monsoon Trough is shifting northward through southern Ethiopia and Somalia.

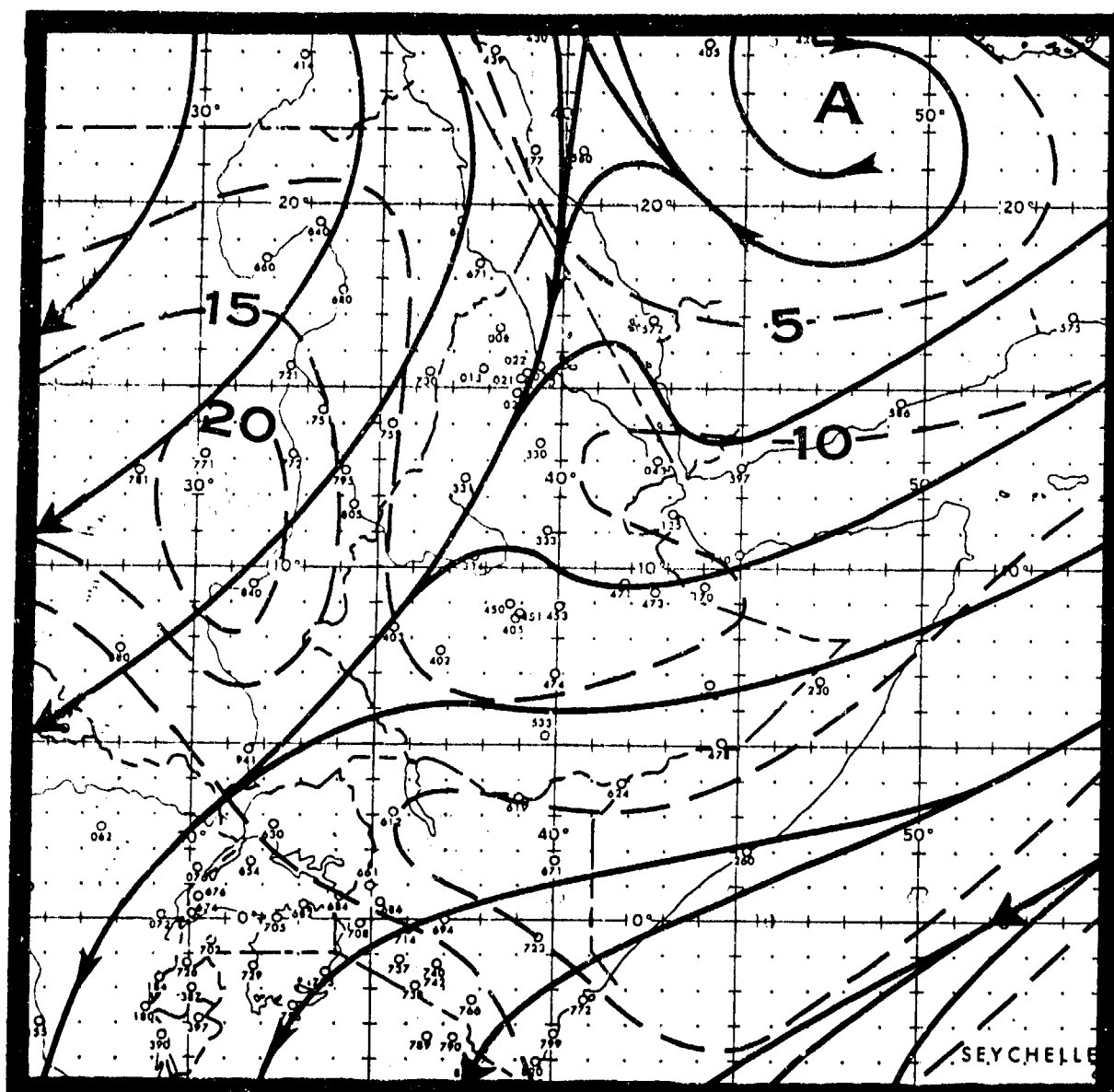


Figure 2-3a. Mean January Gradient Flow. Dashed lines are isotachs at 5-knot intervals.

Flow north of the Trough is still dominated by Azores High outflow west of the Rift, while Northeast Monsoon flow continues east of the Rift System. South of the Monsoon Trough, outflow from the Mascarene High (page 2-13) influences the entire region. By July (Figure 2-3c), Southwest Monsoon air prevails in all areas east of the Rift. Equatorial westerlies--originally South Atlantic

High outflow, but now recurved north of the equator--dominate west of the Rift. By October (Figure 2-3d), Azores High outflow covers the region north of the southward-moving Monsoon Trough, shown here running from east-to-west near 10° N. Modified Southwest Monsoon air--greatly warmed and dried west of the rift--now flows over all the region south of 10° N.

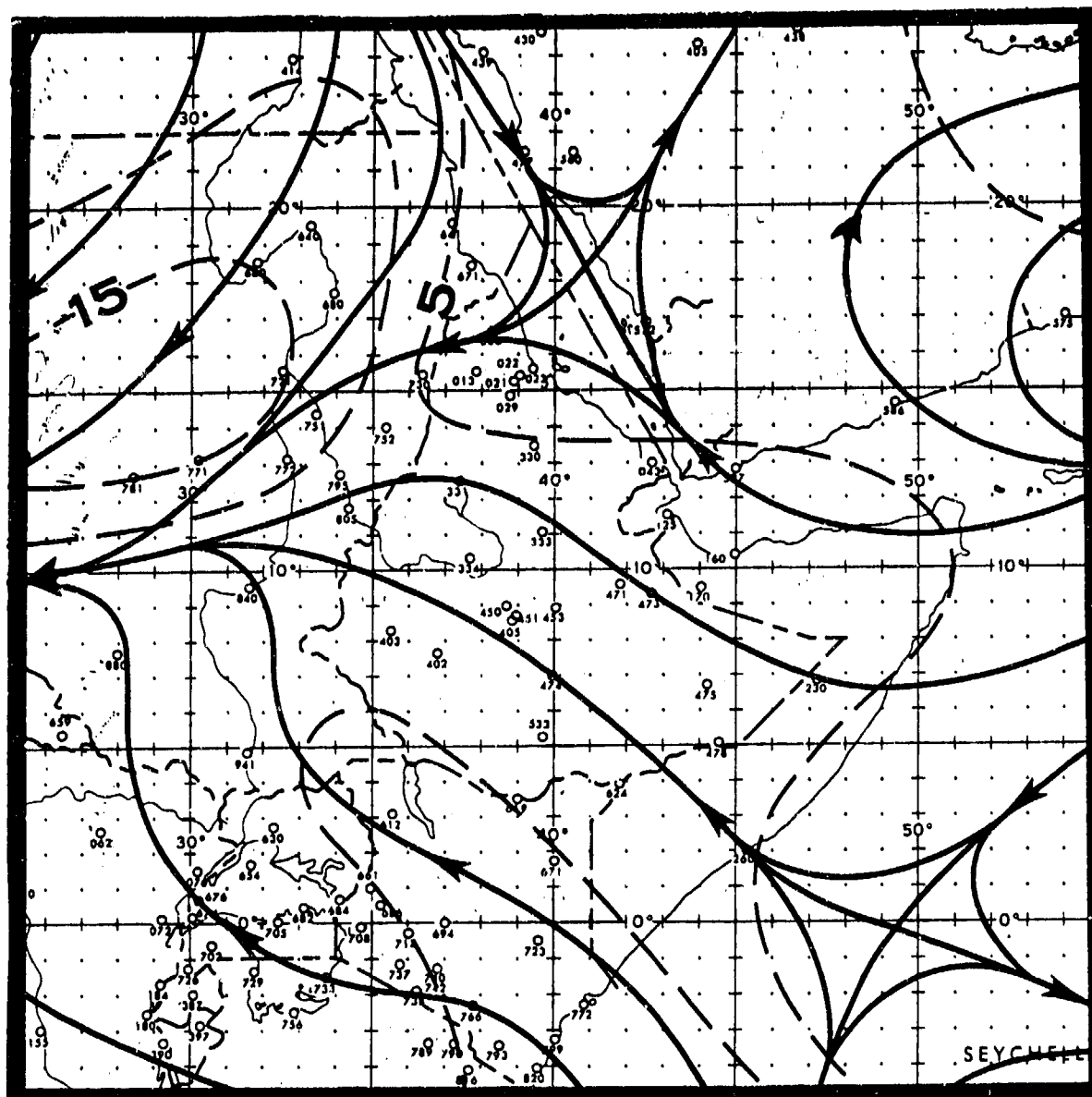
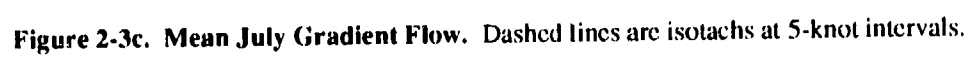


Figure 2-3b. Mean April Gradient Flow. Dashed lines are isotachs at 5-knot intervals.



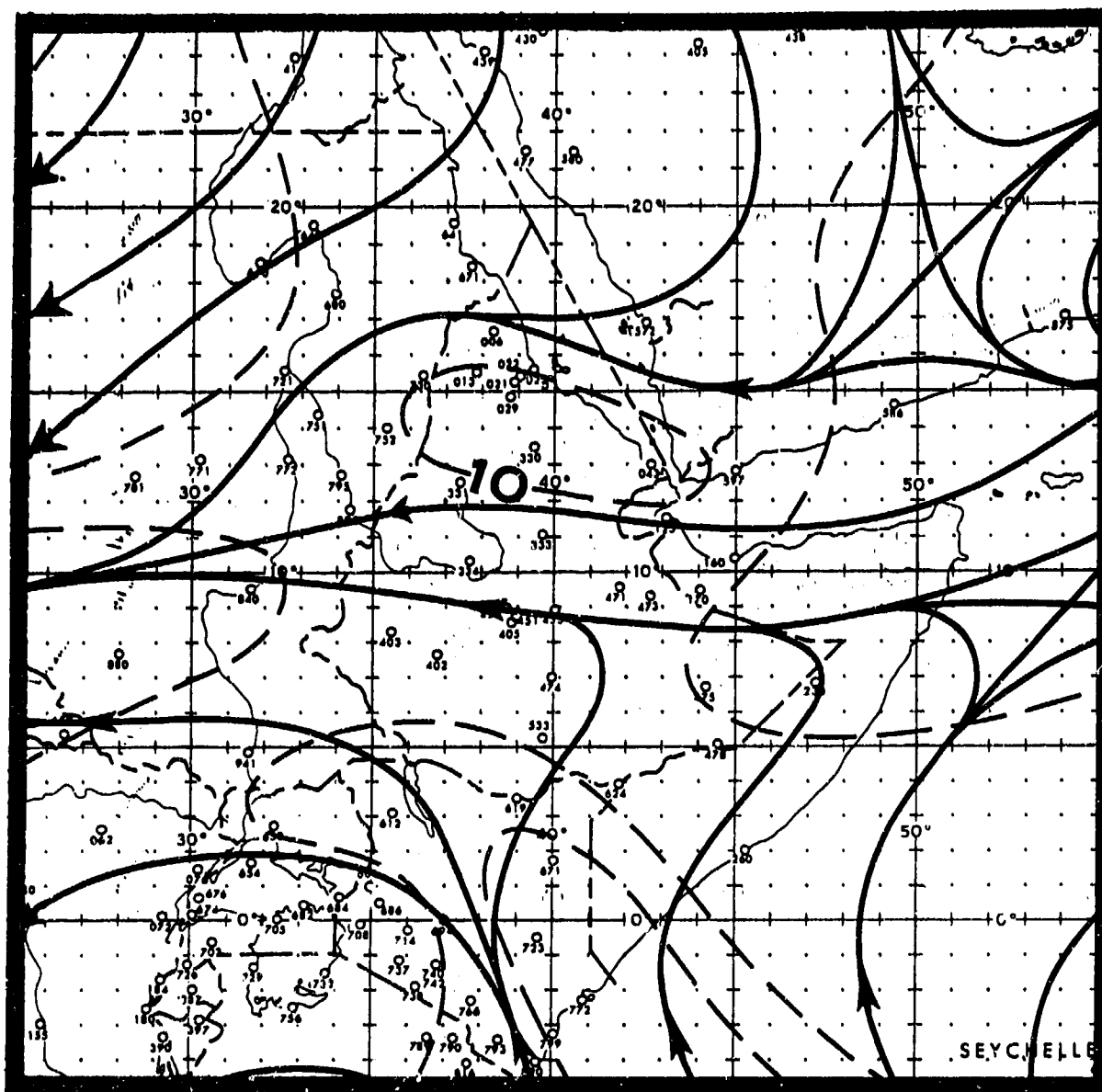


Figure 2-3d. Mean October Gradient Flow. Dashed lines are isotachs at 5-knot intervals.

THE MONSOON CLIMATE. The term "monsoon" (from the Arabic *mawsim*, "seasons") is generally applied to those areas of the world where there is a seasonal reversal of prevailing winds, but the generally accepted definition of a "monsoon" climate includes satisfaction of these four criteria (after Ramage, 1971):

- Prevailing seasonal wind direction changes by at least 120 degrees between summer and winter,

- Summer and winter mean wind speeds both equal or exceed 10 knots (5 meters/sec),

- Wind directions and speeds must remain steady, and

- No more than one cyclone/anticyclone couplet may occur during January or July in any 2-year period within any 5-degree grid square.

Figure 2-4 shows the extent of the "monsoon climate" according to Ramage's criteria throughout the world and across the African continent.

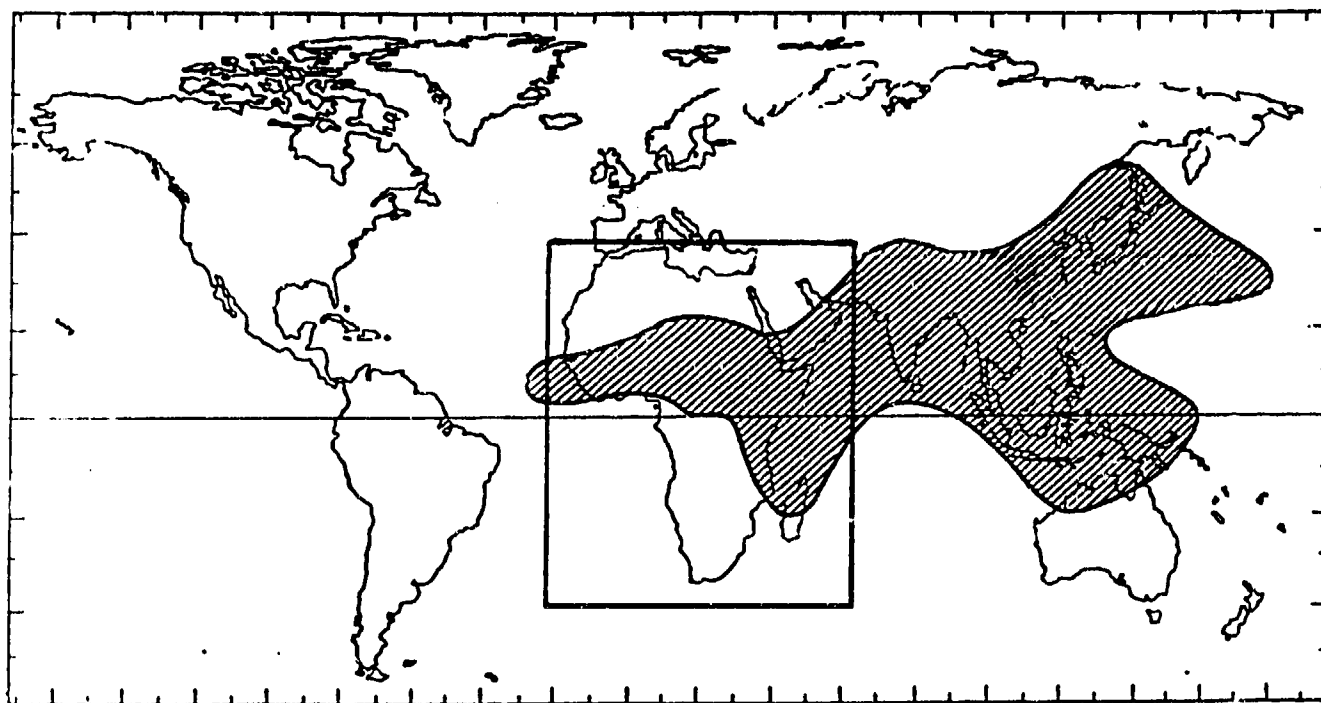


Figure 2-4. Extent of the Monsoon Climate (shaded area) Across the World.

THE SOUTHWEST MONSOON is at full strength between June and September. Rainfall near the Equator (the southern Indian Ocean Plain and southwestern Ethiopian Highlands) begins in April and ends in October. Complex interactions among a number of synoptic-scale features during northern hemisphere summer produce a marked interannual variability in rainfall throughout the Horn of Africa. In Chapters 3 to 6, the Southwest Monsoon season is clearly defined for each subregion. Note that Southwest Monsoon onset, duration, and weather may vary in each of the four subregions from one year to the next.

Figure 2-5 is a three-dimensional view of Southern Asia and the Indian Ocean from 40° to 100° E and from 10° S to 40° N; it shows the most important features of the Southwest Monsoon as it affects the Horn of Africa. The western portion of the Ethiopian Highlands from 33° to 40° E and from 5° to 18° N is affected by tropical easterlies above the 10,000-foot (3,050-meter) or 700-millibar level, but low-level circulation is altogether different. The surface Monsoon Trough discussion in this section describes the differences between Indian Ocean and African low-level circulations.

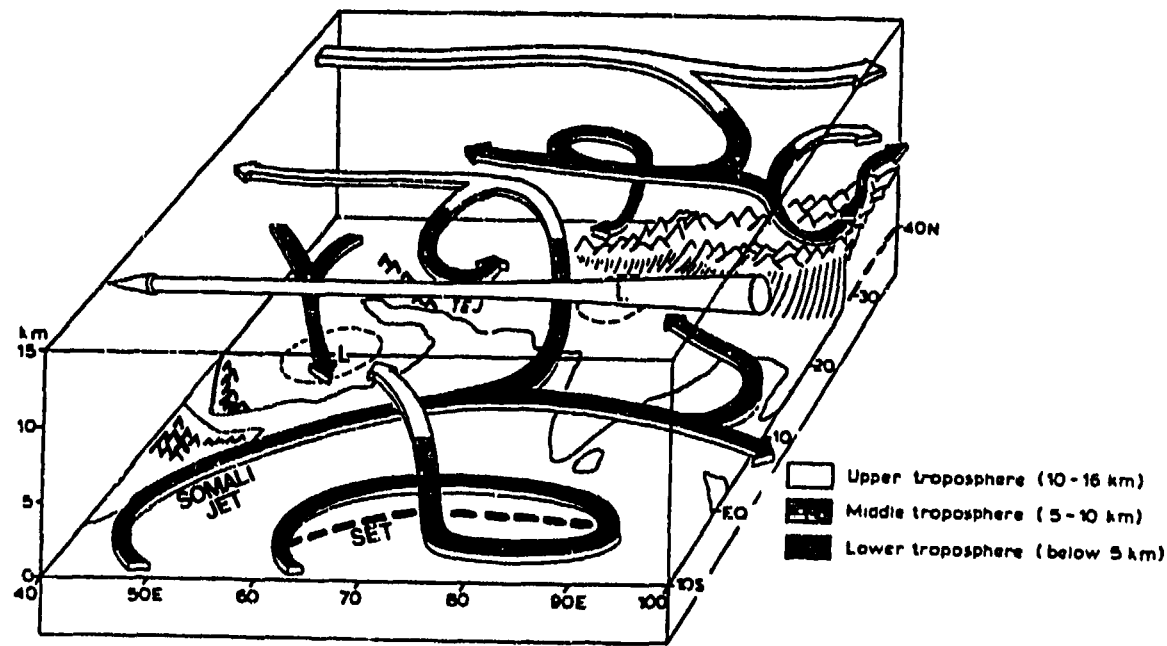


Figure 2-5. Southwest Monsoon Circulation Over Southern Asia and the Indian Ocean (from Hamilton, 1987). The Tropical Easterly Jet (TEJ) is shown in Figure 2-7. The Southern Equatorial Trough (SET) is also shown in Figure 2-20a-c.

THE TIBETAN 200-MB ANTICYCLONE. This semipermanent upper-air cell acts not only as an upper-level heat source, but as an outflow mechanism for sustaining surface Monsoon Trough convection between May and October. Latent heat of condensation from widespread convection over Burma begins anticyclone formation in late April and early May. Strong surface heating on the Tibetan Plateau shifts this massive upper-level high to Tibet in mid- to late May. The mean July 200-mb flow pattern over south central Asia (Figure 2-6a) shows the large-scale anticyclonic circulation anchored over the Tibetan Plateau by strong early and mid-summer surface heating.

By August, moderate snow cover produced by strong Southwest Monsoon convection begins to lower surface temperatures on the elevated Tibetan Plateau.

The energy that normally goes into surface heating is now used to melt the snowfall and evaporate the runoff. Surface temperatures are affected immediately, but cooling aloft is gradual because it usually takes 1 to 2 months for surface effects to reach upper levels. Satellite research shows that the Tibetan Plateau is snow-free 80% of the time during the early Southwest Monsoon months. The upper-level anticyclone weakens by October because the surface "trigger" is eliminated and upper-level westerlies move southward over the Plateau.

Note that the anticyclone first appears in May to the southeast of the Tibetan Plateau as intense convection warms the upper troposphere. The anticyclone forms over northern Burma (see Figure 2-6b) but moves northwest with intense surface heating over the Tibetan Plateau, the surface of which lies at about 500 mb.

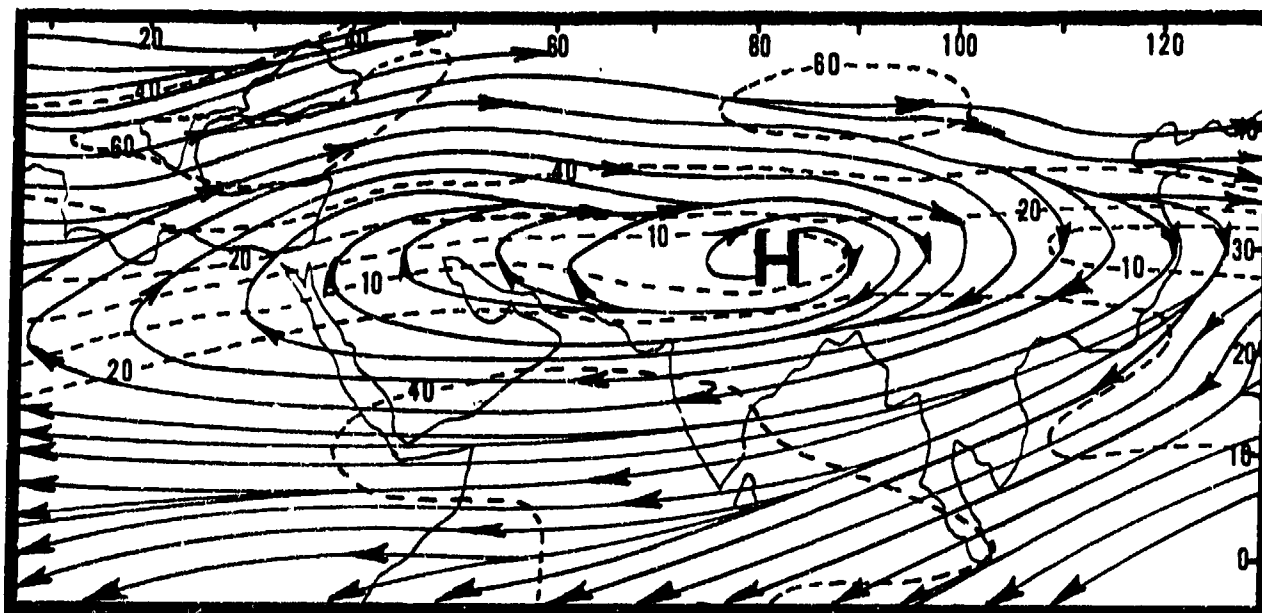


Figure 2-6a. Mean July 200-mb Flow Over the North Indian Ocean and Arabian Sea. The "H" marks the mean position of the Tibetan 200-mb Anticyclone. Dashed lines are isotachs (kts).

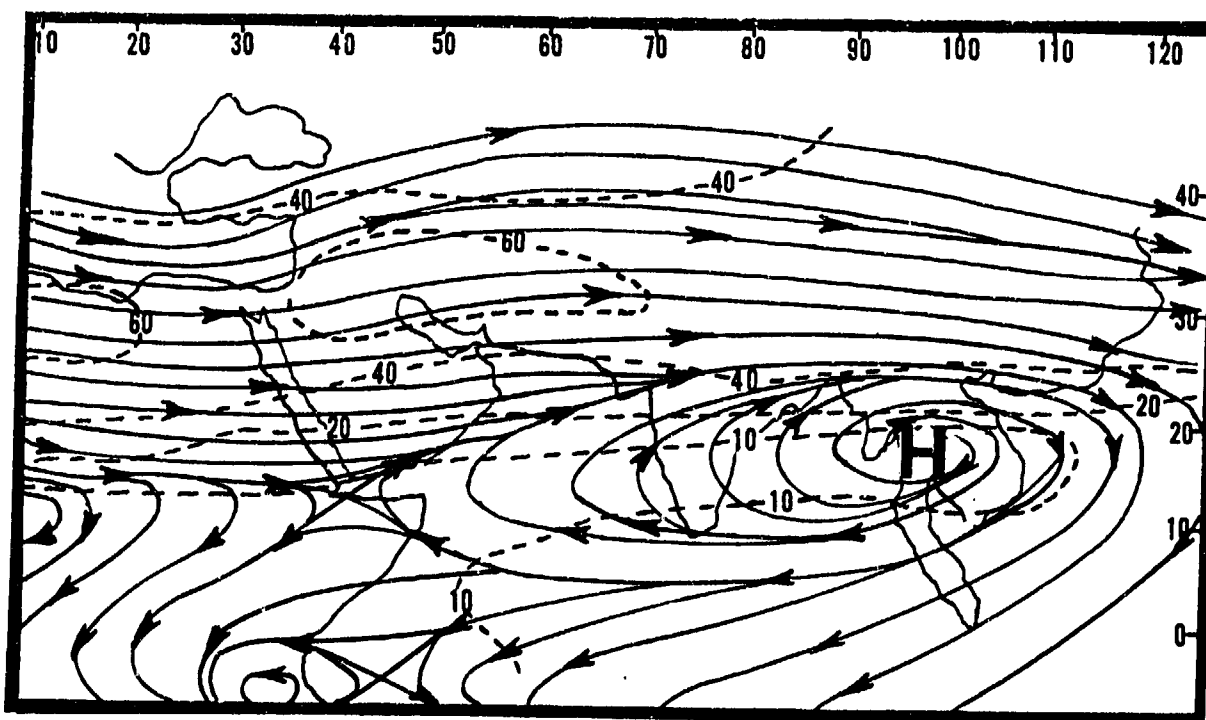


Figure 2-6b. Mean May 200-mb Flow Over the North Indian Ocean and Arabian Sea. Researchers believe that heavy convection initiates the anticyclonic couplet responsible for the Southwest Monsoon's upper-level flow pattern over the western Indian Ocean. The "H" marks the mean position of the Tibetan 200-mb anticyclone. Dashed lines are isotachs (kts).

THE TROPICAL EASTERLY JET (TEJ). This summer feature in the upper-level easterlies develops as outflow from the southern edges of Tibetan 200-mb circulation. The TEJ provides an outflow mechanism for

sustaining heavy Southwest Monsoon convection. Its mean position is at about 11° N, but it oscillates between 7° $30'$ N and 18° N. Highest wind speeds (90 knots) are found between 100 and 200 mb.

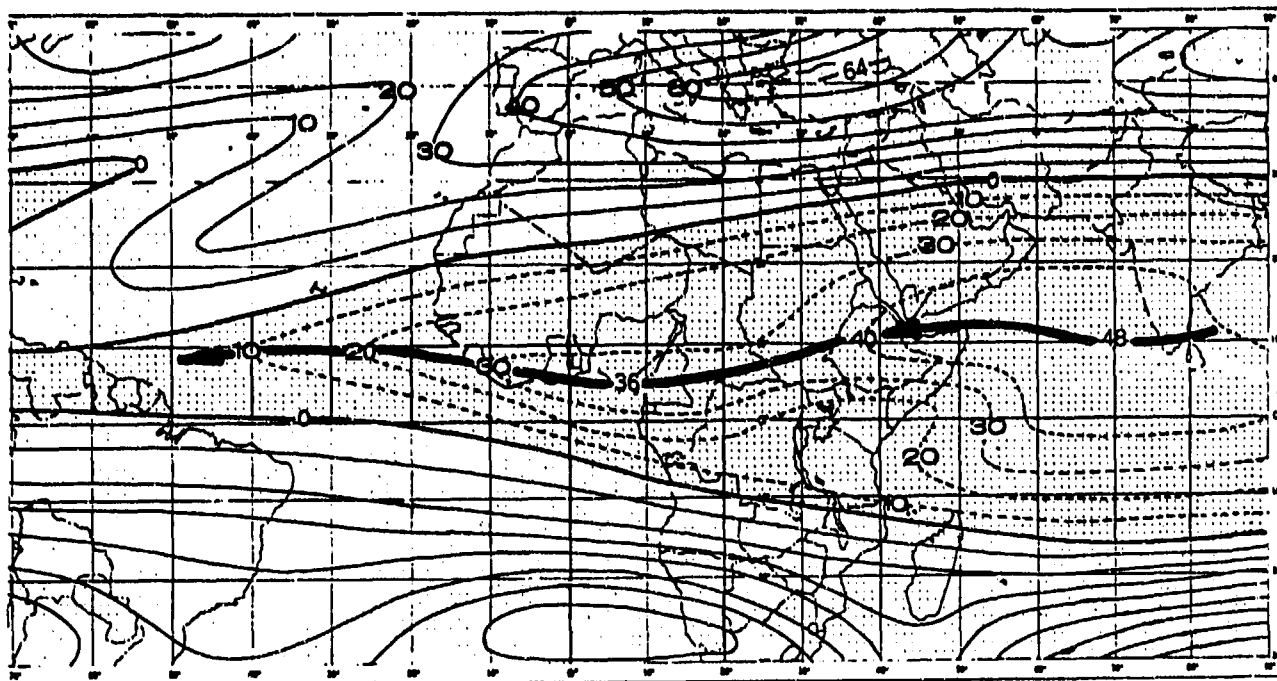


Figure 2-7. Mean July 200-mb Zonal Flow. The dark arrow is the TEJ. The stippled area represents easterly flow. Dashed lines are isotachs in knots. Solid lines are westerly flow isotachs.

THE MASCARENE (SOUTH INDIAN OCEAN) HIGH. This semipermanent southern hemisphere high-pressure cell provides cross-equatorial flow (through the Somali Jet) from April through October. Figures 2-8a-d show mean large-scale surface pressure patterns over the Indian Ocean during the Southwest Monsoon. Note that mean surface pressure patterns (like the ones shown in these figures) do not reflect actual surface flow in the tropics. As a result, wind data and streamline analyses are required to extract the Somali Jet from the broad-scale flow pattern.

The Mascarene High's mean April position (Figure 2-8a) is 32° S, 83° E, with a central pressure of 1021 mb. By July (Figure 2-8b), it strengthens to 1023 mb and shifts northwest to a mean position near 28° S, 65° E. In August (Figure 2-8c), mean central pressure peaks at 1028 mb and the High migrates southeastward to 30° S, 68° E. Maximum low-level cross-equatorial flow peaks between July and August. In October (Figure 2-8d), the High migrates further eastward to 29° S, 80° E; central pressure weakens to 1023 mb.

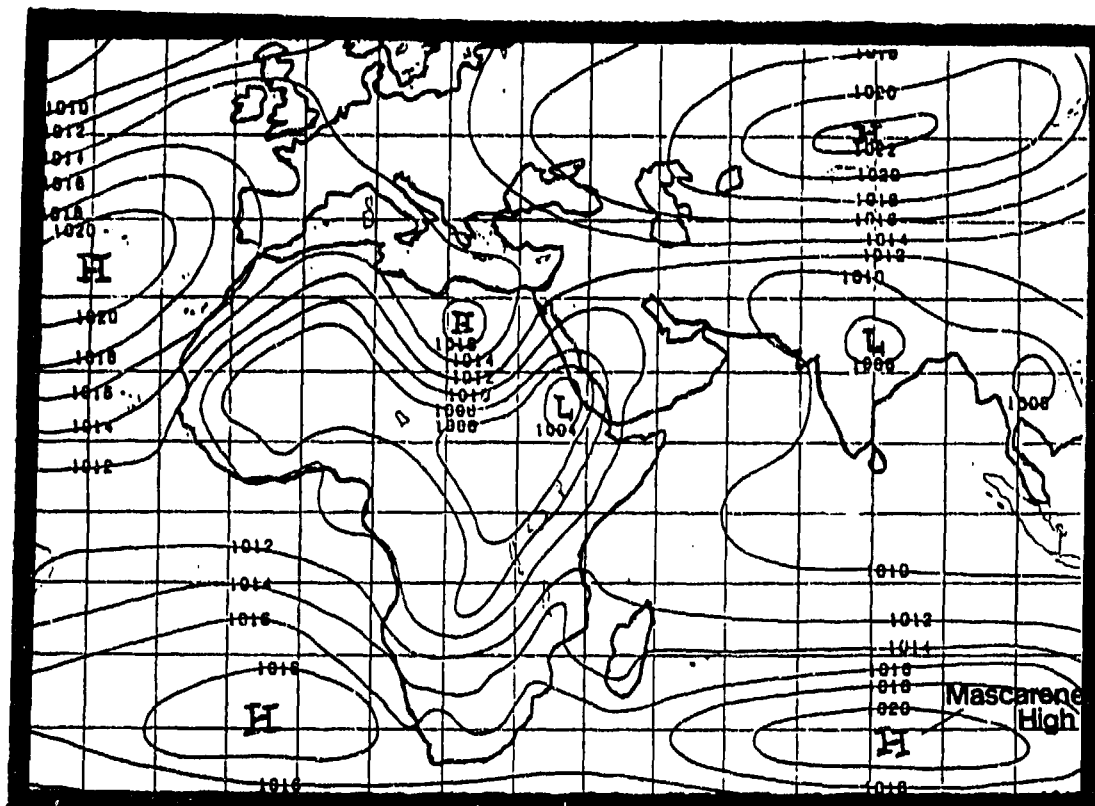


Figure 2-8a. Mean April Surface Position of the Mascarene High.

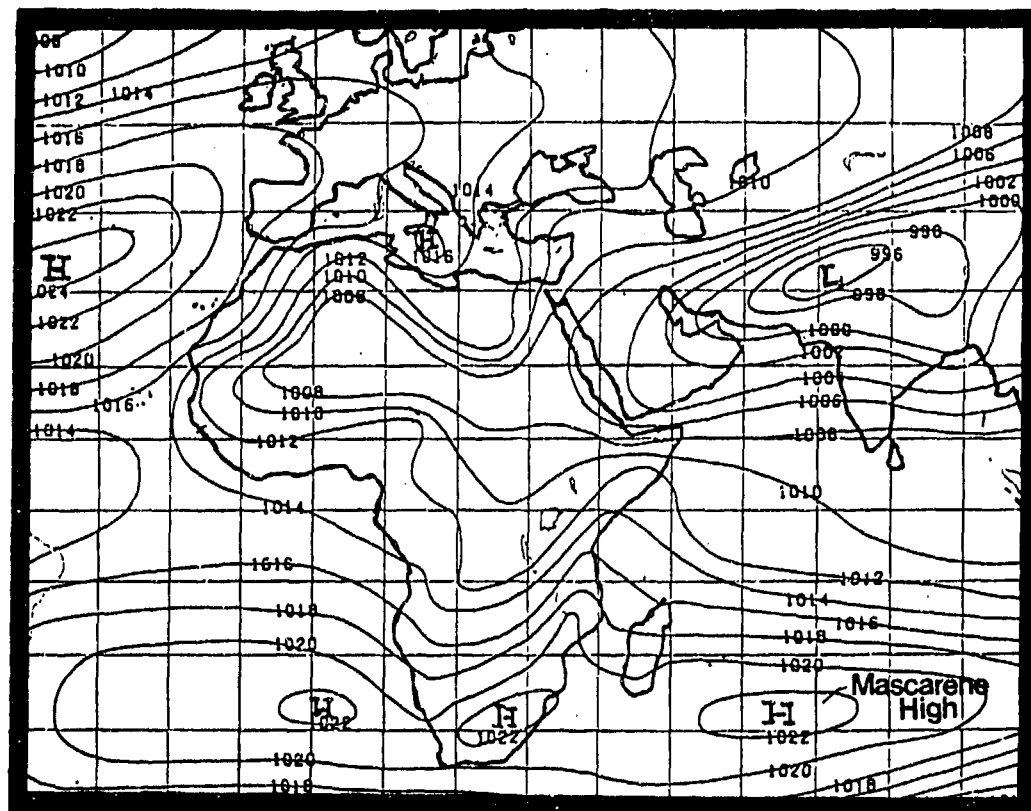


Figure 2-8b. Mean July Surface Position of the Mascarene High.

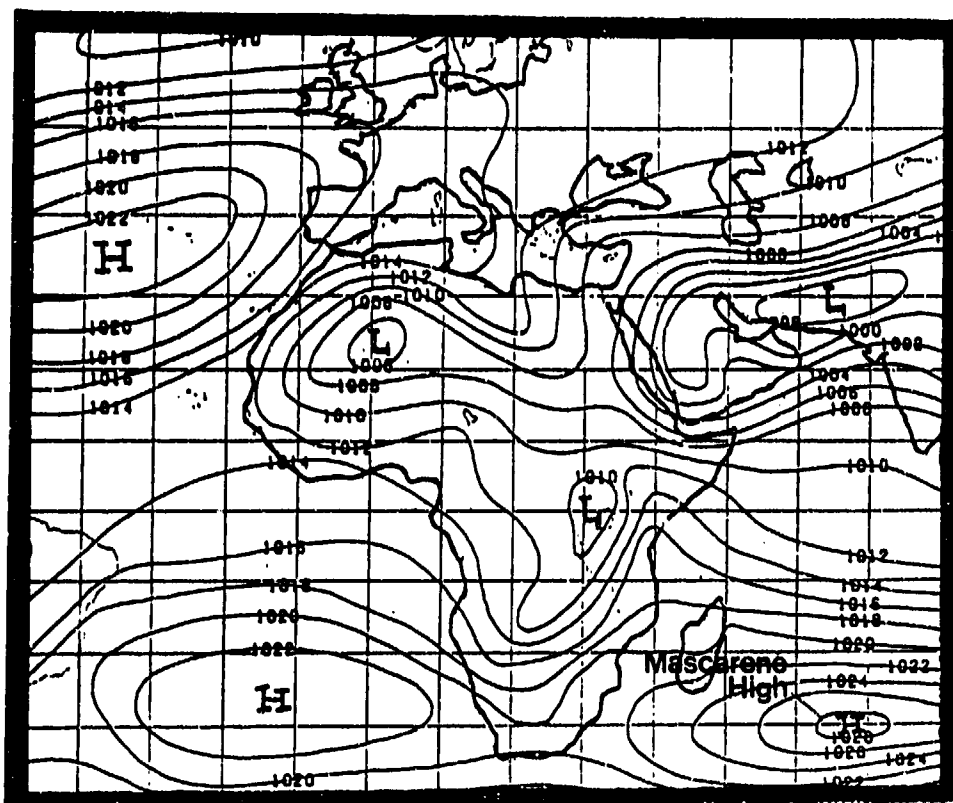


Figure 2-8c. Mean August Surface Position of the Mascarene High.

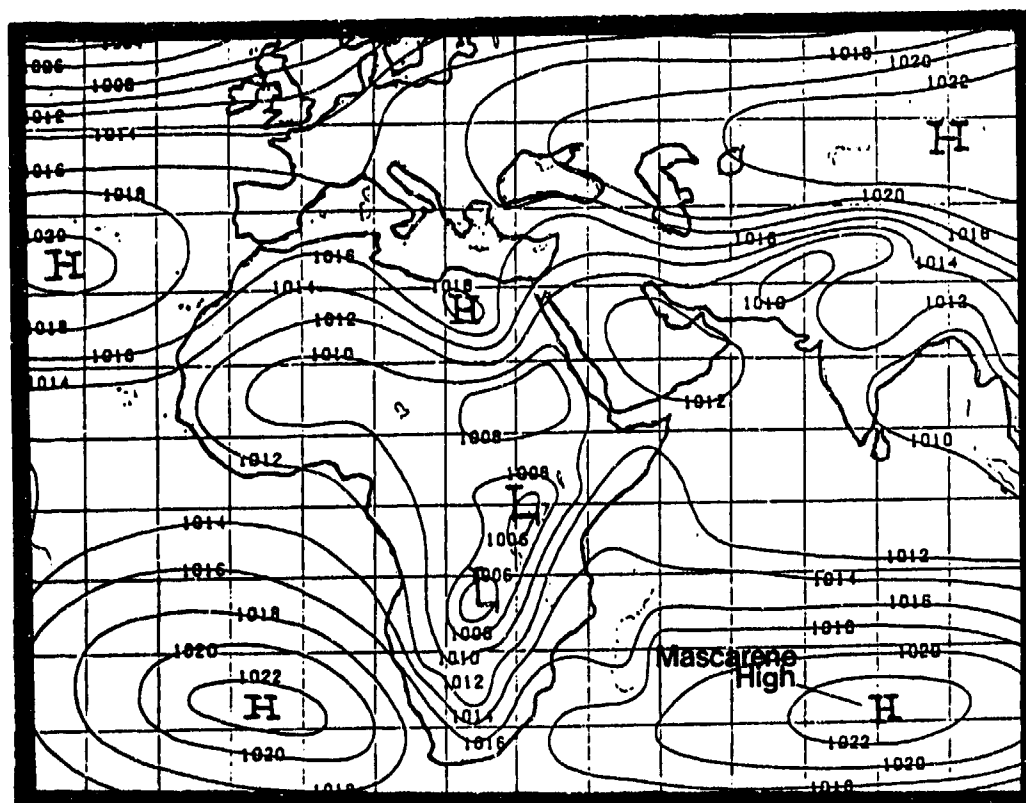


Figure 2-8d. Mean October Surface Position of the Mascarene High.

The Mascarene High's semiannual oscillation provides low-level support for Southwest Monsoon circulation; between April and October, it produces nearly all low-level flow into the Horn of Africa, except for extreme western Ethiopia. Cross-equatorial flow is

concentrated between 39° and 43° E--see Figure 2-9. East African terrain compresses the flow into what we know as the Somali Jet--the most important Southwest Monsoon weather feature in the Indian Ocean Plain and Ethiopian Highlands subregions.

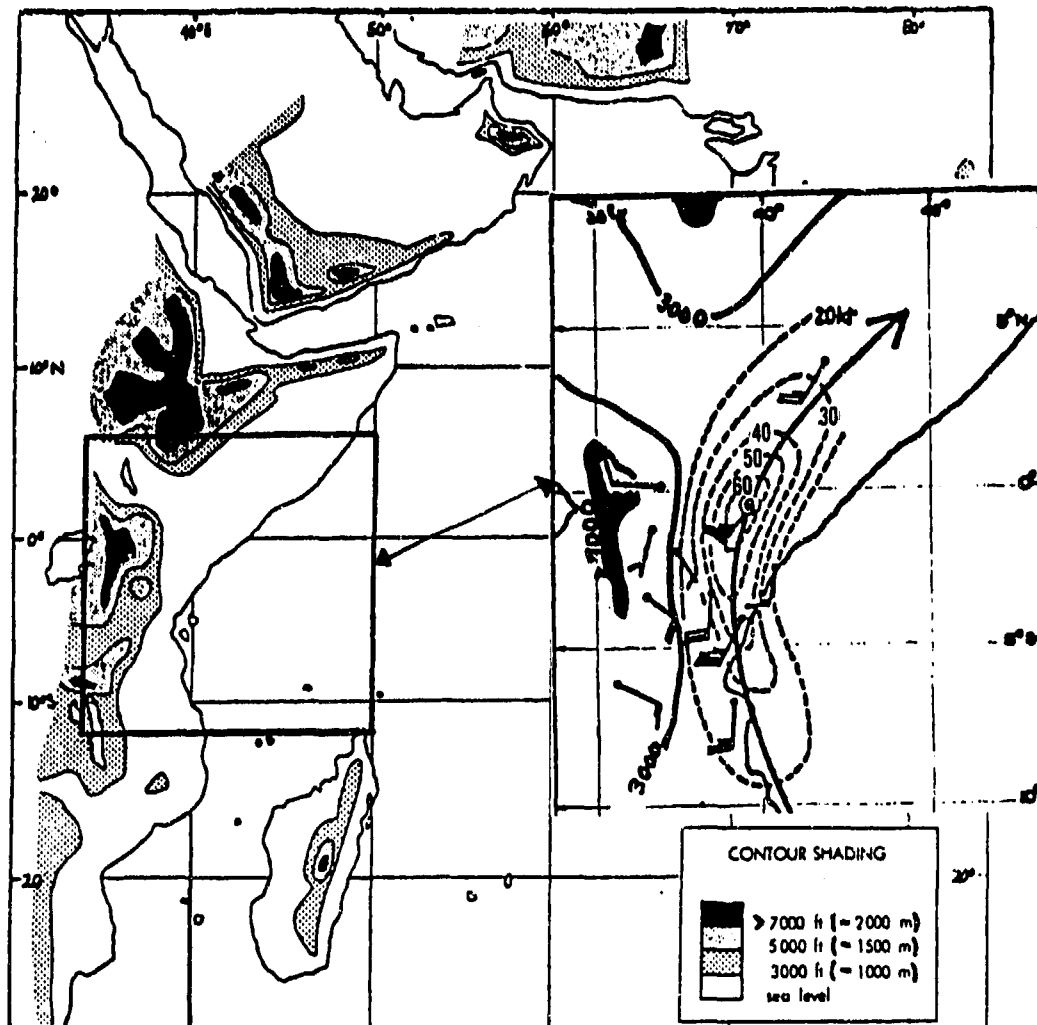


Figure 2-9. Entry Point for Cross-Equatorial Outflow from the Mascarene High into the Indian Ocean Plain and Eastern Ethiopian Highlands. Inset detail shows actual 5,000-foot wind speed (kts) and direction on 27 June 1964. The Somali Jet core is shown as the curved arrow.

THE SOMALI JET. From April to late October, the Somali Jet enters the Northern Hemisphere between 4,000 and 7,000 feet (1,220-2,134 meters) MSL near the Kenya-Somalia border at 39-43° E. Mascarene High outflow is compressed into a high-speed jet core along the eastern edge of Africa's Great Rift System between

5° S and the Equator. The Jet has the usual low-level jet diurnal speed variation. Research shows that mean core speeds are between 25 and 40 knots. Large-scale "forcing" causes mean monthly jet core wind speeds to oscillate northward from April to July (see Figure 2-10), then back south between August and October.

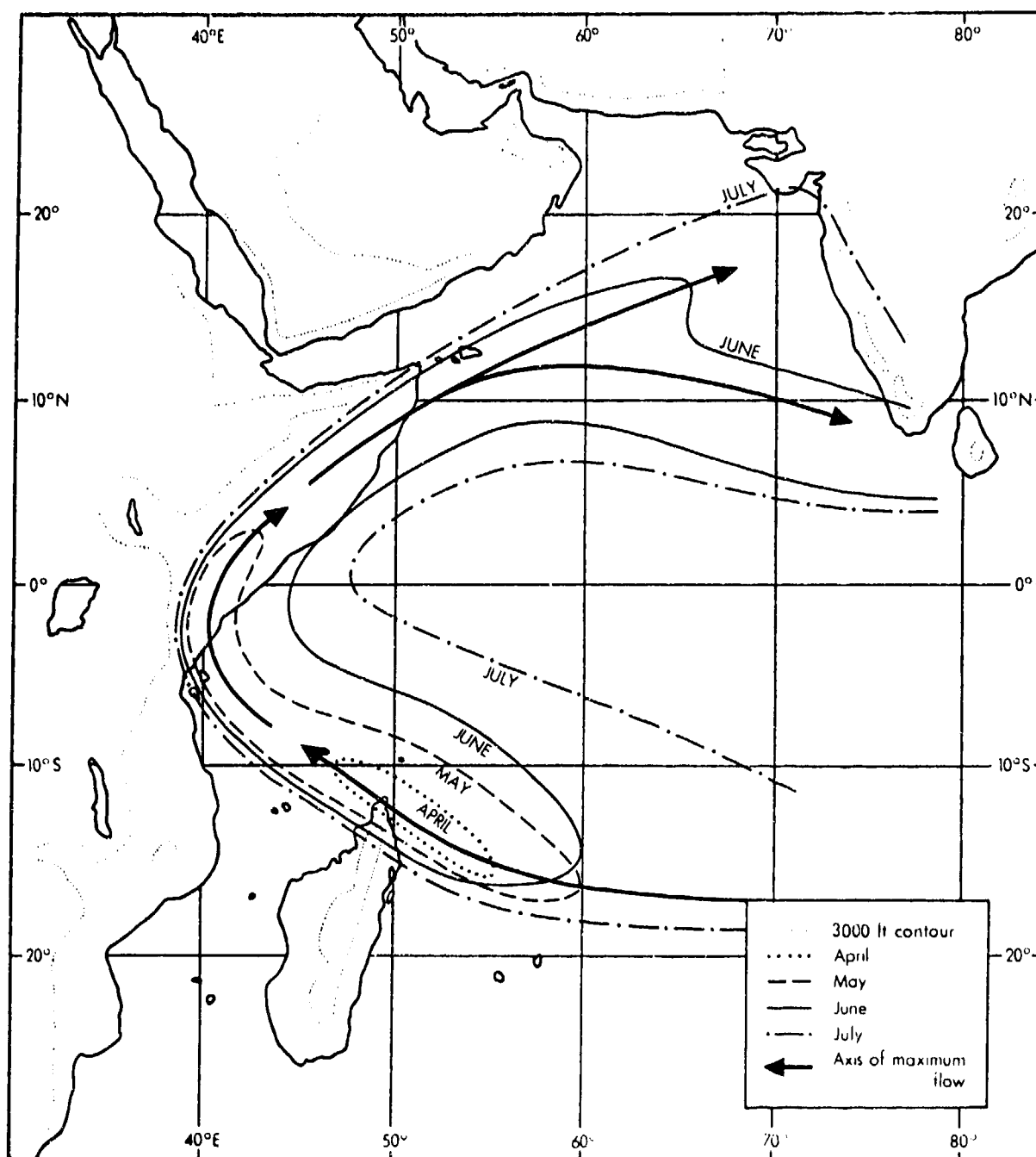


Figure 2-10. Successive Positions of the 20-Knot Isotach at 3,000 Feet (915 meters) AGL Between April and July (from Findlater, 1971). August-September positions are not shown.

Day to day flow often shows more than one maximum wind speed core. As a result, mean monthly 850-mb flow patterns do not always depict the actual daily Somali Jet core position. Figure 2-11 shows a single jet core cross-section between 1 and 2° S and

39-41° E. Typically, the jet loses moisture over land north of the equator, but meso- and synoptic-scale moisture conditions may produce cloud cover along the entire jet axis.

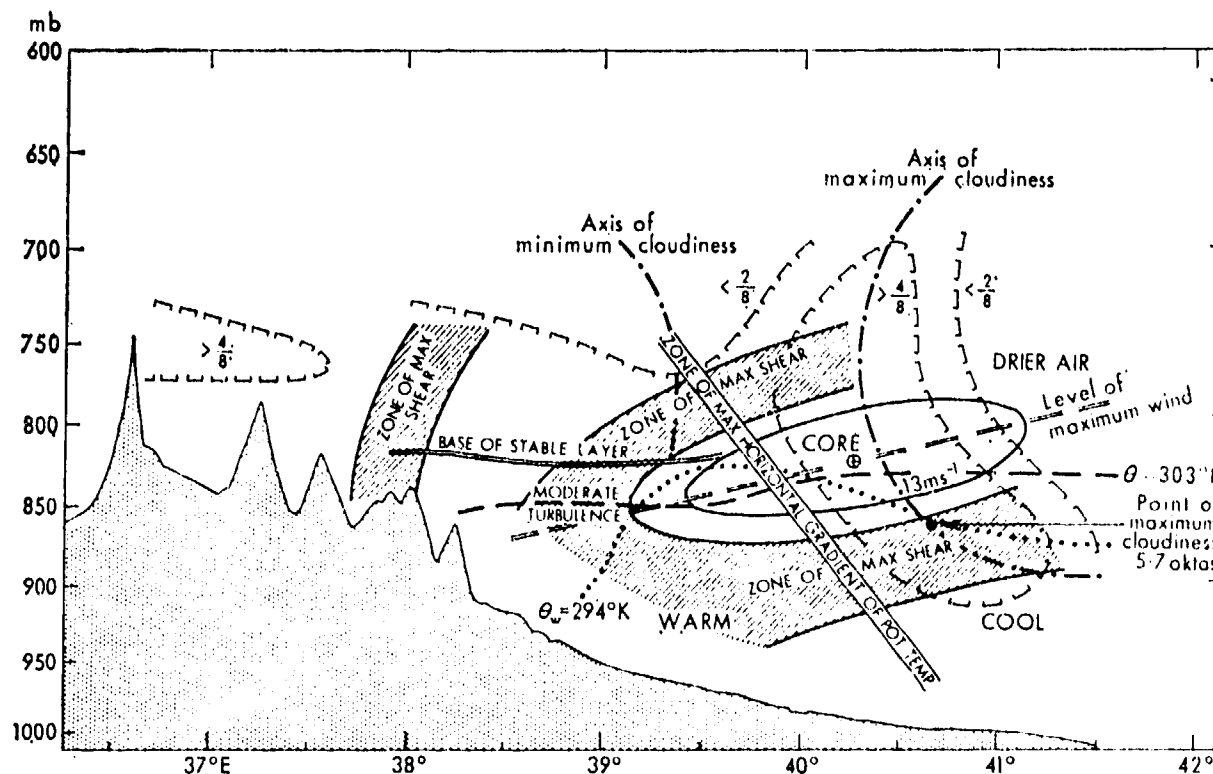


Figure 2-11. Observed Characteristics (Shear Zones/Cloudiness) of the Somali Jet (from Findlater, 1972). Shaded regions represent zones of maximum shear. Areas enclosed in brackets represent typical cloud cover patterns around the jet core, in eighths. Other displays are self-explanatory.

Normally, the Somali Jet crosses the equator as moist southerly flow that turns northeastward along the Indian Ocean Plain/Eastern Ethiopian Highlands from the equator to 11° N. It leaves the study area near Cape Guardafui. North of 6° N, the Jet is very dry. Differential land-ocean heating and jet-induced upwelling (positive "feedback" mechanism) off the Somalia coast may further intensify it. A 100-knot wind speed at 660 feet (200 meters) AGL has been recorded at Cape Guardafui. Eastward-moving southern hemisphere perturbations also cause 12-48 hour fluctuations in speed. Height and speed variations in single or multiple low-level jets are primarily produced by synoptic-scale surges. Individual jet core wind speeds run from 40 to

65 knots. Several branches often form south of the equator, but the East African Plateau compresses the flow into one 4,000- to 7,000-foot (1,220- to 2,134-meter) MSL jet north of the equator. Other low-level jets often develop below 2,000 feet (610 meters) MSL during the day.

Figure 2-12 illustrates the variable height and speed in a single jet stream movement over the region. Figure 2-13 shows multiple low-level jets entering the northern hemisphere; it does not represent a constant level or pressure surface because jet cores meander vertically as well as horizontally.

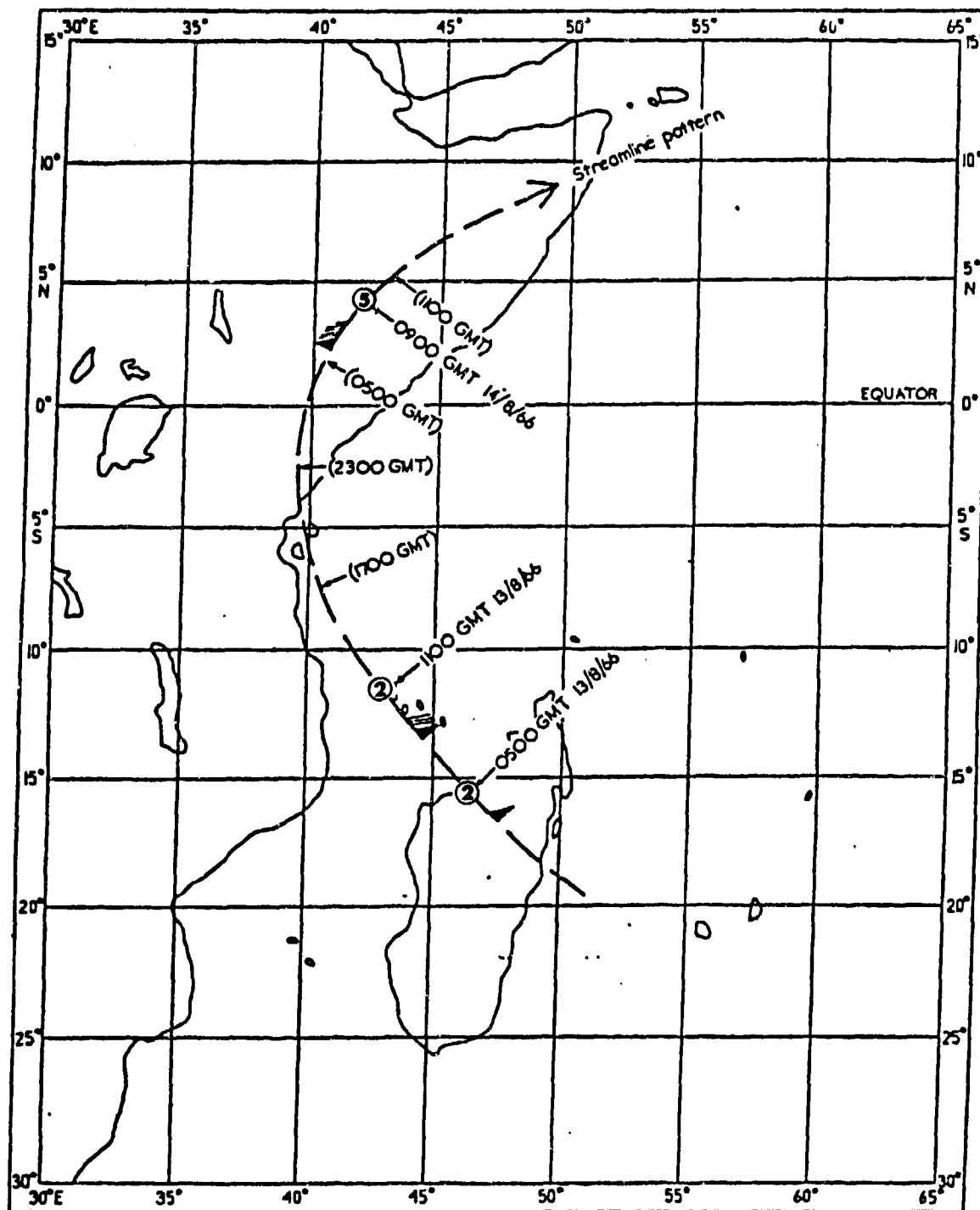


Figure 2-12. Movement of the Somali Jet Core, 13-14 August 1966 (from Findlater, 1969). Note the maximum wind speed fluctuation with height (numbered circles at point of wind arrow in thousands of feet MSL) between 0500Z on 13 Aug 1966 and 1100Z on the 14th.

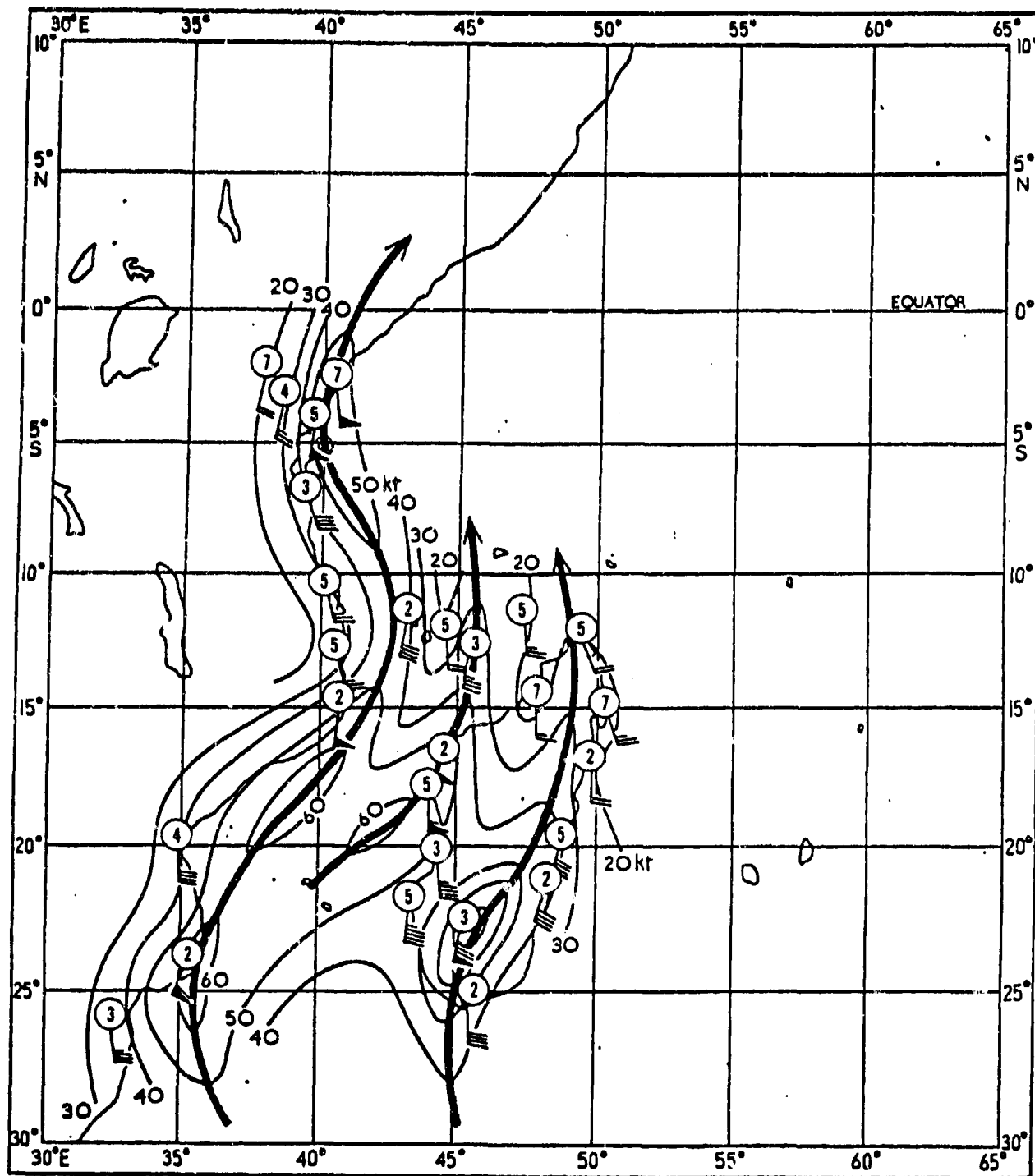


Figure 2-13. Multiple Low-Level Jets on 26 July 1966 (from Findlater, 1969). Thick black arrows represent individual jet cores. Circled numbers represent height (AGL) in thousands of feet.

Note that while the synoptic conditions shown below in Figure 2-14 favor Somali Jet flow "surges," they do not necessarily cause all fluctuations in Somali Jet wind speed. Research confirms that surges in cross-equatorial flow are related to southern hemisphere low-pressure

trough passages; the intensity of the Somali Jet surge lags passage of southern hemisphere troughs through the Mozambique Channel by a day to a day and a half. Surges may produce sudden increases in cloudiness and precipitation.

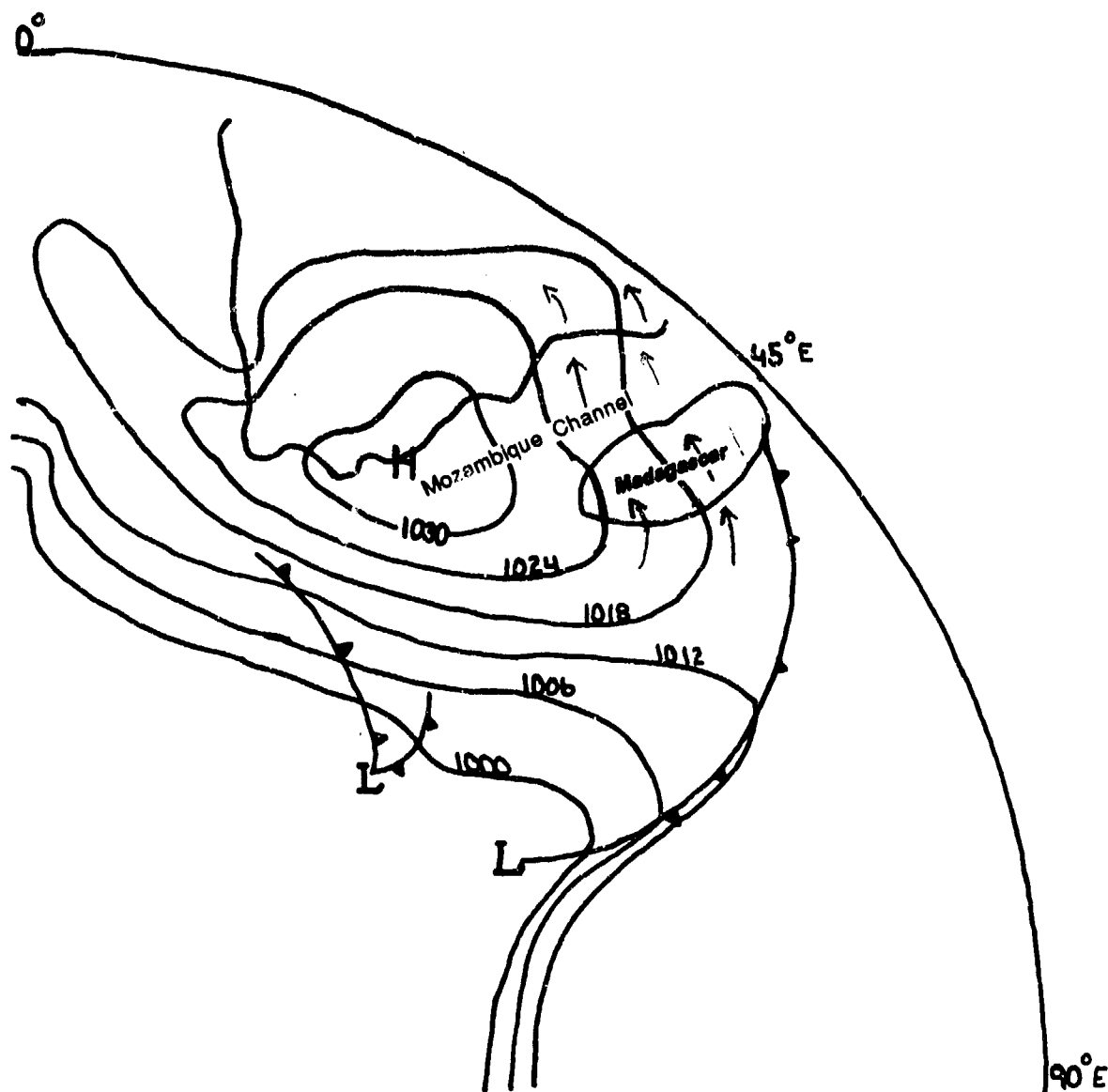


Figure 2-14. A Southern Hemisphere Frontal Passage Typical of Those That May Produce Air Flow Surges in the Somali Jet. This southern polar view shows a southern hemisphere frontal passage through the Mozambique Channel-- a passage that creates favorable conditions for cross-equatorial surges in Somali Jet flow.

Figures 2-15a-b show 3-hour wind speed profiles of sounding composites taken between 23 June and 1 July 1977 for Burao (elevation 3,421 feet/1,043 meters) and

Obbia (39 feet/12 meters). The diurnal oscillation cycle is apparent. The relative locations of Burao and Obbia are shown in Figure 3-1.

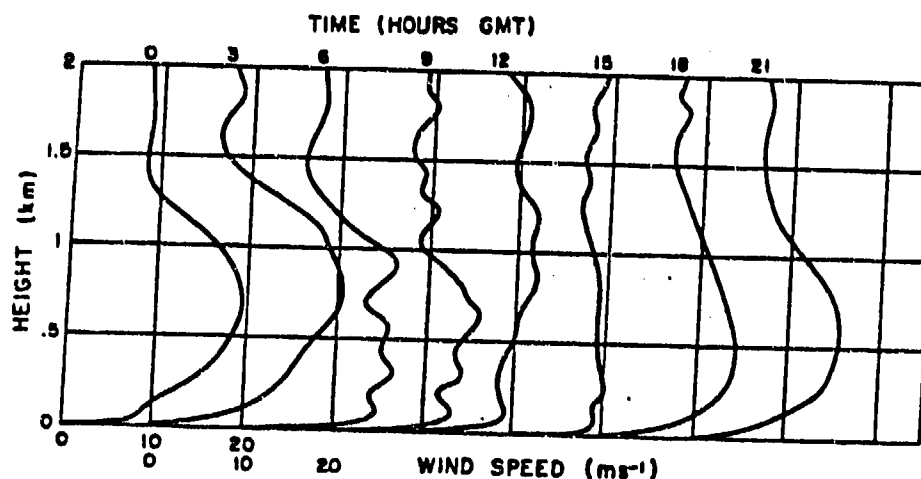


Figure 2-15a. Composite 3-Hour Wind Speed (m/s) Profiles for Burao, SI. The strongest wind speeds aloft are found overnight, peaking at 40 knots by dawn near 2,500 feet (750 meters) AGL.

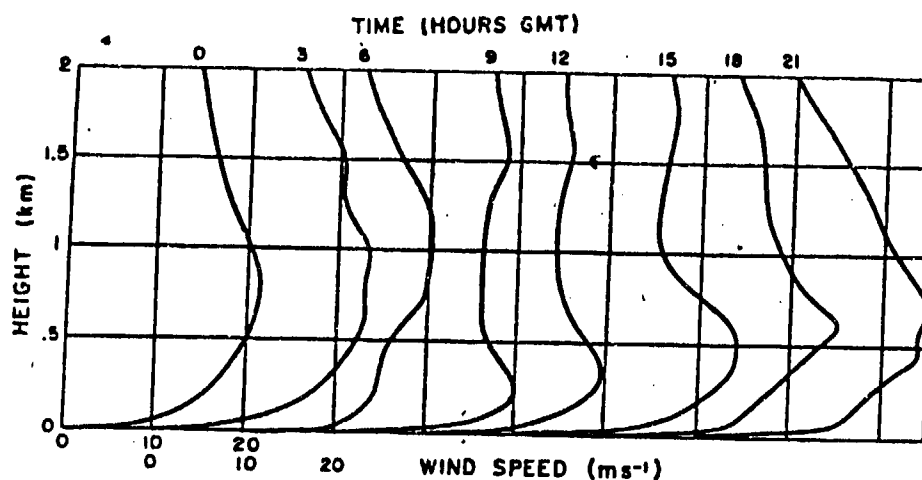


Figure 2-15b. Composite 3 Hour Wind Speed (m/s) Profile for Obbia, SI. A nocturnal jet is also present at Obbia. Maximum speed (50 knots at 2,500 feet/750 meters) AGL occurs at midnight.

THE PAKISTANI HEAT LOW. This low-level feature (normally cloud-free) is present over northwestern India and southern Pakistan between May and early October. It usually breaks down in October as insolation decreases and the Asiatic High becomes established over south central Asia. Intensification of the Pakistani Heat Low forces the mean Somali Jet core

position (the 20-knot isotach) to oscillate northward and southward over the Horn of Africa between May and October--see Figure 2-10. As shown in Figure 2-16a, the low anchors the eastern edge of the larger scale trough extending from India to the Sahara Desert during northern hemisphere summer. Central pressure ranges from 992 to 996 mb by late June.

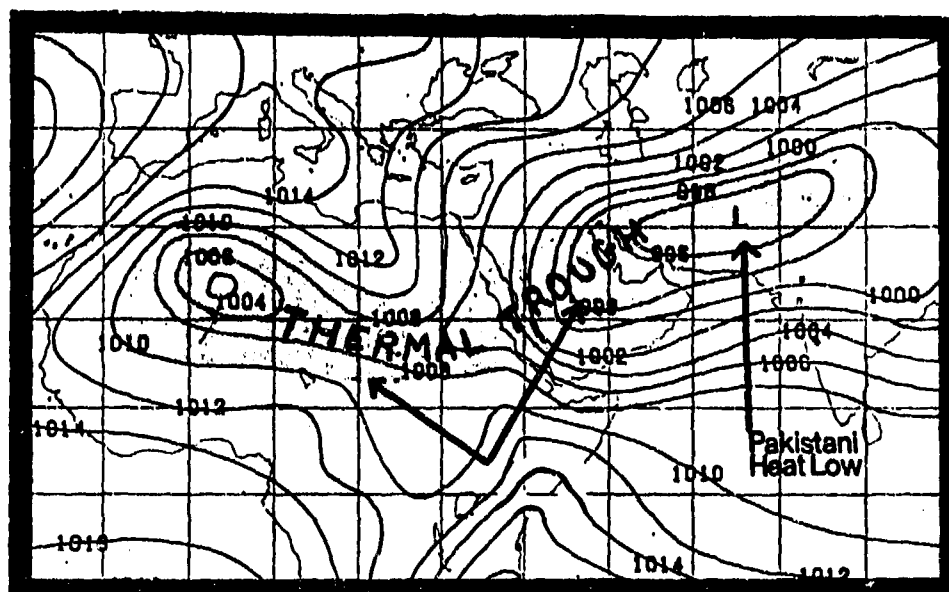


Figure 2-16. The Pakistani Heat Low in Association with a Large-Scale Thermal Low Pressure Trough (shaded) Over SWANEA Region During Northern Hemisphere Summer.

THE MONSOON TROUGH. Movement of the surface Monsoon Trough over the Horn of Africa is extremely complex because of topography. The Ethiopian Highlands, for example, form a natural barrier to airflow from the surface to 850 millibars; they split the surface Monsoon Trough into two distinctly separate axes. West of the Ethiopian Highlands, the convergent wind fields that produce surface Monsoon Trough oscillations originate in the equatorial South Atlantic/equatorial Africa and the Sahara Desert. East of

the Highlands, cross-equatorial outflow from the Mascarene High is the only factor in surface Monsoon Trough movement and position. The Turkana Channel (in northwestern Kenya/southeastern Sudan--see Figure 1-3) and the Red Sea/Gulf of Aden corridor are the only areas where both Trough axes (Interior Africa and Indian Ocean) can temporarily link up along the Horn of Africa. Figure 2-17 shows the surface Monsoon Trough's mean position and movement over the region from April through November.

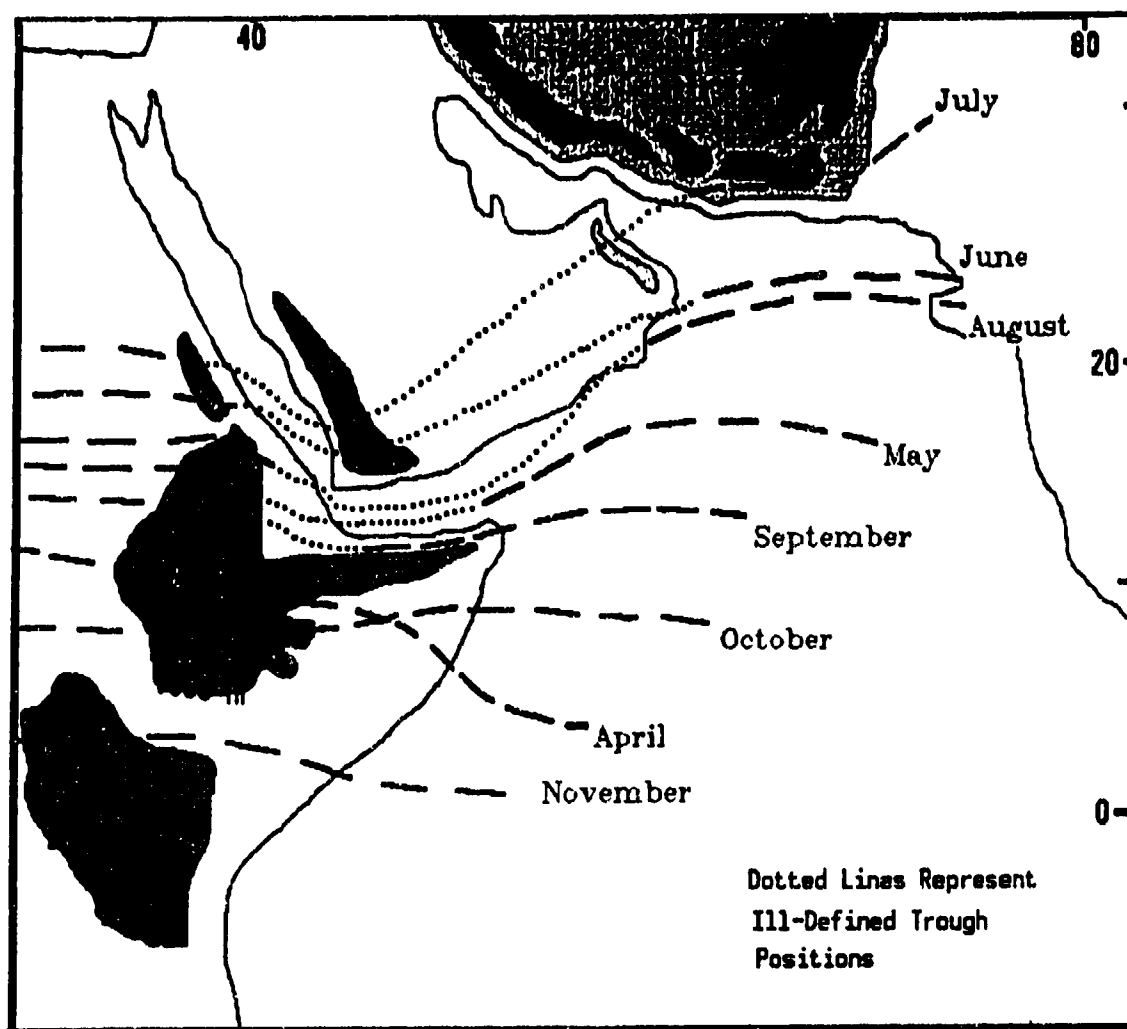


Figure 2-17. Mean Surface Monsoon Trough Positions: April through November. Grey shading represents elevations above 3,000 feet (915 meters); dark shading, elevations above 6,560 feet (2,000 meters). Dotted lines over the Red Sea/Gulf of Aden corridor represent fragmented or discontinuous surface Monsoon Trough positions.

The surface Monsoon Trough lies across the African interior and along the axis of converging wind fields produced by the Azores and South Atlantic Highs. This "Interior Africa" Monsoon Trough is made up of a series of thermal lows oriented WSW to ENE across central and west central Africa. Flow into these lows separates subtropical northeasterlies from cross-equatorial southwesterlies. Typically, the "Interior Africa" Monsoon Trough's northward migration (from April to June) is gradual, but the equatorward oscillation (September to November) is abrupt.

Short-term northward surges occur continually between late March and late April, lasting for 12-36 hours. They occur when a burst of cross-equatorial moisture from equatorial Africa enters southwestern

Ethiopia. Another source of equatorial moisture is the Turkana Channel. Weak (7- to 11-knot) southeasterlies generated by the Somali Jet recurve through the Channel northward along the southern and western Ethiopian Highlands. On rare occasions, a deep migratory mid-latitude low-pressure cell induces strong southerly flow ahead of a modified cold front between February and May. Such frontal-type events may produce Turkana Channel winds up to 60 knots, with the highest speeds in the morning hours.

The surface Monsoon Trough axis over the African interior produces abrupt surface discontinuities in specific and relative humidity. The Intertropical Discontinuity (ITD) forms the boundary between moist southwesterlies and dry northeasterlies aloft. The ITD

slopes southward (as shown in Figure 2-18) to (XX) mb about 250 NM south of the surface Monsoon Trough axis; the zone of maximum convergence, cloudiness, and precipitation is found here, as well. Rugged terrain in east Africa disrupts the well-defined ITD above 3,000

feet (915 meters), but moist low-level flow often penetrates the deep river valleys of western Ethiopia--see Figure 2-19. The maximum moisture influx into western Ethiopia is in July and August, resulting in massive orographic uplift and deep vertical mixing.

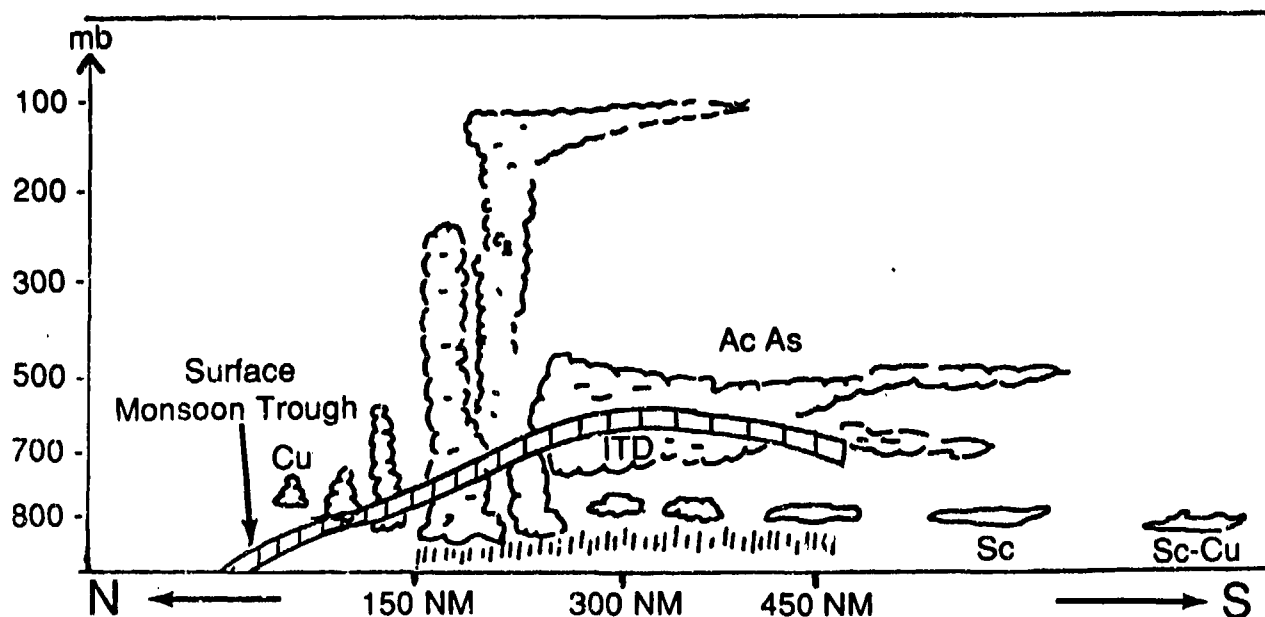


Figure 2-18. Vertical Cross Section of the "African Interior" Monsoon Trough and the Intertropical Discontinuity (ITD) (from Omotosho, 1984).

Over the African interior, cloudiness and rainfall rarely surge north of 16° N until the surface Monsoon Trough merges with the "Indian Ocean" surface Monsoon Trough in July and August over the Red Sea

and Gulf of Aden. When this happens, expect maximum cloud cover and precipitation in the western Ethiopian Highlands. Figure 2-19 shows favorable low-level moisture pathways into the western Highlands.

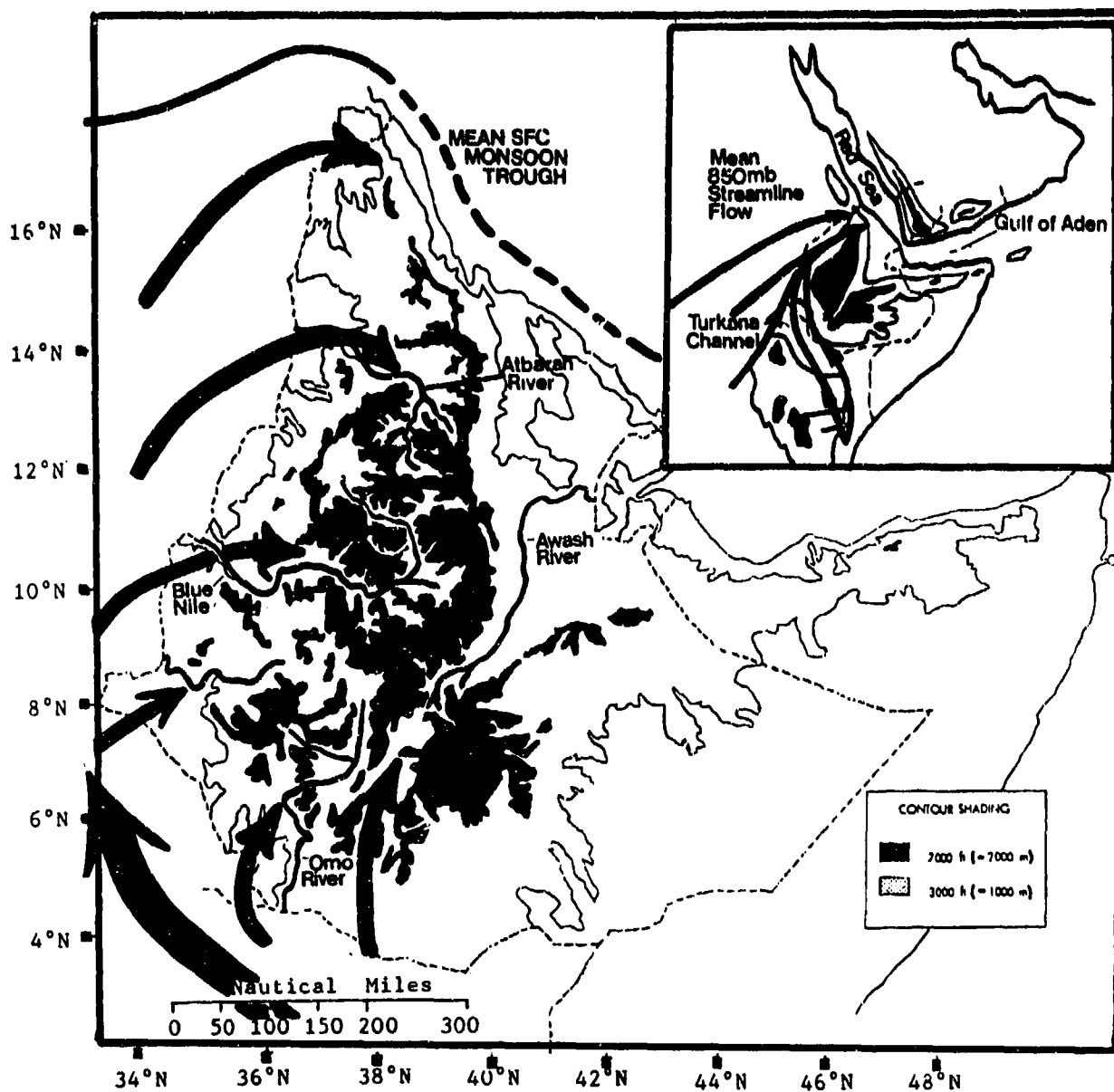


Figure 2-19. Mean Surface Monsoon Trough Position and Natural Pathways (Arrows) for Low-Level Inflow. The inflow pictured produces heavy convection in the western Ethiopian Highlands during July and August. The darkened areas are above 2,000 meters (6,560 feet). The inset shows mean 850-mb streamline flow.

The surface Monsoon Trough position over the western Indian Ocean is controlled entirely by the Somali Jet. Dry Sahara Desert air does not penetrate eastward across the Ethiopian Highlands; as a result, the "Indian Ocean" segment of the surface Monsoon Trough over the Horn of Africa and adjacent Indian Ocean is without an ITD. Furthermore, the Mascarene High is solely responsible for initiating and sustaining the Somali Jet during the Southwest Monsoon.

In summer, there are two trough axis lines in the western Indian Ocean; these are referred to by some meteorologists as the "Northern Equatorial Trough" (NET) and the "Southern Equatorial Trough" (SET).

The NET (the Indian Ocean surface Monsoon Trough) oscillates across 30° of latitude over the Indian Ocean during the Southwest Monsoon (see Figures 2-20a-c). The Somali Jet (southerly low-level flow) controls the position of the NET axis. By late June, the

"Indian Ocean" surface Monsoon Trough is positioned over the northern Arabian Sea. However, the mean SET axis oscillates only 11° of latitude between 7° S and 4° N. Weak large-scale equatorial flow occurs over the equatorial Indian Ocean between 50° and 75° E. Normally, a band of weak low-level equatorial westerlies associated with broad cross-equatorial flow over the equatorial Indian Ocean (not with the Somali Jet) oscillates along and north of the equator between June and August. These equatorial westerlies lie between the NET and SET. Cloud bands frequently develop along

the SET where cyclonic vorticity and convergence is present. A double cloud band has been observed on satellite imagery during some southwest monsoons between June and August. SET cloudiness may propagate westward over Somalia when the SET cloud cover organizes into a significant synoptic weather system. Figures 2-20a-c show NET and SET positions during June, July, and August. Note that the surface Monsoon Trough positions shown in Figure 2-17 do not differ significantly from Findlater's 3,000-foot (915-meter) NET positions in Figures 2-20a-c.

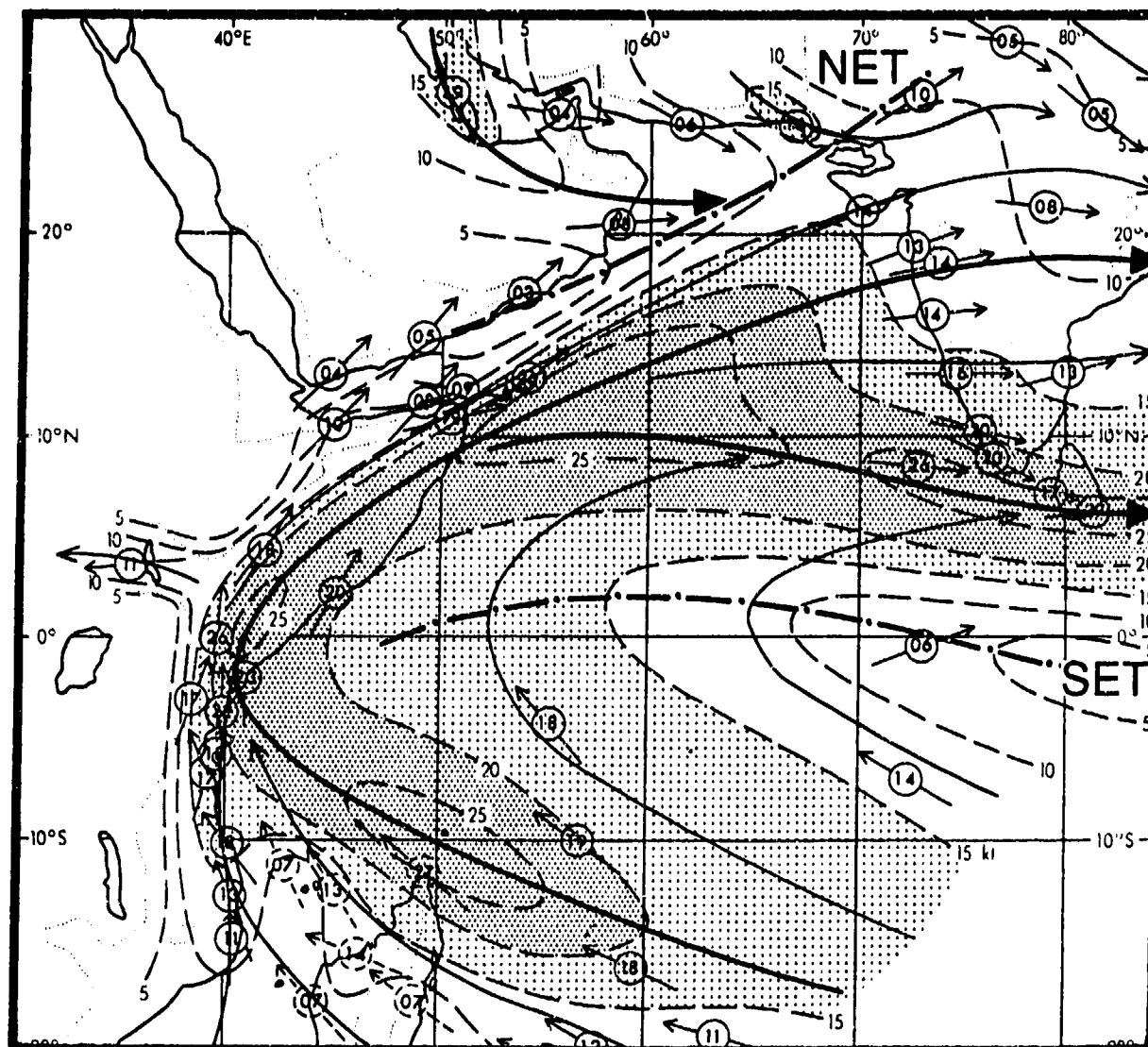


Figure 2-20a. Mean June Positions of the 3,000-foot Monsoon Trough (NET) and the Southern Equatorial Trough (SET) (from Findlater, 1971).

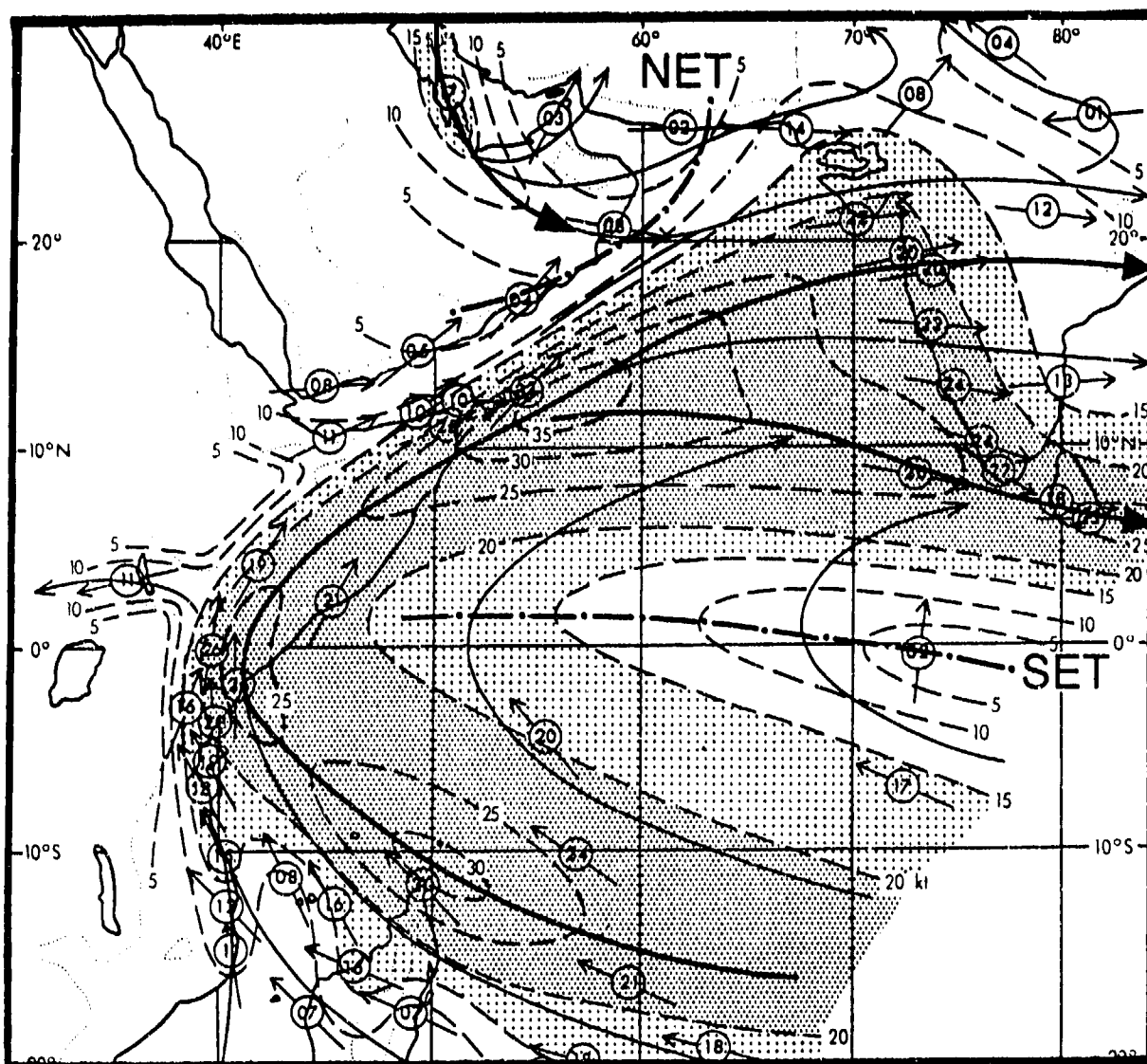


Figure 2-20b. Mean July Positions of the 3,000-foot Monsoon Trough (NET) and the Southern Equatorial Trough (SET) (from Findlater, 1971).

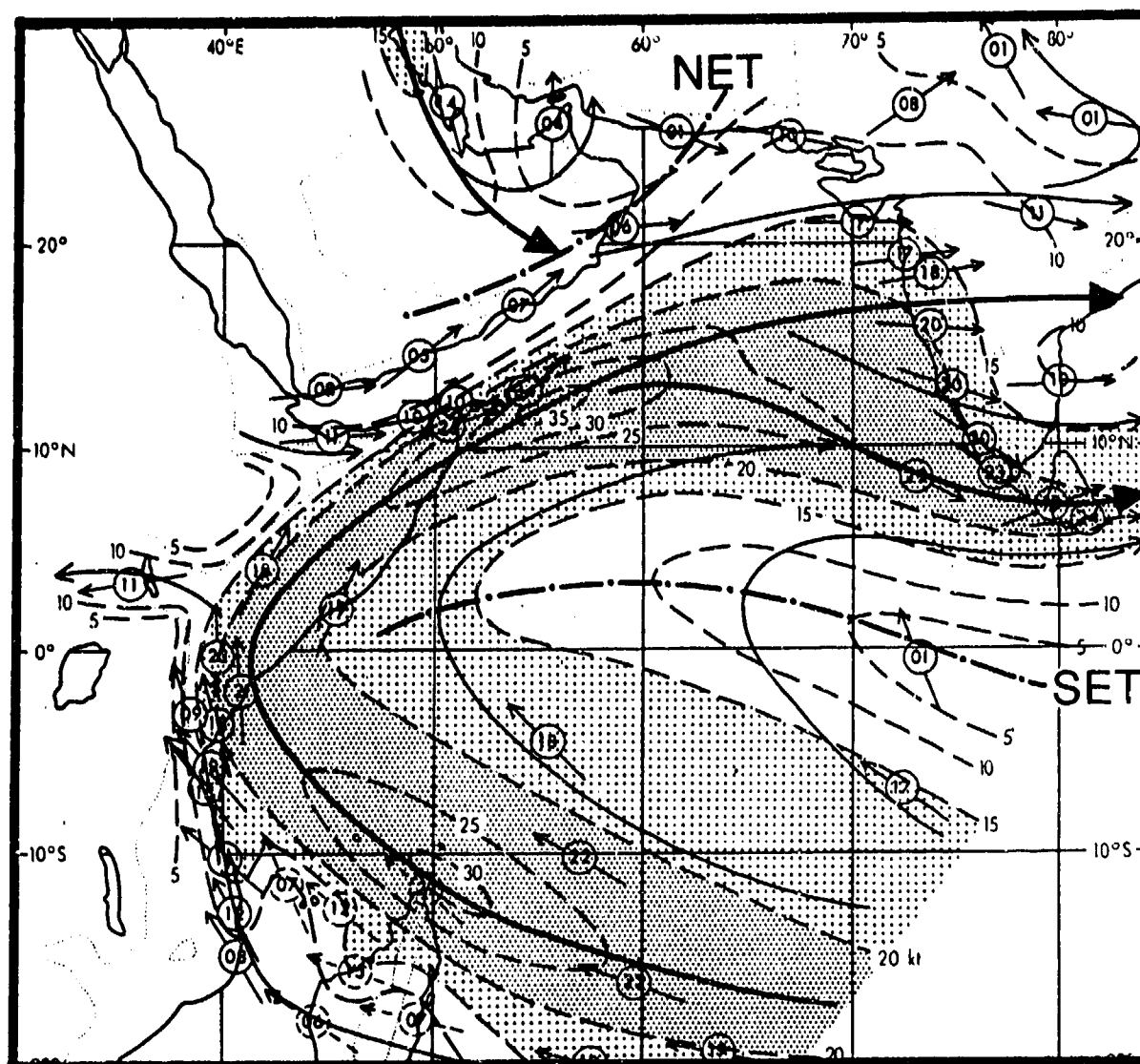


Figure 2-20c. Mean August Positions of the 3,000-foot Monsoon Trough (NET) and the Southern Equatorial Trough (SET) (from Findlater, 1971).

THE NORTHEAST MONSOON. Between December and March, Northeast Monsoon circulation dominates the Horn of Africa. Generally, the Northeast Monsoon (winter) is the "dry" season, and the Southwest Monsoon (summer) the "wet" season. But complex terrain features can result in "wet" Northeast Monsoon conditions along the Red Sea/Gulf of Aden corridor. In Chapters 3-6, Northeast Monsoon flow (December-March) is referred to as the dominant weather feature. Readers should review the "General Weather" sections with care, since Northeast Monsoon flow also affects both transition periods (October-November and April-May).

Any discussions of the Northeast Monsoon must include the Asiatic High, the Saharan High, and the Saudi Arabian High. Surface outflow from these high-pressure cells combine with topography along the Red Sea/Gulf of Aden corridor to produce orographic uplift and the Red Sea Convergence Zone (RSCZ). The Saharan High (by itself) may also contribute to atypical "Northeast Monsoon" weather in northwestern Ethiopia.

THE ASIATIC HIGH. This strong but very shallow system dominates much of the Asian continent from late September to late April. Radiation cooling is the primary mechanism for its formation and intensification. Migratory Arctic air masses moving southward into central Asia temporarily reinforce and intensify this high. Mean central pressure (1035 mb) is over Western Mongolia. Pressure is stronger in January and February, but vertical extent rarely exceeds 850 mb.

Figure 2-21a shows the Asiatic High's mean October position. Mean central pressure (1023 mb) is near 48° N, 90° E. Note that the Pakistani Heat Low (1010 mb) and thermal trough are also shown; the broad-scale thermal trough (shaded) is much weaker because global radiation levels are decreasing rapidly from north to south. In turn, radiation cooling strengthens the Asiatic High over south central Asia. The transition from Southwest to Northeast monsoon flow soon follows.

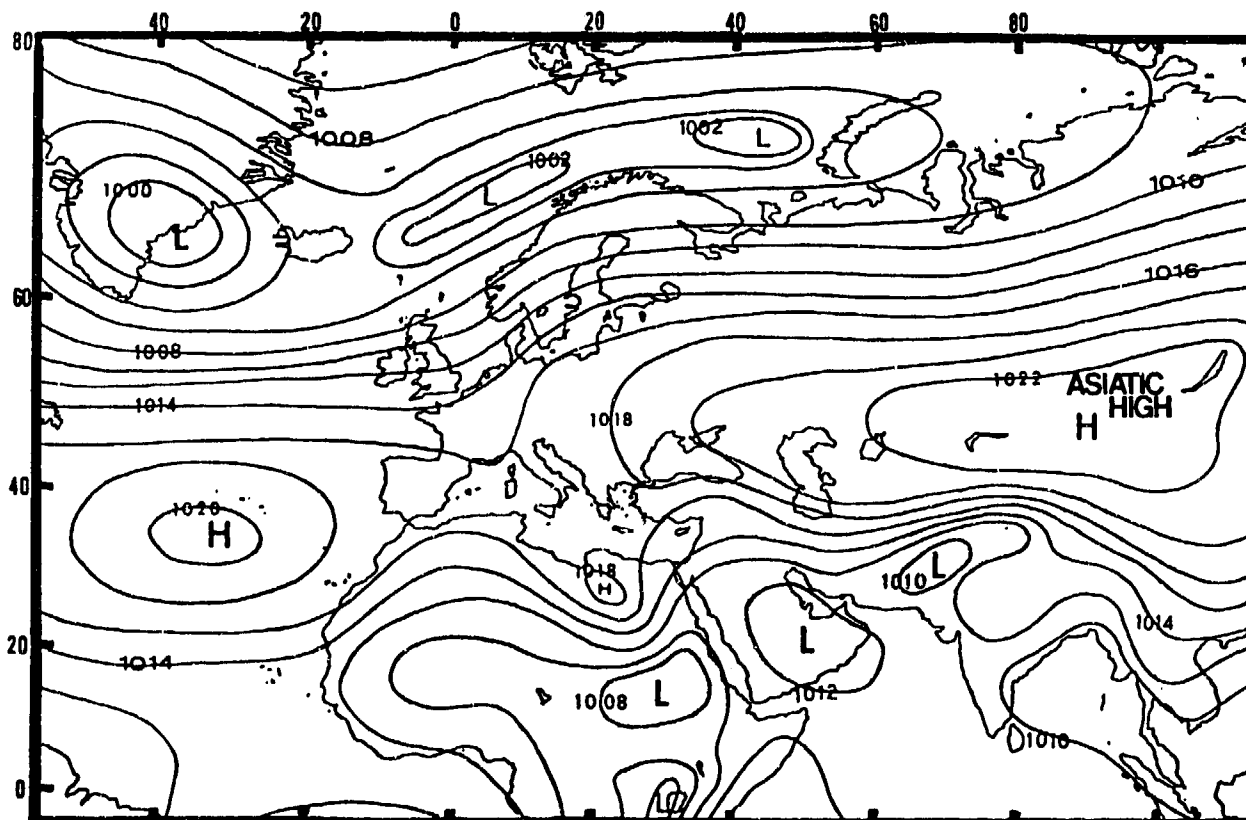


Figure 2-21a. Mean October Surface Position of the Asiatic High. The Pakistani heat low and broad-scale thermal trough (shaded) are also shown.

The mean November surface pressure pattern (Figure 2-21b) shows the mean Asiatic High near 48° N, 80° E. Central pressure has strengthened to 1031 mb. The broad thermal trough that anchors the surface Monsoon Trough, however, is no longer present. As a

result, low-level northeasterly flow penetrates into the Horn of Africa. Northeast Monsoon flow is sustained until late March, when the Asiatic High weakens and intense surface heating again produces the broad-scale thermal trough and Pakistani Heat Low.

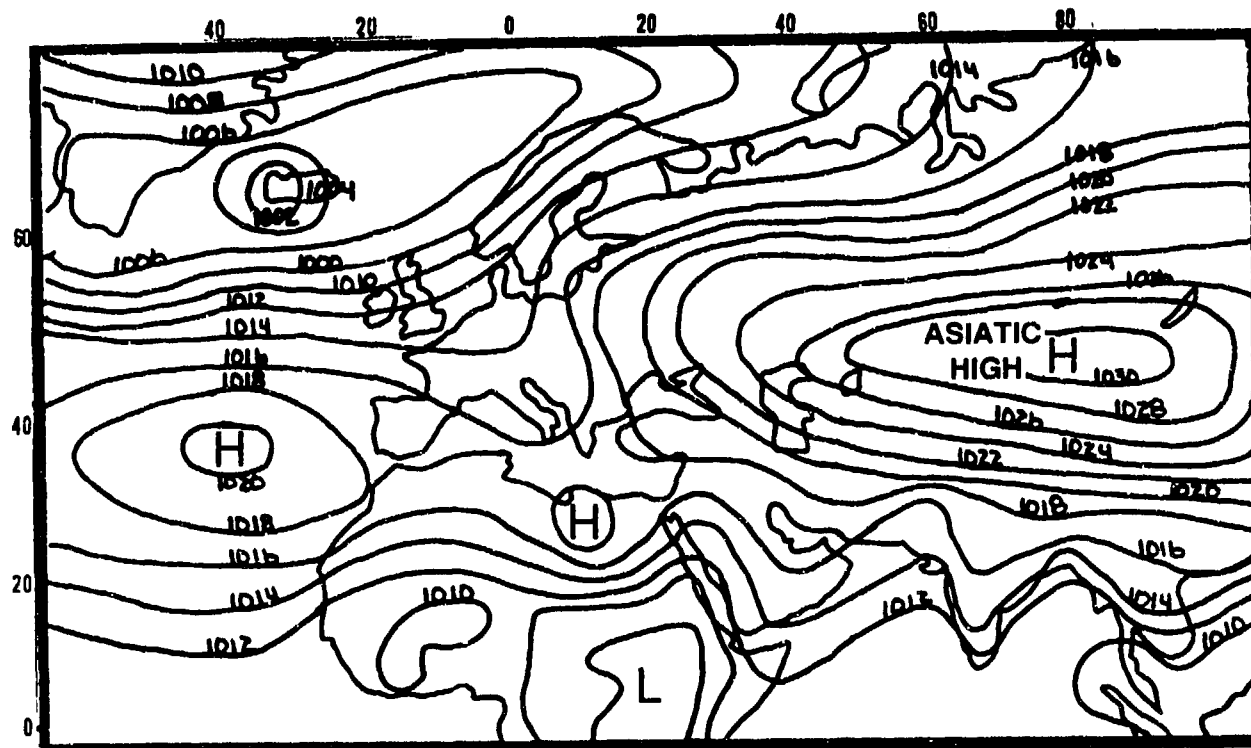


Figure 2-21b. Mean November Surface Position of the Asiatic High. Note the surface trough in the mean surface pressure field at 50° E (dashed line). The trough axis separates Northeast Monsoon flow from weak mean westerly flow from the Azores and Saharan Highs.

Figure 2-21c shows the Asiatic High at its mean peak strength (1035 mb) near 49° N, 97° E. Maximum low-level northeasterly flow is in January and February because south-central Asia is extremely cold. The

Asiatic High may exceed 1050 mb for 1-3 day periods; the highest recorded surface pressure is 1083 mb. Extremely strong highs may intensify northeasterly flow despite the "blocking" effects of the Himalayas.

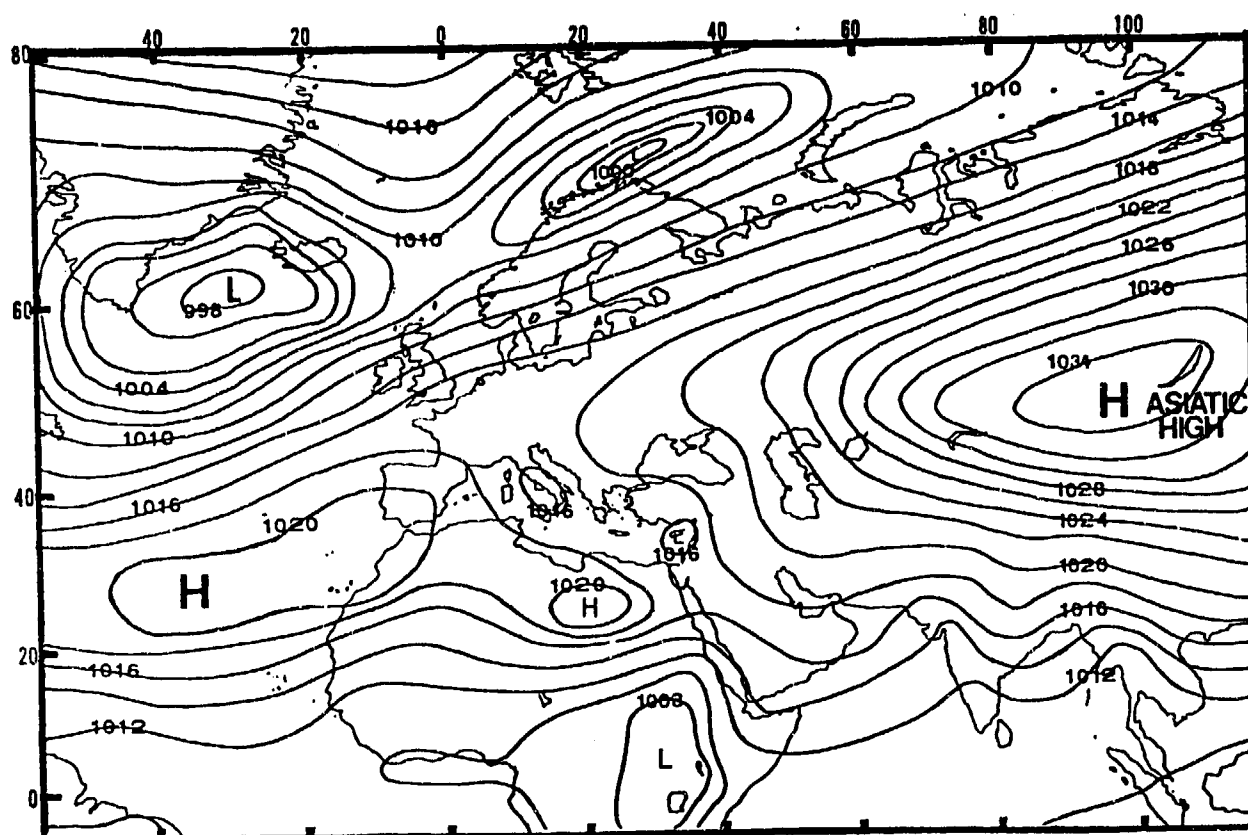


Figure 2-21c. Mean January Surface Position of the Asiatic High.

The mean March surface position of the Asiatic High is 53° N, 82° E; mean central pressure is now 1029 mb. Since the cell migrates northward and weakens with northern hemisphere warming in the mid-latitudes, northeasterly flow over the Horn of Africa is reduced. Initially, the Northeast Monsoon retreats along the

equator. By the end of March, northeasterly flow penetrates southward to only 10-11° N. The weak Asiatic High surface pressure pattern and reduced northeasterly flow over the Horn of Africa is quickly replaced by lower surface pressure (the shaded region in Figure 2-21e) in the subtropics.

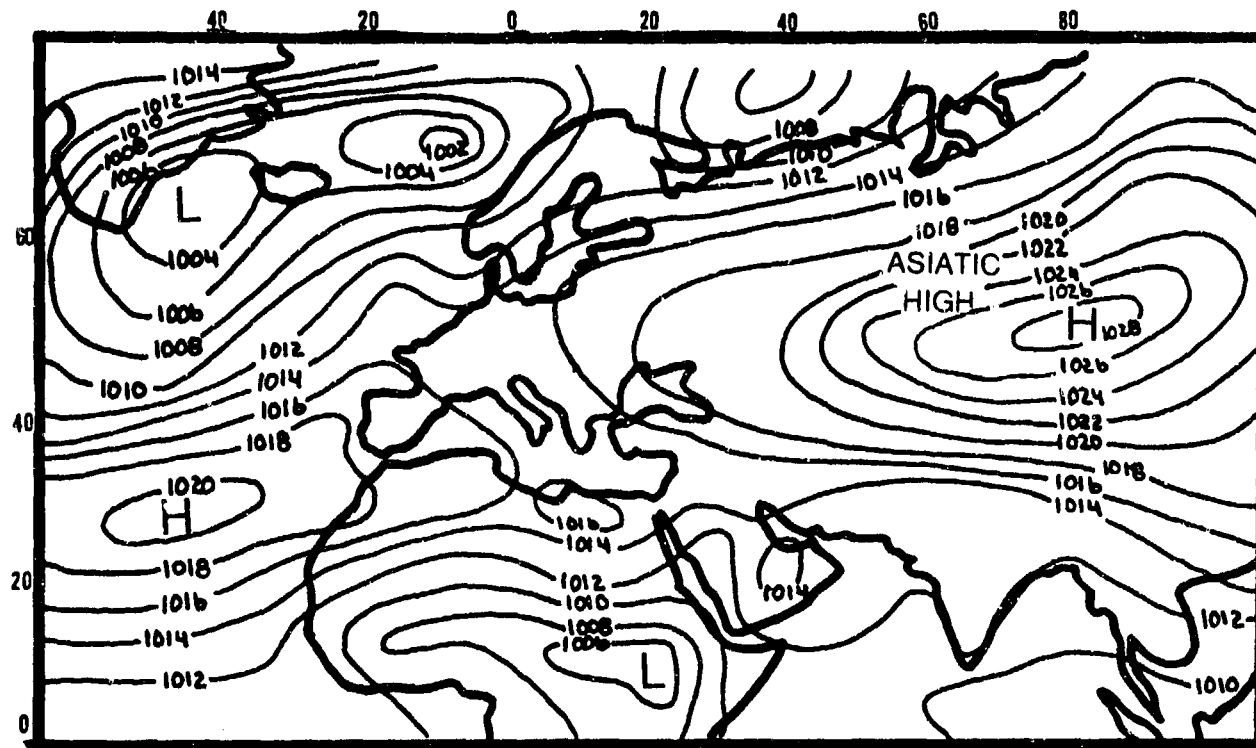


Figure 2-21d. Mean March Surface Position of the Asiatic High.

In April, increasing solar radiation weakens the Asiatic High's mean central pressure to 1022 mb. The broad-scale thermal trough reappears over India, Saudi

Arabia, and northeastern Sudan. Northeasterlies disappear altogether.

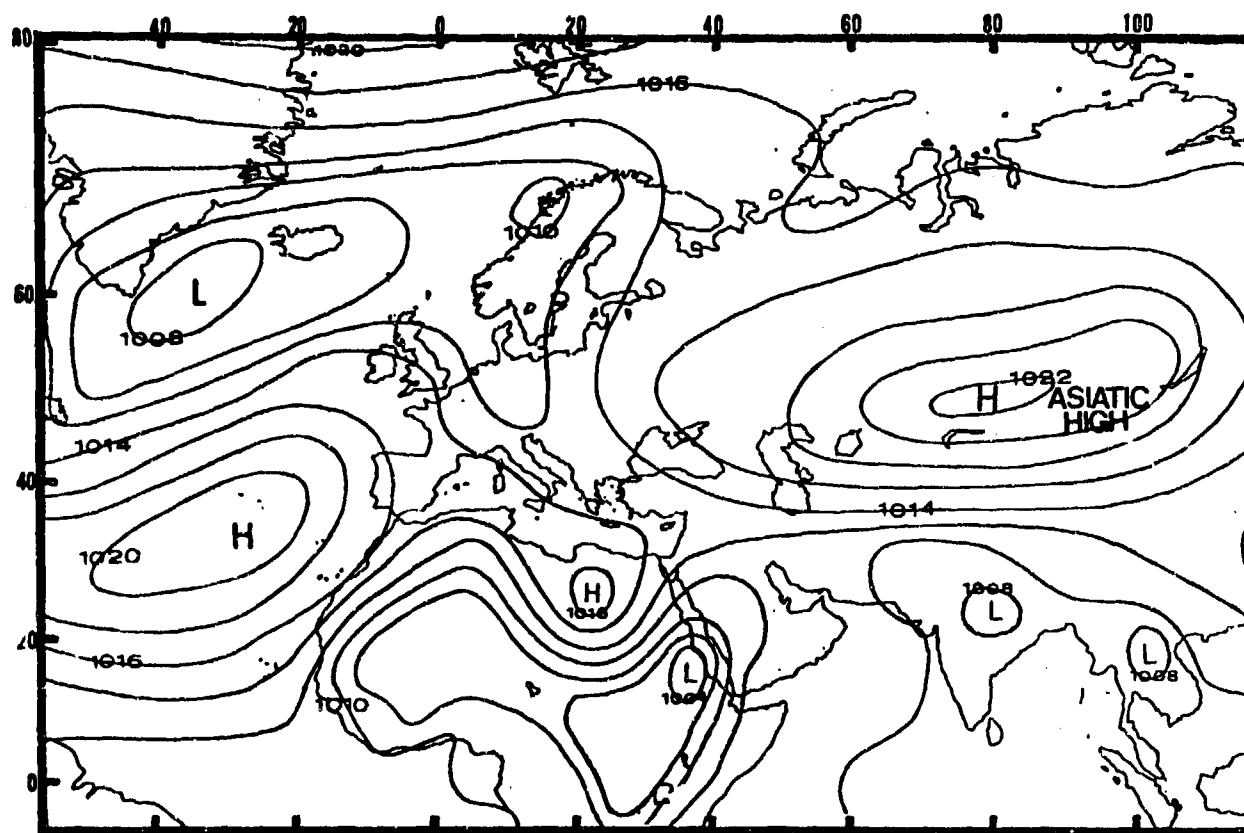


Figure 2-21e. Mean April Surface Position of the Asiatic High. The broad-scale thermal trough is shaded.

THE SAHARAN HIGH. The Saharan High (an apparent extension of the Azores High) provides weak surface flow to the Yemen Highlands and northwestern Ethiopian Highlands between December and early April. Actually a mean position of transitory high cells, its mean January position (26° N, 20° E) is shown in Figure 2-22a; central pressure is 1021 mb. The mean April position (25° N, 22° E) is shown in Figure 2-22b; mean April central pressure is 1018 mb. Because moisture advection and cyclonic activity rarely affect the north and central Sahara south of 20° N, Saharan High outflow is dry and cool. The dry desert air, along with radiation cooling, intensifies the High and makes it a mean surface feature from December to early March.

Mean global sea level pressure charts typically show the Saharan High extending eastward from the Azores High. Undisturbed synoptic weather patterns in the Sahara often produce an extensive high pressure ridge over northern Libya and west-central Egypt, but the Saharan High is actually a transitory cold core high-pressure cell. Its transitory nature is most evident between late January and early April when deep polar troughs enter north Africa. The Saharan High generally moves eastward ahead of the disturbance or disappears from synoptic charts entirely. It usually reforms at the surface within 12-24 hours after a frontal passage.

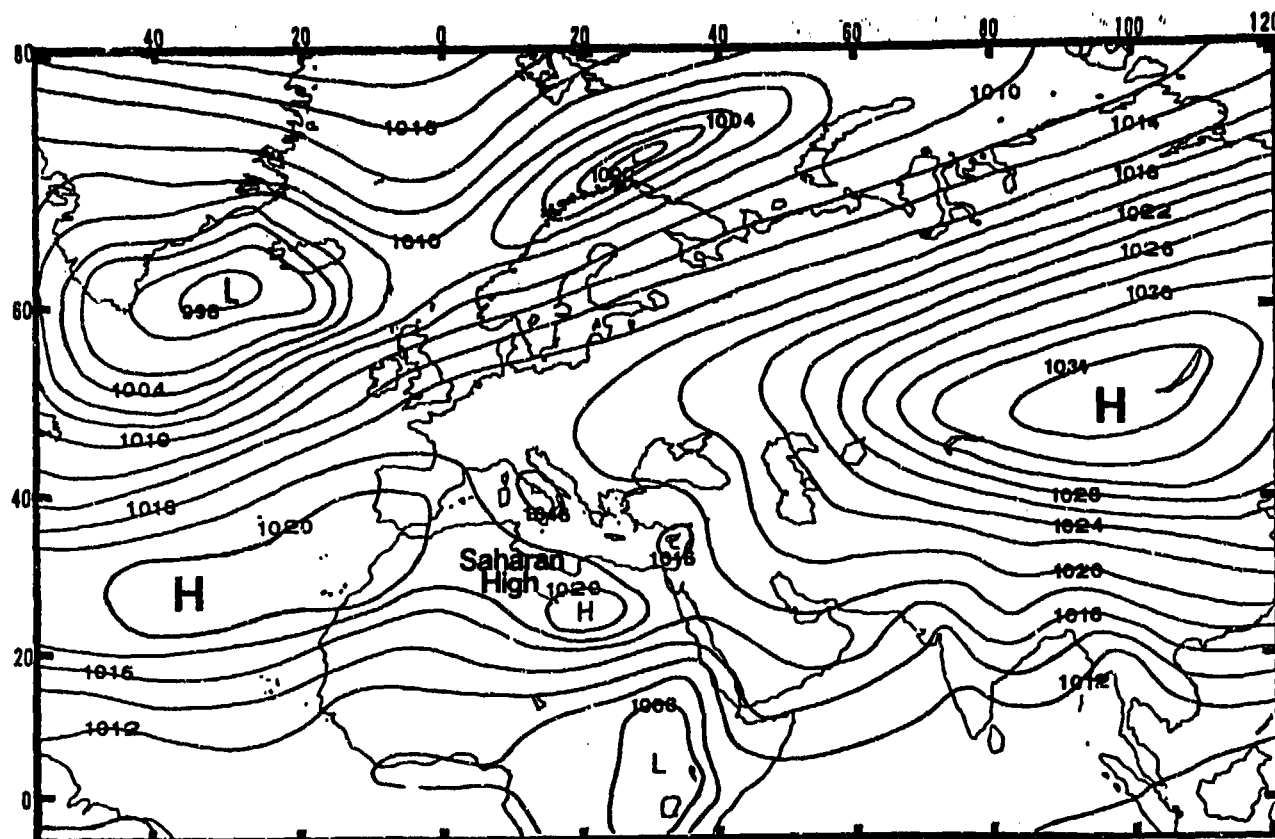


Figure 2-22a. Mean January Surface Position of the Saharan High.

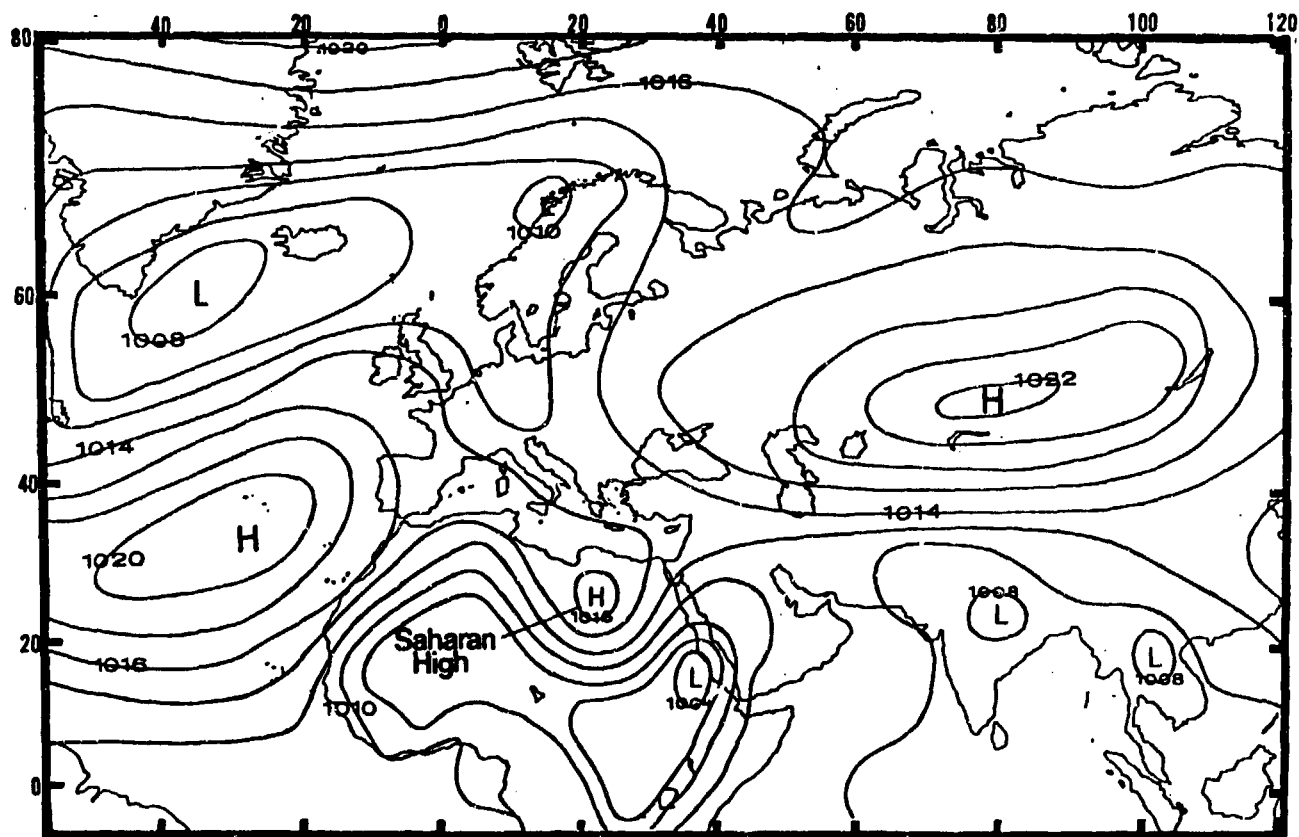


Figure 2-22b. Mean April Surface Position of the Saharan High.

In the rare case of a strong transitory high pressure cell that supports a deep mid-latitude trough passage across the central Red Sea basin, northwesterlies penetrate southward (to 8° N) over North Africa. The western Ethiopian Highlands' rugged north-south terrain from 16° to 4° N normally prevents Saharan High outflow from penetrating east of 37° degrees.

Frequent undisturbed weather patterns along the central and southern Red Sea basin and the southeastern Sahara Desert allow the persistent Saharan High to generate weak west-northwesterly surface flow around the Ethiopian Highlands. North of 16° N, terrain averages only 2,000 feet (610 meters) MSL; as a result, northwesterlies extend southward to 16° N over the Red Sea's open waters. The weak but persistent northerly wind component and the associated shallow air mass over open water represent the Saharan High outflow boundary's southeastern limit.

THE SAUDI ARABIAN HIGH, centered over northwestern Saudi Arabia, is an eastward extension of the Azores-Saharan High pressure ridge in undisturbed synoptic conditions. It is well-defined over the Saudi Arabian peninsula on synoptic charts during extended fair weather periods. Its surface and mid-level anticyclonic circulation is common throughout the December-March Northeast Monsoon. Westerly outflow from the cell's northern edges steers Mediterranean low-pressure systems and their trailing cold fronts into the northern Red Sea and north central Saudi Arabia. East-northeasterly flow prevails along the cell's southern flanks, helping to regulate Northeast Monsoon flow into the Gulf of Aden and the eastern Yemen Highlands. The cell's November position strengthens northeasterly flow into the western Gulf of Aden, through the Straits of Bab al Mandab, and into the southern Red Sea. The High's November and January positions are shown in Figure 2-23a & b. It reaches its southernmost position in March, as shown in Figure 2-23c.

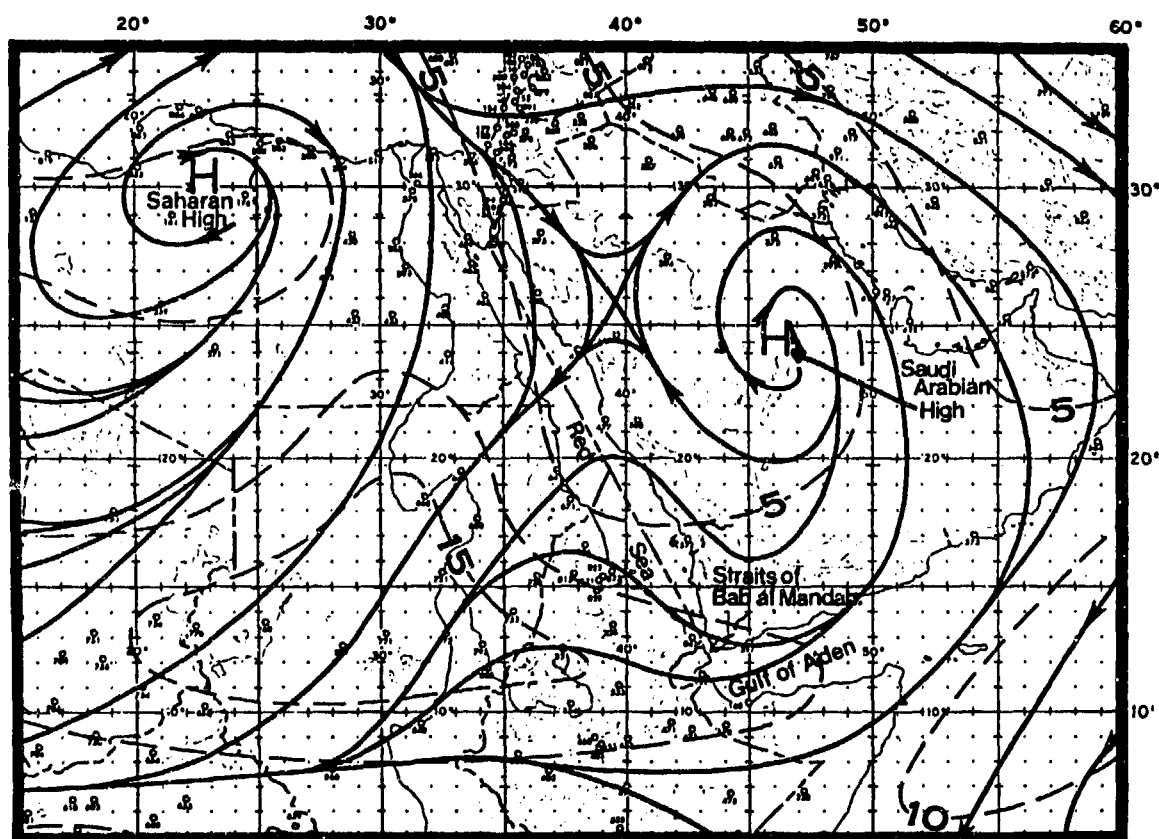


Figure 2-23a. Mean November Gradient Flow and Position of the Saudi Arabian High. Dashed lines are isotachs (kts).

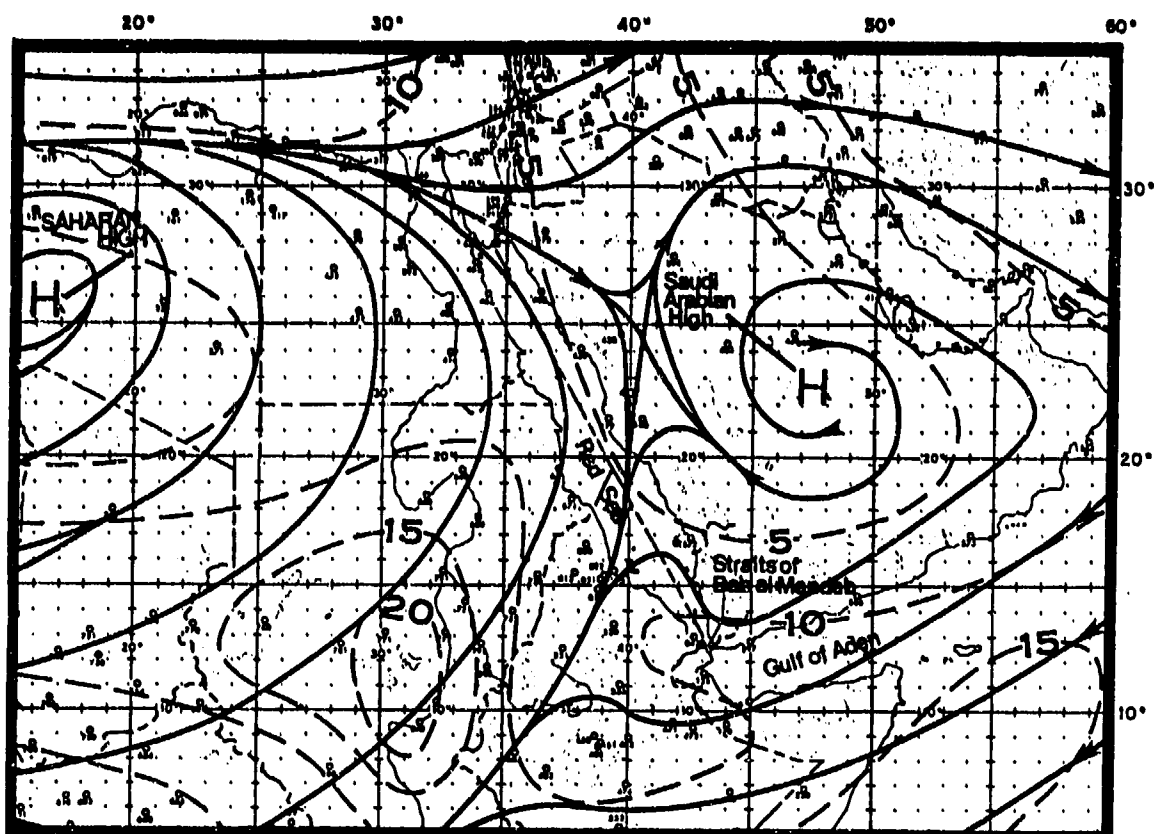


Figure 2-23b. Mean January Gradient Flow and Position of the Saudi Arabian High.

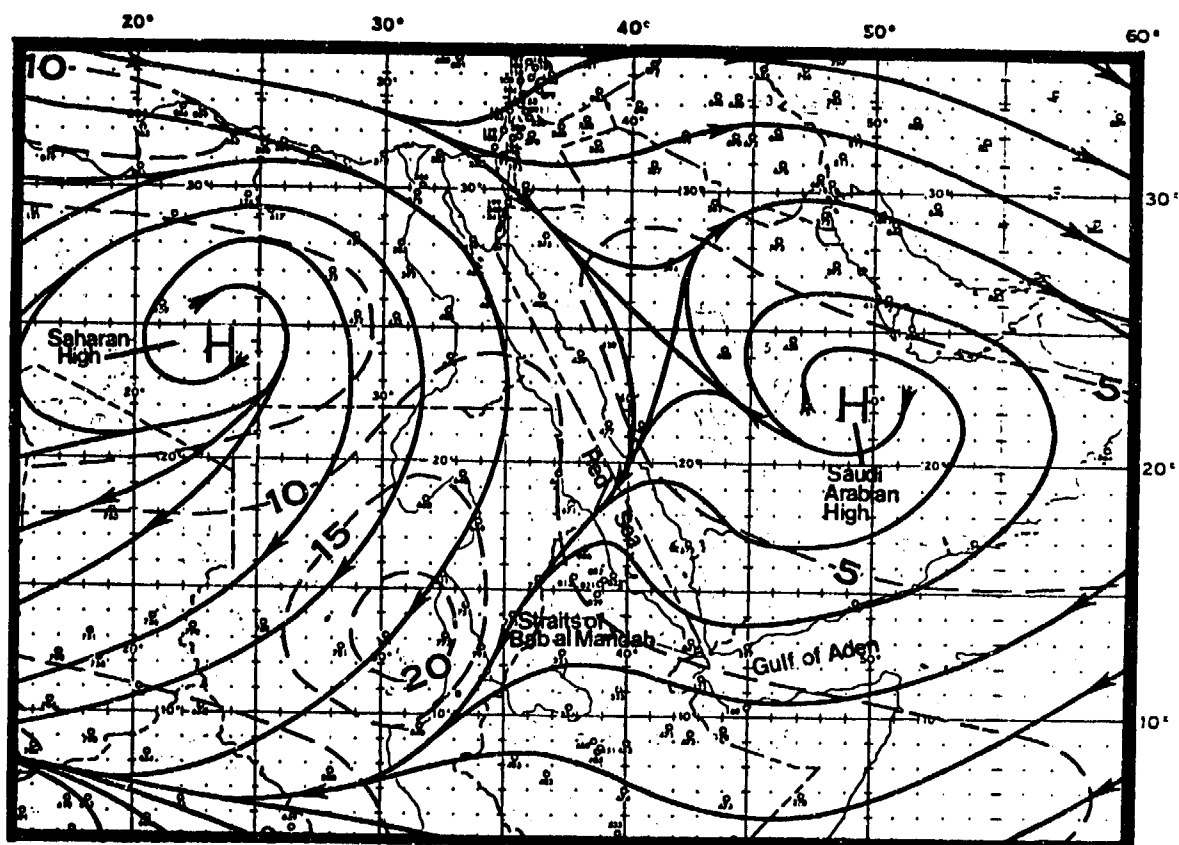


Figure 2-23c. Mean March Gradient Flow and Position of the Saudi Arabian High.

THE RED SEA CONVERGENCE ZONE. Terrain along the Gulf of Aden channels Saudi Arabian High outflow and Northeast Monsoon flow northwestward into the Red Sea. The flow becomes southerly north of

the Straits of Bab al Mandab, where it converges with weak northerly flow from the Saharan High to produce the Red Sea Convergence Zone (RSCZ), shown in Figure 2-24.

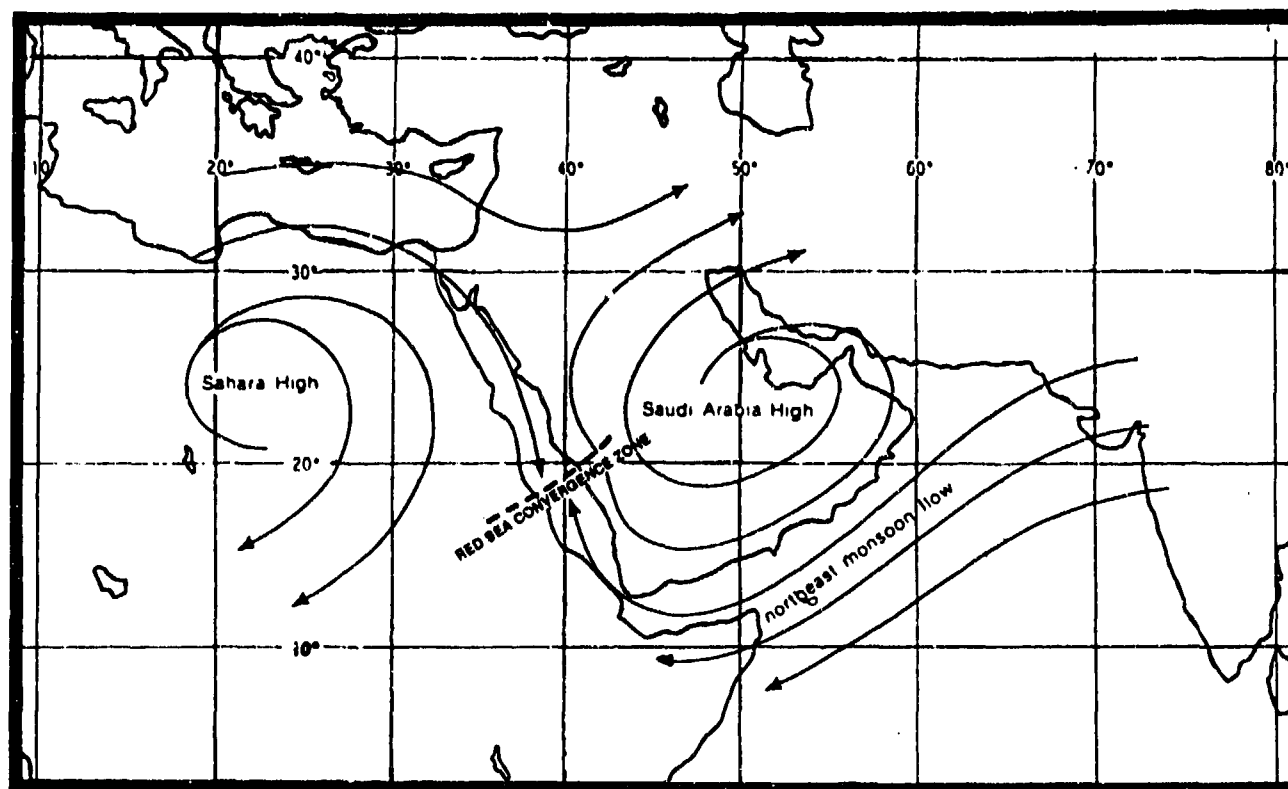


Figure 2-24. Interaction of Saudi Arabian and Saharan High Surface Flow Produces the Red Sea Convergence Zone (RSCZ) (from Fett, 1980).

As shown above, The Red Sea Convergence Zone (RSCZ) forms a continuous band of stratocumulus (oriented WSW-ENE) over open water, but mountains in the Yemen and Ethiopian Highlands break up the feature over land. Figure 2-25 shows the October-April sequence of this feature. Weak surface convergence first appears as a trough line between 18° and 20° N in early October. Between October and April, the Saharan and

Saudi Arabian Highs usually set up weak convergent flow, with Northeast Monsoon circulation supporting daily and monthly oscillations in the trough axis position. October and November flow is shown in the figures by wind speed increases north of the Straits of Bab al Mandab. The RSCZ's mean monthly position is shown by the thick dashed lines.

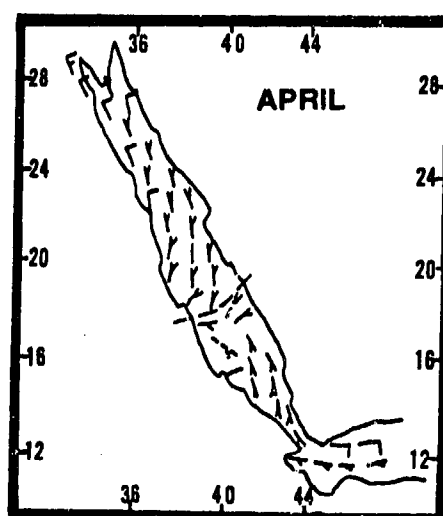
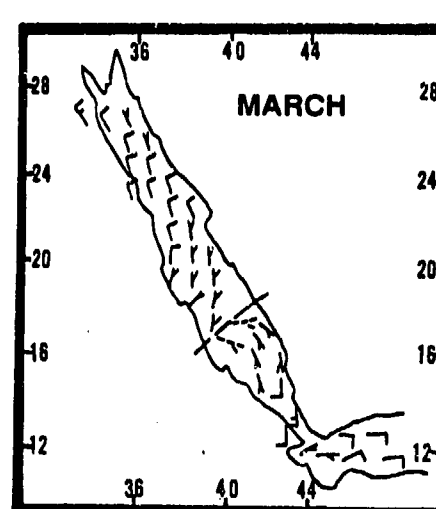
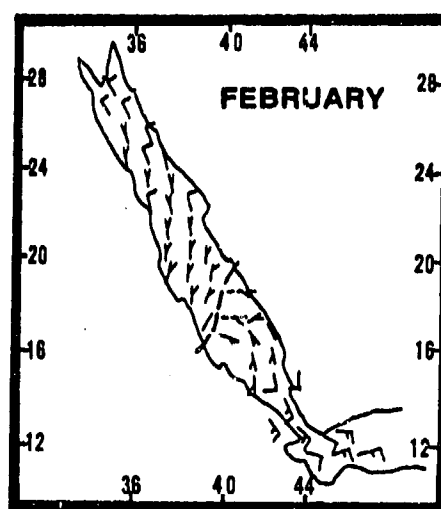
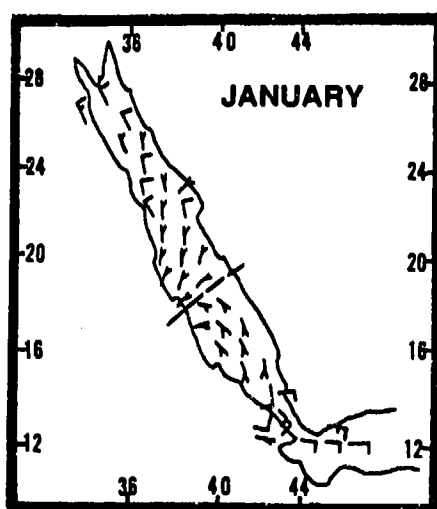
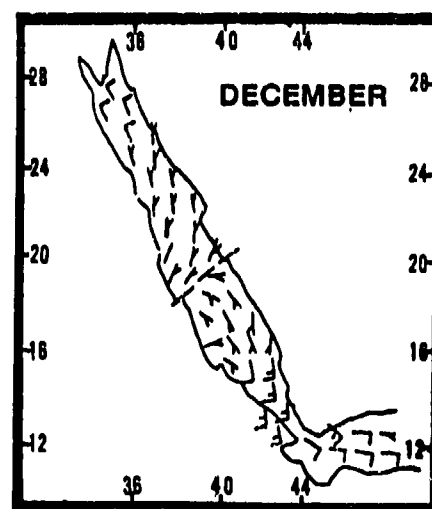
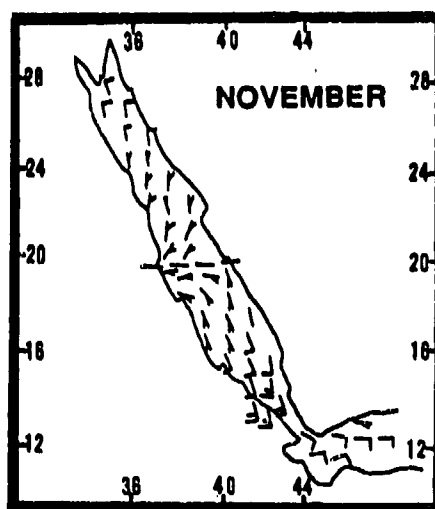
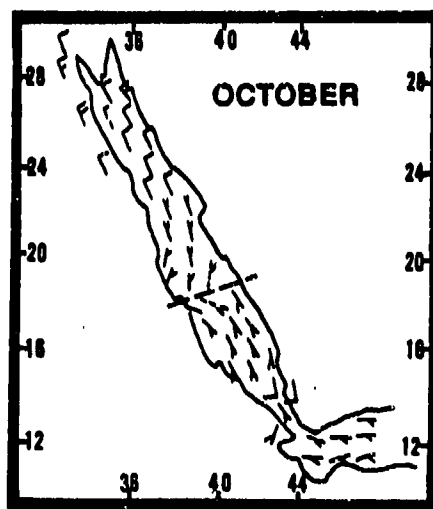


Figure 2-25. RSCZ Positions: October-April.

The trough oscillates little during undisturbed weather periods because of weak winds. The RSCZ, however, oscillates under three conditions:

(1) *When* a southward displacement--on the order of 1-3 days--occurs as shortwave troughs pass over the Red Sea. These shortwaves, with strong northwesterly flow, move the RSCZ to between 13° and 15° N.

(2) *When* warm air advection from interior Africa produces northward movements in the RSCZ. Typically, deep upper-level troughs penetrate low latitudes in January and February. Warm equatorial air and southerly flow--ahead of the cold front--surges northeastward into the central Red Sea. Low-level flow lifts orographically along the north Yemen Highlands subregion. Convergence between the warm front and RSCZ also occurs. The RSCZ may shift to 20-22° N with strong southerly flow, but it recovers to its normal position quickly after the upper-level disturbance drifts

over Saudi Arabia. Depending on its strength, an upper-level shortwave following the frontal passage may push the RSCZ southward again.

(3) *When* there is an increase in Northeast Monsoon flow through the Straits of Bab al Mandab, possible during extended fair weather periods. Southerly flow--deflected through the Straits--may increase with a strengthening Saudi Arabian or Asiatic High.

RSCZ oscillations often converge with land/sea breeze circulations along Red Sea Coasts. The additional convergence may trigger orographic showers and thundershowers on the nearby slopes of the northwestern Ethiopian and Yemen Highlands.

MID- AND UPPER-LEVEL FLOW PATTERNS. Figures 2-26 through 2-29 show January, April, July, and October streamline flow at 850, 700, 500, 300, and 200 millibars over the entire SWANEA study area.

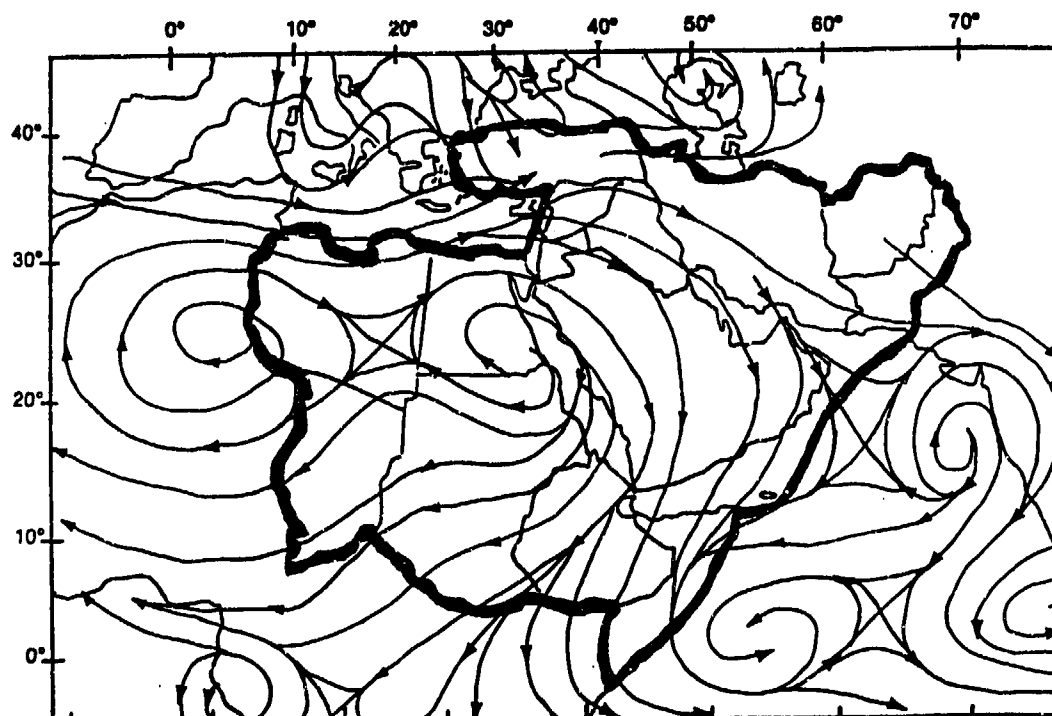


Figure 2-26a. Mean January Upper-Air Flow Patterns, 850 mb.

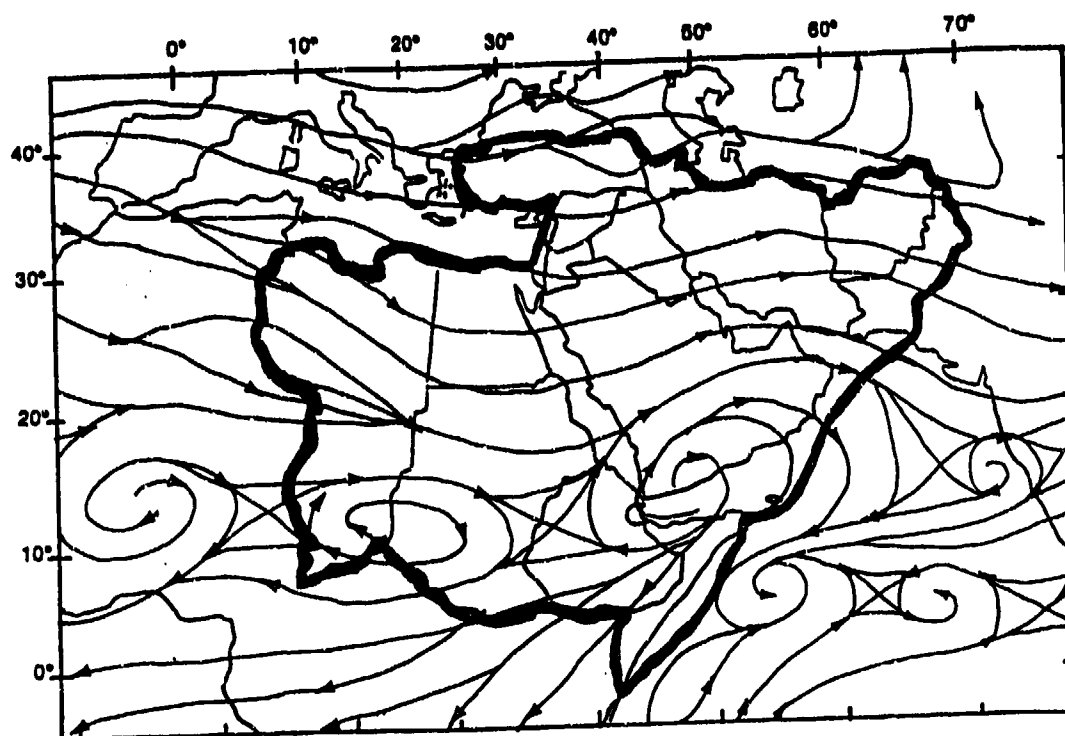


Figure 2-26b. Mean January Upper-Air Flow Patterns, 700 mb.

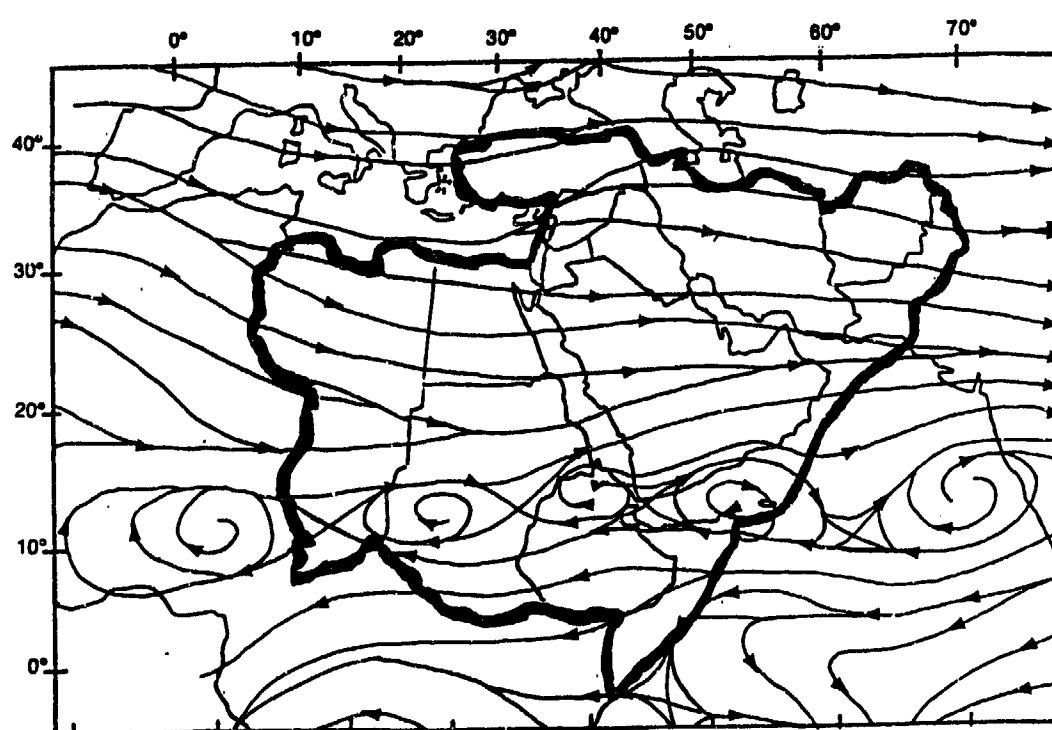


Figure 2-26c. Mean January Upper-Air Flow Patterns, 500 mb.

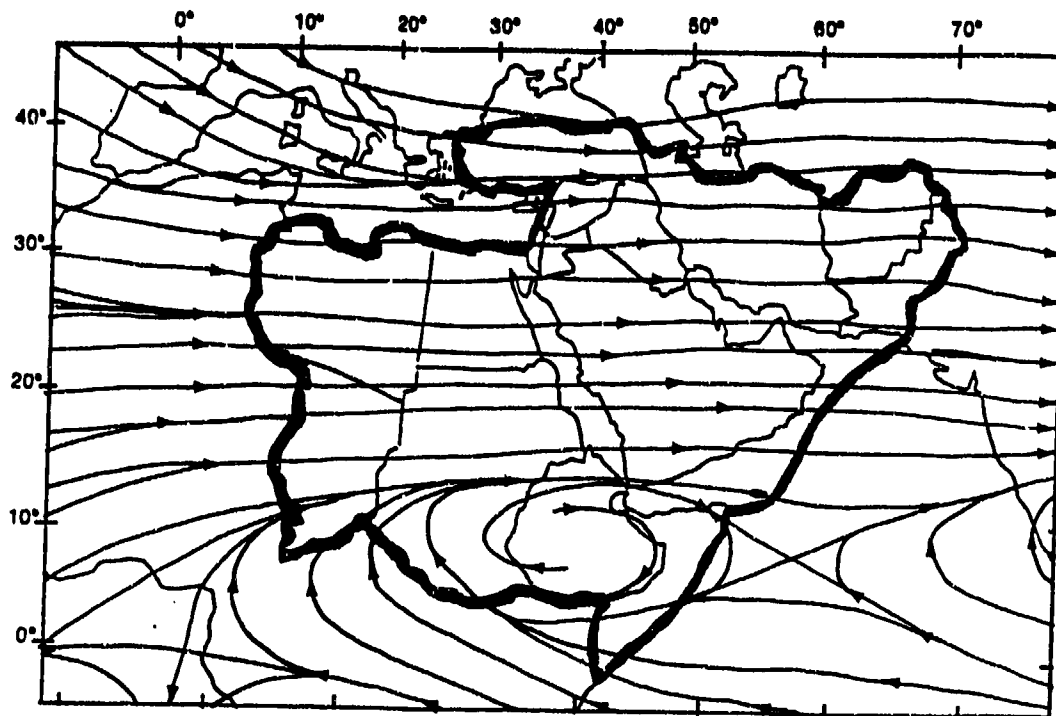


Figure 2-26d. Mean January Upper-Air Flow Patterns, 300 mb.

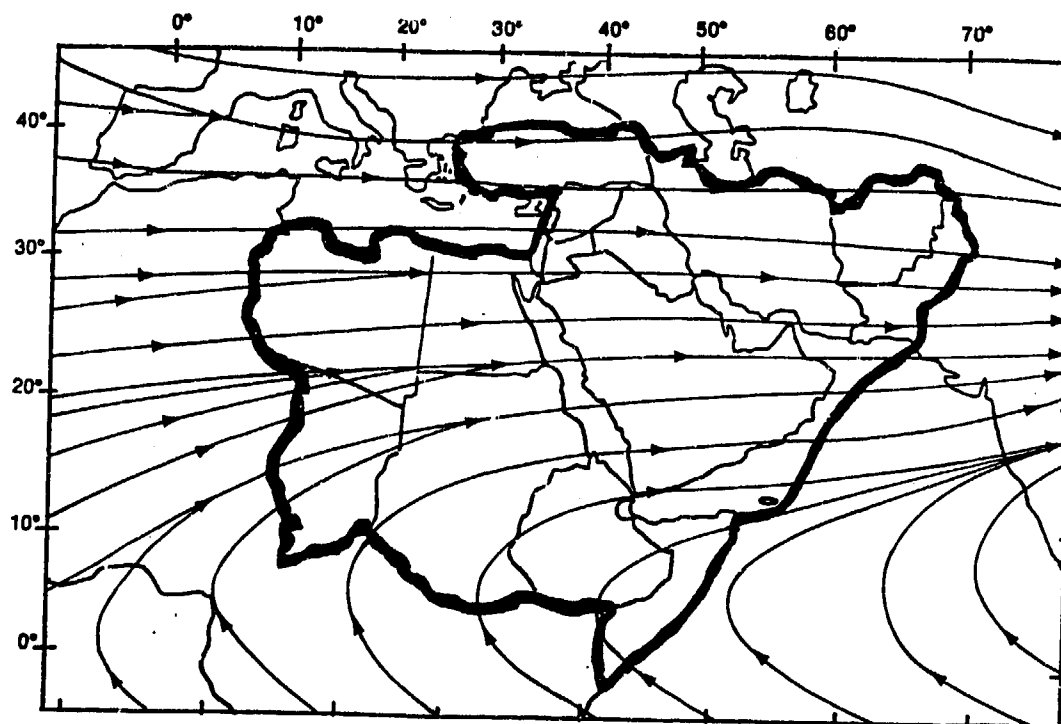


Figure 2-26e. Mean January Upper-Air Flow Patterns, 200 mb.

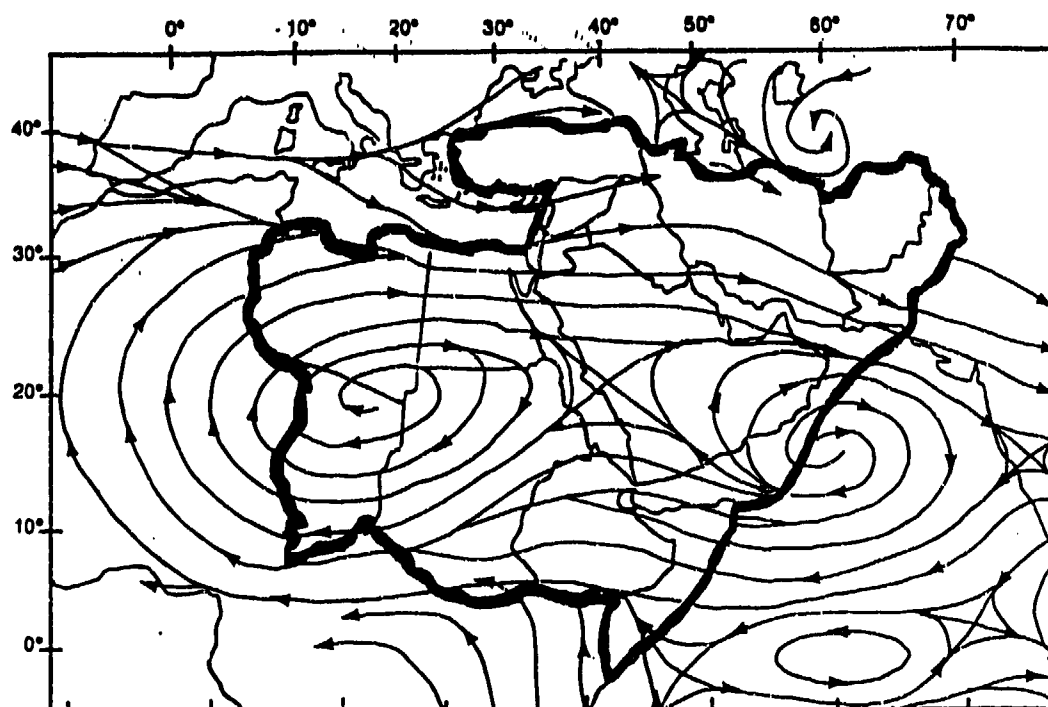


Figure 2-27a. Mean April Upper-Air Flow Patterns, 850 mb.

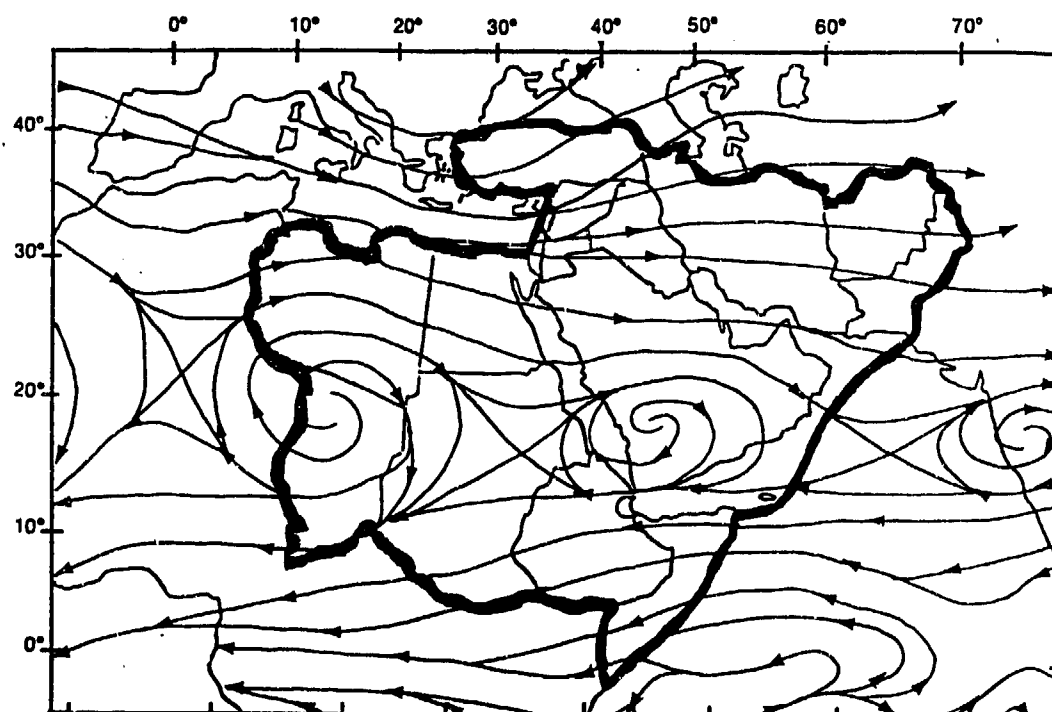


Figure 2-27b. Mean April Upper-Air Flow Patterns, 700 mb.

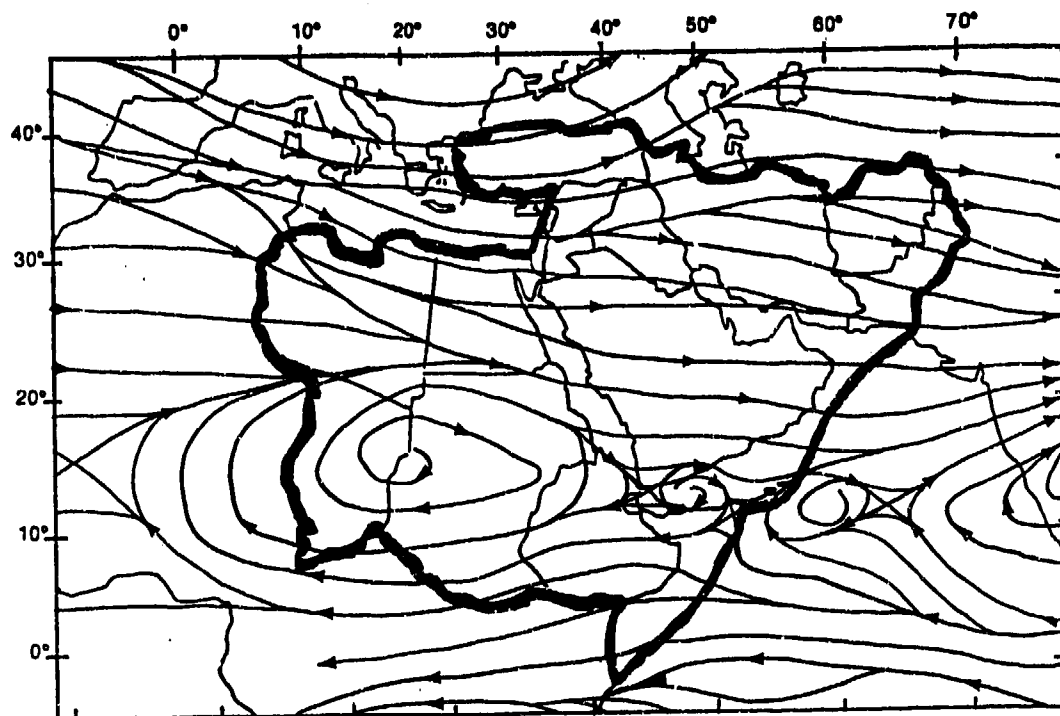


Figure 2-27c. Mean April Upper-Air Flow Patterns, 500 mb.

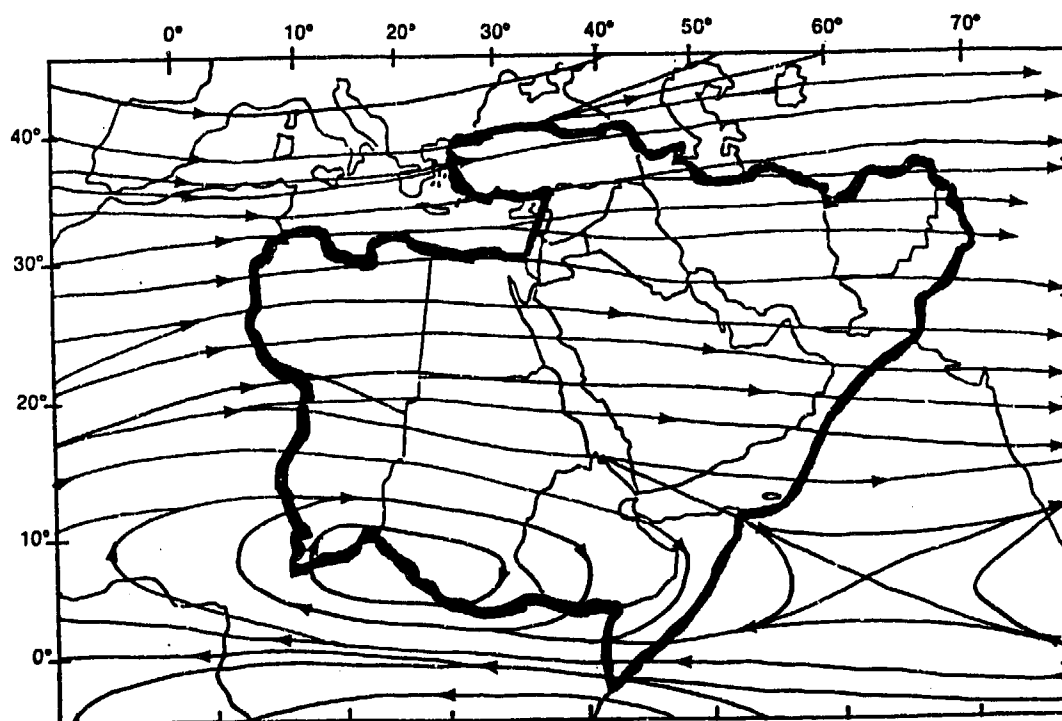


Figure 2-27d. Mean April Upper-Air Flow Patterns, 300 mb.

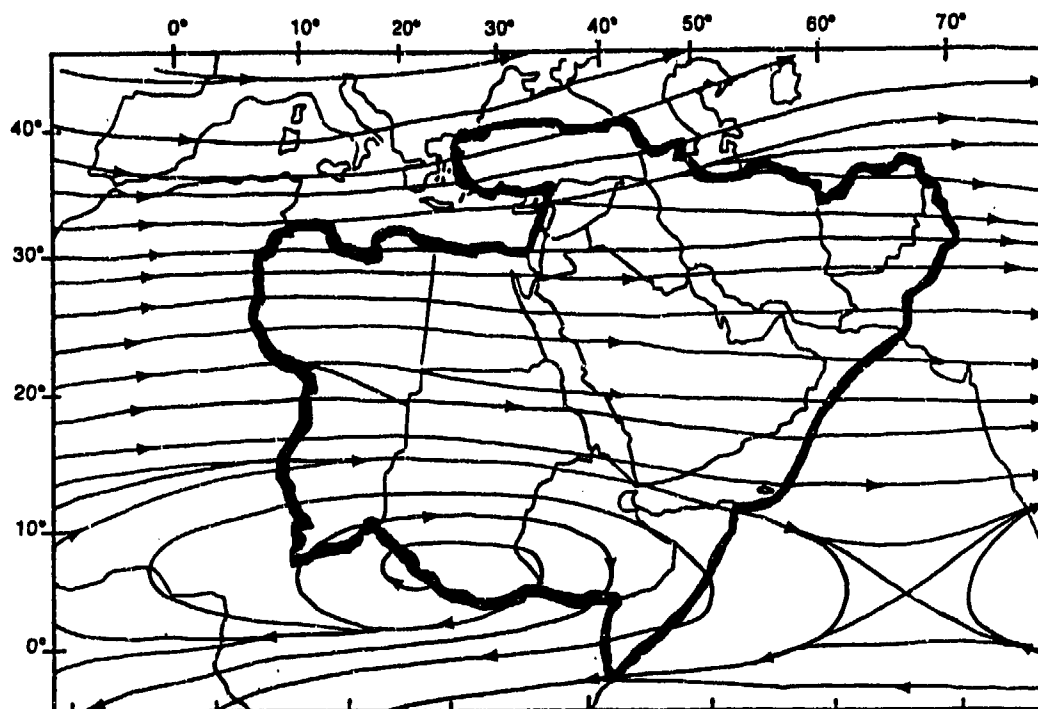


Figure 2-27e. Mean April Upper-Air Flow Patterns, 200 mb.

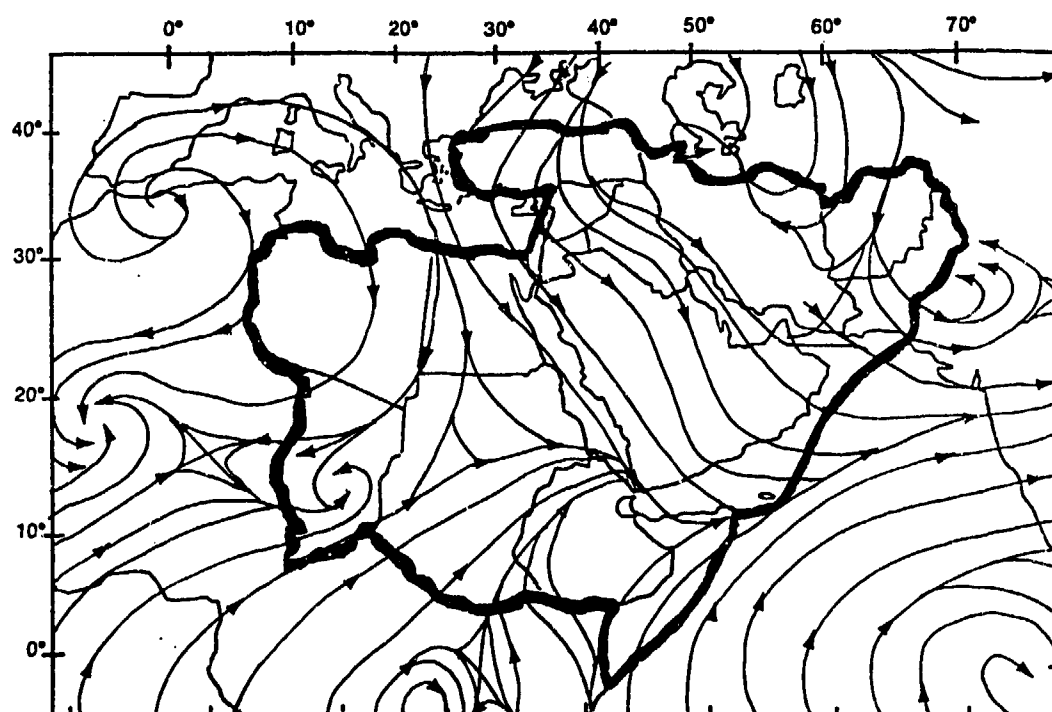


Figure 2-28a. Mean July Upper-Air Flow Patterns, 850 mb.

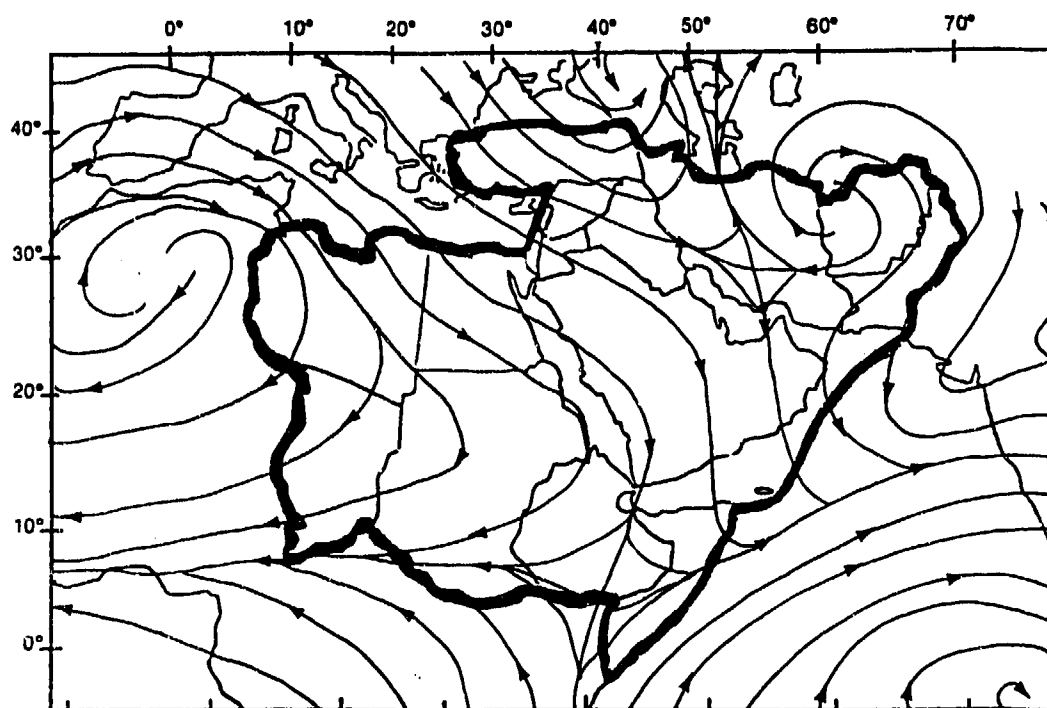


Figure 2-28b. Mean July Upper-Air Flow Patterns, 700 mb.

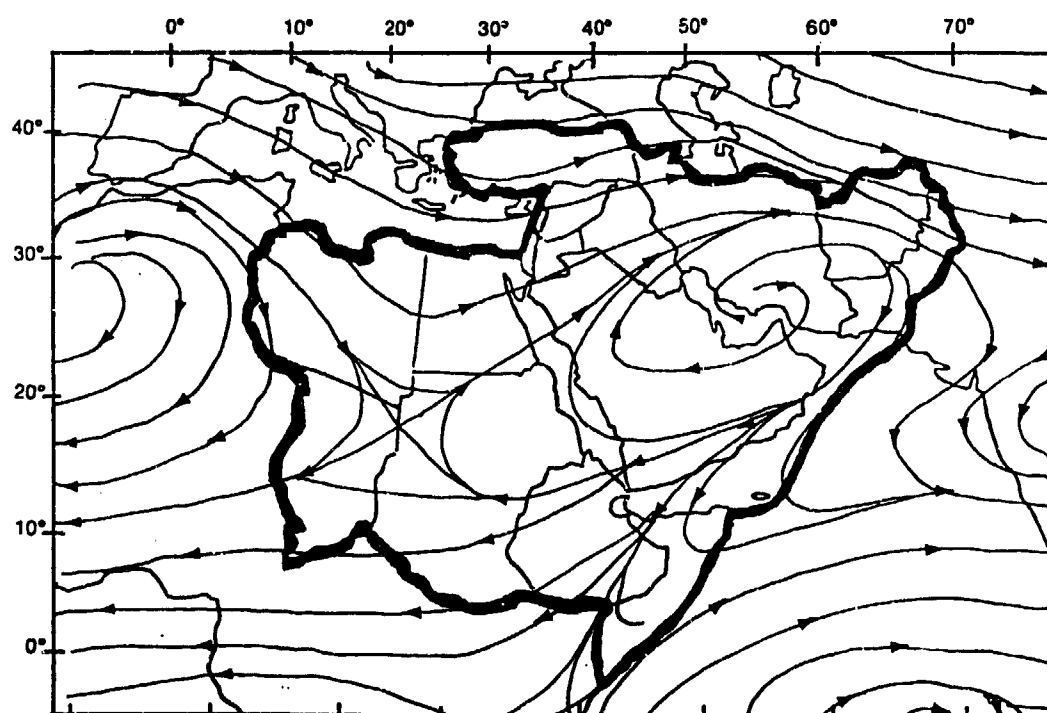


Figure 2-28c. Mean July Upper-Air Flow Patterns, 500 mb.

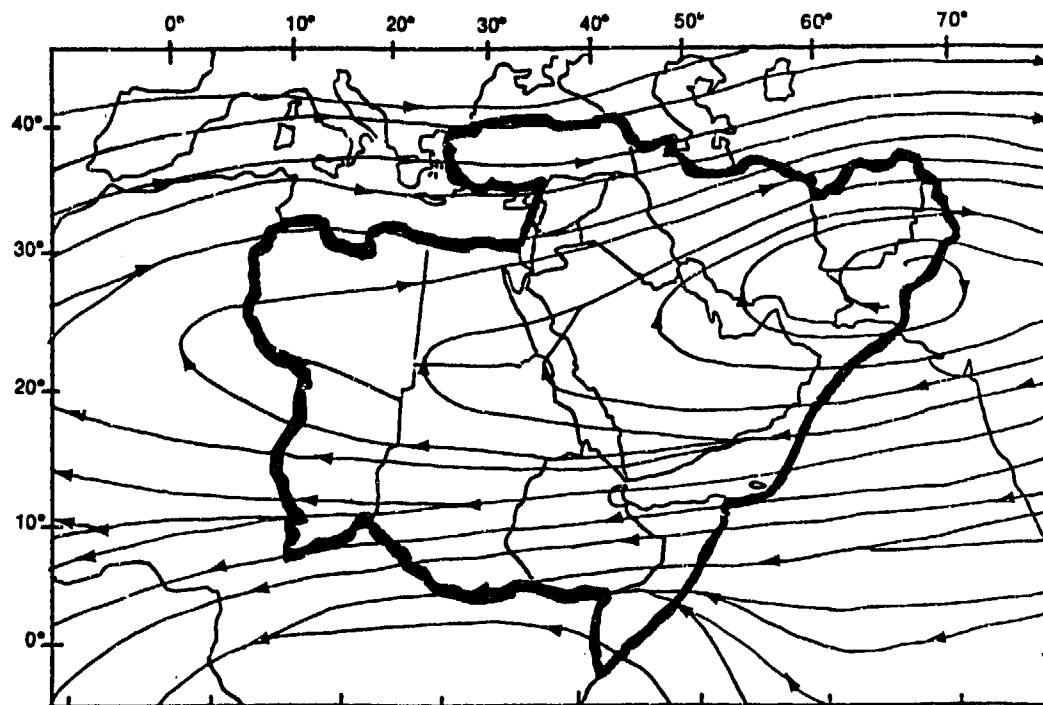


Figure 2-28d. Mean July Upper-Air Flow Patterns, 300 mb.

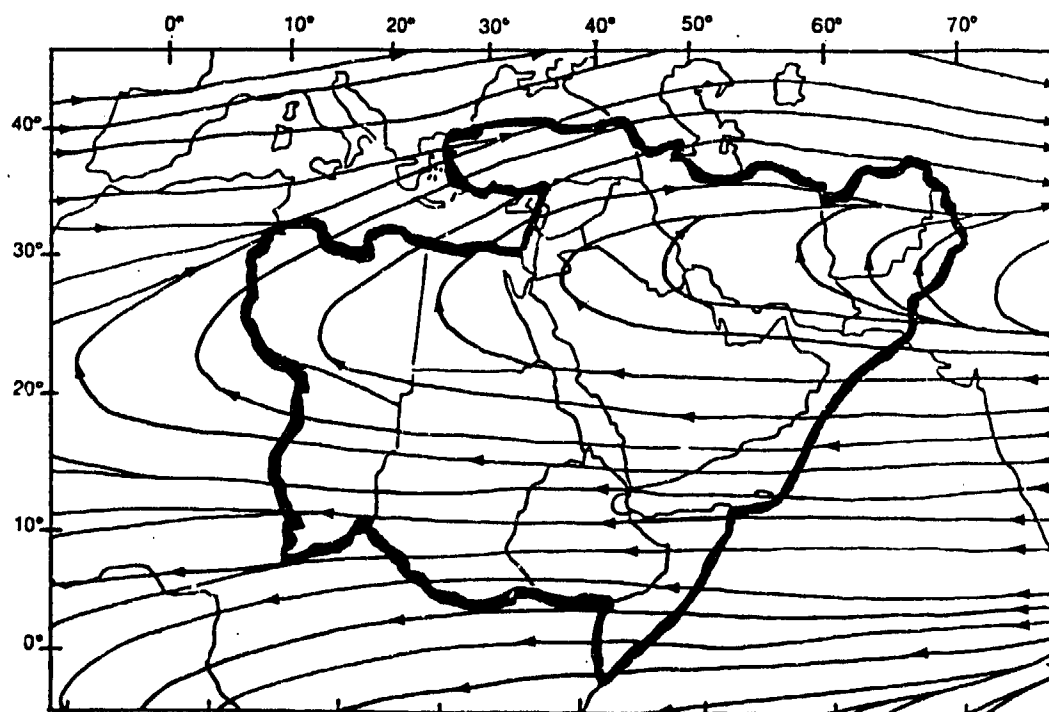


Figure 2-28e. Mean July Upper-Air Flow Patterns, 200 mb.

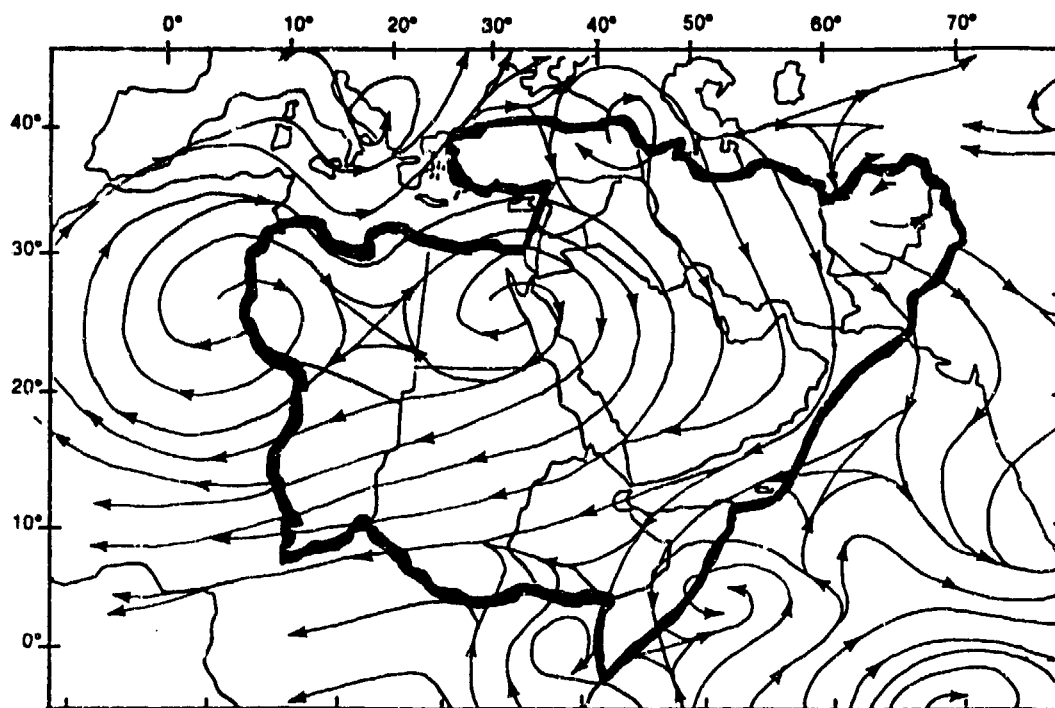


Figure 2-29a. Mean October Upper-Air Flow Patterns, 850 mb.

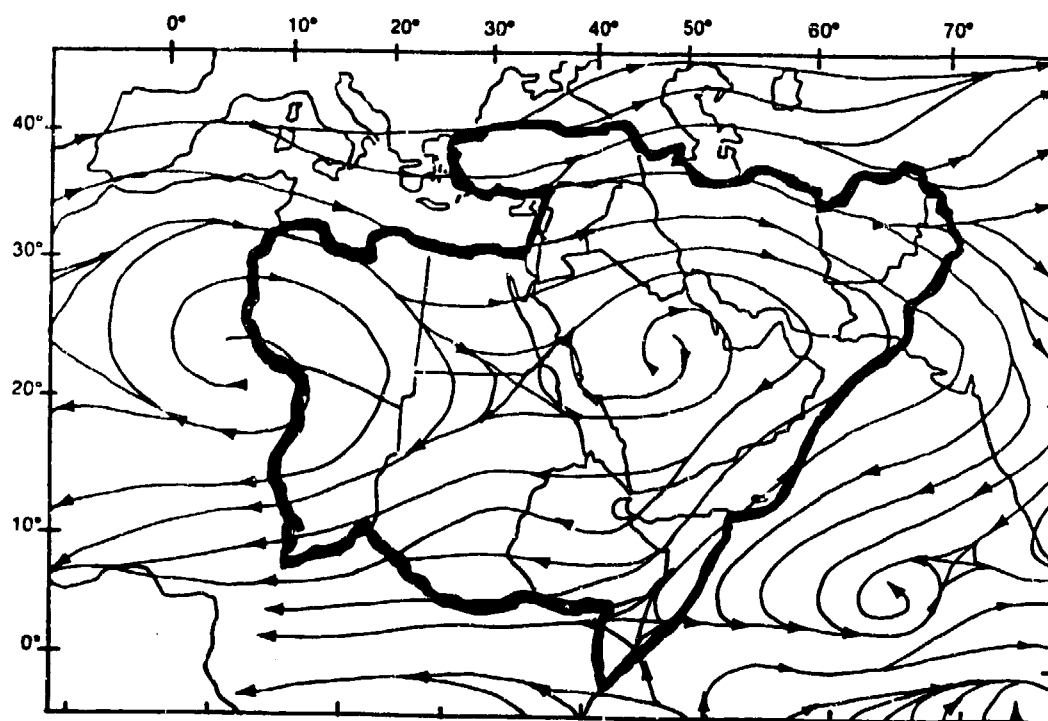


Figure 2-29b. Mean October Upper-Air Flow Patterns, 700 mb.

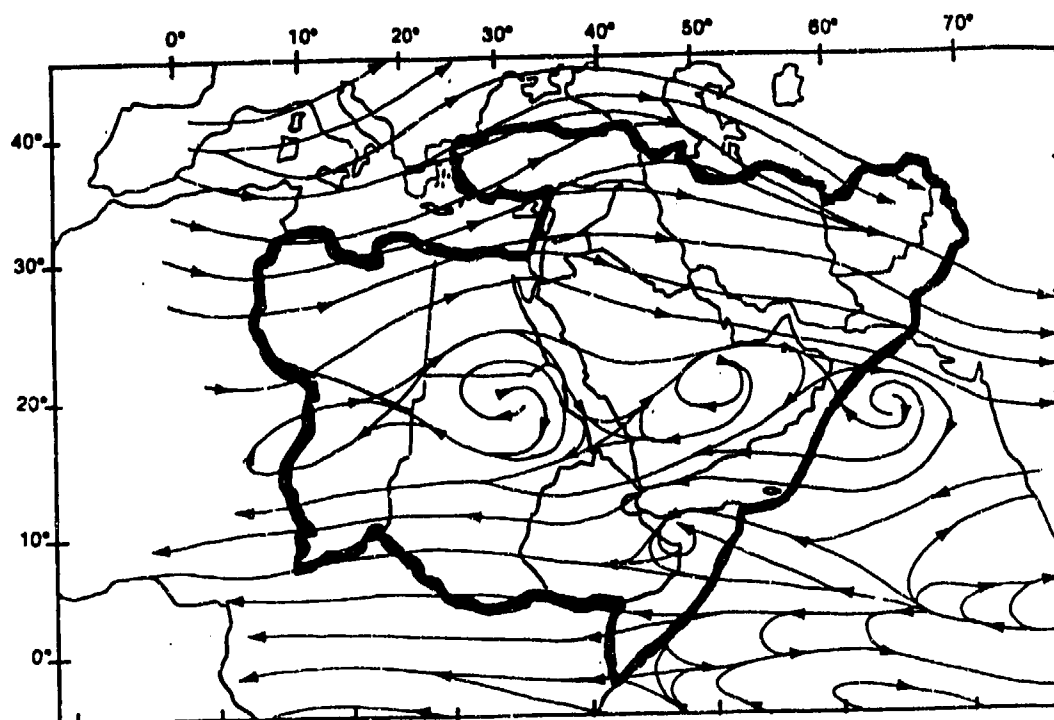


Figure 2-29c. Mean October Upper-Air Flow Patterns, 500 mb.

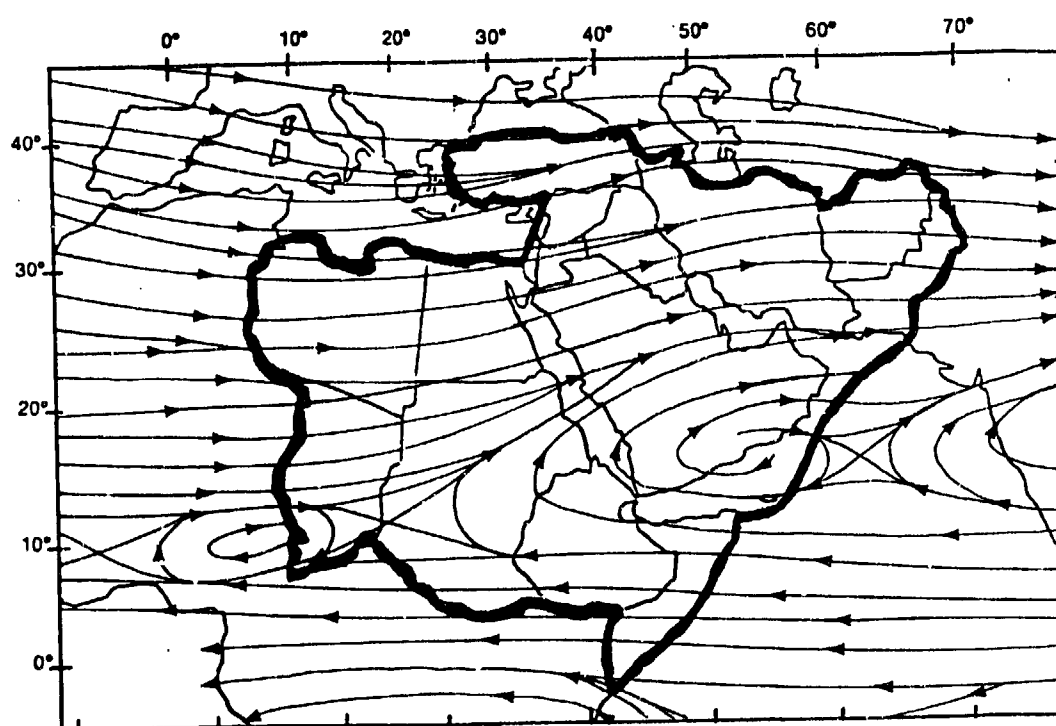


Figure 2-29d. Mean January Upper-Air Flow Patterns, 300 mb.

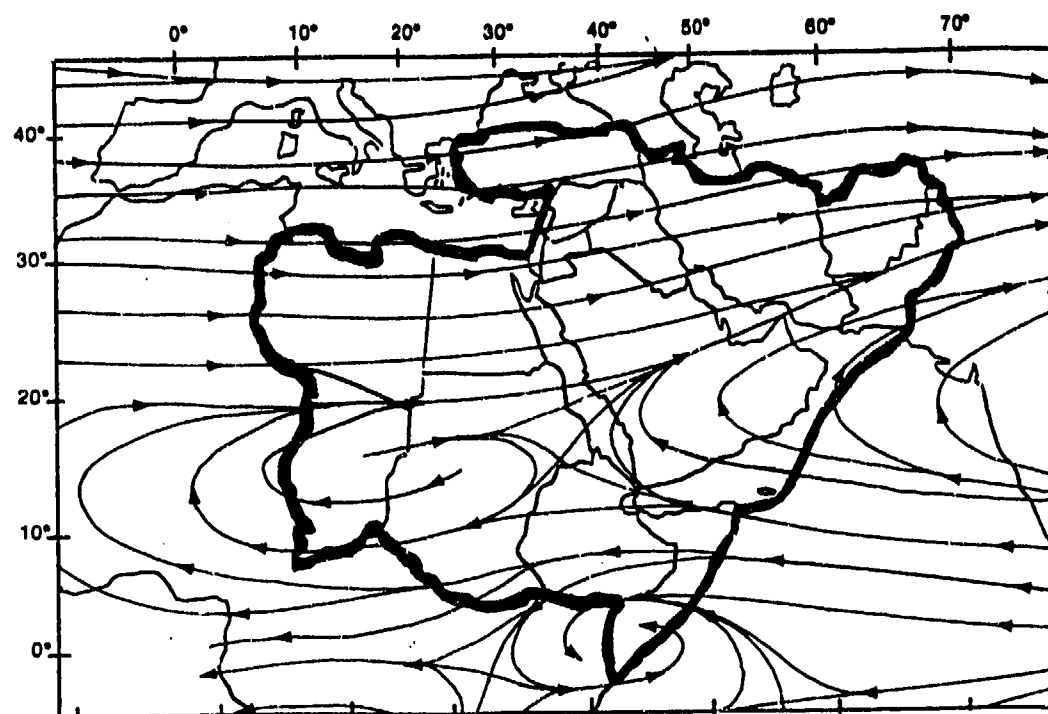


Figure 2-29e. Mean October Upper-Air Flow Patterns, 200 mb.

THE SUBTROPICAL RIDGE. This upper-level feature, represented graphically by the 200-mb anticyclonic ridge axis line, is the division between upper-level westerly and easterly flow. During transitions (October-November and April-May), the Ridge allows both westerly and easterly upper-level flow over the Horn of Africa. Its July position finds it anchored by the Tibetan 200-mb anticyclone north of the study area.

The Subtropical Ridge oscillates from 6° N in January (Figure 2-30a) to 24-27° N in July (Figure 2-30b). These oscillations result in alternating periods of westerly and easterly upper-level flow. Westerly flow (December through late February) supports occasional Mediterranean cyclonic activity across the northern Horn of Africa. Although January's and July's are the only Subtropical Ridge positions provided here, readers may infer April and October positions from Figures 2-27e and 2-29e.

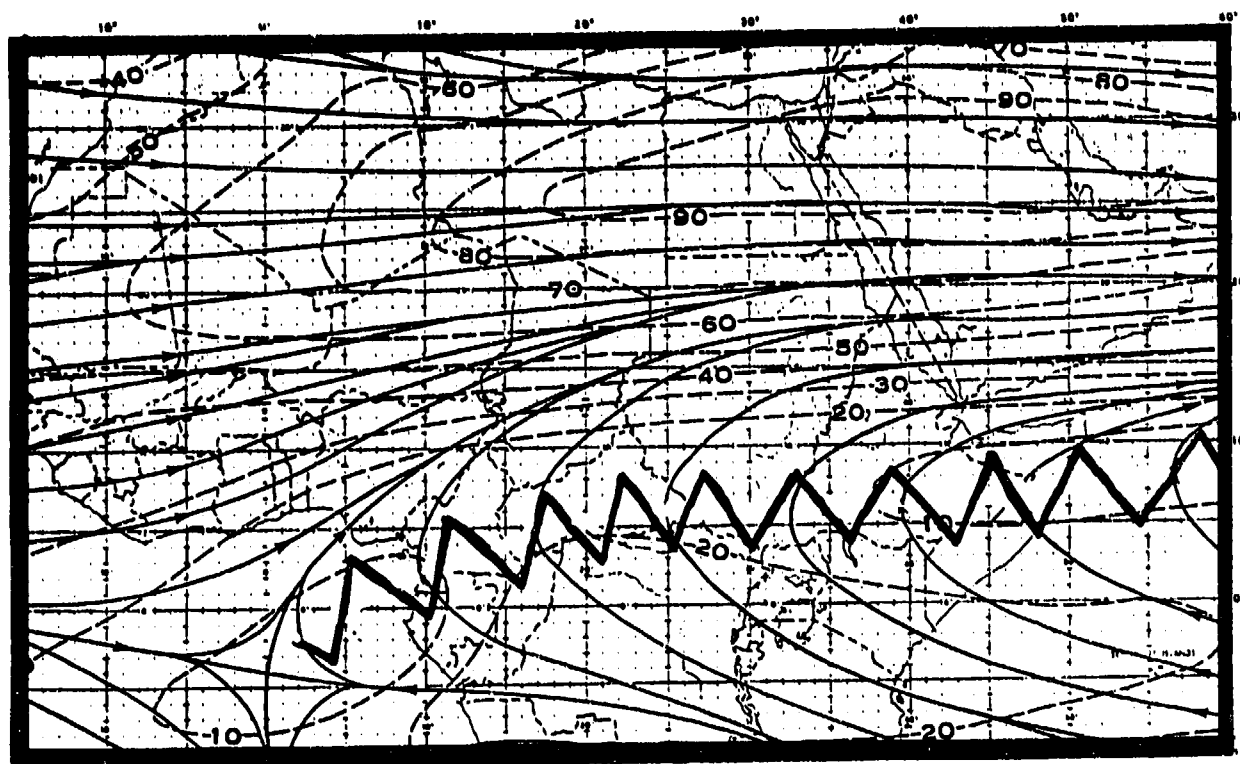


Figure 2-30a. Mean January Position of the Subtropical Ridge. The jagged line denotes the mean ridge axis position. Dashed lines are isotachs (kts).

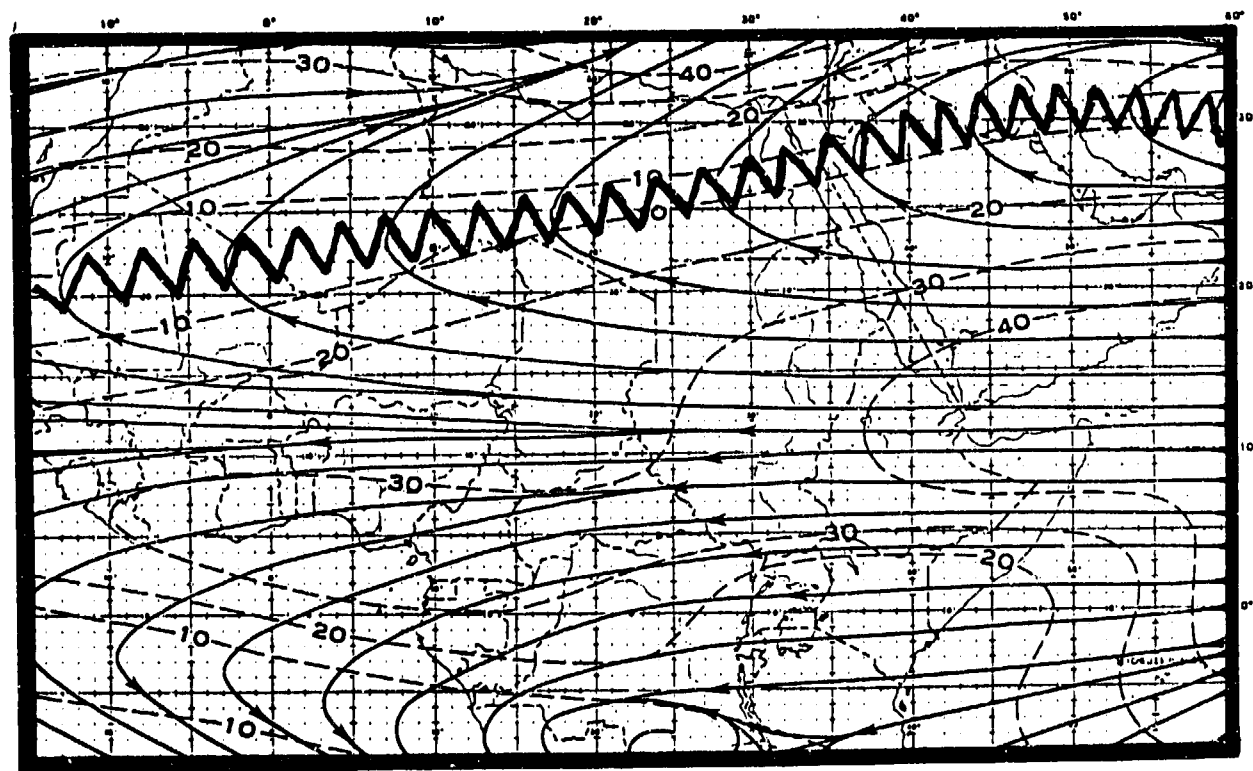


Figure 2-30b. Mean July Position of the Subtropical Ridge. The jagged line denotes the mean ridge axis position. Dashed lines are isotachs (kt).

SYNOPTIC DISTURBANCES

JET STREAMS. The dominant jet streams that affect the Horn of Africa are the Polar Jet (PJ) and the Subtropical Jet (STJ). The former's position and movement control cold air advection and mid-level direction for developing Mediterranean cyclones, while the STJ provides steering, shear, and outflow in the upper layers.

Mean daily PJ position deviates north-to-south from the mean by 10-300 NM. Maximum wind speeds from December to March vary from 60-160 knots. The PJ is usually found near 30,000 feet (9,146 meters). Southward deviations (to 30-45° N) are most frequent between December and March, but on rare occasions in April, May, or June, the PJ enters the eastern Sahara and

Saudi Arabian peninsula. The April-June PJ is found between 30,000 and 34,000 feet (9,146-10,365 meters); maximum wind speeds are between 60 and 140 knots.

Although the STJ shows less variability in its daily position, its seasonal variability is greater than that of the PJ. Mean STJ positions over the subtropics range from 25-30° N (Figure 2-31a) to 40-45° N (Figure 2-31b). Maximum wind speeds between December and April run from 80 to 200 knots at a mean height of 39,000 feet (11,890 meters) MSL. Speeds between May and November are from 30 to 60 knots at 39,000-43,000 feet (11,890-13,110 meters) MSL. The STJ is weakest (30 knots) in July and August, but it may exceed 50 knots north of 30° N.

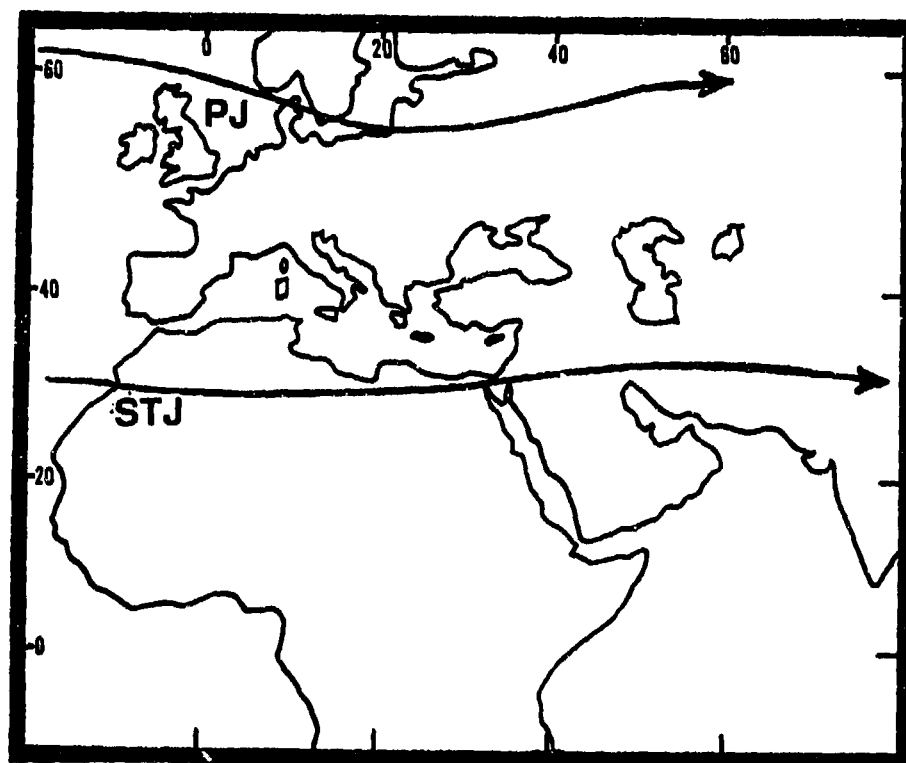


Figure 2-31a. Mean January Positions of the Polar and Subtropical Jet Streams.

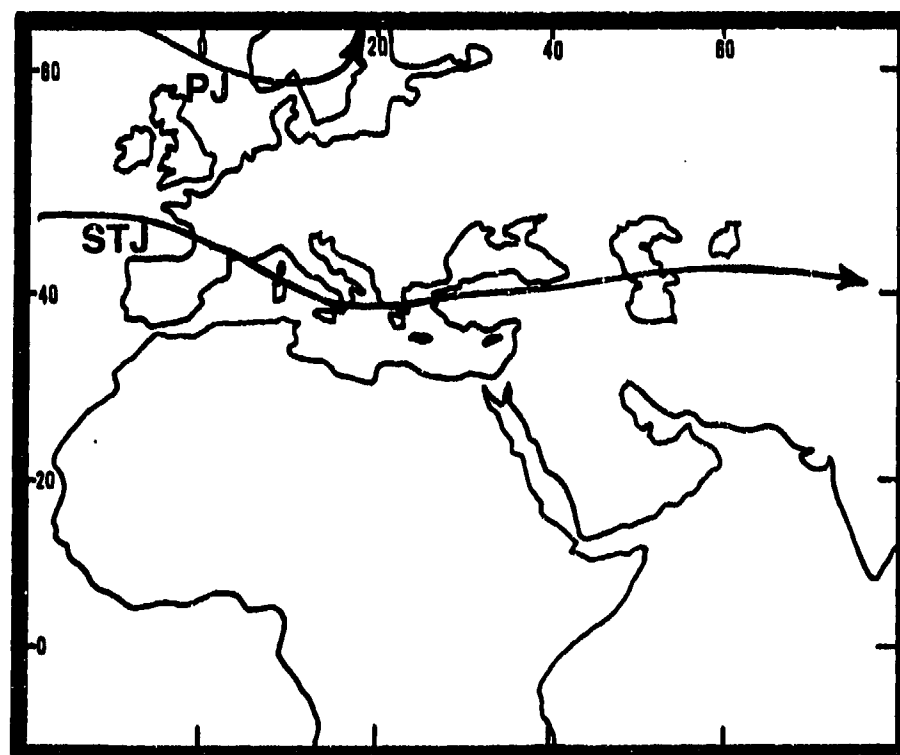


Figure 2-31b. Mean July Positions of the Polar and Subtropical Jet Streams.

The greatest effects of either jet stream are seen between December and April, when cyclonic activity in the Mediterranean Sea basin is most common. Surface low-pressure cells develop when a strong Polar Jet digs southward of 30° N and forms a deep upper-level trough. Northerly flow often develops on the east side of a blocking high-pressure ridge over the eastern Atlantic. The PJ and upper-level trough may intensify surface lows over the Mediterranean Sea and in the lee of the northwest Africa's Atlas Mountains. Northerly flow insures that the trough and the surface cyclone move southeastward into the central (sometimes eastern) Sahara Desert, but other factors are necessary for strong surface cold fronts to penetrate to the central and southern Red Sea. Surface cold fronts usually affect the Horn of Africa north of 15° N when the STJ moves northward to join the PJ and intensify lows over the Sahara Desert still further. The preferred area of surface

low-pressure center intensification during PJ/STJ interaction is often under the southeast quadrant of the upper-level trough. The low often deepens in the area between the two jet streams. Jet stream interaction most frequently occurs with Atlas surface low-pressure formations because they are generated between 25 and 30° N--nearest the mean position of the STJ. Figures 2-32a, b, & c illustrate generalized PJ/STJ interaction and low-pressure intensification areas.

Neither jet has much effect on the Horn of Africa in the summer, but on rare occasions, a strong Polar Jet may push a mid-level trough southward into the STJ as late as early June. For significant weather to reach the Horn of Africa, the deep eastward-moving trough must move over the Red Sea. Otherwise, only a temporary increase in mid-level cloud cover extends into extreme northern sections of the Yemen Highlands subregion.

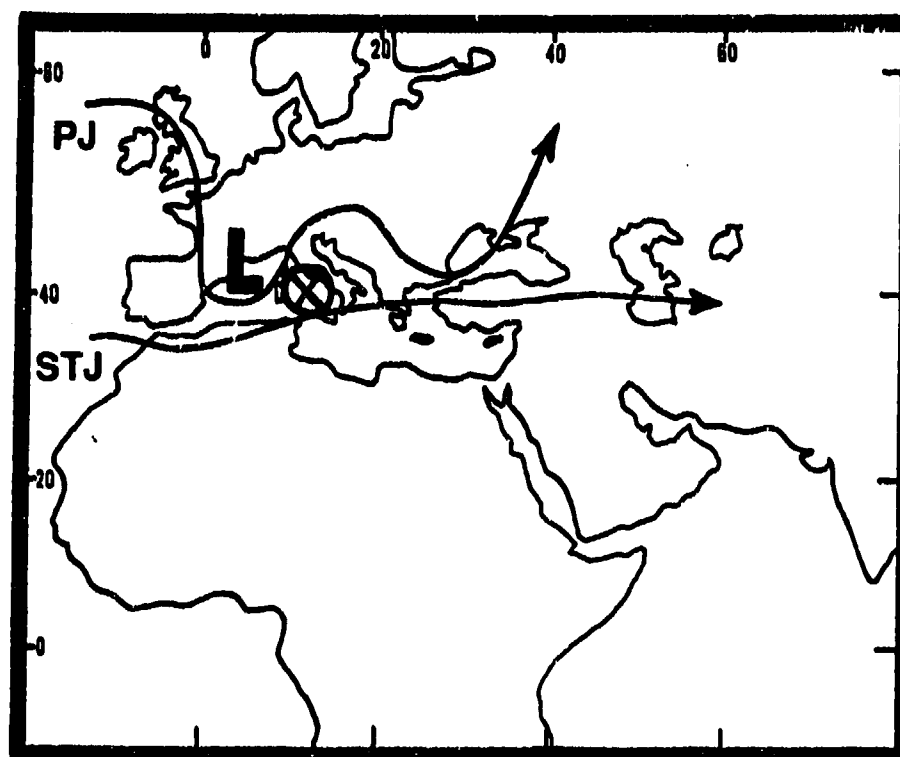


Figure 2-32a. Typical Jet Positions During Formation of Genoa Low. Surface low formation/intensification area is marked by the "X."

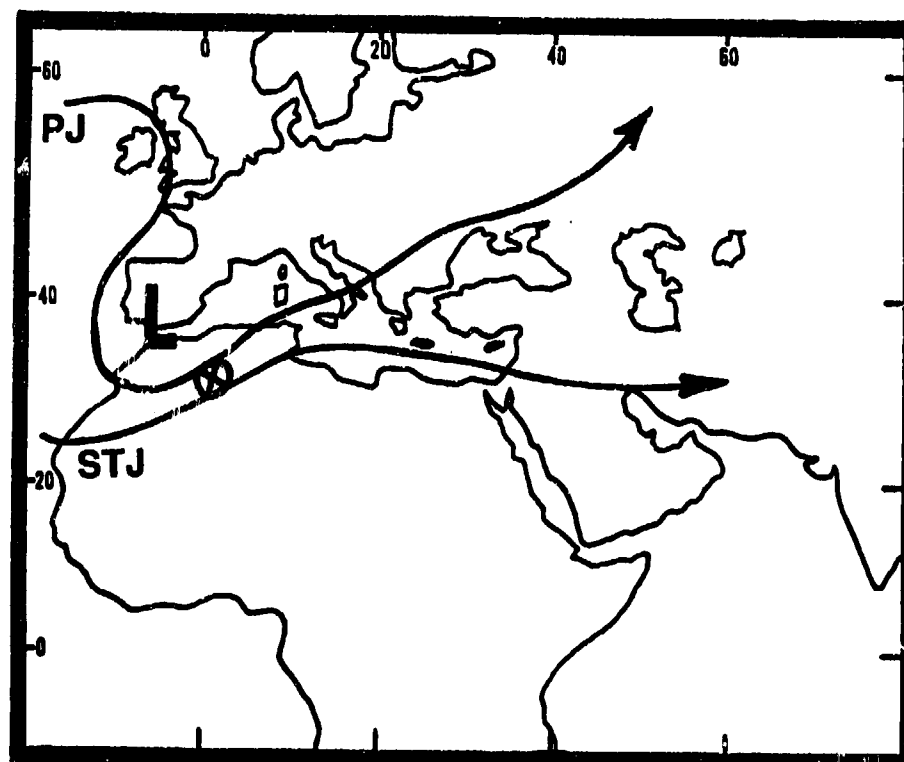


Figure 2-32b. Typical Jet Positions During Formation of Atlas Low. Surface low formation/intensification area is denoted by the "X."

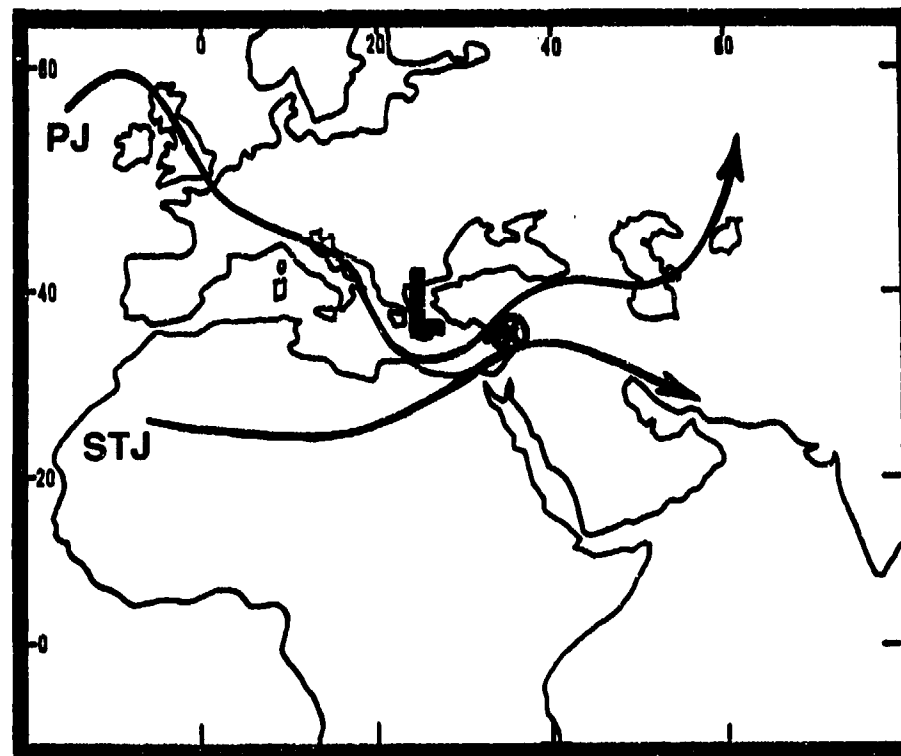


Figure 2-32c. Typical Jet Positions During Formation of Cyprus Low. Surface low formation/intensification area is denoted by "X."

CYCLONIC ACTIVITY. Three primary cyclogenesis regions in the Mediterranean Sea basin affect the northern Horn of Africa between December and April. Their locations and movement are shown in Figure 2-33.

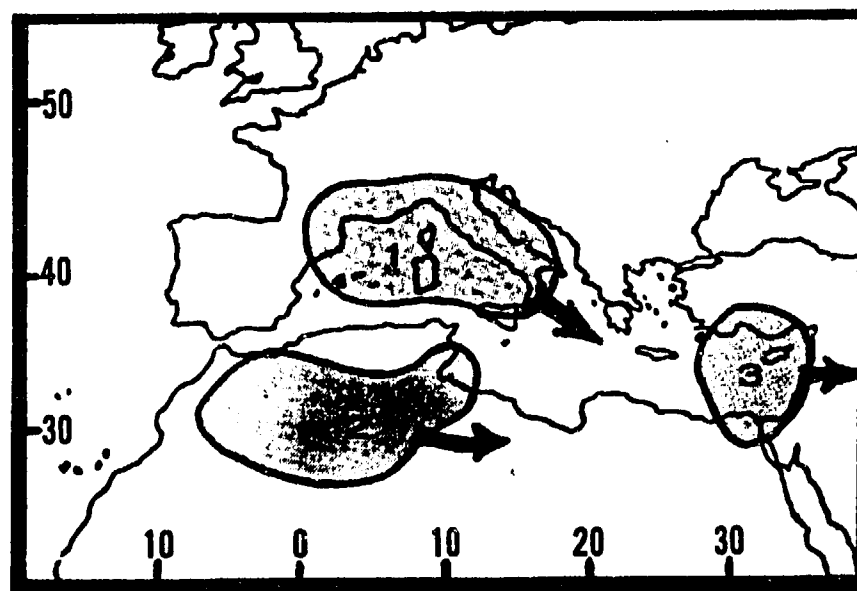


Figure 2-33. Mediterranean Cyclogenesis Regions. (1) The Genoa Low in the Gulf of Genoa and Adriatic Sea, (2) The Atlas Low in the northwest Africa interior, and (3) The Cyprus Low in the eastern Mediterranean Sea. Arrows show general direction of movement away from cyclogenesis areas.

Low-pressure systems and surface cold fronts affect weather in the Horn of Africa between December and April. Synoptic considerations dictate system movement in the northern fringes. Associated weather varies significantly with each frontal passage.

Although Atlas and Cyprus Lows may move cold fronts into the region, very deep low-pressure systems with upper-level support are necessary for heavy showers or thunderstorms.

Typically, one or two fronts and their upper-level troughs pass through the region between December and April. Intense upper-level polar troughs, moving to the southeast, often support isolated thundershower activity along the northwestern Ethiopian Highlands and Yemen Highlands subregions.

On rare occasions, a cold front may reach the Gulf of Aden, as shown in Figure 2-34.

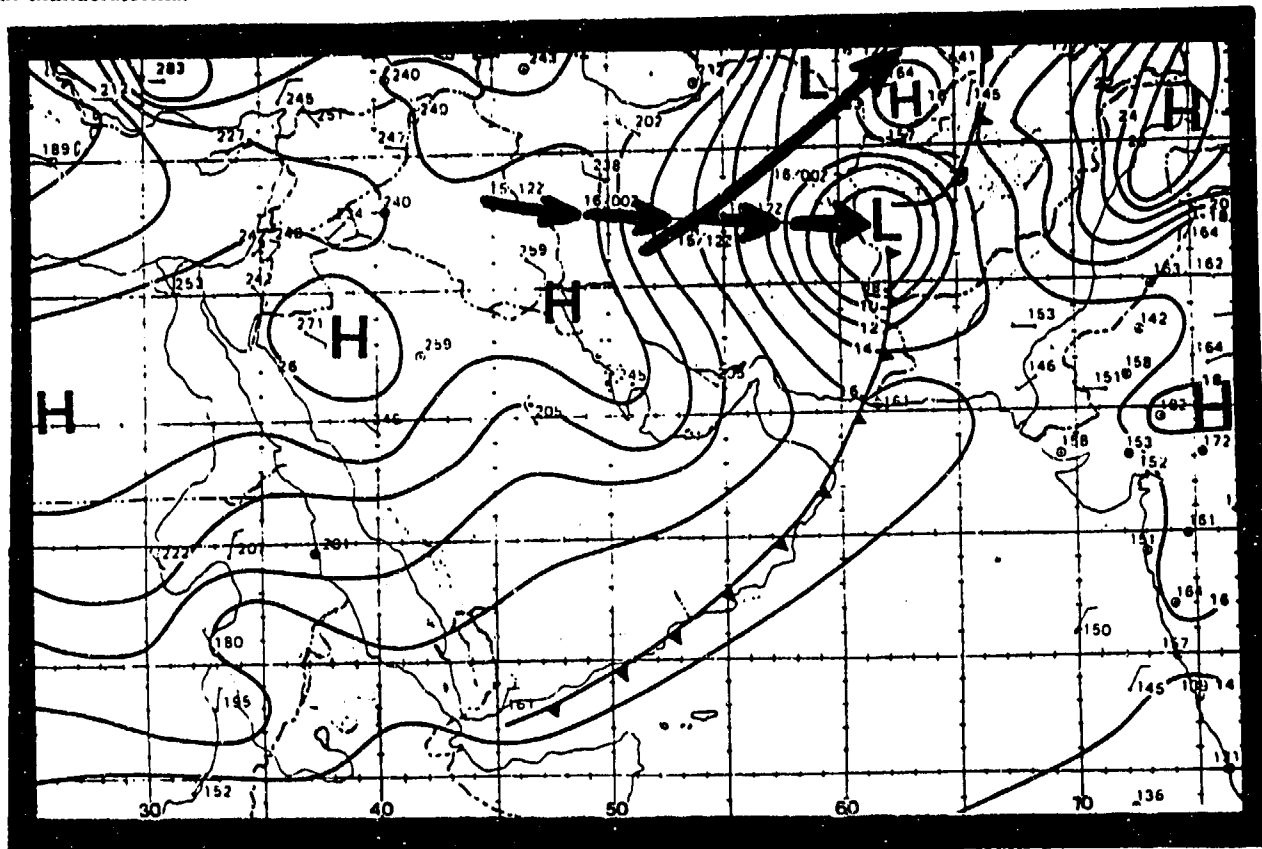


Figure 2-34. Mediterranean-Generated Cyclonic Activity and Trailing Cold Front Entering the Gulf of Aden. The Cyprus Low in this case developed along a cold front extending from southern Europe. The solid arrow shows the path of the southern European cold front, while the dashed arrow represents movement of the Cyprus Low.

The Genoa Low. Transient upper-level and surface disturbances intensify in this low before migrating into the Mediterranean and north Africa. Genoa Lows seldom affect the Horn of Africa, however, because the trailing cold front is modified significantly before reaching the north African coast and central Sahara. Genoa Low cold fronts usually reach the northern Horn of Africa as weak surface wind shifts with little or no cloud development.

The Atlas Low. From March to April or between October and early December, transitory lows form in the north-central interior of Algeria southeast of the Atlas Mountains near 30° N, 62° E. Atlas Lows generally form when a mid-or upper-level trough (oriented NE-SW) over Spain is positioned over a surface low moving southeastward across Europe. In March and April, the mean Azores High position moves north-

westward. The result is a subtle shift in the mean mid-level flow pattern from zonal to meridional. Meridional (northerly) flow favors a southward movement of transient European disturbances along the Polar Jet, which often digs along the backside of the 500-mb trough to produce uplift along the Atlas Mountains. Mid-level cold air and moisture crosses the Atlas range as a cold-core "cut-off" low or shortwave. These storms seldom develop or penetrate very far into the Eastern Sahara Desert and northwestern Ethiopia without strong northerly flow and cold mid-level support. But if this flow persists for more than 3 days and intense polar air surges south of 30° N, the Polar Jet and the mean Atlas Low storm track temporarily shift southward into the north central Sahara. As a result, storms move due east across the northern Sahara into the central Red Sea. Steep pressure gradients along the frontal boundary increase the warm and dry southeasterly Sahara surface flow ahead of the developing surface Atlas Low. Without sustained northerly flow, Atlas Low movement is northeastward over the south-central Mediterranean along the polar-subtropical jet axes (WSW zonal flow). Very deep upper-level troughs produce severe polar outbreaks over the Sahara Desert in either case, but northerly flow insures that the surface polar air mass pushes the Atlas Low cold front deep into the Sahara Desert. The surface trough is often followed by strong surface high pressure that accelerates the frontal boundary southeastward across the central Red Sea. An Atlas Low cold front cannot move southeastward into the central and southern Red Sea Basin without sustained northerly flow. A well-defined cold front that remains intact and moves into southeastern Egypt ($22-25^{\circ}$ N) may also develop a secondary surface low-pressure cell along the surface cold front.

The Subtropical and Polar Jets may intensify disturbances at mid-and upper levels. A mean wind speed maxima (80 knots in the Subtropical Jet) occurs over west Africa in March and April. Strong outflow and

divergence aloft is often coupled with a southward surge of the Polar Jet, adding cold air and instability to the system. A significant southward displacement in both jets must occur for a strong Atlas Low to continue tracking eastward toward the Red Sea basin. Without Polar Jet support, the strong Subtropical Jet produces upper-level shearing over the central Sahara and prevents further easterly movement of the surface trough.

Intense Atlas Lows seldom track eastward across the entire Sahara Desert because many synoptic variables must combine perfectly to sustain continuity over the dry desert. When such combinations occur, however, Atlas Lows and their trailing cold fronts produce surface winds greater than 25 knots and widespread dust/sandstorms across the northwestern Horn of Africa. When an intense Atlas Low reaches the Nile River Valley intact, a secondary or "cut-off" surface low-pressure cell often develops along the primary Atlas Low cold front.

In Figure 2-35a, the 16 April 1964 (1200Z/1500 LST) synoptic chart shows an Atlas Low (1001 mb) over west central Saudi Arabia. To the southeast, the plateaus of western Ethiopia and extreme east central Sudan have produced a transitory thermal trough feature, or Sudanese Low (which see) that appears on mean pressure charts as an inverted low-pressure trough. Although the map (typical for this time of year) shows the inverted trough (solid lines extending to the south and west of the Sudanese Low) looking much like a mid-latitude front, it is only a resemblance.

Figure 2-35b shows the synoptic pattern 24 hours later, on 17 April at 1200Z/1500 LST. The Atlas Low storm track has turned northeastward and a secondary low has formed along the cold front. The Sudanese Low remains stationary. The high-pressure cell centered in the south central Mediterranean builds into the Red Sea and pushes the cold front southeastward.

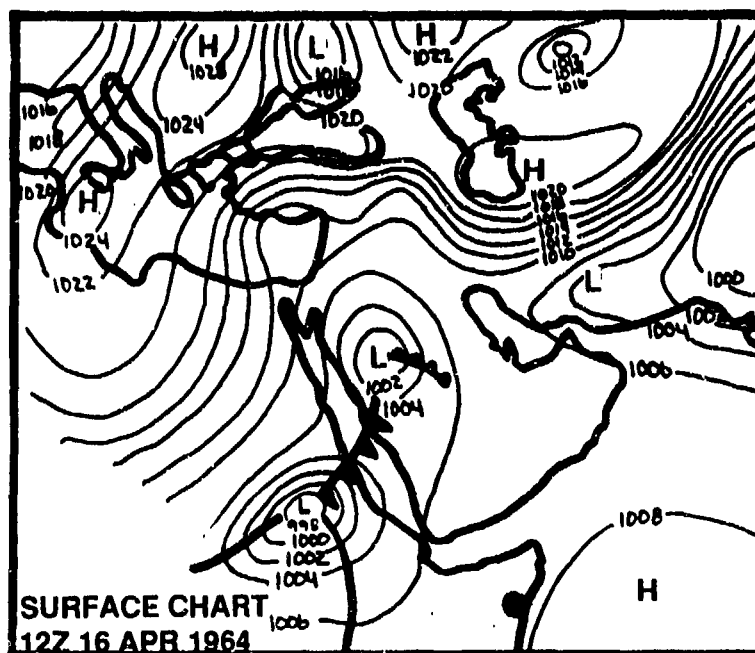


Figure 2-35a. Synoptic Surface Chart (16 April 1964, 1200Z/1500 LST) Showing an Eastward-Tracking Atlas Low. The surface trough (Atlas Low) extends a well-defined cold front across the central Red Sea. The deeper 998-mb Sudanese thermal low enhances the surface trough.

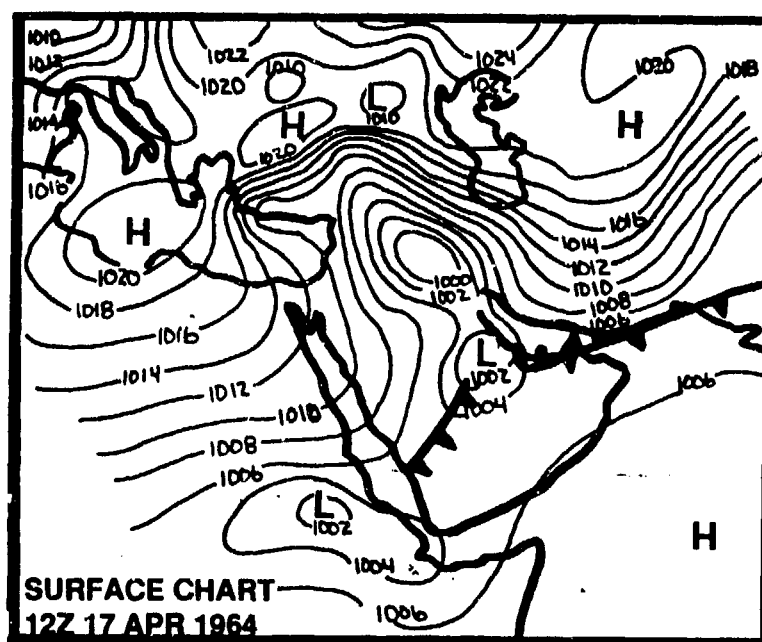


Figure 2-35b. Synoptic Surface Chart (17 April 1964, 1200Z/1500 LST) Showing Secondary Low Formation Along the Active Cold Front.

The Cyprus Low. This migratory low may spawn intense thunderstorm activity over the eastern Sahara Desert, central Red Sea, and northern Horn of Africa between December and March. The two factors contributing to Cyprus Low cyclogenesis are:

- Low-level (below 850 mb) inflow of north-westerlies from the Aegean Sea over warm eastern Mediterranean waters (63-65°F/18°C).
- Instability aloft caused by cold slow-moving migratory (mid-and upper-level) polar troughs.

From December through March, one or two active surface cold fronts accompanying a Cyprus Low move into the north Horn of Africa. These fronts may produce extensive thunderstorm outbreaks in the northern Yemen Highlands and Ethiopian Highlands subregions.

A thunderstorm outbreak with significant rainfall requires cold air between 700 and 500 mb, usually 15-18°F/8-10°C colder than the environment. Occasionally, very cold polar troughs penetrate northern Egypt with moist low-level support generated from Mediterranean and Aegean Sea moisture. Warm Saharan surface air--with Red Sea moisture advected ahead of the surface cold front--may set off severe thunderstorms. Significant positive vorticity advection (PVA) can allow a cold mid-or upper-level trough to deepen and set off thunderstorm activity in the northern Horn of Africa.

Cyprus Lows most frequently track eastward or southeastward into northern Saudi Arabia. These tracks maximize southwesterly surface flow and moisture advection into the Cyprus Low ahead of the cold front. A deep trough with strong southwesterly surface flow produces greater orographic uplift and offers a better chance for thunderstorm activity to spread southward along the Red Sea to 16° N.

STORM TRACKS. Figure 2-36a shows typical December-February storm tracks as they affect the Horn of Africa. Primary tracks (thick lines) pass through the Gulf of Genoa and eastern Mediterranean Basin. Secondary tracks (dashed lines) over the northern Arabian Peninsula reflect surface cyclogenesis along active Cyprus Low cold fronts.

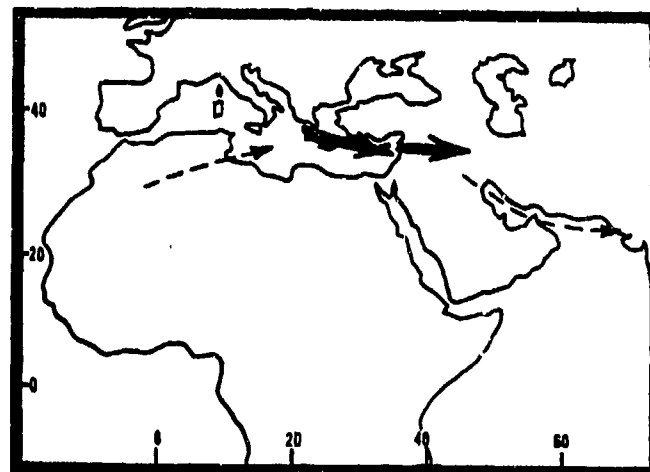


Figure 2-36a. Primary (solid arrow) and Secondary (dashed arrow) Mid-Latitude Storm Tracks, December, January, and February.

Figure 2-36b shows the storm tracks that affect the Horn of Africa in March and April. Leaside troughing along the Atlas Mountains initiates Atlas Low cyclogenesis inland over northwest Africa. The Atlas Low track produces all mid-latitude frontal-type weather in the Horn of Africa in March and April. Secondary storm tracks over the subtropical Sahara reflect surface cyclogenesis along active Atlas Low cold fronts, which remain strong while migrating eastward into the Red Sea basin.

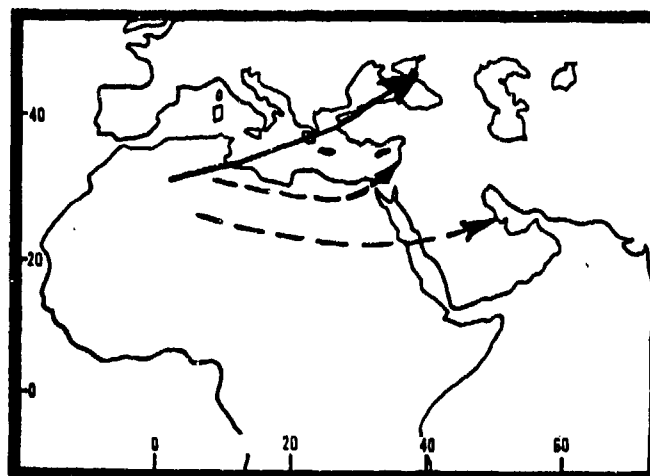


Figure 2-36b. Primary (solid arrow) and Secondary (dashed arrow) Mid-Latitude Storm Tracks, March and April.

Mid-latitude storm tracks between May and October are so rare that an attempt to produce a mean or "typical" track would be impractical. Upper-level troughs only migrate into the northern Horn of Africa once every 4-7 years during this period. The mean November storm tracks shown in Figure 2-36c reflect the southward movement of the Polar Jet. The primary November track (not shown here) results from Genoa Low formation and runs east-northeastward across southern Europe. Most November cyclonic activity in the northern Horn of Africa involves secondary cyclogenesis only along active Genoa Low cold fronts moving through the central and eastern Mediterranean Sea.

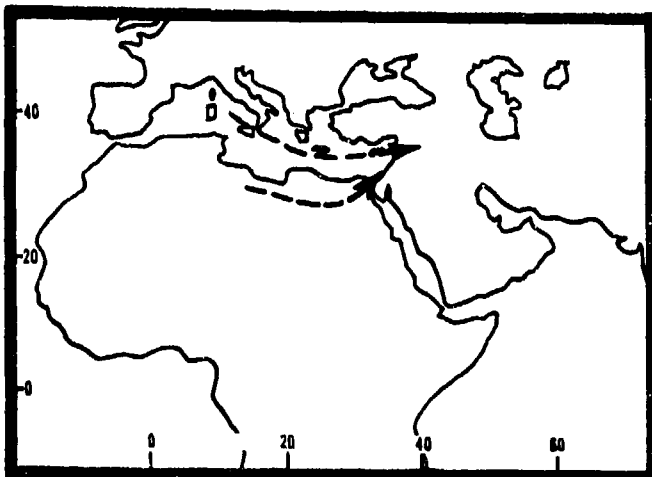


Figure 2-36c. Mid-Latitude Storm Tracks, November.

SOUTHERN HEMISPHERE POLAR SURGES. Southern Hemisphere cyclonic activity between May and October produces fluctuations in Somali Jet flow. This directly affects the Somali Jet's intensity because frontal passages temporarily displace the Mascarene High's position and alter its cross-equatorial outflow.

A low-level wind shift along the cold front increases low-level flow through the Mozambique Channel. Generally, the frontal boundary does not cross the equator, but flow "surges" affect the Northern Hemisphere and eastern Horn of Africa 1-3 days after the front leaves the Mozambique Channel.

This "cause and effect" relationship is shown in Figures 2-37a-k, in which satellite-derived wind vectors (kts) over the western equatorial Indian Ocean during a "surge" episode are compared with surface charts. This 6-day sequence shows how southern hemisphere cyclonic activity and polar surges affect Somali Jet intensity and location over the eastern Horn of Africa.

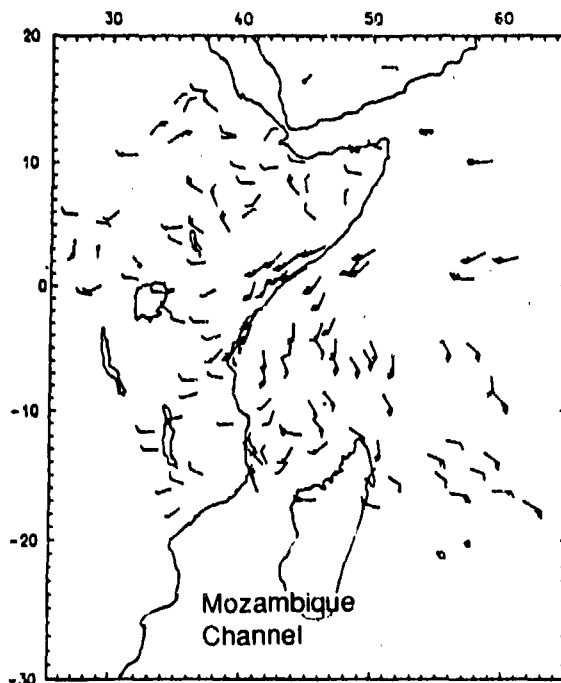


Figure 2-37a. 11 July 1978 Satellite-Derived Wind Vectors Over the Equatorial Western Indian Ocean (from Cadet and Desbois, 1981). Strong flow at 20-35 knots is evident between 40-45° E and 1° S-4° N. This is the "normal" Southwest Monsoon cross-equatorial flow pattern for the period.

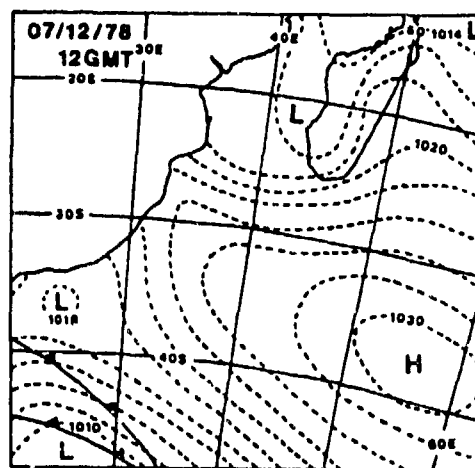


Figure 2-37b. 12 July 1978 Synoptic Chart (1200Z/1500 LST) for the Southeast African Coast and the Large Island of Madagascar (from Cadet and Desbois, 1981). The Mascarene High (1031 mb) is firmly established at 37° S, 56° E.

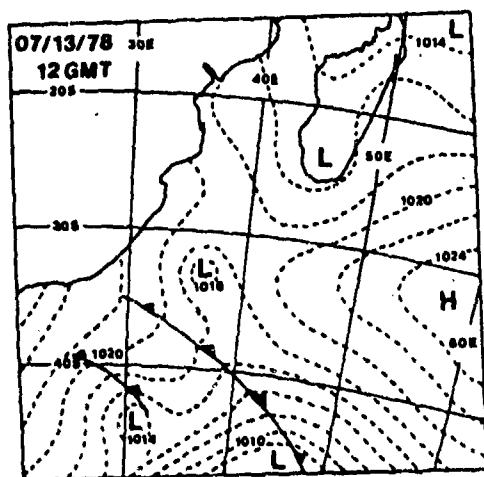


Figure 2-37c. 13 July 1978 Synoptic Chart (1200Z/1500 LST) for the Southeast African Coast and Madagascar (from Cadet and Desbois, 1981). The low-pressure system moves northeastward toward the Mozambique Channel, causing the Mascarene High to shift eastward. The Mascarene High weakens to 1025 mb; its center is at 32° S, 58° E.

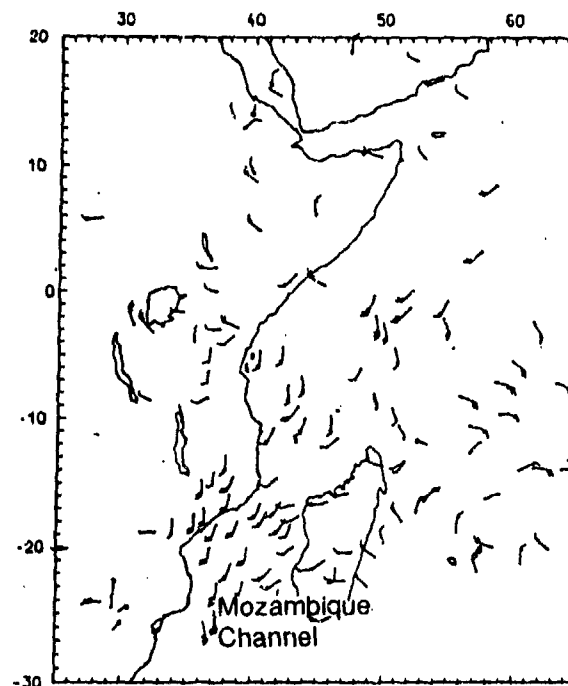


Figure 2-37e. 14 July 1978 Satellite-Derived Wind Vectors Over the Equatorial Western Indian Ocean (from Cadet and Desbois, 1981). Circulation north and west of Madagascar is disorganized, while flow over the Indian Ocean near 2° S, 50° E is 20-30 knots. The Mascarene High's eastward shift alters the "normal" entry point for cross-equatorial flow into the Horn of Africa.

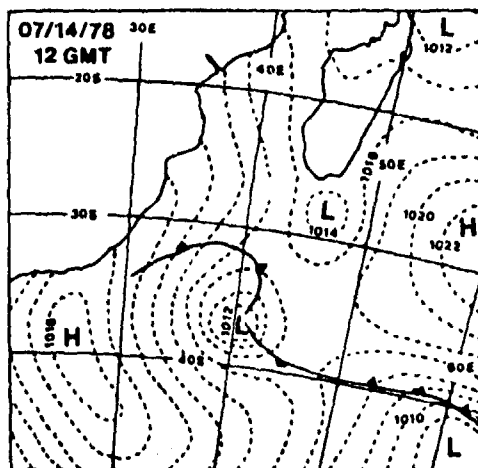


Figure 2-37d. 14 July 1978 Synoptic Chart (1200Z/1500 LST) for the Southeast African Coast and Madagascar (from Cadet and Desbois, 1981). The low-pressure cell and cold front prepare to enter the Mozambique Channel. The Mascarene High weakens further to 1023 mb. High pressure behind the front reinforces surface flow into the Channel.

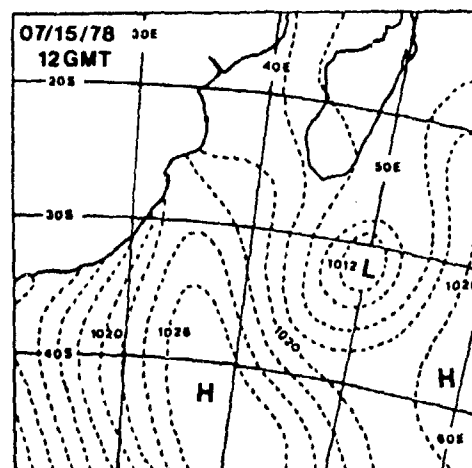


Figure 2-37f. 15 July 1978 Synoptic Chart (1200Z/1800 LST) for the Southeast African Coast and Madagascar (from Cadet and Desbois, 1981). The Mascarene High is shown as a broad and weak pressure cell in the lower right-hand corner. The low (and the high to its southwest) concentrate cross-equatorial flow into the Mozambique Channel.

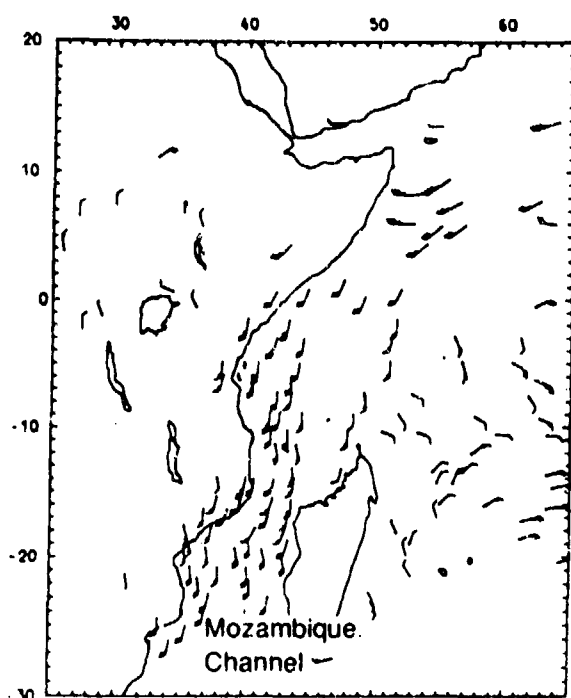


Figure 2-37p. 15 July 1978 Satellite-Derived Wind Vectors Over the Equatorial Western Indian Ocean (from Cadet and Desbois, 1981). Note the concentration of 20-knot wind vectors from 27-15° S. A cross-equatorial flow surge into the eastern Horn of Africa is apparent, but it originates in the Mozambique Channel (frontal passage), and not with Mascarene High outflow. Notice the weak, disorganized flow east of Madagascar.

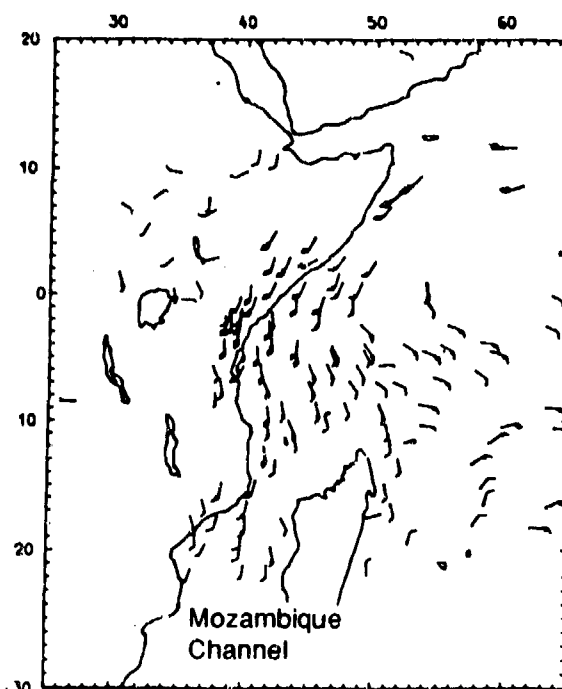


Figure 2-37i. 16 July 1978 Satellite-Derived Wind Vectors Over the Equatorial Western Indian Ocean (from Cadet and Desbois, 1981). Looking back to the flow surge through the Mozambique Channel on the 15th (Figure 2-37g), it's apparent that the surge has crossed the equator. Lighter winds in the Channel on the 16th reflect a southeastward movement in the low-pressure trough.

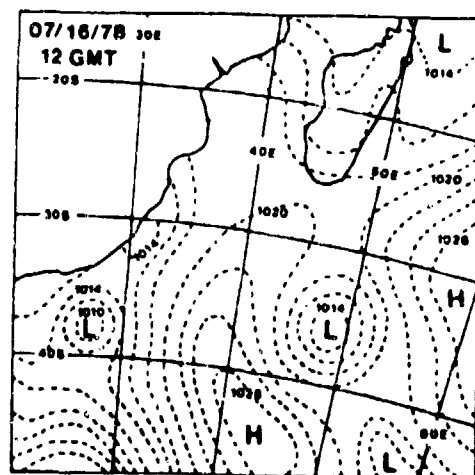


Figure 2-37h. 16 July 1978 Synoptic Chart (1200Z/1800 LST) for the Southeast African Coast and Madagascar (from Cadet and Desbois, 1981). The 1014-mb low at 36° S, 49° E, moves southeastward over the high pressure ridge to its right.

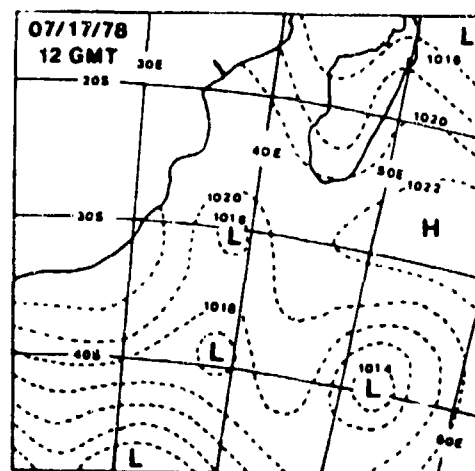


Figure 2-37j. 17 July 1978 Synoptic Chart (1200Z/1500 LST) for the Southeast African Coast and Madagascar (from Cadet and Desbois, 1981). A weak (1022 mb) Mascarene high reestablishes its position southeast of Madagascar.

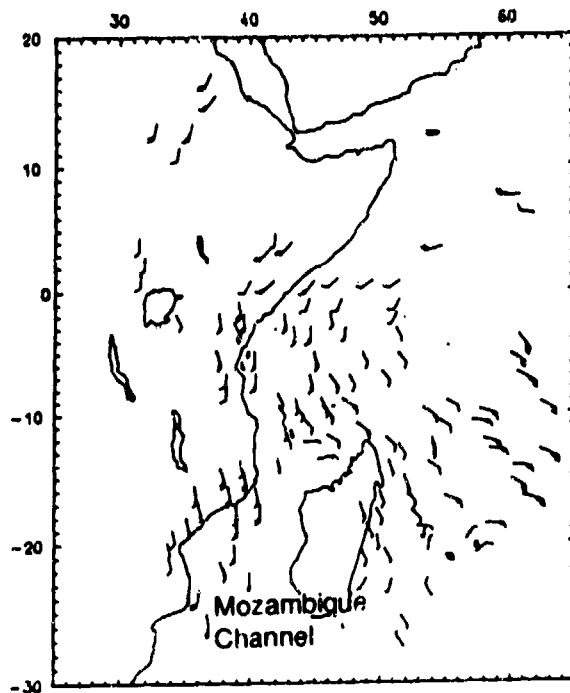


Figure 2-37k. 17 July 1978 Satellite-Derived Wind Vectors Over the Equatorial Western Indian Ocean (from Cadet and Desbois, 1981). The wind field reflects the reappearance of southeasterlies to the north and east of Madagascar.

TROPICAL DISTURBANCES. Massive Monsoon Trough convection organizes into intense tropical disturbances over the southern Arabian Sea and western Indian Ocean. On rare occasions, these disturbances propagate westward into the eastern Gulf of Aden and Somalia.

Squall Lines. Synoptic-scale squall lines occur only along the Monsoon Trough over southern Ethiopia and the Somalia Coast; they usually migrate westward at 20-30 knots. Mesoscale squall lines may occur anywhere in the region, but the Red Sea/Gulf of Aden corridor are preferred regions for development. Squall line clusters that develop off the Somalia Coast may also propagate westward and move inland. These are short-lived north of 6° N, however, because dry air and subsidence aloft over the Indian Ocean Plain dissipate heavy convection rapidly. Three conditions are necessary for squall line development:

- Convective instability along the Monsoon Trough and Intertropical Discontinuity (ITD).
- The Monsoon Trough well to the north (15-20° N) over Africa and between 10-15° N over the Indian Ocean during summer.
- Convergence occurring through a deep layer of the mid-troposphere.

Typically, the leading edge of a squall line assumes the form of a sharply-defined convex arc aligned north to south. This line contains cumulus or cumulonimbus in various stages of growth, as shown in Figure 2-38. Clouds build along outflow boundaries created by old convective lines at various levels, and upper-level portions of the outflow boundaries fuse into a massive precipitating anvil.

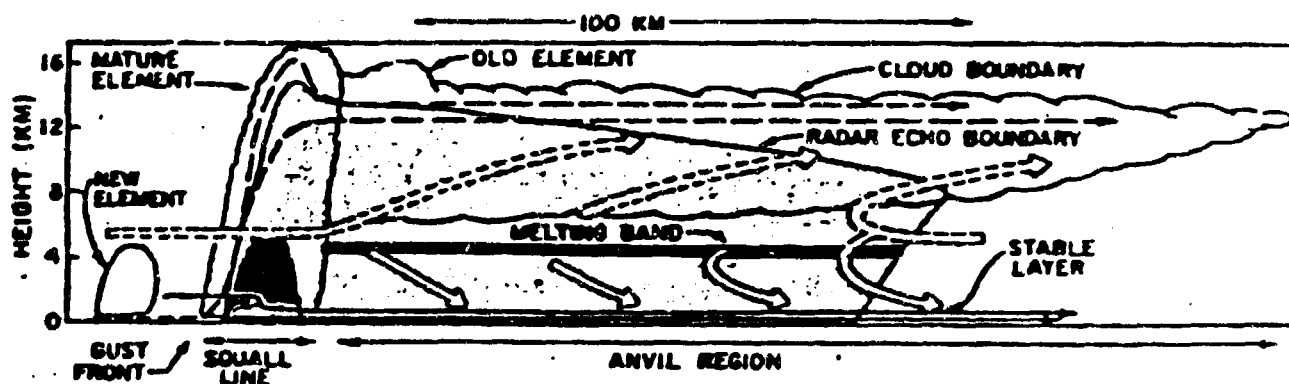


Figure 2-38. Schematic Cross-Section Through Squall Line System (from Gamache and Houze, 1982).

Air temperature gradients are not important for squall line development in the tropics and subtropics. Instead, air mass convergence and local vorticity maxima derived by mid-tropospheric winds trigger these violent weather systems, which are fueled by Monsoon Trough moisture. Squall lines are strictly summertime phenomena south of 16° N. There are winter squall lines associated with intense mid-latitude frontal passages, but these are not tropical systems.

Tropical squall lines are different in at least two important respects: First, the anvil cloud extends *behind*, (not in front of) the squall line. Second, new convective squall lines develop to the west of the downdraft zone (outflow boundary).

The thunderstorm cluster produced by tropical and subtropical squall lines creates intense downburst and outflow boundary winds beneath individual convective cells. Cold downdrafts (rapid temperature decreases) produce strong gust fronts that can lift large amounts of

dirt and dust into the atmosphere and drop visibilities to less than half a mile. Brief, intense rainfall is common, but extremely variable in coverage.

Downdrafts average 21-30 knots over flat terrain, and 40 knots in the deep valleys of the Ethiopian Highlands. Strong winds of the outflow boundaries range from 5-150 NM north to south.

Tropical Cyclones. On very rare occasions, tropical cyclones move into the eastern Gulf of Aden during seasonal transitions. These cyclones propagate westward along the Monsoon Trough at 10-25 knots. Heavy rain and high winds occur over the open Indian Ocean, but isolated showers and gusty winds (30-40 knots) embedded in the cyclone's spiral cloud bands may affect Socotra and the extreme northeastern sections of the region. Figures 2-39a-c show tropical depression and cyclone tracks over the western Indian Ocean/Arabian Sea.

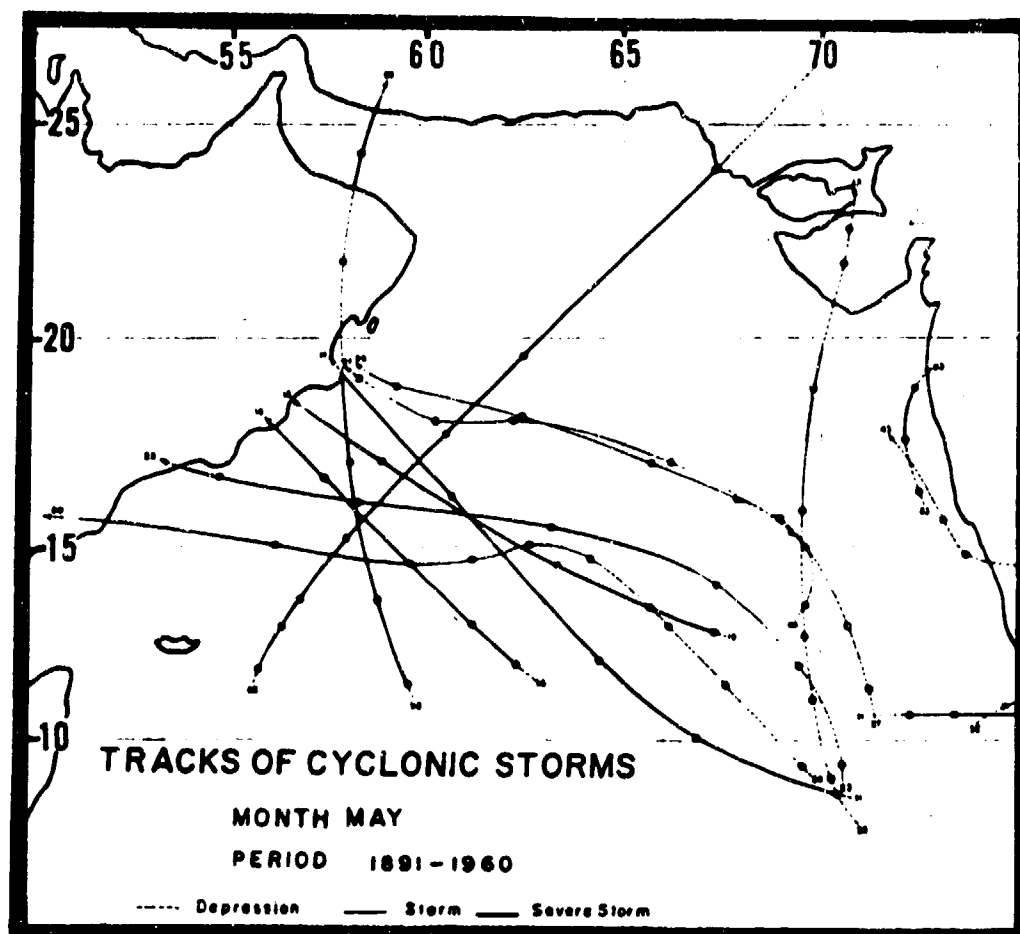


Figure 2-39a. May Tropical Depression and Cyclone Tracks, 1891-1960 (from Indian Met Dept, 1964).

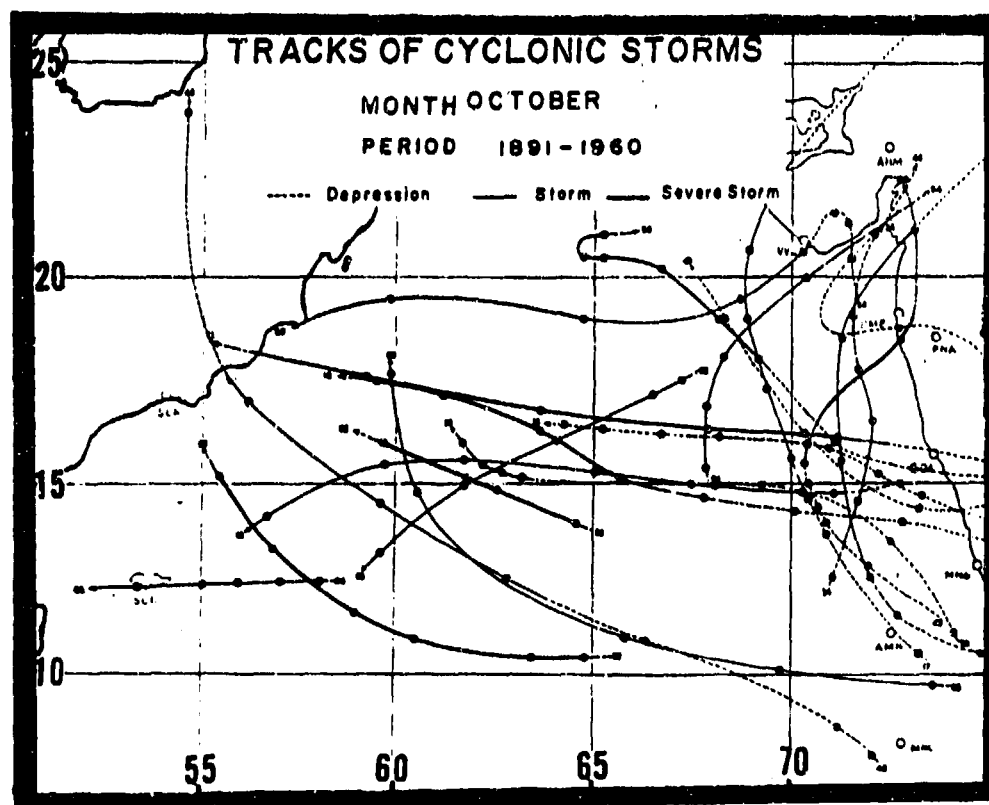


Figure 2-39b. October Tropical Depression and Cyclone Tracks, 1891-1960 (from Indian Met Dept, 1964).

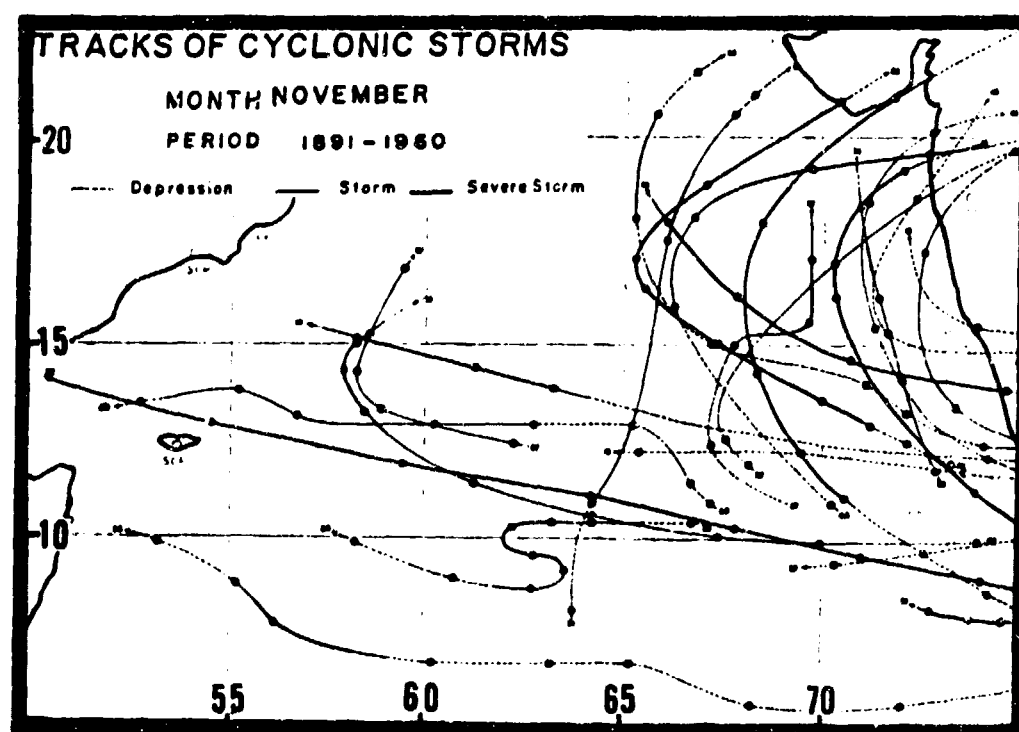


Figure 2-39c. November Tropical Depression and Cyclone Tracks, 1891-1960 (from Indian Met Dept, 1964).

THERMAL LOWS. Large-scale thermal (heat) low formation areas affecting the Horn of Africa are shown in Figure 2-40. Four well-defined thermal low circulations directly or indirectly affect Horn of Africa surface flow during different parts of the year; they are the Saharan Heat Low, the Sudanese Heat Low, and the Saudi Arabian heat low. All are discussed in this section.

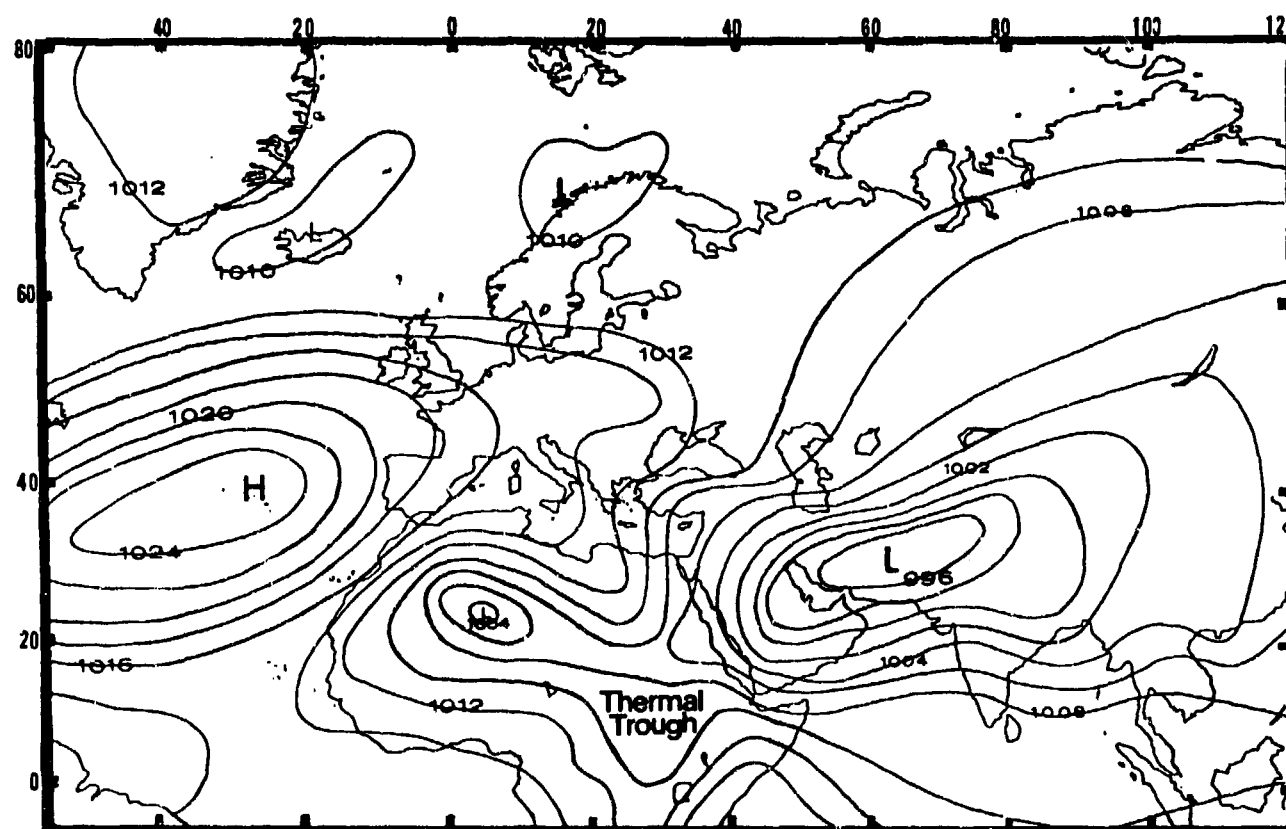


Figure 2-40. Large-Scale Thermal Trough Position (shaded area), July.

The Saharan Heat Low. Between late March and mid-October, the Saharan Low develops over the Sahara desert near 25° N, 3° E. Dry low-level easterlies (varying between 040 and 170 at 8-15 knots) dominate the west and central Sahara Desert. The low anchors the surface Monsoon Trough over the African interior and draws equatorial moisture into western Ethiopia. In

March and April, this low sends hot, dust-laden air masses into the northern Horn of Africa. By July, it has a mean surface pressure of 1004 mb and anchors the western edge of the massive thermal trough that is present during the Southwest Monsoon. Figure 2-41 shows a well-developed Saharan Heat Low during July.

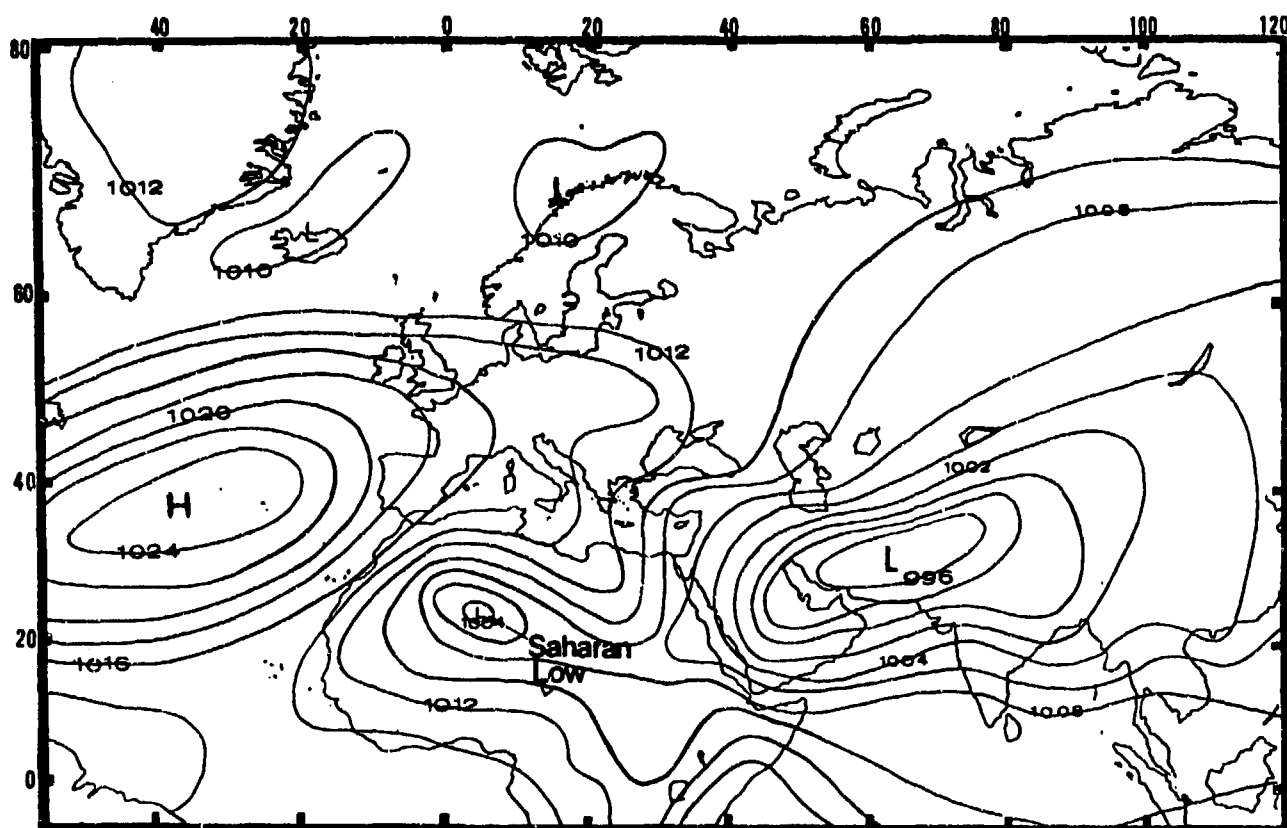


Figure 2-41. Mean July Position of the Saharan Low.

The Sudanese Heat Low. Varying from 1004 to 1012 mb, this low often marks the eastern edge of large-scale equatorial African low pressure in winter. The Sudanese Low is responsible for advecting moist warm-sector southwesterlies ahead of Atlas Low migrations into the Red Sea basin. The Sudanese Low lies over the elevated plateaus of southwestern Ethiopia and southeastern

Sudan (7° N, 32° E) between December and March (Figure 2-42a), but it migrates northward to $15\text{--}20^{\circ}$ N in April and May (Figure 2-42b). Between June and September, it becomes the broad, poorly defined low-pressure area shown in Figure 2-42c, but reappears in October as the closed circulation shown in Figure 2-42d.

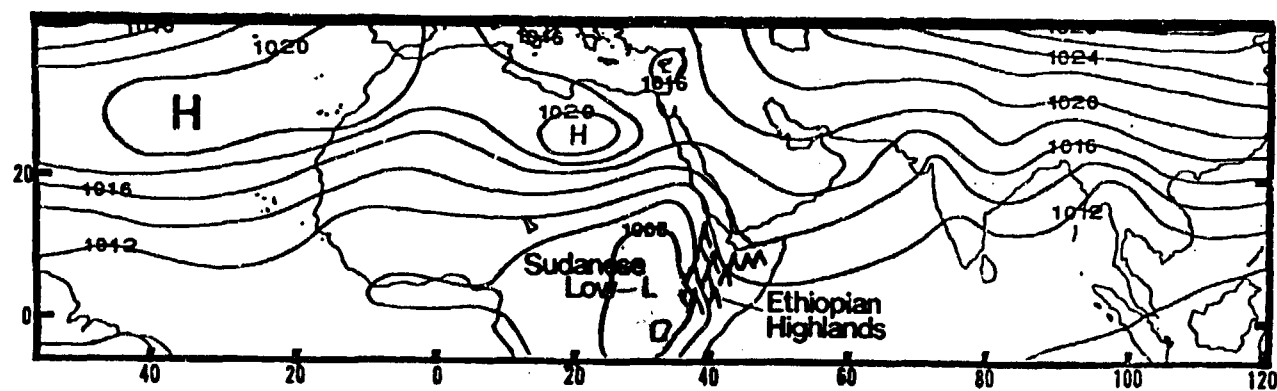


Figure 2-42a. Mean January Surface Position of the Sudanese Low.

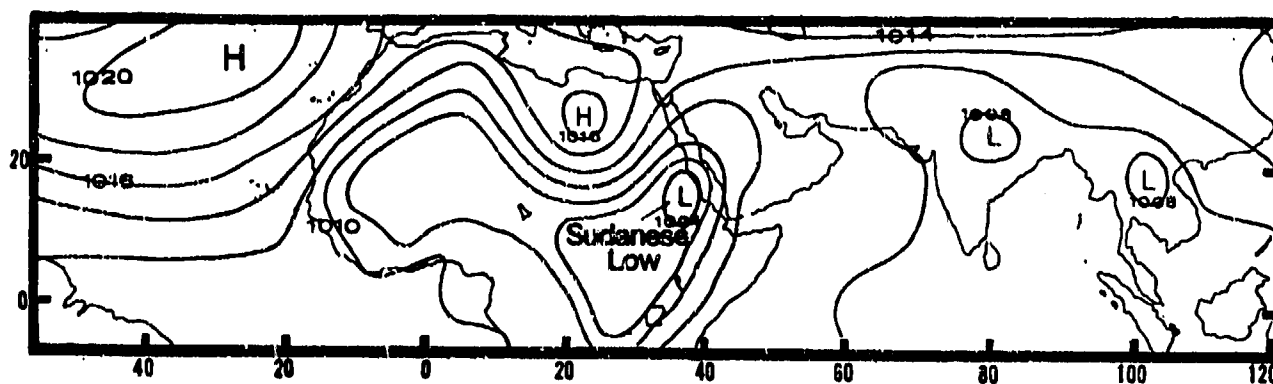


Figure 2-42b. Mean April Surface Position of the Sudanese Low.

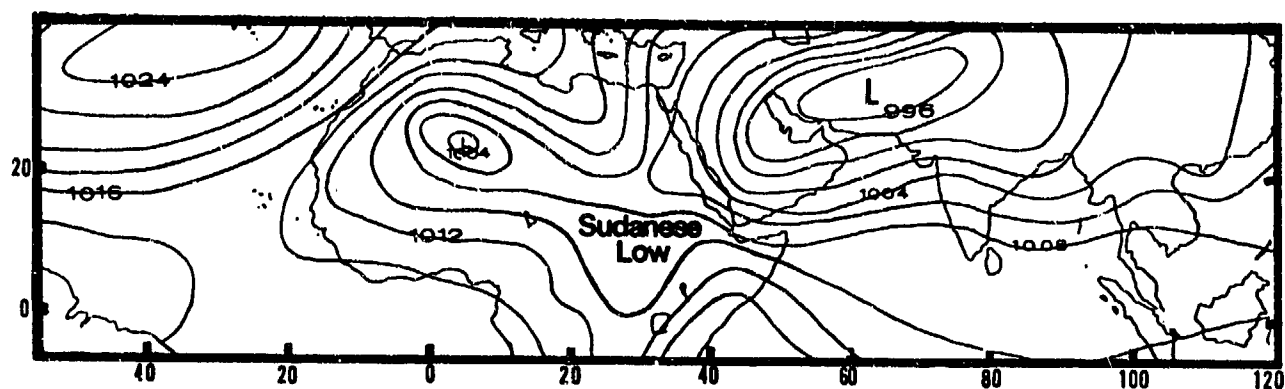


Figure 2-42c. Mean July Surface Position of the Sudanese Low.

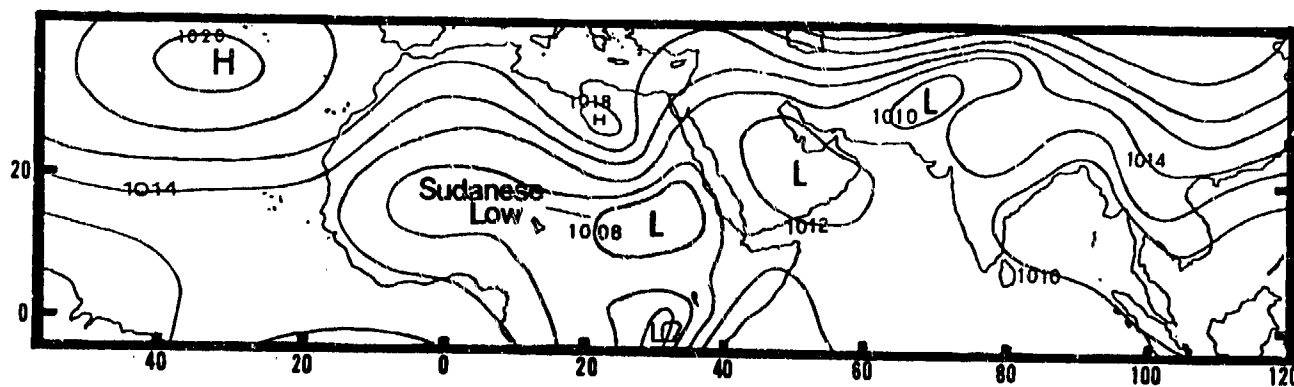


Figure 2-42d. Mean October Surface Position of the Sudanese Low.

The Saudi Arabian Heat Low extends to 650 mb from April to late October. Its mean July position and strength is regulated by intense surface heating over the Rub al

Khali Desert. Since the feature does not appear on mean surface charts for July, gradient-level streamline flow over the Horn of Africa is provided in Figure 2-43.

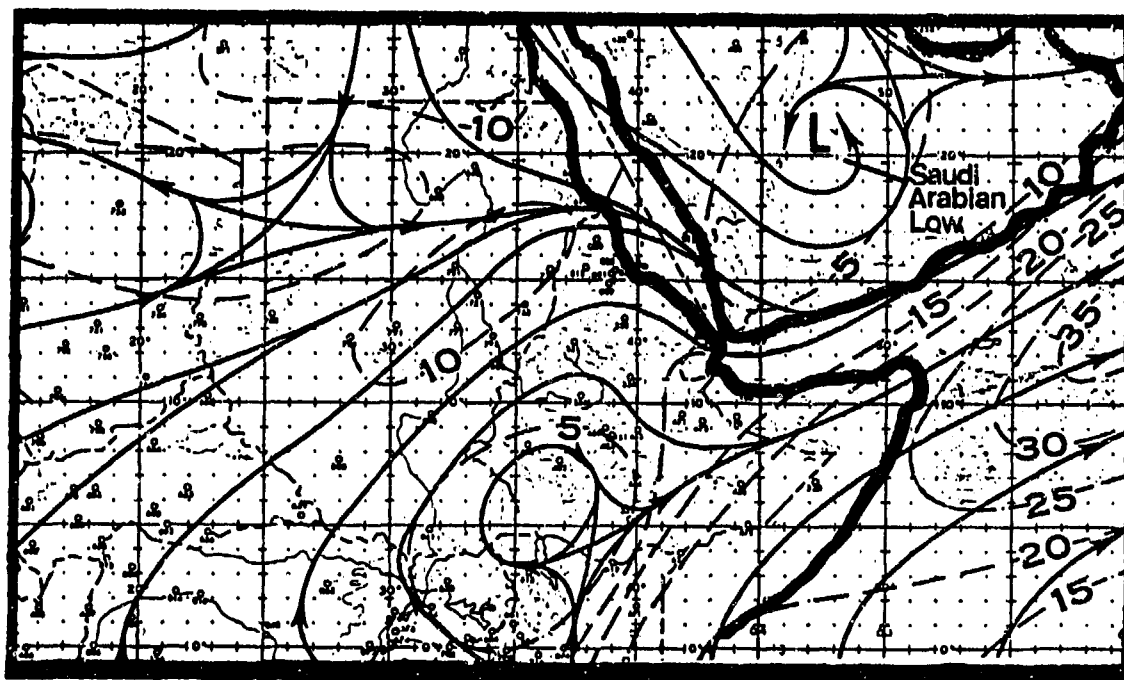


Figure 2-43. Mean July Gradient-Level Flow Showing the Position of the Saudi Arabian Low. Dashed lines are Isotachs (kts).

The mean position (20° N, 48° E) of the Saudi Arabian Heat Low varies little, but its vertical persistence and strength varies diurnally because of an extensive dust layer aloft. Weak low-level convergence associated with the Saudi Arabian Heat Low circulation is capped by a region of subsidence between 850 and 700 mb; convergence dominates above 700 mb. This phenomenon (unlike warm surface lows with high pressure aloft) is unique to the Saudi Arabian Low

because the dust layer prevents anticyclonic development aloft during the day.

During the night, subsidence is present at all levels. Except for very weak convergence near 750 mb, divergent flow dominates from the surface to 550 mb. Descending flow produces northeasterly surface flow at 5-15 knots along the northern and eastern Yemen Highlands.

MESOSCALE AND LOCAL FEATURES

MOUNTAIN-VALLEY WINDS are common in the Yemen Highlands and Ethiopian Highlands subregions. Orographic uplift may accentuate mountain-valley convergence above 6,000-7,000-feet (1,830-2,134 meters), producing short-lived convective cells with isolated rainshowers. Isolated mesoscale convection caused by orographic uplift and mountain-valley convergence is common in the Yemen Highlands and Ethiopian Highlands' coastal ranges, where sea breeze moisture is available. In the western Ethiopian Highlands west of 39° E, the surface Monsoon Trough over the African interior combines low-level moisture with complex diurnal mountain-valley circulations to result in massive orographic uplift and heavy convection every day between June and August.

Two types of terrain-induced winds affect the Horn of Africa; these are the mesoscale mountain-valley wind

and the localized, microscale "slope" (upslope/downslope) wind. The key differences lie in their temporal and spatial scales.

Mesoscale Mountain-Valley Winds average 6-12 knots. Daytime valley winds (Figure 2-44a) are strongest, averaging 10-15 knots between 200 and 400 meters (660 and 1,310 feet) AGL. Nighttime mountain winds (Figure 2-44b) average only 3-7 knots at the same level. Deep valleys develop more nocturnal cloud cover than shallow valleys because nocturnal air flow convergence is stronger. Mesoscale mountain-valley circulation has a maximum vertical extent of 6,560 feet (2,000 meters) AGL, depending on valley depth and width, the strength of prevailing winds in the mid-troposphere, and the breadth of microscale slope winds.

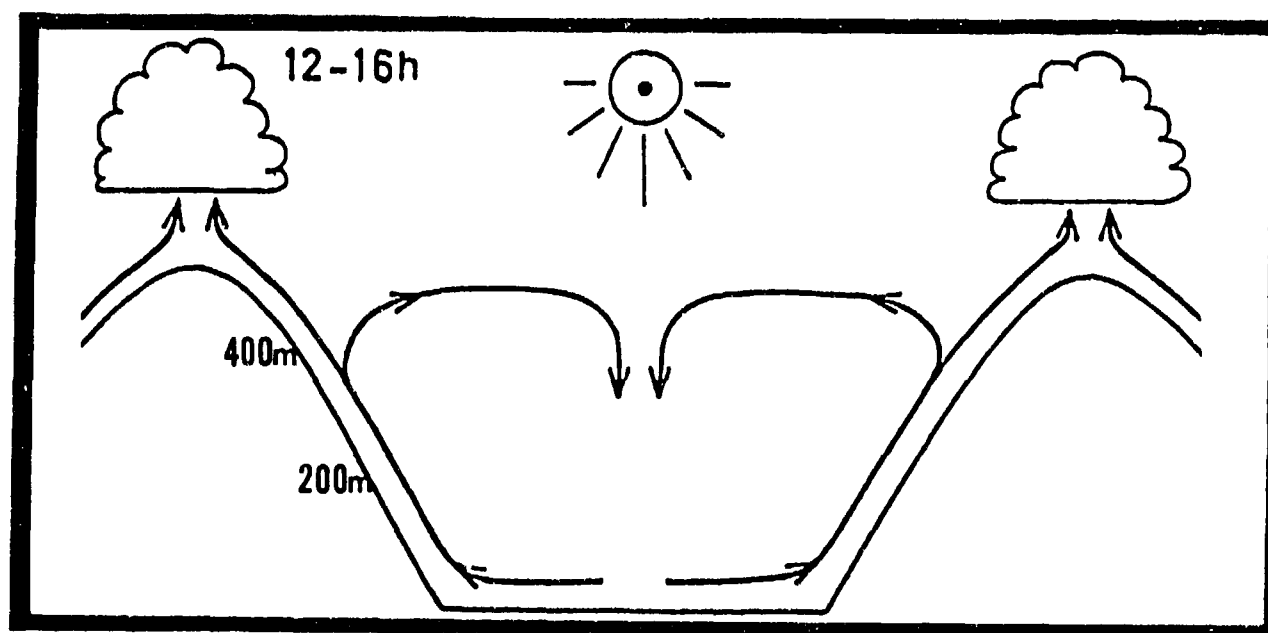


Figure 2-44a. Typical Daytime Valley Circulation (After Flohn, 1969).

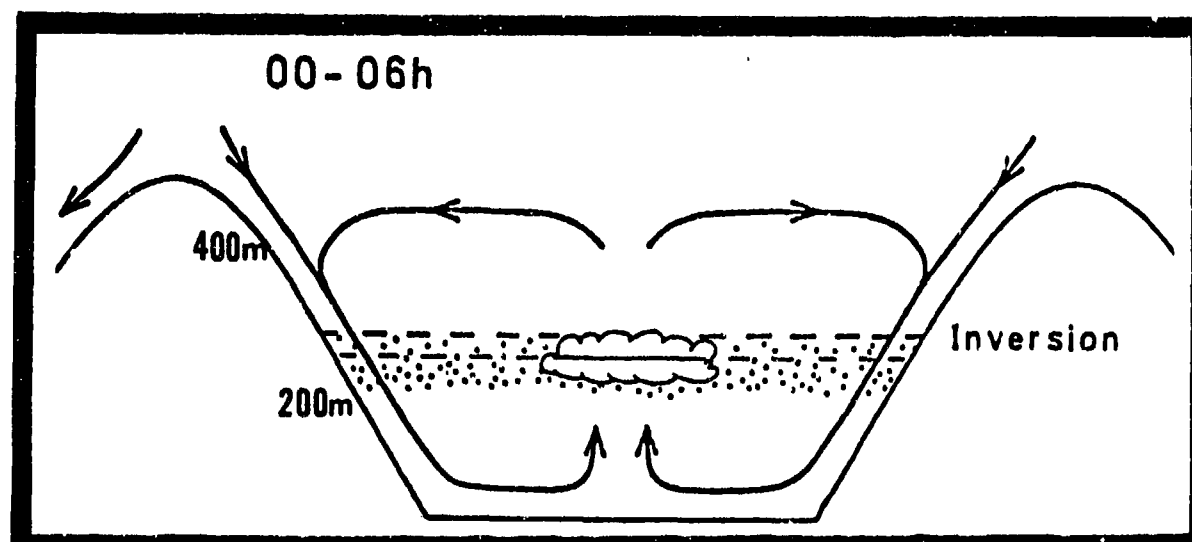


Figure 2-44b. Typical Nighttime Mountain Circulation (After Flohn, 1969).

Microscale Slope Winds develop along the surface boundary layer (0-500 feet/0-152 meters) of mountains and large hills. Mean daytime upslope wind speeds are 6-8 knots; mean nighttime upslope speeds are 4-6 knots. These speeds are found at elevations no higher than 130 feet (40 meters) AGL. Downslope mountain winds are strongest between November and March, while upslope valley winds are strongest between April and October. Upslope winds are strongest on slopes with southerly exposures. Figures 2-45a-h (from Geiger, 1961) show the life cycle of a typical mountain-valley wind circulation. The light arrows represent *microscale* circulation; the dark arrows, *mesoscale* circulation.

microscale upslope wind, which is not fully-developed until the entire valley surface is heated enough to stop the mesoscale downslope mountain wind.

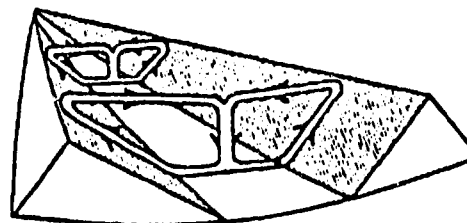


Figure 2-45b. LATE MORNING. Widespread surface heating continues to generate microscale upslope flow, and cuts off any downslope support to the mesoscale Mountain circulation; downslope mountain circulation stops.

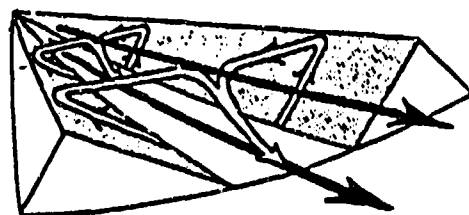


Figure 2-45a. SUNRISE. Sunshine almost immediately starts upslope wind development, but the downslope mountain wind persists because mesoscale flow overrides microscale flow. Generally, the transition between Figures 2-45a and b is 0700-1000 LST, but local terrain determines how soon sunlight can start the

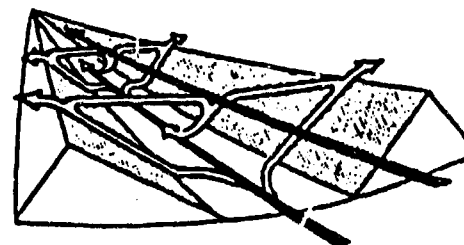


Figure 2-45c. MIDDAY. Sunshine covers the entire valley floor, and upslope flow feeds valley circulation.

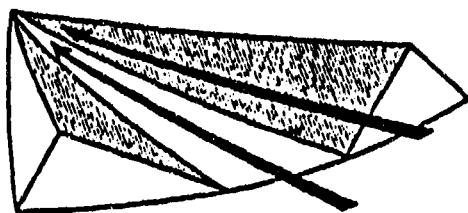


Figure 2-45d. LATE AFTERNOON. East-facing slopes begin to cool; upslope flow weakens.

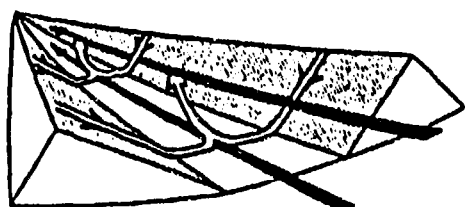


Figure 2-45e. SUNSET. Although microscale downslope wind components dominate the surface boundary layer, mesoscale upslope valley flow retains weak momentum.

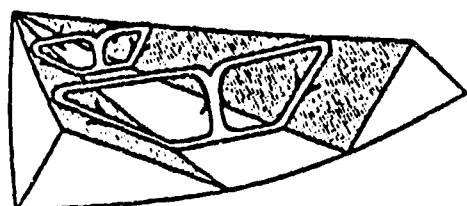


Figure 2-45f. LATE EVENING. Downslope winds dominate.

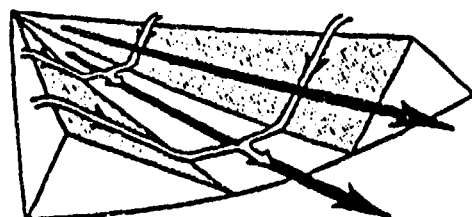


Figure 2-45g. MIDNIGHT. Downslope winds feed the mountain circulation.

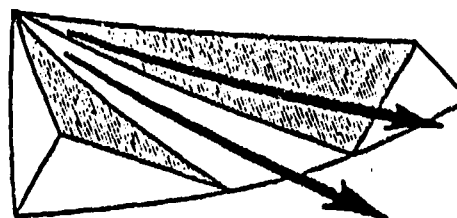


Figure 2-45h. PRE-DAWN. Winds are calm just before surface heating begins at the microscale; the mesoscale downslope mountain circulation retains its momentum. Microscale downslope winds end just after sunrise; upslope winds begin again at first light.

Mountain inversions develop when cold air builds up along wide valley floors where nocturnal downslope wind convergence is weak. The cold air descends from the slopes above the valley at 8-12 knots, but loses momentum when it spreads out over the valley floor. A macroscale example of this situation occurs in the central and southern Great Rift Valley, where steep terrain brackets a level, gently-sloping valley 10-15 NM wide. By the time nocturnal downslope flow down both slopes can converge, wind speeds average only 2-4 knots. The cold air replaces warm, moist valley air at the surface and produces a thin smoke and fog layer near the base of the inversion. First light here initiates upslope wind components by warming the cold air trapped on the valley floor. By late morning, more than 70 percent of the valley surface is exposed to sunlight. Warming of the entire boundary layer commences near the 500-foot (152-meter) level AGL.

MOUNTAIN WAVES. Mountain wave turbulence is usually moderate to severe. Rotor clouds produce the strongest turbulence due to sudden directional shears, but they are rarely seen over the Horn of Africa. Between December and March, the Taurus and Himalaya Mountains in Turkey and northern India block large-scale southward movement of cold air from Asia into the Arabian Sea and western Indian Ocean, but occasional mid-and upper-level troughs in the westerlies may produce potentially dangerous mountain waves over the Ethiopian and Yemen Highlands. Deep troughs reaching these subregions may form leeside gravity waves. Criteria for mountain wave formation includes sustained speeds between 15-25 knots with flow within 30 degrees of perpendicular to the ridge. Waves develop when air at lower levels is forced up over the windward side of a ridge, as shown in Figure 2-46.

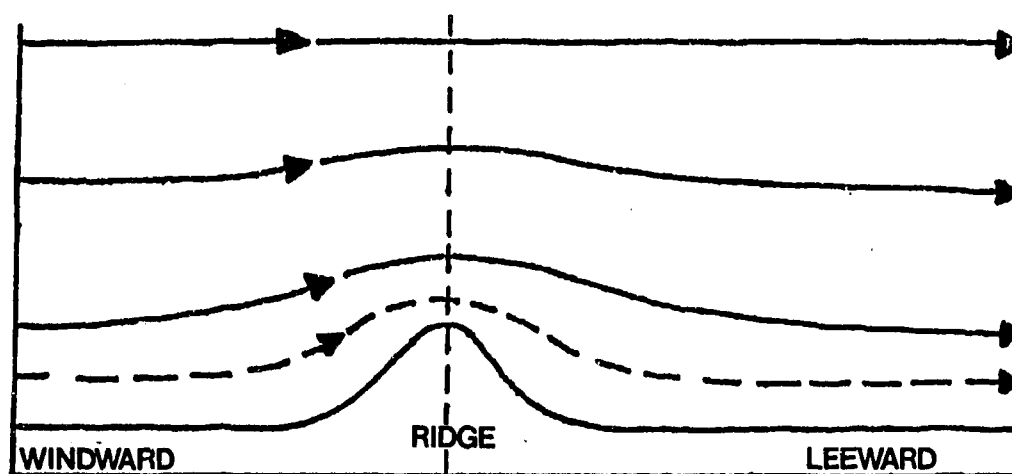


Figure 2-46. Initial Flow Pattern Over Topographic Barrier; Wind Speed Less Than 15 Knots (from Barry, 1981).

Wavelength amplitude is dependent on wind speed and lapse rate above the ridge. Light winds follow the contour of the ridge with little displacement above and rapid dampening beyond. Stronger winds displace air above the stable inversion layer; average upward

displacement is 10 times the ridge height. Downstream, the wave propagates for an average distance of 50 times the ridge height. Figure 2-47 illustrates the leeside gravity wave formation.

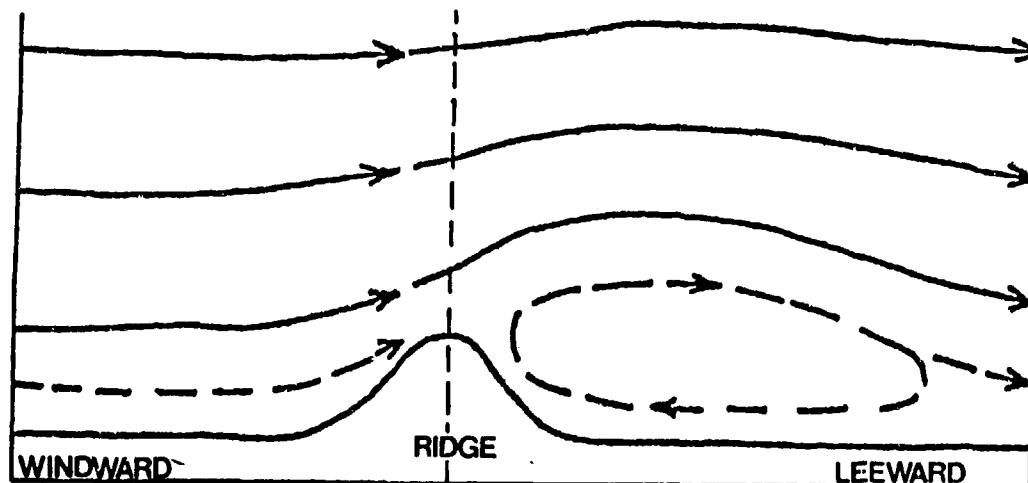


Figure 2-47. Vertical Cross-Section of Mountain Lee Wave (Gravity Wave) Formation (from Barry, 1981).

DUSTSTORMS. Given the right conditions, duststorms dominate terrain below 4,000 feet (1,220 meters) MSL. They occur primarily in the Great Rift Valley, along the Red Sea/Gulf of Aden coastline, and in interior sections of Somalia and eastern Ethiopia. Duststorms carry suspended particles over large distances, often reducing visibility to less than 30 feet (10 meters). Season of occurrence, wind direction, and amount of particulate matter vary by locality. Large-scale duststorms often persist for 1 or 2 days before a frontal passage (such as

with an Atlas or Cyprus Low) or with synoptic-scale squall lines. Mesoscale squall lines may reduce visibility to less than 1/2 mile for a few minutes to an hour along sandy coastlines.

Dust devils are, in effect, miniature tornados set off by intense summer heating. Diameters range from 10-300 feet (3-91 meters). Dust devils may last 1-5 minutes. They occur most frequently along the sandy coastal zones of Somalia, Yemen (Aden) and Djibouti.

Surface temperature inversions tend to dampen turbulent mixing in the lowest layers and reduce the effects of sand/dust storms from day to day. These inversions are the diurnal control observed with most duststorm activity. Typically, inversions break down several hours after sunrise, allowing turbulent mixing in the lower layers; however, large-scale synoptic disturbances may override the nocturnal duststorm minima.

The origin and nature of duststorms depend on general synoptic conditions, local surface conditions, and diurnal/seasonal considerations, as shown below:

Synoptic Conditions--

Active cold fronts. Between November and April, duststorms may develop with frontal passages in the western and northern fringes of the Horn of Africa. Gusts of 15-20 knots are enough to lift dust and sand, but a pressure gradient of 6 to 8 mb/100 NM produces widespread airborne dust/sand over a 100 sq NM area. Stronger fronts may carry Sahara Desert dust/sand across the Red Sea into the western Yemen Highlands subregion. (See Chapter 4--Southwest Monsoon Visibilities).

Convective activity. Convection produces local cumulus downdrafts up to 30 knots, while squall lines organize over a larger area, producing cloud bands up to 100 NM long and 10-20 NM wide, with easterly winds. Wind speeds in Indian Ocean squall lines are much greater; these systems suspend particulates in the atmosphere for longer periods of time and reduce visibilities to 4-7 miles over a larger area. Organized convection may transport dust/sand 100-200 NM inland from the Somali coastline.

The Somali Jet. Between late April and early October, the Somali Jet may produce strong southerly flow (15-25 knots) over the western Indian Ocean Plain (Somalia and eastern Ethiopia). When it does, visibility is 2-6 miles during the day in this isolated, sparsely-populated area. The air and the surface are abnormally dry, and a thin haze with 4-to 7-mile visibilities may persist for up to a week.

Local Surface Conditions--Soil type and condition control the amount of particulate matter that can be raised into the atmosphere. Dry sand or silt, for example, is easily lifted by a 10-to 15-knot wind. From December to February, thin haze is a persistent feature north of 6° N and east of 43° E because of sustained 15-knot northeasterly flow along the Aden Coastal Fringes and Indian Ocean Plain. Although larger particles quickly settle to the surface after a duststorm, finer sediments remain suspended in the atmosphere for days. Fine dust, sand, salt, or silt may travel hundreds of miles from its source. Distant, large-scale sources of material provide most storm debris over western Ethiopia/Yemen (San'a) and the Red Sea.

Seasonal Considerations--

November to March. Thin dust or haze are the most frequently observed obstructions to vision. Several weeks of fair and dry weather allows surface heating and sea breeze to put an accumulation of fine silt into the air. Duststorms associated with frontal boundaries are uncommon but severe; visibility can be 1-3 miles over large areas. Every other year between November and March, 20-knot winds lasting for 3-9 hours occur in northwest Ethiopia. Similar conditions occur with abnormally strong (15- to 25-knot) Northeast Monsoon flow in the eastern and southern Gulf of Aden.

April to October. Late-April frontal boundaries, thermal convection, and mesoscale squall lines produce most duststorms and low visibilities. The Somali Jet Stream is another source.

Diurnal Considerations--

Daytime. Hot and dry surface conditions in June, July, and August across northern Somalia, Djibouti, and the northern Great Rift Valley of Ethiopia produce considerable dust and haze. Persistent dryness raises dust to 10,000 feet (3,050 meters) MSL.

Nighttime. Cooler surface temperatures result in stability; turbulent mixing is minimized, along with the threat of duststorms.

LAND/SEA BREEZE. Differential surface heating along coasts generates this diurnal phenomenon. The marine boundary layer rarely extends above 2,000 feet (610 meters) AGL or 15 NM inland without synoptic assistance. Two types of land/sea breezes are found in the Horn of Africa: "common," and "frontal."

"Common" land/sea breezes affect Gulf of Aden and Somali coastlines. The southern Aden Coastal Fringe is an exception because of the Somali Jet that produces persistent southerly winds that overrides the "common" sea breeze. All coastal areas are affected by the land/sea breeze during the Northeast Monsoon, but wind directions along the immediate coastline can vary from northeasterly by 45 degrees or more. Figure 2-48 illustrates the "common" land/sea breeze circulation under calm synoptic conditions, with uniform coastline configurations, and no topographic influences. Onshore (A) and offshore (B) flow intensifies in proportion to daily heat exchange between land and water. Common land/sea breezes always reverse at dawn and dusk.

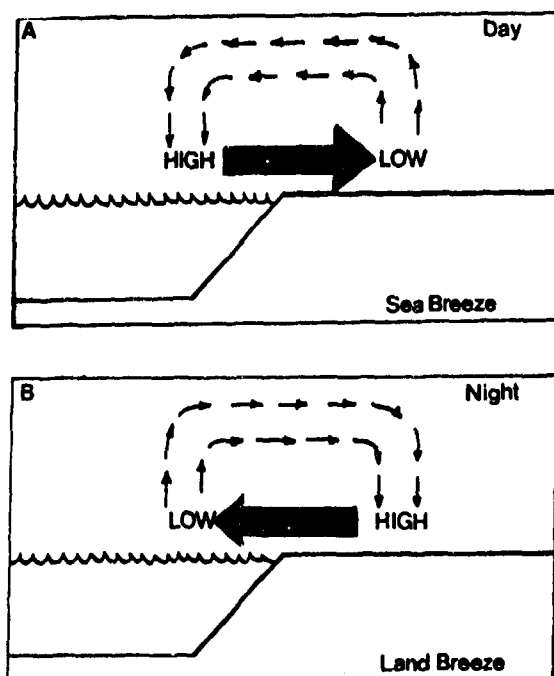


Figure 2-48. The "Common" Daytime Sea Breeze (A) and Nighttime Land Breeze (B). Thick arrows represent pressure gradient and direction of flow.

"Frontal" land/sea breezes are the product of the "front" between the land and sea air masses. The transition for wind reversal is delayed by 1-4 hours because gradient flow prevents the sea breeze boundary layer or "front" from moving ashore. Figures 2-49a-f show a typical "frontal" land/sea breeze sequence. Solid blocks denote the land surface, while dashed lines represent water. Vertical lines show the sea breeze boundary layer and arrows represent wind circulation.



Figure 2-49a. Gradient Flow With Offshore Wind Component Slopes Gently Over Dense, Cooler Marine Boundary Layer. Shearing action along the "front," or land/sea air mass interface, compacts the layer. Gradient flow strength determines the magnitude of compacting.



Figure 2-49b. Increased Compacting Tightens Pressure Gradient Along Land/Sea Interface. If the gradient is weak, land surfaces heat rapidly. As a result, the surface pressure gradient and winds resemble those in Figure 2-49a.



Figure 2-49c. Maximum Compacting of the Marine Boundary Layer. At this instant, the surface winds inside the marine boundary layer show onshore direction. The marine layer surface flow may take several hours to reach the coast. Momentum accelerates wind speed with time.



Figure 2-49d. Frontal Sea Breeze Accelerates Towards Shore. Initial "frontal" sea breezes may sustain 20-knot winds for 15-45 minutes.

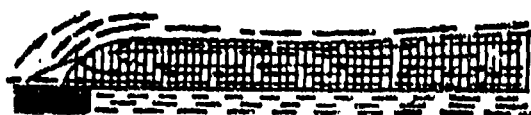


Figure 2-49e. Sea Breeze "Front" Reaches The Coast. Note the increased depth of onshore flow in the marine boundary layer. Compare with Figure 2-49c.



Figure 2-49f. Land/Sea Breeze Mechanism in Full Swing. Offshore flow aloft, onshore flow at surface.

Topography perpendicular to shorelines modifies the land/sea breeze in several ways. Orographic uplift induces sea breeze-stratiform/cumuliform cloudiness and deflects surface winds. The mesoscale mountain circulation accelerates the land breeze over open water. Elevated coastal topography produces steep nocturnal temperature gradients. Strong offshore gradient flow produces frontal land/sea breezes like those illustrated above; the Ethiopian and Yemen Highlands are examples. Socotra Island is another example, but on a smaller scale.

Coastal configuration also has an effect on land/sea breeze--the most obvious with the onshore sea breeze. Coastlines parallel to sea breezes impede the progress of onshore flow to produce localized upwelling and low-level divergence.

Coastlines perpendicular to onshore flow promote maximum sea breeze penetration and low-level convergence. However, hot and dry land surfaces modify moist onshore flow within 20 NM of the coast. Without orographic lift, cumulus rarely develops beyond immediate coastlines.

Synoptic-scale effects on land/sea breezes are best exemplified near Cape Guardafui, as shown in Figures 2-50a-c. This unique location combines topography and complex coastal configuration with low-level synoptic flow--the Somali Jet.

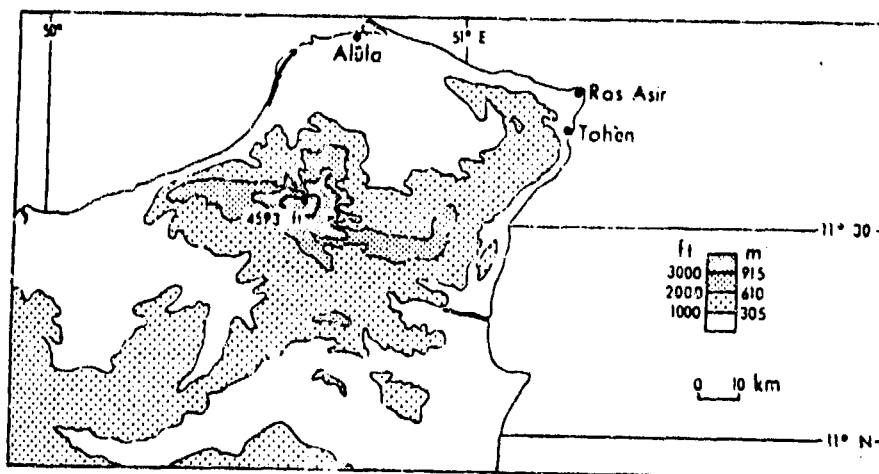


Figure 2-50a. Local Topography at Cape Guardafui (Ras Asir) (from Findlater, 1971).

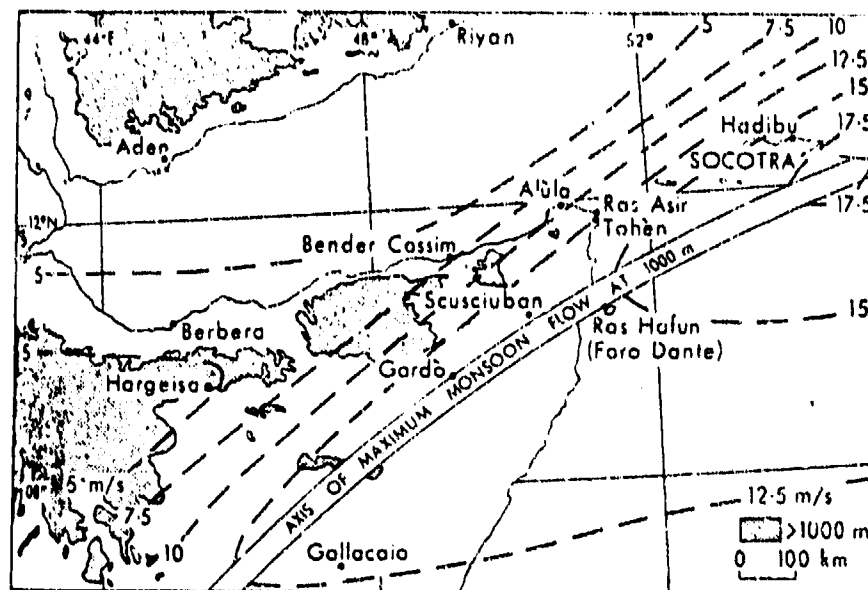


Figure 2-50b. Synoptic Scale Winds at Cape Guardafui (Ras Asir) (from Findlater, 1971). Isotachs (dashed lines) are in meters/sec.

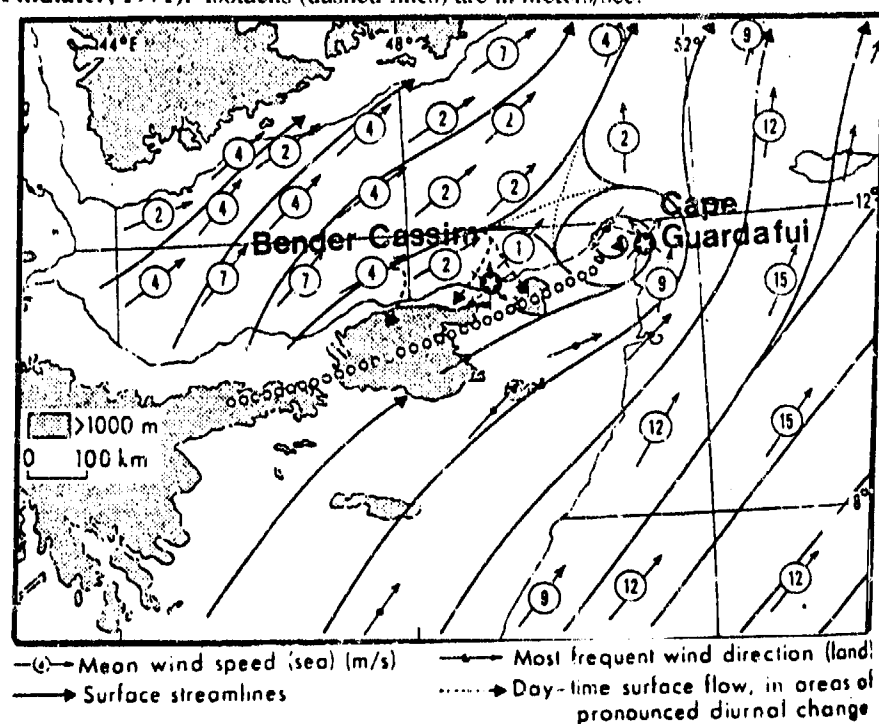


Figure 2-50c. Mean July Surface Streamline Flow (from Findlater, 1971).

WET-BULB GLOBE TEMPERATURE (WBGT) HEAT STRESS INDEX. The WBGT heat stress index provides values that can be used to calculate the effects of heat stress on individuals. WBGT is computed by using the formula:

$$WBGT = 0.7 WB + 0.2 BG + 0.1 DB,$$

where: WB = wet bulb temperature
BG = Vernon black globe temperature
DB = dry bulb temperature

A complete description of the WBGT heat stress index and the apparatus used to derive it is given in Appendix A of TB MED 507, *Prevention, Treatment and Control of Heat Injury*, July 1980, published by the Army, Navy and Air Force. The physical activity guidelines shown in Figure 2-51 are based on those used by the three services. Note that the wear of body armor or NBC gear adds 10°F to the WBGT, and activities should be adjusted accordingly.

WBGT (°F)	WATER REQUIREMENT	WORK/REST INTERVAL	ACTIVITY RESTRICTIONS
90-up	2 quarts/hour	20/40	Suspend all strenuous exercise.
88-90	1.5-2 quarts/hour	30/30	No heavy exercise for troops with less than 12 weeks hot weather training.
85-88	1-1.5 quarts/hour	45/15	No heavy exercise for unacclimated troops, no classes in sun, continue moderate training 3rd week.
82-85	.5-1 quart/hour	50/10	Use discretion in planning heavy exercise for unacclimated personnel.
75-82	.5 quart/hour	50/10	Caution: Extremely intense exertion may cause heat injury.

Figure 2-51. WBGT Heat Stress Index Activity Guidelines.

Figures 2-52a-d, on the following pages, give average maximum WBGTs for January, April, July, and October. They were traced from the full-color WBGT charts given in *Global Climatology for the Wet Bulb Globe Temperature (WBGT) Heat Stress Index*, published by the U.S. Army Research Institute of Environmental Medicine, Natick MA 01760-5007. Quoting from that document: "This climatological atlas was compiled using a variety of sources because the WBGT index is unique and no single data base or publication contained this type of information. Units used in this atlas are degrees fahrenheit. Four parameters [sic] have been

mapped in this atlas: the average maximum dry-bulb temperature, the average maximum wet-bulb temperature, the average maximum black globe temperature and the average maximum WBGT. These parameters were chosen because they reflect the average of the greatest heat stress that would be encountered by a combat soldier during the day, and are most representative of the 1300 to 1500 local time frame. A local, diurnal temperature curve should be taken into consideration when attempting to gauge heat stress for other times of the day, or for a 24 hour period."

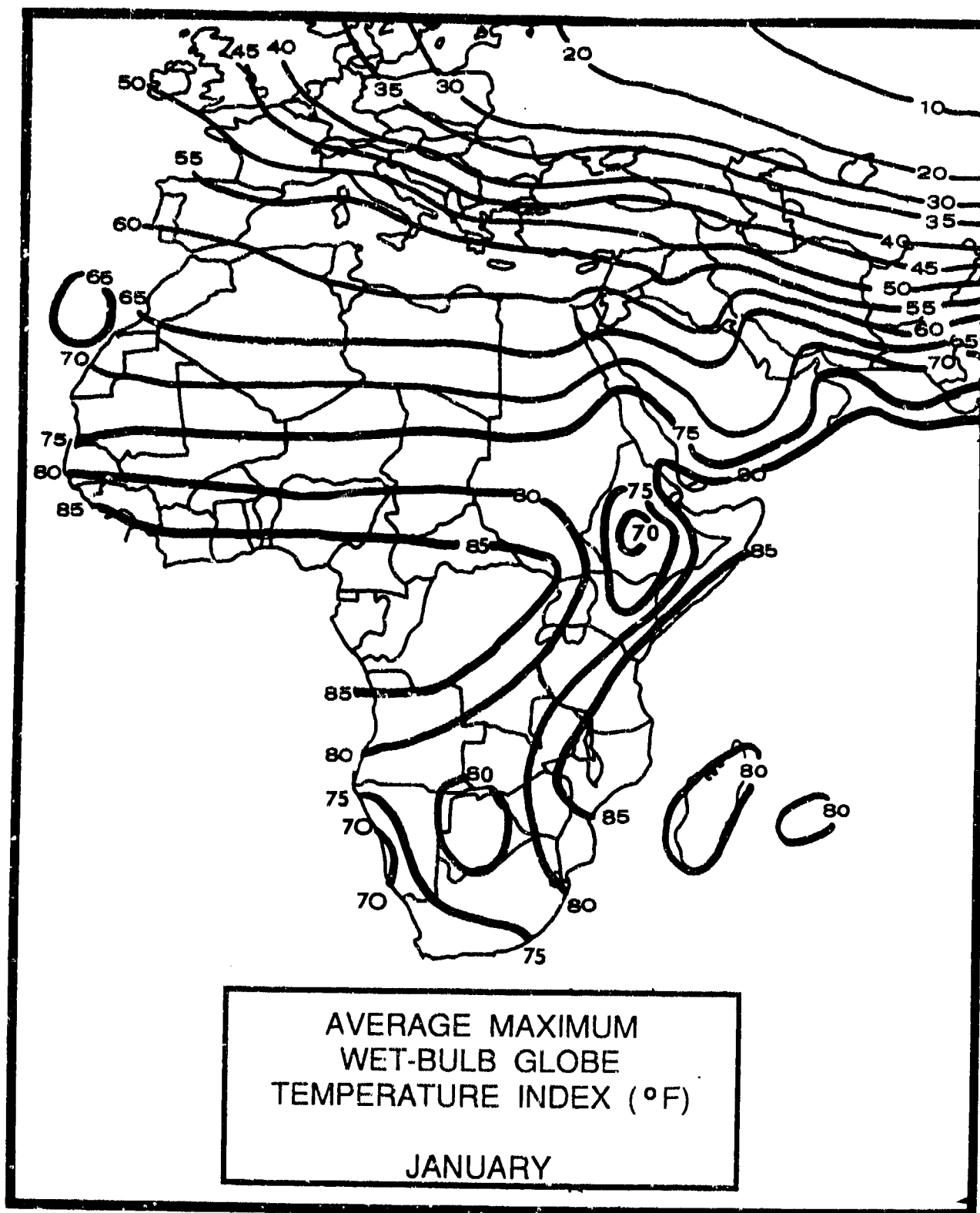


Figure 2-52a. Average Maximum WBGT--January. The Ethiopian Highlands see January WBGTs between 70° F (21°C) and 75° F (24°C) because of lower dry-bulb temperatures above 5,000 feet (1,524 meters) MSL. Along the Somalia coastline, WBGTs reach 85° F (29°C) as ocean moisture raises wet-bulb temperatures.

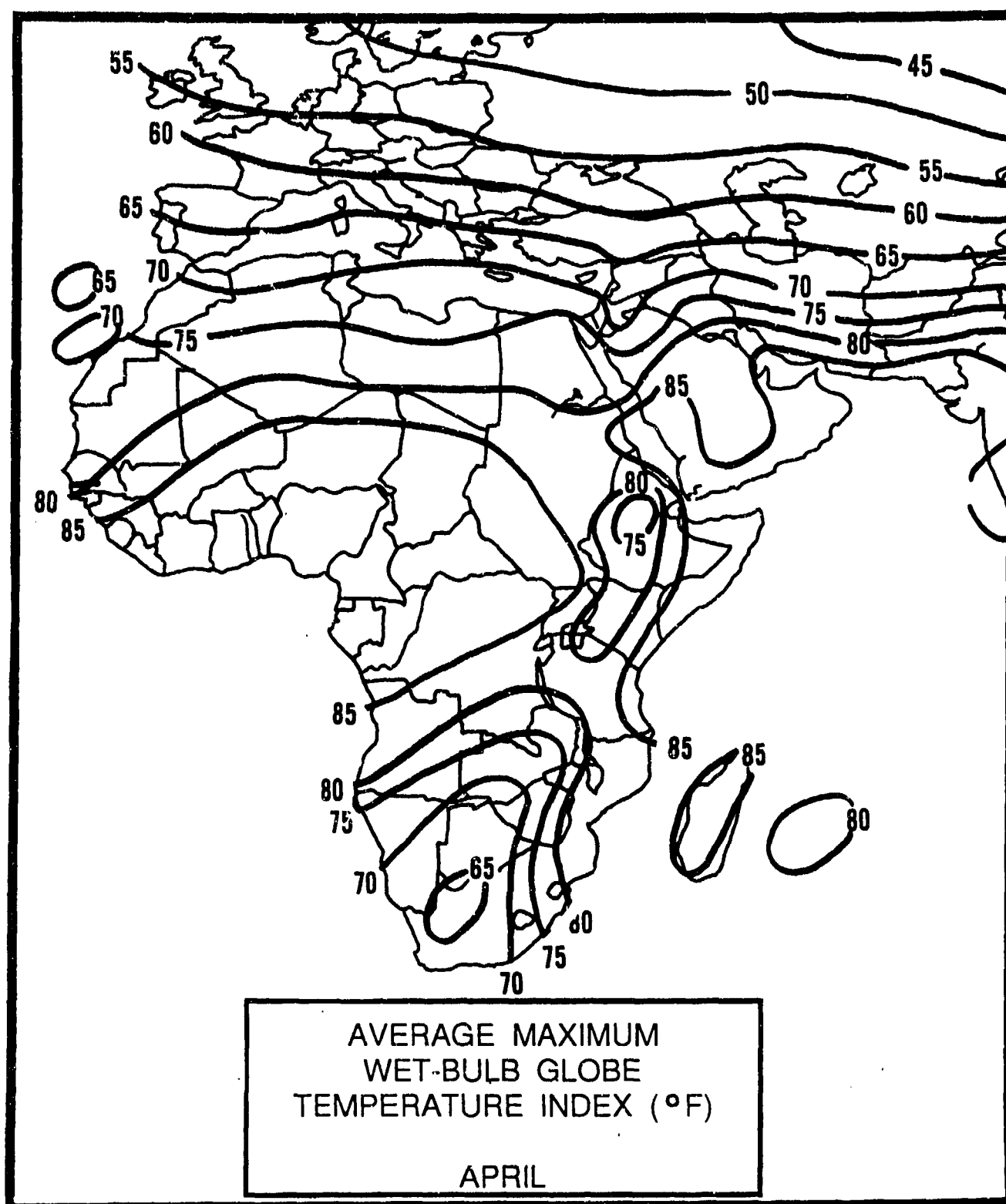


Figure 2-52b. Average Maximum WBGT--April. By April, the 85°F (29°C) WBGT isoline surges northward and westward over Somalia and extreme eastern Ethiopia. Only mountainous areas above 8,000 feet (2,439 meters) MSL see WBGTs between 75°F (24°C) and 80°F (27°C). The expansion of higher WBGTs across the Horn of Africa are caused by northward movements in the surface Monsoon Trough and Somali Jet core.

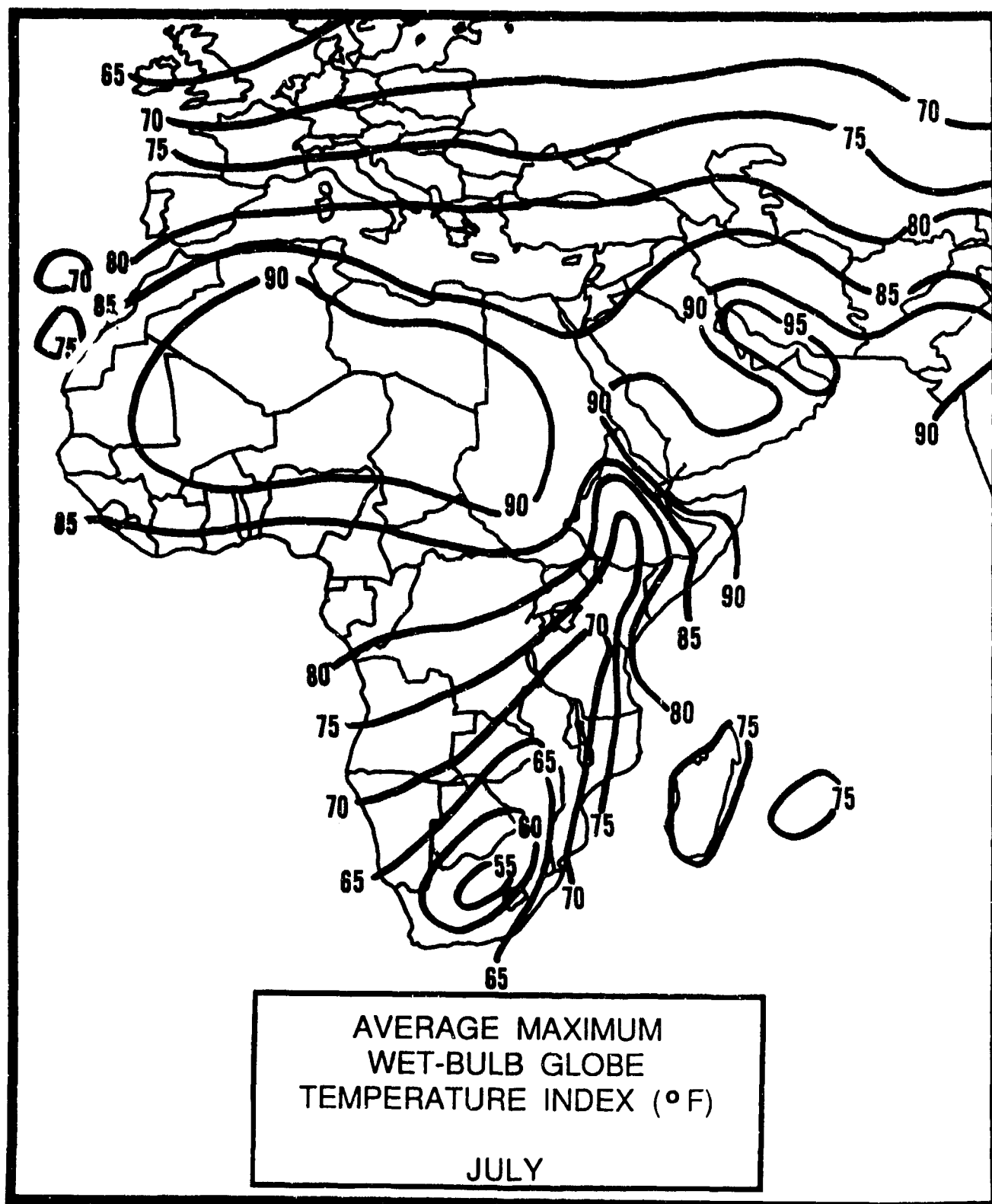


Figure 2-52c. Average Maximum WBGT--July. In July, there are large WBGT variations across the Horn of Africa. The higher WBGTs (above 80°F/27°C) are found in those areas with scant rainfall, searing heat, and high humidities. Elevations above 7,000 feet (2,134 meters) MSL are humid, but heavy rainfall, extensive cloud cover, and low temperatures cause average maximum WBGTs to remain below 80°F (27°C). Average maximum WBGTs over the entire Yemen Highlands and Aden Coastal Fringe are consistently above 90°F (32°C) in July.

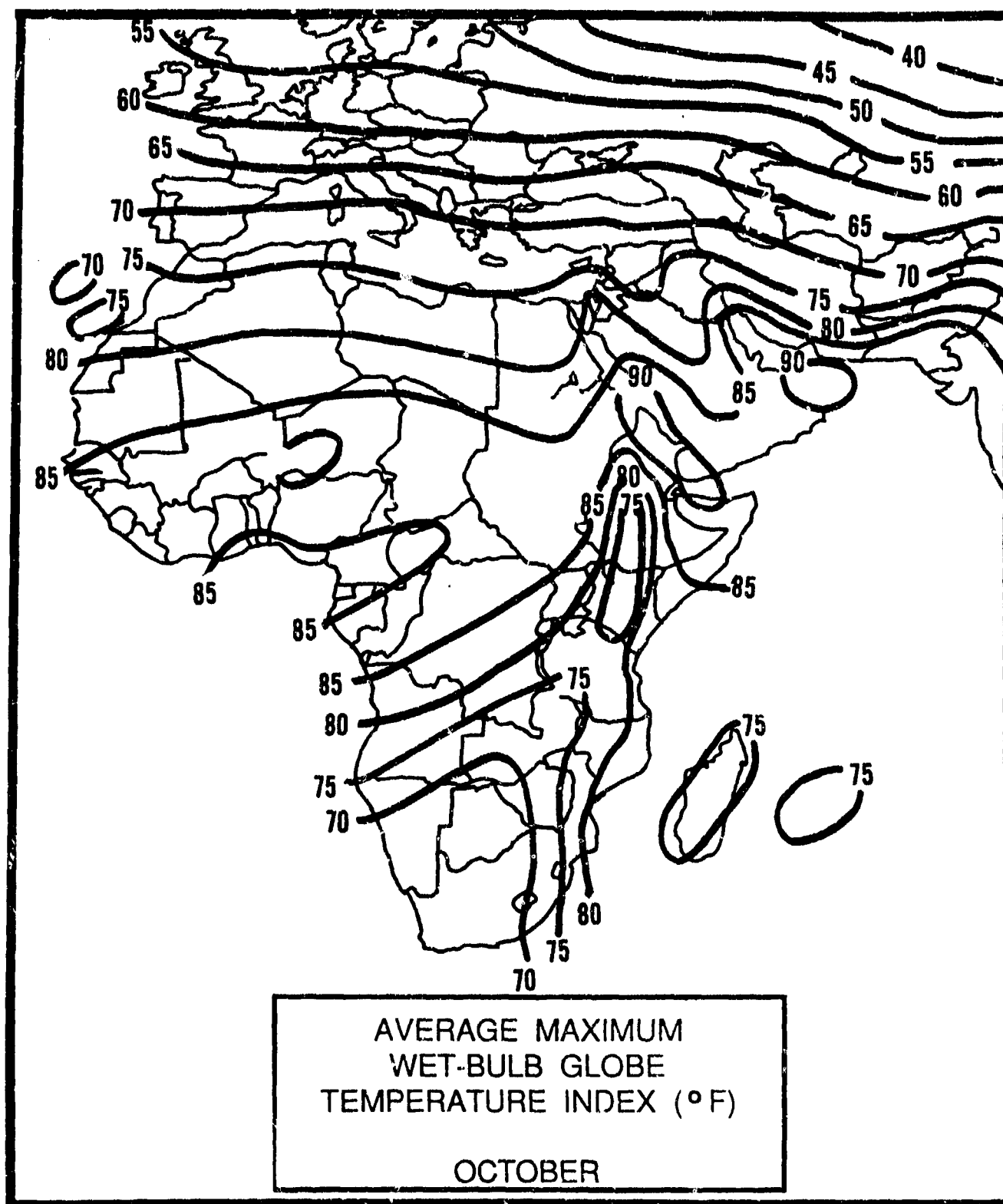


Figure 2-52d. Average Maximum WBGT--October. There is little change in average maximum WBGT from July. The only difference is a smaller area of 90°F (32°C) in the Gulf of Aden.

Chapter 3

INDIAN OCEAN PLAIN

The "Indian Ocean Plain" encompasses most of Somalia (SI) and parts of eastern Ethiopia (ET). After describing this area's situation and relief, this chapter discusses "typical weather conditions" by season. Local names for the seasons here ("Hagai," "Der," "Gilal," and "Gu"), are as shown.

Situation and Relief	3-2
The Southwest Monsoon ("Hagai")--July-September	3-7
General Weather	3-7
Sky Cover	3-7
Visibility	3-8
Winds	3-9
Precipitation	3-11
Temperature	3-13
Southwest to Northeast Monsoon Transition ("Der")--October-November	3-14
General Weather	3-14
Sky Cover	3-15
Visibility	3-17
Winds	3-18
Precipitation	3-19
Temperature	3-20
Northeast Monsoon ("Gilal")--December-March	3-21
General Weather	3-21
Sky Cover	3-21
Visibility	3-22
Winds	3-23
Precipitation	3-24
Temperature	3-24
Northeast to Southwest Monsoon Transition ("Gu")--April-June	3-26
General Weather	3-26
Sky Cover	3-26
Visibility	3-28
Winds	3-29
Precipitation	3-30
Temperature	3-32

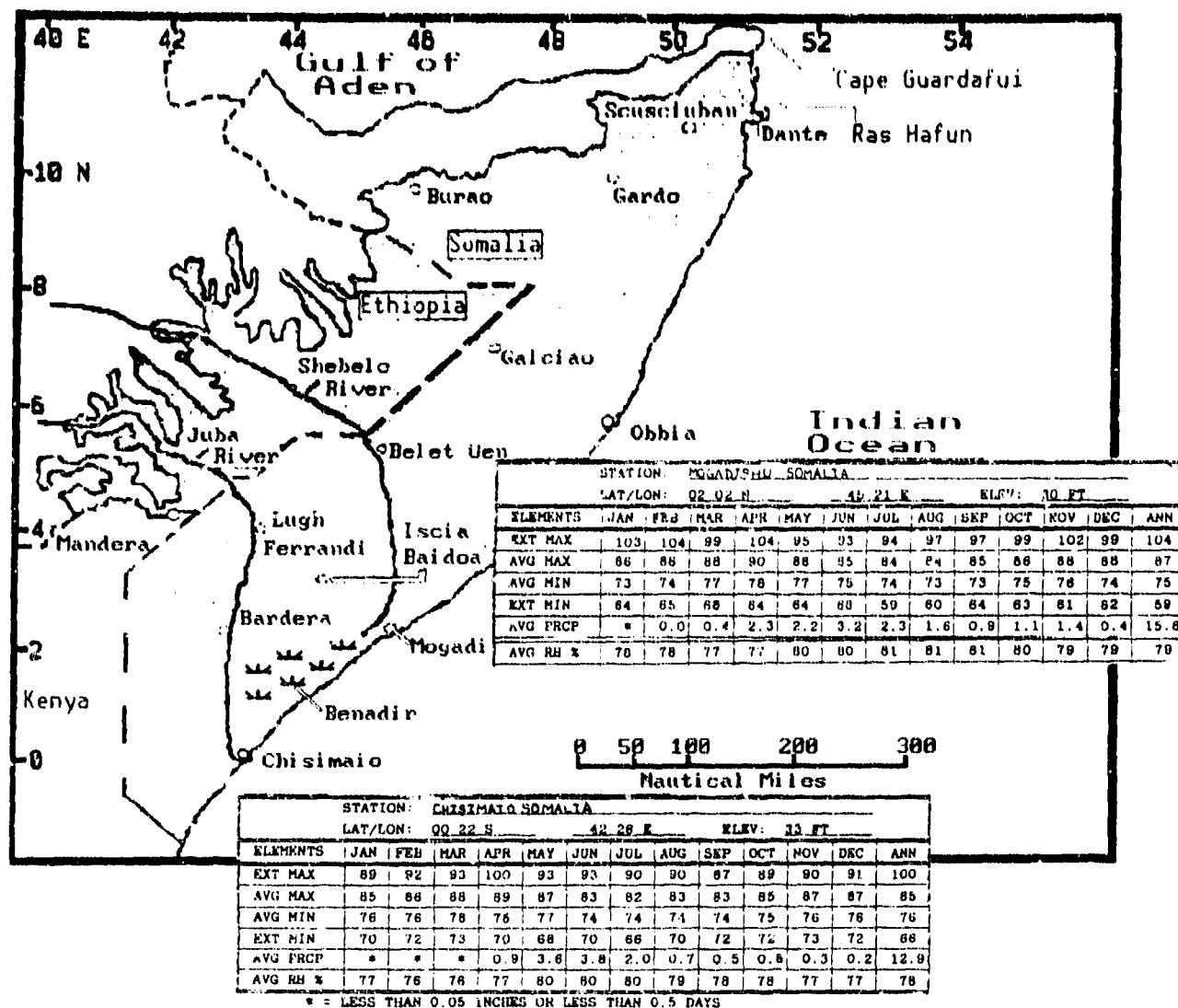


Figure 3-1. The Indian Ocean Plain. The Indian Ocean Plain includes most of Somalia and part of southeastern Ethiopia. It slopes gently upward from the Indian Ocean to the foothills of the Eastern Ethiopian Highlands. Its eastern boundary is the Indian Ocean from just south of Cape Guardafui to the Kenya border. The southern border is the Kenya-Somalia political boundary. The western and northern boundaries are SSW to NE from the Kenya-Ethiopia-Somalia border at 40° E along the 3,280-foot (1,000-meter) contour to about 11° N, 50° E before extending due east along 11° N to the Indian Ocean 30 NM south of Cape Guardafui. The northwest corner of the region includes the Juba and Shebele River Valleys of Ethiopia. Inset tables provide climatological summaries for Chisimaio and Mogadishu; periods of record were varied.

INDIAN OCEAN PLAIN

SITUATION AND RELIEF

ZONES OF RELIEF. The Indian Ocean Plain is separated into three distinct zones of relief, each of which will be discussed in turn. These zones, shown and

described below, are the "coastal dunes and lowlands" (Figure 3-2a), the "dissected hills" (Figure 3-2b), and the "elevated western plateau" (Figure 3-2c).

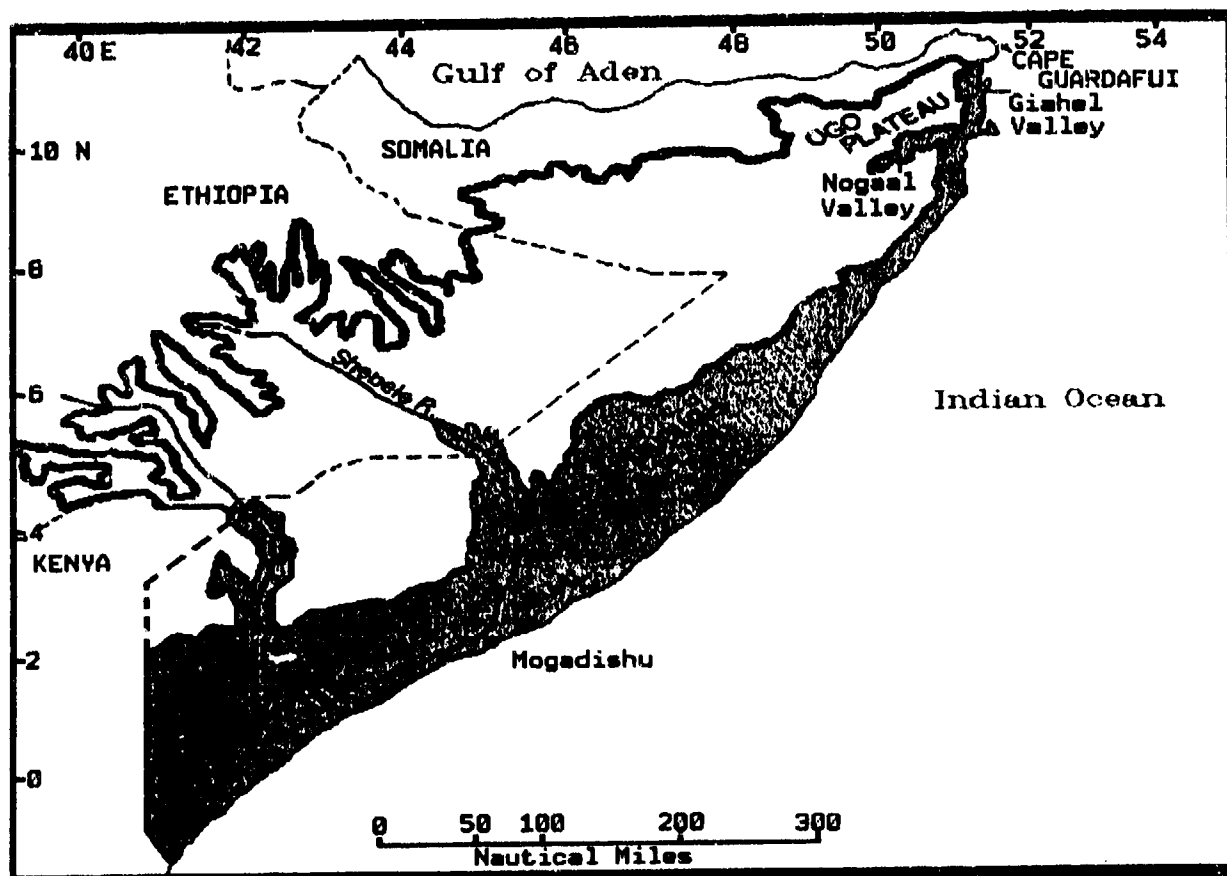


Figure 3-2a. The Coastal Dunes and Lowlands. This low coastal zone lies below 656 feet/200 meters along the Indian Ocean Plain's eastern fringes. Portions extend inland for 160 NM. The coastline from 30 NM south of Cape Guardafui to the Kenya border spans 1,200 NM. This coastal lowland zone is oriented NNE to SSW over 13 degrees of latitude from 11° N to 2° S.

The northernmost sections (8-11° N) of this zone are extremely narrow; flat coastal dunes and lowland plains range from 2 to 10 NM in width. The Indian Ocean on the east and the steep bluffs of the Ogo Plateau on the west are the boundaries. The Gishel Valley, just north of the Nogaal Valley, runs west to east toward the coast and extends 20 NM inland to the plateau. The Nogaal Valley (Nogaal is Somali for "fertile land") runs WNW to ESE to the coast for 120 NM. It is well-watered, but contains no permanent streams.

The central section of the lowlands, known as the Mudugh Plain, extends inland 160 NM from the coast. This area (4-8° N) contains extensive dune formations oriented NNE to SSW along the Indian Ocean shoreline. The dunes' heights reach 600 feet (195 meters); they are 1-3 NM in width and may stretch continuously for 20-30 NM. The interior Mudugh Plain contains ancient sand dunes, low hills, and a poor intermittent drainage network. Shallow stream beds average several miles in length and only 33 feet (10 meters) in width.

INDIAN OCEAN PLAIN

SITUATION AND RELIEF

The southern sections of the lowlands (from 4° N to the Kenya border) are traversed by two large rivers, the Shebele and the Juba. Their river valleys extend 250 NM inland and contain natural levees. Between these river valleys lies the Benadir, an extensive marshland. The

southern lowlands average 70 NM in width and 700 NM in length. The Abgal, 40 NM north of Mogadishu, Somalia contains extensive coastal sand dunes that merge into the Mudugh Plain.

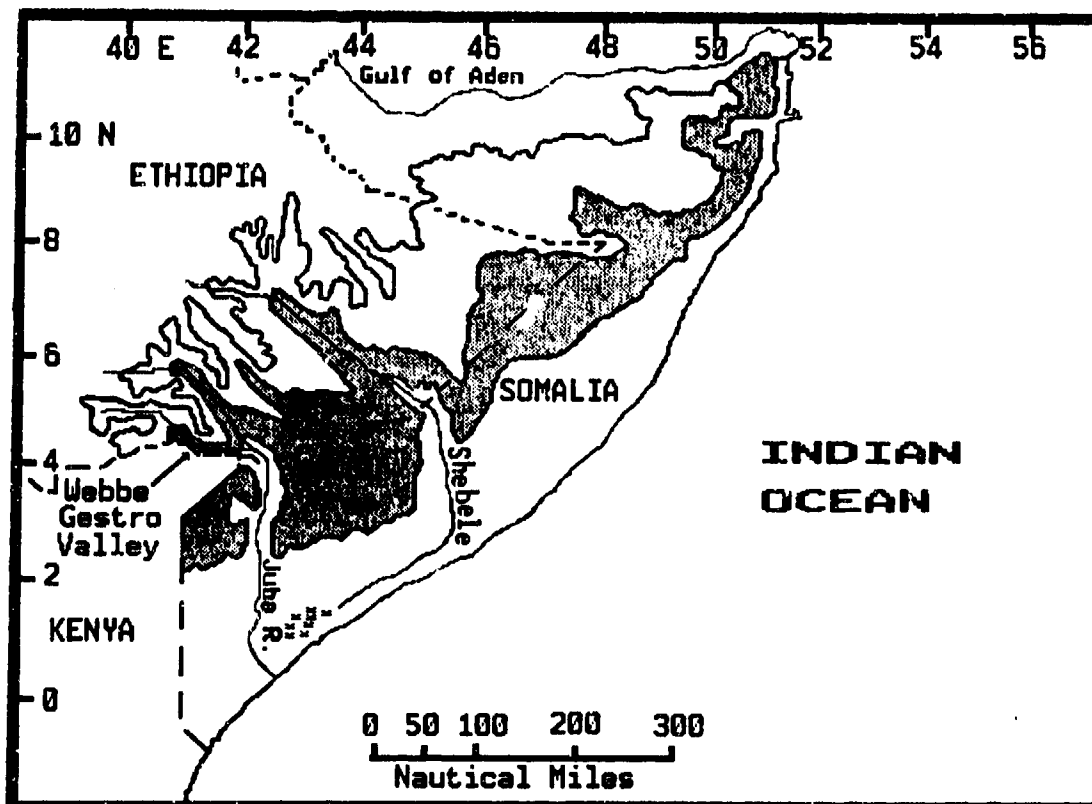


Figure 3-2b. The Dissected Hills. This zone comprises 15-20 percent of the Indian Ocean Plains. The hills lie exclusively within the 656-to 1,620-foot (200-500 meter) range and mark the transition zone between the western plateau and eastern lowlands. This zone is extremely narrow and rugged in the north, gradually widening near the Ethiopia-Somalia-Kenya borders. Here, the gently rolling hills are eroded by seasonal rains that create wide gullies and narrow (33 feet/10 meters) canyons. Several long valley systems run northwest to southeast through the dissected hills. The Juba and Shebele river valleys parallel each other and extend 200 NM into Ethiopia.

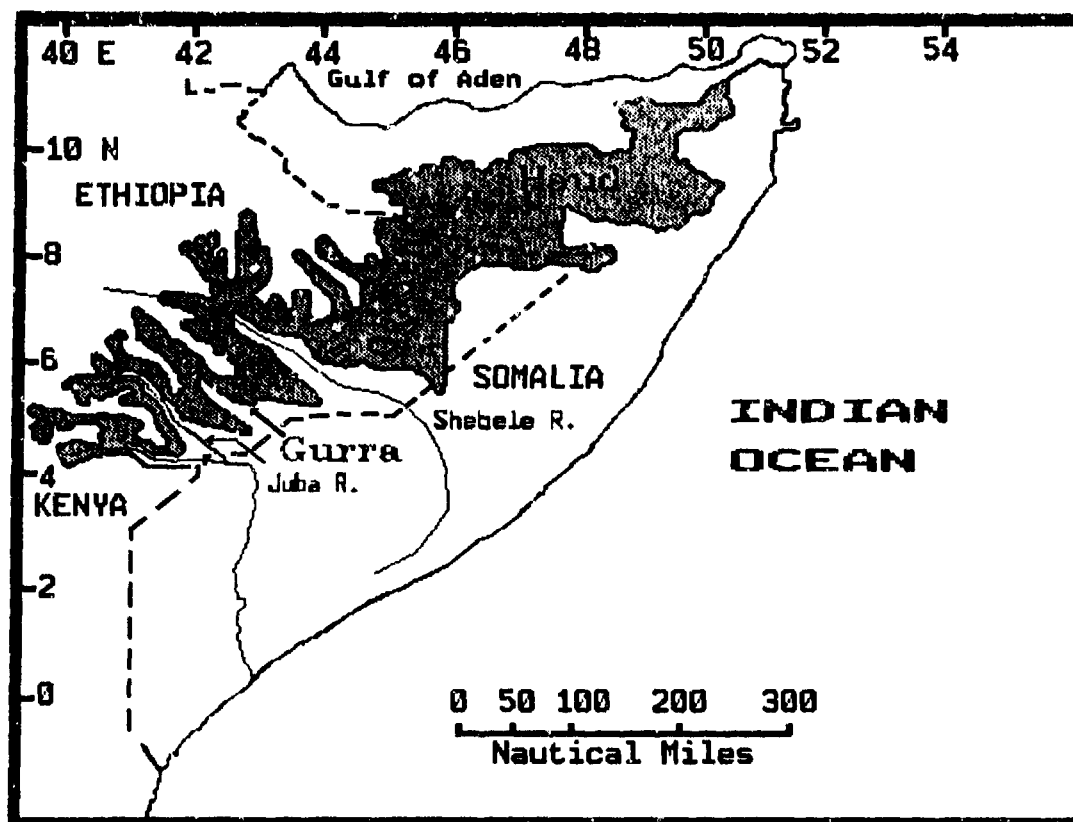


Figure 3-2c. The Elevated Western Plateau. This zone comprises highlands with elevations from 1,620 to 3,280 feet (500 to 1,000 meters).

The Elevated Western Plateau can be divided into three distinct plateau formations:

The Haud Plateau forms the southern foothills of the Ogo Highlands, an eastern range paralleling the Gulf of Aden. This is a level, largely alluvial plain that slopes gently southward. About 330 NM long and 100 NM wide, the plateau extends eastward to within 30 NM of the Indian Ocean near 9° N.

The Ogaden Plateau is 250 NM long (west to east) and 180 NM wide. Elevations average 1,620-3,000 feet (500-915 meters). It lies to the immediate south of the Haud Plateau, inside the borders of Ethiopia. Its southern and southwestern edges are defined by the Shebele River Valley.

The Gurra Plateau, in southeastern Ethiopia is bordered by the Shebele River valley on the north and the Juba River valley on the south.

RIVER SYSTEMS. The Shebele and Juba Rivers originate in the Mendebo Range of Ethiopia (7° N, 38° 30' E). They provide the only perennial water sources on the Indian Ocean Plain. Their courses run for 1,200 and 545 NM, respectively. The rivers parallel each other to within 30 NM of the Indian Ocean. They flow northwest to southeast toward the Somalia-Ethiopia border, then south through Somalia. The Juba (average width 500 feet/152 meters) flows into the sea at Chisimaio, while the Shebele (average width 200 feet/61 meters) turns abruptly southwestward 30 NM from the Indian Ocean coastline to run along the coastal dunes towards the Benadir lowlands. During wet seasons, the Shebele and Juba are connected by a wide flood plain. Both rivers cut broad, extensive valleys through the western plateaus. Below 1,620 feet (500 meters), they create natural levees along their banks that reach 33 feet (10 meters) in height. Numerous small depressions called "descecks" flank the river floodplains during wet seasons.

INDIAN OCEAN PLAIN

VEGETATION. The plateaus of the Indian Ocean Plain are primarily covered by open bush, with scattered deciduous trees. Savannah grasslands are concentrated south of 6° N, where adequate rainfall supports them. The dissected hills contain small shrubs and grass clumps. Intermittent stream beds and the Juba-Shebele

SITUATION AND RELIEF

River valleys contain scattered open woodland along the river edges. The coastal lowlands north of 8° N contain short grasses with isolated trees and brush. Southward towards the Kenya border, the land is grass-covered, with mangroves concentrated south of the Equator.

INDIAN OCEAN PLAIN SOUTHWEST MONSOON ("Hagal")

July-September

GENERAL WEATHER. The low-level Somali Jet (see Chapter 2) has the greatest single influence on Southwest Monsoon weather. The jet's daily position determines prevailing surface winds, cloud cover, and rainfall across the region. Instability showers near the jet axis are common south of 6° N, but moisture in the fast-moving flow is squeezed out before the jet leaves the Indian Ocean Plain near 11° N. Except for local land/sea breezes, southwesterly surface flow dominates.

SKY COVER. Moist southerly low-level flow convergence near the Somali Jet determines mean seasonal and diurnal cloud cover distribution. The daily jet position regulates cross-equatorial moisture across the entire region. Diurnal cloud cover distribution is determined by the jet's core speeds. A distinct nocturnal wind speed maximum produces patchy stratus and stratocumulus south of 6° N. These clouds often parallel the SSW-NNE Somali Jet axis and seldom extend to more than 20-30 NM on either side of the maximum wind speed core. Nocturnal cloud distribution decreases north of 6° N because of decreasing low-level moisture.

Mid-afternoon cloud cover is controlled by surface heating. Occasionally, morning stratus develops into stratocumulus with 2-6/8ths sky cover along the Somali Jet. Cloud cover decreases rapidly along the jet axis north of Galcaio, Somalia, where very dry air aloft inhibits development. Midday sea breeze cumulus and patchy stratocumulus develop along the immediate coastline north of Mogadishu; to the south, the coastline is often clear. Shallow cumulus bands are aligned north to south farther inland where the Somali Jet enters the southern Indian Ocean Plain. These cloud bands result from sea breeze moisture convergence with Somali Jet flow over land. Cumulus mixed with stratus and stratocumulus covers 4 to 6/8ths before 1000-1100 LST. By late afternoon, coverage averages 1 to 3/8ths.

Figure 3-3 shows large variations in north-south cloudiness. Mean cloudiness is better than 55% in the south, but less than 45% in the north. Midday cloud cover (1100-1500 LST) dominates in the north, but there is extensive cloud cover around the clock in the south--up to 71% at Chisimaio--due to persistent low-level instability in the Somali Jet.

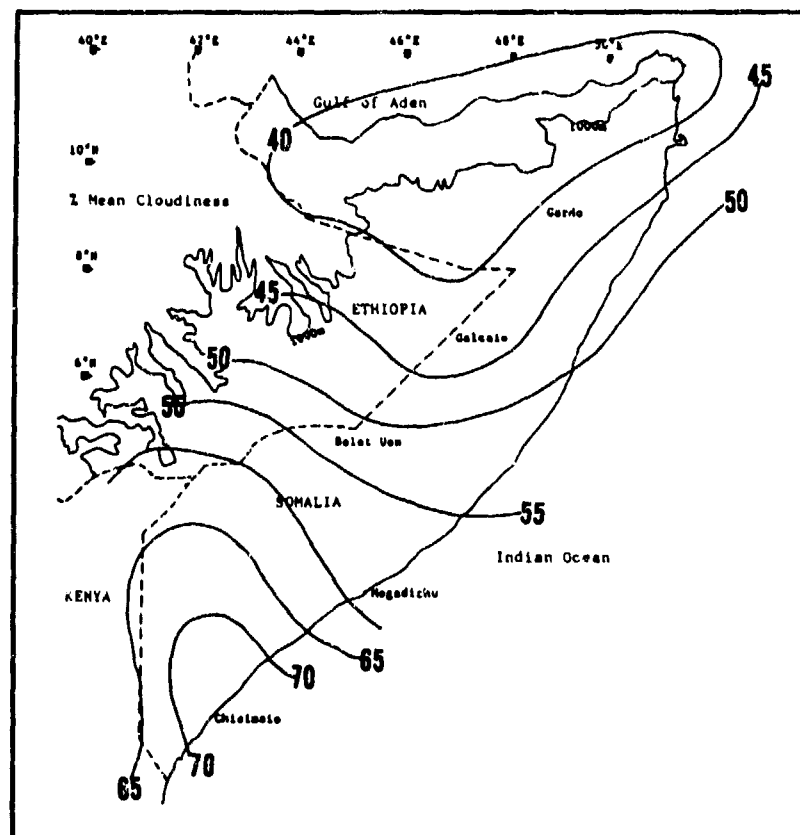


Figure 3-3. Mean Southwest Monsoon Cloudiness Frequencies, Indian Ocean Plain. Isolines are in 5% intervals. Data was derived by calculating the grand mean for National Intelligence Summary (NIS) mean cloudiness percentages for specific sites between July and September.

INDIAN OCEAN PLAIN **SOUTHWEST MONSOON ("Hagal")**

July-September

Predominant Southwest Monsoon cloud types are stratus and stratocumulus. Bases average 1,000-3,000 feet (305-915 meters) AGL; tops are 3,000-5,000 feet (915-1,524 meters) MSL. Diurnal convection produces isolated cumulus with 3,000-foot (915-meter) bases and 5,000-to 6,000-foot (1,524-to 1,830-meter) tops near the Somali Jet. Towering cumulus rarely develops over land. Dry air aloft and subsidence may inhibit vertical cumulus growth. Low-level shear along the jet may also prevent substantial cumulus development. Most high cloudiness approaches the coast from the east, and the

interior from the west or east. Both are the result of thunderstorm "blow-off" from heavy convection over the Indian Ocean and the eastern Ethiopian Highlands, respectively.

Percent frequency distributions of ceilings below 3,000 feet (915 meters) in Figure 3-4 show a distinct daytime low ceiling maximum north of Belet Uen, and a slight diurnal increase at Chisimaio. At Mogadishu, low ceiling frequencies are greater at night.

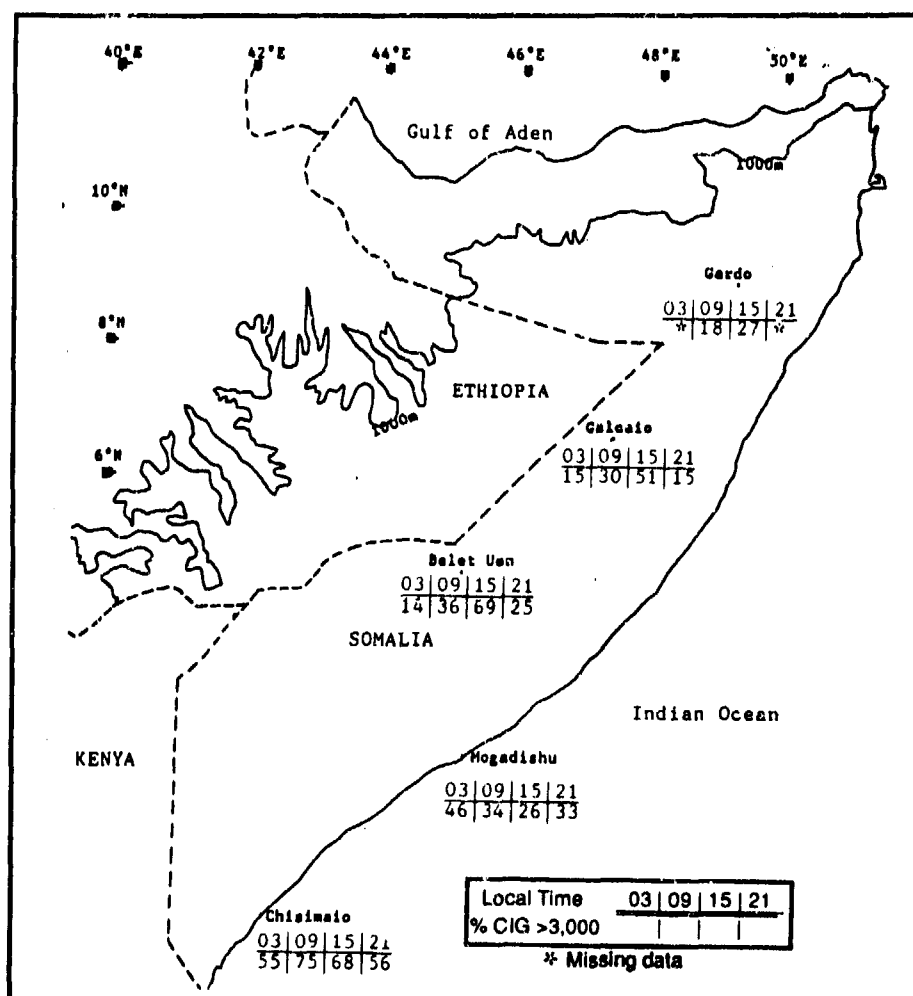


Figure 3-4. Southwest Monsoon Frequencies of Ceilings Below 3,000 Feet (915 meters), Indian Ocean Plain.

VISIBILITY. High frequencies of low visibility (Figure 3-5) are associated with duststorms or heavy rainshowers over the interior. On the coast from Mogadishu to Ras Hafun, shallow nocturnal marine inversions and thick

localized sea fog, mist, or haze account for most visibilities below 3 miles. Strong upwelling produces a seasonal temperature contrast between the sea (74-80°F/24-26°C) and the land (78-83°F/26-27°C).

INDIAN OCEAN PLAIN **SOUTHWEST MONSOON ("Hagal")**

July-September

Dense early morning sea fog forms off the coast as a result of the nocturnal land breeze, then moves inland with the sea breeze. These fogs can be thick along the entire coastal region, extending, in rare cases, as far inland as 200 NM.

Blowing dust/sand is common with surface winds greater than 15 knots. The highest occurrence of dust-related low visibilities is in July and August when the Somali Jet is strongest. Localized duststorms

frequently lower visibility to less than 2 1/2 miles north of 6° N due to the much drier surface conditions there.

More than half the low visibilities at Belet Uen are dust/sand related but moderate to heavy rain/rainshowers are also common south of 6° N. Fog and occasional haze are reported in only 5% of all observations beyond 30 NM inland. Low visibility in rain or rainshowers is uncommon north of 6° N.

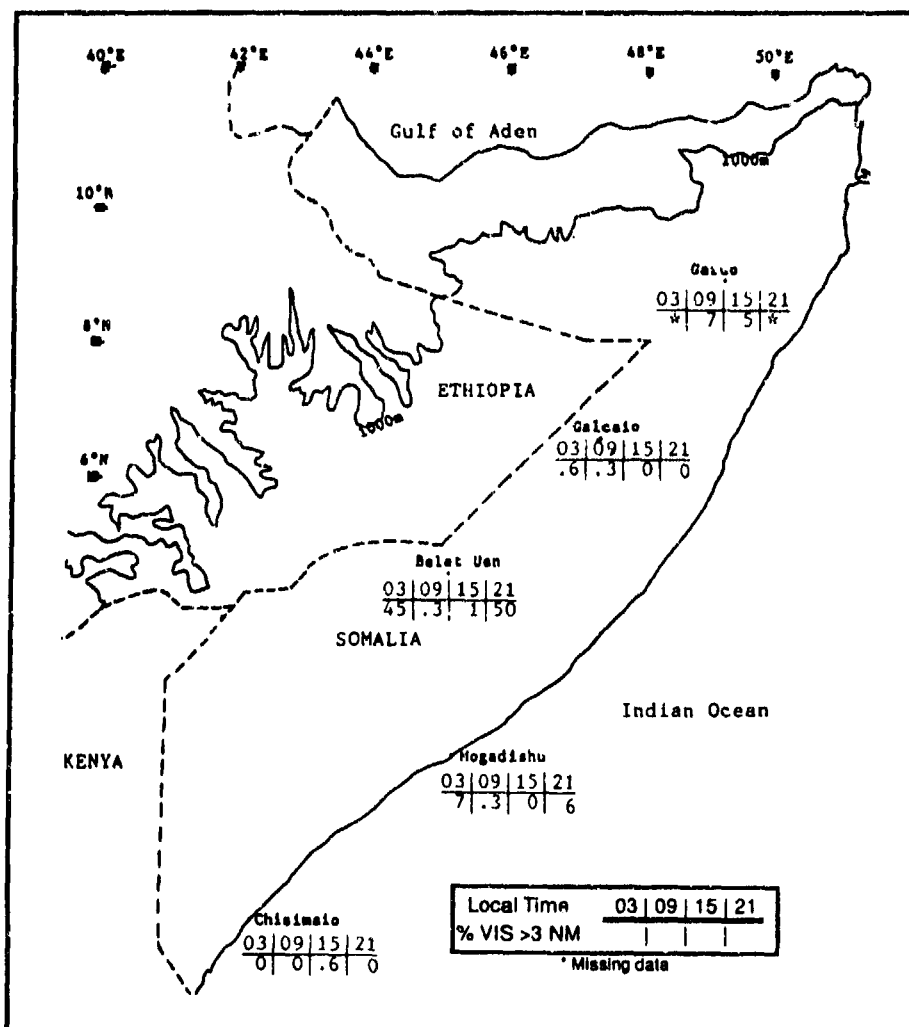


Figure 3-5. Southwest Monsoon Frequencies of Visibilities Below 3 Miles, Indian Ocean Plain.

WINDS. Mean surface wind speed and direction reflect the Somali Jet's dominance. Figure 3-6 shows mean surface wind speeds and prevailing directions shown in at least 85% of all surface observations for the entire Southwest Monsoon season. Prevailing winds veer from southerly at Chisimaio (0° 22' S, 42° 26' E) to west and

southwesterly at Gardo (9° 31' N, 49° 05' E). There is a noticeable speed maximum in August. The strong, dry, and hot southwesterlies at Galkaio (6° 51' N, 47° 16' E) and Gardo also support moisture depletion at low levels and result in higher duststorm frequencies.

INDIAN OCEAN PLAIN
SOUTHWEST MONSOON ("Hagel")

July-September

SSE-SSW
WSW-S
WSW-S
W-SW

	JUL	AUG	SEP
Chisimaio	9.90	10.50	9.60
Isola Baldoa	10.00	10.70	10.00
Galeaio	24.70	24.20	18.30
Gardo	20.80	22.10	15.50

Figure 3-6. Mean July-September Wind Speed (kts) and Prevailing Direction, Indian Ocean Plain.

Jet core wind speeds average 25-35 knots, but may exceed 70 knots for 12- to 36-hour periods. Core heights are extremely variable because the flow is sensitive to terrain and thermal energy exchanges. Jet core oscillations of 1,000-2,000 feet (305-610 meters) over 200 NM are common. Typically, the broad southerly current is found between 3,000-7,000 feet (915-2,134 meters) with one or more wind speed maxima.

The inadequate upper-air data network in this region is supplemented by the mean wind direction profile at Mandera, Kenya ($3^{\circ} 54' N$, $41^{\circ} 52' E$), on the Kenya-Somalia-Ethiopia border. Mean annual winds here (shown in Figure 3-7) provide an accurate representation of conditions below 500 millibars over the entire Indian Ocean Plain. Note the south to southwesterly flow at all levels in July. Mean Southwest Monsoon wind speeds are shown for each level.

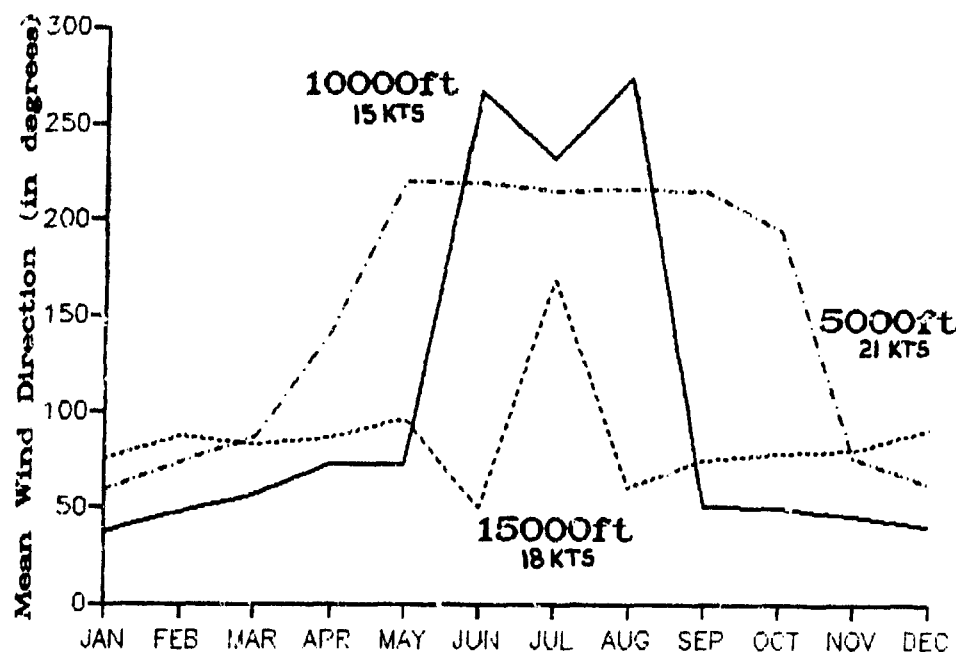


Figure 3-7. Mean Annual Wind Direction for Mandera, Kenya.

INDIAN OCEAN PLAIN **SOUTHWEST MONSOON ("Hagal")**

July-September

PRECIPITATION. The Somali Jet establishes a low-level south to north moisture gradient across the region throughout the Southwest Monsoon. The jet core and sufficient tropical moisture near the equator are the main reasons for a wet Southwest Monsoon season south of 5° N (Figure 3-8).

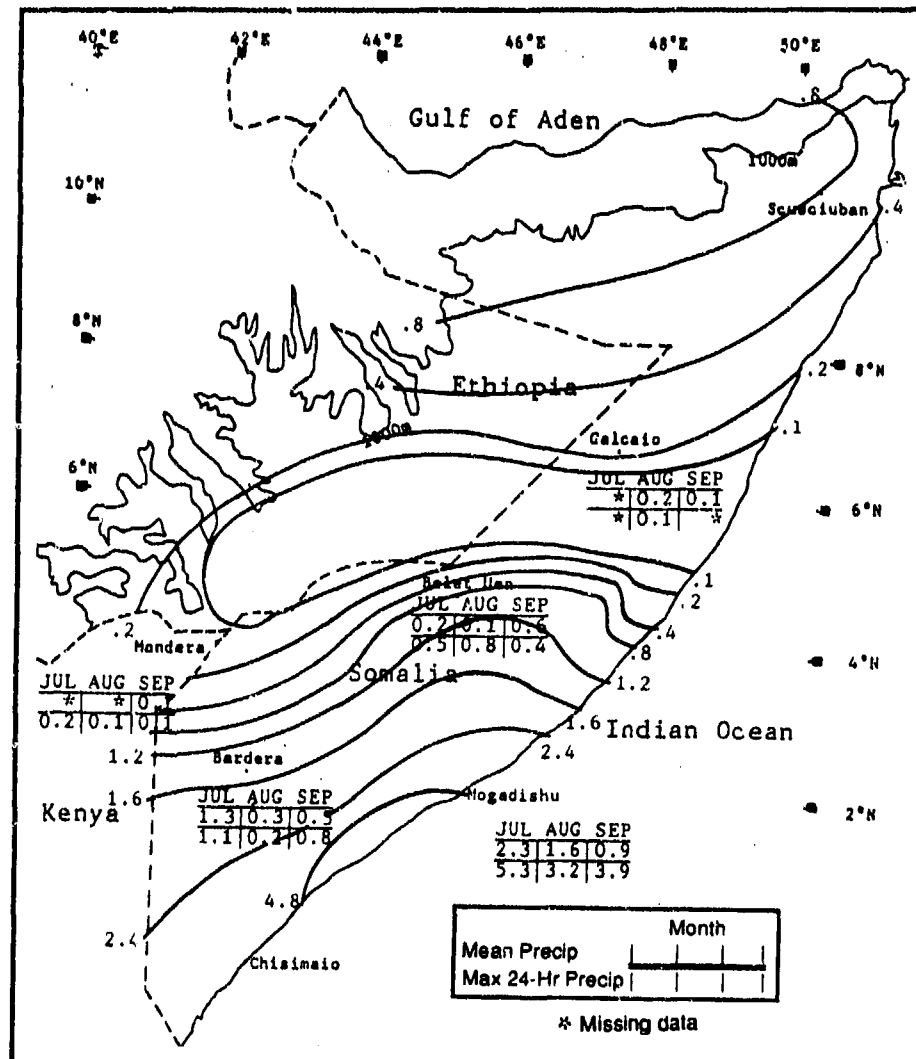


Figure 3-8. Mean Southwest Monsoon Monthly/Maximum 24-Hour Precipitation, Indian Ocean Plain. Isohyets represent mean seasonal rainfall totals (inches).

Southwest Monsoon precipitation usually occurs beneath the zone of maximum winds, as shown in Figure 3-9. However, equatorial moisture and rainfall decrease significantly north of the jet core. Sea breezes help support standing convection lines (oriented southwest-to-northeast along the jet axis) south of 5° N. Storm movement is northeasterly, with moderate to heavy rainfall concentrated in narrow bands. These

convection lines often form 10-20 NM east of the Great Rift System--mountain ranges immediately south of the Equator in Kenya--but dissipate before reaching 6° N. South of Mogadishu, moist sea breezes cause inland convection during daylight hours, with individual cells moving NNE at 15-30 knots. These convective cells are often sheared by the Somali Jet.

INDIAN OCEAN PLAIN
SOUTHWEST MONSOON ("Hagal")

July-September

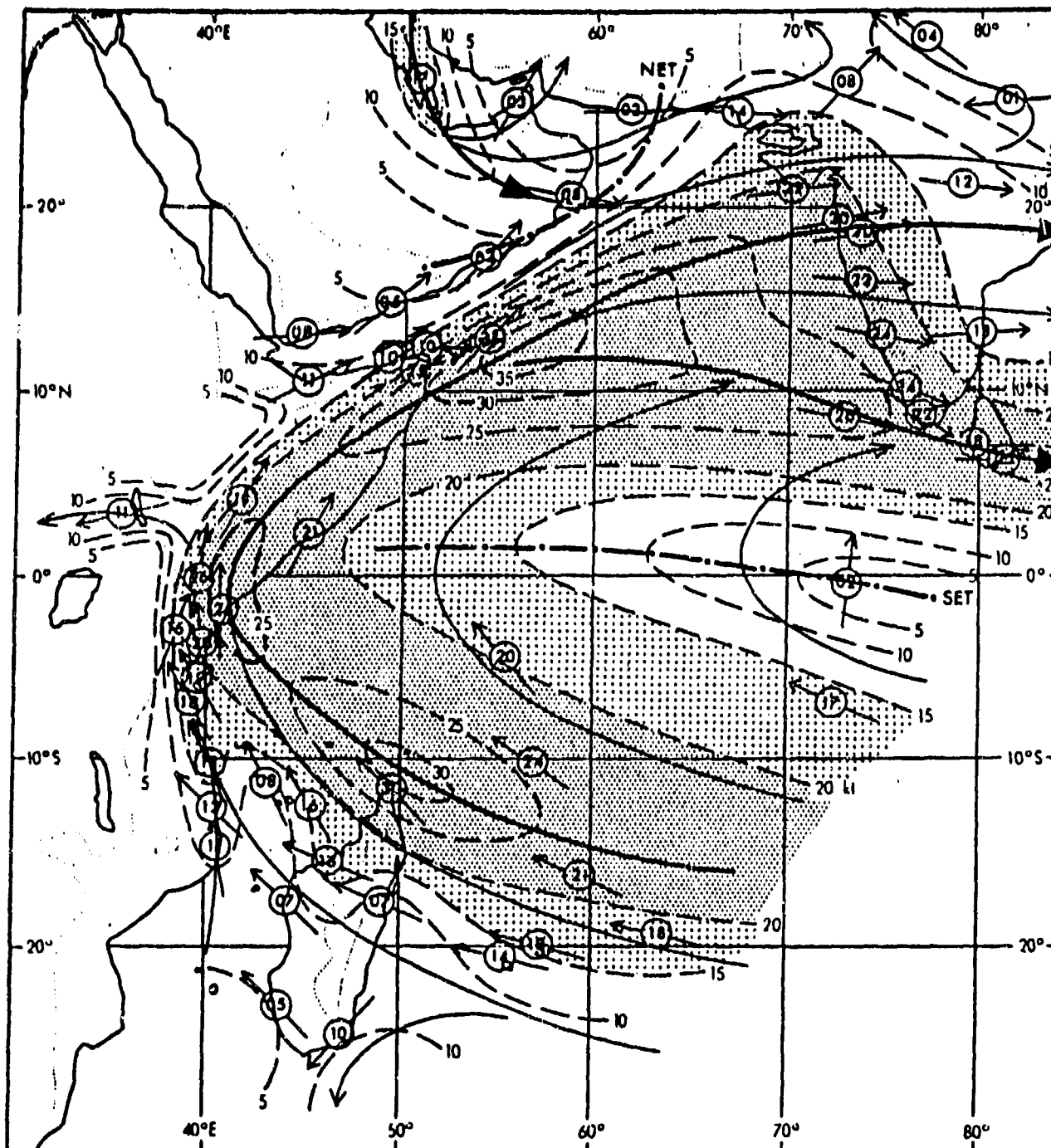


Figure 3-9. Mean July Flow Pattern at 3,000 Feet (915 meters) AGL (from Findlater, 1970). Speeds are in knots. Note that the Southern Equatorial Trough (SET) lies just east of the Somali coastline between Chisimaio and Mogadishu. See Chapter 2 for more on the SET.

INDIAN OCEAN PLAIN **SOUTHWEST MONSOON ("Hagal")**

July-September

North of 5-6° N, the Southwest Monsoon becomes a "dry" season because of upwelling along the Somalian coastline and a reduced sea breeze effect. The "dry" Somali Jet produces little cloud cover of significance. Deep convection and thunderstorm activity are rare as convergence aloft and large-scale subsidence cap the shallow cumulus. Maximum 24-hour rainfalls are associated with thunderstorms. Thunderstorm development occurs with either isolated squall lines or weakly organized tropical disturbances propagating westward along the Southern Equatorial Trough (SET) shown in Figure 3-9. Southern hemisphere polar surges (see Chapter 2) that intensify Somali Jet flow into the Indian Ocean Plain may also trigger isolated thunderstorm activity.

TEMPERATURE. The high (55-71%) Southwest Monsoon mean cloud cover frequency, along with

continentality--the degree to which a climate has continental qualities--regulate temperatures. Coastal locations in the cool sea breeze boundary layer average 82-88°F (28-31° C), while continental (inland) sites average 90-102°F (32-39°C). Highs reach 108°F (42°C) inland and north of 6° N, while the lowest record high along the coast is only 87°F (31°C), at Chisimaio. Inland daytime temperatures vary with latitude from day to day because the Somali Jet distributes a narrow (50-150 NM wide) SSW-NE cloud band. South of 6° N, mean daily highs are at their lowest of the year during the Southwest Monsoon.

Average lows range from 70°F (21°C) at Bardera to 77°F (25°C) at Scusciuban. A low of 59°F (15°C) at Mogadishu has occurred in July, but lows near 72°F/22°C at Chisimaio in September are more common south of 6° N.

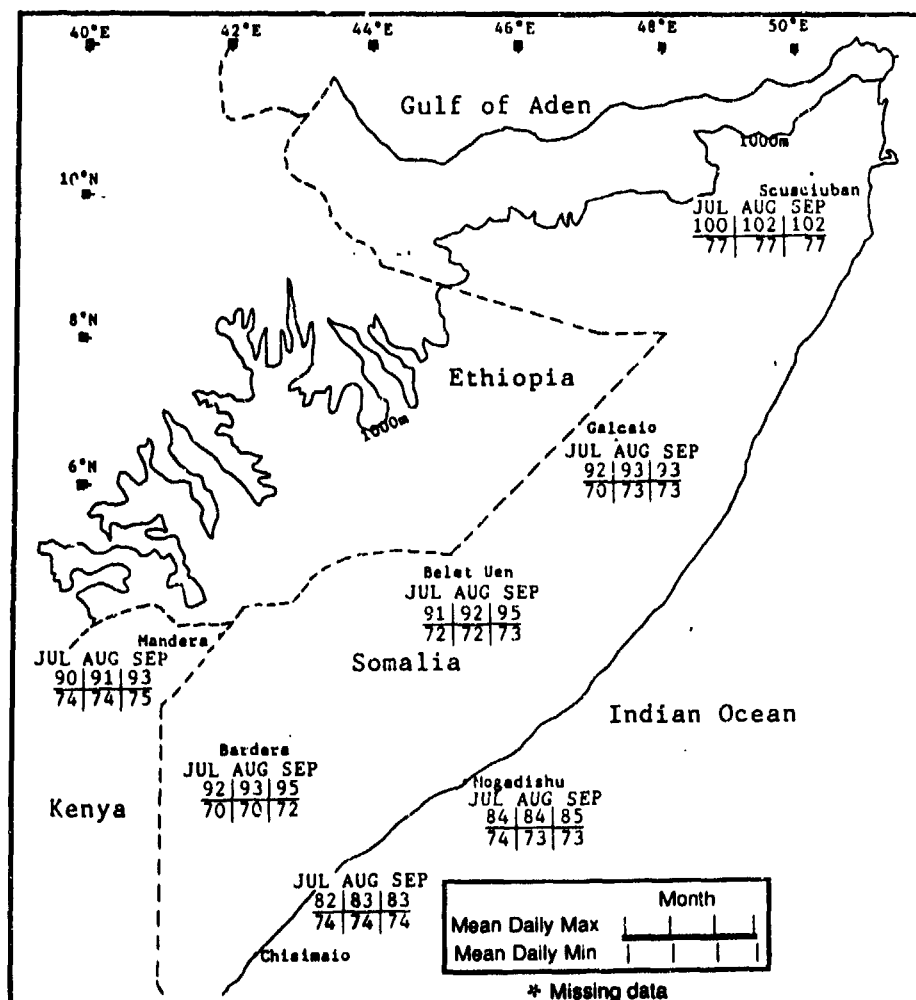


Figure 3-10. Mean Southwest Monsoon Daily Maximum/Minimum Temperatures (°F), Indian Ocean Plain.

INDIAN OCEAN PLAIN

SOUTHWEST TO NORTHEAST MONSOON TRANSITION ("Der")

October-November

GENERAL WEATHER. The transition from the Southwest to the Northeast Monsoon (locally, "Der," or "short rains") is marked by the cessation of cross-equatorial flow into the region. In October, southerly low-level flow weakens north of 4° N. As shown in Figure 3-11, mean maximum winds in the Somali Jet core shift to south of the equator. Weather associated with the jet occurs near the equator. The surface Monsoon Trough moves rapidly southward

without sustained southerly flow to support its previous Southwest Monsoon seasonal position. Northeasterly flow along the Monsoon Trough's north axis begins to advance into the northern Indian Ocean Plain when the Trough oscillates equatorward. A brief wet season ("the short rains") occurs as the Trough moves quickly through the region. By November, only the extreme southern Indian Ocean Plain has not been affected by Northeast Monsoon flow.

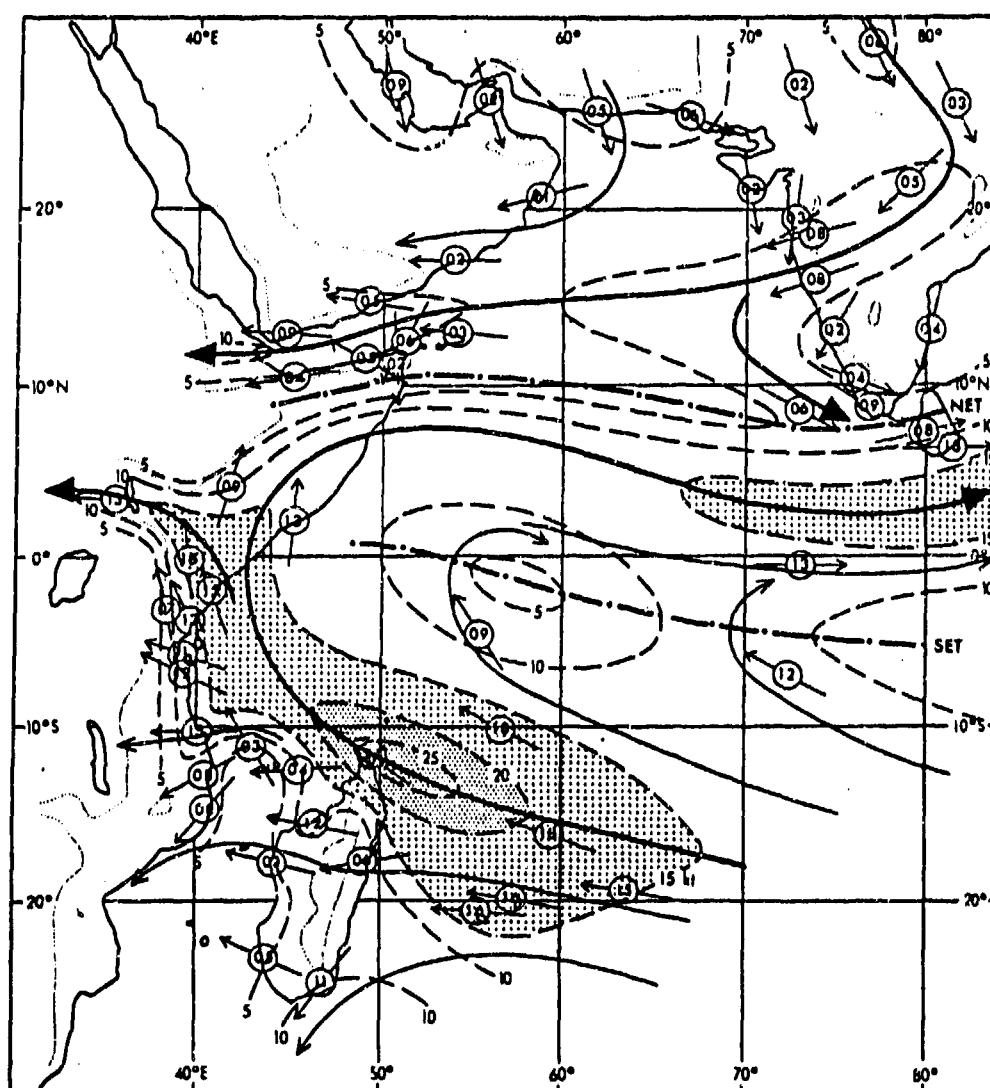


Figure 3-11. Mean October Flow Pattern at 3,000 Feet (915 meters) AGL (from Flindater, 1971). Speeds are in knots.

INDIAN OCEAN PLAIN

SOUTHWEST TO NORTHEAST MONSOON TRANSITION ("Der")

October-November

SKY COVER. Mean cloudiness on the Indian Ocean Plain (Figure 3-12) is dependent on the Somali Jet and the Monsoon Trough. Highest mean cloudiness (greater than 60 percent) during the transition is oriented SSW-NNE from the Kenyan border to 5° N, 42-46° E. Cloud cover is typically stratus, stratocumulus, and isolated cumulus. Mean cloud cover decreases

northeastward where the Somali Jet lacks sufficient moisture for stratus and dense stratocumulus development. North of 5° N, mean cloudiness is less than 50 percent; sky cover is mostly shallow midday cumulus generated through intense diurnal surface heating.

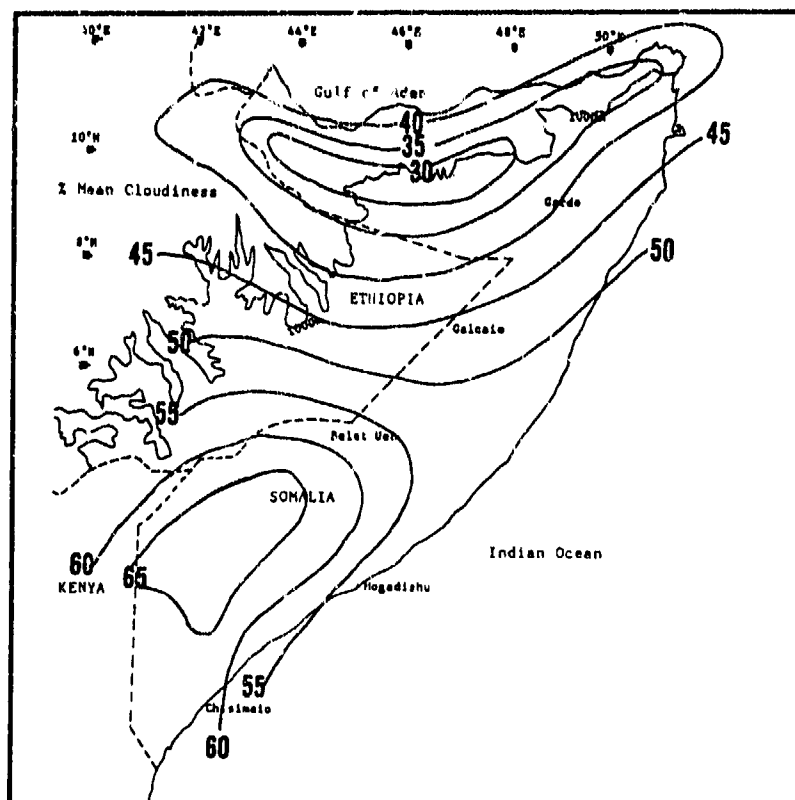


Figure 3-12. Mean SW/NE Monsoon Transition Cloudiness Frequencies, Indian Ocean Plain. Isolines are in 5% intervals. Data was derived by calculating the grand mean from National Intelligence Summary (NIS) mean cloudiness data for specific sites during October and November.

North of 5° N, shallow cumulus cover averages 4/8ths between 0900-1500 LST. Cover is 2/8ths or less at all other times over the interior. Thin cirrus from thunderstorm "blowoff" in the Ethiopian Highlands is often seen over the Ogaden Plateau. Although deep convection forms along the Monsoon Trough, it is concentrated 100-200 NM offshore and rarely reaches the northern Indian Ocean Plain coastline. Coastal sea breeze stratus and stratocumulus (3-5/8ths coverage) occurs from 0600 to 0900 LST. These clouds seldom penetrate more than 20 NM inland. All clouds normally dissipate by 1000 LST.

South of 5° N, early morning stratus and stratocumulus develop in the sea breeze boundary. South of Mogadishu, sea breeze moisture often interacts with Somali Jet low-level southerly flow. In contrast, coastal locations north of Mogadishu are rarely affected by the jet core after early October. Skies are 6/8ths to overcast between 0600-1000 LST, but only 3/8-5/8ths between 1100-1500 LST because of the deep turbulent mixing below 5,000 feet (1,534 meters). North of Mogadishu, however, cloud cover is 3-5/8ths from 0600 to 1000 LST, decreasing to less than 2/8ths sky cover between 1100 and 1500 LST. Surface turbulence rapidly

INDIAN OCEAN PLAIN **SOUTHWEST TO NORTHEAST MONSOON TRANSITION ("Der")**

October-November

dissipates stratus/stratocumulus except immediately adjacent to the Somali Jet core or along a well-defined and unstable surface Monsoon Trough axis. Stratus bases are near 1,500 feet (457 meters), while bases of the thin scattered stratocumulus average 3,500-5,000 feet (1,067-1,524 meters). By 1100 LST, isolated cumulus with bases near 4,000-5,000 feet (1,220-1,534 meters) and tops to 8,000 feet (2,439 meters) develop inland near the Somali Jet.

Occurrence of broken-to-overcast ceilings at or below 3,000 feet (915 meters) across the Indian Ocean Plain averages 39%. Ceilings at or below 1,000 feet (305 meters) account for only 13% of all Indian Ocean Plain ceilings. Figure 3-13 gives diurnal low ceiling frequency differences for selected stations. The highest frequency of low ceilings is found between Chisimaio and Galcaio, an area that shows the mean transition position of the Somali Jet.

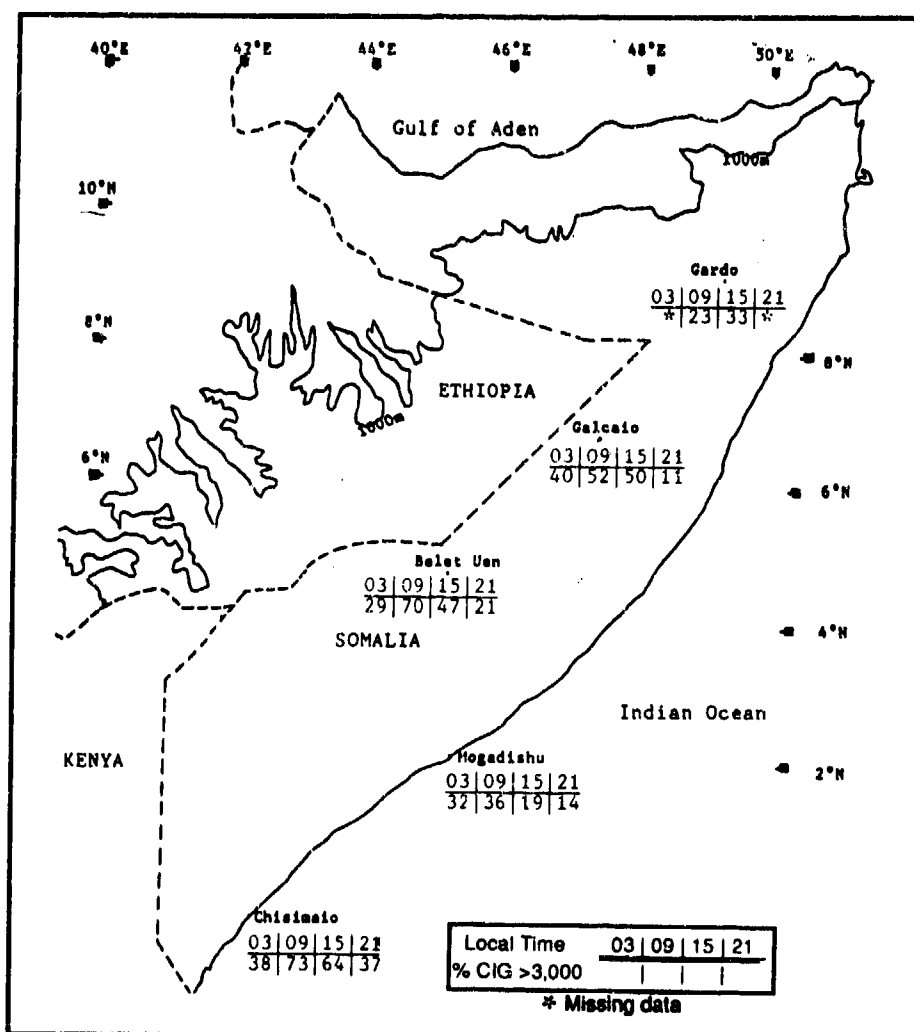


Figure 3-13. SW-NE Monsoon Transition Frequencies of Ceilings Below 3,000 Feet (915 meters), Indian Ocean Plain.

INDIAN OCEAN PLAIN **SOUTHWEST TO NORTHEAST MONSOON TRANSITION ("Der")**

October-November

VISIBILITY. Precipitation is the main obstruction to vision during the transition; at least 72% of all visibilities below 3 miles are in rain and/or rainshowers. Because of the wetter soil, blowing dust/sand causes only 13% of all reported low visibilities. Fog is most frequent at Belet Uen, while mist/haze is more frequent at Mogadishu.

Radiation inversions and local terrain make ground fog at Belet Uen common between 2100-0300 LST, while mist/haze frequencies at Mogadishu reduce visibility to less than 3 miles about 10-14% of the time between 2100-0300 LST. Figure 3-14 gives low visibility occurrence frequency at selected stations.

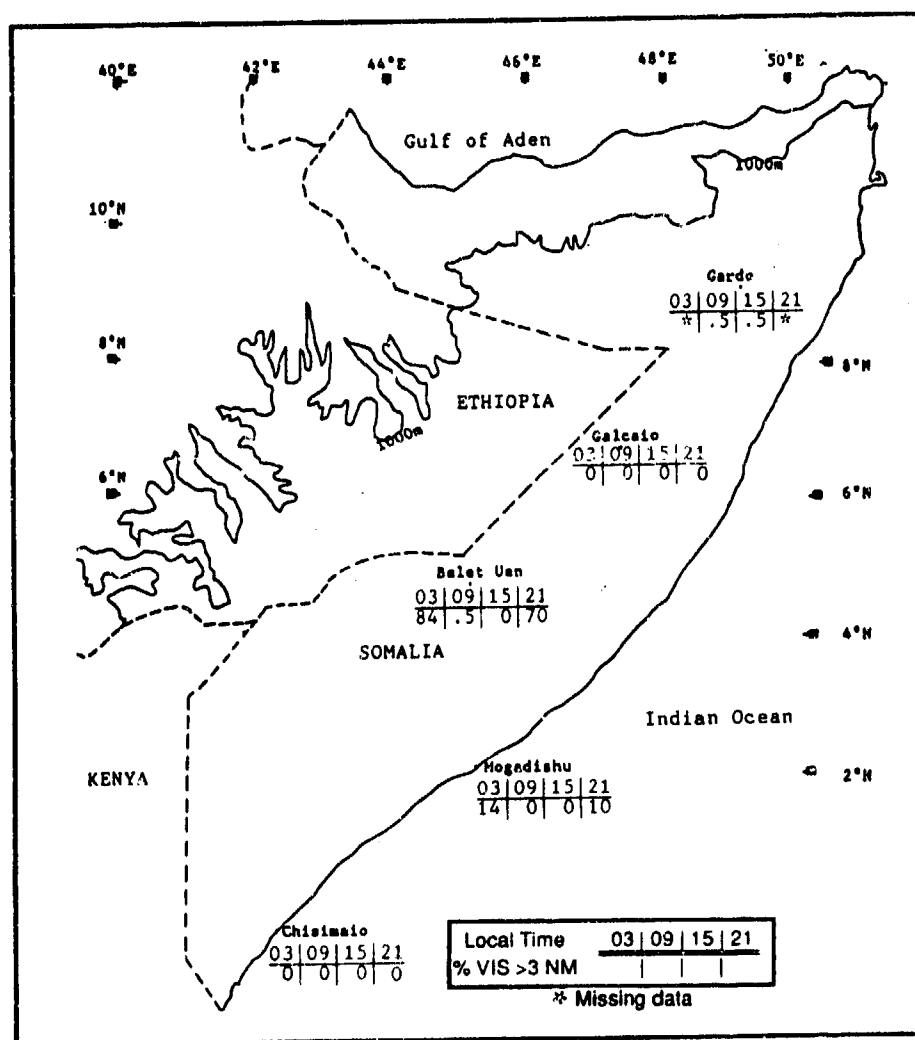


Figure 3-14. SW-NE Monsoon Frequencies of Visibilities Below 3 Miles, Indian Ocean Plain.

INDIAN OCEAN PLAIN**SOUTHWEST TO NORTHEAST MONSOON TRANSITION ("Der")****October-November**

WINDS. Mean surface wind speed and direction (Figure 3-15) illustrates several important transition flow characteristics. During the transition, mean wind speeds are decreased at all locations, reflecting the weakening of the Somali Jet. At Chisimaio and Iscia Baidoa, south to east flow decreases slightly through the transition, but speeds at Galcaio and Gardo--3-4 times less than those of the Southwest Monsoon shown in Figure 3-6--show a

slight increase from October to November as Northeast Monsoon flow begins to affect these two northern Indian Ocean Plain stations. Note that prevailing directions at Gardo are E and NE, while Galcaio flow is SW and SE in October, E and NE in November. The surface wind shift shows the surface Monsoon Trough axis moving southward from Galcaio/Gardo (7-9° N) in October to Galcaio/Ischia Baidoa (3-7° N) by late November.

S-E
S-E
SW-SE/E-NE
E-NE

	OCT	NOV
Chisimaio	8.60	7.00
Ischia Baidoa	7.20	5.50
Galcaio	7.30	7.70
Gardo	5.90	6.40

Figure 3-15. Mean October-November Wind Speed (kts) and Prevailing Direction, Indian Ocean Plain.

INDIAN OCEAN PLAIN **SOUTHWEST TO NORTHEAST MONSOON TRANSITION ("Der")**

October-November

PRECIPITATION. The "Der" (or "short rains") season consists of instability showers concentrated in low-level wind convergence zones. Localized showers often develop near the Monsoon Trough, with northeasterly winds at 5-8 knots. There are also showers at the northern tip of the Somali Jet, where winds are southerly at 15-20 knots.

North of 6° N, October rainfall is 4-20 times greater than in September (late in the Southwest Monsoon), as

the Monsoon Trough and the mean Somali Jet wind maximum migrate through the area together.

Instability moves rapidly equatorward by mid-November as the Somali Jet weakens considerably. November rainfall distributions follow the southward migration of both features. As shown in Figure 3-16, only Chisimaio is affected by instability and rainfall in November because of its proximity to the surface Monsoon Trough axis.

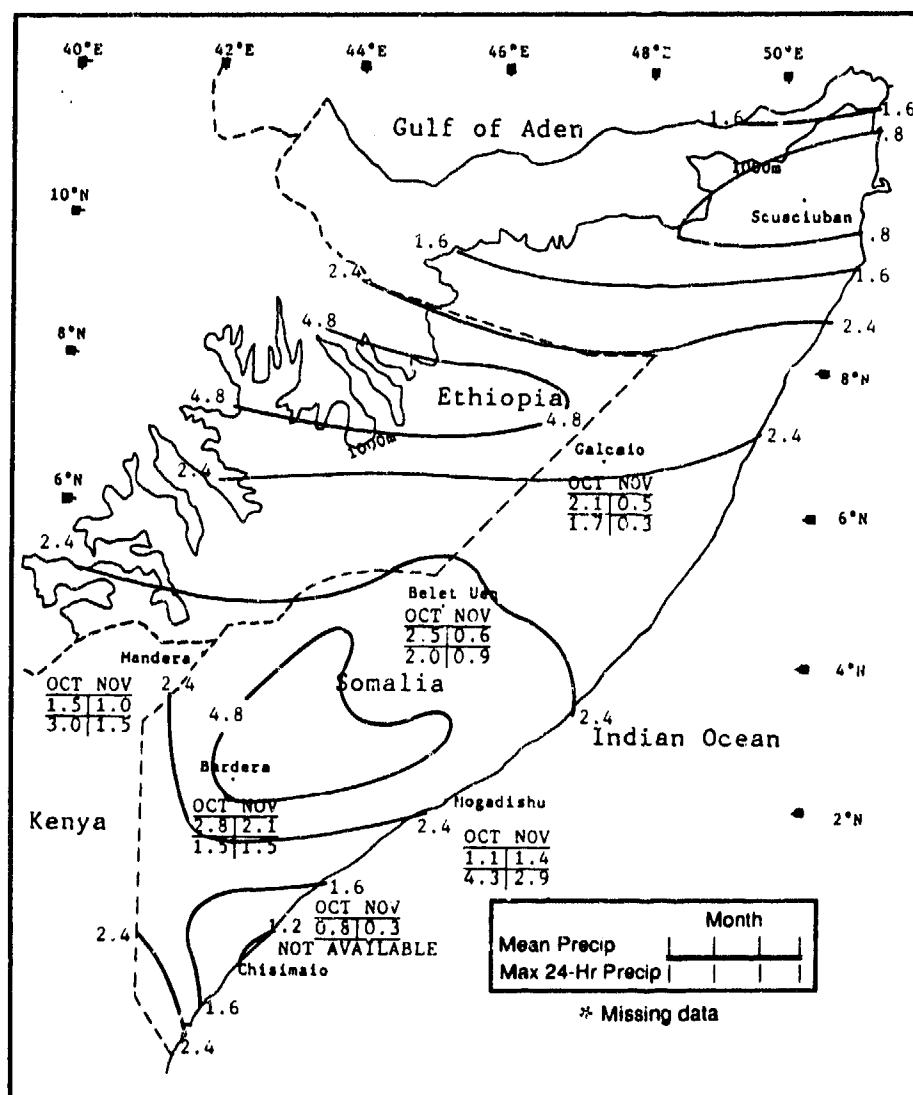


Figure 3-16. Mean SW/NE Monsoon Transition Monthly/Maximum 24-Hour Precipitation, Indian Ocean Plain. Isohyets show mean seasonal rainfall totals (inches).

INDIAN OCEAN PLAIN **SOUTHWEST TO NORTHEAST MONSOON TRANSITION ("Der")**

October-November

TEMPERATURE. Mean daily highs range from 85°F (29°C) at Chisimaio to 97°F (36°C) at Bardera. Daily highs are 5-9°F (3-5°C) cooler on the coast than in the interior. Absolute highs have reached 107°F (42°C) at Bardera, but only 89°F (32°C) at Chisimaio. Mean daily November lows average 66°F (19°C) at Scusciuban, and

up to 76°F (24°C) at Chisimaio. An extremely rare mid-latitude cold front resulted in Scusciuban's absolute low of 57°F (14°C). The absolute low of 73°F (23°C) at Chisimaio shows the Indian Ocean's ability to moderate coastal locations. Figure 3-17 gives mean daily highs and lows for selected stations on the Indian Ocean Plain.

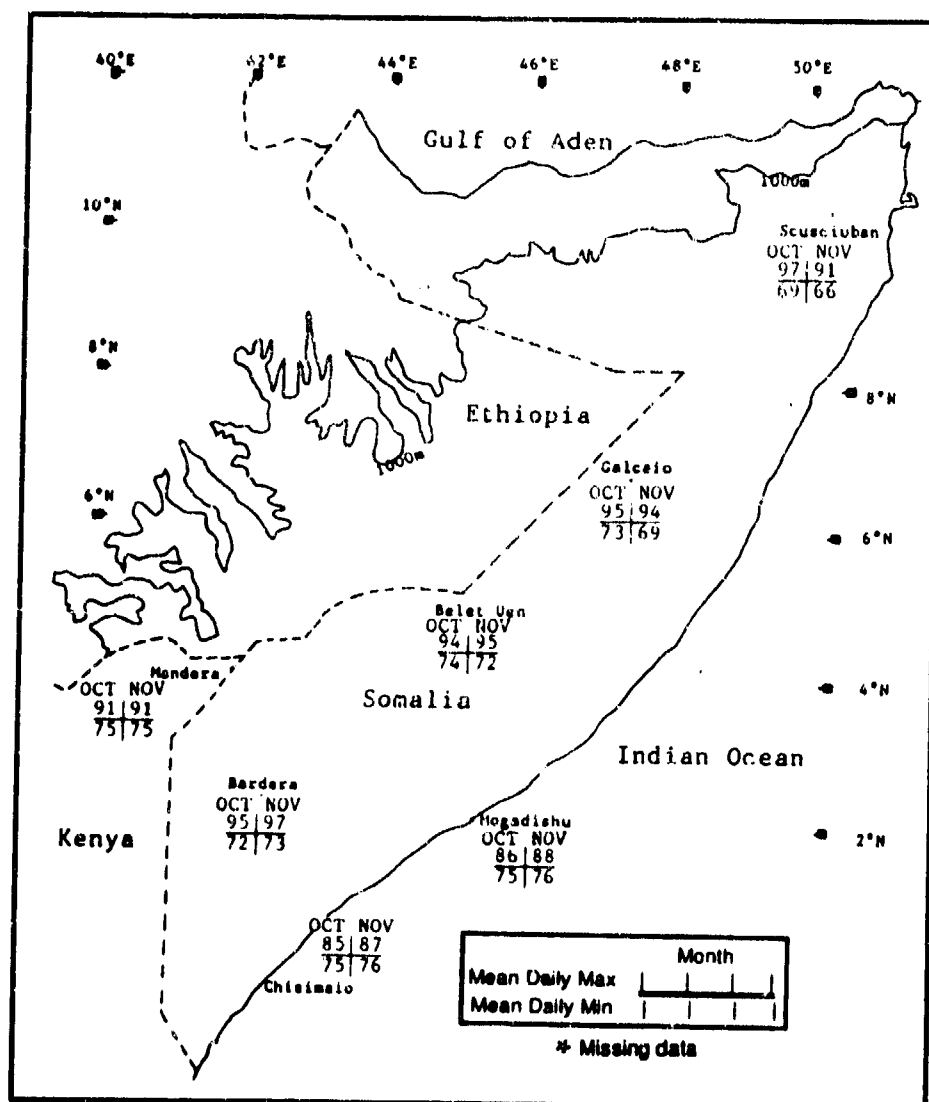


Figure 3-17. Mean SW/NE Monsoon Transition Daily Maximum/Minimum Temperatures (°F), Indian Ocean Plain.

INDIAN OCEAN PLAIN NORTHEAST MONSOON ("Gital")

December-March

GENERAL WEATHER. Northeast Monsoon flow results in the southward migration of dry conditions across the Indian Ocean Plain. The northeasterly flow converges into the surface Monsoon Trough--the only weather-producer of significance--and strengthens through February. Initially, moderate (7-11 knots) northeasterly surface flow sweeps over the northern Indian Ocean Plain in December, but doesn't reach the Equator with similar force until February. As a result, surface Monsoon Trough instability is located near and south of the Equator. Rainfall is irregularly distributed along the Monsoon Trough, which is oriented west to east; instability rarely remains stationary for more than 12 hours. Brief, southward-moving showers are typical Northeast Monsoon features. Locations affected by Monsoon Trough instability receive light showers for only 1-3 weeks during each Northeast Monsoon season.

SKY COVER. Northeasterlies dominate the entire region except for weak low-level easterly flow south of the Equator. Northeasterly flow, nearly parallel to the

coastline, results in limited moisture transport from ocean to land, and there is less overall cloud development. Generally, skies are clear to partly cloudy, with no more than 3/8ths coverage. If daytime surface heating is accentuated by light northeast breezes, fair weather cumulus develops by 1400 LST and thickens to 4/8ths coverage; bases are at 2,500-3,000 feet (762-915 meters), and tops to 8,000 feet (2,439 meters). Cirrus above 15,000 feet (4,573 meters) is also of the "fair weather" variety. All clouds dissipate by sunset.

Mean cloudiness at the selected stations shown in Figure 3-18 reflects the Northeast Monsoon's southward migration. Highest mean cloudiness--greater than 55 percent--is concentrated south of 2° N. December and March cloud cover is greatest because of weak cross-equatorial flow, a strong sea breeze, and the presence of abundant equatorial moisture. In January and February, Northeast Monsoon circulation extends to the Equator.

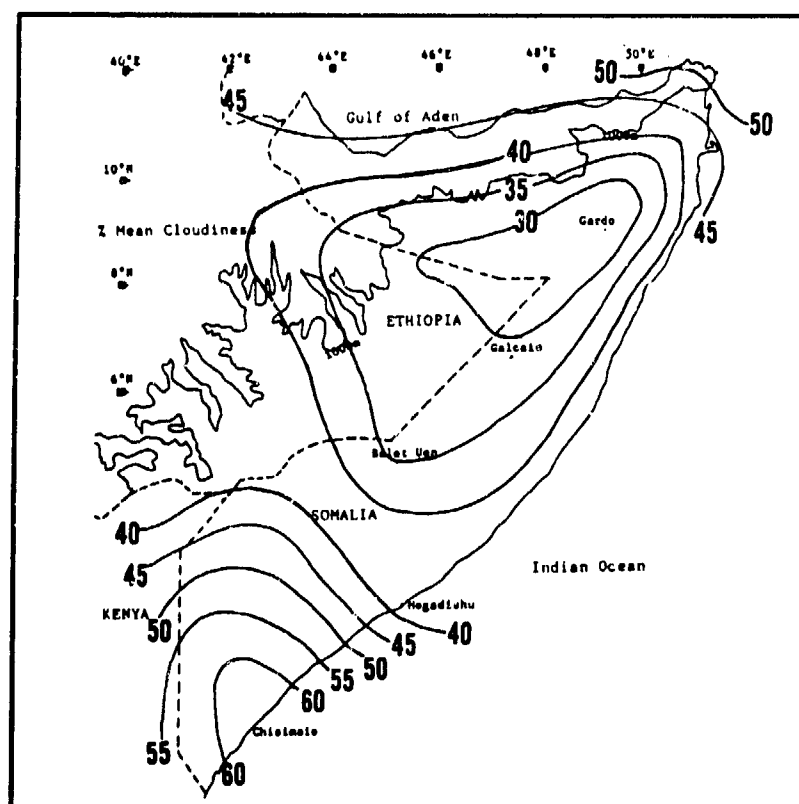


Figure 3-18. Mean Northeast Monsoon Cloudiness Frequencies, Indian Ocean Plain. Isolines are in 5% intervals. Data was derived by calculating the grand mean from National Intelligence Summary (NIS) mean cloudiness data for specific sites between December and March.

INDIAN OCEAN PLAIN **NORTHEAST MONSOON ("Gillal")**

December-March

Frequency of ceilings below 3,000 feet (915 meters) averages 20%, but ceilings at or below 1,000 feet (305 meters) average only 3%. Low ceilings at Chisimaio result from stratus/stratocumulus decks; cumulonimbus

may be embedded during disturbed weather periods. Figure 3-19 gives frequency of ceilings below 3,000 feet at selected Indian Ocean Plain stations.

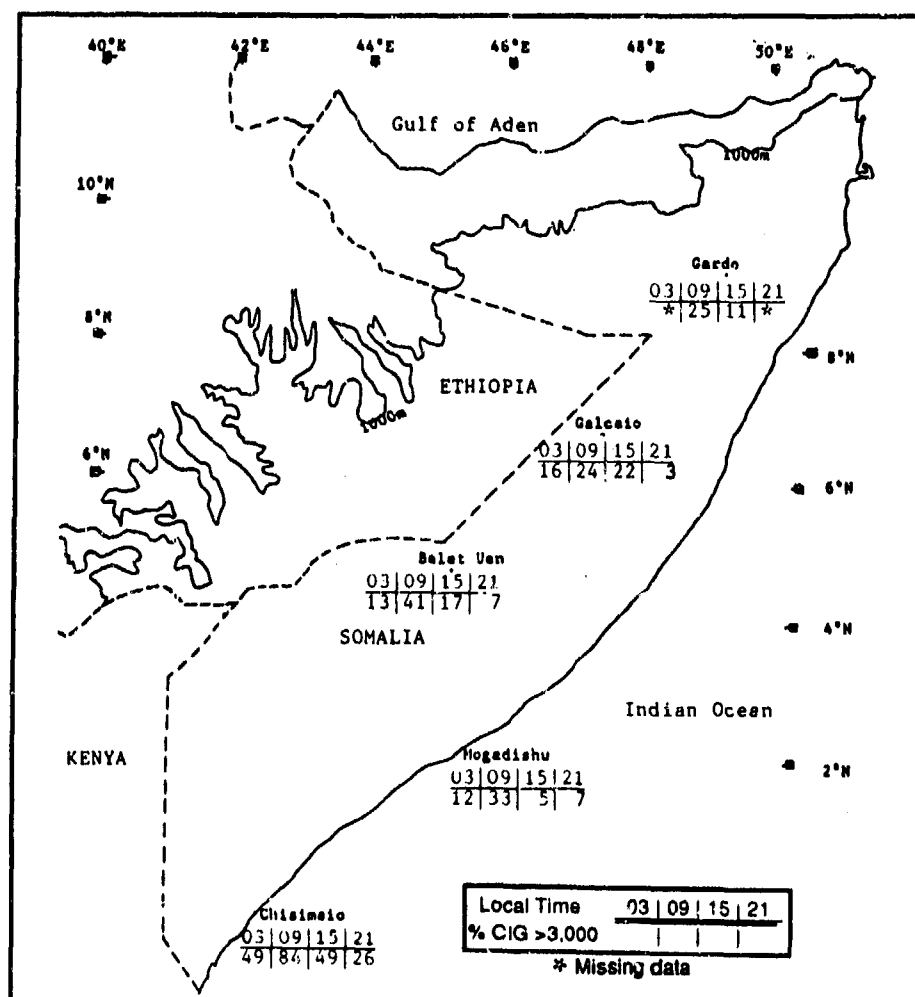


Figure 3-19. Northeast Monsoon Frequencies of Ceilings Below 3,000 Feet (915 meters), Indian Ocean Plain.

VISIBILITY. The land/sea breeze circulation produces shallow sea fog, mist, and haze, but low visibility frequencies in fog are only 0-5%. Coastal fog frequency decreases from south to north. Dante, on the northern coast, rarely sees fog during the Northeast Monsoon. In December, visibilities below 3 miles occur with early morning ground/sea fog between Chisimaio and Mogadishu.

Dry weather and soil conditions inland allow blowing dust/sand to be the major obstruction to vision. Blowing

dust/sand accounts for visibilities below 3 miles in 79% of cases, except at Belet Uen, where a local moisture source (the Shebele River) produces fog and extremely high (55-85%) frequencies of visibility below 3 miles from 2100 LST through dawn. Located near an extensive lowland marsh, and with hills on three sides of the station, Belet Uen is in an ideal location for stable, calm evenings and fog formation. Figure 3-20 shows the relatively low frequency of low visibility across most of the Indian Ocean Plain.

**INDIAN OCEAN PLAIN
NORTHEAST MONSOON ("Gila")**

December-March

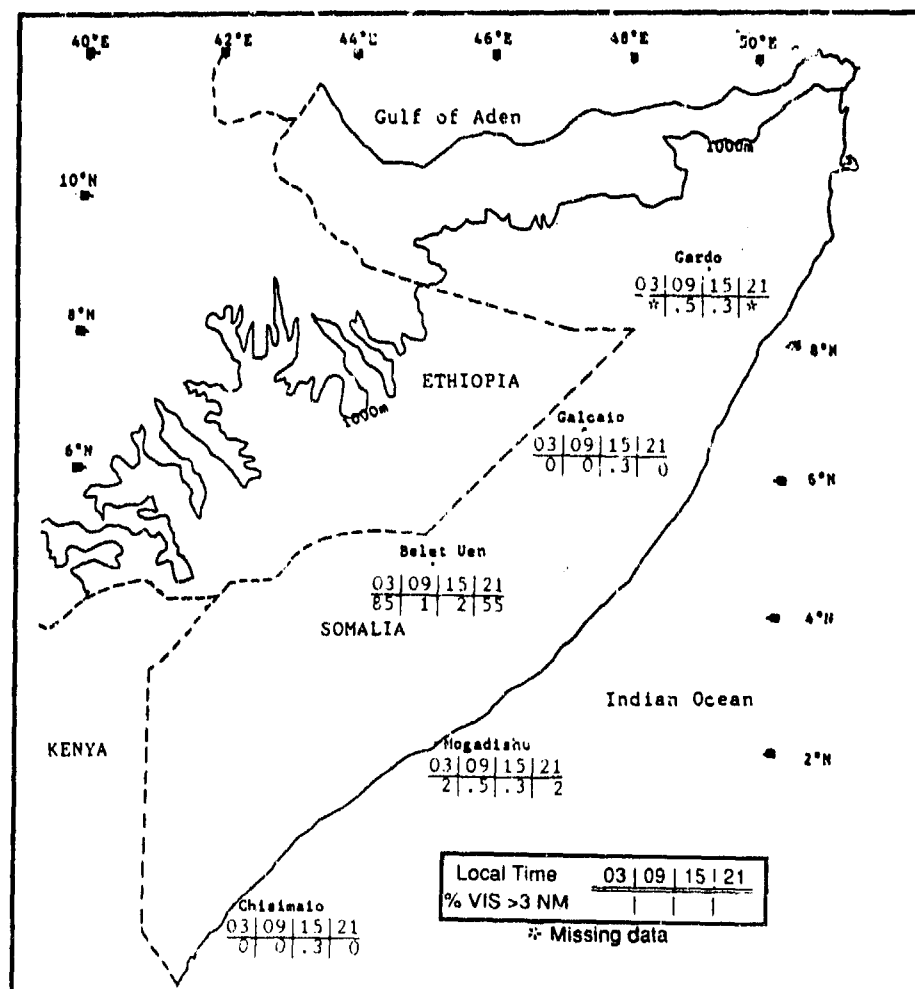


Figure 3-20. Northeast Monsoon Frequencies of Visibilities Below 3 Miles, Indian Ocean Plain.

WINDS. Mean surface wind speeds and prevailing directions (shown in Figure 3-21) show the distinctive Northeast Monsoon circulation. Light northeasterlies at Gardho in March indicate a gradual large-scale decrease in

the Northeast Monsoon at higher latitudes. Wind speeds above 5,000 feet (1,524 meters) MSL are easterly at 10-15 knots.

**E-NE
ESE-NE
E-NNE
E-NE**

	DEC	JAN	FEB	MAR
Chisimaio	9.50	11.40	10.90	9.10
Ischia Baidera	7.20	8.60	8.40	3.60
Galcaio	10.60	11.80	12.10	9.60
Gardho	8.20	9.30	7.90	4.80

Figure 3-21. Mean Northeast Monsoon Wind Speed (kts) and Prevailing Direction, Indian Ocean Plain.

**INDIAN OCEAN PLAIN
NORTHEAST MONSOON ("Gilal")**

December-March

PRECIPITATION. Northeast Monsoon ("Gilal") precipitation is light to non-existent. Rainfall averages less than 0.7 inches (17.5 mm) a month. Only Bardera, in the south, receives some rainfall every month. Figure

3-22 indicates a slight precipitation maximum (oriented southwest to northeast) over Bardera. This area lies under a weak wind maximum, the remnants of cross-equatorial flow in December and March.

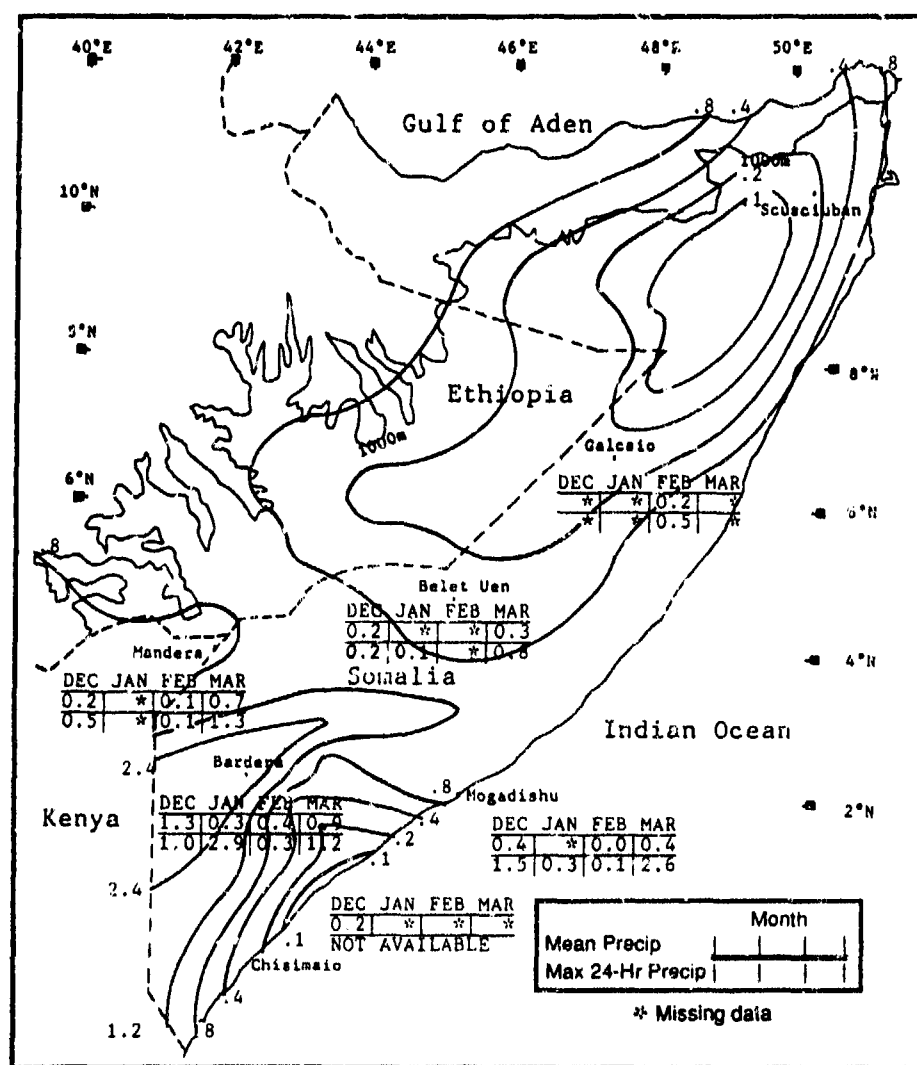


Figure 3-22. Mean Northeast Monsoon Monthly/Maximum 24-Hour Precipitation, Indian Ocean Plain. Isohyets represent mean seasonal rainfall totals (inches).

INDIAN OCEAN PLAIN **NORTHEAST MONSOON ("Gillal")**

December-March

TEMPERATURE. The Northeast Monsoon is a very warm season, especially in March when northeasterly flow decreases in strength. Mean daily highs range from 85° to 104° F (29-40° C). Because of the intense sunshine there, only southern inland locations (south of 4° N) reach 100°F (38°C) on a daily basis. Coastal air temperatures remain below 90°F (32°C) because of the extremely moist boundary layer air and sea breezes that moderate climate and produce small diurnal temperature ranges. The marine layer is very shallow (less than 1,000 feet/305 meters) and extends 5-10 NM inland. Absolute

highs range from 89°F (32°C) in January at Chisimaio to 113°F (45°C) in March at Bardera. With little cloud cover or precipitation in the northern Indian Ocean Plain, low temperatures can reach 53-55°F (11-12°C), except on the coast, where 70°F (21°C) or less is extremely rare. Mean daily lows range from 64°F (18°C) at Scusciuban to 78°F (26°C) at Chisimaio. Absolute lows from 53°F (11°C) in February at Scusciuban to 73°F (23°C) at Chisimaio in March. Figure 3-23 summarizes Northeast Monsoon temperatures across the Indian Ocean Plain.

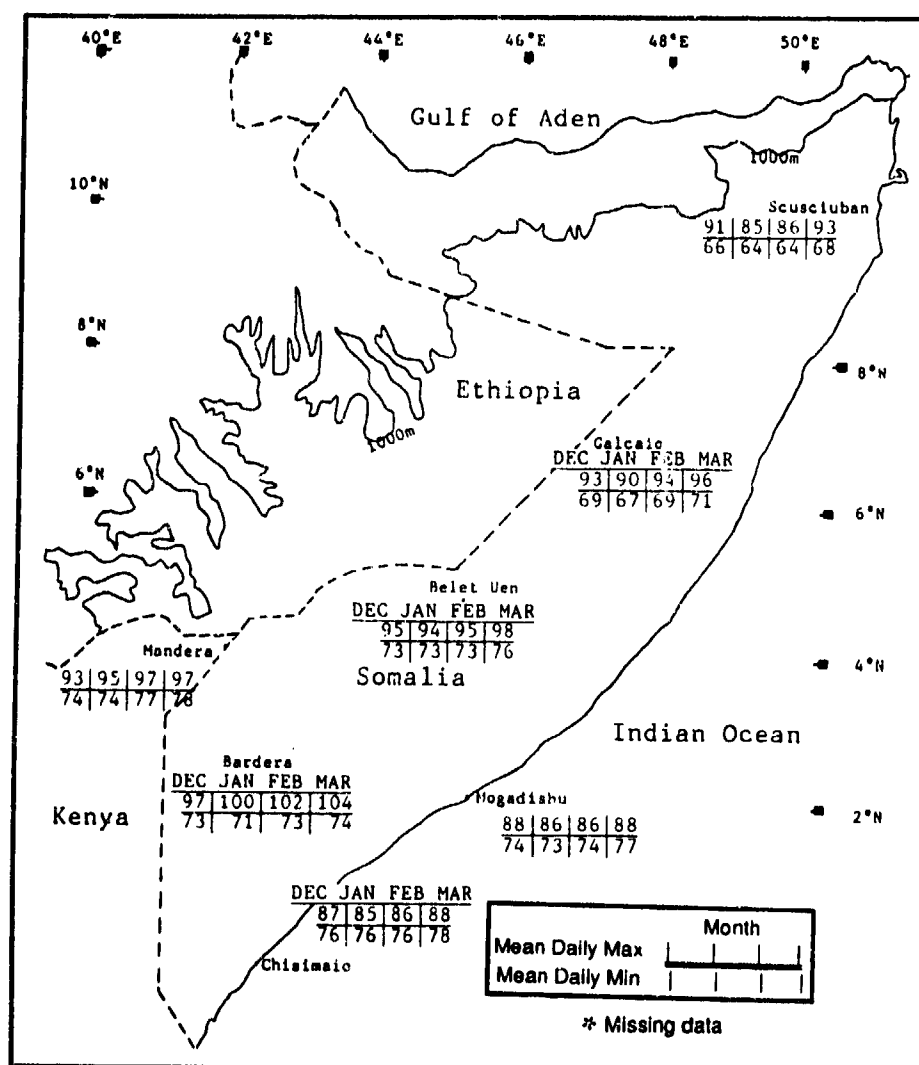


Figure 3-23. Mean Northeast Monsoon Daily Maximum/Minimum Temperatures (F), Indian Ocean Plain.

INDIAN OCEAN PLAIN NORTHEAST-TO-SOUTHWEST MONSOON TRANSITION ("Gu")

April-June

GENERAL WEATHER. Prolonged rains, extensive cloud cover, and southerly flow associated with the return of the Somali Jet dominate the transition from Northeast to the Southwest Monsoon, referred to locally as "Gu," or the "long rains." Significant weather occurs near the Somali Jet core as it flows SSW to NNE across the region by mid-May.

Precipitation initially develops in the south where low-level Monsoon Trough convergence and Somali Jet flow is strongest. Moderate shower activity migrates slowly northward, with a resurgence of strong southerly flow into higher latitudes. In many locations, the transition is the wettest season of the entire year.

SKY COVER. The mean seasonal cloudiness increase shown in Figure 3-24 is a direct result of the Somali Jet's strong low-level southerly component. Moist cross-equatorial flow returns in April to push the Monsoon Trough axis northward. Low-level instability and cloud cover parallels the jet core axis. Weak northeasterly flow and Northeast Monsoon cloud patterns are evident 100 NM north of the Monsoon Trough, but Southwest Monsoon flow dominates south of the Trough axis. Mean cloud cover ranges from over 75% in the Southwest to less than 50% in the northeast. Mean Monsoon Trough instability, rainfall, and Somali Jet flow remain south of 6° N until early May. Higher percentages in the south reflect heavy April rainfall, thick cloud cover, and strong low-level Somali Jet flow.

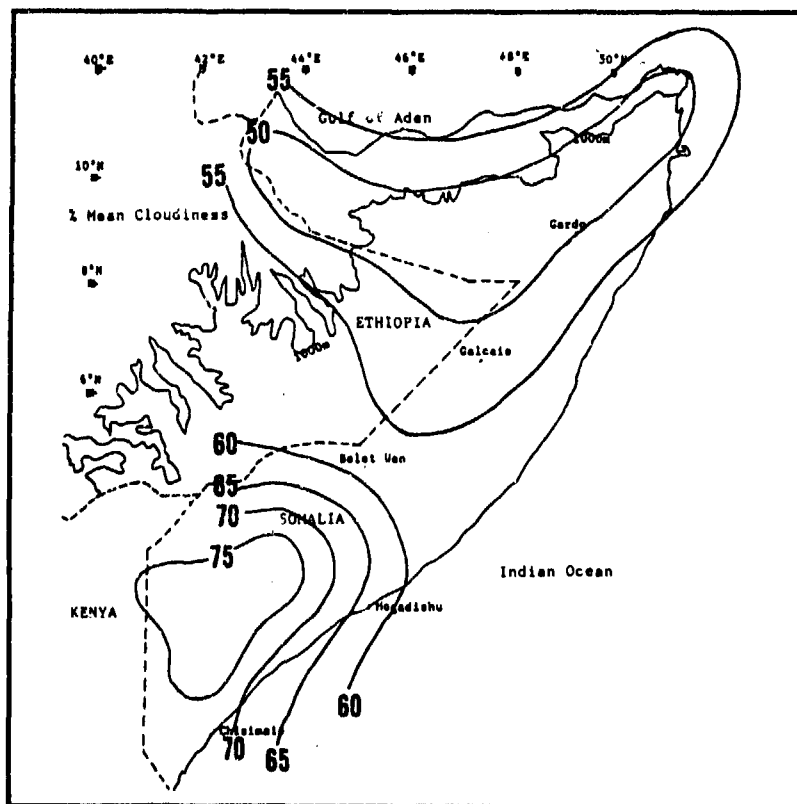


Figure 3-24. Mean NE-SW Monsoon Transition Cloudiness Frequencies, Indian Ocean Plain. Isolines are in 5% intervals. The data is derived by calculating the grand mean from National Intelligence Summary (NIS) mean cloudiness data for specific sites during April, May, and June.

INDIAN OCEAN PLAIN **NORTHEAST-TO-SOUTHWEST MONSOON TRANSITION ("Gu")**

April-June

At the selected stations shown in Figure 3-25, low ceiling frequencies range from 21 to 62%. Immediately north of the mean surface Monsoon Trough position, ceilings are below 3,000 feet (915 meters) AGL primarily during daylight hours as light northeasterly winds let diurnal convective heating and fair weather cumulus development mix with Somali Jet flow. South of the Trough axis, the diurnal cycle is present except at Mogadishu. The higher frequency of nocturnal low ceiling observations are associated with the Somali Jet. Ceilings below 1,500 feet (457 meters) AGL are not uncommon at Belet Uen, Chisimaio, and Mogadishu,

where high humidity and calm winds prevail at night. Cloud bases near the Somali Jet average 2,500-3,000 feet (762-915 meters) AGL. Stratocumulus is the dominant cloud type. Tops only reach 8,000 feet (2,439 meters) MSL. Short-lived cumulus squall lines usually move onshore with the sea breeze between 0800-1100 LST. Squall line cloud bases average 2,000 feet (610 meters) AGL, and cloud tops may reach 15,000 feet (4,573 meters) MSL over water. Strong low-level shear near the Somali Jet dissipates squall lines and heavy cumulus development.

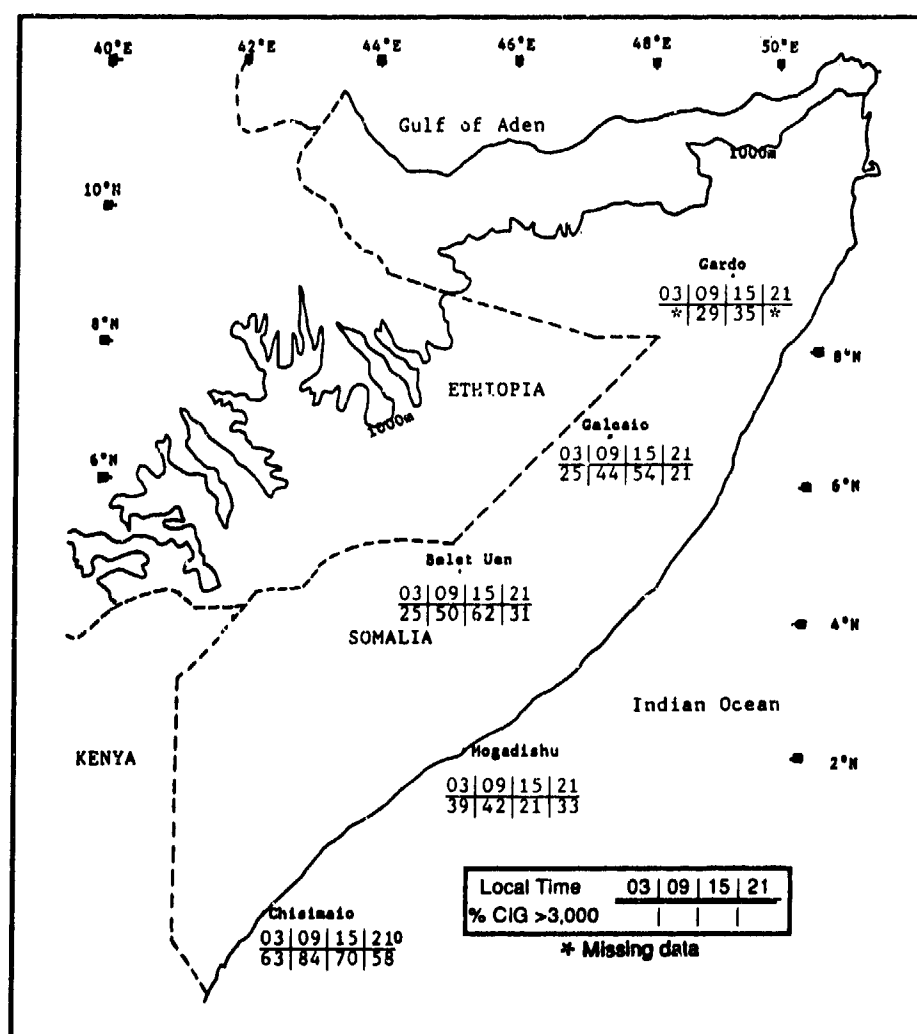


Figure 3-25. NE-SW Monsoon Transition of Ceilings Below 3,000 Feet (915 meters), Indian Ocean Plain.

INDIAN OCEAN PLAIN **NORTHEAST-TO-SOUTHWEST MONSOON TRANSITION ("Gu")**

April-June

VISIBILITY. Although low visibility frequencies (Figure 3-26) increase slightly during the transition, they remain low everywhere except Belet Uen, where the topography and moisture produce thick ground fog that usually dissipates by 0900 LST. Heavy rainshowers, dust, and fog are the principal visibility restrictions. Early morning sea fog is responsible for most visibilities below 3 miles along the coast, but shower activity and squall lines can raise dust along coastal dunes. Dust and

haze account for most low visibilities in the northern Indian Ocean Plain interior under stable conditions. Convective activity near the Monsoon Trough/Somali Jet increases surface wind speeds. If rainfall is sparse, localized duststorms occur; however, visibility rarely drops below 3 miles for more than an hour. Heavy rains rarely drop visibility below 3 miles for more than 30 minutes.

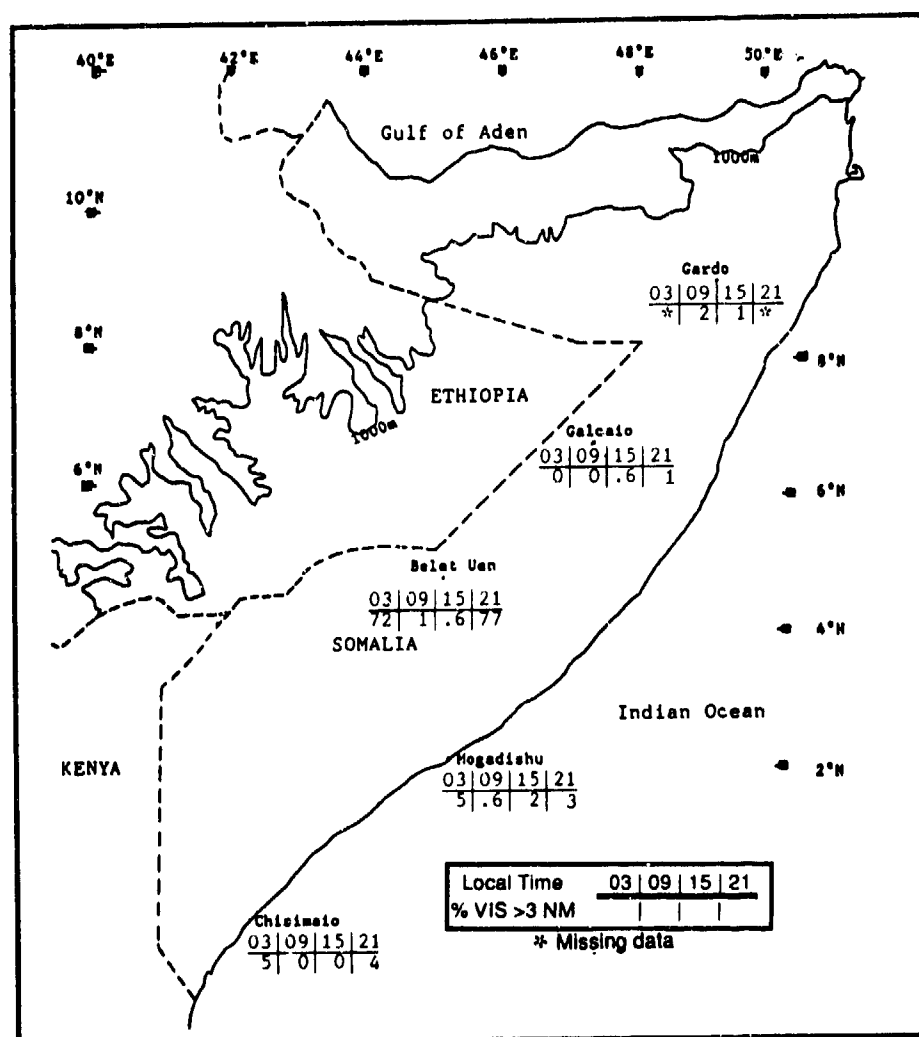


Figure 3-26. NE-SW Monsoon Transition Frequencies of Visibilities Below 3 Miles, Indian Ocean Plain.

**INDIAN OCEAN PLAIN
NORTHEAST-TO-SOUTHWEST MONSOON TRANSITION ("Gu")**

April-June

WINDS. Surface wind convergence into the Monsoon Trough produces the "Long Rains" or "Gu". Figure 3-27 gives mean surface wind speeds and prevailing directions during the transition. An important transition feature

shown here is the steady increase in southerly flow. In April, only Gardo has light ESE-NE winds, while southeasterlies dominate the rest of the region. By May, strong southerly winds affect the entire region.

**S-E/S-SSW
S-E/S-WSW
SE-E/S-WSW
ESE-NE/W-SW**

	APR	MAY	JUN
Chisimadio	6.90	9.80	10.50
Isalo Baldaa	6.50	6.90	10.00
Galeadio	6.40	10.70	17.90
Gardo	4.60	9.60	17.10

Figure 3-27. Mean NE-SW Monsoon Transition Wind Speed (kts) and Prevailing Direction, Indian Ocean Plain.

Somali Jet speeds average 25-40 knots at 4,000-6,000 feet (1,220-1,829 meters) MSL, but speeds in excess of 50 knots are not uncommon. The jet core may split into two or three ill-defined wind maxima. Typically, these wind maxima occur at different levels between 2100 and 0700 LST when the jet is at maximum strength. Daylight jet speeds are 10-15 knots weaker than at night.

Above 10,000 feet (3,050 meters) MSL, light easterlies (10-15 knots) dominate south of the Monsoon Trough. In June, 15,000-foot (4,573-meter) flow shifts briefly to southerly. North of the Trough, easterlies increase with height above 10,000 feet (3,050 meters) because the Tropical Easterly Jet near 200 millibars flows east to west across the region; mean speed in June is 40-60 knots, but speeds greater than 70 knots may occur.

PRECIPITATION. This is the wettest period of the year. Because the Somali Jet migrates from south to north, and because the Northeast Monsoon retreats northwards with increased Somali Jet flow, surface convergence along the Monsoon Trough and Indian Ocean Plain is persistent. The northern edge of the Somali Jet increases instability above the surface trough. Heaviest rainfall is located beneath and to the immediate east and north of the jet core wind maximum, but isolated heavy convection and showers may be present

along the entire surface Monsoon Trough, where weak northeasterlies and persistent southerlies converge. Normally, April and May are wettest in the interior, while May and June are wettest on the coasts. This is the result of subtle shift in mean Somali Jet orientation.

By the end of May, the mean Somali Jet core is over the southern Indian Ocean Plain from the Kenya-Somalia border to 4° N, as shown in Figure 3-28. Heaviest rainfall occurs south of 5° N, beneath the jet core. Steady showers and occasional moderate rainfall prevails for 3-7 weeks. Thunderstorms are rare, but they may form beneath or east of a southern Somali Jet core wind maximum between 3-6° N.

Rainfall amounts slacken North of 5° N, but light rainshowers along the Monsoon Trough persist for several days. Heavy showers are triggered by flow surges in the Somali Jet. Normally, a 10-to 25-knot increase in Somali Jet flow lets moisture and instability surge northward into the Monsoon Trough. Heavy rainfall is localized near where the northern edge of the flow surge and surface Monsoon Trough intersect. Such events can be forecast by observing a SE to S wind shift in the northern Mozambique Channel--see Figures 2-37a-k. Although this figure represents a July moisture surge, a mid-or late June synoptic situation is also very common.

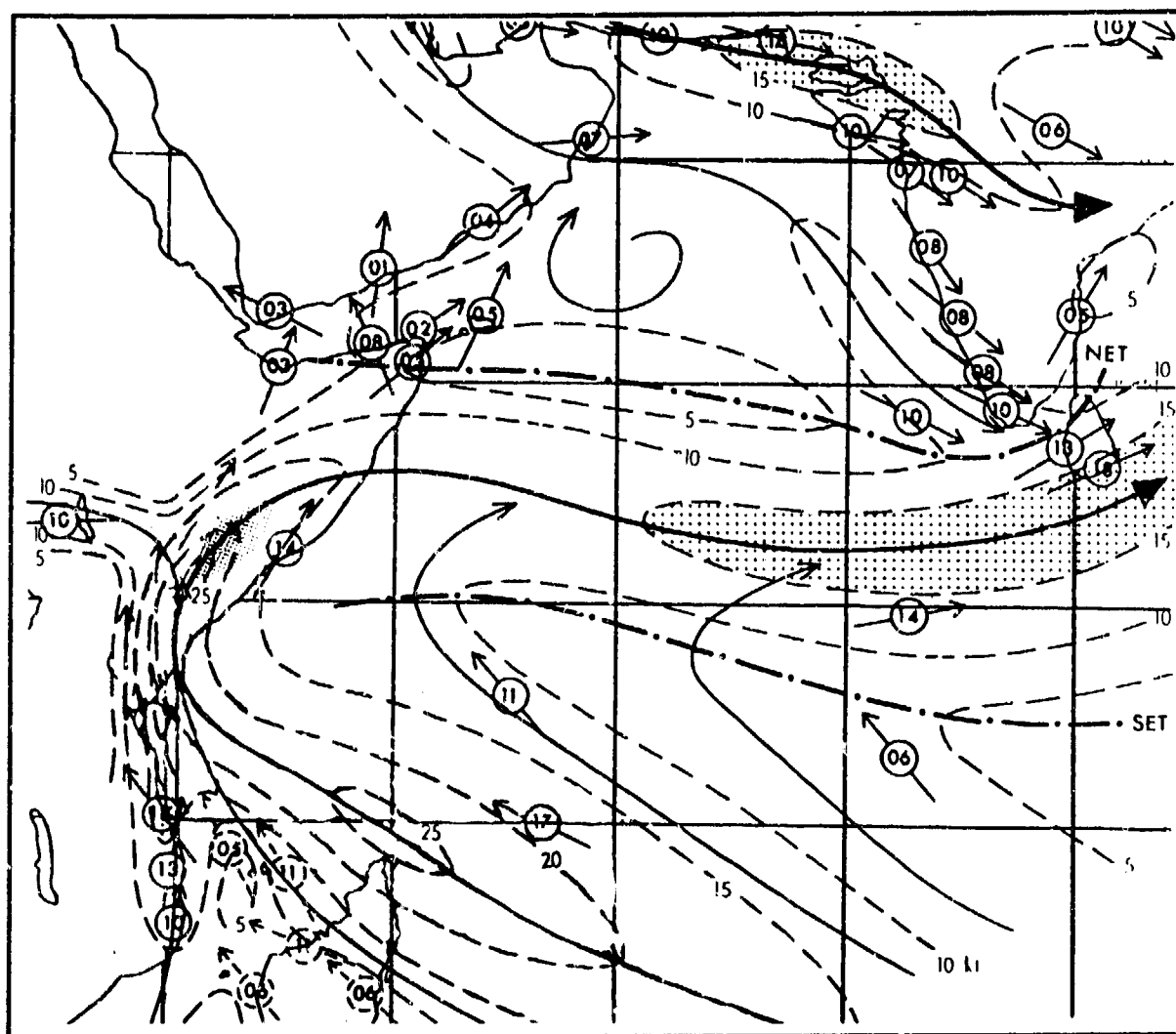


Figure 3-28. Mean May Flow Pattern at 3,000 Feet (915 meters) AGL (adapted from Findlater, 1971). Heaviest precipitation areas (Shaded) are shown to the immediate north and east of the Somali Jet wind core.

The isohyets in Figure 3-29 show a broad transition rainfall zone of more than 7.2 inches (183 mm) between Bardera and Mogadishu, and another in the extreme southern tip of the region. Both regions lie beneath persistent Somali Jet flow and abundant moisture. Between 4-7° N and 44-50° E, and north of 9° N to east of 49° E, less than 2.4 inches (61 mm) of rain falls

during the transition. In the extreme north, Somali Jet moisture is insufficient to produce as much rainfall as in the south. Nearly all rainfall in the extreme north is caused by surface convection generated by the Monsoon Trough. On rare occasions, orographic uplift of Somali Jet flow in the eastern Ethiopian Highlands generates light showers in the interior.

INDIAN OCEAN PLAIN
NORTHEAST-TO-SOUTHWEST MONSOON TRANSITION ("Gu")

April-June

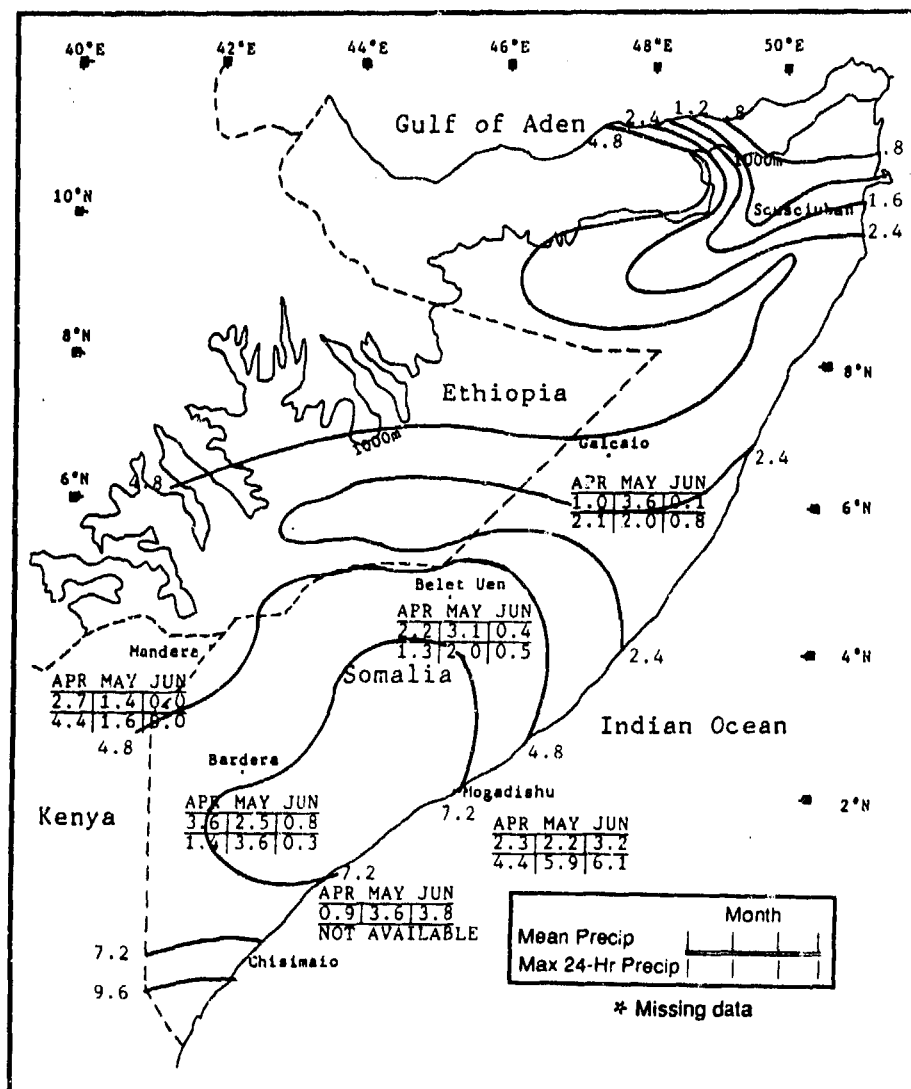


Figure 3-29. Mean NE-SW Monsoon Transition Monthly/Maximum 24-Hour Precipitation, Indian Ocean Plain. Isohyets give mean seasonal rainfall totals (inches).

TEMPERATURE. Maximum temperatures here result from the clear skies, light winds, and intense solar radiation in early April, before Somali Jet/Monsoon Trough cloudiness migrates northward. The absolute maximum (122°F/ 50°C) was recorded at Lugh Ferrandi in April; the record high on the coast was 93°F (34°C), recorded at Mogadishu in June. Mean daily highs range from 91°F to 105°F (33-41°C) in the interior. Most 100°F+ (38°C) temperatures occur north of 5° N. The

coastline up to 10 NM inland is moderated by the marine boundary layer. Average diurnal temperature ranges inland exceed 30°F (17°C) in April and May, but they rarely exceed 14 F°(8°C) on the coast. Mean daily lows range from 72°F (22°C) at Galcaio to 78°F (26°C) at many coastal sites. Record lows range from 61°F (16°C) in April at Scusciuban to 70°F (21°C) in June at Chisimaio. Figure 3-30 gives mean daily highs and lows for selected stations.

INDIAN OCEAN PLAIN
NORTHEAST-TO-SOUTHWEST MONSOON TRANSITION ("Gu")

April-June

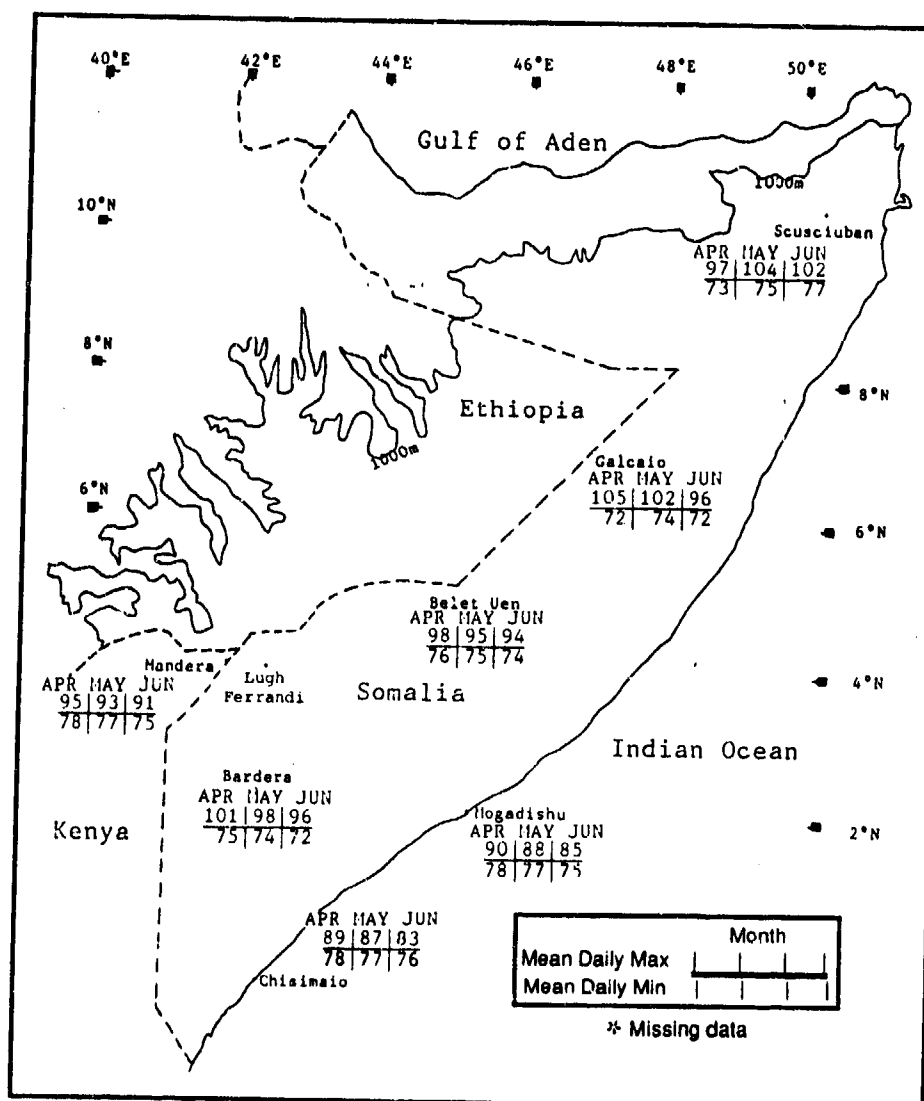


Figure 3-30. Mean NE-SW Monsoon Transition Daily Maximum/Minimum Temperatures (°F), Indian Ocean Plain.

Chapter 4

ETHIOPIAN HIGHLANDS

The "Ethiopian Highlands" region encompasses most of Ethiopia (ET) and small portions of Djibouti (DJ), Somalia (SI), and Sudan (SU). After describing the area's situation and relief, this chapter discusses typical weather conditions by season. Seasons here have local names ("Krempt," "Tsedia," and "Belgh"), as shown.

Situation and Relief	4-4
The Southwest Monsoon ("Krempt")--June-September	4-8
General Weather.....	4-8
Sky Cover.....	4-8
Visibility.....	4-10
Winds	4-11
Precipitation	4-15
Temperature	4-16
Southwest-to-Northeast Monsoon Transition ("Tsedia")--October-November	4-17
General Weather.....	4-17
Sky Cover.....	4-17
Visibility.....	4-19
Winds	4-19
Precipitation	4-20
Temperature	4-22
The Northeast Monsoon--December-March	4-23
General Weather.....	4-23
Sky Cover.....	4-24
Visibility.....	4-25
Winds	4-26
Precipitation	4-29
Temperature	4-31
Northeast-to-Southwest Monsoon Transition ("Belgh")--April-May.....	4-33
General Weather.....	4-33
Sky Cover.....	4-33
Visibility.....	4-35
Winds	4-36
Precipitation	4-37
Temperature	4-39

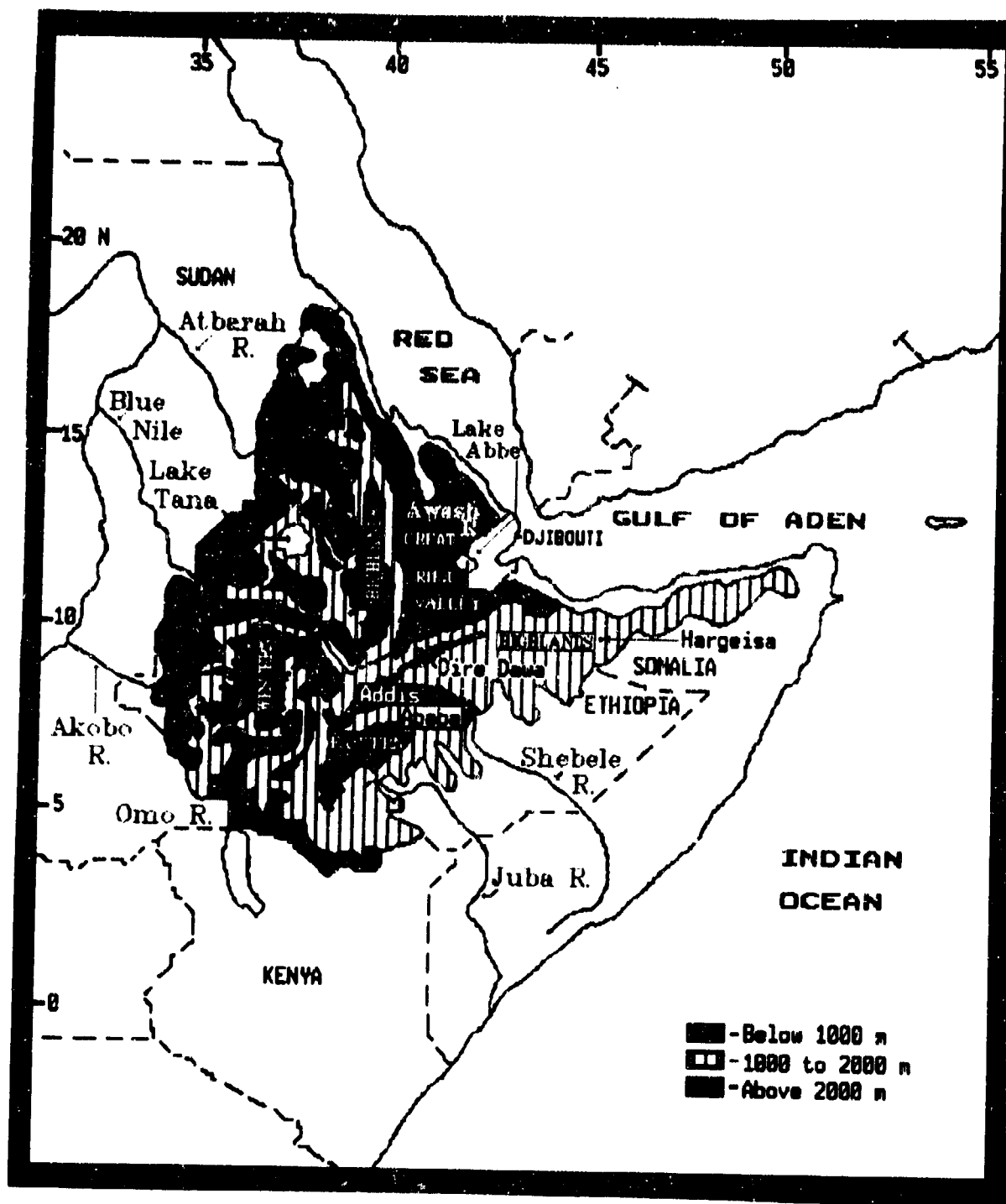


Figure 4-1a. The Ethiopian Highlands. This region includes most of Ethiopia, northern Somalia, extreme eastern Sudan, and western Djibouti.

STATION: ADDIS ABABA ETHIOPIA													
LAT/LON: 09 09 N 38 48 E ELEV: 7823 FT													
ELEMENTS	JAN	FEB	MAR	APR	MAY	JUN	JUL	AUG	SEP	OCT	NOV	DEC	ANN
EXT MAX	82	88	85	88	95	84	88	84	81	91	81	82	86
AVG MAX	74	78	77	77	77	74	69	69	71	74	73	73	74
AVG MIN	43	48	49	50	49	49	51	51	49	48	41	41	47
EXT MIN	27	32	34	37	38	38	37	41	38	38	29	28	27
AVG PRCP	0.8	1.7	2.8	3.4	3.7	5.4	11.1	11.7	7.6	0.8	0.8	0.2	49.8
MAX MON	4.1	0.9	9.8	12.4	11.9	14.8	18.7	18.7	22.4	5.6	3.8	2.7	78.3
MIN MON	0.0	0.0	0.0	0.0	0.1	0.2	4.8	6.8	2.0	0.0	0.0	0.0	36.7
MAX DAY	1.4	2.9	3.2	2.4	3.1	2.1	2.8	3.0	3.0	2.9	1.4	2.0	3.2
DUST DAYS	0	0	1	0	0	0	1	0	0	0	0	*	1
TS DAYS	1	1	8	7	7	15	17	20	15	5	0	0	98

* = LESS THAN 0.05 INCHES OR LESS THAN 0.5 DAYS

STATION: ASMARA ETHIOPIA													
LAT/LON: 15 17 N 39 54 E ELEV: 7626 FT													
ELEMENTS	JAN	FEB	MAR	APR	MAY	JUN	JUL	AUG	SEP	OCT	NOV	DEC	ANN
EXT MAX	86	88	88	88	88	88	85	81	82	83	79	82	88
AVG MAX	73	75	77	77	78	79	72	72	74	72	72	72	74
AVG MIN	48	48	50	52	54	54	53	53	51	48	48	48	50
EXT MIN	32	32	34	39	41	41	41	43	41	37	38	31	31
AVG PRCP	*	*	0.3	1.2	1.9	1.3	6.8	6.1	1.3	0.4	0.4	0.1	20.0
MAX MON	0.9	1.2	1.4	4.2	8.2	4.8	16.6	14.3	4.7	0.9	3.0	0.8	35.8
MIN MON	0.0	0.0	0.0	0.0	0.0	0.0	1.1	2.4	*	0.0	0.0	0.0	12.4
MAX DAY	0.5	0.7	1.0	2.2	3.6	2.4	2.8	4.2	2.5	0.9	1.3	0.5	4.2
DUST DAYS	0	*	*	*	*	1	*	0	0	0	0	0	0
TS DAYS	*	0	4	7	8	7	19	17	6	2	2	1	73

* = LESS THAN 0.05 INCHES OR LESS THAN 0.5 DAYS

STATION: DIRE DAWA ETHIOPIA													
LAT/LON: 02 38 N 41 51 E ELEV: 3759 FT													
ELEMENTS	JAN	FEB	MAR	APR	MAY	JUN	JUL	AUG	SEP	OCT	NOV	DEC	ANN
EXT MAX	95	99	100	102	102	100	100	99	99	99	97	93	102
AVG MAX	8	88	90	88	93	95	91	88	90	91	88	84	90
AVG MIN	59	61	64	66	68	68	64	63	63	63	61	57	63
EXT MIN	41	43	48	48	48	50	43	41	48	48	46	43	41
AVG PRCP	0.8	1.1	1.7	3.3	1.2	0.9	4.3	6.5	2.8	0.5	0.7	0.4	24.2
MAX MON	3.4	10.7	6.7	7.4	5.1	3.8	9.0	9.5	5.3	1.7	4.4	2.7	30.3
MIN MON	0.0	0.0	0.0	0.0	0.0	0.0	1.0	3.3	1.1	0.0	0.0	0.0	14.5
MAX DAY	2.0	2.7	2.5	2.1	1.0	1.2	2.6	2.0	2.6	1.0	1.8	2.1	2.7
TS DAY	0	1	4	2	2	1	3	4	6	1	0	0	2

* = LESS THAN 0.05 INCHES OR LESS THAN 0.5 DAYS

STATION: HARGEISA SOMALIA													
LAT/LON: 02 29 N 44 05 E ELEV: 4423 FT													
ELEMENTS	JAN	FEB	MAR	APR	MAY	JUN	JUL	AUG	SEP	OCT	NOV	DEC	ANN
EXT MAX	88	90	91	91	94	93	93	92	91	89	88	84	94
AVG MAX	75	81	84	84	87	88	86	84	88	82	79	77	83
AVG MIN	54	55	61	63	64	64	63	64	63	59	55	54	59
EXT MIN	37	37	39	44	52	53	50	50	50	45	39	40	37
AVG PRCP	0.1	0.3	1.0	2.4	2.4	2.3	1.7	3.2	2.3	0.4	0.3	*	16.4
MAX MON	2.7	4.7	9.0	7.4	4.8	7.4	4.8	7.0	5.3	2.5	2.8	0.7	32.0
MIN MON	0.0	0.0	0.0	0.0	0.2	0.7	0.5	0.5	0.7	0.0	0.0	0.0	10.2
MAX DAY	1.8	1.7	2.4	2.3	1.9	2.0	2.0	2.4	1.9	1.3	1.5	0.8	2.4
TS DAYS	*	*	2	4	7	9	7	8	7	1	1	0	48

* = LESS THAN 0.05 INCHES OR LESS THAN 0.5 DAYS

Figure 4-1b Climatological Summaries for Selected Stations in the Ethiopian Highlands.

ETHIOPIAN HIGHLANDS

SITUATION AND RELIEF

SITUATION AND RELIEF. The Ethiopian Highlands Region includes all land above 3,280 feet (1,000 meters), as well as a 100 by 20 NM portion of the area between 1,620 and 3,280 feet (500 and 1,000 meters) in the northern Great Rift Valley where the Awash River drains into Lake Abbe. The western boundary extends from the Kenya-Ethiopia border northward into Sudan, 20 NM west of the Red Sea. The northern boundary of the region includes all mountainous terrain parallel to the Red Sea and Gulf of Aden to about 50° 30' E. The

eastern boundary arcs northeast to southwest over northern Somalia and eastern Ethiopia to the Kenya border.

ZONES OF RELIEF. The Ethiopian Highlands region contains enough distinctly different relief features to warrant its separation into three zones; *The Western Highlands* (Figure 4-2a), *The Great Rift Valley* (Figure 4-2b), and *The Eastern Highlands* (Figure 4-2c).

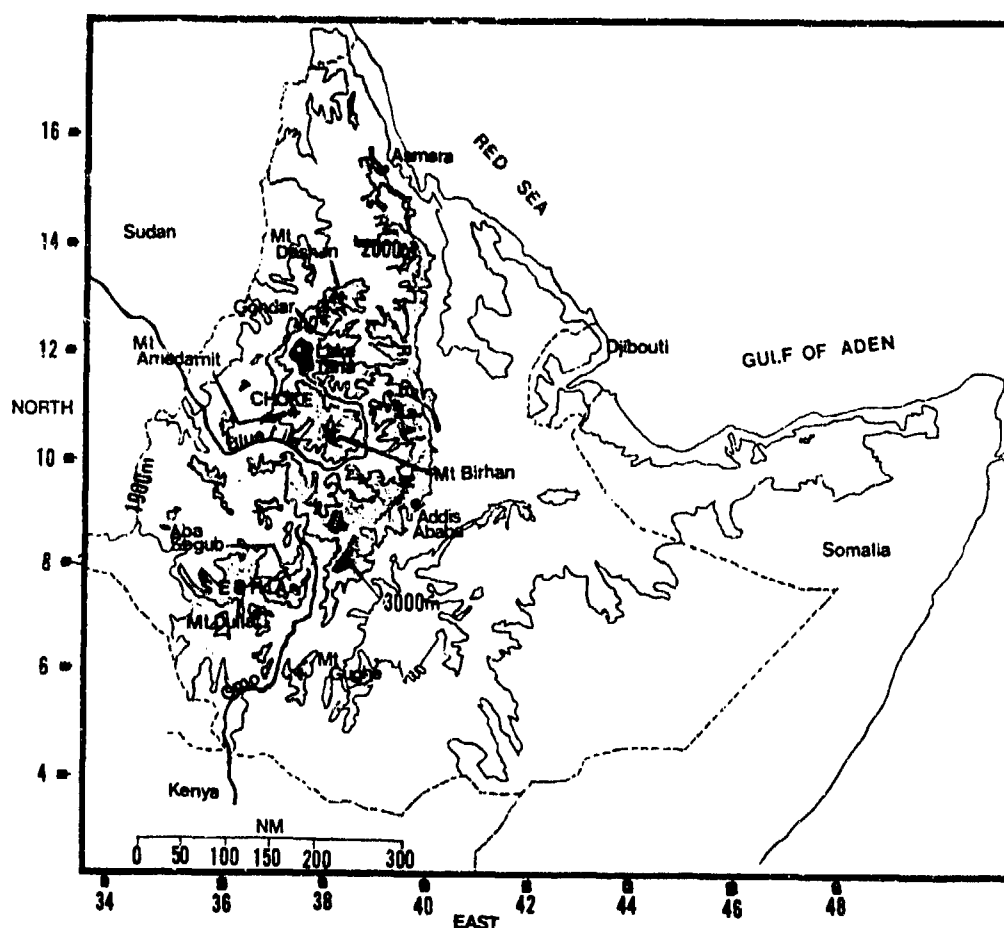


Figure 4-2a. The Western Highlands. This zone averages 250 NM in width and contains the highest mountain peaks in the Ethiopian Rift System.

The Western Highlands are characterized by volcanic peaks and rugged escarpments. It contains several large lakes and waterfalls. Volcanic ranges run south to north, from Kenya to the Red Sea and Sudan, for 950 NM. Elevations average 8,000 feet (2,440 meters), and numerous peaks rise above 14,000 feet (4,420 meters)

MSL. The extremely rugged terrain keeps low-level flow from interior Africa from reaching the Indian Ocean. Western Highlands weather is influenced only by synoptic weather features common to the subtropical African continent.

ETHIOPIAN HIGHLANDS

SITUATION AND RELIEF

The major ridge system runs from north to south along the western edge of the Great Rift Valley. The Eritrean Mountains ($10-15^{\circ}$ N, $39-40^{\circ}$ E) form the northernmost portions of the Western Highlands. The highest elevation in the Horn of Africa (15,158 feet/4,620 meters) is here, at Mount Dashan. Average elevation is 11,000 feet (3,354 meters) along the central Great Rift Valley's western edge.

Isolated interior ranges to the west of the valley include the Choke Mountains (11° N, 38° E), which contain Mount Birhan (13,625 feet/4,154 meters) and Mount Amedamit (11,870 feet/3,619 meters). The Seshia Mountains (8° N, $36-37^{\circ}$ E) occupy the southwestern fringes of the Highlands. Mount Dulla is the highest peak (12,093 feet/3,686 meters).

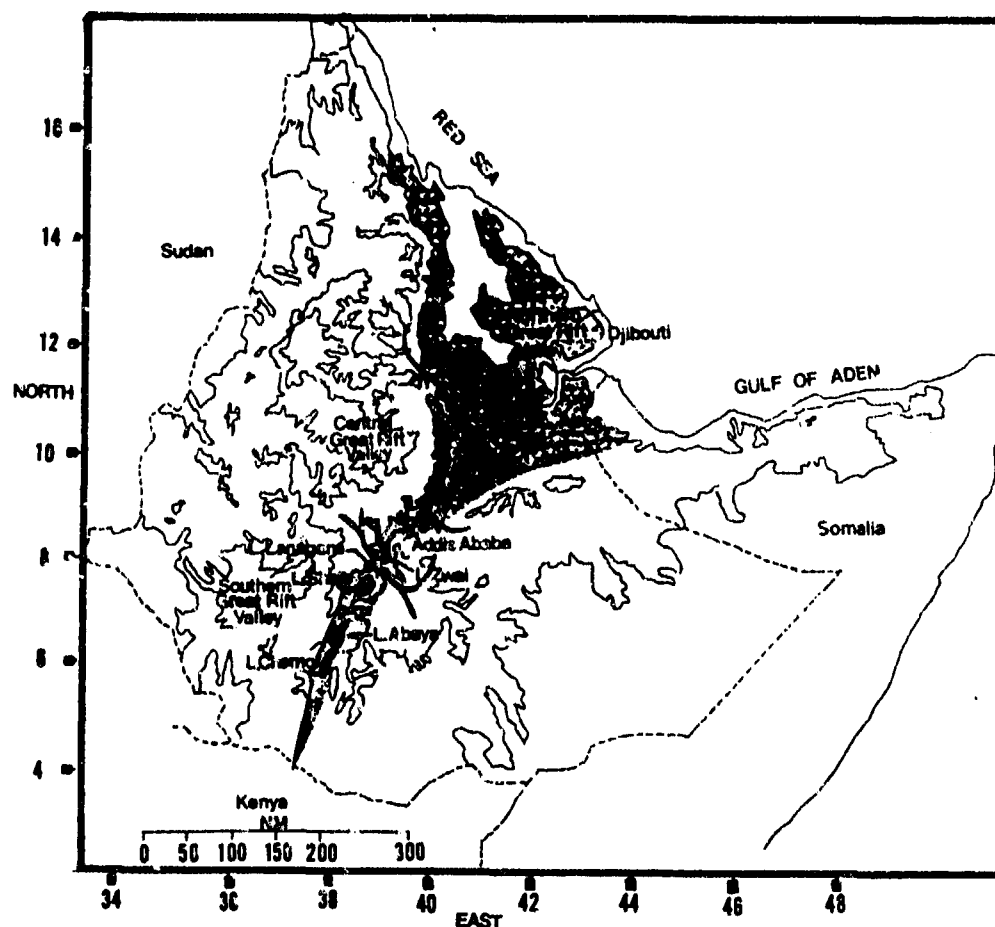


Figure 4-2b. The Great Rift Valley. The valley is a flat, V-shaped depression that slopes upward from NNE to SSW. Elevations average 4,000-5,000 feet (1,220-1,515 meters).

The Great Rift Valley floor gradually narrows from 250 NM near the Red Sea-Gulf of Aden coast to 10 NM southeast of Addis Ababa, Ethiopia. Near the Red Sea-Gulf of Aden coast, the broad valley floor is an ancient sea bed of sand and rocky stubble. It is extremely arid and desolate, with several small deserts. The small mountainous portion of the Danakil Desert covers 800 sq NM between the eastern slopes of the

Eritrean Mountains and the Djibouti border near 13° N, 41° E. A chain of large, brackish lakes (see "Lakes and Reservoirs") in the southern valley separates the extensive volcanic ridges of the Western Highlands from the older, weathered Eastern Highlands. The lakes--oriented N-E to SSW along the valley floor--are spring-fed.

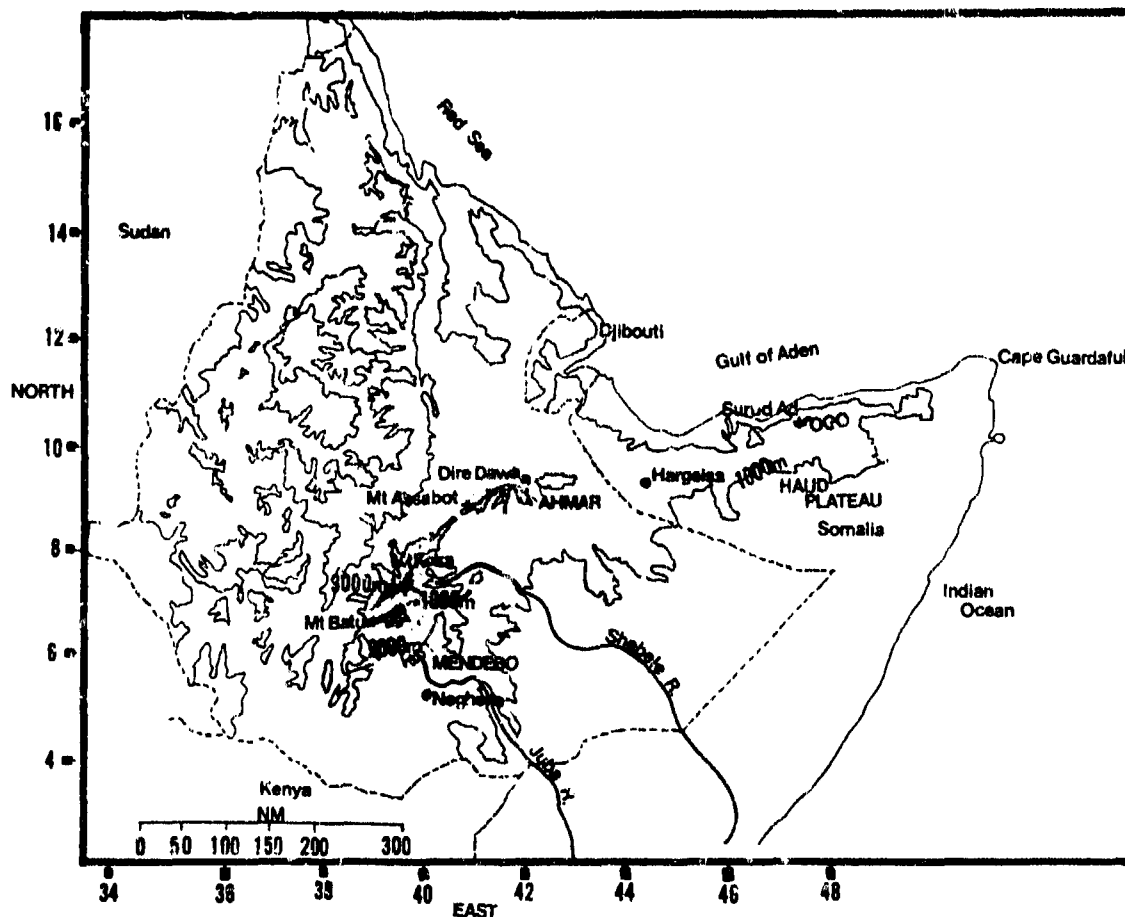


Figure 4-2c. The Eastern Highlands form the eastern boundary of the Ethiopian Highlands region. Oriented SW-NE, they extend 900 NM from south central Ethiopia to northeastern Somalia. Elevations average 7,000 feet (2,745 meters), but several peaks reach 13,000 feet (3,963 meters).

The Eastern Highlands contain three distinct mountain ranges: the Mendebo Mountains, the Ahmar Range, and the Ogo Highlands of northern Somalia.

The Mendebo Chain is the highest and most rugged in the Eastern Highlands. Mount Koka (13,747 feet/4,190 meters) and Mount Batu (14,131 feet/4,307 meters) rise near the source of the Juba and Shebele Rivers, both of which flow southeastward toward the Indian Ocean. Spectacular gorges and waterfalls are common.

The Ahmar Range consists of weathered volcanic peaks with gradually sloping terrain on both sides of the ridge crests. Located near 9° N, the range runs west to east from 40 to 43° E. Many streams radiating from this ranges become semipermanent waterways over the

semiarid Ogaden Plateau (see Figure 3-2c) and the Great Rift Valley. The highest peak (8,212 feet/2,503 meters) is Mount Assabot.

The Ogo Highlands are the highest in Somalia; their highest point (7,900 feet/2,408 meters) is at Surud Ad. The Highlands extend 470 NM west to east along the Gulf of Aden to within 75 NM of Cape Guardafui. In northern Somalia, they become eroded, discontinuous ranges 50-75 NM wide with several peaks that reach 7,000 feet (2,134 meters). Ridge lines are separated by weathered plateaus that average 1,900 feet (579 meters) high and 5-10 NM wide. Plateaus contain one or more shallow intermittent stream beds. Northern slopes of the Ogo are steep, but southern slopes descend gradually to the semiarid Haud Plateau.

ETHIOPIAN HIGHLANDS

SITUATION AND RELIEF

RIVER SYSTEMS. The Ethiopian Highlands contain numerous river systems and mountain lakes. Most rivers originate in the Western Highlands; three of these (flowing from south to north) are the Omo, the Awash and the Blue Nile. The Omo flows 500 NM south from the Seshia Mountains into Kenya. The Awash originates along the western slopes of the Great Rift Valley and flows northeastward through deep gorges south of Addis Ababa into the Great Rift Valley towards Lake Abbe, a total run of 500 NM. The Blue Nile begins at Lake Tana (12° N, 37° 20' E) and flows southeast, south, then west around the Choke Mountains before entering Sudan.

The eastern Ethiopian Highlands contain the Juba and Shebele Rivers. Both originate in the Mendebo Mountains. Their flow cuts deep gorges, some 4,920 feet (1,500 meters) deep. Many small streams originate on the southern slopes of the Ogo Highlands, all flowing intermittently below 3,280 feet (1,000 meters).

LAKES AND RESERVOIRS. The southern Great Rift Valley contains numerous lakes, all above 4,000 feet (1,220 meters). Lake Tana, at 6,004 feet (1,829 meters) MSL is the largest, covering 1,400 sq mi. Lake Zwai (150 sq mi), Lake Lanagana (80 sq mi), and Lake Shala form a chain of lakes near the apex of the Great Rift Valley. These lakes contain natural hot springs located above the 5,000-foot (1,620-meter) level. Lake Zwai (elevation 6,056 feet/1,846 meters) contains five inhabited islands; the largest (Tulugudu) is 2 NM long. Near 6° 20' N, 38° E, Lake Abaya (485 sq mi, elevation 4,160 feet/1,267 meters) and Lake Chamo (210 sq mi, elevation 4,045 feet/1,231 meters) form a wide elevated basin containing hot springs and marshlands. During the rainy season, these lakes are connected by a semipermanent river.

VEGETATION. The Ethiopian Highlands contain varied vegetation types. Tropical forests flourish above

6,000 feet (1,829 meters); alpine forests grow above 8,200 feet (2,500 meters). Semiarid shrub and savannah grasses cover lower elevations.

Above 6,560 feet (2,000 meters), the Western Highlands contain a mixture of tropical evergreen forest and deciduous woodland. Scattered alpine vegetation grows above 8,200 feet (2,500 meters), especially in and along the deeper elevated gorges of the Eritrean and Choke Mountains. To the south, tropical savannahs dominate below 6,560 feet (2,000 meters). Along the western slopes and high plateaus bordering Sudan, there is a transition to a semiarid zone that contains scattered open woodland and thorny shrubs.

The Great Rift Valley has two distinct vegetation zones. The narrow southern valleys containing the lakes have savannah grasslands and scattered open woodland. Some aquatic grasses inhabit the lake fringes and seasonal swamplands. As the Rift Valley widens, vegetation reflects the distinctly semiarid environment within 50 NM of the Red Sea-Gulf of Aden coastal plain. The savannahs in the south become short thorny scrub and grass clumps as moisture decreases toward the north and northeast. Only short, isolated trees grow north of 12° N.

The Eastern Highlands south of 7° N have tall grass savannah intermixed with thorn trees between 4,920-6,560 feet (1,500-2,000 meters). Above the 6,560-foot (2,000-meter) level, isolated evergreen vegetation grows, but it is confined primarily to the deep valleys in the rugged ridges of the Mendebo Range. The Ahmar and Ogo Highlands contain short savannah grasses and thorny acacia trees above 4,920 feet (1,500 meters). Below the 4,920-foot (1,500-meter) level, vegetation becomes the semiarid scrub familiar throughout Africa.

ETHIOPIAN HIGHLANDS SOUTHWEST MONSOON ("Kremp")

June-September

GENERAL WEATHER. Widespread convection dominates the Western Highlands and the Mendebo Mountains of the Eastern Highlands. Monsoon Trough moisture "surges" into the numerous canyons, ravines, and valleys, where orographic uplift forces moisture to the 700- to 500-mb layer. Heaviest rainfall, thunderstorms, and occasional small hail affect the highest ridges immediately, while moderate rainshowers or continuous drizzle fall downwind from massive cloud clusters. The Ethiopian Highlands region's complex terrain produces widely variable precipitation patterns because synoptic circulation and moisture distributions below 850 mb are so complex. Moist low-level currents only affect certain sections of the Ethiopian Highlands.

SKY COVER. Extensive cloudiness in all of the Western Highlands and in the extreme southern portions of the Eastern Highlands and Great Rift Valley is produced by heavy Monsoon Trough convection. Moist southerly flow from the African interior produces orographic convection along the Choke, Seshia, and Eritrean Ranges. Low-level moisture comes from the African Monsoon Trough and the Turkana Channel through the western branch of the Somali Jet, which see. Heavy convection drifts slowly northeastward into the southern Great Rift Valley. Although strong surface heating assists in convective cell intensification, upper-level easterlies often prevent eastward movement of convective activity in the Western Highlands beyond 43° E.

East of 43° E, the Somali Jet and dry low-level flow (rather than the African Monsoon Trough) dominate the Eastern Highlands. The Mendebo and Ahmar Mountains are consistently cloud-covered because of abundant

Turkana Channel moisture. Orographic uplift on west, south, and east slopes are continuously fueled by moist low-level flow between June and August. A reduction in Turkana Channel flow ends widespread convection abruptly. By mid-September, an intense surface heating mechanism temporarily replaces the broad low-level moisture source.

Orographic effects provide only isolated convective activity east of the Ahmar Mountains and Hargeisa. African Monsoon Trough moisture rarely penetrates eastward beyond the Western Highlands. As a result, only the fast-moving Somali Jet or intense surface heating can generate orographic showers. The dry low-level flow is deflected eastward and upward along the Ogo Highlands southern slopes. Stratocumulus forms above 5,000 feet (1,524 meters) AGL, then moves ENE with the Somali Jet. If upper-level easterly flow is less than 15 knots, and if there is enough low-level heating and deep vertical moisture, cumulus develops. Otherwise, cloud development along the Ogo Highlands' southern slopes is rapidly sheared at the mid- and upper levels.

In general, mean cloudiness shown in Figure 4-3 for the entire Ethiopian Highlands varies from less than 45% in the east to more than 70% in the west. At remote elevations above 10,000 feet (3,050 meters) MSL, Southwest Monsoon mean cloudiness is much higher, running from 78 to 95%. Since orographic cloud cover depends on orientation to prevailing flow and available moisture, mean cumulus/stratocumulus cover in the Great Rift Valley may vary by 25-35% over a distance of 25-30 NM.

ETHIOPIAN HIGHLANDS SOUTHWEST MONSOON ("Kremp")

June-September

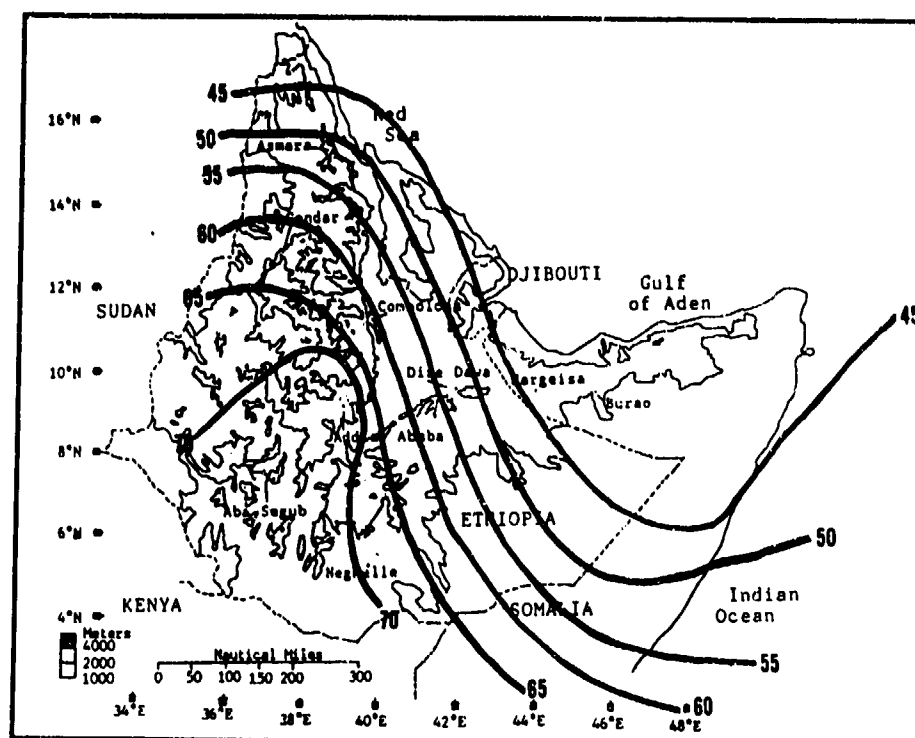


Figure 4-3. Mean Southwest Monsoon Cloudiness Frequencies, Ethiopian Highlands. Isolines are in 5% intervals. The data is derived by calculating the grand mean from National Intelligence Summary (NIS) mean cloudiness percentages for specific sites between June and September.

Dominant cloud types throughout the region are cumulus and cumulonimbus. Intense surface heating along the plateaus of extreme western Ethiopia and Great Rift Valley (all above 6,000 feet/1,829 meters MSL) produce diurnal cumulus or cumulonimbus development. Midday (1100-1500 LST) cloud bases average 6,000-8,000 feet (1,829-2,439 meters) AGL, with tops exceeding 40,000 feet (12,195 meters) MSL. Thunderstorm tops reach 50,000 feet (15,244 meters). Cirrus and altocumulus most often occur over the Great Rift Valley and Eastern Highlands as the result of thunderstorm "blow-off" from heavy convection along the Eritrean/Choke Mountains and the Mendebo/Ahmar Mountains respectively.

Extensive stratus or stratocumulus decks form in the early morning along the southern Great Rift Valley.

Light mountain breezes and residual moisture from heavy precipitation produce strong inversions at 1,000-3,000 feet (305-915 meters) AGL. Bases below 1,000 feet (305 meters) are not uncommon, but they give way to extensive cumulus buildup after 1100 LST.

Diurnal variation in ceilings below 3,000 feet (915 meters) is apparent from Figure 4-4. Although not apparent in the figure because there are no weather reports from the Great Rift Valley, the numerous large lakes there result in a high frequency of low ceilings between 2100 and 0900 LST. Ceilings in the Great Rift Valley fall below 1,000 feet (305 meters) on 1 day in 3. Frequencies of ceilings below 3,000 feet (915 meters) are shown in Figure 4-4; they range from 44% at Neghelle to only 1% at Dire Dawa, both at (0900) LST.

ETHIOPIAN HIGHLANDS SOUTHWEST MONSOON ("Kremp")

June-September

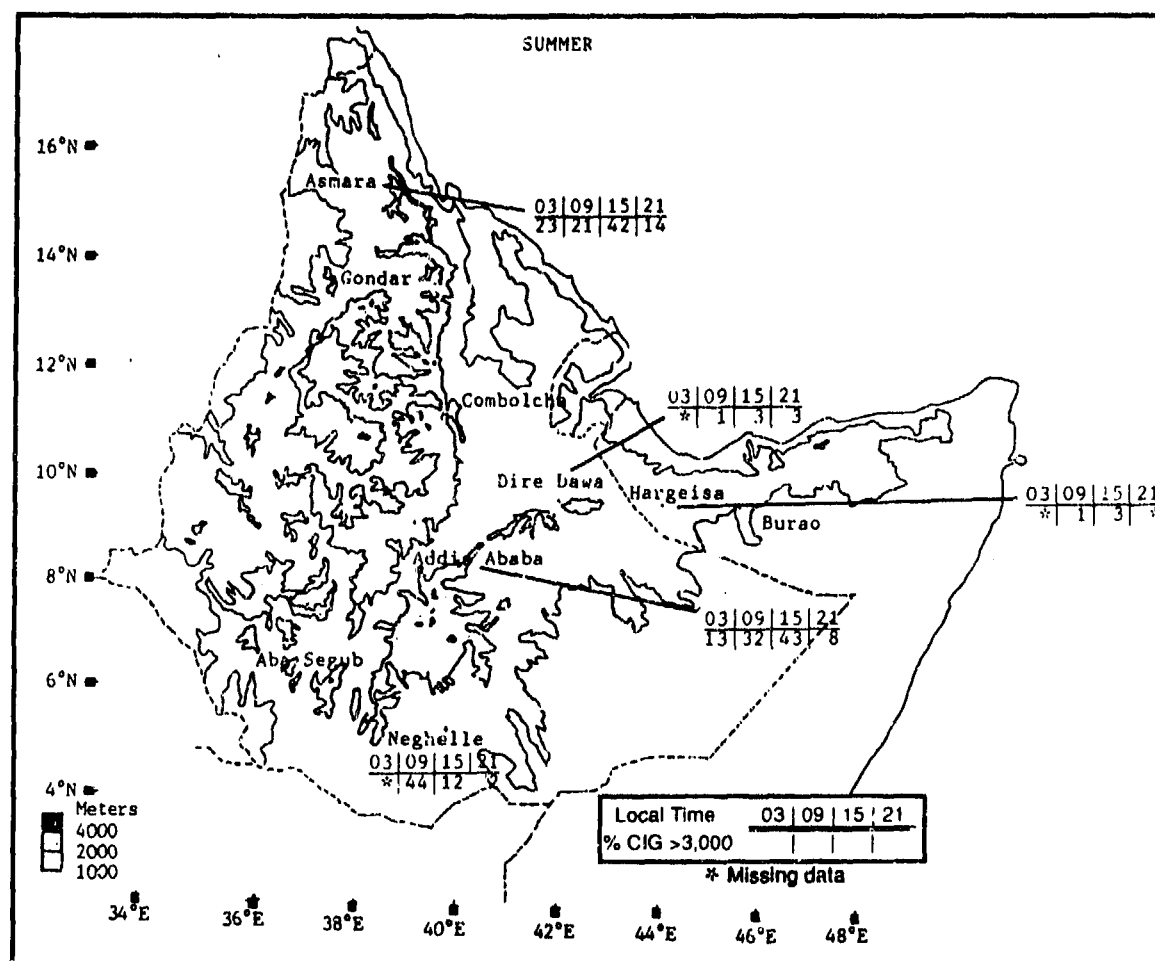


Figure 4-4. Southwest Monsoon Frequencies of Ceilings Below 3,000 Feet (915 meters), Ethiopian Highlands.

VISIBILITY. Southerly flow results in an influx of moisture during the Southwest Monsoon. The rugged terrain produces orographic uplift and heavy rains or thundershowers. Figure 4-5 shows the highest frequency of visibilities below 3 miles to be 6% (at Asmara), but most visibilities below 3 miles occur in remote locations over rugged terrain, in heavy orographic cloud cover. A high incidence of ground fog and heavy mist can also be expected along remote Western Highland mountain tops,

ravines, and valleys where light early morning winds and residual moisture from heavy convection lower visibility between (0500) and (0800) LST. "Dust haze" is a localized low-visibility phenomenon in the northern Great Rift Valley. Since the region has so few reporting stations, conditions there must be inferred by analyzing coastal data, soil moisture conditions, and soil type. Minimum visibilities here are believed to average more than 3 miles; in isolated cases, they may go as low as 1/2 mile.

ETHIOPIAN HIGHLANDS SOUTHWEST MONSOON ("Kremp")

June-September

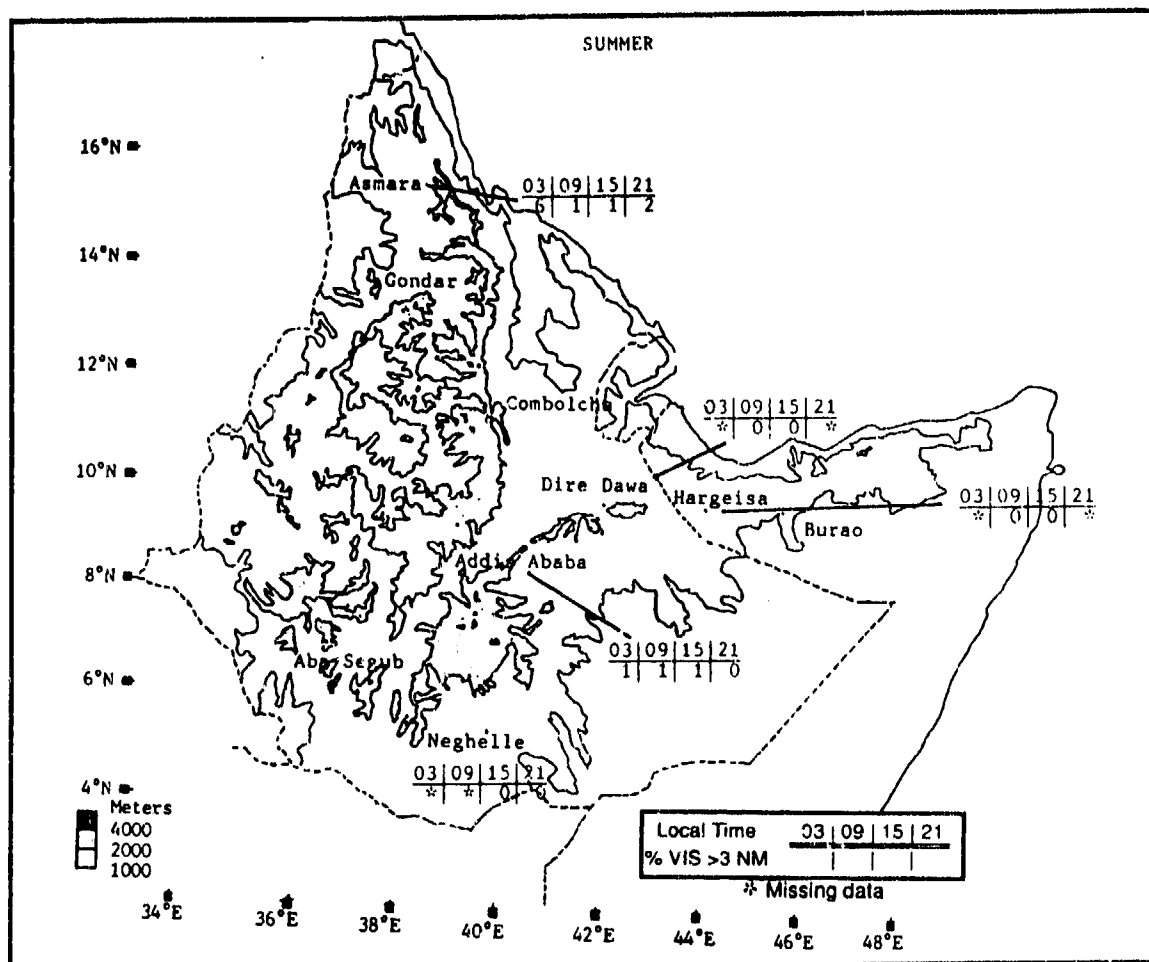


Figure 4-5. Southwest Monsoon Frequencies of Visibilities Below 3 Miles, Ethiopian Highlands.

WINDS. Complex interactions between local mountain/valley circulation and prevailing synoptic flow produce widely variable surface wind patterns throughout the Ethiopian Highlands. Elevation and ridge orientation are important in determining to what degree low-and mid-level circulation will affect a specific area. Only general trends can be inferred from the low-density surface observation network in this region. Forecasters should be most concerned with prevailing synoptic flow patterns because increased boundary layer moisture penetration signifies deep recurving southerly flow and Southwest Monsoon conditions (see Chapter 2).

Normally, Monsoon Trough and Somali Jet position determine low- and mid-level circulation. The surface Monsoon Trough lies between 17° and 20° N in June, between 19° and 22° N in July, and between 12° and 18° N in September. However, 90% of the Ethiopian Highlands region lies above 850 mb; only the peripheral plateaus and the northern Great Rift Valley are below 850 mb. As a result, the surface Monsoon Trough is discontinuous over the rugged mountainous interior and ill-defined when joined over the Red Sea and Gulf of Aden.

ETHIOPIAN HIGHLANDS SOUTHWEST MONSOON ("Krempf")

June-September

Southwest Monsoon surface flow below 850 mb is southerly, but the Western Highlands, the Eastern Highlands, and the Great Rift Valley receive unequal amounts of southerly flow during the Southwest Monsoon because the surface Monsoon Trough is divided into two distinct segments by topography. Above 760 mb, which is Addis Ababa's mean pressure

during the Southwest Monsoon, weak easterlies dominate. Aloft, there is a 27- to 48-knot wind maximum at the 200- and 100-mb levels--see "Tropical Easterly Jet," Chapter 2. Easterly synoptic flow prevails throughout the region until deep southerly flow migrates northward. Even then, mean southerly flow only persists below 760 mb during July.

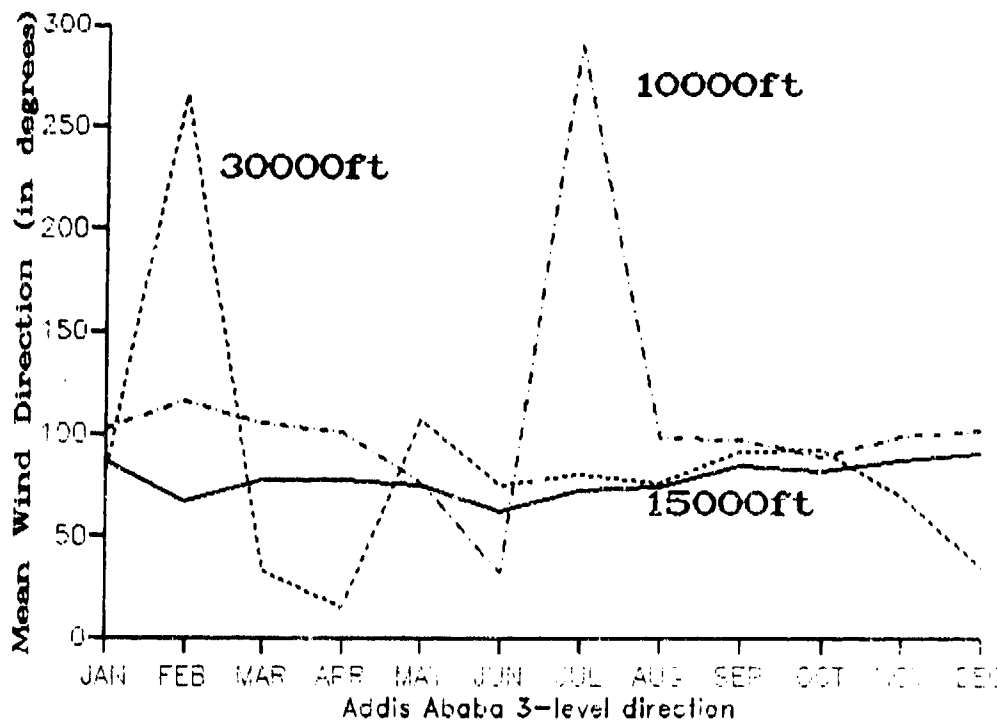


Figure 4-6. Mean Annual Wind Direction, Addis Ababa, Ethiopia. Addis Ababa is at 7,624 feet (2,324 meters) above mean sea level.

Southerly flow enters the Western Highlands from points immediately south or west at 5-11 knots. The Seshia Mountains receive initial sustained Southwest Monsoon southerly "moisture bursts" from the Turkana Channel--the Somali Jet's western branch--through late June. Turkana Channel flow alone seldom penetrates into the Seshia Mountains north of 8° N, but normally recurves into the Monsoon Trough over southeastern Sudan. Deep low-level moisture from the Monsoon Trough's northward migration across equatorial Africa seldom penetrates east of 40° E because of the barrier presented by the Western Highlands. Normally, the primary Monsoon Trough current slides northward around the Eritrean Mountains (north of 16° N), but southwesterly flow at 6-10 knots enters the deep gorges, river valleys, and low plateaus that dissect the Western Highlands. During daylight hours, local mountain-valley winds accentuate orographic uplift and deflect southwesterly flow at the microscale. Local valley winds

average 8-11 knots and may deflect Monsoon Trough flow in the deep Omo, Blue Nile, and Atharah River valleys to westerly or northwesterly.

Nocturnal mountain winds oppose prevailing Monsoon Trough flow, but do not override them. Nocturnal convergence with light and variable winds are common to most Western Highland valleys between 2300 and 0600 LST. These winds may become easterly, but speed is usually less than 5 knots.

Figure 4-7 gives mean annual wind directions for three levels at Asmara. Asmara is in the extreme northern part of the Western Highlands. The winds here illustrate the 10,000-foot/3,050-meter deflection of mid-level flow to northerly. By September, mean northeasterly flow signals the Monsoon Trough's southward migration.

ETHIOPIAN HIGHLANDS SOUTHWEST MONSOON ("Krempt")

June-September

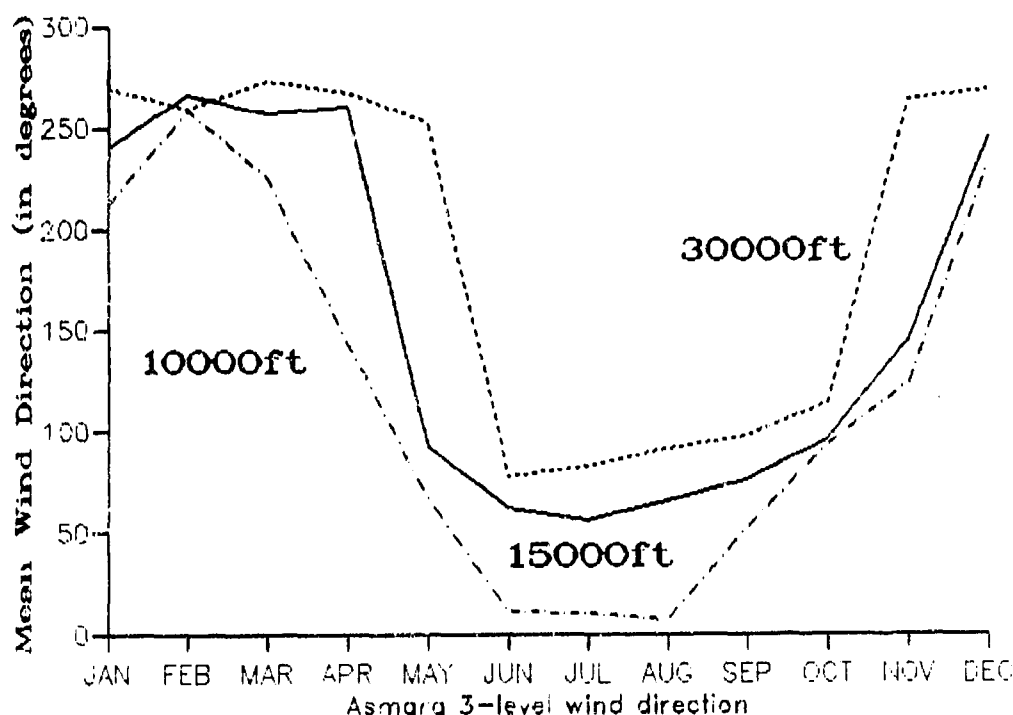


Figure 4-7. Mean Annual Wind Direction, Asmara, Ethiopia. Asmara is 7,627 feet (2,325 meters) above sea level.

The Great Rift Valley gets a shallow SSW stream of Southwest Monsoon air at 4-7 knots through the high plateaus dividing the Seshia Mountains in the Western Highlands and the Mendebo Mountains in the Eastern Highlands. This moist southerly flow doesn't regularly override prevailing mid-level easterly flow until mid-July. Normally, southerlies increase to 8-11 knots before easterly flow is reversed. The Great Rift Valley is affected by mesoscale mountain-valley winds as well as synoptic flow. The northern half of the Great Rift Valley is in a rain shadow, sheltered from Monsoon Trough southerlies by the Western and Eastern Highlands. Daytime valley winds are dry northerlies that travel upslope along the valley floor. This surface flow (6-9 knots) produces hot and dry conditions in the northern Great Rift Valley throughout the Southwest Monsoon. The high-altitude southern Great Rift Valley is a surface wind transition zone. By day, moist southerlies and dry but weak northerlies converge near Addis Ababa. Wind directions are variable, but average 8-9 knots. At night, mountain winds are southerly or easterly at 4-7 knots.

The Eastern Highlands are also affected by Monsoon Trough flow, but the mechanism is different than in the

Great Rift Valley or Western Highlands. The Somali Jet provides southerly flow to the Mendebo, Ahmar, and Ogo Ranges, but available moisture decreases rapidly northward as the Eastern Highlands deflect the Somali Jet ENE toward the Indian Ocean. As a result, moist southerlies (9-13 knots) produce massive uplift along the Mendebo Mountains, but only weak (7-11 knots) Somali Jet flow enters the southern Great Rift Valley between July and September.

The southern Ahmar Mountains also get Somali Jet flow (SSW at 10-14 knots), but it is very dry. The swift low-level current deflects towards the Indian Ocean--east of Hargeisa--before leaving the region in the southeastern Ogo Highlands. Wind speeds near the exit region are 17-25 knots by day and 25-35 knots at night. Figure 4-8 gives mean surface wind speeds and prevailing directions at four Ethiopian locations. At Addis Ababa and Asmara, mean direction shifts to easterly in September, while prevailing direction at Neghelle and Dire Dawa remains southerly throughout the Southwest Monsoon. These regional differences illustrate the Monsoon Trough's effect on the Western and Eastern Highlands.

ETHIOPIAN HIGHLANDS
SOUTHWEST MONSOON ("Kremp")

June-September

		JUN	JUL	AUG	SEP
<div style="display: flex; flex-direction: column; align-items: center;"> <div>S-SW/E</div> <div>NW/E</div> <div>S-W</div> <div>S</div> </div>	Addis Ababa	9.10	8.50	9.10	9.60
	Asmara	9.10	10.30	8.60	9.70
	Neghelle	9.10	7.30	8.30	5.30
	Dire Dawa	9.20	10.30	8.50	7.90

Figure 4-8. Mean Southwest Monsoon Surface Wind Speed (kts) and Prevailing Direction, Ethiopian Highlands.

Figure 4-9 shows generalized late Southwest Monsoon season 850-mb moisture flow over the Ethiopian Highlands. The dashed flow arrows represent Somali Jet flow, while the solid arrows denote Turkana

Channel flow and interior African Monsoon Trough flow. The Monsoon Trough's position in late July and early August results in the maximum moist southerly flow into the region.

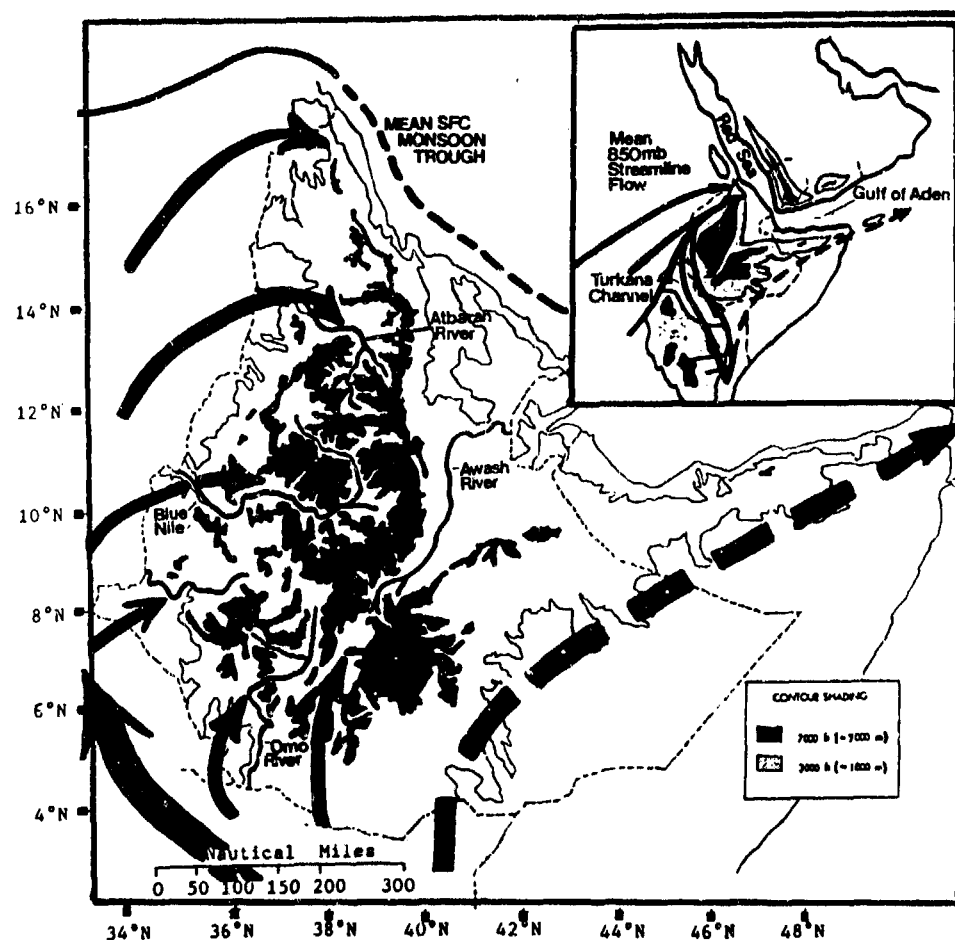


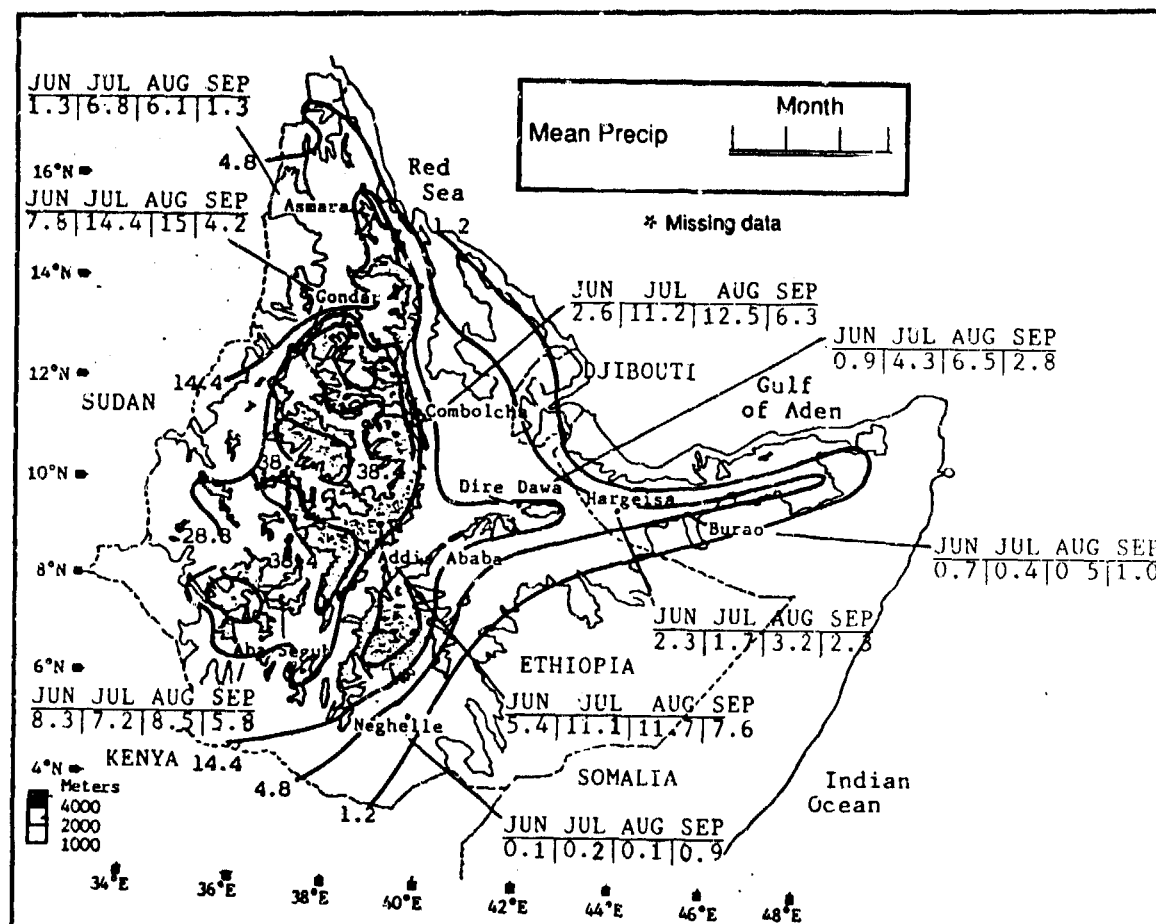
Figure 4-9. Generalized Southwest Monsoon 850-mb Streamline Flow Pattern and Low-Level Moisture Inflow Trajectories. Dashed line is Somali Jet flow; solid lines are Turkana Channel and interior African Monsoon Trough flow.

ETHIOPIAN HIGHLANDS SOUTHWEST MONSOON ("Kiremt")

June-September

PRECIPITATION. Between 55 and 90% of Ethiopian Highland total annual rainfall occurs during the Southwest Monsoon--see Figure 4-10. Heavy isolated convective activity develops daily along the rugged, sparsely populated western and southern slopes of the Western Highlands' Choke, Seshia, and Eritrean Mountains, as well as the Eastern Highlands' Mendebo

Mountains. Southerly low-level flow is lifted orographically to produce massive convective cells that form, dissipate, then regenerate in mid-and upper-level easterlies aloft. Widespread areas of continuous rainshowers or steady drizzle spread downwind from the Mendebo Mountains into the southern Great Rift Valley when mid-level easterly flow is from 12 to 18 knots.



ETHIOPIAN HIGHLANDS SOUTHWEST MONSOON ("Krempi")

June-September

ridges above 10,000 feet (3,050 meters) have a greater frequency of 0900-1300 LST thunderstorms because the initial convective activity develops at these higher elevations before moving downwind. July and August are also the primary thunderstorm months in the central and northern Western Highlands as strong surface heating and deep moisture penetrations (south of the Monsoon Trough) from interior equatorial Africa consistently invade from the southwest. Peak thunderstorm days in the southern Western Highlands (the Seshia Mountains) are in June and July. As a result, the Monsoon Trough's migration along the western periphery of the Ethiopian Highlands produces a similar migration of peak thunderstorm frequency northward. Hail occurs on 6 days during the Southwest Monsoon, but is extremely variable in size and duration.

TEMPERATURE. Typically, mean daily maximum temperatures (see Figure 4-11) are lower during the Southwest Monsoon than in any other period because of the heavy convection that prevents intense surface heating. Mean daily highs range from 69°F (21°C) at Addis Ababa, where rain falls nearly every day, to 95°F (35°C) at Dire Dawa, located on the leeward (north) slopes of the Ahmar Mountains of the Eastern Highlands. Record highs range from 86°F (30°C) at Asmara to 112°F (44°C) at Burao, both recorded in June. Elevation determines diurnal temperature ranges; normally, there is only a 10 to 20°F (11°C) range during the Southwest Monsoon. Mean daily lows range from 49°F (9°C) at Addis Ababa to 68°F (20°C) at Dire Dawa. Record lows include readings of 36°F (2°C) at Addis Ababa in June and 50°F (10°C) at Hargeisa in August.

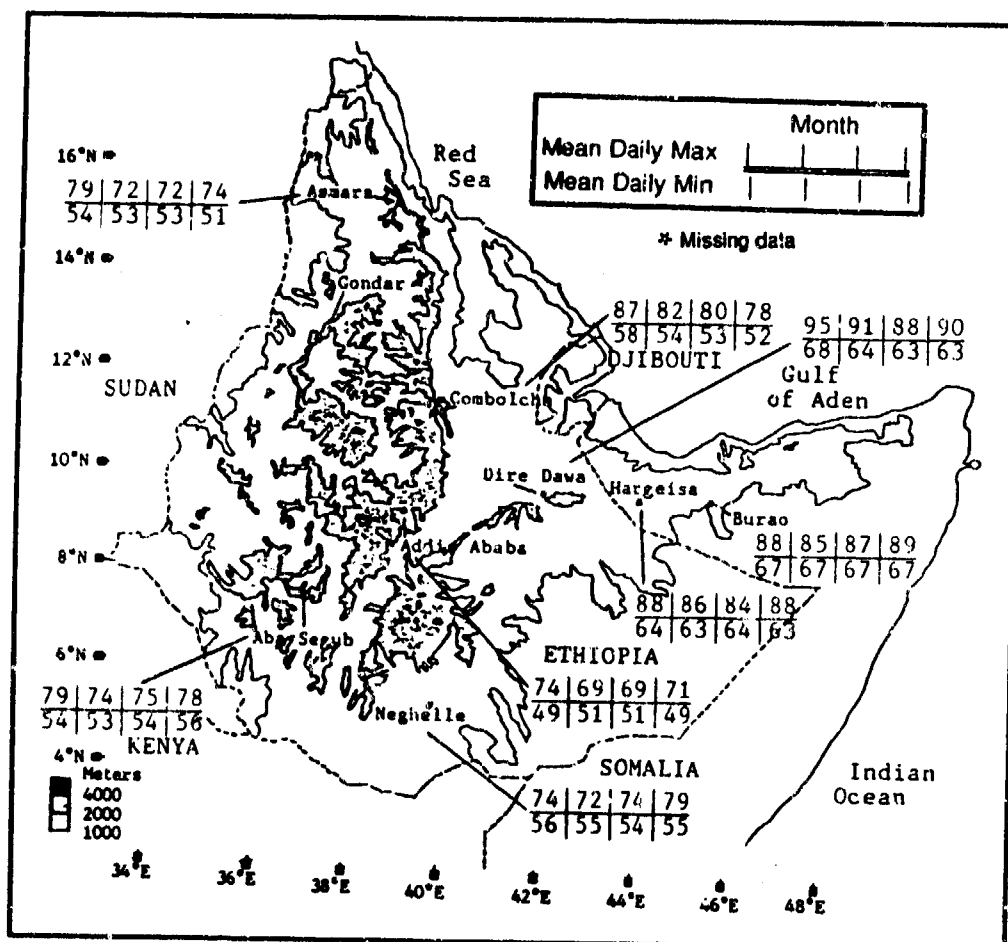


Figure 4-11. Mean Southwest Monsoon Daily Maximum/Minimum Temperatures (°F), Ethiopian Highlands.

ETHIOPIAN HIGHLANDS SOUTHWEST-TO-NORTHEAST MONSOON ("Kremp")

October-November

GENERAL WEATHER. Transition weather is characterized by a gradual large-scale wind reversal. The Monsoon Trough's rapid southward migration confines southerly flow and moisture to the Western Highlands south of 8° N during October and early November. However, dry easterlies prevail north of the Monsoon Trough, and the effects--decreased moisture and rainfall--move southward with the Monsoon Trough. By the end of the transition in November, fair weather dominates, with isolated showers and significant cloud cover found only in the southern parts of the Western and Eastern Highlands.

The Somali Jet rapidly weakens in strength by mid-October. The Monsoon Trough--positioned north of the Somali Jet's southerly flow--is backed by deep but weak (4- to 8-knot) northeasterlies that migrate slowly southward into the southern Eastern Highlands. Dry conditions and fair weather dominate by early November. The only significant weather occurs when

scattered shower activity occurs along the surface Monsoon Trough's western axis (Indian Ocean segment) on the eastern slopes and adjacent Eastern Highlands' plateaus. The Great Rift Valley is dominated by dry easterly flow at all levels. Significant weather only occurs in the extreme southern Great Rift Valley whenever southerly flow temporarily penetrates to 7° N. Orographic uplift produces brief afternoon showers over this area. Clouds are mostly stratocumulus and cumulus.

SKY COVER. Mean cloudiness (Figure 4-12) decreases from south to north across the region with reduced southerly flow and available moisture. The northern parts of the region see less than 35% mean cloud cover during the transition; most is from isolated convection produced by diurnal surface heating. Higher mean cloudiness percentages in the south are attributed to the effects of the Somali Jet and Monsoon Trough that may persist through the transition.

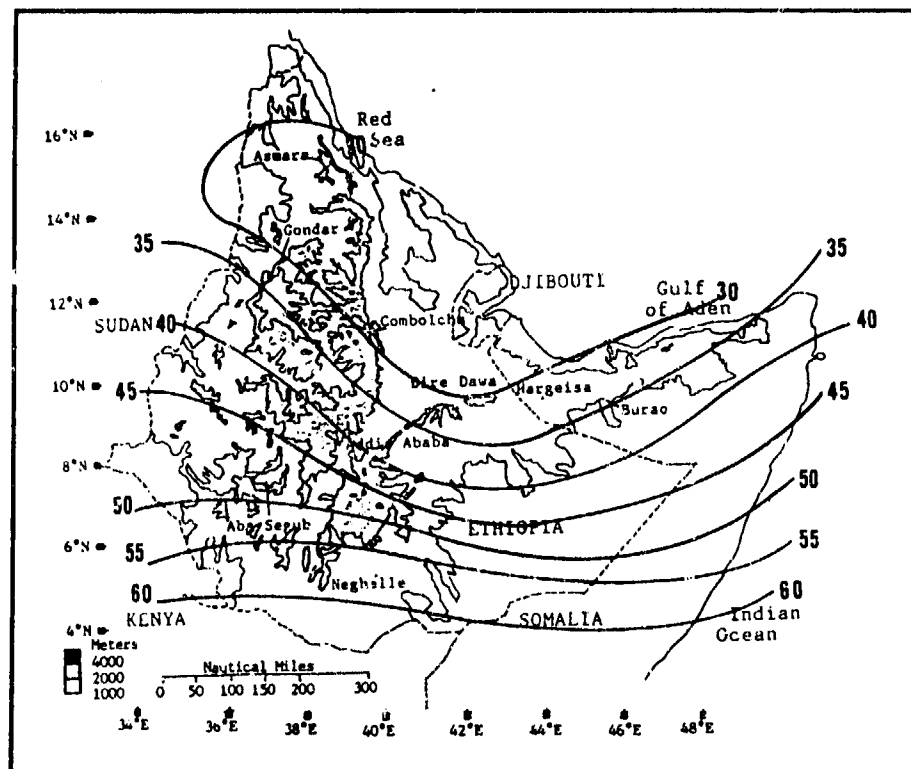


Figure 4-12. Mean SW-NE Monsoon Transition Cloudiness Frequencies, Ethiopian Highlands. Isolines are in 5% intervals. The data was derived by calculating the grand mean from National Intelligence Summary (NIS) mean cloudiness data for specific sites between June and September.

ETHIOPIAN HIGHLANDS

SOUTHWEST-TO-NORTHEAST MONSOON ("Kremp")

October-November

The mean cloudiness shown in Figure 4-12 ranges from 27% at Asmara to 58% at Neghelle. Mid-afternoon cumulus and cumulonimbus are the main cloud types. Bases average 4,000 feet (1,220 meters) AGL. Tops occasionally reach 40,000 feet (12.2 km) MSL in early October along the Western Highlands. In November, tops seldom reach 20,000 feet (6.1 km), but towering cumulus and isolated thunderstorms, associated with strong mid- and upper-level troughs, may occur in the Eritrean Mountains; tops may reach 35,000 feet (10.7 km). Most clouds dissipate by 1100 LST.

Low ceiling frequencies (Figure 4-13) vary throughout the Ethiopian Highlands. Typically, the highest frequency of ceilings below 3,000 feet (915 meters) is between 0600 and 1500 LST because of orographic lift and surface heating along the windward slopes of the Seshia, Choke, and Mendebo Mountains. Ceilings below 5,000 feet (152 meters) due to thick stratus formation after sunrise in Western Highlands valleys are most common between 0600 and 0900 LST. High mountain peaks and their adjacent slopes and valleys see low clouds, or are even obscured, every day.

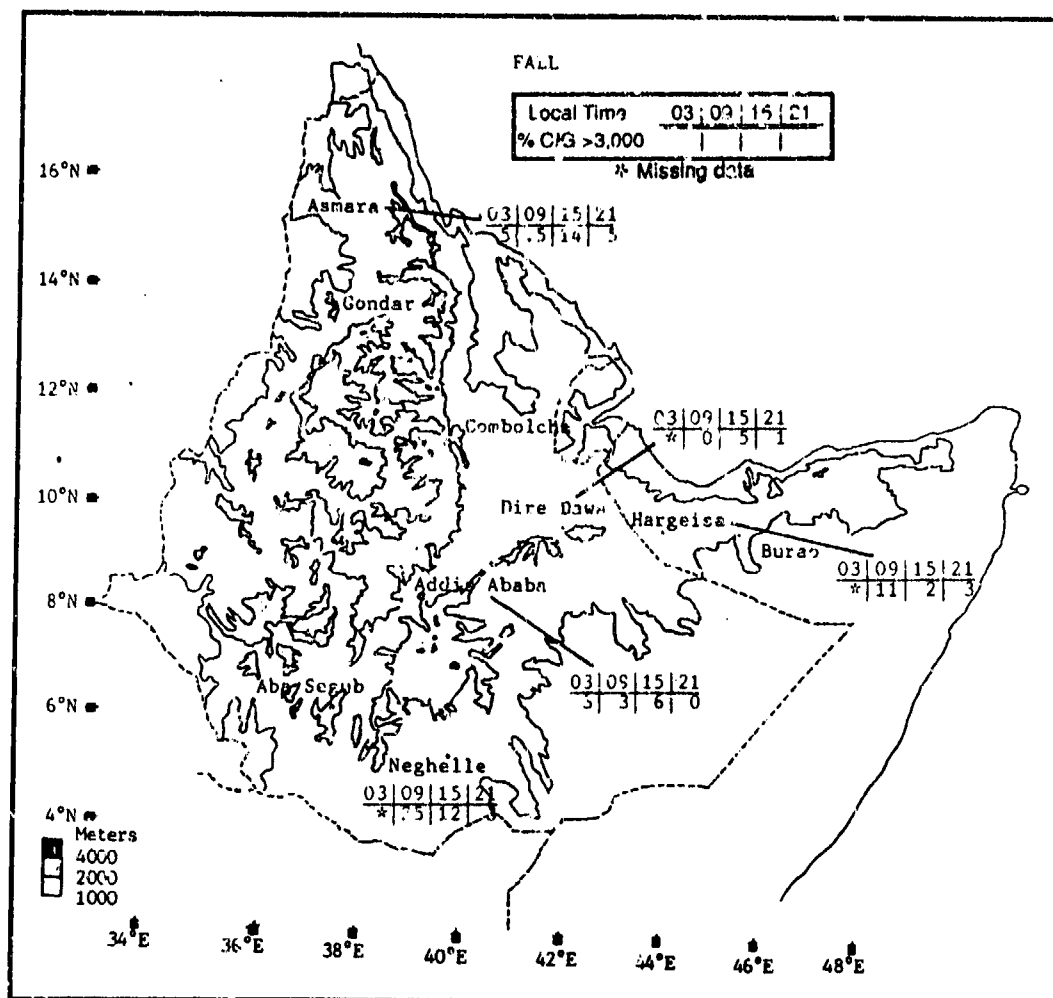


Figure 4-13. SW-NE Monsoon Transition Frequencies of Ceilings Below 3,000 Feet (915 meters), Ethiopian Highlands.

ETHIOPIAN HIGHLANDS SOUTHWEST-TO-NORTHEAST MONSOON ("Krempt")

October-November

VISIBILITY. Visibilities in the Ethiopian Highlands are greater than 6 miles more than 95% of the time during the transition, they are below 3 miles less than 3% of the time. Figure 4-14 shows the frequency

distribution of low visibilities across the Ethiopian Highlands. Note that remote mountain valleys and ridges may see visibilities near zero for 2-4 hours during heavy rains or early morning ground fog.

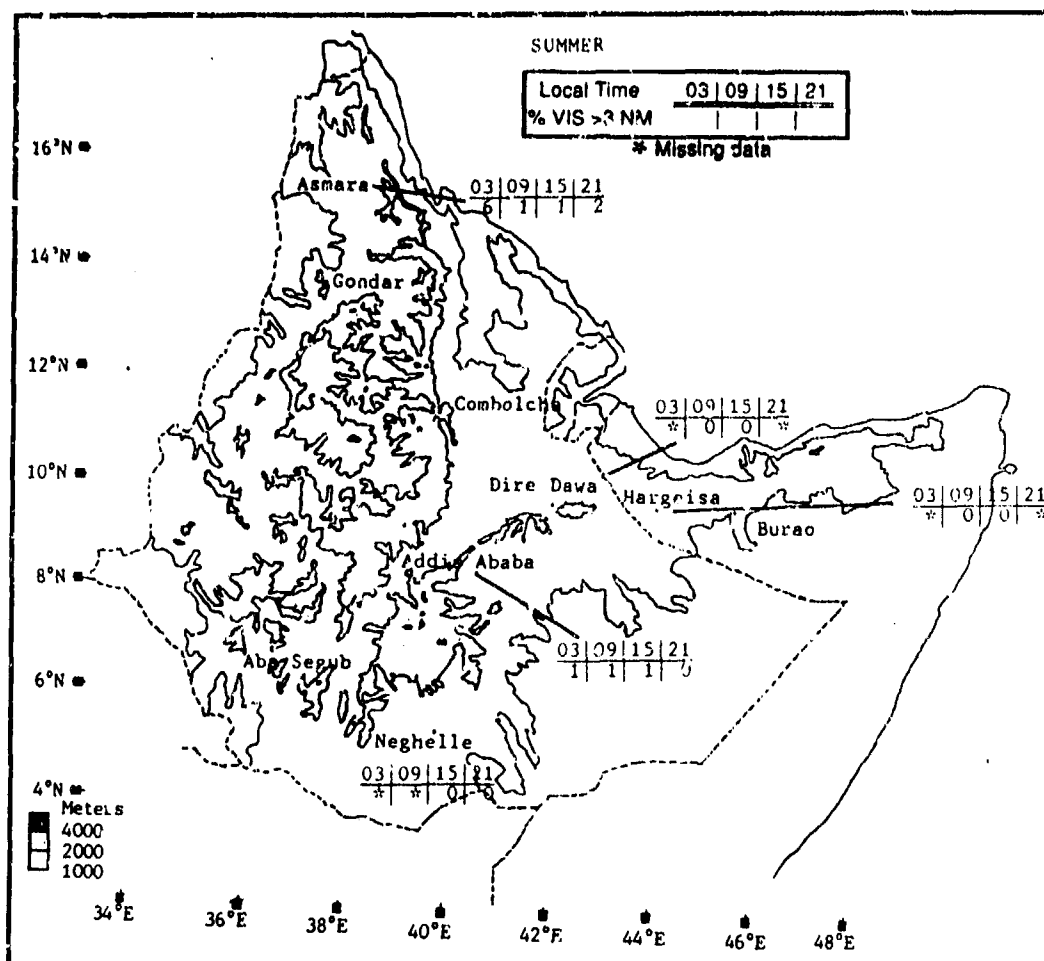


Figure 4-14. SW-NE Monsoon Transition Frequencies of Visibilities Below 3 Miles, Ethiopian Highlands.

WINDS. The Monsoon Trough moves rapidly southward through the Ethiopian Highlands during the transition, preceded by light and variable winds and followed by drier air currents from the northeast. The northeasterlies affect the northern Ethiopian Highlands--the Ogo, Ahmar, and Eritrean Ranges--and northern Great Rift Valley sites by mid-October. Weak southerly flow still dominates the southern Ethiopian Highlands and its Choke, Seshia, and Mendebo Ranges.

Mean surface wind speeds and prevailing directions (Figure 4-15) show prevailing easterly flow in the

Western Highlands (Addis Ababa-Asmara). Speeds average 7-11 knots. At night, local mountain winds average only 3-7 knots. The south to east prevailing winds at Dire Dawa and southeast to east winds at Neghelle show the Somali Jet's influence in October. By late November, wind direction is northeasterly. At Dire Dawa, the northerly wind component represents a localized upsloping daytime circulation.

Northeasterly flow produces local orographic uplift along the northern Ogo Highlands, as well as in the Ahmar and eastern Eritrean Mountains. Low-level

ETHIOPIAN HIGHLANDS SOUTHWEST-TO-NORTHEAST MONSOON ("Kremp")

October-November

easterly flow is relatively dry, but mid- and upper-level easterlies accentuate orographic uplift into the northern half of the Ethiopian Highlands. Cumulus development through orographic uplift now occurs on the north and

eastern slopes but is less extensive during the transition because of the relative dryness of the low-level northeasterlies.

E-ESE
E-ESE
SE-E/E-NE
S-E/E-N

	OCT	NOV
Addis Ababa	10.70	9.60
Asmara	8.70	7.90
Neghelle	5.10	7.30
Dire Dawa	5.50	5.00

Figure 4-15. Mean SW-NE Monsoon Transition Wind Speed (kts) and Prevailing Direction, Ethiopian Highlands.

PRECIPITATION. October rainfall at Aba Segub (in the southern Seshia Mountains) is 5.5 inches (140 mm); Neghelle gets 3.3 inches (84 mm); Gondar, 2.1 (53 mm). The other stations shown in Figure 4-16 get 1 inch (25 mm) or less in October. Moderate to heavy precipitation rarely occurs below 10,000 feet (3,050 meters), but heavy convection, generated by moist southerly low-level flow near the Monsoon Trough, builds along the southern Seshia, Choke, and Mendebo Mountains. Convective cells move slowly westward with light rain showers and continuous drizzle spreading downwind from the main convective cells.

The eastern Eritrean Mountains and northern Ahmar/Ogo Ranges see orographic showers with northeasterly flow. Isolated towering cumulus brings light showers to the northern Great Rift Valley, but the low-level north-easterlies lack the moisture to form massive convective cells. Convective cloudiness and low-level moisture are normally confined to the first mountain slopes that lift the flow. By November, northeasterly low-level flow penetrates to 6° N, and

significant localized Gulf of Aden moisture ascends the northern Ogo/Ahmar and eastern Eritrean Mountains. However, orographic rainshowers are light because the large-scale air mass is extremely dry. Isolated convective activity rarely regenerates into massive cloud clusters. Often, the original convective cell dissipates with only a trace or 0.01 inches (0.025 mm) of rainfall below 5,000 feet (1,524 meters) MSL. From 0.25 to 0.50 inches (6-13 mm) may fall along higher ridge crests.

In November, moist southerly flow along the Monsoon Trough penetrates only to the extreme southern Mendebo Seshia, and Choke Mountains. Normally, the Trough is too far south for widespread heavy convection and significant rainfall to persist for more than 12 hours. November rainfall is primarily generated by diurnal convective heating and isolated orographic uplift of localized moisture from lakes and marshlands. Moderate showers may occur above 10,000 feet (3,050 meters), but they are extremely variable in duration and intensity. Light rainshowers and drizzle are common downwind from convective activity.

ETHIOPIAN HIGHLANDS
SOUTHWEST-TO-NORTHEAST MONSOON ("Kremp")

October-November

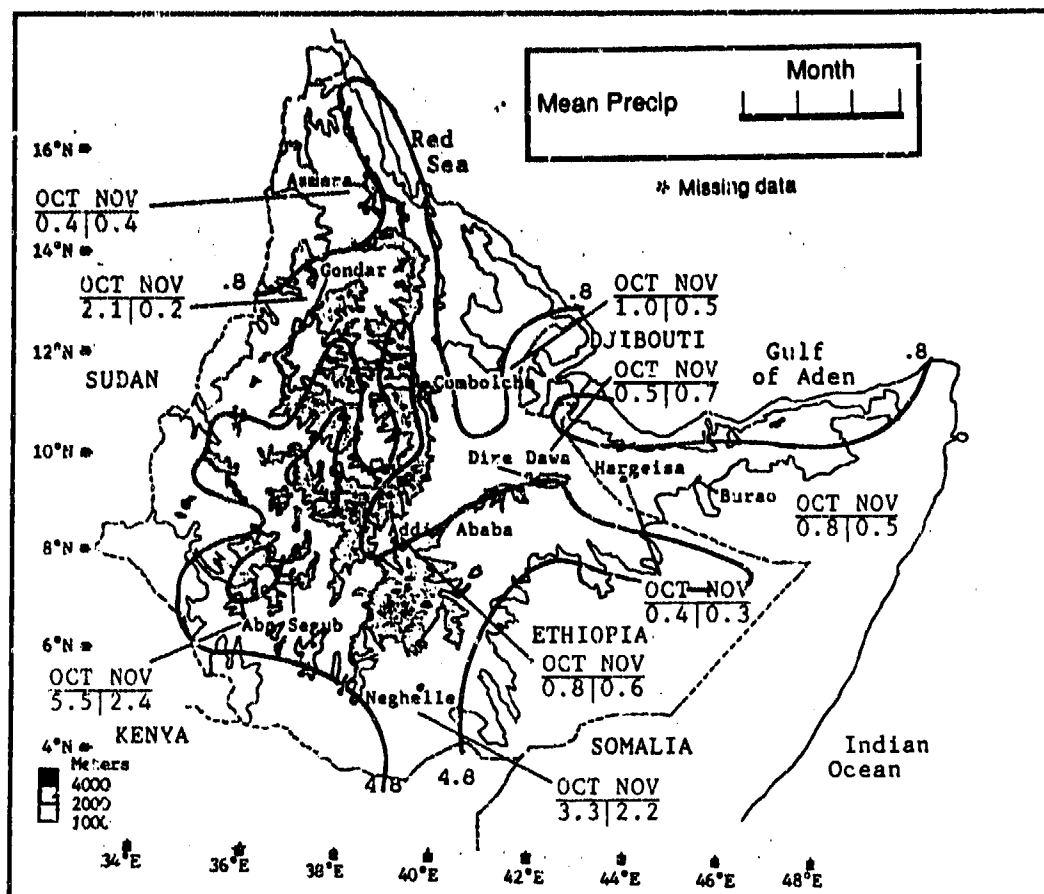


Figure 4-16. Mean SW-NE Monsoon Transition Monthly Precipitation, Ethiopian Highlands. Isohyets represent mean seasonal rainfall totals (inches).

ETHIOPIAN HIGHLANDS SOUTHWEST-TO-NORTHEAST MONSOON ("Kremp")

October-November

TEMPERATURE. Mean daily highs average 72-91°F (22-33°C). Record highs range from 86°F at Asmara in October to 100°F at Neghelle, also in October. Radiation cooling, clear skies, and low mid-level air temperatures result in lower mean daily minimum temperatures above 7,000 feet/ 2,134 meters (Addis

Ababa, Asmara, Combolcha) than at 4,000 feet/1,220 meters (Burao, Dire Dawa). Mean daily lows average 43-63°F (6-17°C) with record lows of 29°F (-2°C) at Addis Ababa and 46°F (8°C) at Dire Dawa, both in November.

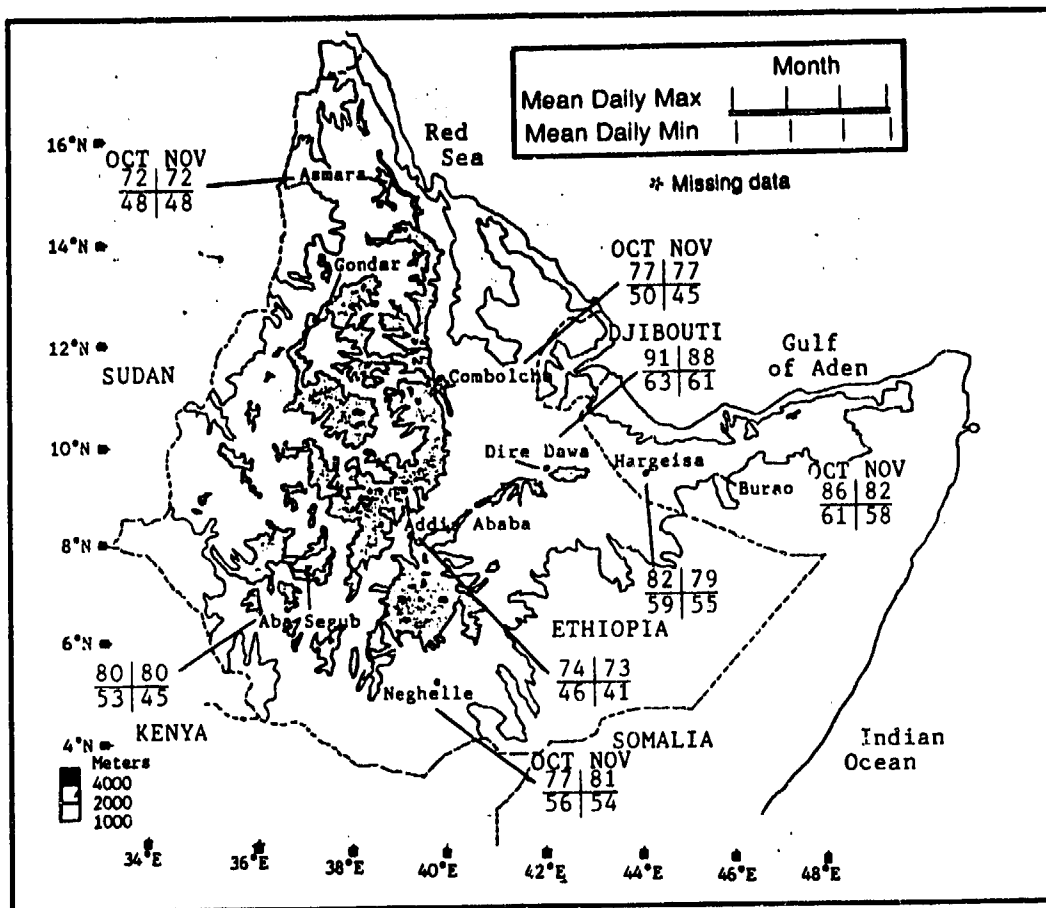


Figure 4-17. Mean SW-NE Monsoon Transition Daily Maximum/Minimum Temperatures (°F), Ethiopian Highlands.

ETHIOPIAN HIGHLANDS NORTHEAST MONSOON

December-March

GENERAL WEATHER. Northeast Monsoon circulation dominates most of the region during fair weather, but the Western Highlands and its complex terrain create a unique low-level transition zone for African and Asian flow. These two low-level circulations--the Northeast Monsoon and Sahara Desert westerly flow--converge in the southern Red Sea. The Western Highlands force the recurvature of low-level westerlies around the northern tip of the Eritrean Mountains. The Red Sea Convergence Zone (RSCZ)--see Chapter 2--represents the low-level transition zone.

When cyclonic activity and disturbed weather migrates eastward across the northern Ethiopian Highlands, low-level westerlies temporarily override Northeast Monsoon flow in the northern Great Rift Valley and Eastern Highlands. Mid-level flow funnels southward through the northern Great Rift Valley. Normally, the low-level Northeast Monsoon flow extends westward to the western edge of the Great Rift Valley in fair weather. However, a frontal passage may

temporarily reverse the flow for 4-12 hours. West-northwesterlies may reach the eastern Ogo Highlands before the Northeast Monsoon regains its momentum and reverses low-level flow.

At the upper levels, the Subtropical Ridge is oriented WSW-ENE above the region during the Northeast Monsoon. This splits upper-level circulation into westerly and easterly branches. The southernmost extent of westerly upper-level flow affects the northern two-thirds of the Western Highlands and Great Rift Valley, as well as the extreme west edge of the Eastern Highlands, between mid-January and late February. By March, only the extreme northern tip of the Western Highlands are affected by westerly upper-level flow because the Subtropical Ridge has migrated to 15° N. See the mean monthly 200-mb flow patterns in Chapter 2 to understand the Subtropical Ridge's seasonal oscillation path over the region. A three-level wind direction profile at Addis Ababa (Figure 4-18) illustrates the upper-level wind shift over the Ethiopian Highlands between mid-January and late February.

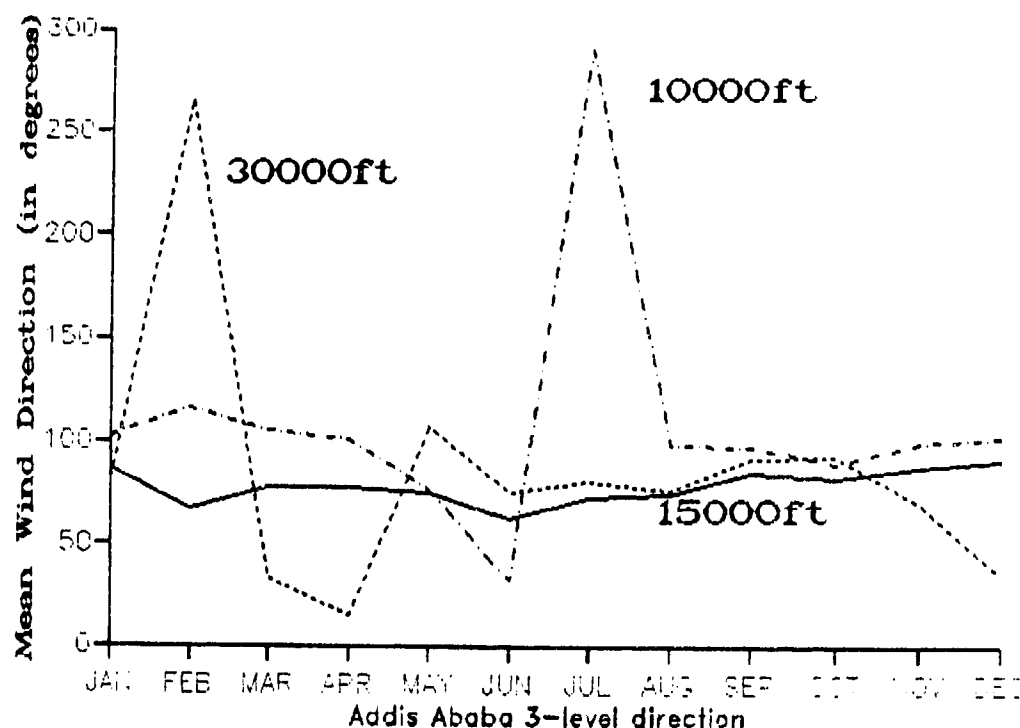


Figure 4-18. Mean Annual Wind Direction, Addis Ababa, Ethiopia. Note the consistent mid-level easterly flow during the Northeast Monsoon, as well as the mean upper-level (30,000-foot/9,146 meter) westerly flow during mid-January through late February.

ETHIOPIAN HIGHLANDS NORTHEAST MONSOON

December-March

SKY COVER. Orographic uplift and diurnal surface heating produce nearly all daytime low-and mid-level cloud cover. The southern Great Rift Valley sees the most daytime cloud cover, but low clouds (scattered cumulus and stratocumulus) average 6,000 to 8,000 feet (1,829-2,439 meters) AGL and cover only 2-3/8ths. Evening sees stratus and stratocumulus forming as strong radiative cooling produces shallow temperature and moisture inversions; bases average 4,000-6,000 feet (1,220-1,829 meters) AGL. Most nocturnal cloud cover is thin, except for occasional thick ground fog that develops near large lakes. The numerous water bodies in the southern Great Rift Valley often produce fog or very low stratus in the early morning because the water temperature is often 10-15°F (4-6°C) warmer than the land.

orographic uplift only occurs along the Western/Eastern Highlands' north- and east-facing slopes, which are perpendicular to the prevailing flow and produce the greatest uplift. Extensive cumulus development is limited to ridge crests above 10,000 feet (3,050 meters) MSL in the Ahmar Mountains near Dire Dawa and eastern Eritrean Mountains between Combolcha and Addis Ababa. Thin cirrus is also common.

When the rare cyclonic storm extends a weak cold front into the southern Red Sea and Gulf of Aden, westerly flow produces strong orographic uplift against the western Eritrean Mountains between Asmara and Gondar. However, most of Asmara's scant Northeast Monsoon cloud cover and precipitation occurs with low-level convergence along the Red Sea Convergence Zone (RSCZ)--see Chapter 2--rather than from weak frontal passages.

Figure 4-19 shows mean Northeast Monsoon cloudiness across the Ethiopian Highlands. Typically,

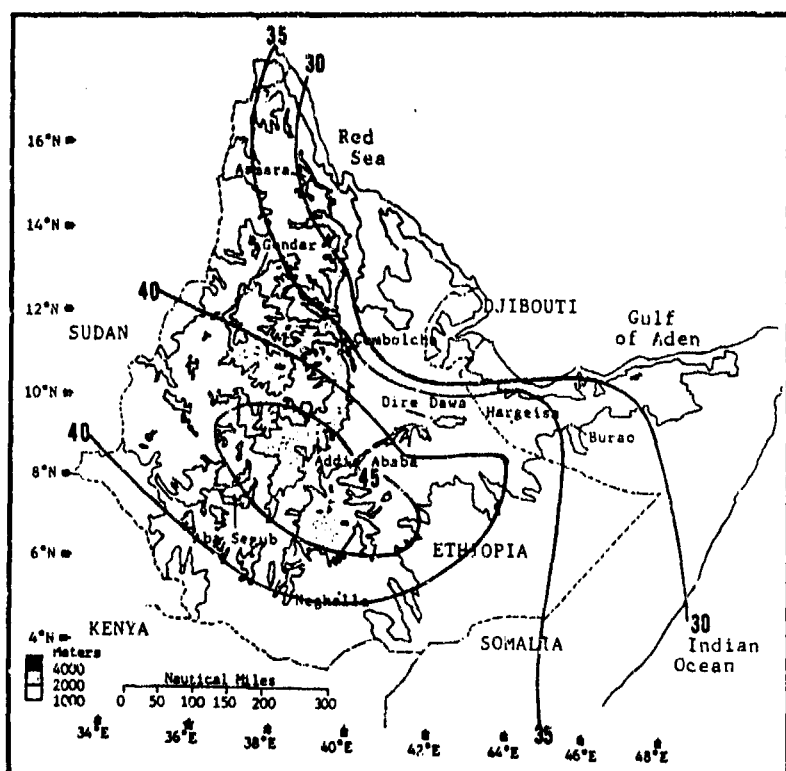


Figure 4-19. Mean Northeast Monsoon Cloudiness Frequencies, Ethiopian Highlands. Isolines are in 5% intervals. The data is derived by calculating the grand mean from National Intelligence Summary (NIS) mean cloudiness data for specific hours between December and March.

ETHIOPIAN HIGHLANDS NORTHEAST MONSOON

December-March

Ceilings at or below 3,000 feet (915 meters) AGL average less than 25% (see Figure 4-20). Note that several stations (Hargeisa, Dire Dawa, and Neghelle) do not report 0300 LST ceiling data. Hargeisa's 24% low ceiling frequency (Figure 4-20) at 0900 LST is mostly stratus and stratocumulus that dissipate by 1100 LST. Ceiling frequencies at or below 1,000 feet (305 meters)

AGL are only 1-5%, and occur most frequently in the morning. Typically, ceilings at or below 3,000 feet/915 meters AGL occur at mid-morning (0900 LST) in the southern Ethiopian Highlands and at night in the northern Eritrean/Great Rift Valley. At Dire Dawa, low ceiling frequencies are higher in afternoon and early evening than at night because of uplift in the Ahmer Mountains.

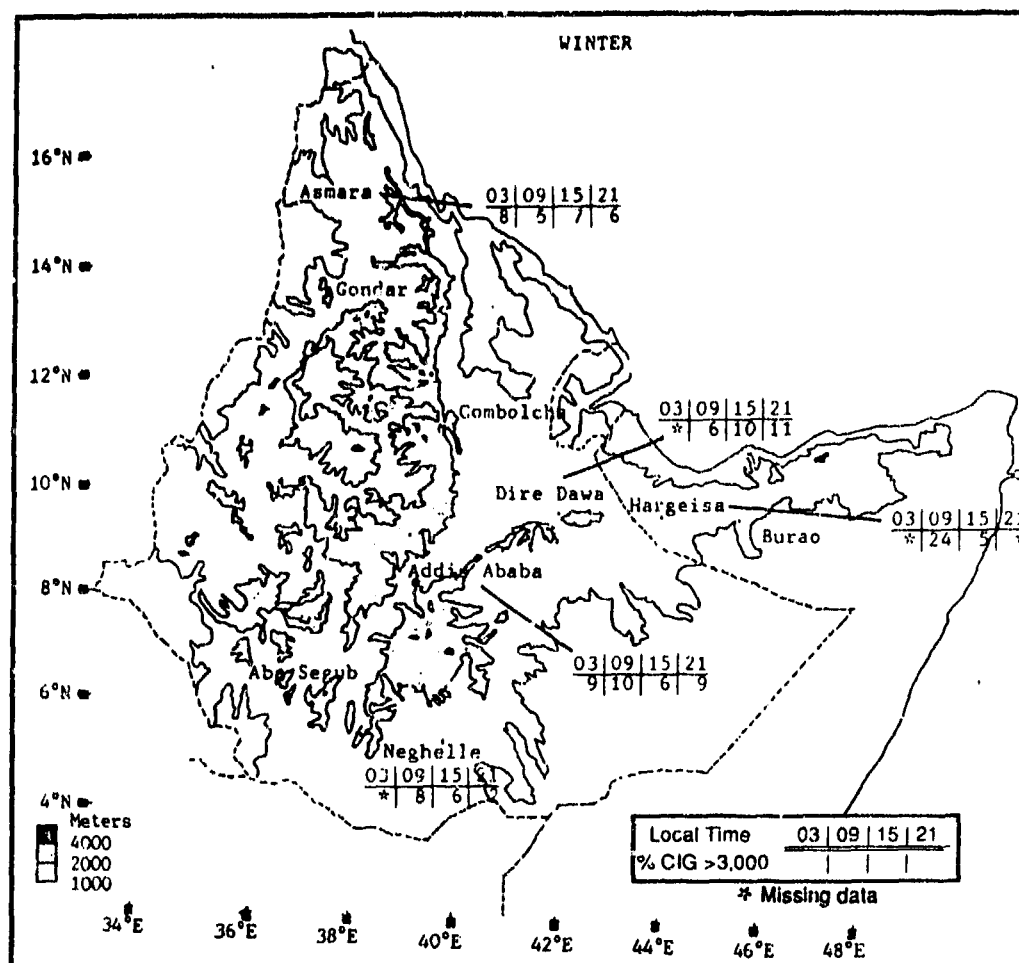


Figure 4-20. Northeast Monsoon Frequencies of Ceilings Below 3,000 Feet (915 meters), Ethiopian Highlands.

VISIBILITY. As shown in Figure 4-21, visibilities below 3 miles are very rare during the Northeast Monsoon. Radiation fog (from 0300 to 0800 LST) is the primary cause of low visibilities in high mountain valleys above 10,000 feet (3,050 meters).

Dust/sandstorms may limit visibilities in the lower elevations (below 5,000 feet/1,524 meters) as high winds lift the drier soil. Local visibilities below 3 miles occur in the Western Highlands with most frontal passages, regardless of strength.

ETHIOPIAN HIGHLANDS NORTHEAST MONSOON

December-March

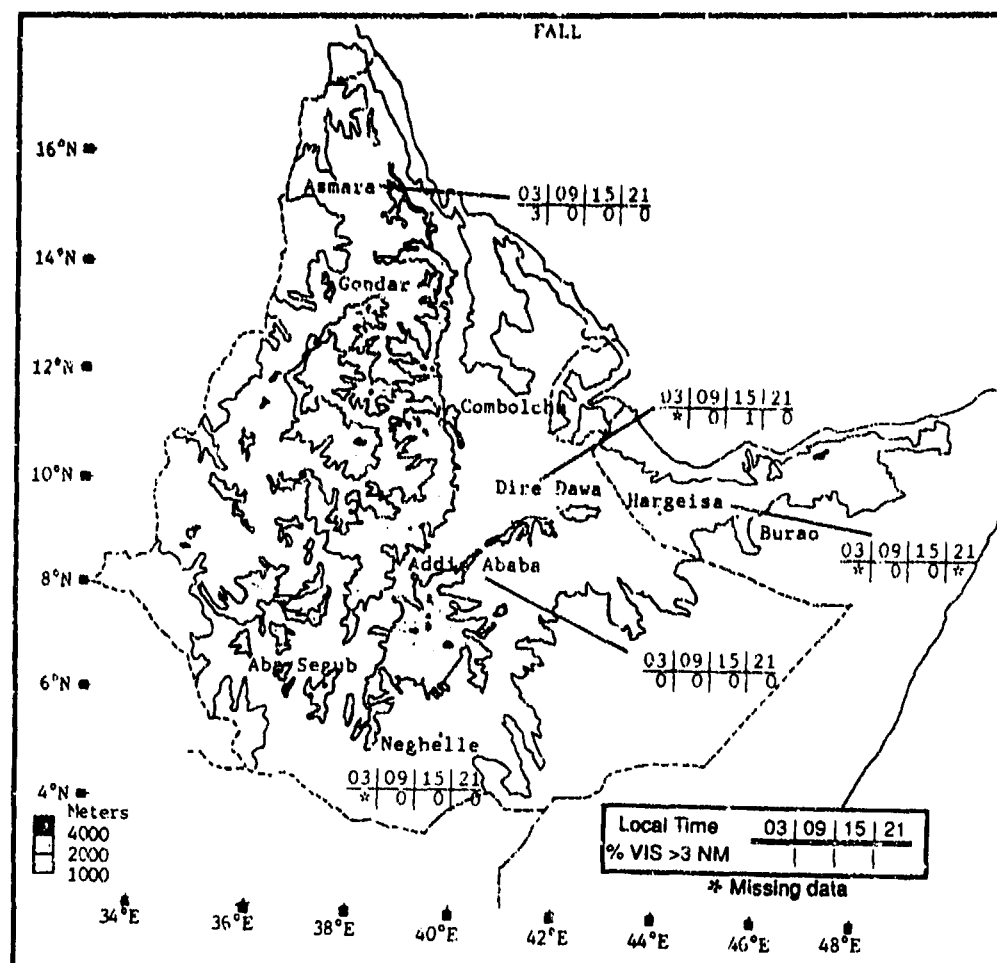


Figure 4-21. Northeast Monsoon Frequencies of Visibilities Below 3 Miles, Ethiopian Highlands.

WINDS. Prevailing wind directions and speeds shown in Figure 4-22 vary significantly because of the complex topography in the Ethiopian Highlands. Low-level convergence between Northeast Monsoon and Sahara Desert flow occurs in the southern Red Sea north of the region. It also affects the Eritrean Mountains' northern tip, near Asmara. East of Asmara, wind shifts are often dramatic. East-southeasterly flow at 8-11 knots during fair weather shifts to northwesterly (5-10 knots) with frontal passages. By March, west southwesterly flow affects Asmara regularly. The rugged western interior of the Eritrean, Choke, and Seshia Mountain Ranges have complex mid- and upper-level flow patterns. These are

the only places in the Ethiopian Highlands where mid- and upper-level conditions deviate from easterly flow.

Through February, weak upper-level westerlies at 10-15 knots may migrate southward to 7-8° N and penetrate to the western edges of the Great Rift Valley. Fair-weather mid-level flow is easterly at 10-15 knots. When upper-level troughs move over the interior Western Highlands, weak west-southwesterlies and orographic uplift are temporarily established at the mid-levels, but easterly flow is reestablished after the trough passes.

**ETHIOPIAN HIGHLANDS
NORTHEAST MONSOON**

December-March

	DEC	JAN	FEB	MAR
ESE				
SE/WSW				
E-NE				
W-N				
Addis Ababa	8.40	9.10	8.50	9.10
Asmara	7.90	8.10	9.00	8.60
Neghelle	7.30	7.00	8.90	7.50
Dire Dawa	4.10	4.40	4.90	6.80

Figure 4-22. Mean Northeast Monsoon Wind Speed (kts) and Prevailing Direction, Ethiopian Highlands.

The Eastern Highlands (shaded in Figure 4-23) split the persistent low-level northeasterly Monsoon flow into a relatively moist Gulf of Aden current and a very dry low-level Indian Ocean current.

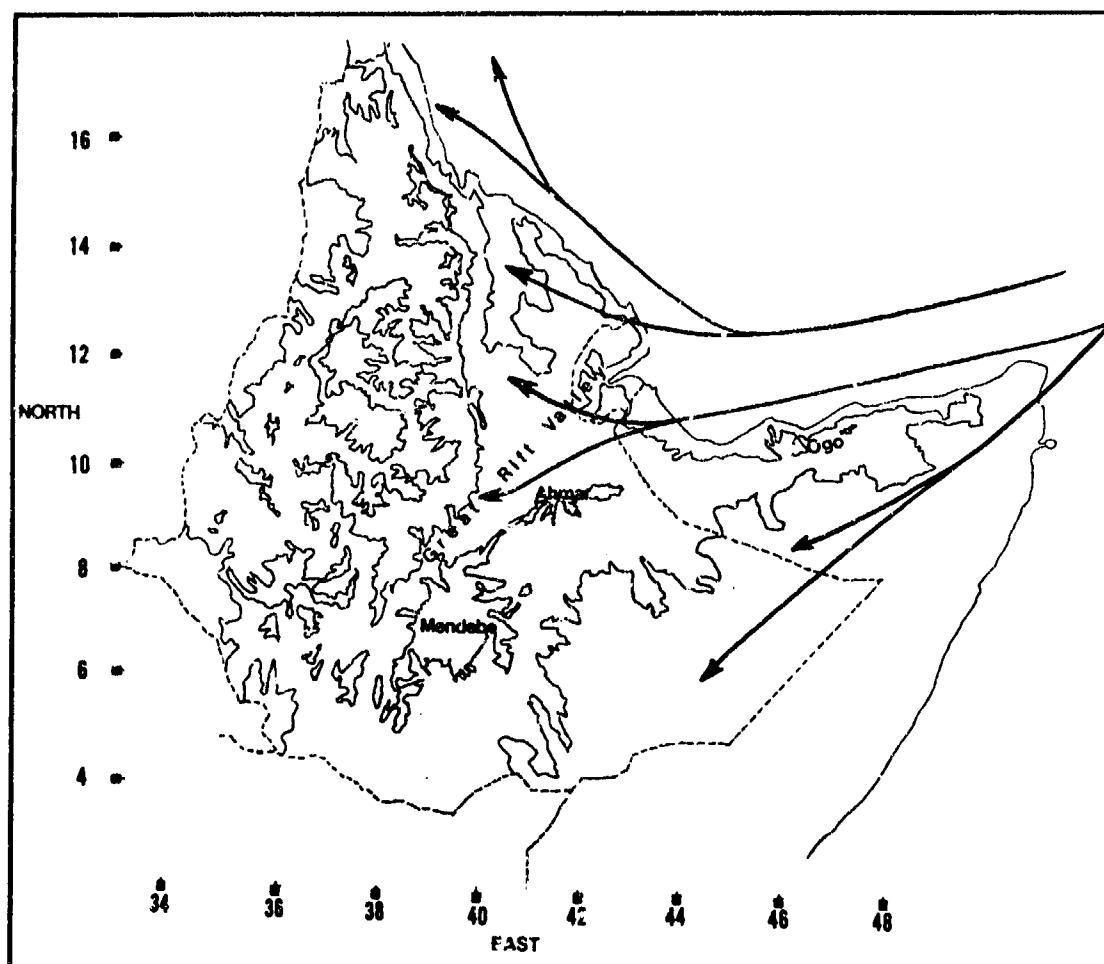


Figure 4-23. Generalized Low-Level Flow Across the Eastern Highlands (shaded) During the Northeast Monsoon.

ETHIOPIAN HIGHLANDS NORTHEAST MONSOON

December-March

The dry current shown in Figure 4-23 flows along the southern Eastern Highland slopes of the Ogo, Ahmar, and Mendebo Ranges and the plateaus of southeastern Ethiopia. The moist current advects west-southwestward along the northern Ogo and Ahmar Ranges in the northern Eastern Highlands, then recurves southward into the northern and central Great Rift Valley as far as Addis Ababa. During fair weather, Northeast Monsoon flow crosses the entire northern Great Rift Valley and ascends the eastern Eritrean Mountains between 12° and 14° N. To the north and west of the eastern Eritrean Ranges, northeasterlies recurve northward into the southern Red Sea. It is rare for low-level Northeast Monsoon flow to penetrate the rugged Western Highlands interior. The Western Highlands are a transition zone for airflow below 5,000 feet (1,524 meters) MSL. The eastern

Eritrean Mountains between Asmara and Addis Ababa block low-level northeasterly flow from entering the Seshia, Choke and interior Eritrean Ranges. As a result, a Northeast Monsoon/Sahara desert/Mediterranean Sea low-level airflow boundary is established along these ranges. In the western and interior Western Highlands, Mediterranean low-level flow, modified by the desert, can dominate the Northeast Monsoon. Light westerlies at the surface, 10- to 15-knot easterlies between 8,000 and 20,000 feet (2,439-6,097 meters) MSL, and westerlies (15-20 knots) above 30,000 feet (9,146 meters) MSL are common in the Western Highlands when the Subtropical Ridge is south of 12° N. Figure 4-24 shows mean low-level (850 mb) Northeast Monsoon flow across the Western Highlands.

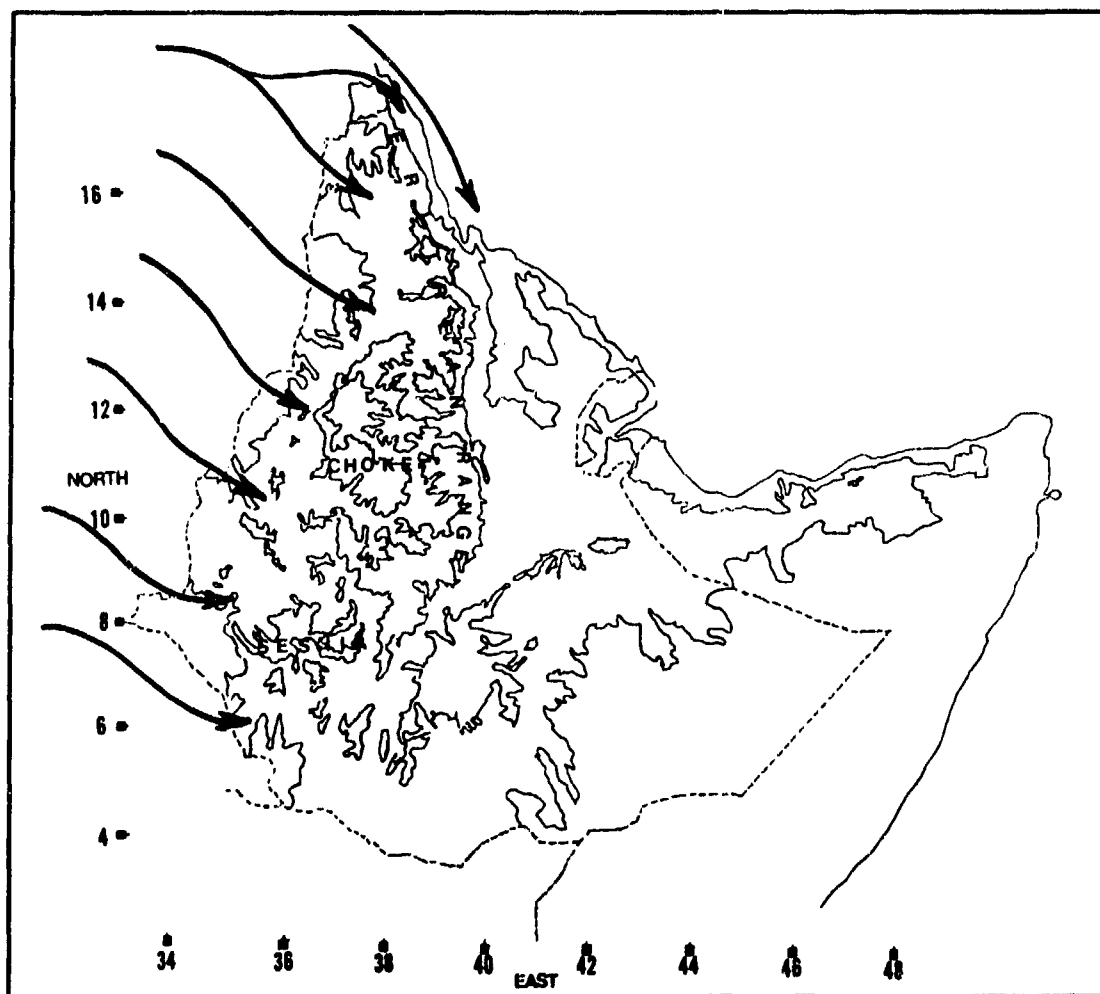


Figure 4-24. Generalized Low-level Flow Across the Western Highlands (shaded) During the Northeast Monsoon.

ETHIOPIAN HIGHLANDS NORTHEAST MONSOON

December-March

Mean mid- and upper-level wind speeds average 10-20 knots. The Subtropical Ridge is oriented WSW-ENE across the region during the Northeast Monsoon. North of the Ridge axis, westerlies (at 15-20 knots) reach Addis Ababa by late February. To the south of the Ridge, easterlies (at 10-15 knots) dominate upper-level flow. By March, the Subtropical Ridge migrates northward. Only the extreme northern tip of the Western Highlands is influenced by upper-level westerly flow.

PRECIPITATION. December is the driest month of the year in the Ethiopian Highlands, but northeasterly flow produces some localized convection along the Eastern Highlands and northern Great Rift Valley. As shown in Figure 4-25, mean precipitation increases are most dramatic in the Great Rift Valley as broad-scale Northeast Monsoon flow becomes well-established in the western Gulf of Aden between January and early March.

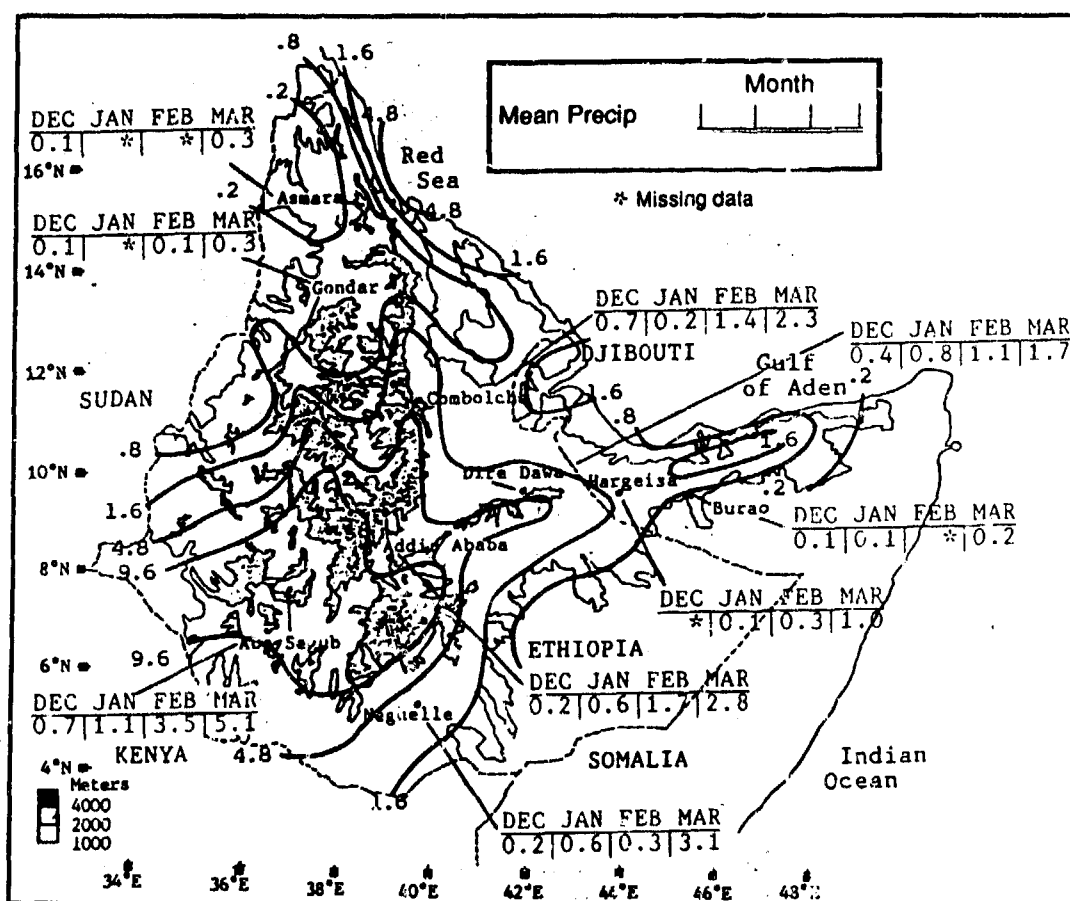


Figure 4-25. Mean Northeast Monsoon Monthly Precipitation, Ethiopian Highlands. Isohyets represent mean seasonal rainfall totals (inches).

Mid-level easterlies increase orographic uplift over the Eastern Highlands and eastern Eritrean Mountains at the lower levels. In the extreme southern Ethiopian Highlands, mean March rainfall is greatest as abundant equatorial moisture begins to surge northward with the Monsoon Trough and Somali Jet Stream. The heaviest rainfall is normally confined to the north-facing ridge crests of the Ogo Highlands and Ahmar Mountains, but rainshowers and drizzle can spread westward with the

easterly mid-level flow along the northern Ogo Highlands and Ahmar Mountains into the northern Great Rift Valley. Normally, precipitation in the Western Highlands only occurs when weak cyclonic activity moves southeastward across the Sahara Desert or when low-level northeasterlies reach the northeastern Eritrean Mountains. These frontal passages affect Asmara most often, but they produce little rainfall beyond 39° E--the eastern edge of the Western Highlands. Approaching

ETHIOPIAN HIGHLANDS NORTHEAST MONSOON

December-March

troughs normally intensify low-level easterly flow and moisture into the western Great Rift Valley. Figures 4-26a and b show a trough approaching Asmara from the

northwest during the Northeast Monsoon. Although enough snow occurs to produce shallow snow depths, the snow line is above 12,000 feet (3,659 meters) MSL.

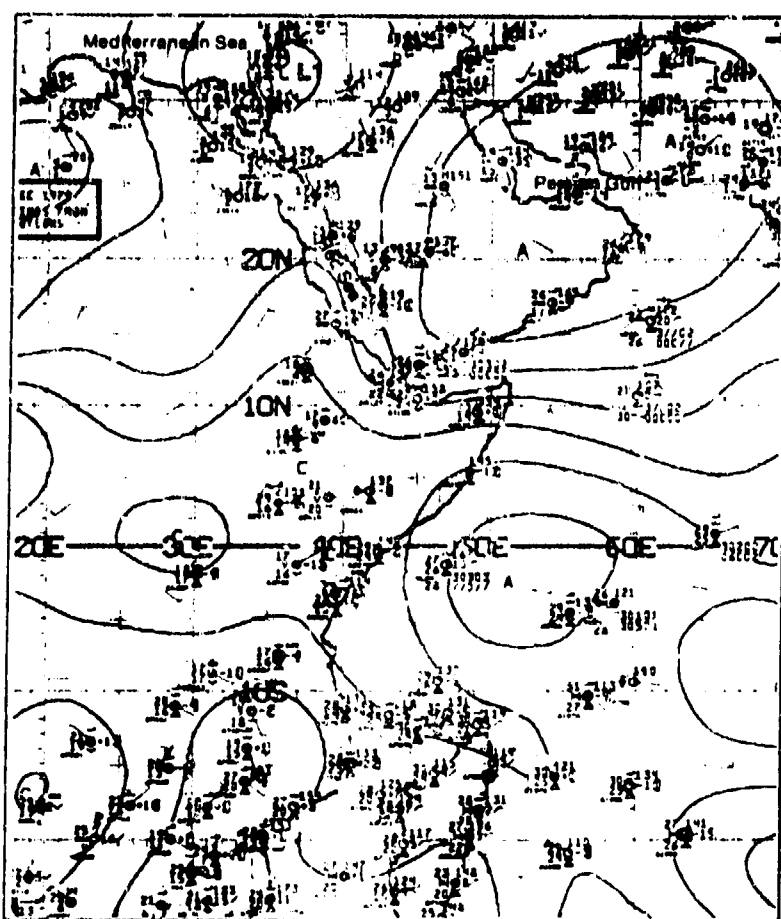


Figure 4-26a. Surface Streamline Analysis, 19 December 1979, (0600Z/0900 LST).

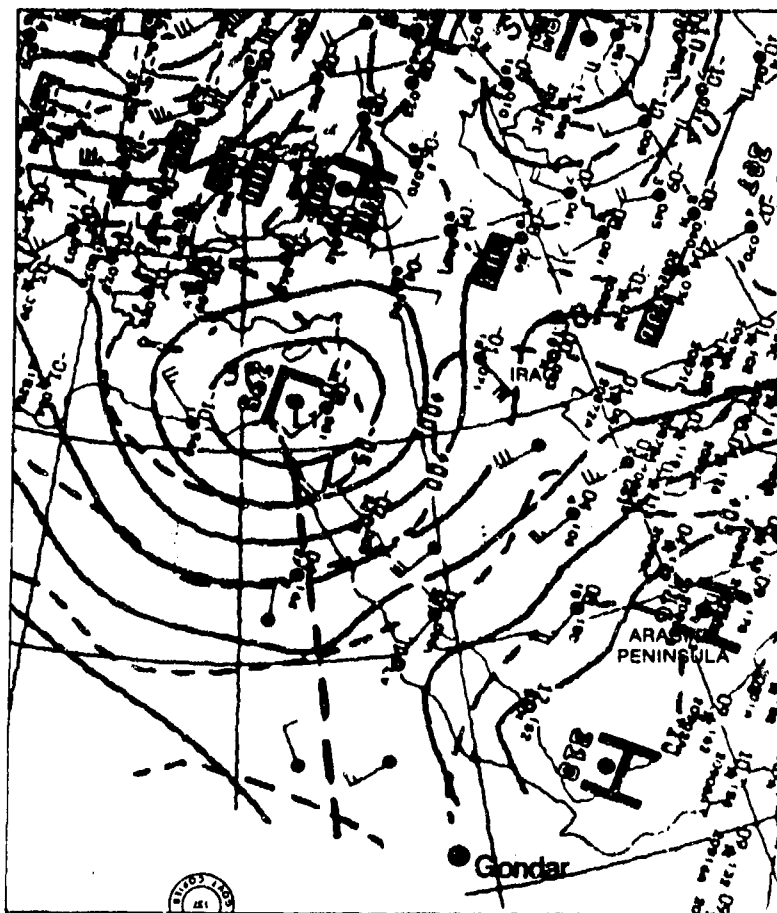


Figure 4-26b. 700-mb Analysis, 19 December 1979, (0000Z/0300 LST). At 0300 LST, the trough line extends to 120 NM WNW of Gondar, Ethiopia.

TEMPERATURE. Although Ethiopian Highland temperatures are very high during the Northeast Monsoon, they decrease 3-4°F (2°C) for every 1,000-foot (305 meter) increase in elevation--see Figure 4-27. Mean daily highs range from 71°F (22°C) at Asmara in December to 90°F (33°C) at Dire Dawa in March. Above 10,000 feet (3,050 meters), mean daily highs are at or below 70°F (21°C). Elevations between 3,280-6,560 feet (1,000-2,000 meters) are consistently in the 80-89°F (27-31°C) range. Record highs range from

85°F (30°C) at Addis Ababa in February to 100°F (38°C) at Dire Dawa in March. The highest diurnal temperature range found in the Northeast Monsoon (40°F (22°C) is at Aba Segub. Mean daily lows range from 40°F (4°C) at Aba Segub to 64°F (18°C) at Dire Dawa. Lowest temperatures are in January. The 27°F (-3°C) reading at Addis Ababa and the 41°F (5°C) at Dire Dawa are the record lows in the Western/Eastern Highlands.

ETHIOPIAN HIGHLANDS NORTHEAST MONSOON

December-March

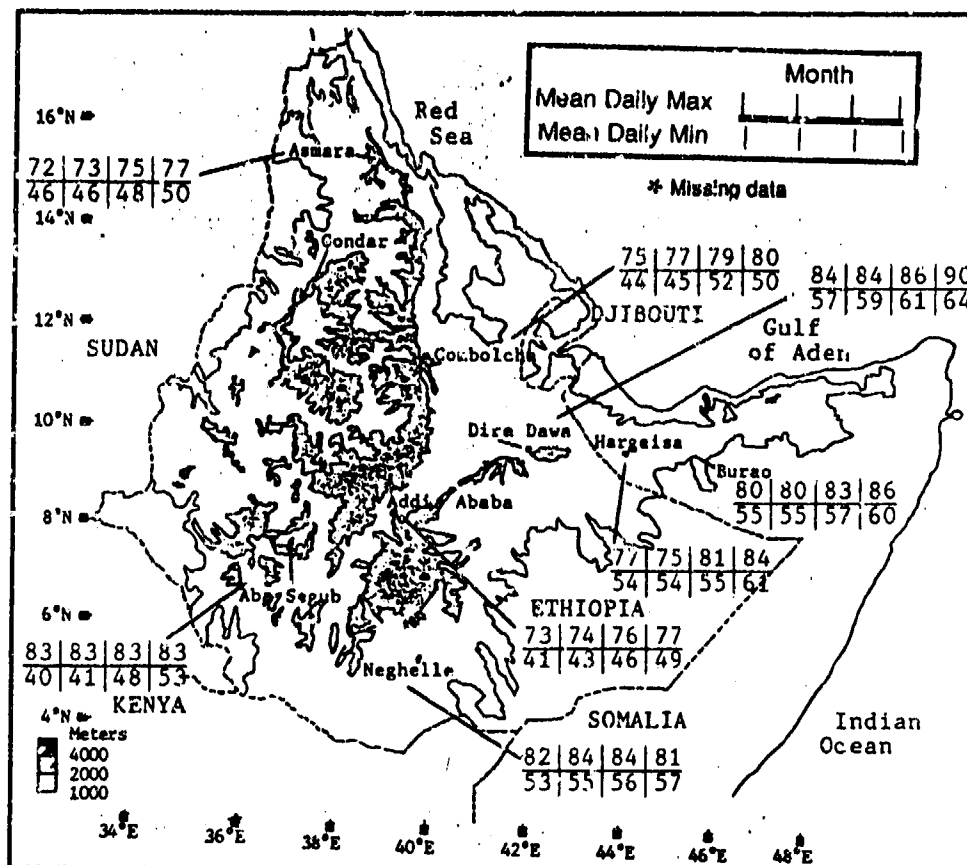


Figure 4-27. Mean Northeast Monsoon Daily Maximum/Minimum Temperatures (°F), Ethiopian Highlands.

ETHIOPIAN HIGHLANDS NORTHEAST-TO-SOUTHWEST MONSOON TRANSITION ("Belgh")

April-May

GENERAL WEATHER. The transition from the Northeast to the Southwest Monsoon is a 2-month period during which northeasterly flow diminishes in the northern Ethiopian Highlands and moist, southerly flow patterns reappear in the southern Seshia and Mendebo Mountains.

The surface Monsoon Trough and Somali Jet Stream oscillate northward--with a continuous flow of tropical moisture--into the southern Ethiopian Highlands by early April. The Monsoon Trough supplies southerly flow and abundant moisture to the Seshia and southern Choke Mountains, while the Somali Jet Stream brings southerly flow and moisture into the Eastern Highlands' Mendebo Mountains. The northern Great Rift Valley is usually sheltered from southerly flow until late May because the Monsoon Trough and low-level moisture remains south of 8° N.

The Monsoon Trough and Somali Jet transport moisture in uneven 3-7 day "bursts". By early April, these bursts affect the southern Eritrean Mountains, the

central Great Rift Valley, and the Ogo Highlands. Weak Northeast Monsoon conditions continue prior to the arrival of the Monsoon Trough and Somali Jet in the north. Typically, the onset of persistent southerly flow is preceded by a 1- to 3-week period of light and variable winds mixed with short (1-6 hour) bursts of strong (10-to 15-knot) southerly flow. Southerly flow eventually persists.

SKY COVER. Cirrus and convective cloud clusters form over the Ethiopian Highlands due to the orographic lifting of the moist southerly flow. The Seshia range in the Western Highlands and the Mendebo Mountains in the Eastern Highlands are initially affected. As shown in Figure 4-28, areas affected by southerly flow and equatorial moisture throughout the transition show high (greater than 55%) mean cloudiness frequencies. The steep south-to-north gradient in mean cloudiness (63% at Neghelle, 34% at Asmara) illustrates the slow northward migration of Monsoon Trough moisture through the Ethiopian Highlands.

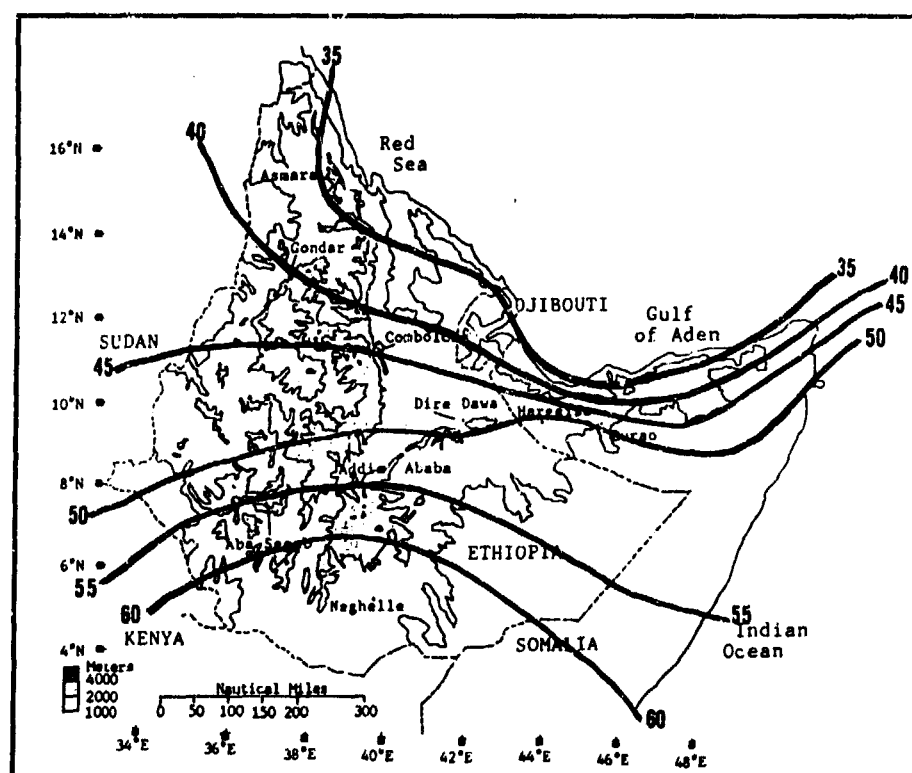


Figure 4-28. Mean NE-SW Monsoon Transition Cloudiness Frequencies, Ethiopian Highlands. Isolines are in 5% intervals. The data is derived by calculating the grand mean from National Intelligence Summary (NIS) mean cloudiness data for specific sites during April and May.

ETHIOPIAN HIGHLANDS

NORTHEAST-TO-SOUTHWEST MONSOON TRANSITION ("Dolgh")

April-May

Sky condition during the transition deteriorates from north to south. Tropical moisture influx to the Eastern Highlands is caused by the Somali Jet. Low-level flow splits along the Mendebo Mountains into two branches. A westward branch of Somali Jet flow passes through the Turkana Channel and along the northern slopes of the Mendebo Mountains. Main Somali Jet flow slides northward along the southeastern slopes of the Mendebo and Ahmar Mountains. Orographic uplift occurs frequently in these mountainous areas, but heavy orographic convection dissipates into altocumulus and altostratus when individual cell movement is to the east or northeast. Southern and eastern slopes of the Mendebo and Ahmar Mountains average 4-5/8ths sky cover at all hours because the Somali Jet is stronger at night. Cumulus, towering cumulus, and cumulonimbus predominate. Bases are 3,000-4,000 feet (915-1,220 meters) AGL; tops, 16,000 feet (3,050 meters). The Jet is the sole source of ascending air that converges with mountain breezes at night, while diurnal mountain slope heating assists the weaker Jet during the day.

East of the Ahmar Mountains, Somali Jet flow is nearly parallel to the southern Ogo Highlands, and much drier. Cumulus sky cover averages 2-5/8ths in May, but in early April, the Northeast Monsoon (low-level northeasterly flow) still affects the Ogo Highlands' northern slopes. As a result, orographic uplift in May reverses along the Ogo Highlands from the northern to the southern slopes. Similar cloud cover distributions affect the Ahmar Mountains. These clouds form at about 5,000 feet (1,524 meters) AGL.

In the Western Highlands, some Turkana Channel flow reaches the southeastern Seshia Mountains and extreme southern Great Rift Valley. The Monsoon Trough, however, induces most orographic uplift. In early April, moist but shallow low-level southerly flow consistently penetrates the sinuous Omo River Valley in the Seshia Mountains. Heavy convection builds through late morning. Sky cover is consistently 5-7/8ths, decreasing to 4-5/8ths overnight.

In April, initial convective cloud clusters that develop between 0600 and 0900 LST have bases between 1,000 and 4,000 feet (305 and 1,220 meters) AGL, with tops to 30,000 feet (9,145 meters) MSL. By mid-day, most convective clusters dissipate as orographic uplift squeezes out moisture. By mid-afternoon, extensive fair weather cumulus with tops to 15,000 feet (4,573 meters) covers the Seshia and southern Choke/Eritrean Mountains.

By May, the Monsoon Trough migrates northward along the Western Highlands to 12-15° N and establishes a deeper moisture layer into the Western Highlands; heavy convective cloudiness begins to enter the southern Great Rift Valley and north-central Eritrean Mountains. The new Trough position increases low-level moisture penetration into the southern Great Rift Valley as well as into the Blue Nile Valley of the Choke and central Eritrean Mountains. Widespread convection continues to develop through midday in the Seshia Mountains, but now the Choke and southern Eritrean Mountains also develop heavy convection between 0600 and 0900 LST. Cloud bases run from 4,000 to 6,000 feet (1,220 to 1,829 meters) AGL; tops may exceed 20,000 feet (6,097 meters).

The mean frequency of ceilings below 3,000 feet/915 meters AGL (as shown in Figure 4-29) is 7% for the entire Ethiopian Highlands. Higher frequencies occur at Neghelle, as well as at other Ethiopian Highlands locations south of 8° N. Normally, peak low ceiling frequencies at 0900 LST indicate that a sustained low-level flow mechanism is helping to sustain heavy convection. A low ceiling frequency peak at 1500 LST, on the other hand, implies a diurnal heating mechanism. Asmara, Dire Dawa, and Addis Ababa see more radiation ground fog than other locations because local terrain produces a high number of nocturnal inversions with calm and stable conditions.

ETHIOPIAN HIGHLANDS NORTHEAST-TO-SOUTHWEST MONSOON TRANSITION ("Belgh")

April-May

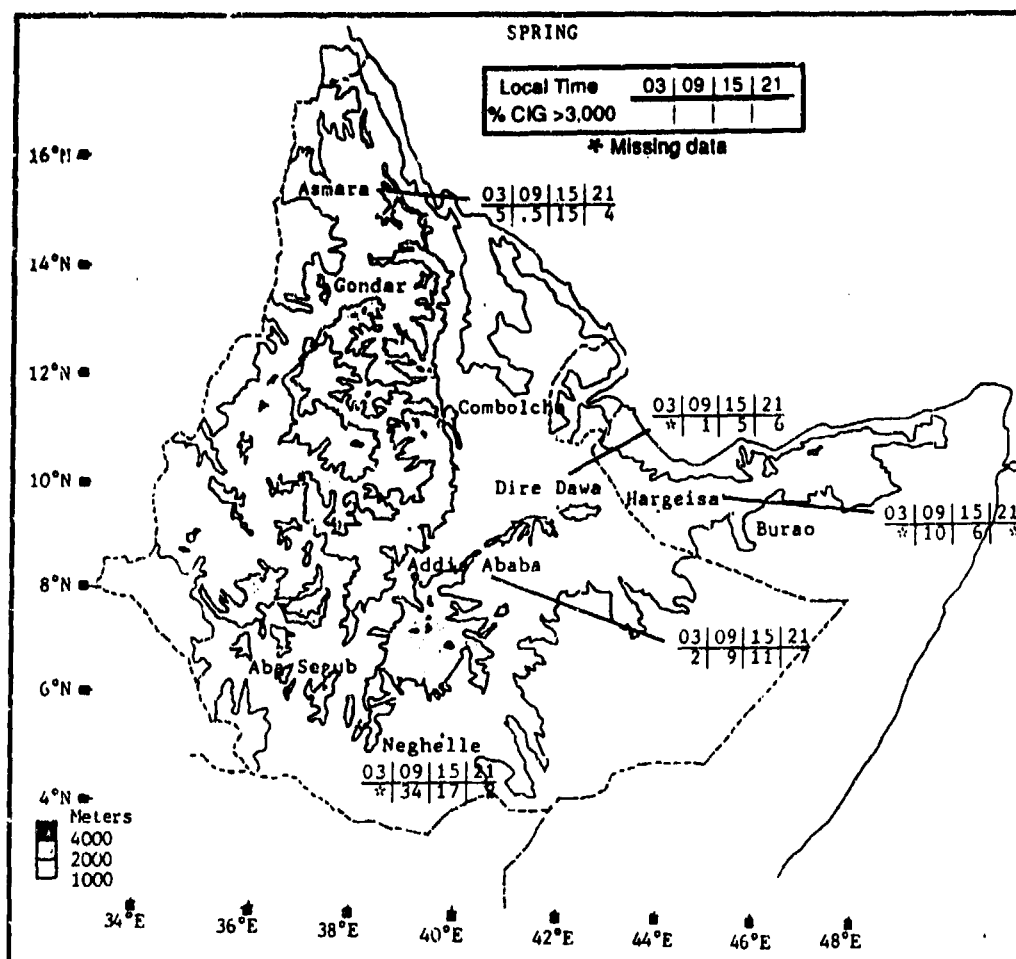


Figure 4-29. NE-SW Monsoon Transition Frequencies of Ceilings Below 3,000 Feet (915 meters), Ethiopian Highlands.

VISIBILITY. Ground fog is the main cause of low visibilities recorded during the transition. The overall frequency of visibilities below 3 miles is low, as shown in Figure 4-30. Radiation fog appears in the Great Rift Valley with calm conditions during the night and early morning hours. In the northern Great Rift Valley, light northeasterly winds allow nocturnal radiation inversions

to occur. In the central and southern Great Rift Valley, the warm valley floor combines with weak, moist southerly flow to produce a moist, 3-knot upslope wind during undisturbed weather conditions. The moist upslope flow condenses in cooler air to produce mid-afternoon fog or mist during April and early May.

ETHIOPIAN HIGHLANDS NORTHEAST-TO-SOUTHWEST MONSOON TRANSITION ("Belgh")

April-May

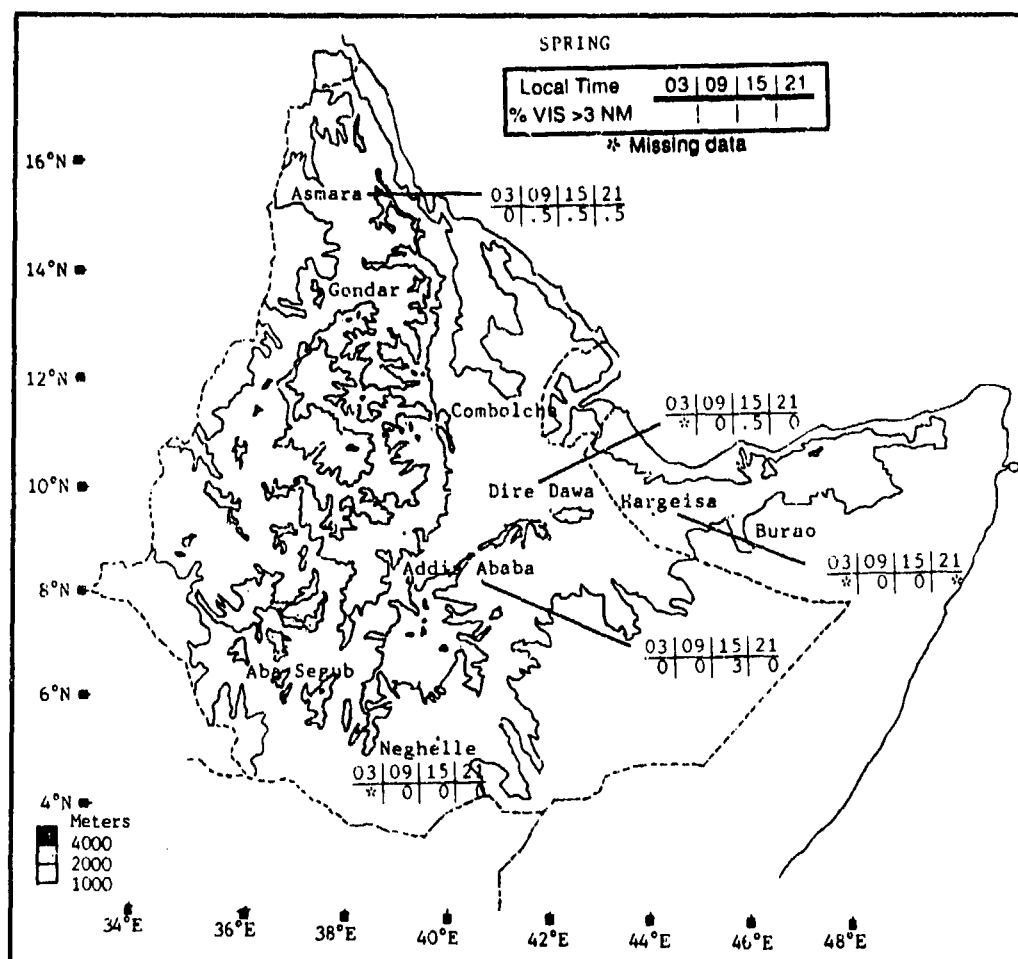


Figure 4-30. NE-SW Monsoon Transition Frequencies of Visibilities Below 3 Miles, Ethiopian Highlands.

WINDS. Sudden low-level wind shifts occur in the Eastern Highlands as the Somali Jet surges spontaneously into the region. Figure 4-31 shows that April-May wind shift phenomenon at Neghelle and Dire Dawa. Prevailing wind direction at Addis Ababa reflects its location on the eastern edge of the Western Highlands where it is sheltered from the Somali Jet and Monsoon

Trough. Surface flow at Addis Ababa is dominated by prevailing flow in the central Great Rift Valley. Prevailing surface winds reflect the sustained Northeast Monsoon circulation through May. Northeasterly flow channels through the Gulf of Aden--over open water--into the area before the surface Monsoon Trough reaches this far north.

ETHIOPIAN HIGHLANDS

NORTHEAST-TO-SOUTHWEST MONSOON TRANSITION ("Belgh")

April-May

ESE-E
ESE-ENE
E-NE/S-W
S-W/S

	APR	MAY
Addis Ababa	8.40	9.10
Asmara	7.90	8.10
Neghelle	5.90	6.20
Dire Dawa	7.40	9.80

Figure 4-31. Mean NE-SW Monsoon Transition Wind Speed (kts) and Prevailing Direction, Ethiopian Highlands.

Because mean surface flow during the transition is so complicated, it is best described in three categories: (1) *Northeast Monsoon* circulation that affects the northern Ogo Highlands, the northern and central Great Rift Valley, and the eastern Eritrean Mountains; (2) the *Transition Zone*--a narrow east-to-west band of light and variable winds that represent the surface Monsoon Trough and boundary between the Northeast/Southwest Monsoons; and (3) the *Southwest Monsoon*, which accounts for all southerly flow and which migrates northward along the Eastern Highlands much faster than the Western Highlands.

Northeast Monsoon Flow. Although the Asiatic High (see Chapter 2) is no longer producing low-level northeasterly flow across the Arabian Sea, the final flow surge in Northeast Monsoon flow enters the Gulf of Aden in late April or early May. Low-level Northeast Monsoon flow passes westward across the northern Ogo Highlands and into the northern half of the Great Rift Valley. After a final northeasterly surge, winds become light and variable on both sides of the Ogo Highlands and Ahmar Mountains.

Transition Zone Flow. The transition zone between northeast and southwest flow is an east-to-west belt of light easterly to southeasterly flow at 4-7 knots. This wind shift zone marks the surface Monsoon Trough along the Ethiopian Highlands' periphery, but the surface trough is often ill-defined. The zone does not exist above 5 000 feet (1,524 meters) MSL because of terrain in the Highlands. The surface Monsoon Trough and wind shift zone migrates rapidly northward (from

Neghelle in mid-April to Burao in early May) along the Eastern Highlands as the Somali Jet produces a synoptic scale burst of southerly flow. The light and variable wind belt affects Eastern Highland plateau locations for less than a 2-week period during each transition. The wind shift zone along the Western Highlands has no cross equatorial jet streams to concentrate southerly flow; as a result, surface Monsoon Trough axis movement to the north is a gradual broad-scale event. Light and variable winds may persist over a Western Highland plateau location for 2-4 weeks before southerly flow is sustained.

Southwest Monsoon flow along the southern Eastern Highlands (10-20 knots) and the southern Western Highlands (7-10 knots) is separated by rugged terrain. Although the transition begins in the south, the Southwest Monsoon does not affect the entire Ethiopian Highlands until late May. When synoptic scale southerly flow is sustained, there is an immediate increase in relative humidity, cloud cover, and rainfall, a signal that the transition from the Northeast to the Southwest Monsoon is complete.

PRECIPITATION. Referred to locally as "Belgh" (or "small rains") the NE-SW Monsoon Transition sees precipitation becoming a daily occurrence with the south-to-north oscillations in the Monsoon Trough and influx of moist southerly flow. Figure 4-32 shows mean April and May rainfall across the Ethiopian Highlands. Note the large 2-month rainfalls (greater than 19.2 inches/488 mm) across the Mendebo, Seshia, and southern Choke Mountains.

April-May

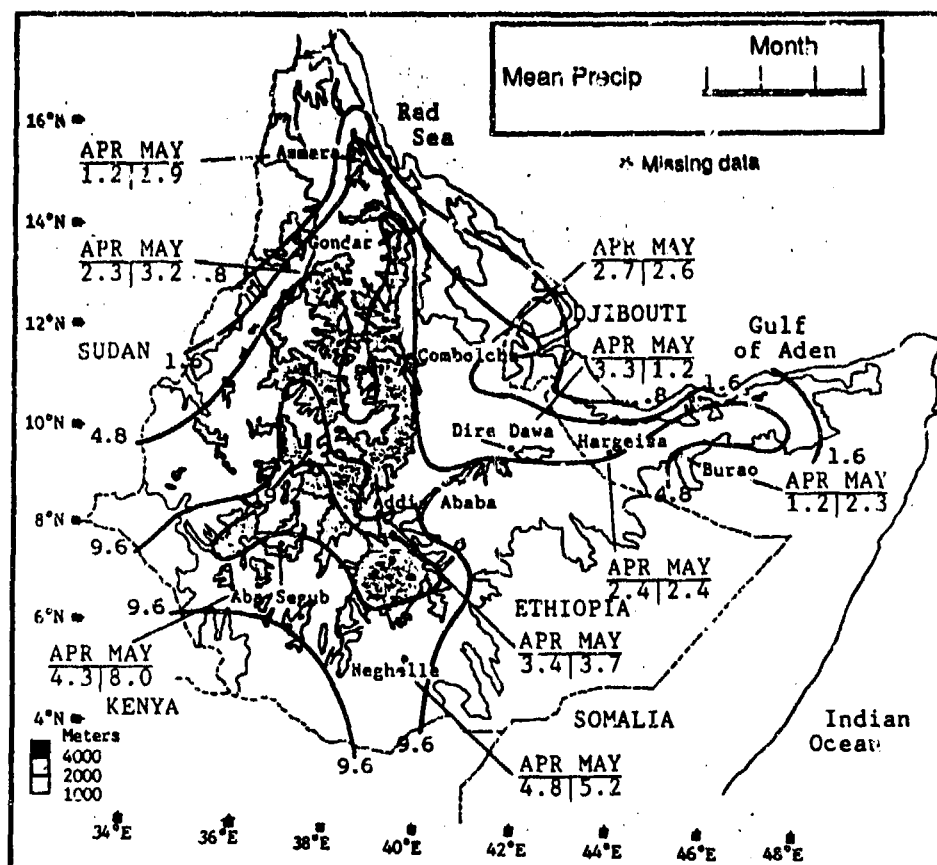


Figure 4-32. Mean NE-SW Monsoon Transition Monthly Precipitation, Ethiopian Highlands. Isohyets represent mean seasonal rainfall totals (inches).

indicates that the Monsoon Trough is not consistently north of that city during the transition. In fact, cyclonic activity provides most transition rainfall. In the northern Great Rift Valley at Gombolcha and Dire Dawa, mean transition rainfall actually decreases from April to May as northeasterly flow weakens through the period and terrain prevents moist southerly flow from reaching those areas.

Thunderstorms are frequent in the Mendebo and Seshia Mountains, occurring on 6-8 days a month during the transition. Maximum frequency is between (0600 and 0900) LST. Hail is rare in the southern Ethiopian Highlands, but lightning and thunder are reported frequently.

ETHIOPIAN HIGHLANDS

NORTHEAST-TO-SOUTHWEST MONSOON TRANSITION ("Belgh")

April-May

TEMPERATURE. Mean daily highs (see Figure 4-33) range from 76°F (24°C) at Neghelle to 93°F (34°C) at Dire Dawa. Record highs across the region include an 86°F (30°C) reading at Asmara in May and a 102°F (39°C) at Dire Dawa, also in May. Most absolute highs occur prior to the onset of moist southerly flow, but northern Great Rift Valley locations reach their maximum temperatures of the year in May when winds

are light and sunshine is intense. The lower mean daily highs in the southern Ethiopian Highlands are the result of moist southerly flow that increases cloud cover and rainfall. Mean daily lows range from 49°F (9°C) at Addis Ababa to 68°F (20°C) at Dire Dawa. Absolute lows range from 36°F (2°C) at Addis Ababa in May to 50°F (10°C) at Neghelle, also in May.

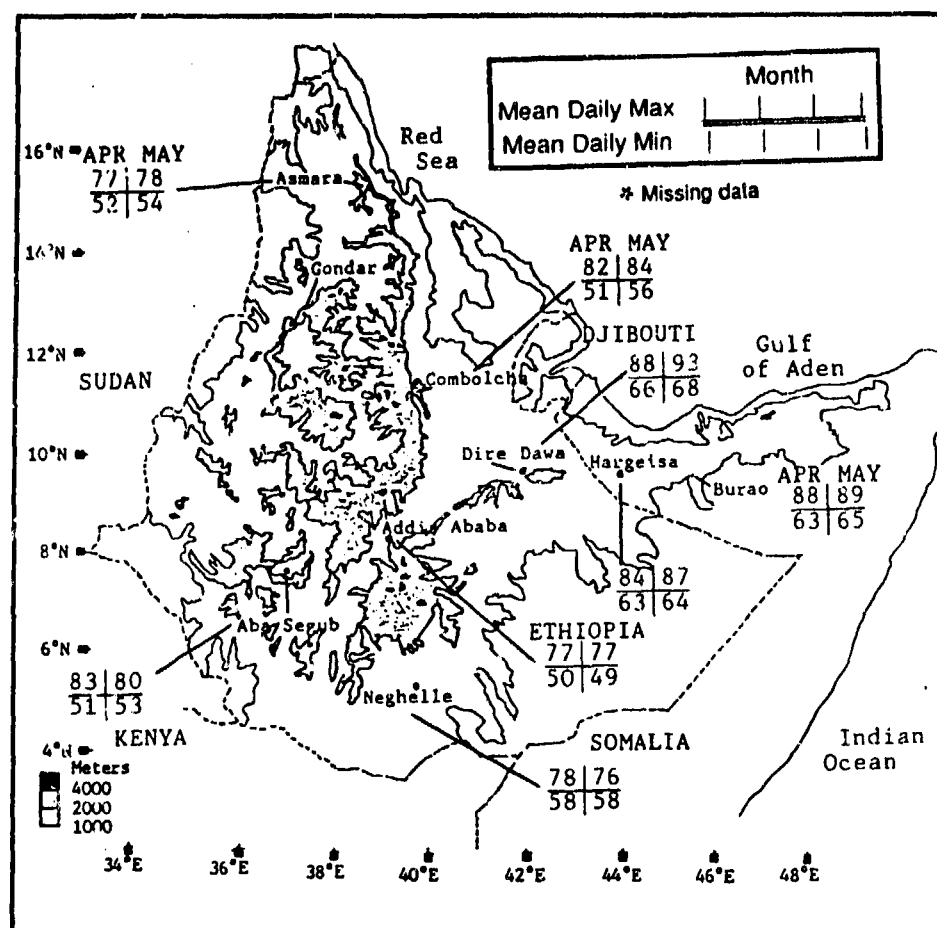


Figure 4-33. Mean NE-SW Monsoon Transition Daily Maximum/Minimum Temperatures (°F), Ethiopian Highlands.

Chapter 5

ADEN COASTAL FRINGE

The "Aden Coastal Fringe" includes coastal portions of Somalia (SI), Djibouti (DJ), Yemen Aden (AD) and all of Socotra Island (AD). After describing the area's situation and relief, this chapter discusses typical weather conditions by season. Seasons here have local names ("Hagai," "Der," "Gilal," and "Gu"), as shown. Note that the local names here are the same as those used in the Indian Ocean Plain (Chapter 3). Note also that, because of rainfall, June in the Aden Coastal Fringe is a part of the Southwest Monsoon proper, rather than of the transition.

Situation and Relief	5-4
Southwest Monsoon ("Hagai") June-September	5-5
General Weather	5-5
Sky Cover.....	5-5
Visibility	5-7
Winds	5-8
Precipitation	5-11
Temperature	5-12
Southwest-to-Northeast Monsoon Transition ("Der") October-November	5-13
General Weather	5-13
Sky Cover.....	5-13
Visibility	5-15
Winds	5-15
Precipitation	5-16
Temperature	5-17
Northeast Monsoon ("Gilal") December-March	5-18
General Weather	5-18
Sky Cover.....	5-19
Visibility	5-20
Winds	5-20
Precipitation	5-21
Temperature	5-23
Northeast-to-Southwest Monsoon Transition ("Gu") April-May	5-24
General Weather	5-24
Sky Cover.....	5-25
Visibility	5-27
Winds	5-27
Precipitation	5-28
Temperature	5-29

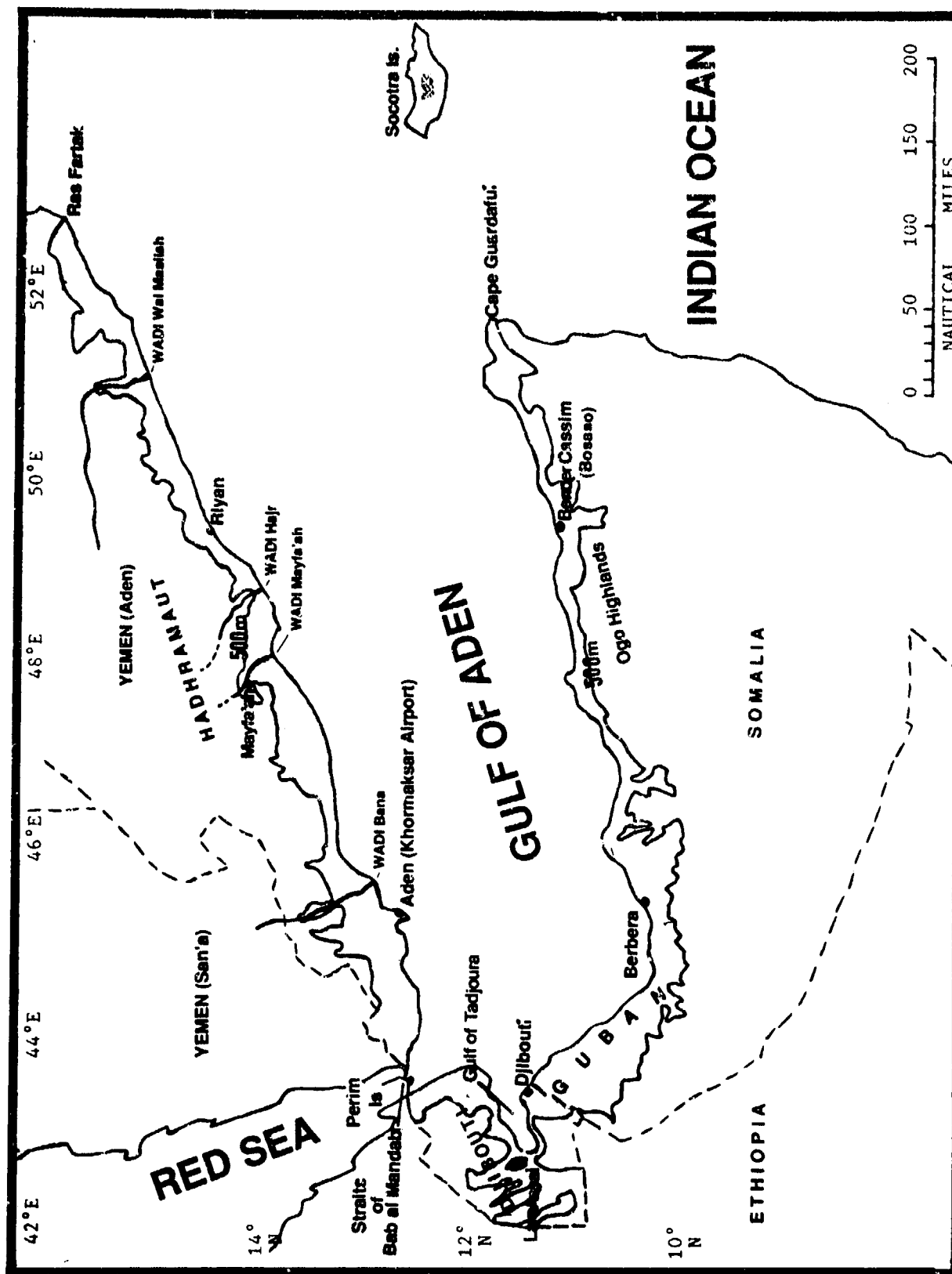


Figure 5-1a. The Aden Coastal Fringe. This region comprises the Gulf of Aden's immediate coastlines. It extends from Ras Fartak in Yemen to Djibouti, then back east to Cape Guardafui, Somalia, and Socotra Island.

STATION: ADEN KHORMAKSAR YEMEN													
LAT/LON: 12 50 N 45 02 E ELEV: 12 FT													
ELEMENTS	JAN	FEB	MAR	APR	MAY	JUN	JUL	AUG	SEP	OCT	NOV	DEC	ANN
EXT MAX	92	91	98	102	107	112	109	107	105	101	97	93	112
AVG MAX	80	81	84	88	93	95	93	92	93	90	85	81	88
AVG MIN	73	73	75	78	82	84	83	81	83	78	75	73	78
EXT MIN	56	61	58	66	70	73	70	63	71	59	61	59	56
AVG PRCP	0.2	0.1	0.2	*	*	*	0.1	*	0.1	*	0.1	0.1	1.0
MAX MON	3.3	2.3	6.6	3.9	1.4	1.3	0.9	2.0	1.9	2.2	1.3	1.6	8.6
MIN MON	0.0	0.0	0.0	0.0	0.0	0.0	0.0	0.0	0.0	0.0	0.0	0.0	0.1
MAX DAY	2.2	2.3	3.0	2.6	1.4	1.0	0.6	1.4	1.9	2.2	0.8	1.1	3.0
DUST DAYS	4	7	10	8	12	24	29	25	13	5	5	4	146
TS DAYS	0	0	*	*	*	*	2	2	1	*	0	0	5
AVG RH %	70	73	73	74	72	65	65	65	68	68	71	70	70
APP TEMP	83	83	90	100	105	106	104	104	102	100	90	84	

STATION: BERBERA SOMALIA													
LAT/LON: 10 24 N 44 57 E ELEV: 30 FT													
ELEMENTS	JAN	FEB	MAR	APR	MAY	JUN	JUL	AUG	SEP	OCT	NOV	DEC	ANN
EXT MAX	94	92	95	108	112	117	116	116	114	107	98	96	117
AVG MAX	84	84	86	89	96	107	107	106	103	92	88	85	94
AVG MIN	68	71	73	77	80	86	88	87	84	76	71	68	77
EXT MIN	58	60	62	66	69	72	69	68	64	62	61	59	58
AVG PRCP	0.3	0.1	0.2	0.5	0.3	*	*	0.1	*	0.1	0.2	0.2	2.0
MAX MON	2.6	2.2	5.7	3.5	2.6	0.8	0.7	0.7	0.7	1.2	1.9	2.7	7.0
MIN MON	0.0	0.0	0.0	0.0	0.0	0.0	0.0	0.0	0.0	0.0	0.0	0.0	0.1
MAX DAY	1.8	1.5	5.2	2.3	2.6	0.9	0.8	0.6	0.7	1.1	1.9	1.3	5.2
TS DAYS	*	1	1	2	2	1	1	1	1	1	*	0	11
APP TEMP	90	90	90	100	117	127	126	126	125	105	99	89	

STATION: BOSASO SOMALIA													
LAT/LON: 11 17 N 49 11 E ELEV: 7 FT													
ELEMENTS	JAN	FEB	MAR	APR	MAY	JUN	JUL	AUG	SEP	OCT	NOV	DEC	ANN
EXT MAX	101	99	101	108	113	113	113	114	112	113	97	97	114
AVG MAX	85	86	88	94	99	106	106	104	102	91	86	85	94
AVG MIN	69	69	70	74	77	85	86	85	82	73	68	68	76
EXT MIN	54	57	59	62	66	70	73	75	70	57	53	52	52
AVG PRCP	*	0.0	*	0.1	0.1	0.0	0.0	0.0	0.0	0.1	0.3	0.1	0.7
MAX MON	0.1	0.0	0.2	1.2	0.9	*	0.0	0.0	0.0	0.7	1.3	0.9	2.3
MIN MON	0.0	0.0	0.0	0.0	0.0	0.0	0.0	0.0	0.0	0.0	0.0	0.0	0.5
MAX DAY	0.1	0.0	0.2	0.8	0.9	*	0.0	0.0	0.0	0.8	0.9	0.5	0.9
AVG RH %	70	71	68	66	64	52	47	48	56	69	76	73	63
APP TEMP	92	93	100	120	130+	130+	128	130+	130+	110	96	90	

* = LESS THAN 0.05 INCHES OR LESS THAN 0.5 DAYS

Figure 5-1b. Climatological Summaries for Selected Stations in the Aden Coastal Fringe.

ADEN COASTAL FRINGE

SITUATION AND RELIEF. The narrow coastal area that surrounds the Gulf of Aden is about 650 NM long. It includes all the Yemen (Aden) coast west of Ras Fartak that lies below 1,620 feet (500 meters). The region is dominated by sand and lava-covered coastal plains backed by steep volcanic hills and mountain ridges. The coastline widens only where isolated semipermanent stream beds (wadis) cut deep canyons into the mountains and hillsides. Two volcanic peaks on the peninsula at Aden, Yemen, rise above 1,000 feet (305 meters) MSL and are connected to the mainland by a narrow strip of land several miles long. Aden has the only natural harbor on the northern Aden Coastal Fringe. Most of the plain from Wadi Mayfa'ah to Perim Island in the Straits of Bab al Mandab is stone and gravel, but from Ras Fartak to Wadi Mayfa'ah there is mostly sand. The entire northern Aden Coastal Fringe is backed by lava hills and plateaus incised by an extensive system of wadis running north to south from the Yemen Highlands to the Gulf of Aden. The wadis have steep slopes and broad, fertile valleys varying in width from 1-4 NM wide. Wadi Hajr is the only permanent stream flowing to the coast; its valley floor width averages 3-8 NM and is below 1,620 feet (500 meters) up to 40 NM inland.

The area called the "Guban," as shown in Figure 5-1, is a region of barren lava fields surrounded by the volcanic hills and mountain ridges of the Ogo Highlands, which see. The Gulf of Tadjoura (Djibouti) and neighboring lowlands are surrounded by volcanic hills rising to 2,000 feet (610 meters) MSL. Marsh flats and caustic swamplands, some below sea level, dominate the interior sections of Djibouti where the coastal fringe is widest at 40-60 NM.

To the east, the coastline gradually narrows to 1-10 NM near Berbera. This narrow section of coastline is paralleled by steep ridges to its south. The 1,620-foot (500-meter) contour is runs only about 1-3 NM inland from the coast.

East from Berbera to Bender Cassim (Bosaso), SI, the coastline gradually widens from 10 to 40 NM near 49° E, but becomes very narrow again between Bender Cassim (Bosaso) and Cape Guardafui, SI. This section of the Aden Coastal Fringe is backed by elongated plateaus and broad valleys interspersed along the eastern Ogo Highlands which lie to the south of the Coastal Fringe.

SITUATION AND RELIEF

The Island of Socotra lies 150 NM ENE of Cape Guardafui, at the easternmost point in the region. Socotra is 72 NM long and 22 NM wide, and covers 1,200 sq NM. The highest elevation is 4,931 feet (1,503 meters) MSL.

DRAINAGE AND RIVER SYSTEMS. The region is dominated by dry stream beds (wadis) that flow intermittently from the surrounding highlands toward the Gulf of Aden. Wadi floors provide most of the arable land. In the northern sections--from west to east--major wadis include: the Bana (20 NM northeast of Aden); the Mayfa'ah (its mouth near 14° N, 47° 15' E); the Hajr (the only stream considered perennial, near 14° 10' N, 48° 56' E) and the Wal Masilah (15° N, 51° E). All the wadis originate in the Hadhramaut (Yemen Highland plateau) and have steeply terraced slopes. They drain from west to south, with minor systems draining to the east. There are no significant wadi systems in the southern half. Stream beds run perpendicular to the shoreline inland, but within a mile of the coast they are indistinguishable.

LARGE WATER BODIES. The Gulf of Aden is 550 NM long and 330 NM across between Ras Fartak and Cape Guardafui. It encompasses nearly 300,000 sq NM. The only lake of significance is Lake Assal, in central Djibouti. This is a salt water lake 10 NM long and 4 NM wide. The adjacent brackish marshland lies 500 feet (-154 meters) below sea level at its lowest point. The lake, which serves as its own internal 150 sq NM drainage basin, is wedged between several isolated volcanic peaks in the Great Rift Valley.

VEGETATION. The northern half of the region is dotted with coconut palms and sparse grasses. In the major wadi valleys and canyons, the floors are scattered with thorny shrubs and palms. Some crops are dispersed along the wadi fringes. On adjacent slopes, isolated pockets of open woodland coexist with scattered terrace agriculture, but the majority of these slopes are uncultivated and contain small grass clumps.

The southern half is dominated by isolated thorny brush and acacia trees inland for 3 NM or more. Small shrubs dot the slopes of most bluff walls, but along the coastline the vegetation is limited to isolated grass clumps and shallow rooted shrubs.

ADEN COASTAL FRINGE SOUTHWEST MONSOON ("Hagal")

June-September

GENERAL WEATHER. Somali Jet Stream flow and Gulf of Aden sea surface temperatures (SSTs) are the primary climatic features. Except for isolated locations in the east, this season is extremely dry. Scant rainfall, high temperatures, and westerly surface winds dominate west of Berbera and Aden--areas where the Somali Jet does not affect the weather.

Somali Jet Stream flow has a significant effect, however, on the southern half of the region. Its WSW-SW flow leaves the mainland near Cape Guardafui and passes over the extreme southeastern Gulf of Aden and Socotra Island. The Jet is deflected by the Ogo Highlands, which parallel the entire southern Aden Coastal Fringe. Terrain establishes a complex surface circulation pattern (which includes vortices) between Cape Guardafui and Socotra Island. This pattern brings descending motion and adiabatic warming to the north side of the Ogo Highlands between Bender Cassim (Bosaso) and Berbera.

SST distributions, which grow warmer from east to west in the Gulf of Aden, accentuate surface moisture and temperature patterns. The immediate coastline to 2

NM inland stays cool during the day. In the northeast, the Somali Jet causes strong upwelling near Ras Fartak, where there is a high incidence of early morning coastal stratus.

SKY COVER. In early June, surges of strong southwesterly flow in the Somali Jet affect the southern part of the Aden Coastal Fringe. Persistent southerly flow descends from the Ogo Highlands and warms adiabatically. The flow opposes a weak sea breeze by day and reinforces offshore flow at night. Both diurnal circulations are too dry for significant cloud development, but southwesterly Somali Jet flow produces extensive cloud cover on Socotra Island. Moist air is lifted along the west and south sides of Socotra's only mountain range (the Haggier). Maximum ridge crest elevation is 4,931 feet (1,503 meters).

Southwest Monsoon mean cloudiness distribution (Figure 5-2) varies from 44 percent near Ras Fartak in the north to 17 percent at Berbera, in the south. Percentages are probably even lower in the "Guban" between Djibouti and Berbera.

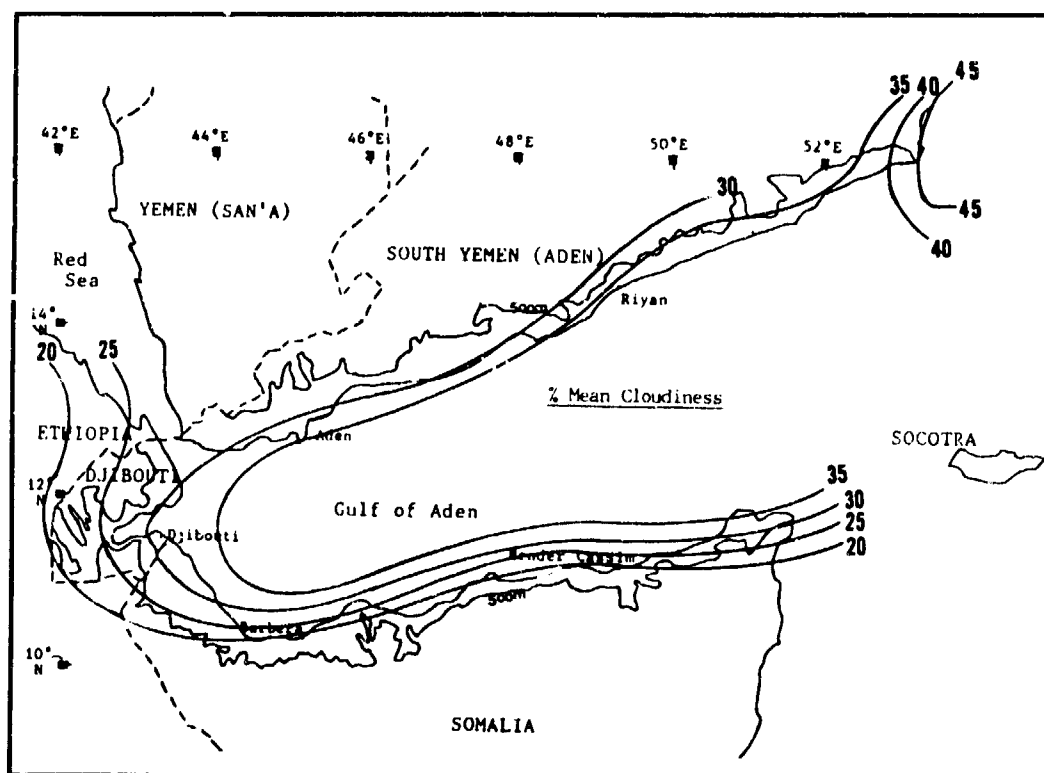


Figure 5-2. Mean Southwest Monsoon Cloudiness Frequencies, Aden Coastal Fringe. Isolines are in 5% intervals. The data is derived by calculating the grand mean from National Intelligence Summary (NIS) cloudiness data for specific sites from June to September.

ADEN COASTAL FRINGE SOUTHWEST MONSOON ("Hagal")

June-September

The northern and southern halves of the Aden Coastal Fringe region see different mean cloudiness. Somali Jet flow does not normally reach the northern half, but a strong daytime sea breeze produces fair weather cumulus on the immediate coastline. A weak surface Monsoon Trough (see Chapter 2) over the northern Aden Coastal Fringe strengthens onshore flow, but inland temperatures are too high, and the boundary layer too dry, for extensive cumulus development.

The southern half averages only 1-2/8ths sky cover, mostly cirrus blowoff from convection over the Ogo Highlands. Thin stratocumulus and stratus (rarely constituting a ceiling) appear between (0400 and (0700 LST between Djibouti and Bender Cassim (Bosaso). Near Cape Guardafui, cloud cover averages 2-4/8ths stratus and stratocumulus during land/sea breeze transition hours (0600-0800 LST and 1900-2100 LST). Bases average 3,300 feet (1,006 meters) AGL. On Socotra, southern mountain slopes see 3 to 5/8ths cumulus by mid-afternoon, but little cumulus development on northern slopes. Bases average 2,500-3,000 feet (762-915 meters), but tops rarely exceed 8,000 feet (2,439 meters). Strong Somali Jet flow over

Socotra produces distinct windward/leeward cloud cover patterns.

The northern half sees moderate (2-4/8ths) cumulus development along immediate coastlines by day. Bases average 4,000 feet (1,220 meters), but tops rarely exceed 6,000-7,000 feet (1,829-2,134 meters). Early morning stratus and stratocumulus bases range from 2,000 to 3,000 feet (610 to 915 meters). These clouds develop offshore between Riyan and Ras Fartak due to upwelling. Low stratus moves onshore between (0500 and 0700 LST with bases at 1,000-2,500 feet (305-762 meters). Clouds dissipate rapidly away from immediate coastlines. Near the city of Aden, there is localized convection near the twin volcanic cones of Shamsan and Ihsan. Cumulus rarely covers more than 2 or 3/8ths of the sky during daylight. Bases average 3,000-4,000 feet (915-1,220 meters), with tops to 8,000 feet (2,439 meters).

Frequencies of ceilings below 3,000 feet (915 meters) vary widely because of wind flow and topography. Highest frequencies seem to be in mid-morning and early evening (Figure 5-3).

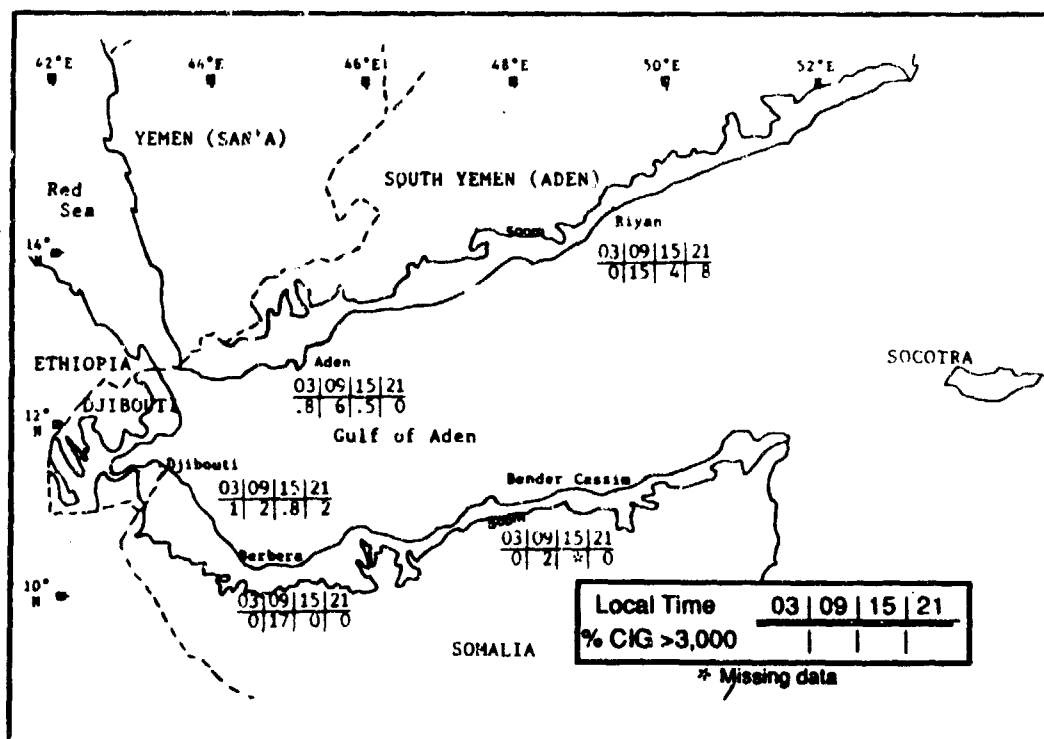


Figure 5-3. Southwest Monsoon Frequencies of Ceilings Below 3,000 Feet (915 meters), Aden Coastal Fringe.

ADEN COASTAL FRINGE **SOUTHWEST MONSOON ("Hagal")**

June-September

The extreme northeastern and southeastern parts of the Aden Coastal Fringe are affected by strong offshore upwelling that produces coastal stratus. The cold water and surface Monsoon Trough are responsible for most low ceilings (15%) at Riyan in June and September.

During July and August, the air over land is too dry for extensive low cloud anywhere but around Ras Farak's immediate shoreline. Predominant low clouds are early morning stratus and stratocumulus. At Berbera, low cloud (17% at 0900 LST) is also stratus and stratocumulus, now caused by land/sea breeze convergence.

VISIBILITY. The frequency of visibilities below 3 miles (Figure 5-4) is less than 5% across the entire

region, all the result of strong sea breeze winds that raise sand and dust. The extreme dryness of the Southwest Monsoon normally results in thin haze with visibilities of 4-7 miles. In the southern part of the Aden Coastal Fringe between Cape Guardafui and Berbera, weak southerly flow from the Somali Jet descends from the Ogo Highlands; warming adiabatically, it carries dust/sand onto the coastal plains below. If downslope flow is strong (15-20 knots), visibility may drop to a mile or less for brief periods.

East of Riyan, early morning fog and stratus are the main obstructions to vision. Strong coastal upwelling along the northern shore east of Riyan may produce extensive thin fog that may persist along the water and immediate coastline until 1600-1700 LST.

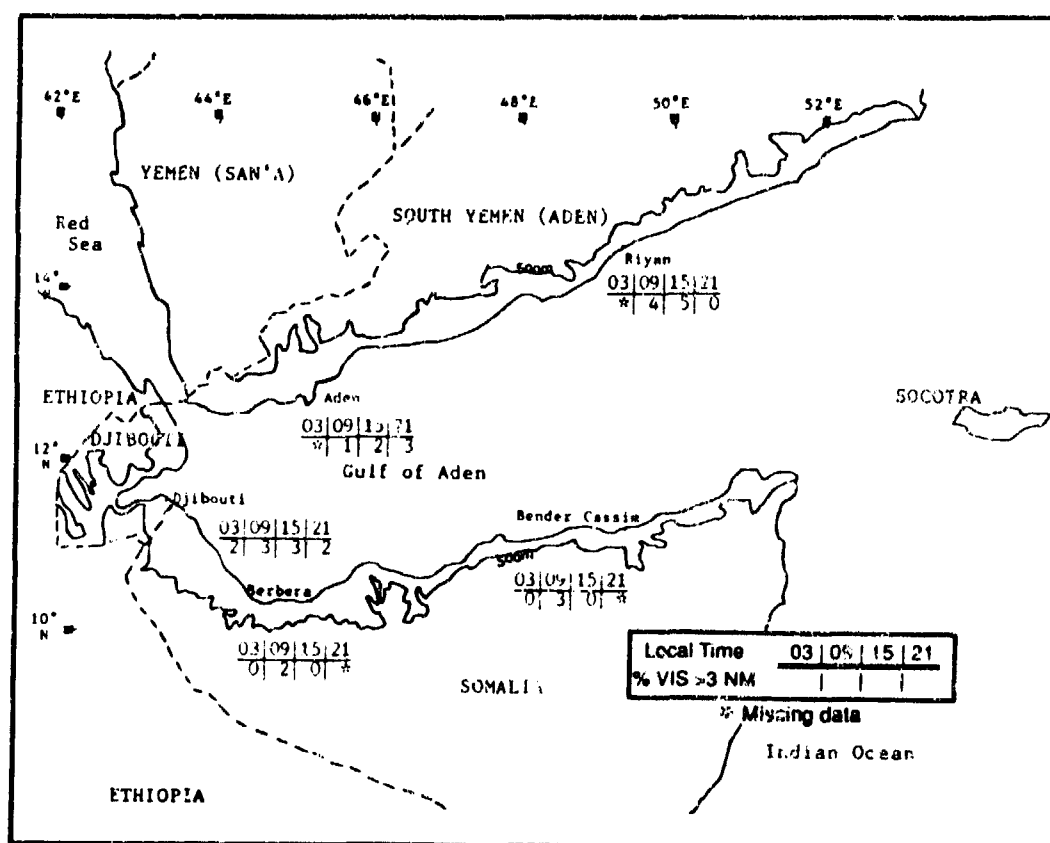


Figure 5-4. Southwest Monsoon Frequencies of Visibilities Below 3 Miles, Aden Coastal Fringe.

ADEN COASTAL FRINGE **SOUTHWEST MONSOON ("Hagal")**

June-September

WINDS. Surface wind circulations along the southeastern Aden Coastal Fringe shoreline between Bender Cassim (Bosaso) and Cape Guardafui are extremely complex because the Somali Jet and Ogo Highlands produce an anomalous low-level flow pattern. Figure 5-5a shows surface streamline flow during a typical July over the southeast tip of the region. The vortices that develop from topographic effects on Somali

flow produce wide variations in local surface winds between Cape Guardafui and Bender Cassim (Bosaso). Local diurnal land/sea breeze circulations further complicate diurnal speed and direction along the immediate coastline, at Bender Cassim in particular. Figure 5-5b is a closeup of a vortex directly above Cape Guardafui. The mean wind speed (in the center of the circle) is in meters per second.

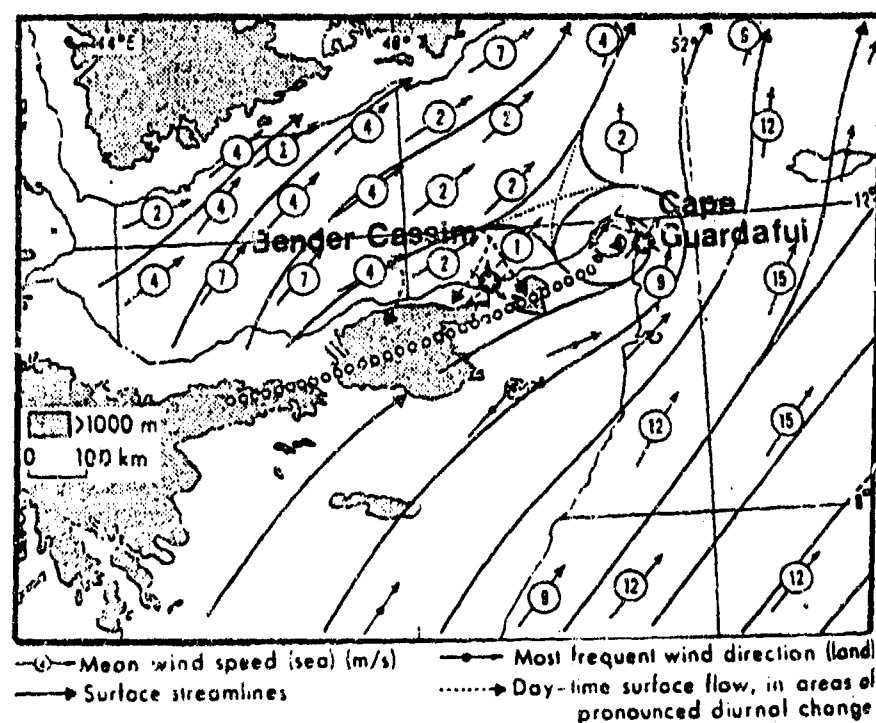


Figure 5-5a. Complex Surface Circulation on the Southeastern Aden Coastal Fringe. Surface streamlines were created by Findlater (1971) to show mean July surface flow along the northern Somalia coast. Local cloud cover patterns vary slightly with circulation.

ADEN COASTAL FRINGE SOUTHWEST MONSOON ("Hagal")

June-September

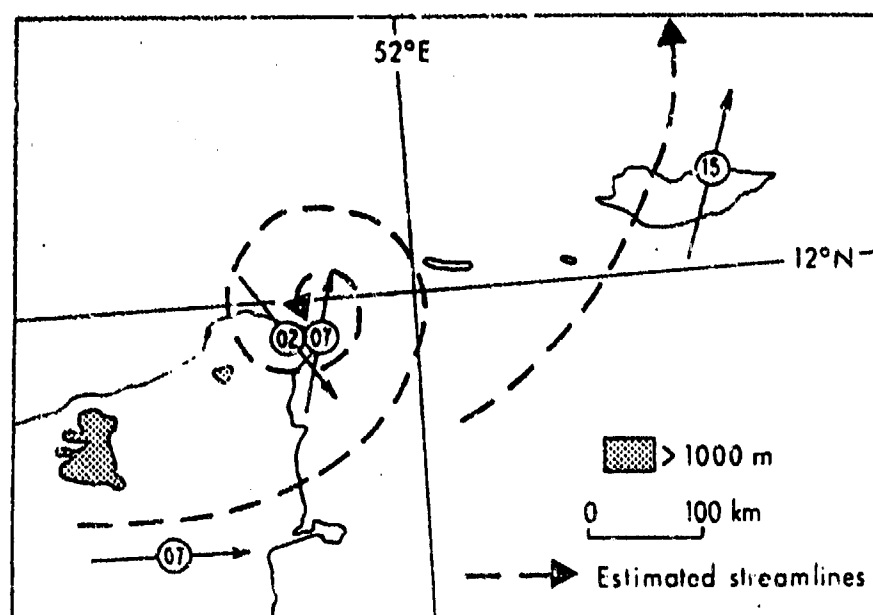


Figure 5-5b. Closeup View of Individual Vortex Over Cape Guardafui, Somalia (from Findlater, 1971). Dashed lines with arrows represent estimated streamline between 1,000-2,000 feet (305-610 meters) AGL. Circled numbers give wind speed in m/s.

Figure 5-6 gives mean monthly wind speeds and prevailing wind directions for Aden, Djibouti and Riyan (Riyan is on the northeastern edge of the Aden Coastal Fringe). The prevailing surface wind direction at Djibouti shows the combined influence of northerly mid-level flow and the low-level sea breeze circulation.

Aden and Riyan data shows that a moderate sea breeze (7-10.5 knots) is dominant at the surface. Strong surface west-southwesterlies (15-20 knots) occurs at Cape Guardafui. However, wind speed reaching 60 to 70 knots are not uncommon in July and August.

	JUN	JUL	AUG	SEP
SE-SW				
E-SW				
W				
Riyan	9.00	10.50	9.70	7.80
Aden	7.80	10.30	9.90	7.80
Djibouti	8.70	12.20	11.90	9.30

Figure 5-6. Mean Southwest Monsoon Wind Speeds and Prevailing Directions, Aden Coastal Fringe. Prevailing directions in boldface on left.

ADEN COASTAL FRINGE SOUTHWEST MONSOON ("Hagal")

June-September

Figures 5-7a and b give mean annual wind directions for three levels at Aden and Djibouti. There are striking differences between the two stations in June and September. The Somali Jet rarely affects the northern Aden Coastal Fringe because it is deflected by the Ogo Highlands. As a result, Southwest Monsoon low-level

moisture and rainfall during the day must be drawn from sea breezes. However, mid-level monthly Southwest Monsoon wind direction shows offshore (20-70) components, and dry air aloft suppresses widespread sea breeze cumulus between Riyan and Aden.

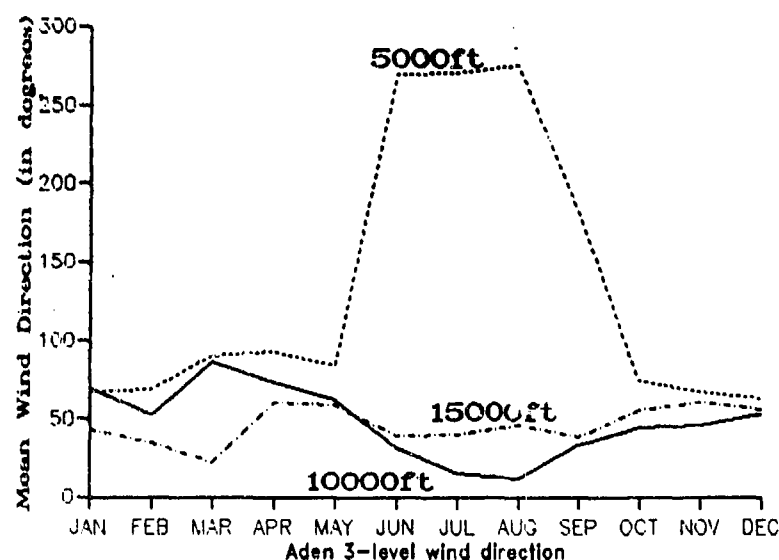


Figure 5-7a. Mean Annual Wind Direction, Aden, AD. Note the abrupt wind shift at 5,000 feet (1,524 meters) from easterly (87°) to west-northwesterly (280°) by June. In September, the mean 5,000-foot wind direction backs to south-southwesterly (200°) just before the transition to Northeast Monsoon flow. The low-level wind shift is not present at the higher levels.

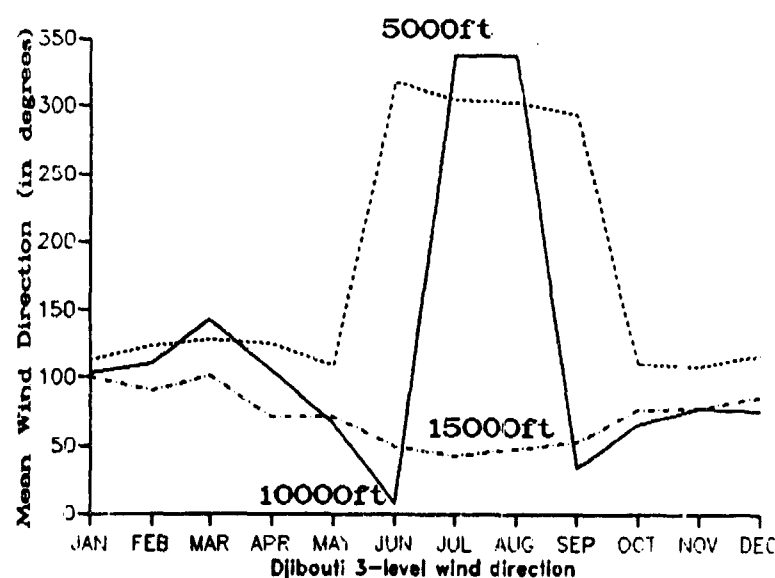


Figure 5-7b. Mean Annual Wind Direction, Djibouti, DJ. Djibouti's wind profile shows a northerly ($340-015^{\circ}$) component to 10,000 feet (3,050 meters) MSL throughout the Southwest Monsoon. This 10-15 knot flow doesn't provide much mid-level moisture along the southwestern Aden Coastal Fringe, but it reinforces orographic lift of sea breeze moisture.

ADEN COASTAL FRINGE SOUTHWEST MONSOON ("Hagai")

June-September

PRECIPITATION. The Southwest Monsoon--known locally as "Hagai"--is extremely dry because the Somali Jet is now confined to the extreme southeastern parts of the Aden Coastal Fringe. Many locations across the region get only a trace of rain during the entire Southwest Monsoon. Bender Cassim (Bosaso) normally sees no rain at all during this season. Even though orographic lift in the southern Ogo Highlands produces thundershowers, very little rainfall reaches southern Aden Coastal Fringe coastlines between Cape Guardafui and Djibouti. This region is also a rain-shadow zone with southwesterly flow from the Somali Jet.

Along the northern Aden Coastal Fringe, strong upwelling east of Riyan produces spotty early morning drizzle. Most of the population here is confined to the fertile wadi valleys 200-300 NM west of the strongest offshore upwelling. Most of the drizzle falls east of

Riyan. Surface easterlies are rare and weak, and do not push significant amounts of stratus west of Riyan. On about 1-3 days a season there is a trace to 0.01 inch (0.25 mm) from low stratus with light southeasterly or easterly winds.

Thunderstorms reach their highest frequency (1-3 a month) during the Southwest Monsoon. Although thunder is heard along the southern Aden Coastal Fringe, rain stays south of the Ogo Highlands. Frequent thunderstorms with light rain occur after midnight near the city of Aden. Lightning is frequently seen to the north of the Yemen Highlands between 1700 and 2100 LST. Strong sea breeze uplift triggers thunderstorms over high terrain 30 NM north of Aden. Anvil clouds spread south to the coast, with light rain reaching Aden by 1900 LST. Figure 5-8 shows Southwest Monsoon rainfall by month.

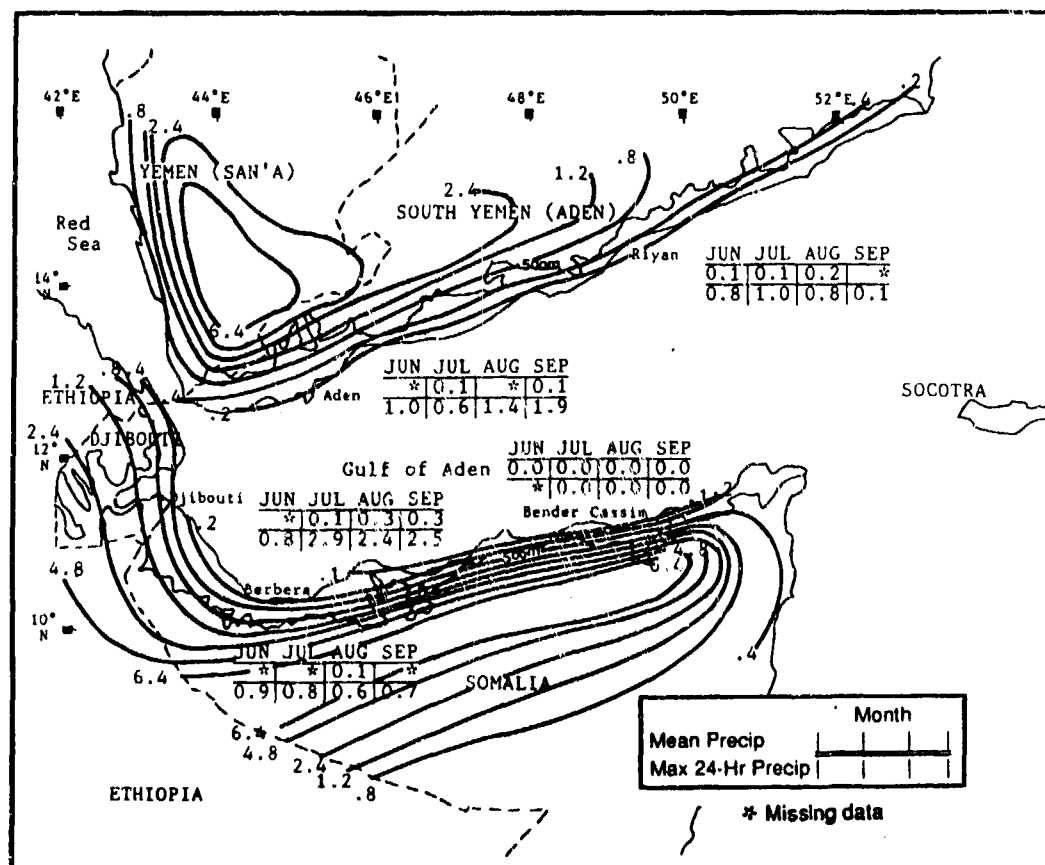


Figure 5-8. Mean Southwest Monsoon Monthly/Maximum 24-Hour Precipitation, Aden Coastal Fringe. Isohyets represent mean seasonal rainfall (inches).

ADEN COASTAL FRINGE **SOUTHWEST MONSOON ("Hagel")**

June-September

TEMPERATURE. Mean daily highs range from 90°F (32°C) at Riyan to 107°F (42°C) at Berbera. The record high at Riyan was 111°F (44°C) recorded in June, and 117°F (47°C) at Berbera, also in June. The record for the region is 121°F (49°C), set at Djibouti. Mean daily

lows are controlled by Gulf of Aden sea surface temperatures; the lowest temperatures are found near coastal upwelling regions between Riyan-Ras Fartak and just south of Cape Guardafui (77-79°F/24-26°C). The highest mean daily low is 88°F (31°C) at Berbera.

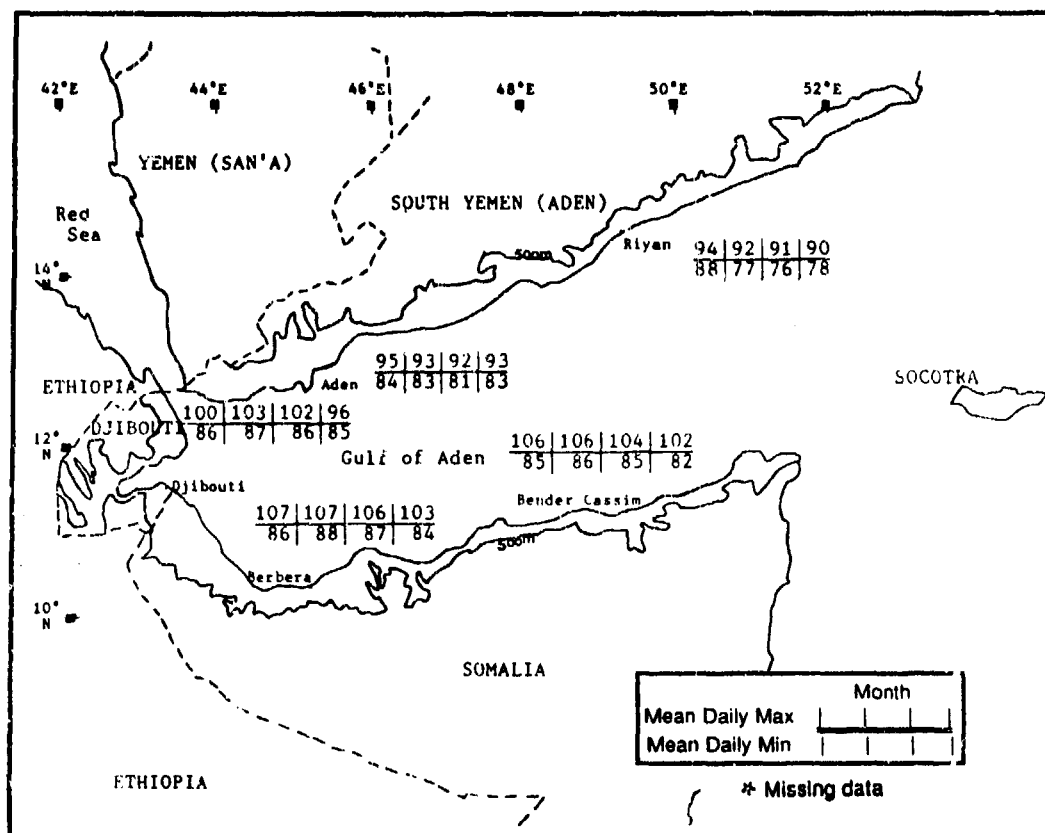


Figure 5-9. Mean Southwest Monsoon Daily Maximum/Minimum Temperatures (°F), Aden Coastal Fringe.

ADEN COASTAL FRINGE SOUTHWEST-TO-NORTHEAST TRANSITION

October-November

GENERAL WEATHER. A subtle shift in low- and mid-level circulation results in light and variable surface winds throughout the region. Along the southeastern Aden Coastal Fringe from Bender Cassim (Bosaso) to Socotra Island, strong southwesterly flow diminishes as the Somali Jet migrates south. To the immediate north of the Jet, the surface Monsoon Trough produces weak, low-level convergence that results in a short-lived period of showers as the Trough moves rapidly south of the area by mid-to late October.

From Bender Cassim (Bosaso) to Perim Island, the Monsoon Trough's southward migration produces weak easterly flow that is easily lifted against the Ogo Highlands to produce light showers along the highest ridges. These showers occasionally fan out onto the adjacent coastal plain. On the northern Aden Coastal Fringe, weak easterly flow allows sea breeze cumulus to form, but dry air inland prevents cloud development past 5 NM inland.

SKY COVER. Mean cloudiness over the Aden Coastal Fringe ranges from 18-26% (Figure 5-10). Low- and mid-level cloud cover (thin stratus and stratocumulus) is greatest from 0800 to 1100 LST and accounts for most of the Aden Coastal Fringe's mean seasonal cloudiness. Between Bender Cassim (Bosaso) and the city of Djibouti, however, most cloud cover occurs in the afternoon (1300-1600 LST) as strong sea breezes produce orographic lift. Cumulus development along the northern Ogo Highlands rarely exceeds 2/8ths. Bases are 3,000 feet (915 meters) AGL with tops to 8,000 feet (2,439 meters) MSL. Clouds move westward along the Ogo Highlands because the southern Aden Coastal Fringe coastline is parallel to northeasterly flow--sea breeze deflection is very strong. Maximum development (2-3/8ths) is near Djibouti where the coastline is perpendicular to the sea breeze and downwind from Ogo Highland cloud cover. Isolated convective activity occasionally produces 4-5/8ths sky cover at Djibouti. Tops may reach 30,000 feet (9,146 meters) MSL.

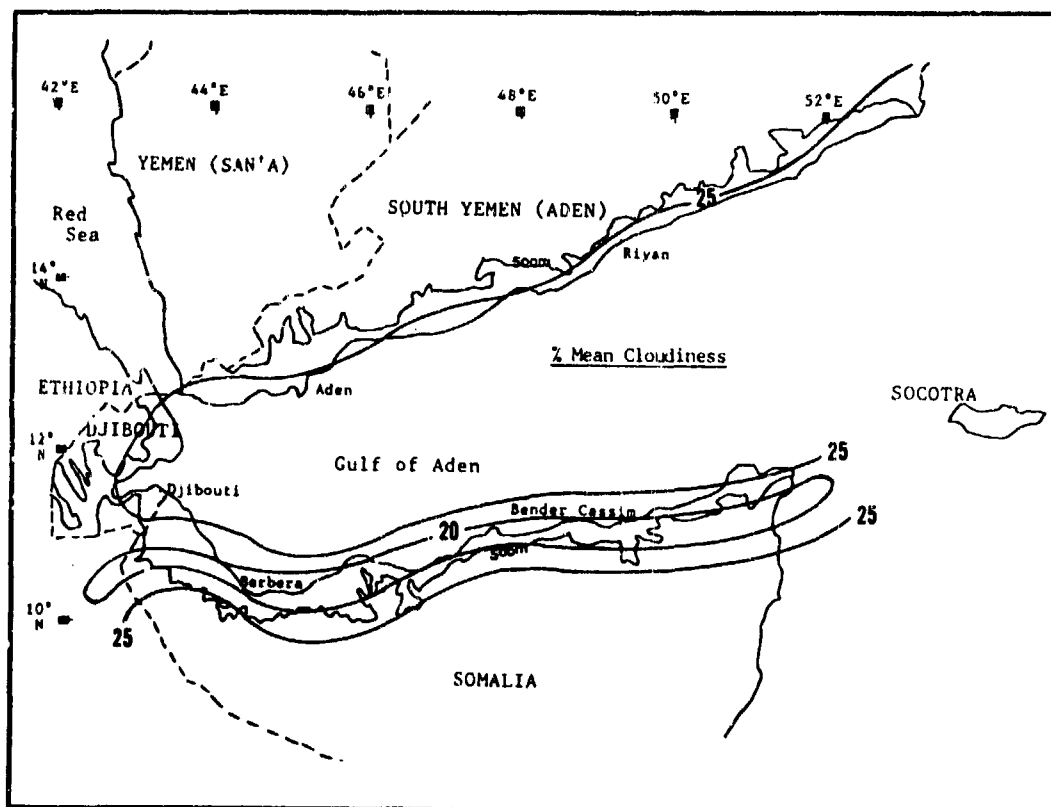


Figure 5-10. Mean SW-NE Monsoon Transition Cloudiness Frequencies, Aden Coastal Fringe. The data is derived by calculating the grand mean from National Intelligence Summary (NIS) mean cloudiness data for specific sites in October and November. Isolines are in 5% intervals.

ADEN COASTAL FRINGE SOUTHWEST-TO-NORTHEAST TRANSITION

October-November

Stratus and stratocumulus forms only during the morning land-to-sea breeze transition (0600-0800 LST); offshore flow is stronger and 5-10°F cooler than the twilight (1900-2100 LST) land breeze, resulting in greater instability over warm coastal waters in the morning. Coastal stratus and stratocumulus have bases between 2,000-2,500 feet (610-762 meters) AGL, but are short-lived as the land-to-sea breeze reversal pushes cloud cover inland. The dry air mass dissipates the cloud cover by 1000-1100 LST. Along the northern Aden Coastal Fringe, synoptic flow and sea breezes rarely

produce anything but light diurnal cloudiness. Isolated fair weather cumulus develops almost every afternoon near the city of Aden along Mt Shamsan and Mt Ihsan. Bases are 3,000-4,000 feet (915-1,220 meters)-- tops may reach 7,000 feet (2,134 meters).

The frequency of ceilings below 3,000 feet (915 meters) ranges from 0 to 13% (Figure 5-11). The highest frequency is just south of Berbera (12% at 0900 LST) and at Bender Cassim (Bosaso).

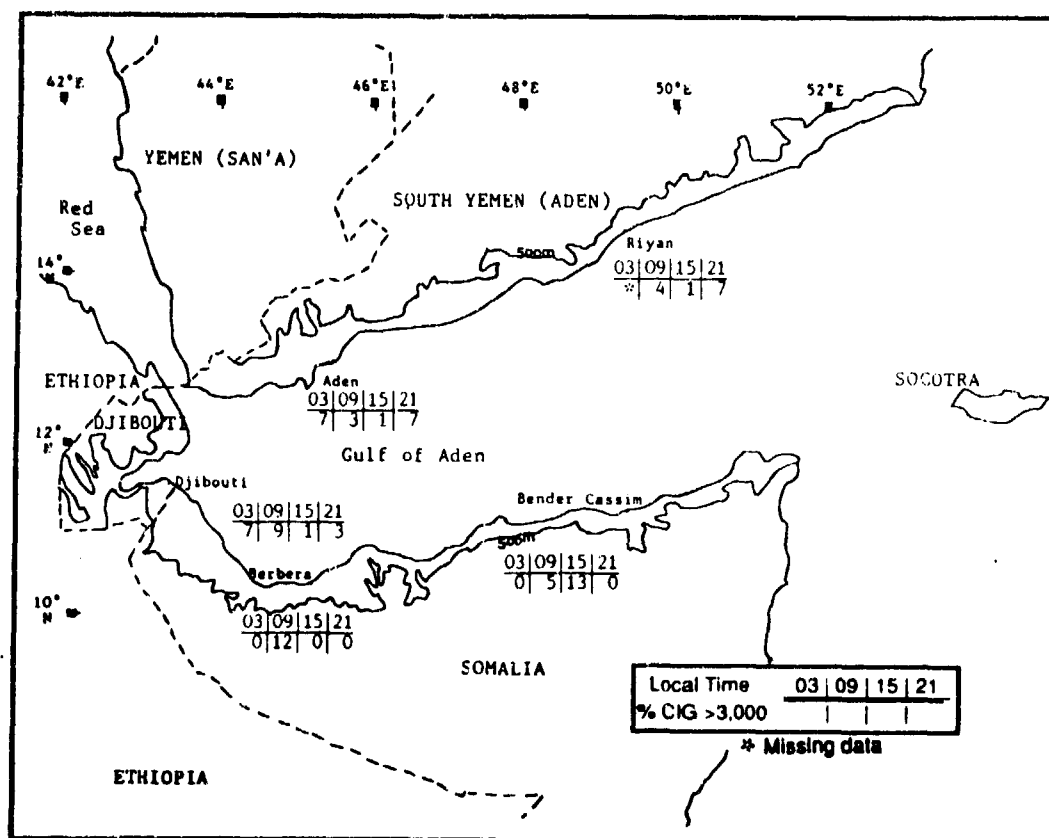


Figure 5-11. SW-NE Monsoon Transition Frequencies of Ceilings Below 3,000 Feet (915 meters), Aden Coastal Fringe.

ADEN COASTAL FRINGE SOUTHWEST-TO-NORTHEAST TRANSITION

October-November

VISIBILITY. The frequency of visibilities below 3 miles (Figure 5-12) is only 0-2%. Nearly all low visibilities during the transition are caused by blowing dust and sand along immediate coastlines. The rare

frontal passage almost always produces widespread dust along the cold front. Visibility drops to less than a mile for up to 4 hours after a frontal passage.

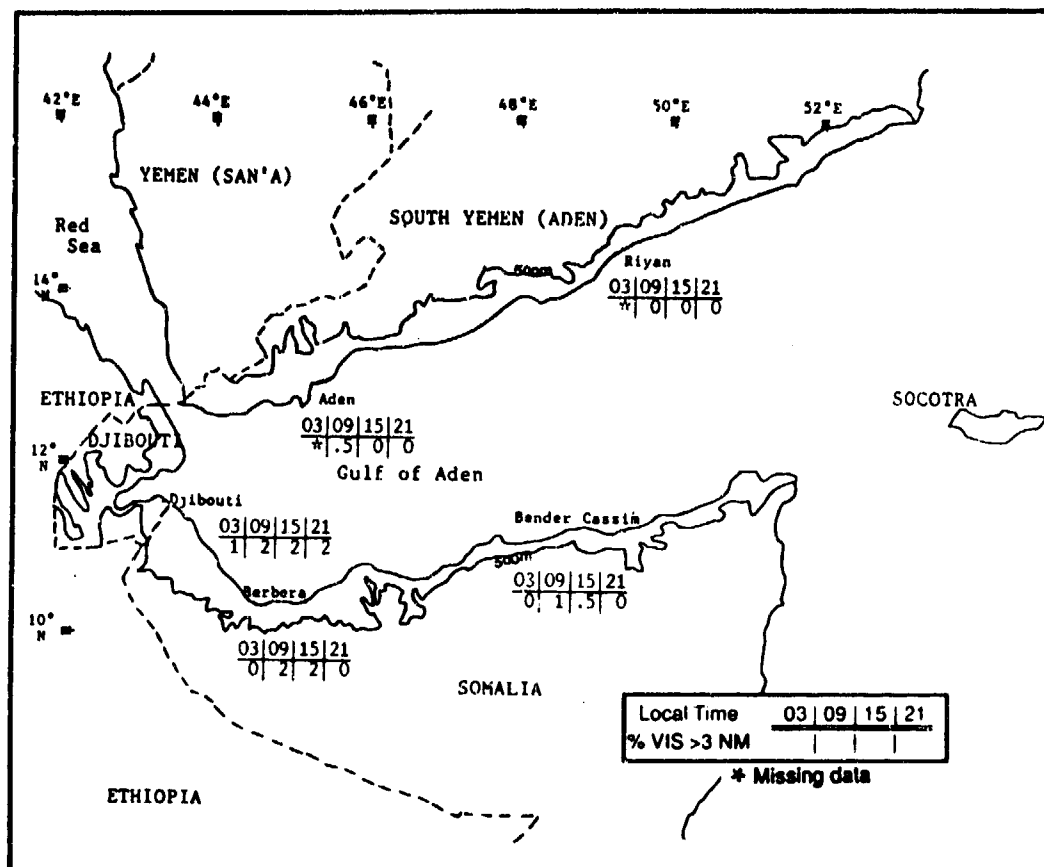


Figure 5-12. SW-NE Monsoon Transition Frequencies of Visibilities Below 3 Miles, Aden Coastal Fringe.

WINDS. Figure 5-13 shows the persistent strengthening of east to southeasterly flow near the surface. When the surface Monsoon Trough migrates south of 8° N, Northeast Monsoon flow strengthens in the eastern Gulf of Aden. The Northeast Monsoon normally arrives in the eastern Gulf by the first week in November, but northeast surface flow in the western Gulf of Aden doesn't become

organized until the third or fourth week in November. Mid- and upper-level wind flow is almost due easterly (080-100°) at 10-15 knots during October and November. On rare occasions, a deep mid-latitude upper-level trough reaches Aden and Riyan. Peak surface winds are north-northwesterly at 20-27 knots.

ADEN COASTAL FRINGE **SOUTHWEST-TO-NORTHEAST TRANSITION**

October-November

E-SE
E-SE
E-SE

	OCT	NOV
Riyan	6.30	6.50
Aden	8.40	10.30
Djibouti	8.50	9.50

Figure 5-13. Mean SW-NE Monsoon Transition Wind Speeds (kt) and Prevailing Directions, Aden Coastal Fringe.

PRECIPITATION. The Aden Coastal Fringe averages less than 1 inch (25 mm) of rain a month in October and November, but mean rainfall amounts are greater than during the Southwest Monsoon because of northeasterly surface flow, Gulf of Aden moisture, and orographic uplift. As shown in Figure 5-14, the eastern Aden Coastal Fringe is drier than the western portion, where topography, coastal configuration, and low-level moisture result in more diurnal convection. Rainfall amounts vary widely across the region. Except for Aden, all extreme maximum 24-hour rainfalls occur in November, when strong northeasterly surface flow penetrates the western Aden Coastal Fringe. Moist onshore flow is available to fuel convection between

Berbera and Djibouti, where topography favors orographic lift. But an unusual mid- or upper-level trigger must have been responsible for the rare 6.1 inch/155 mm 24-hour rainfall maximum recorded at Djibouti. Possible triggers: an upper-level trough or a northward surge of moisture through the Great Rift Valley. November maximum 24-hour rainfalls at Berbera (1.9 inches/48 mm), Bender Cassim (Bosaso)--0.9 inches/23 mm, and Aden (0.8 inches/20 mm) were probably the result of isolated convection. Riyan's 24-hour maximum (4.1 inches/84 mm) occurred with an extremely rare tropical cyclone that made landfall near Ras Fartak.

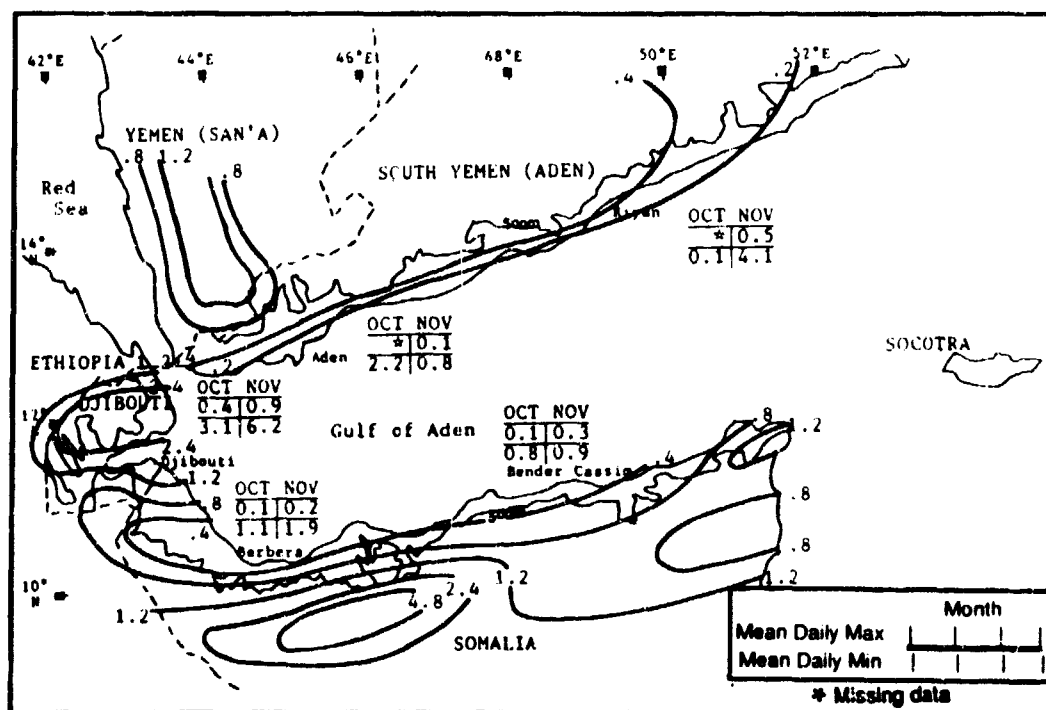


Figure 5-14. Mean SW-NE Monsoon Transition Monthly/Maximum 24-Hour Precipitation, Aden Coastal Fringe. Isohyets represent mean seasonal rainfall totals (inches).

ADEN COASTAL FRINGE **SOUTHWEST-TO-NORTHEAST TRANSITION**

October-November

TEMPERATURE. Mean daily highs (Figure 5-15) range from 85°F/29°C at Aden to 92°F/33°C at Berbera. Record highs include 101°F (38°C) at Aden and 113°F (45°C) at Bender Cassim (Bosaso), both in October.

Mean daily lows range from 68° to 80°F (20-27°C). The record low (53°F/12°C) was recorded in November at Bender Cassim (Bosaso). Djibouti's November record low was 65°F (18°C).

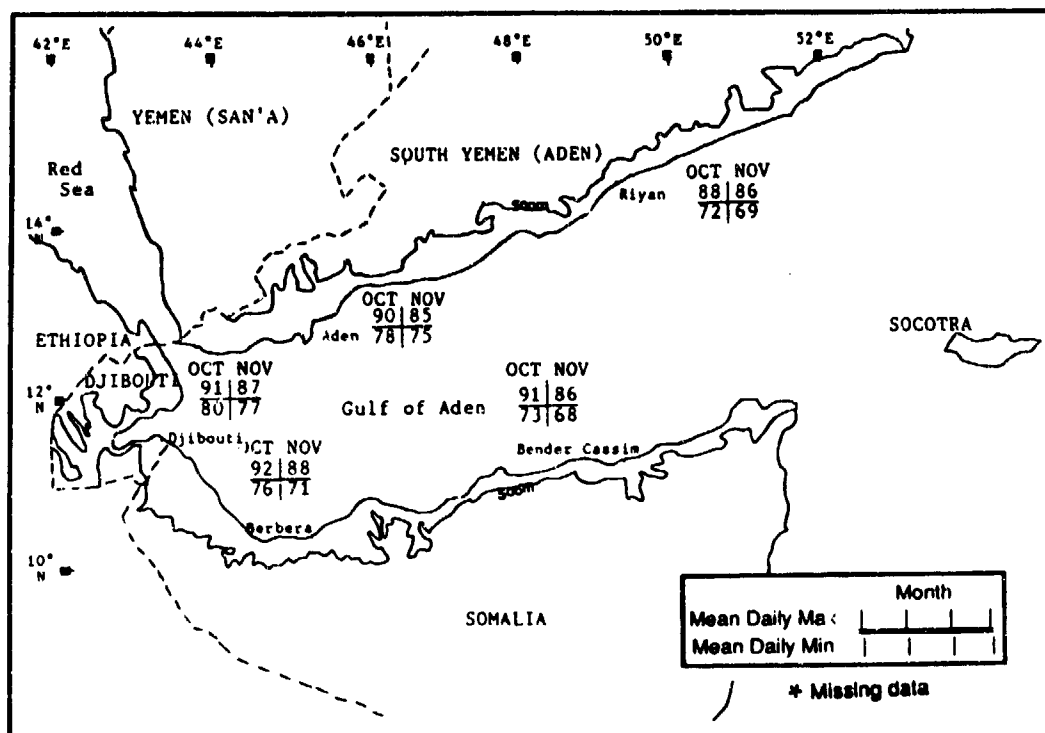


Figure 5-15. Mean SW-NE Monsoon Transition Daily Maximum/Minimum Temperatures (°F), Aden Coastal Fringe.

ADEN COASTAL FRINGE NORTHEAST MONSOON ("Gilal")

December-March

GENERAL WEATHER. Low-level northeasterly flow dominates. Coastline configuration and terrain orientation in the southern half of the region produce two distinct rainfall and cloud cover patterns during the Northeast Monsoon. The southwest and southeast parts are cloudier and wetter than the south-central portion because surface flow is reinforced by the sea breeze and lifted along coastal ranges. There is a narrow leeward rainshadow zone between Bender Cassim and Berbera, where surface flow is parallel to the coast. Upper-level flow (west-southwesterly at 20-30 knots north of the Subtropical Ridge) is dry. Poor upper-level outflow mechanisms do not support widespread low-level convection; as a result, there are very few thunderstorms, even with northeasterly flow, favorable low-level moisture, and uplift.

SKY COVER. Northeasterly flow into the Gulf of Aden and Aden Coastal Fringe is persistent. Surface flow parallels the northern coastline from Riyan to Aden;

synoptic scale moisture transport from the Gulf inland to the elevated interior is minimal. However, Cape Guardafui/Socotra Island and the western Aden Coastal Fringe (Djibouti to Perim Island) are oriented nearly perpendicular to the flow; these areas are the cloudiest in the region.

Figure 5-16 shows mean cloudiness to be lowest (22%) at Berbera, highest (44 percent) at Djibouti. Stratus and stratocumulus with bases near 2,500 feet (762 meters) AGL are the dominant Northeast Monsoon cloud types. Maximum frequency of occurrence is in mid morning. Afternoon (1200-1500 LST) cumulus with bases at 3,000-3,500 feet (915-1,067 meters) AGL and shallow vertical development (tops to 7,000 feet/2,134 meters MSL) contribute to mean seasonal sky cover conditions, which average 3-4/8ths in the morning and 2-3/8ths in the afternoon. The only exception is near Cape Guardafui, where sky cover averages 3-5/8ths, all hours.

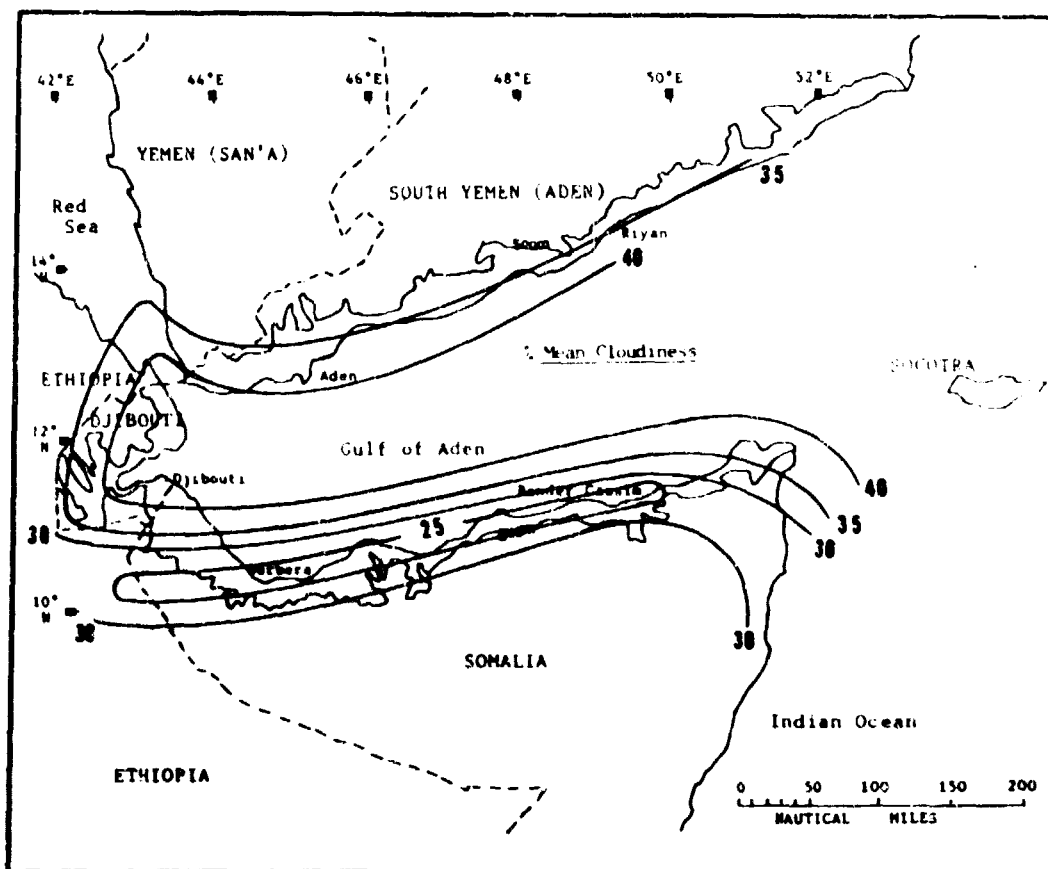


Figure 5-16. Mean Northeast Monsoon Cloudiness Frequencies, Aden Coastal Fringe. The data is derived by calculating the grand mean for National Intelligence Summary (NIS) mean cloudiness data at specific hours from December through March. Isolines are in 5% intervals.

ADEN COASTAL FRINGE NORTHEAST MONSOON ("Gillal")

December-March

The frequency of ceilings at or below 3,000 feet (915 meters) AGL averages 14% for the entire region (Figure 5-17). Regional frequencies vary from 17 to 32 percent between 2100 and 0900 LST at Djibouti to 0 percent between 1500 and 0300 LST at Berbera. Late evening to mid-morning low stratus/stratocumulus ceilings are common along most of the Aden Coastal Fringe; they

are the result of weak surface convergence (land/sea breeze transition) and warm coastal waters. Terrain around the Gulf of Tadjoura helps increase low ceiling frequency around Djibouti. Frontal passages rarely result in little more than slight increases in mid-and upper-level cloudiness.

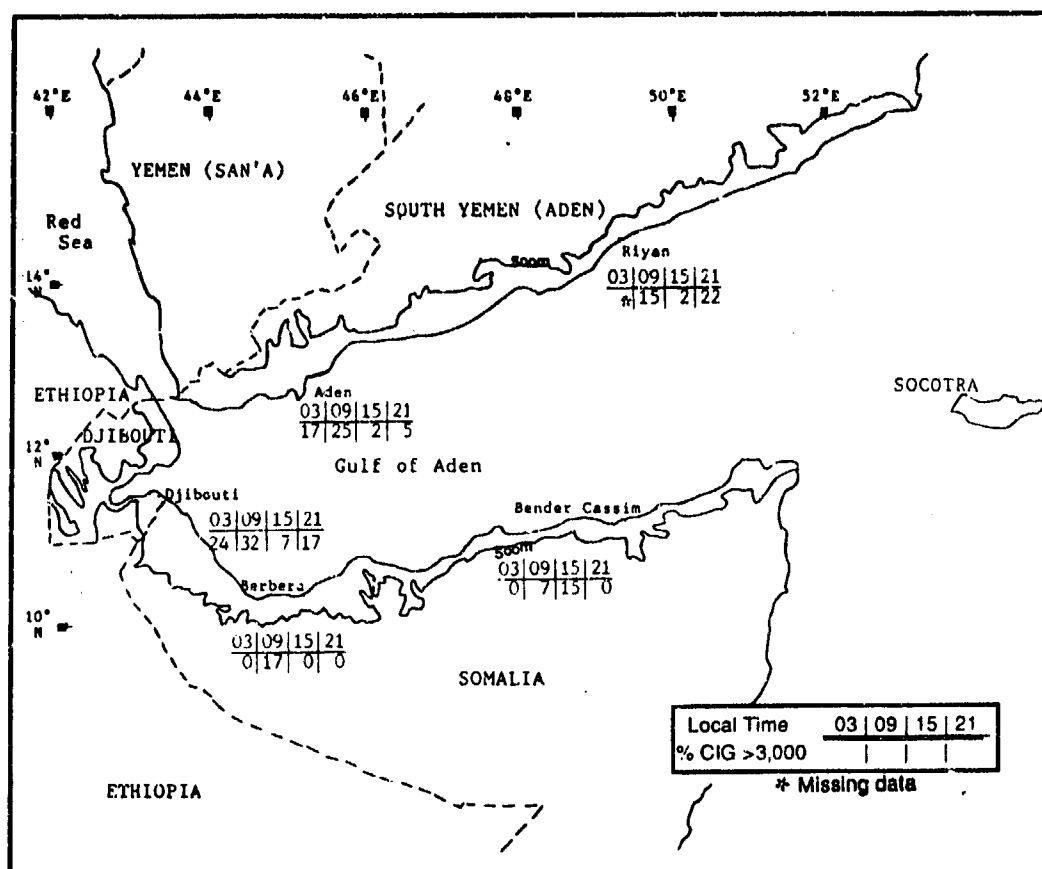


Figure 5-17. Northeast Monsoon Frequencies of Ceilings Below 3,000 Feet (915 meters), Aden Coastal Fringe.

VISIBILITY. Dust and haze are the main causes of low visibilities during the Northeast Monsoon, but frequencies (Figure 5-18) are low. Visibility is below 3 miles on only 8 days during the entire season. On 6 of those 8 days (75% of observations), the obstruction to vision is dust. The rest are accounted for by radiation

fog, haze, or smoke. Most dust-related obstructions to vision occur when strong sea breezes push inland. Coastal dunes and extended fair weather periods--with dry surface conditions--are favorable for sandstorm or duststorm development.

ADEN COASTAL FRINGE **NORTHEAST MONSOON ("Gillal")**

December-March

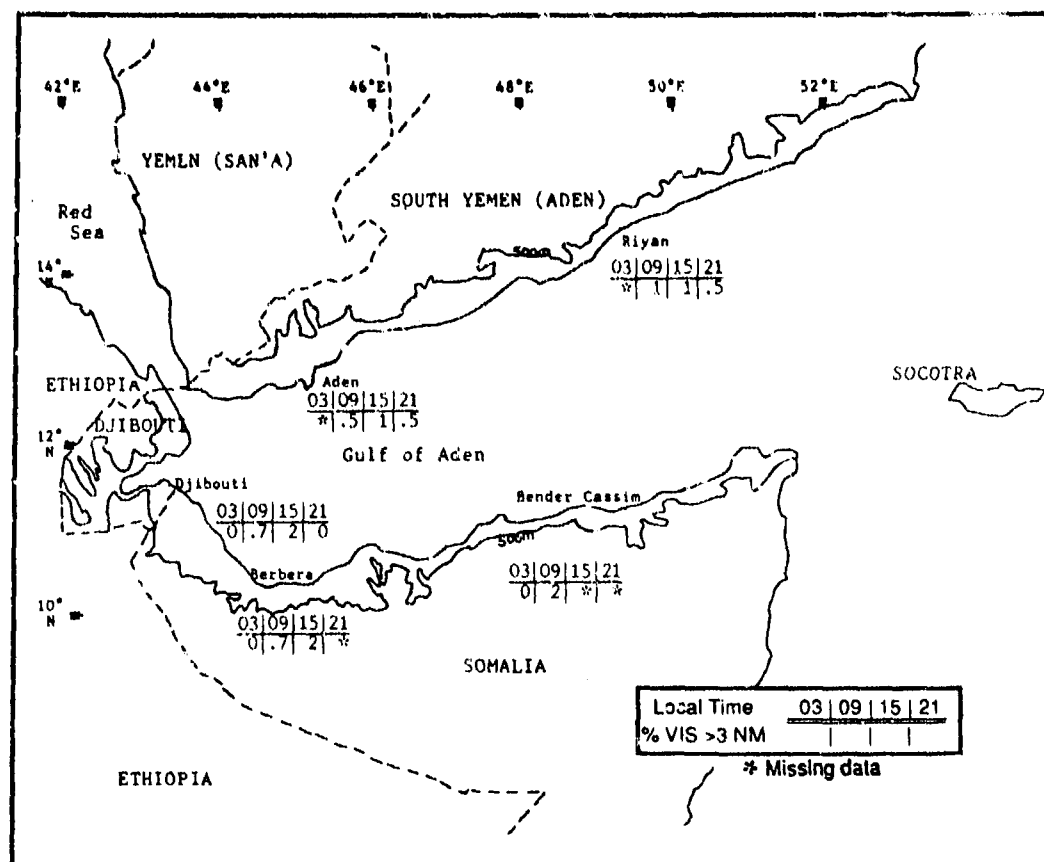


Figure 5-18. Northeast Monsoon Frequencies of Visibilities Below 3 Miles, Aden Coastal Fringe.

WINDS. Figure 5-19 gives mean Northeast Monsoon surface wind speeds and prevailing directions for several Aden Coastal Fringe stations. Easterlies prevail; local variations are a function of sea breeze deflection. Note

that Djibouti's prevailing wind direction changes from E-S to E-NE in March; the slight shift is caused by an increase in weak cyclonic activity (northwesterly flow) that penetrates the southern Red Sea in March.

E-SE
E-SE
E-S/E-NE

	DEC	JAN	FEB	MAR
Riyan	7.50	7.50	7.10	6.80
Aden	11.00	11.40	10.50	11.20
Djibouti	10.40	10.40	10.50	10.30

Figure 5-19. Mean Northeast Monsoon Wind Speed (kts) and Prevailing Direction, Aden Coastal Fringe.

ADEN COASTAL FRINGE NORTHEAST MONSOON ("Ghial")

December-March

A deep upper-level trough and a surface cold front may temporarily (6-24 hours) shift winds in the western and northern Aden Coastal Fringe to northwesterly, with maximum speeds of 25 knots along the cold front. Strongest winds occur near Perim Island and the Straits of Bab al Mandab. The surface front weakens in the central and eastern Gulf of Aden, and northwesterly winds become less than 10 knots.

PRECIPITATION. Mean monthly Northeast Monsoon rainfall (Figure 5-20) is controlled by topography and coastline orientation. Most locations get at least 0.1 inch (2.5 mm) a month. The exception is near Bender Cassim (Bosaso), where localized low-level divergence along the coast produces only trace amounts in January and March, and no rain at all in February.

The southern Aden Coastal Fringe has two zones of maximum Northeast Monsoon precipitation. Near Cape Guardafui (including Socotra Island), the coastline is perpendicular to onshore flow. During early morning (0500-0800 LST), stratus and shallow stratocumulus develop almost every day. Light or intermittent drizzle

falls every third day somewhere along the Cape, and above 1,000 feet (305 meters) MSL on Socotra's northern mountain slopes. More than 0.01 inch (0.25 mm) falls near Cape Guardafui about 9 days in each Northeast Monsoon season. Just inland from Cape Guardafui, nocturnal rainfall may occur if thick coastal stratus and stratocumulus move inland between 0000-0600 LST. Between Cape Guardafui and 46° E, little daytime precipitation occurs because the coastline orientation is parallel to the flow. Forty nautical miles west of Berbera, the coastline turns northwestward and perpendicular to prevailing northeasterly flow. From this point west and north to Perim Island, rainfall is more frequent, and moderate rains are not uncommon.

Half the region's total mean annual precipitation falls during the Northeast Monsoon, but an entire monthly or seasonal mean can occur in only one or three rainshowers. Thunderstorms are rare, with only one or two a season. Since the Aden Coastal Fringe gets only 2-4 inches (51-102 mm) of rain a year, just one isolated thunderstorm could provide that much, or more.

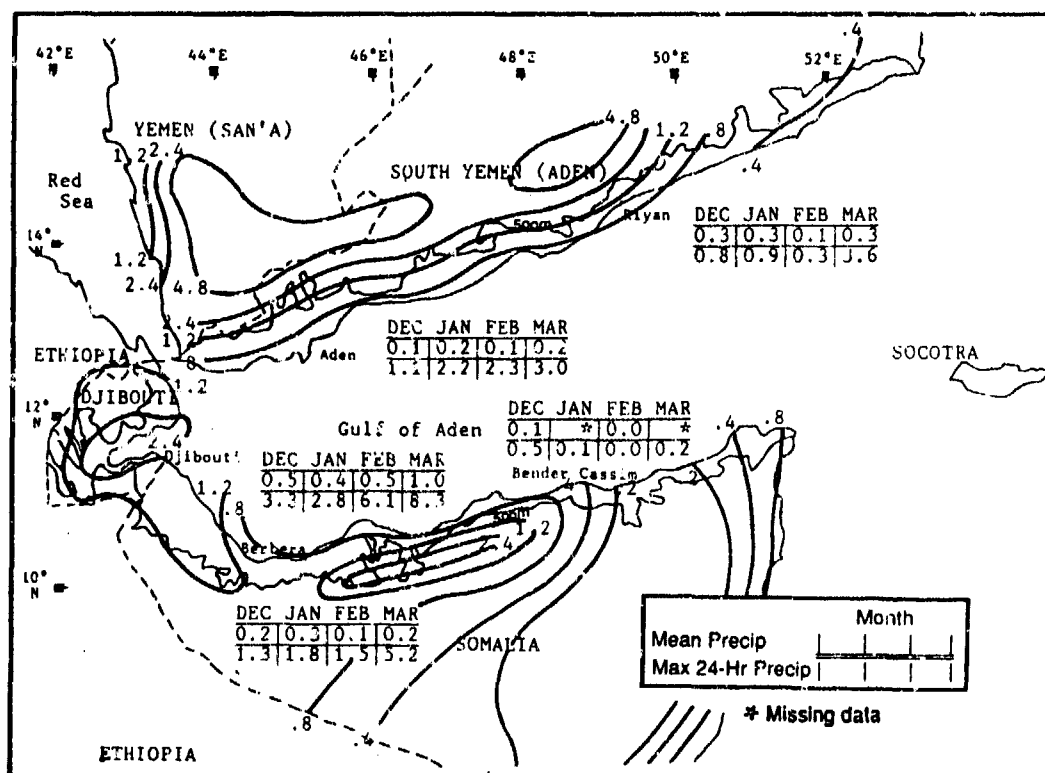


Figure 5-20. Mean Northeast Monsoon Monthly/Maximum 24-Hour Precipitation, Aden Coastal Fringe. Isohyets represent mean seasonal rainfall totals (inches).

**ADEN COASTAL FRINGE
NORTHEAST MONSOON ("Gillal")**

December-March

Occasionally, a mid- or upper-level disturbance brings above normal rainfall to the western parts of the region. Such mid-latitude disturbances most often affect the Aden Coastal Fringe when the Polar Jet moves southward into the central Red Sea. As shown in Figure 5-21, the 300-mb Polar Jet temporarily "shares energy" with the Subtropical Jet. Because both jets deviate southward into the Red Sea, a cold trough aloft descends

abnormally southward. In the figure, the Polar Jet (PJS) and Subtropical Jet (STJ) have two wind speed maxima: the first over the Persian Gulf (PJS/STJ-1) and a second in east central Egypt (PJS/STJ-2). Rare thunderstorms or heavy showers developing over the northern Ethiopian/Yemen Highlands move into the western Aden Coastal Fringe.

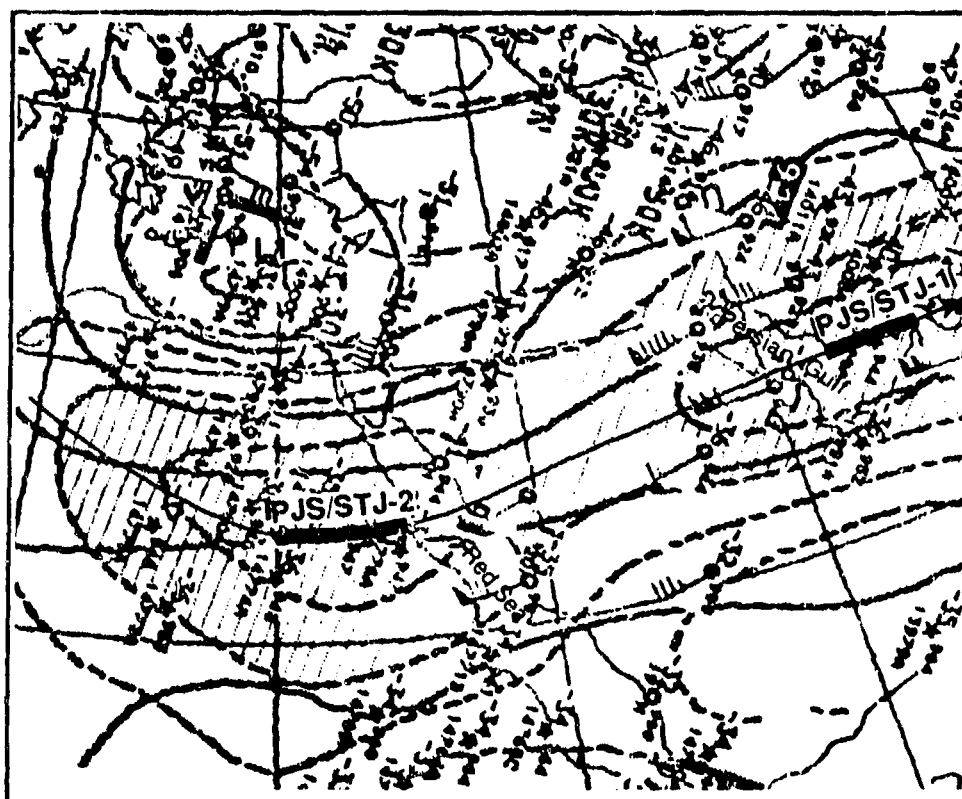


Figure 5-21. The Polar Jet (PJS) and Subtropical Jet (STJ) Interact Over the Subtropics. The PJS/STJ-2 position is critical to abnormally heavy Aden Coastal Fringe precipitation.

ADEN COASTAL FRINGE **NORTHEAST MONSOON ("Gilal")**

December-March

TEMPERATURE. The Northeast Monsoon is the coolest season of the year, but mean daily highs (Figure 5-22) still average 80-88°F (27-32°C). Record highs range from 96°F (36°C) at Berbera in December to 101°F (38°C) at Bender Cassim (Bosaso) in January. Daily highs typically occur just after noon. By 1300

LST, well-developed sea breezes start to cool the coastal plains. The lowest temperatures of the year occur during the Northeast Monsoon, when mean daily minimums range from 67 to 76°F (19 to 24°C). The record lows were recorded in December: 52°F (11°C) at Bender Cassim, and 63°F (17°C) at Djibouti.

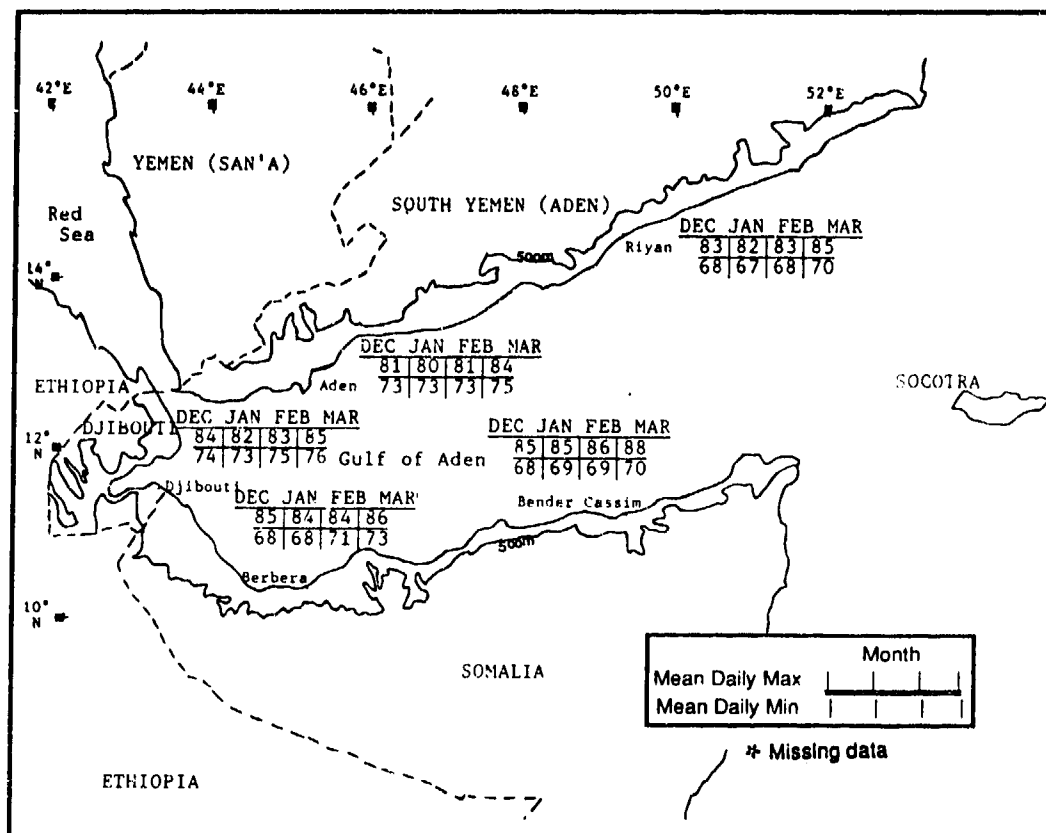


Figure 5-22. Mean Northeast Monsoon Daily Maximum/Minimum Temperatures (°F), Aden Coastal Fringe.

ADEN COASTAL FRINGE **NORTHEAST-TO-SOUTHWEST MONSOON TRANSITION ("Gu")**

April-May

GENERAL WEATHER. The most important feature of the transition is the surface Monsoon Trough's northward migration into the region in early May. This produces a subtle surface wind shift from moist easterly-southeasterly (Figure 5-23a) to dry southerly (Figure 5-23b). Thick arrows are primary streamlines, thin arrows secondary streamlines. Arrows through circles depict surface wind direction, and numbers inside

circles are surface wind speeds in knots. Dashed lines are 5-knot isotachs. The surface Monsoon Trough (dash-dot-dash line) produces weak convergence along its axis, along with showers and increased low- to mid-level cloud cover. Isolated convective cells are short-lived, but occasionally build into towering cumulus.

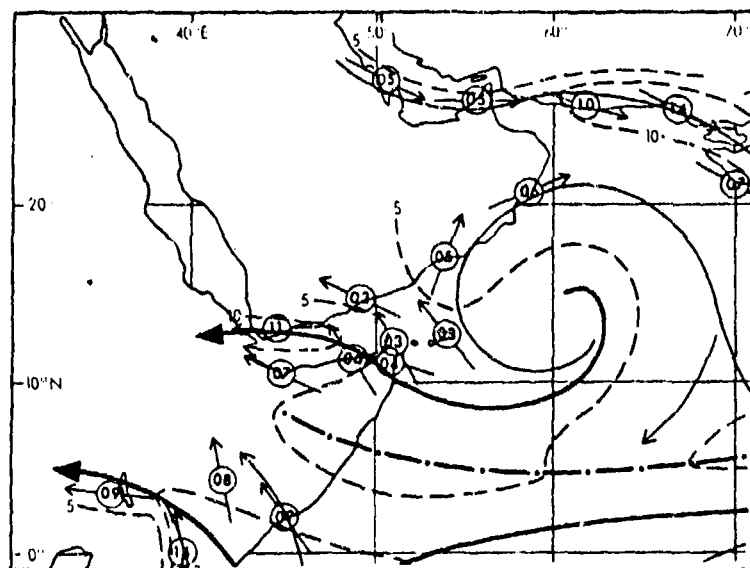


Figure 5-23a. Mean April Gradient Flow, Aden Coastal Fringe.

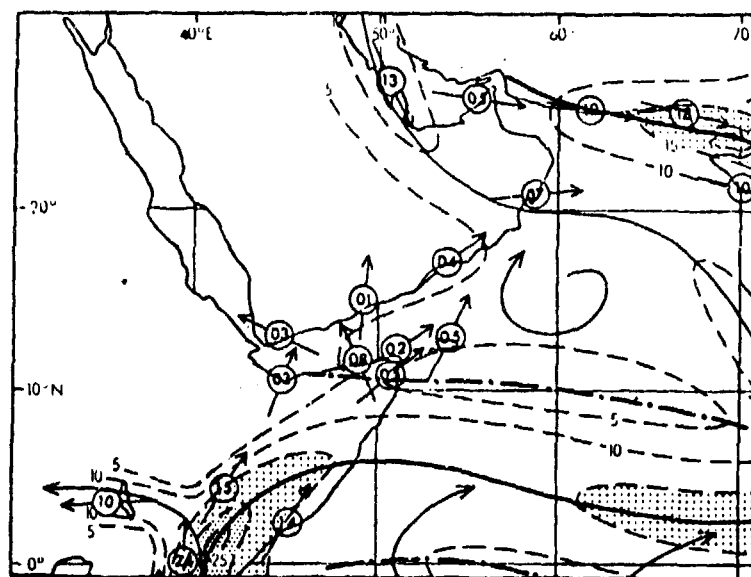


Figure 5-23b. Mean May Gradient Flow, Aden Coastal Fringe.

ADEN COASTAL FRINGE NORTHEAST-TO-SOUTHWEST MONSOON TRANSITION ("Gu")

April-May

SKY COVER. Mean cloudiness varies across the region from 18 to 35% (Figure 5-24). April surface flow in the Gulf of Aden is easterly (ENE-ESE). Western and northern coasts are oriented perpendicular to the moist flow, resulting in higher frequencies of diurnal sea breeze cumulus and early morning stratus and stratocumulus along immediate coastlines. The southern Aden Coastal Fringe between Bender Cassim (Bosaso) and Berbera is sheltered from these easterlies by the Ogo Highlands; this is reflected by lower (20-25%) mean cloudiness here. Less than 2/8ths isolated mid-afternoon fair weather cumulus is typical between Bender Cassim (Bosaso) and Berbera. This cumulus results from intense surface heating, but there is not enough sea breeze moisture for vertical development. Most early and

mid-morning cloud cover is stratus and stratocumulus (3-4/8ths).

Along the western Aden Coastal Fringe (near Aden and Djibouti) in late April and early May, stratocumulus may develop into cumulus (and occasionally cumulonimbus) by mid-afternoon as the surface Monsoon Trough provides weak low-level convergence. Sea breeze moisture penetrates into interior Djibouti with easterly flow to the north of the Trough. Cloud bases average 2,000-2,500 feet (610-762 meters) AGL for stratus and 3,000-4,000 feet (915-1,220 meters) MSL for cumulus and stratocumulus. Cumulonimbus bases are similar to those of the cumulus and stratocumulus, but tops reach 35,000 feet (10.7 km) MSL.

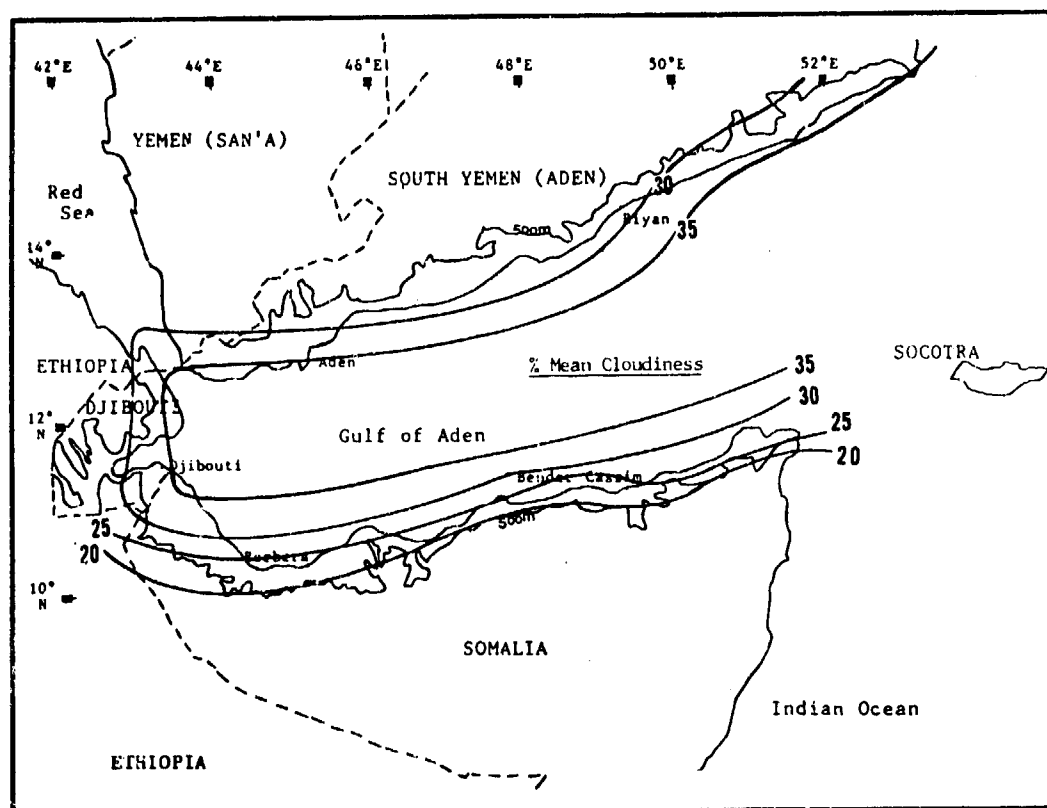


Figure 5-24. Mean NE-SW Monsoon Transition Cloudiness Frequencies, Aden Coastal Fringe. The data is derived by calculating the grand mean from National Intelligence Summary (NIS) mean cloudiness data for specific sites in April and May. Isolines are in 5% intervals.

ADEN COASTAL FRINGE **NORTHEAST-TO-SOUTHWEST MONSOON TRANSITION ("Gu")**

April-May

As shown in Figure 5-25, ceilings at or below 3,000 feet/915 meters AGL occur less than 16% of the time throughout the region. Low ceilings at Riyan (16%) are mostly due to coastal stratus, but at Berbera (12-13%), they are caused by stratocumulus/cumulus buildups along the surface Monsoon Trough.

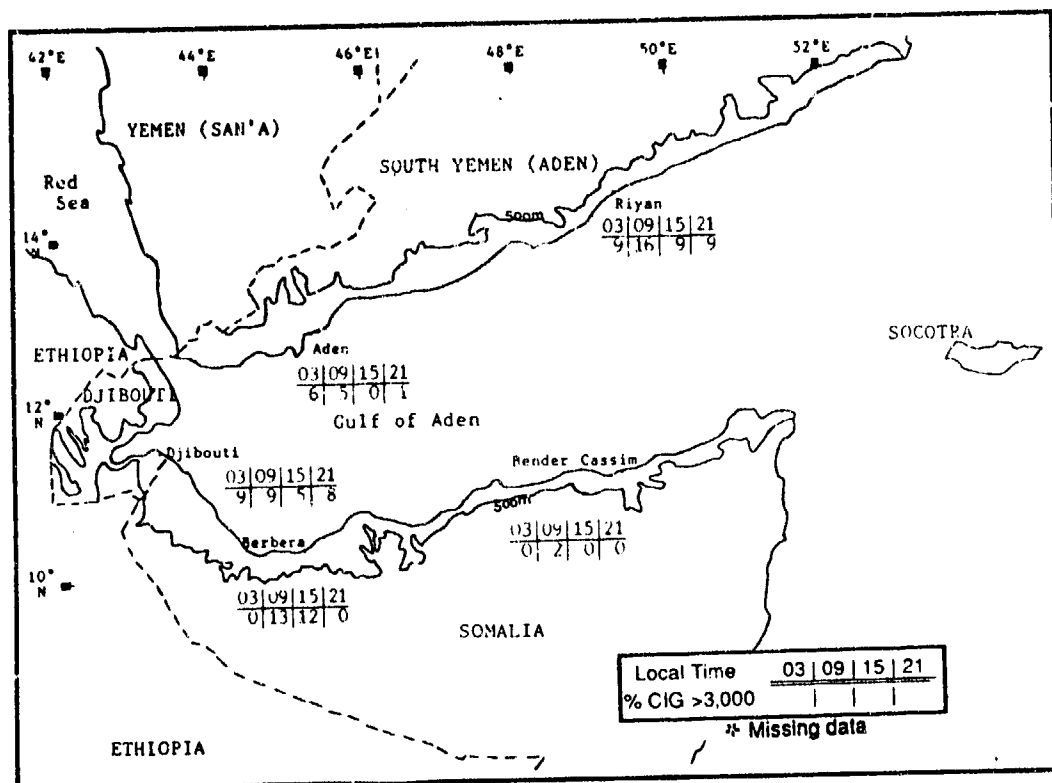


Figure 5-25. NE-SW Monsoon Transition Frequencies of Ceilings Below 3,000 Feet (915 meters), Aden Coastal Fringe.

ADEN COASTAL FRINGE NORTHEAST-TO-SOUTHWEST MONSOON TRANSITION ("Gu")

April-May

VISIBILITY. The Aden Coastal Fringe has a very small (less than 2%) frequency of visibilities below 3 miles. Nearly all low visibilities in the southern part of

the Aden Coastal Fringe are due to duststorms, some of which may reduce local visibility to 300 feet (97 meters) for up to 30 minutes.

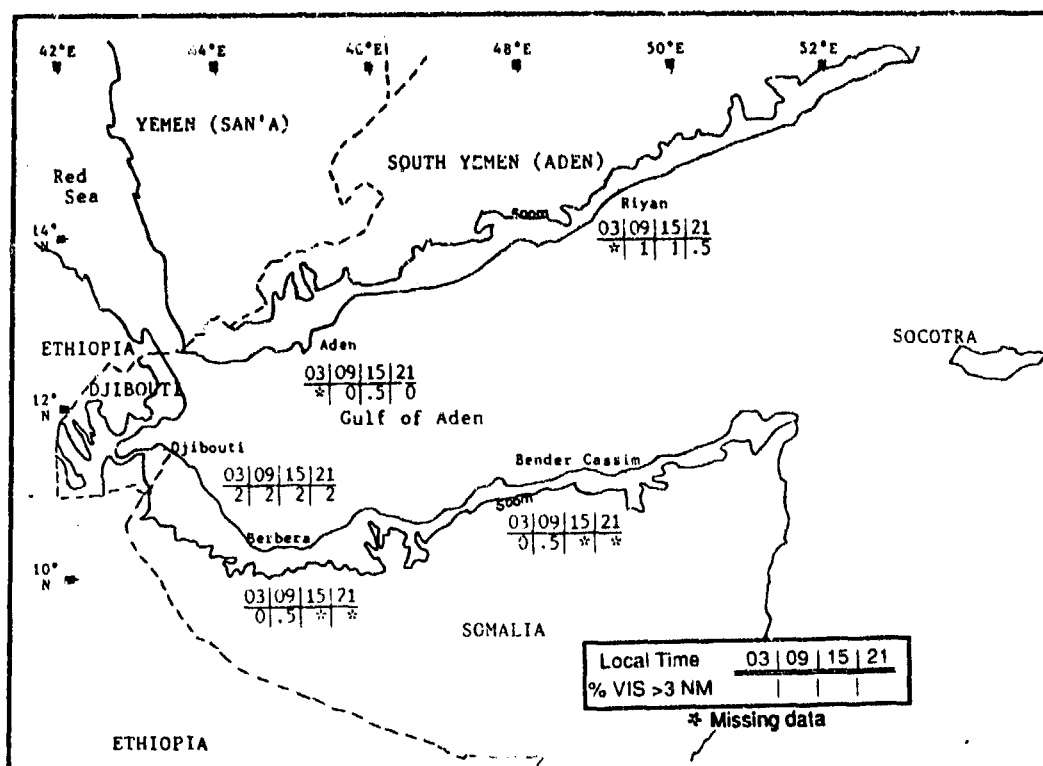


Figure 5-26. NE-SW Monsoon Transition Frequencies of Visibilities Below 3 Miles, Aden Coastal Fringe.

WINDS. In Figure 5-27, mean surface wind speed decreases through May except at Riyan, where there is a small increase. Prevailing directions reflect diurnal land/sea breeze circulation, not the synoptic flow shown in Figures 5-25a and b.

Upper-level flow is easterly at 10-15 knots. The mean position of the Subtropical Ridge is immediately north of the region, but an upper-level trough may sweep through once or twice during the transition. Weak troughs do not create detectable surface wind shifts.

E-S
E-S
E-NE

	APR	MAY
Riyan	6.80	7.10
Aden	10.90	8.60
Djibouti	9.50	7.40

Figure 5-27. Mean NE-SW Monsoon Transition Wind Speed (kts) and Prevailing Direction, Aden Coastal Fringe.

ADEN COASTAL FRINGE **NORTHEAST-TO-SOUTHWEST MONSOON TRANSITION ("Gu")**

April-May

PRECIPITATION. Most transition rainfall occurs with irregular and isolated diurnal convection triggered by brief northward surges of the surface Monsoon Trough. The southwestern Aden Coastal Fringe (Berbera to Perim Island) is affected by localized convection originating in the Ethiopian Highlands to the south and west. Mean April rainfall (0.5 inches/13 mm) at Berbera and Djibouti are the highest in the Aden Coastal Fringe. Little rain falls across the Gulf near the city of Aden. This supports the notion that the isolated Ethiopian Highland convective clusters that move into the southwestern

Aden Coastal Fringe are supported by northward surface Monsoon Trough movements and sustained by low-level sea breeze moisture concentrated at the Gulf's west end. The dry southeastern Aden Coastal Fringe is controlled by the Somali Jet's low moisture content.

Maximum 24-hour April rainfall at Djibouti (7.1 inches/180 mm), at Aden (2.6 inches/66 mm), and at Berbera (2.3 inches/58 mm), illustrate the potential but extremely rare case of Monsoon Trough convection penetrating the western Aden Coastal Fringe.

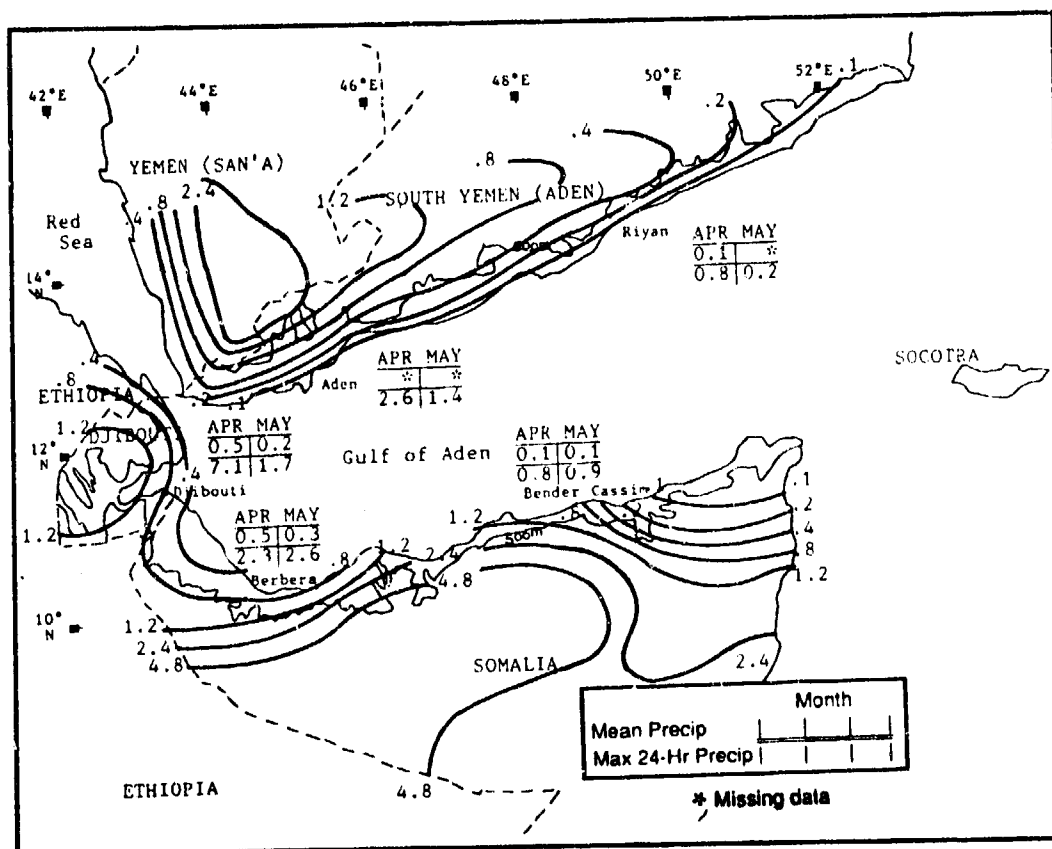


Figure 5-28. Mean NE-SW Monsoon Transition Monthly/Maximum 24-Hour Precipitation, Aden Coastal Fringe. Isohyets represent mean seasonal rainfall totals (inches).

ADEN COASTAL FRINGE **NORTHEAST-TO-SOUTHWEST MONSOON TRANSITION ("Gu")**

April-May

TEMPERATURE. As shown in Figure 5-29, mean daily highs range from 88 to 99°F (31-37°C). May is the warmest month of the year, averaging 93-99°F (33-37°C). Record highs are 104°F (40°C) at Riyan in April and 113°F (45°C) at Bender Cassim in May.

Mean daily lows range from 74°F to 82°F (24-28°C). Temperatures rarely drop below 65°F (18°C)--record lows are 62°F (17°C) at Bender Cassim (Bosaso) and 70°F (21°C) at Djibouti, both in April.

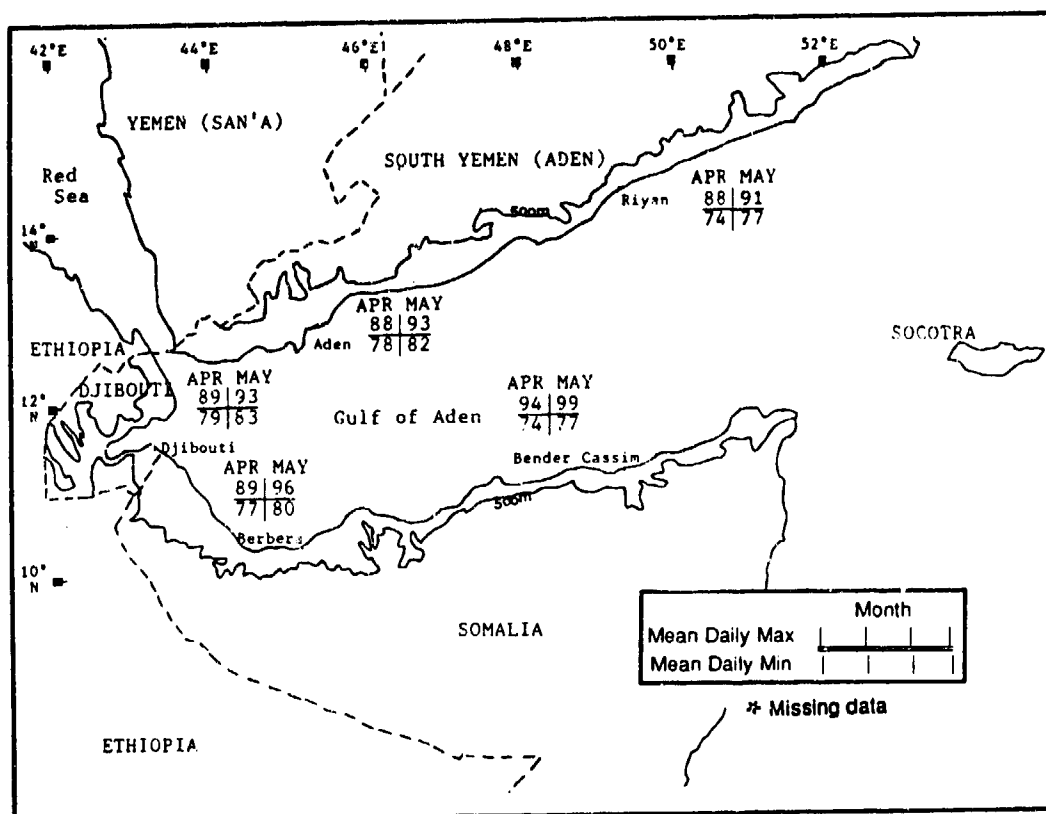


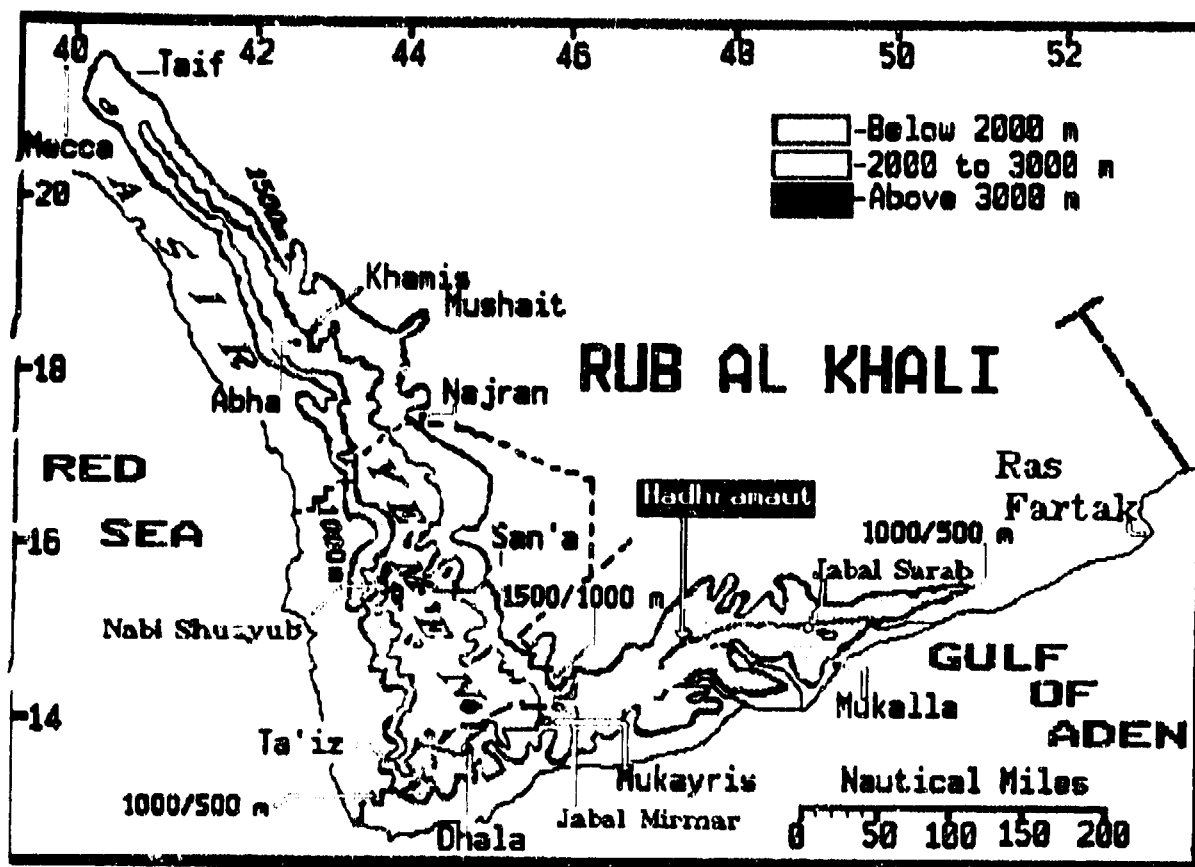
Figure 5-29. Mean NE-SW Monsoon Transition Mean Daily Maximum/Minimum Temperatures (°F), Aden Coastal Fringe.

Chapter 6

YEMEN HIGHLANDS

The region discussed here as the Yemen Highlands includes includes Yeraen--San'a (YD), as well as small portions of Saudi Arabia (SD) and Yemen--Aden (AD). After describing the area's situation and relief, this chapter discusses its "typical weather" by season, as shown below.

Situation and Relief.....	6-3
Southwest Monsoon--June-September.....	6-5
General Weather	6-5
Sky Cover.....	6-5
Visibility	6-7
Winds	6-8
Precipitation	6-10
Temperature	6-11
Southwest-to-Northeast Monsoon Transition--October-November	6-12
General Weather	6-12
Sky Cover.....	6-12
Visibility	6-13
Winds	6-14
Precipitation	6-15
Temperature	6-16
Northeast Monsoon--December-March	6-18
General Weather	6-18
Sky Cover.....	6-18
Visibility	6-20
Winds	6-21
Precipitation	6-23
Temperature	6-24
Northeast-to-Southwest Monsoon Transition--April-May.....	6-25
General Weather	6-25
Sky Cover.....	6-25
Visibility	6-27
Winds	6-27
Precipitation	6-28
Temperature	6-29



STATION: SAN'A YEMEN													
LAT/LON:		15 31 N		44 11 E		ELEV:		7183 FT					
ELEMENTS	JAN	FEB	MAR	APR	MAY	JUN	JUL	AUG	SEP	OCT	NOV	DEC	ANN
AVG MAX	72	75	78	76	79	82	82	80	79	75	72	69	77
AVG MIN	37	43	44	49	49	52	54	54	48	40	38	36	45
AVG PRCP	*	0.1	1.1	1.7	1.3	0.2	2.6	3.5	0.5	*	0.4	0.2	11.7

* = LESS THAN 0.05 INCHES OR LESS THAN 0.5 DAYS

Figure 6-1. The Yemen Highlands. This "L"-shaped region includes most of Yemen (San'a), Yemen (Aden), and a small portion of southwestern Saudi Arabia, from Mecca southeast to Najran. The table summarizes climatology for San'a, Yemen.

YEMEN HIGHLANDS

SITUATION AND RELIEF

SITUATION AND RELIEF. The southern boundary of the Yemen Highlands follows the 1,620-foot (500 meter) contour from the San'a-Aden political boundary ENE to 50° E, or 110 NM WSW of Ras Fartak. The eastern edge includes the Hadhramaut Plateau, which is defined by the 1,620-foot (500 meter) contour on the south and the 3,280-foot (1,000 meter) contour to the north. The 3,280-foot (1,000 meter) contour extends westward along the northern Hadhramaut Plateau and back to the San'a-Aden border. From there, the 6,560 foot (1,500 meter) contour runs northwest into Saudi Arabia to 21° 50' N or 30 NM NE of Mecca, SD. The western boundary follows the 3,280-foot (1,000 meter) contour south to the San'a/Aden border, then rejoins the 1,620-foot (500 meter) contour on Yemen's border.

The western part of the region (the upright bar of the "L") contains rugged terrain produced by massive geologic uplift along Africa's Great Rift System. Volcanic ridges (the Asir and Yemen Mountains) are aligned NNW to SSE for about 630 NM between 13° N and 21° 30' N. These ridges have a significant effect on climate in the Yemen Highlands. An extensive network of dendritic river systems dissect the ridges, but no permanent streams extend westward to the Red Sea or eastward to the Rub al Khali.

In the north, the eroded Asir Mountain ridges extend into Saudi Arabia north of 17° N. The Asirs are only 10-20 NM wide and average 6,890 feet (2,100 meters) MSL in height. The Asirs end just northeast of Mecca, Saudi Arabia. Western slopes are covered by alluvium, while eastern slopes (above 4,920 feet/1,500 meters) are rolling hills, a desert steppe environment. The surface is a mix of rocky stubble, boulders, and isolated sand hills.

Further south, the rugged Yemen Mountains average 8,100 feet (2,500 meters) in height and 100 NM in width between 13° 30' N and 17° N. Numerous volcanic peaks surround San'a and Ta'iz; the highest is Nabi Shuayub at 12,333 feet (3,760 meters). Terrain is isolated; there are few roads or even foot trails in the interior. Western slopes parallel the Red Sea coast and ascend at the rate of 492 feet/150 meters per nautical mile. Terrain rapidly transitions from lava-covered hills to rugged canyons with steep vertical walls that may rise 1,000 feet (305 meters) above the canyon floor. The interior Yemen Mountain network contains rugged granitic mountains with minimal vegetative cover. The dry and desolate eastern slopes trend gradually down to a barren plateau that transitions abruptly to the Rub al Khali Desert--the second largest desert in the world.

The southernmost portion of the Highlands (the bottom of the "L") is known as the Hadhramaut Plateau. It parallels the Gulf of Aden and averages 3,937 feet (1,200 meters) in elevation. Smaller volcanic ridges are aligned WSW-ENE along the plateau's southwest edge. The plateau contains a network of deep and sinuous canyons where numerous semipermanent stream beds (wadis) have cut steep vertical cliffs into the plateau. The tablelands above these canyons are level and barren. The plateau's southern fringes extend to within 20-30 NM of the Gulf of Aden coastline, and are composed of igneous rock, sandstone, and limestone. The area bears a resemblance to South Dakota's Badlands.

The extreme western edge of the Hadhramaut Plateau is an extension of the southeastern Yemen Mountains. Jabal Mirmal is the highest point at 6,360 feet (1,939 meters). To the east, the plateau is flat-topped with isolated hills and sinuous ridges cut by an intricate network of flat-bottomed valleys, gullies and deep canyons. The highest point (40 NM northwest of Mukalla, South Yemen) is Jabal Sarab at 6,980 feet (2,112 meters). The northern and eastern edges of the plateau disappear into the deep sand dunes and barren landscape of the Rub al Khali. The outstanding feature of the plateau is the Wadi Hadhramaut, running west to east through the center of the plateau. Its watershed drains 1,000 sq NM of adjacent wadis. The largest tributary (the Wadi Masilah) carries water towards the Gulf of Aden during heavy rains. Wadi valleys are 1 to 3 NM wide, with level, arable land abruptly edged by natural sandstone and limestone terraces. These slopes can rise to 1,200 feet (365 meters) above the valley floor.

DRAINAGE AND RIVER SYSTEMS. There are few permanent water bodies on the Hadhramaut Plateau except for isolated permanent groundwater sources in deep wadi canyons. The Wadi Hadhramaut is the largest intermittent river valley, extending 350 NM SSW to the Gulf of Aden. As it turns south, the valley becomes the Wadi Masilah. The Wadi Mayfa'ah and Wadi Hajr originate along the southern ridges of the Hadhramaut Plateau and form deep canyons along their courses. Each stream runs about 100 NM northwest to southeast to the coast. The Wadi Mayfa'ah flows throughout the year on a 10 NM stretch of its course, but surface water does not reach the Gulf of Aden. The Wadi Hajr is the only perennial stream that flows through the southern Hadhramaut from its source to the Gulf. The wadi system is shown in Figure 5-1a.

YEMEN HIGHLANDS

SITUATION AND RELIEF

VEGETATION. The western and northern fringes of the Hadhramaut Plateau are covered sparsely by short shrubs and grasses. These regions are transition zones between alpine and desert environments. Above 6,700 feet (2,043 meters), isolated acacia trees, thorn shrubs, and alpine grasses thrive. The canyons and valleys of the Hadhramaut contain diversified vegetation. Palm, acacia and ariata (an ornament tree or shrub with feathery branches) thrive in the moist sands of the wadi channels. Valley floors contrast the barren slopes of canyons. Some isolated agricultural terracing is attempted on the slopes, but most are dotted by shallow rooted shrubs.

Along the western slopes of the Yemen Mountains, there is an evergreen zone between 4,000 and 6,700 feet (1,220-2,043 meters) MSL. Deciduous and mixed forest cling to the rugged terrain, but they thin appreciably northward into Saudi Arabia and the southern Asirs. Below the evergreen zone, acacia trees, small shrubs and grass clumps thrive, but above the evergreen zone, the terrain is treeless. Alpine flowers, grasses and lichens are seasonal forms of vegetation.

YEMEN HIGHLANDS SOUTHWEST MONSOON

June-September

GENERAL WEATHER. Sea breeze circulation and the surface Monsoon Trough are the two most important Southwest Monsoon weather features in the Yemen Highlands. As the sea breeze surges inland against the Asir and Yemen Mountains, orographic lift produces cumulus between 4,000 and 8,000 feet (1,220 and 2,439 meters) from Ta'iz northward to San'a. The uplift occasionally produces a continuous line of convective activity some 400 NM long from SSE-NNW along the southern Asir and Yemen Mountains, with moderate rainshowers and embedded thundershowers. Rainfall often occurs between 1400 and 1800 LST.

The surface Monsoon Trough and its weak low-level convergence occasionally produces isolated convection near the Straits of Bab al Mandab, but the Trough's primary role as a Southwest Monsoon weather-maker is to provide hot and dry northeasterly flow to the Hadhramaut and eastern Yemen and Asir Mountains. A strong thermal low--part of the broad scale thermal trough discussed in Chapter 2--anchors the surface Monsoon Trough over the Rub al Khali Desert during the Southwest Monsoon. Dry northeasterly flow ascends the eastern Yemen Highlands and mixes with ascending sea breeze moisture to the west of the highest ridge crests. The result is a well-defined diurnal cloud and precipitation pattern west-to-east across the Yemen and Asir Mountains. Hot, dry, and cloud-free skies dominate eastern slopes, while moderate convection, substantial rainfall, and cooler daytime temperatures dominate western slopes. Light rain falls on eastern slopes above 8,000 feet/2,439 meters, the product of convective towers originating along western mountain slopes.

On rare occasions, a strong high-pressure ridge disrupts the typical synoptic surface pressure pattern. Cooler and moister Mediterranean-type air masses descend across northern Saudi Arabia. The abnormal synoptic pattern produces temporary (3- to 12-hour) moist mid-level flow along the eastern Yemen Highlands. Nearly all eastern slope rainfall below 8,000 feet (2,439 meters) occurs with high pressure ridging. Note that high pressure ridges are early and late season phenomena only.

SKY COVER. The Southwest Monsoon produces the highest percentage of mean cloudiness for the entire year, but the highest frequencies shown by the isopleths in Figure 6-2 are still less than 45 percent. Most cloudiness is over the southern and central Yemen Mountains, where low-level Red Sea moisture and weak convergence along the surface Monsoon Trough fuel orographic uplift. The sea breeze insures a diurnal cycle of moderate convection all day. The cycle begins between 0900 and 1000 LST and ends before 1800 LST. Orographic uplift occurs along the western Asirs, but to a lesser degree; the convective cycle here stops at 1600 LST.

Mean cloudiness decreases considerably downwind (on leeward slopes) and over the Hadhramaut Plateau as sea breeze moisture is unable to penetrate into the interior. Most leeward and plateau cloud cover here is the result of convective blow-off, while most mid and upper-level cloudiness is determined by synoptic flow. Hot and dry air from the Arabian interior and Rub al Khali keep skies clear east of the highest ridges. With easterly flow aloft, only cirrus or shallow altostratus clouds develop above 15,000 feet (4,573 meters). Sea breezes produce most early morning stratus, stratocumulus, and cumulus, but these are confined to immediate coastal slopes below 6,560 feet (2,000 meters).

Skies are clear in the early morning except for the patchy stratus that develops along immediate coastlines and pushes inland during the land/sea breeze transition between 0600 and 0800 LST. Patchy stratus or shallow stratocumulus rarely constitute a ceiling, and both dissipate quickly with heating. Thin stratus and shallow ground fog may develop in remote canyons and rugged valleys in the southern and western Yemen Mountains. These thin clouds appear along the inversion layer with strong radiation cooling in the evening. Thin cloud cover may persist for several hours if winds remain calm overnight and into mid-morning above 10,000 feet (3,050 meters). Most ground fog and stratus develop at or above 300 feet (91 meters) AGL, but are seldom more than 100 feet (30 meters) thick.

YEMEN HIGHLANDS SOUTHWEST MONSOON

June-September

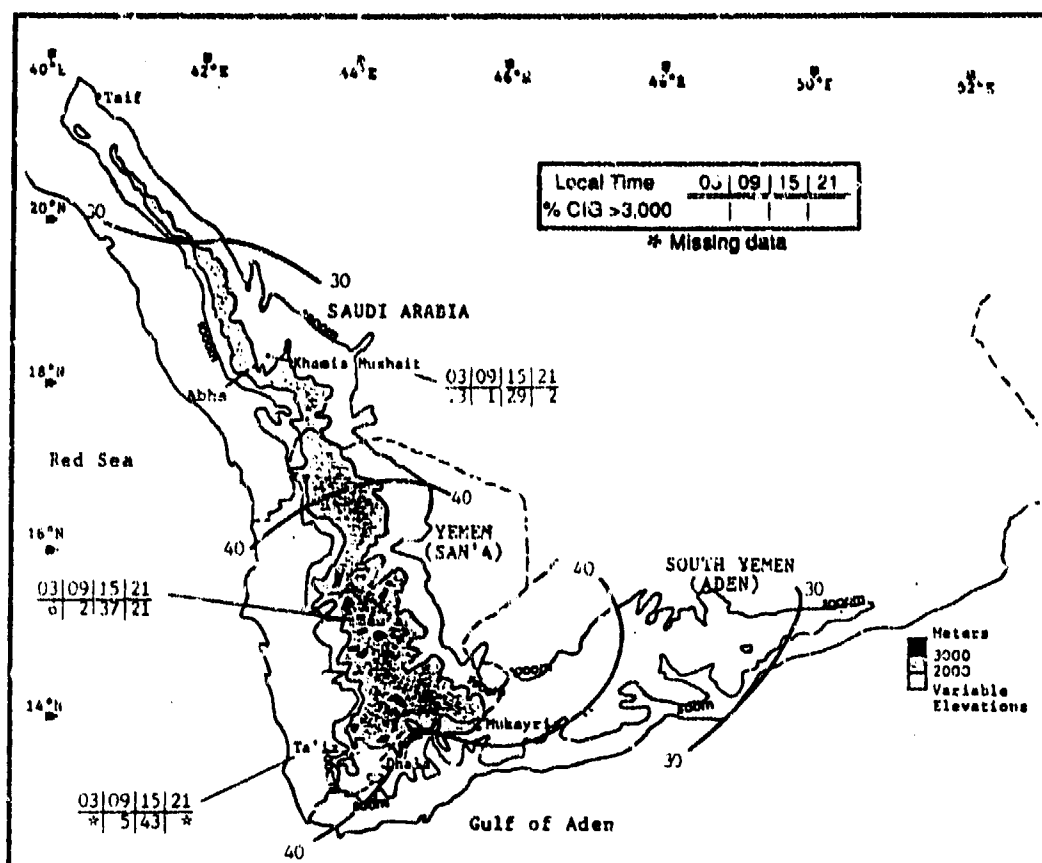


Figure 6-2. Mean Southwest Monsoon Cloudiness (Isolines) and Frequencies of Ceilings Below 3,000 Feet (915 meters), Yemen Highlands. Isopleths are in 10% intervals. The numerical data is derived by calculating the grand mean of National Intelligence Summary (NIS) mean cloudiness data for specific sites between June and September.

Shallow cumulus develops over ridges by late morning or early afternoon during maximum sea breeze penetration into the interior. Rain seldom falls on the leesides of mountains unless cold pockets of air aloft or a northeasterly surface circulation over the interior triggers more convergence along the highest ridge crests. At Khamis Mushait, prevailing winds are northeasterly, but there is enough extensive orographic cumulus for this leeward location to have mid-afternoon cloud cover. Typically, northeasterly flow is too dry for orographic cloud cover to form on the Asir or Yemen Mountains' eastern slopes. Most cumulus dissipates by midnight, with some isolated altostratus or altocumulus drifting eastward in the residual moisture provided by the sea breeze. Typical fair weather cumulus may form a broken cloud line along the western Asir and Yemen Mountains between 7,000 and 9,000 feet (2,134 and 2,744 meters) MSL, but tops rarely exceed 12,000 feet (3,658 meters). This fair weather cumulus rarely continues eastward

along the leeward slopes. When northeasterly flow from the Rub al Khali is weak, a continuous cloud line extends from Ta'iz to Abha. Much of the diurnal cumulus is observed at 2,000-3,000 feet (610-915 meters) AGL on the western slopes of these mountain ranges; tops may exceed 15,000 feet (4,573 meters). With a strong surge in the Southwest Monsoon, convergence over the peaks between Aden and San'a may produce severe thunderstorms with tops to 50,000 feet (15.2 km). Mid-level cloud cover increases temporarily in early June whenever a rare southward surge of the Polar Jet stream brings a weak cold front into the central Red Sea.

Low ceilings are common with sea breeze cumulus or when a high-pressure ridge creates northeasterly circulation with some Mediterranean moisture. Low ceiling frequencies are highest between 1500 and 0000 LST. At San'a, the frequency of ceilings between 1,000 and 3,000 feet (305-915 meters) reaches 54% in August

YEMEN HIGHLANDS SOUTHWEST MONSOON

June-September

between 1600 and 0000 LST. Most ceilings between 2,500-3,000 feet (700-915 meters) at Khamis Mushait and Ta'iz occur when prevailing wind direction is southerly or westerly. On rare occasions, low ceilings occur with northerly flow at Khamis Mushait.

VISIBILITY. Visibilities during the Southwest Monsoon are greater than 3 miles more than 90% of the time, but dust and haze often restrict visibility to 4-6 miles (60% of the time in July) with strong afternoon winds. These winds are generally caused by mountain and valley breezes, but sea breezes also stir up large amounts of dust and sand. At 1500 LST, Ta'iz visibilities are 4-6 miles 82% of the time.

Visibilities below 3 miles (Figure 6-3) occur less than 7% of the time and are rarely below a mile. Duststorms

and sandstorms that lower visibilities to less than a mile along coastlines may become so widespread that locations at elevations between 3,280 and 5,000 feet (1,000 and 1,524 meters) MSL are also affected.

"Dju Farah" is the local name for a duststorm in the Yemen Highlands caused by localized differential surface heating. Although "Dju Farah" may occur at other times, they are most severe during early August, in the afternoon.

Fog is extremely rare during the Southwest Monsoon, but it may occur on 1-2 mornings a season with calm early morning conditions along the southwest facing slopes south of Ta'iz. Visibility in fog is normally less than 2 1/2 miles.

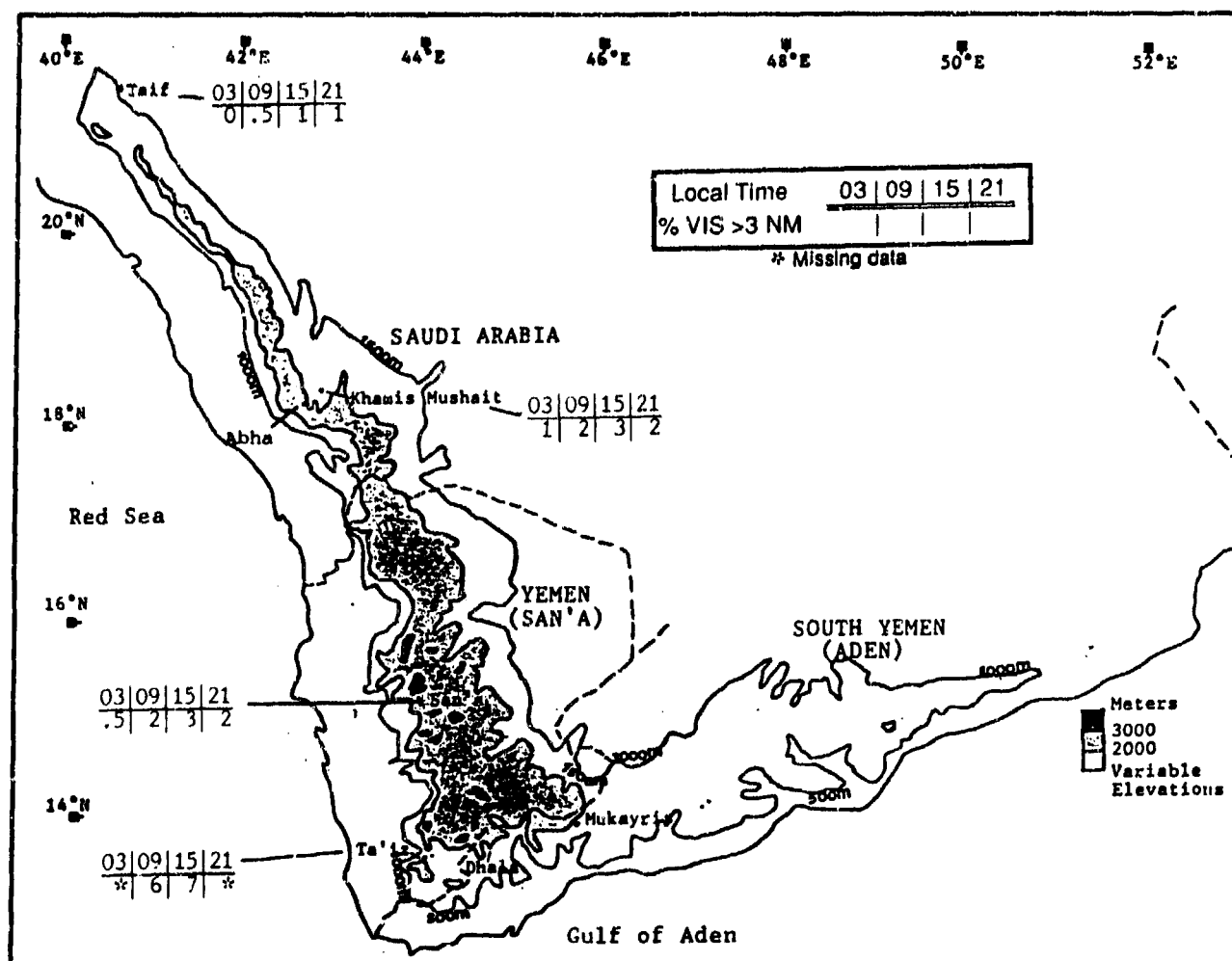


Figure 6-3. Southwest Monsoon Frequencies of Visibilities Below 3 Miles, Yemen Highlands.

YEMEN HIGHLANDS SOUTHWEST MONSOON

June-September

WINDS. Figure 6-4 shows mean monthly surface wind speeds and prevailing directions for three stations in the Yemen Highlands. Note that while the prevailing direction at Khamis Mushait (Kh's Mushait) and San'a is northeasterly, it is westerly at Ta'iz. The surface northeasterlies originate in the northern or northwest quadrant of the Saudi Arabian Heat Low discussed in Chapter 2. The westerlies near Ta'iz are sea breezes at

9-10 knots. Northeasterly flow is also present along the northern Hadhramaut Plateau. Mid- and upper-level winds (Figures 6-5a-c) during the Southwest Monsoon do not necessarily reflect surface conditions. Mean mid-level speeds show little variation during the Southwest Monsoon, averaging 8-11 knots at 10,000 feet (3,050 meters); 12-18 knots at 15,000 feet (4,573 meters); and 10-14 knots at 30,000 feet (9,146 meters).

NNE-ENE
N-NE
WSW-W

	JUN	JUL	AUG	SEP
Kh's Mushait	5.80	5.90	5.60	6.50
San'a	7.50	8.10	7.20	7.30
Ta'iz	9.50	8.90	10.30	9.80

Figure 6-4. Mean Southwest Monsoon Wind Speed (kts) and Prevailing Direction, Yemen Highlands.

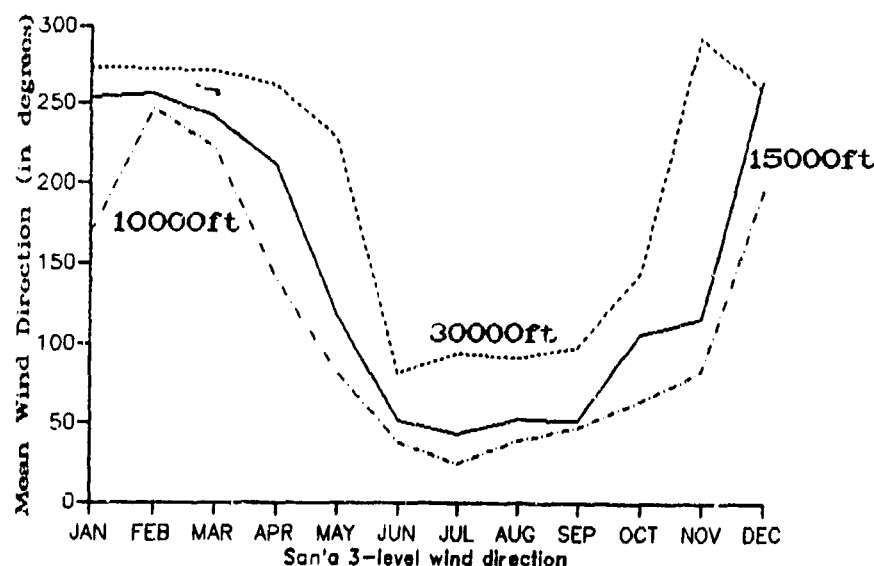


Figure 6-5a. Mean Annual Wind Direction, San'a, YD. Prevailing wind direction at San'a is northeasterly at 10,000 and 15,000 feet (3,050 and 4,573 meters), but easterly at 30,000 feet (9,146 meters).

**YEMEN HIGHLANDS
SOUTHWEST MONSOON**

June-September

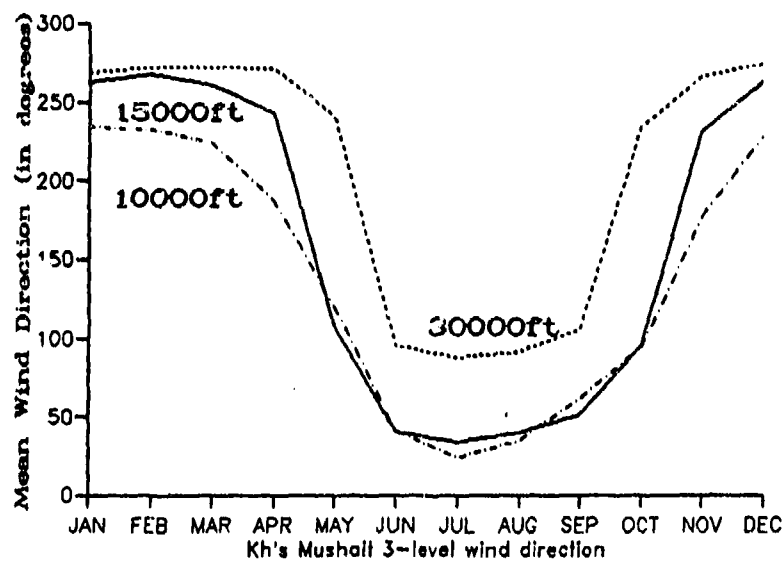


Figure 6-5b. Mean Annual Wind Direction, Khamis Mushait, SD. Winds over Khamis Mushait are similar to those at San'a.

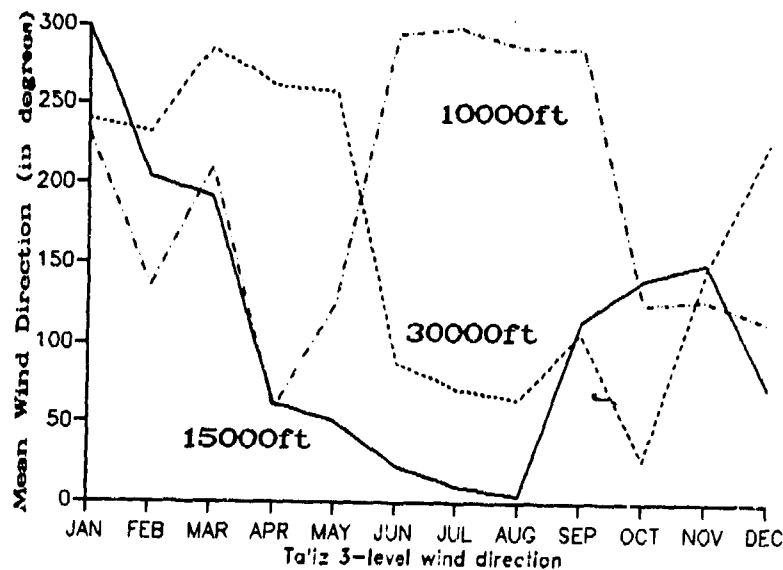


Figure 6-5c. Mean Annual Wind Direction, Ta'iz, YD. At Ta'iz, mid-level winds are westerly. In September, the 15,000-foot (4,573-meter) winds are east-southeasterly, rather than northeasterly as at San'a and Khamis Mushait.

YEMEN HIGHLANDS SOUTHWEST MONSOON

June-September

PRECIPITATION. The heaviest Southwest Monsoon precipitation is confined to the western Asir and western/southern Yemen Mountains, as shown in Figure 6-6). Moist sea breezes fuel orographic convection every day in these areas. Moderate rain showers lasting for 1-2 hours in late afternoon seldom occur north of 17° N.

Only an isolated section of the western Asir Mountains (west of Abha) gets more than 4 inches (102 mm) of rain during the Southwest Monsoon. Highest seasonal rainfall (more than 9 inches/229 mm) is along the Yemen Mountains near 44° E and 13° 45' N, 15° 30' N.

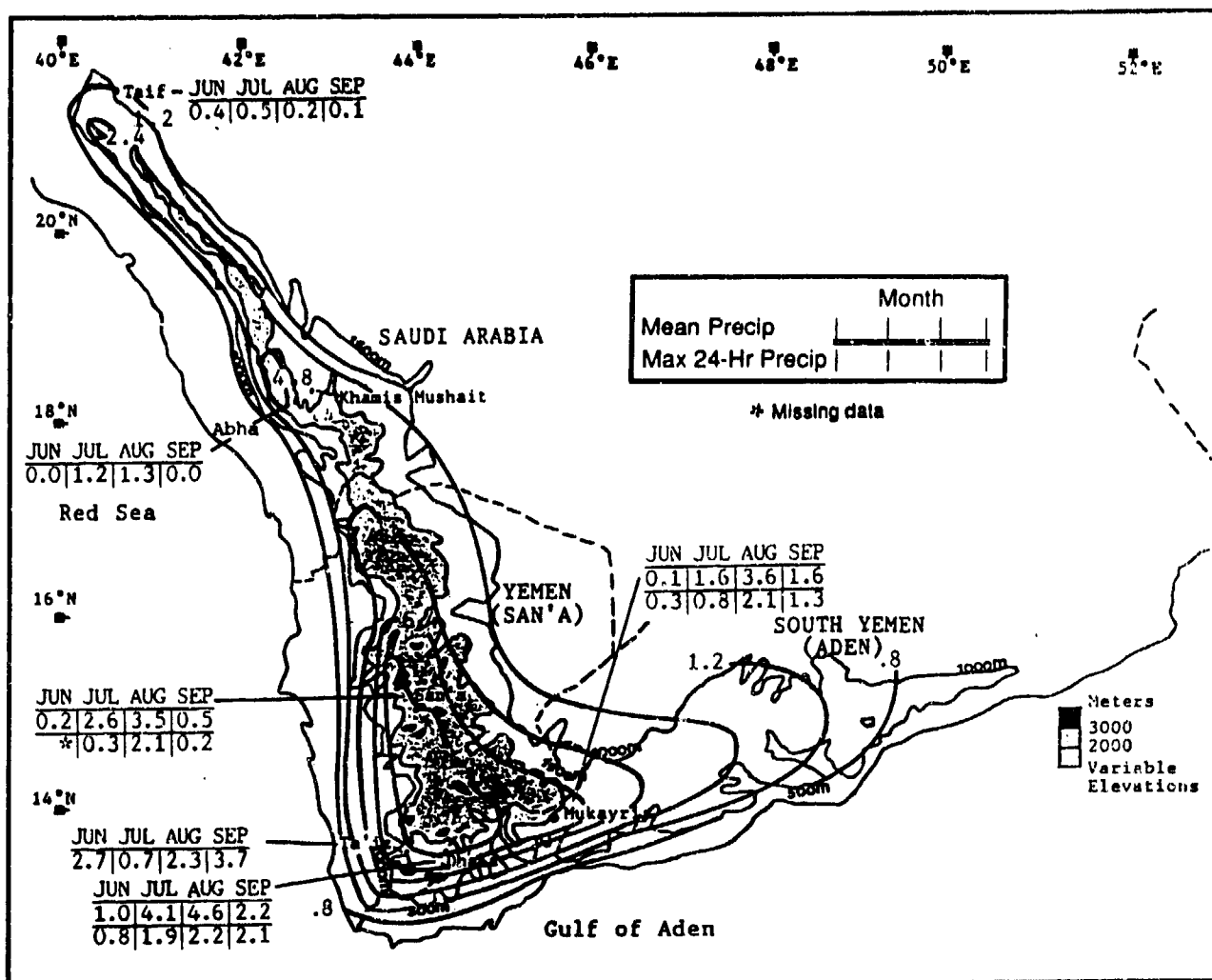


Figure 6-6. Mean Southwest Monsoon Monthly/Maximum 24-Hour Precipitation, Yemen Highlands. Isohyets show mean seasonal rainfall totals (inches).

YEMEN HIGHLANDS SOUTHWEST MONSOON

June-September

TEMPERATURE. The highest temperatures are in June. Mean daily highs (Figure 6-7) range from 75 to 96°F (24-36°C). The record highs in June are 86°F (30°C) at San'a and 104°F (40°C) at Ta'if. The Rub al Khali, in northeastern Yemen, is much hotter; intense surface heating and clear skies can produce temperatures greater than 125°F (52°C). Surface air temperatures may drop by 55°F (30°C) in an hour when a northerly wind

shift occurs before mid-afternoon rains along the Yemen Mountains' leeward slopes. Mean daily lows range from 52 to 77°F (11-25°C). September is coolest, with record lows of 39°F (4°C) at San'a and 57°F (14°C) at Ta'if, both above 5,000 feet (1,524 meters). Although Ta'iz is only at 4,629 feet (1,411 meters), the persistent sea breeze and a marine climate resulted in its record low of 65°F (18°C).

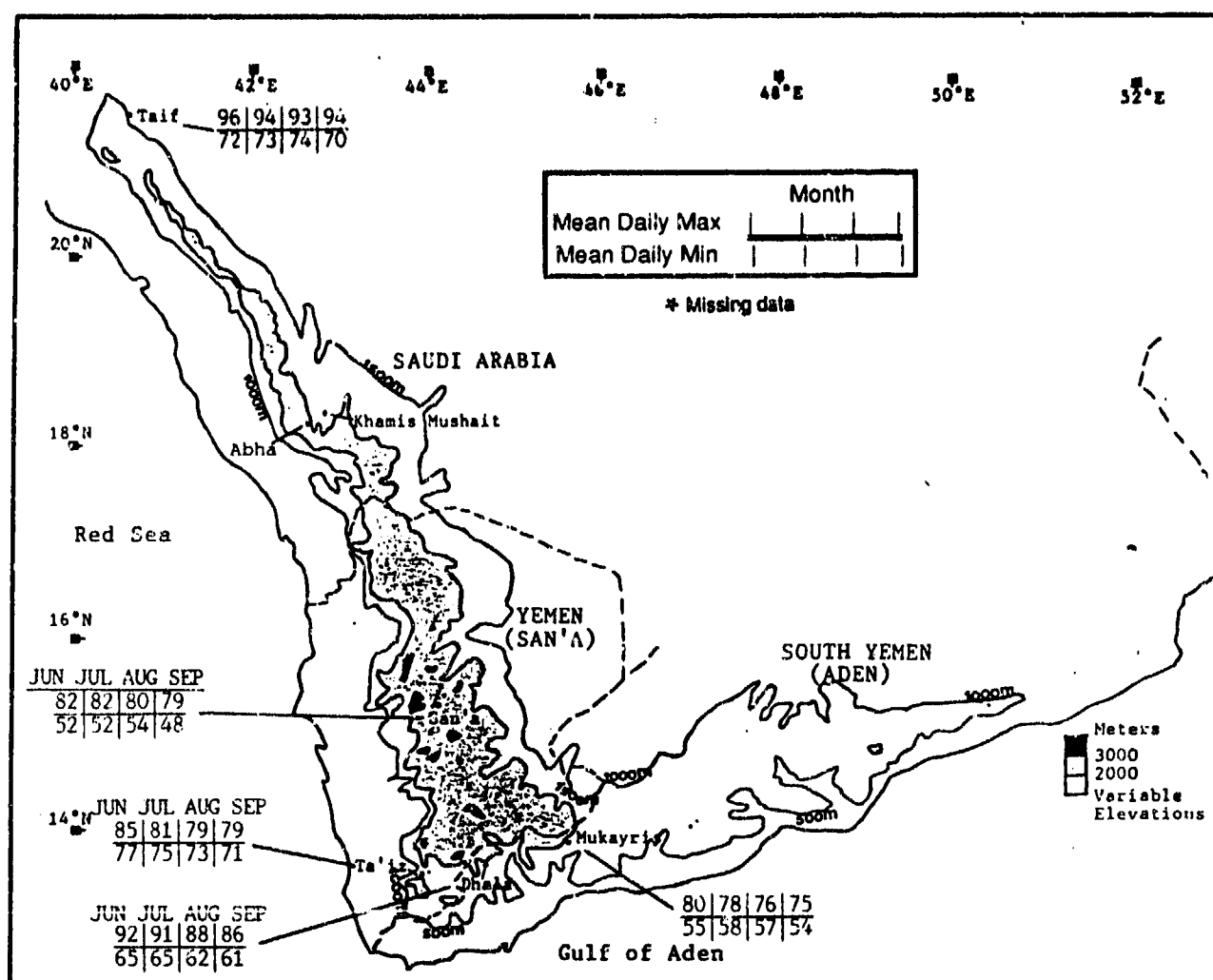


Figure 6-7. Mean Southwest Monsoon Daily Maximum/Minimum Temperature (°F), Yemen Highlands.

YEMEN HIGHLANDS

Southwest-to-Northeast Monsoon Transition

October-November

GENERAL WEATHER. The two most important weather-makers during the transition are the surface Monsoon Trough's southward migration and changes in surface circulation over the Rub al Khali. The southerly retreat of the Monsoon Trough reduces southerly inflow into the Saudi Arabian Heat Low by mid-October. As a result, the sea breeze cannot push inland with enough force to induce massive orographic uplift along the southern Yemen Highlands.

The Saudi Arabian Heat Low's disappearance decreases the amount of hot northeasterly flow into the eastern Yemen Highlands and northern Hadhramaut Plateau. In fact, the Heat Low is replaced in November by the Saudi Arabian High, which induces weak easterly

outflow into the Gulf of Aden and produces fair weather and lower temperatures. The Saudi Arabian High strengthens in November and increases subsidence at the middle levels. Subsidence further reduces the effect of orographic uplift on sea breeze moisture above 6,000 feet (1,829 meters) MSL on the Hadhramaut Plateau and in the southeastern Yemen Highlands.

SKY COVER. Mean cloudiness during the transition is less than 20% except for a small portion of the extreme western Yemen Mountains between 14 and 16° N. Mean cloudiness (shallow fair-weather cumulus and cirrus) on the eastern slopes of the Yemen Highlands and the northern Hadhramaut Plateau is 15% or less--see Figure 6-8.

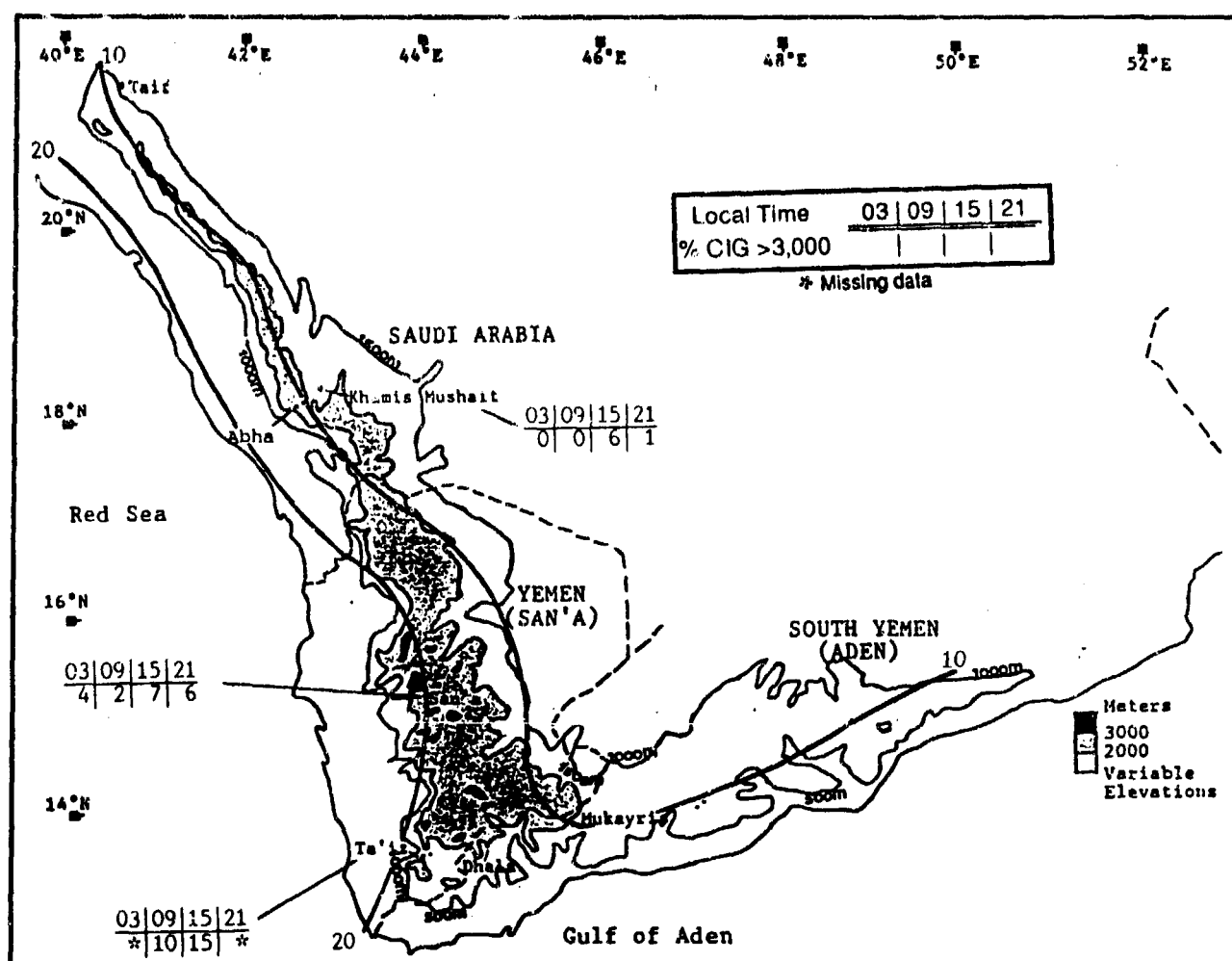


Figure 6-8. Mean SW-NE Monsoon Transition Cloudiness (Isolines) and Frequencies of Ceilings Below 3,000 Feet (915 meters), Yemen Highlands. Isopleths are in 10% intervals. The numerical data is derived by calculating the grand mean from National Intelligence Summary (NIS) mean cloudiness data for specific sites in October and November.

YEMEN HIGHLANDS

Southwest-to-Northeast Monsoon Transition

October-November

Persistent high surface pressure over the Saudi Arabian peninsula produces weak easterly low-level flow into the eastern Yemen Highlands and northern Hadhramaut Plateau by early November. Light sea breezes may generate shallow convective cumulus cloud cover along the Yemen Highlands' western and southwestern slopes. Stratocumulus with embedded cumulonimbus occurs with the divergence that precedes upper-level troughs.

Westerly or southwesterly flow signals a weak frontal passage. Such shifts increase altocumulus and cirrus cloud cover, but may also produce stratocumulus in the valleys and plateaus east of the Asir and Yemen Mountains. Although only cirrus is present with weaker troughs, well-organized systems produce isolated altocumulus, altostratus and stratocumulus. Bases average 5,000-7,000 feet (1,524-2,134 meters) AGL, and tops reach to 15,000 feet (6,097 meters) MSL.

Along the southern Yemen Mountains and the southern Hadhramaut Plateau, a southeast wind increases orographic uplift and the amount of low cloud. Ceilings of 3,500 feet (1,067 meters) are common at Khamis Mushait; tops reach 10,000 feet (3,050 meters) MSL. Most low ceilings are in diurnal cumulus resulting from orographic lift, but they occur during late evening, too. Evening cloudiness is the result of local mountain and valley wind convergence on the western slopes of the Yemen and Asir Mountains. Along eastern slopes, evening air is too dry for local mountain and valley wind convergence to produce low cloud cover.

VISIBILITY. Visibilities are excellent. They are 6 miles or more 90% of the time, and frequencies below 3 miles are lowest of the year (Figure 6-9). Best chance for visibility below 6 miles is 0900-1200 LST. At Ta'iz and Khamis Mushait, 3- to 6-mile visibility frequency reaches a high of 8% in November. Visibilities below 2 miles, although extremely rare, are usually reported with ground fog.

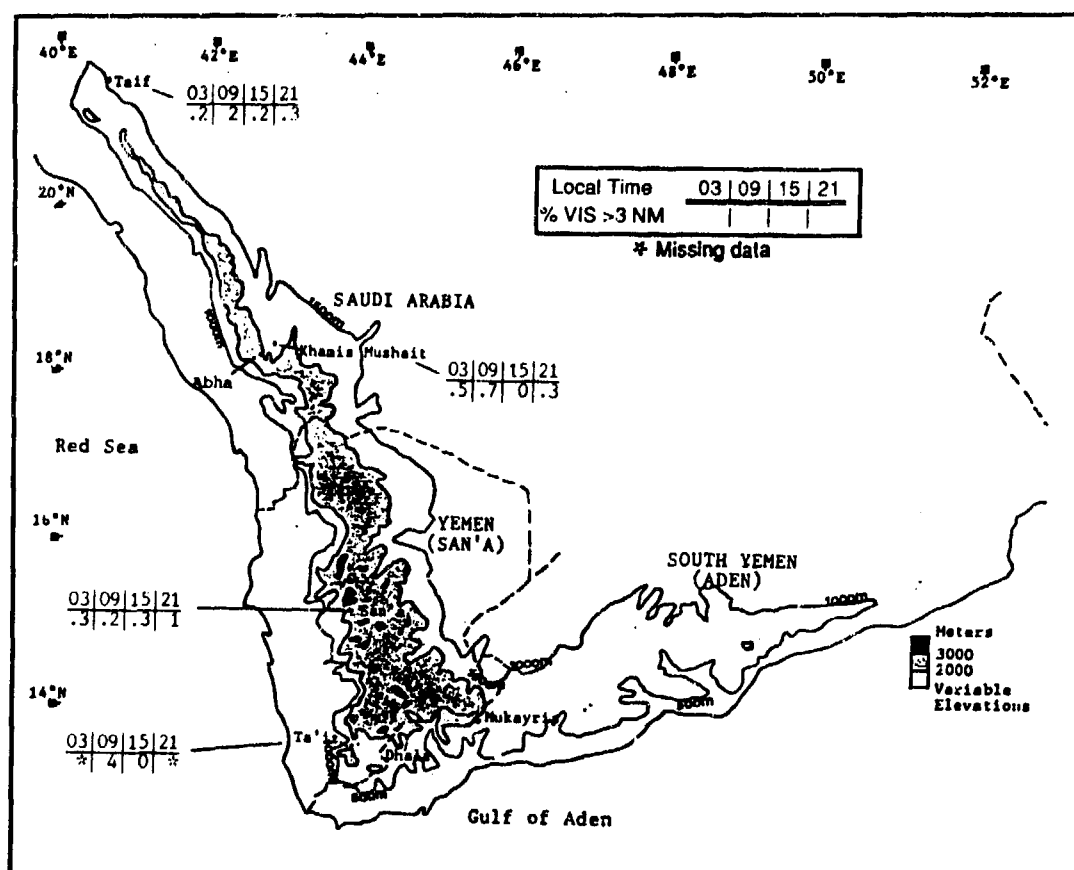


Figure 6-9. SW-NE Monsoon Transition Frequencies of Visibilities Below 3 Miles, Yemen Highlands.

YEMEN HIGHLANDS **Southwest-to-Northeast Monsoon Transition**

October-November

WINDS. In October, the surface Monsoon Trough produces light and variable winds along its axis, but by November, weak easterly synoptic flow develops at the lower levels. Figure 6-10 gives mean surface wind speeds and prevailing directions for Khamis Mushait (Kh's Mushait), San'a, and Ta'iz. Winds are weaker over the interior Yemen Highlands because the sea

breeze cannot reach that far unless reinforced by synoptic flow; i.e., southeasterlies in the Gulf of Aden or westerlies in the Red Sea. Figures 6-11a and b give mean annual mid- and upper-level wind directions at Khamis Mushait (representative of the north) and at San'a (representative of the south).

		OCT	NOV
E-S NE SE	Kh's Mushait	5.20	5.50
	San'a	5.00	5.10
	Ta'iz	8.90	9.00

Figure 6-10. Mean SW-NE Monsoon Transition Wind Speed (kts) and Prevailing Direction, Yemen Highlands.

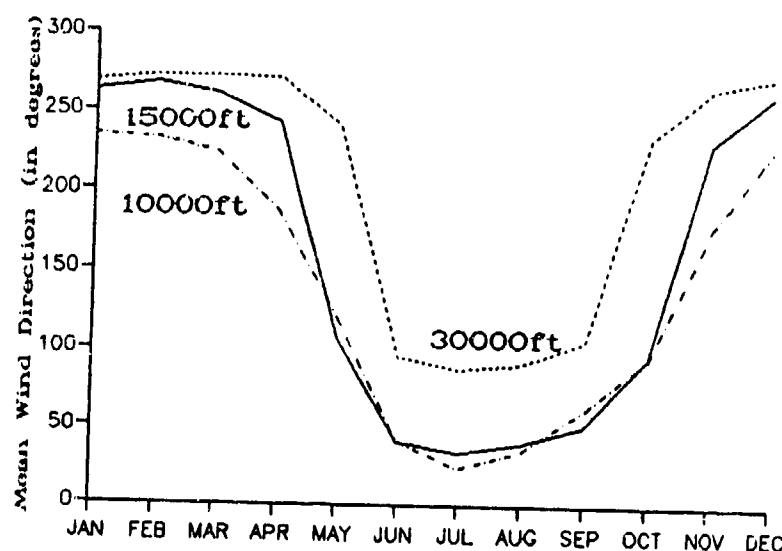


Figure 6-11a. Mean Annual Wind Direction, Khamis Mushait, SD. Upper-level (30,000-foot/9.1 km MSL) westerlies increase from 14 knots in October to 25 knots in November. At mid- and upper-levels, winds shift from northeasterly to west-southwesterly. The upper-level shift is caused by the southward movement of the Subtropical Ridge.

YEMEN HIGHLANDS

Southwest-to-Northeast Monsoon Transition

October-November

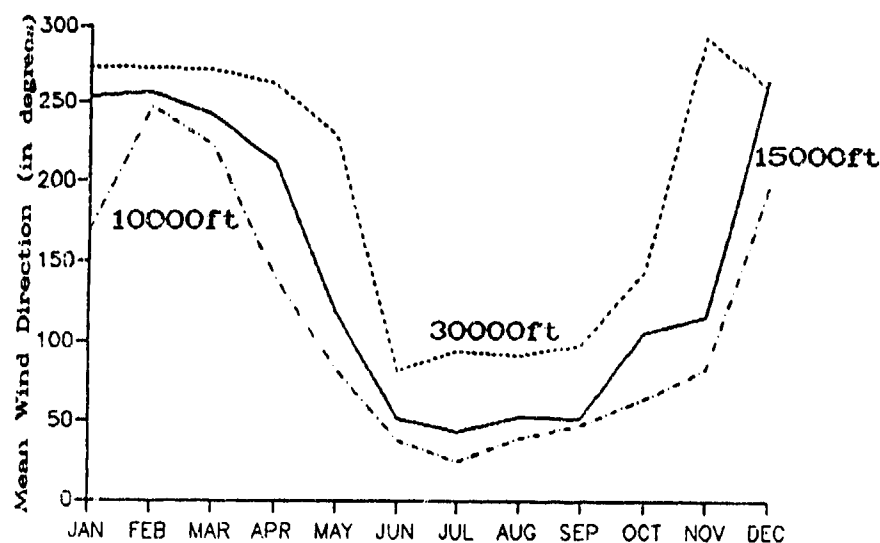


Figure 6-11b. Mean Annual Wind Direction, San'a, YD. Winds remain easterly (050-120°) in the south, but average only 12-16 knots.

PRECIPITATION. The transition from the Southwest to the Northeast Monsoon is the driest period of the year, thanks to weak convergence between the surface Monsoon Trough and the sea breeze. Mean monthly precipitation averages 1.2 inches (30 mm) or less; most locations get less than 0.5 inches (13 mm). The weak sea breeze doesn't regularly penetrate to the Yemen Highlands; orographic lift, diurnal convection, and rainfall are minimized in October and November. On the rare occasion that sea breeze moisture does generate orographic lift, moderate to heavy rainshowers can occur.

The areas of heaviest rainfall are shown (in Figure 6-12) by the closed (2.4 inch/61 mm) isohyets in the western Yemen Mountains. Upper-level troughs may trigger additional rainfall in November, but these disturbances only occur on 1-2 days a season. Heavy dew is common on clear, cold mornings. Expect snow above 10,000 feet (3,050 meters) by the end of November. Snow depth rarely exceeds 6 inches (152 mm) unless an unusually high number of upper-level troughs (2-4 a month) penetrate the Yemen Highlands during November.

YEMEN HIGHLANDS

Southwest-to-Northeast Monsoon Transition

October-November

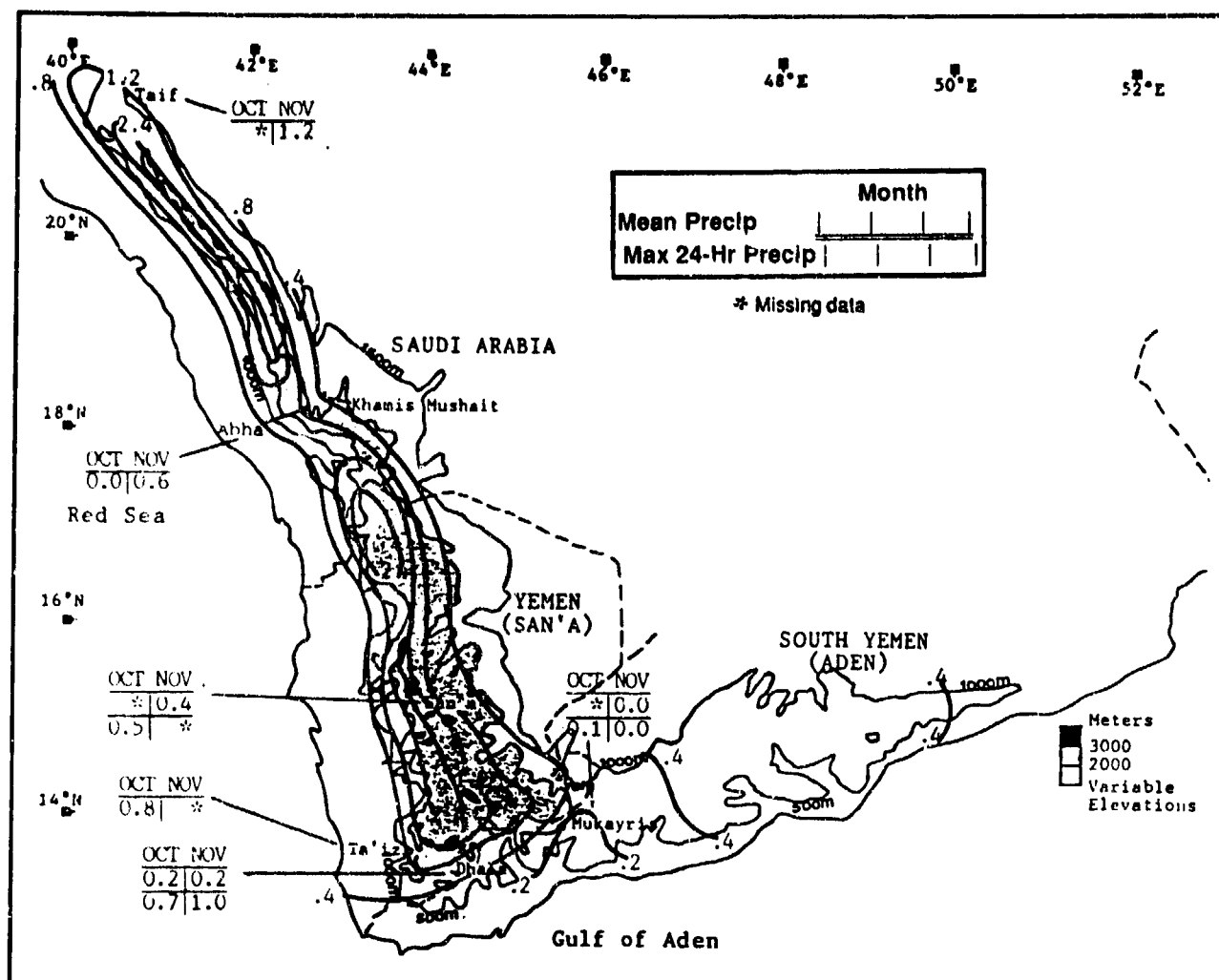


Figure 6-12. Mean SW-NE Monsoon Transition Monthly/Maximum 24-Hour Precipitation, Yemen Highlands. Isohyets represent mean seasonal rainfall totals (inches). Maximum 24-hour precipitation values were available for San'a, Mukayris, and Ta'iz only.

TEMPERATURE. Transition temperatures shown in Figure 6-13 depend on elevation and topography. Mean highs range from 68 to 87°F (20-31°C). Record highs include 78°F (26°C) at Mukayris and 93°F (34°C) at Ta'if, both in October. Mean daily lows range from 38 to 58°F (3-14°C), but locations near the marine

boundary layer (such as Ta'iz) are greatly modified (69°F/21°C) by the sea breeze. Record lows at San'a and Ta'if were 27°F (-3°C) and 45°F (7°C), both in November. The record low at Ta'if was 63°F (17°C), set in October.

YEMEN HIGHLANDS

Southwest-to-Northeast Monsoon Transition

October-November

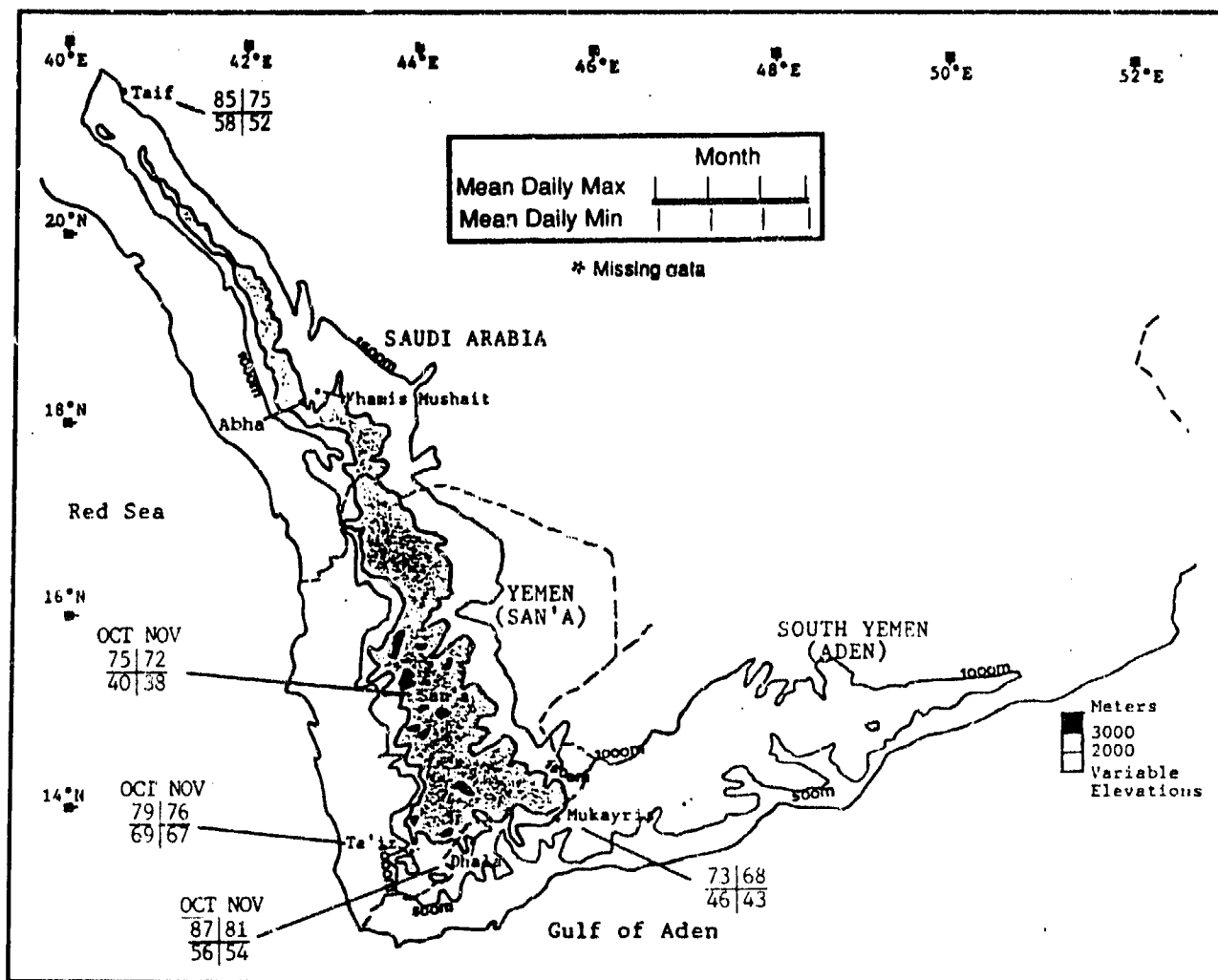


Figure 6-13. Mean SW-NE Monsoon Transition Daily Maximum/Minimum Temperatures (°F), Yemen Highlands.

YEMEN HIGHLANDS NORTHEAST MONSOON

December-March

GENERAL WEATHER. Periodic cyclonic activity, migratory upper-level troughs, and low-level convergence along the Red Sea Convergence Zone (RSCZ--see Chapter 2) produce most of the Northeast Monsoon's significant weather. Every 5 to 10 days, a surface cold front moves southeast or eastward across the Asir and northern Yemen Mountains. Light rain, increased mid- and upper-level cloud cover and southwesterly-to-southerly surface flow precedes the front.

Northeast Monsoon flow into the Straits of Bab al Mandab converges with weak northwesterly outflow from the Saharan High along the southern Red Sea. Weak low-level convergence combines with sea breezes along the western Yemen Highlands between 16 and 21 N to produce the RSCZ. Isolated rainshowers and occasional thundershowers are common along the RSCZ's eastern edge.

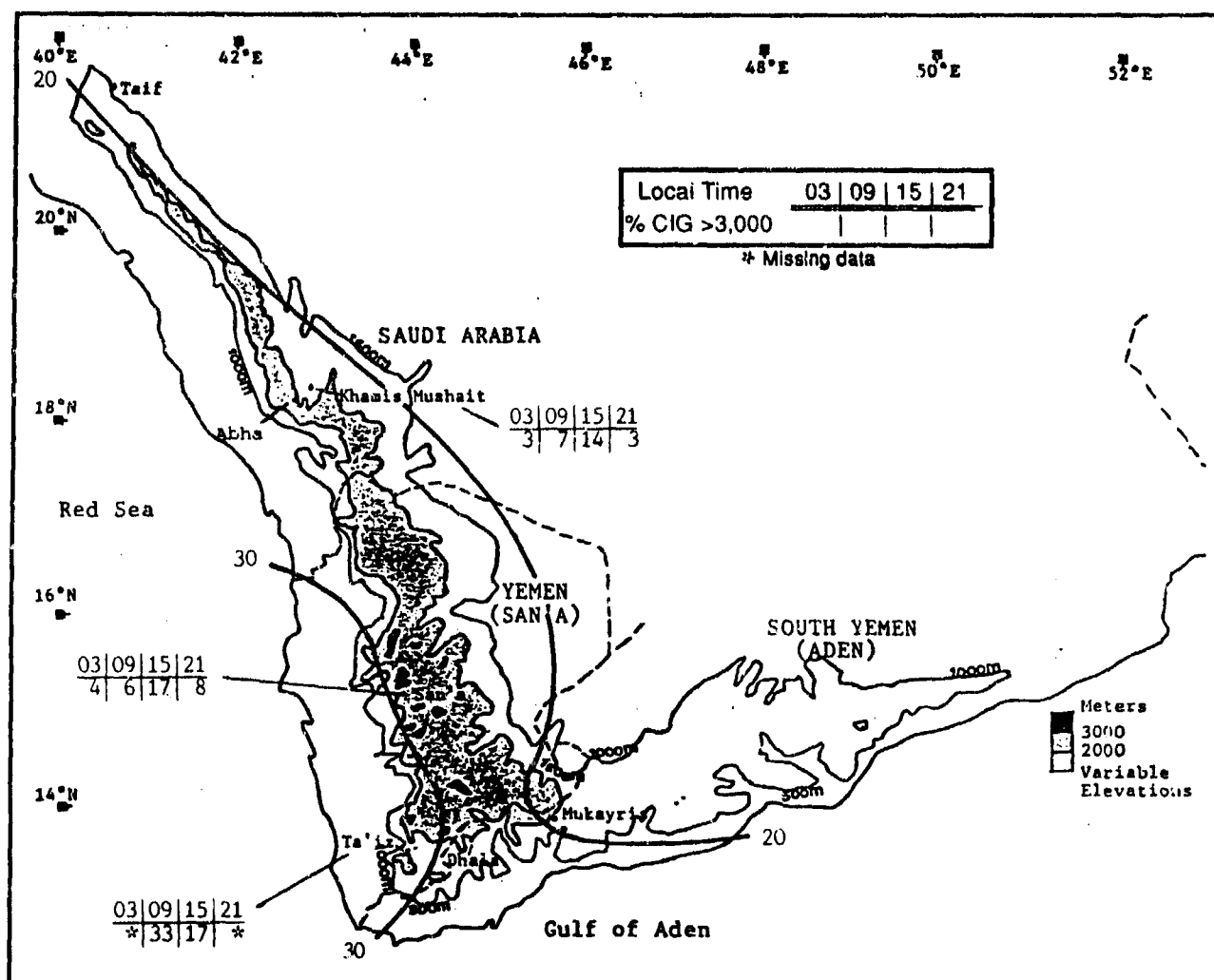


Figure 6-14. Mean Northeast Monsoon Cloudiness (Isolines) and Frequencies of Ceilings Below 3,000 Feet (915 meters), Yemen Highlands. Isopleths are in 10% intervals. Numerical data was derived by calculating the grand mean of National Intelligence Summary (NIS) mean cloudiness data for specific sites from December to March.

SKY COVER. Northeast Monsoon mean cloudiness (shown above in Figure 6-14) averages 20-30 percent along the Yemen and Asir Mountains, and less than 20

percent over the Hadhramaut Plateau, where northeasterly flow provides little low-level moisture. Although the plateau generally sees less cloudiness (now

YEMEN HIGHLANDS NORTHEAST MONSOON

December-March

mostly cirrus and cirrostratus), northeasterly flow induces some orographic fair-weather cumulus along the southeastern Yemen Mountains between Mukayris and Dhala.

Along the Western Yemen and Asir Mountains, cyclonic activity, the Red Sea Convergence Zone (RSCZ) and persistent westerly synoptic flow produce more orographic lift. The uplift produces cumulus as well as mid- and upper-level cloudiness. Bases are 5,000-7,000 feet (1,524-2,134 meters) AGL, and tops reach 10,000 feet (3,050 meters) MSL.

Ceilings below 3,000 feet (915 meters) generally occur with south or southwest winds. Southeast winds only produce low clouds (cumulus and stratocumulus) along the southern Yemen Mountains in mid-afternoon, and over the southwest Hadhramaut Plateau in early and mid-morning. Ceilings of 1,000 and 1,500 feet (305-453 meters) are possible along the western and southern Yemen Mountains. Ceilings at or below 1,000 feet (305 meters) are most common between January and March, from 0600 to 0900 LST. Ceilings from 1,000 to 3,000 feet (305-to 915-meter) are most common in the western and southern Yemen Highlands between 1600 and 2100

LST. Clear skies are common with undisturbed weather during the Northeast Monsoon. However, infrequent mid-latitude cold fronts (Cyprus Lows) pass the area on 2-3 days a month and increase mid- and upper-level cloud cover for 6 to 18 hours. Weak frontal passages produce scattered to broken ceilings. Skies include a mixture of cumulus, stratocumulus, and altocumulus over the Asirs, while extensive cumulus forms along the western Yemen Mountains above 10,000 feet (3,050 meters) MSL.

Strong cold fronts occasionally penetrate the northern half of the region to 18° N. Above the surface cold front, the Polar Jet (PJS) and Subtropical Jet (STJ) may merge and "share energy" over the northern Asirs, as shown in Figure 6-15. Moist low-level southwesterly flow develops along the surface warm front. Common warm front sky conditions include multilayered clouds with isolated cumulonimbus embedded in low stratus decks. Isolated cumulus bases run from 6,000 to 8,000 feet (1,838 to 2,439 meters) AGL, with tops 10,000-15,000 feet (3,050-4,573 meters) MSL. Stratus deck bases run from 2,000 to 4,000 feet (610-1,220 meters) MSL. Surface cold fronts moving over the Red Sea have isolated cumulus and/or cumulonimbus immediately ahead, but little or no cloud behind.

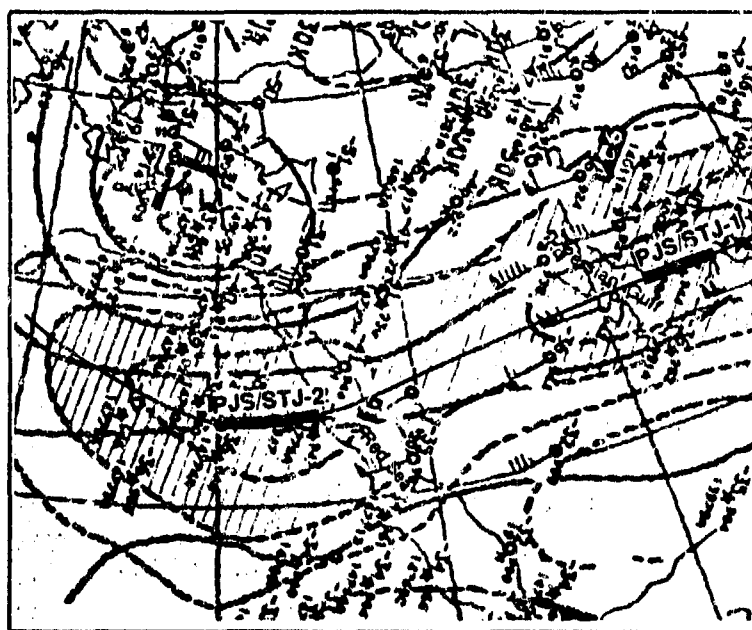


Figure 6-15. Upper-Level (300-mb) Flow Supporting an Intense Frontal Passage into the Northern Yemen Highlands. PJS = Polar Jet Stream; STJ = Subtropical Jet Stream. The map shows two areas of jet stream interaction, but PJS/STJ-2 is important to this discussion.

YEMEN HIGHLANDS NORTHEAST MONSOON

December-March

When the Subtropical Jet is the only feature present in the flow pattern, dense cirrus covers the region. Scattered altostratus with bases between 15,000 and 18,000 feet (4,573-5,487 meters) AGL is possible.

Between 16° and 21° N, the Red Sea Convergence Zone (RSCZ--see Chapter 2) produces weak low-level convergence and cloud cover along its axis. At the eastern edge of the RSCZ axis, convective cells concentrate development along a 10-30 NM section of the western Asir and northern Yemen Mountains in mid-morning. The precise location for isolated cumulus development varies from day to day and month to month. If an upper-level trough lies to the west of the RSCZ, cumulus with tops to 20,000 feet (6,097 meters) MSL may form parallel to a large (200 NM north to south) portion of the western Yemen Highlands; they may spill 10-20 NM east of the highest ridge lines by late afternoon. When they do, leeward slopes see scattered

altocumulus with ceilings at or above 5,000 feet (1,524 meters) AGL. Cloud cover on windward slopes remains for up to 6 hours after trough passage; the line of cumulus and cumulonimbus with tops to 18,000-20,000 feet (5,487-6,097 meters) MSL and bases at or above 3,000 feet (915 meters) AGL dump heavy rainfall on the western Yemen Highlands.

VISIBILITY. Dust and haze are the primary visibility restrictions. Afternoon visibilities are between 3 and 6 miles 36 percent of the time at Ta'iz (January) and San'a (March). Visibilities below 3 miles are rare; frequencies at Ta'iz are 5% at 0900 LST. Morning haze is the most frequently observed obstruction to vision at Ta'iz. Most inland and high-altitude locations see a few dust- or haze-related low visibilities, but the mean frequency is low. Lowest visibilities occur with strong southwesterly flow immediately ahead of a surface cold front.

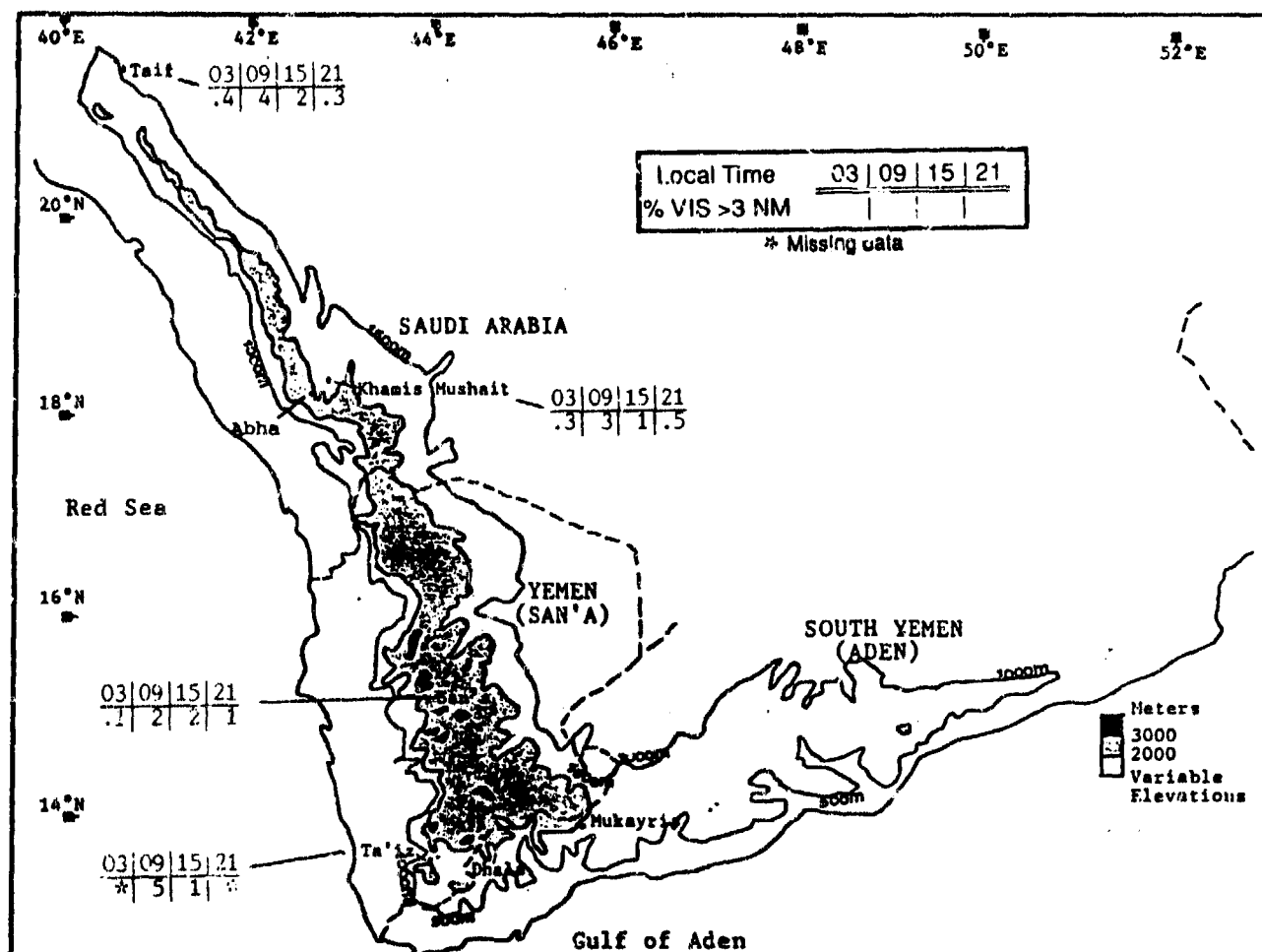


Figure 6-16. Northeast Monsoon Frequencies of Visibilities Below 3 Miles, Yemen Highlands.

YEMEN HIGHLANDS NORTHEAST MONSOON

December-March

WINDS. Surface winds vary from northwest to southeast as two-large scale surface circulations--Northeast Monsoon flow and northwesterly Saharan High outflow--converge in the southern Red Sea. Yemen Highlands topography limits this convergence to the Red Sea area between the surface and 5,000 feet (1,524 meters) MSL.

Figure 6-17 gives mean surface wind speeds and prevailing directions at Kh's Mushait (Khamis Mushait), San'a, and Ta'iz. Winds are southeasterly in the western Yemen and Asir Mountains below 5,000 feet (1,524 meters) MSL and south of the RSCZ. Northeasterly low-level flow deflects to the right (to southerly/southeasterly) upon entering the Straits of Bab al Mandab and southern Red Sea. Wind speeds in the Straits and foothills of the southeastern Yemen Highlands (Ta'iz) average 15-20 knots over water and 10-15 knots in the foothills.

As Northeast Monsoon surface flow enters the Straits from the south, northwesterly-to-northerly flow enters the Red Sea from the Sahara. The Saharan High (see Chapter 2) produces this northerly surface wind component. Northwesterlies are weak (3-5 knots) in the central and southern Red Sea during undisturbed weather, but surface flow reinforces the sea breeze along the western Yemen Mountains. Resultant synoptic wind direction (Saharan High/sea breeze flow) along the extreme northern Yemen Mountains and the Asirs is southwesterly, although surface wind direction along the extreme eastern edge of the RSCZ may be variable.

When cyclonic activity enters the Red Sea, southwesterlies at 8-15 knots precede frontal passage by 6 to 36 hours, depending on the speed of the front. Some move eastward or northeastward quickly (10-20 knots), but others move only at 5-10 knots.

		DEC	JAN	FEB	MAR
S-SW SW-W SE-SSE	Kh's Mushait	6.40	7.70	8.60	8.50
	San'a	6.00	6.00	8.50	6.90
	Ta'iz	10.50	11.50	10.60	13.30

Figure 6-17. Mean Northeast Monsoon Wind Speed (kts) and Prevailing Direction, Yemen Highlands.

Although mid- and upper-level wind directions are less affected by terrain, some southern Yemen Mountain locations are in a transition zone between subtropical African mid-level westerlies and easterly mid-level flow during different months of the season. Mean mid-level flow averages only 9-12 knots regardless of direction. Upper-level flow is westerly because the Subtropical Ridge is south of the region. Mean upper-level flow averages 18-26 knots in the southern Yemen Mountains (at Ta'iz and San'a), but 38-47 knots in the Asirs (at Khamis Mushait).

The mid-level flow transition zone is best illustrated by comparing mean annual wind directions at Ta'iz

(Figure 6-18a) and San'a (Figure 6-18b). At Ta'iz, the mean December direction at 10,000 feet (3,050 meters) is southeasterly; at 15,000 feet (4,573 meters), it's northeasterly. Mean wind direction at 15,000 feet (4,573 meters) reverses in January (300°) and February (205°). In March, both levels are south southwesterly (190-210°). Note that surface wind direction at Ta'iz (elevation 4,629 feet/1,411 meters) is southerly to southeasterly. At San'a (elevation 7,237 feet/2,206 meters), 15,000-foot (4,573 meter) wind direction is west-southwesterly to westerly between December and March, southerly at 10,000 feet (3,050 meters) from December to January, and southwesterly in February and March.

**YEMEN HIGHLANDS
NORTHEAST MONSOON**

December-March

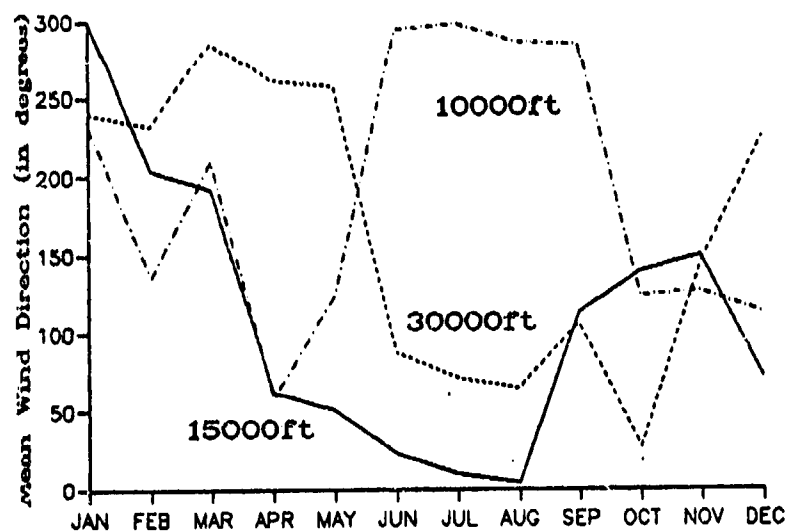


Figure 6-18a. Mean Annual Wind Direction, Ta'iz, YD.

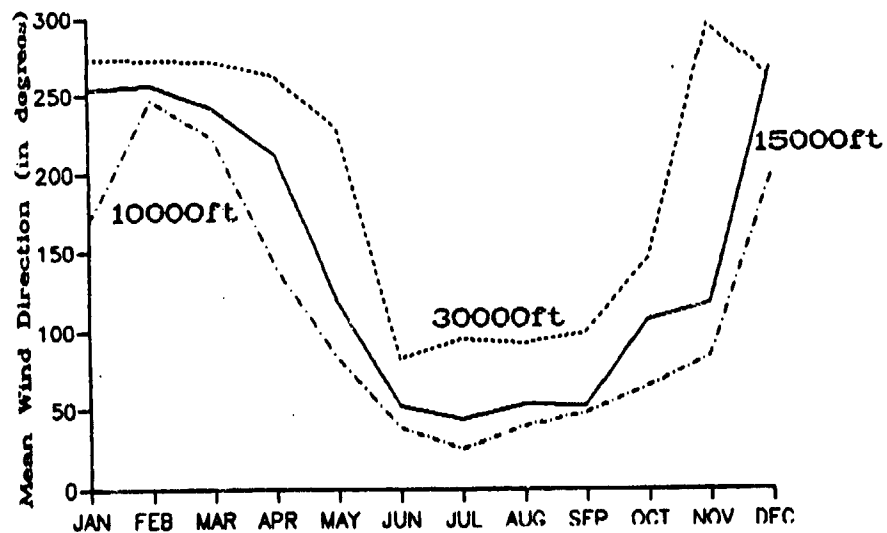


Figure 6-18b. Mean Annual Wind Direction, San'a, YD.

YEMEN HIGHLANDS NORTHEAST MONSOON

December-March

PRECIPITATION. Nearly all Northeast Monsoon season rainfall occurs north of 14° N as cold upper-level troughs pass over the Yemen Highlands. Significant rainfall (0.05 inches/1.3 mm or greater) falls when the Polar Jet descends into the central Red Sea and Saudi Arabian Peninsula. The Polar Jet's southward surge of cold air aloft into the subtropics may merge with the Subtropical Jet. When the two jets interact (or "share energy"), moisture increases at the upper levels. If a low-level cyclonic circulation develops beneath the upper-level trough, southwesterly or southerly winds push warm moist air from the Red Sea deep into the western Asir and Yemen Mountains. The cold air in the upper-level trough helps generate isolated thunderstorm activity and moderate rainfall on the western Yemen

Highlands. Three or four upper-level troughs move into the central Red Sea during each Northeast Monsoon season, but only one or two superimpose themselves over a surface cyclone or cold front. Snow occurs above 10,000 feet (3,050 meters) with most cold upper-level troughs, but accumulations of 6 inches (152 mm) or more are extremely rare. Snow below 6,000 feet (1,829 meters) has not been documented. Figure 6-19 shows mean monthly precipitation across the region. Only Dhala, Mukayris, and Taif get more than 0.2 inches (5 mm) in each month of the Northeast Monsoon. Dhala and Mukayris rainfall is caused by cold upper-level troughs, but by northeasterly low-level Northeast Monsoon flow and orographic lift.

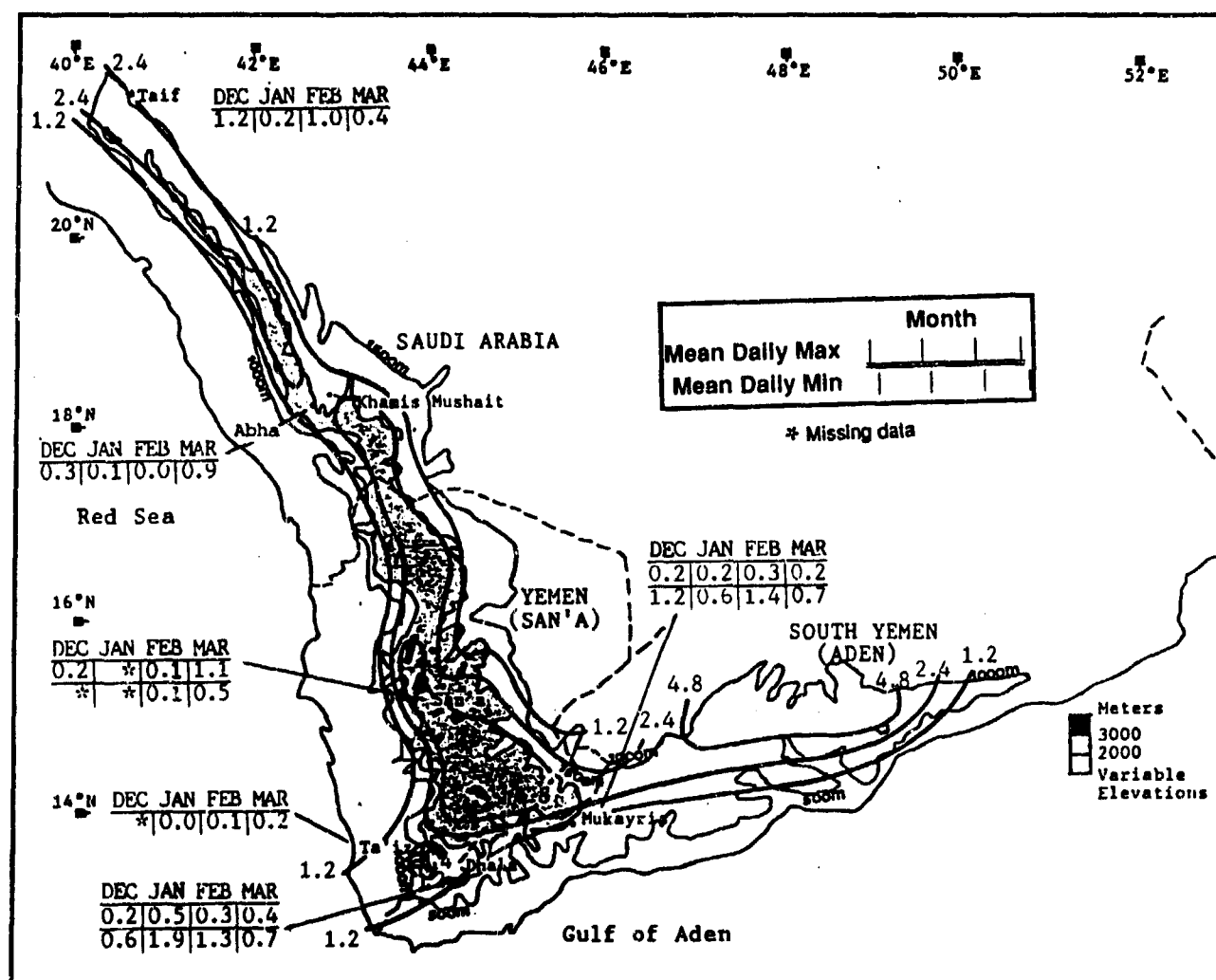


Figure 6-19. Mean Northeast Monsoon Monthly/Maximum 24-Hour Precipitation, Yemen Highlands. Isohyets represent mean seasonal rainfall totals (inches). 24-hour data was not available for Abha and Ta'iz.

YEMEN HIGHLANDS NORTHEAST MONSOON

December-March

TEMPERATURE. Above 5,000 feet (1,524 meters), temperatures vary with elevation and topography, but prevailing low-level wind direction has an effect below 5,000 feet (1,524 meters). On southern Yemen Mountain hillsides below 5,000 feet (1,524 meters) between Ta'iz and Mukayris, temperatures are moderated by sea breeze moisture. On eastern Red Sea hillsides, the sea breeze moderates temperature, but does not normally affect nighttime temperatures above 5,000 feet (1,524 meters)

Mean daily highs range from 64 to 82°F (18-28°C). The record March high at Mukayris (elevation 6,720 feet/2,049 meters) is 77°F (25°C). At Ta'if (elevation

4,500 feet/1,372 meters), the record is 90°F (32°C). Extended (3-7-day) periods of undisturbed weather allow larger diurnal temperature ranges at higher elevations. For example, the January diurnal range at San'a (elevation 7,237 feet/2,206 meters) is 35°F (19°C), but at Ta'iz (elevation 4,629 feet/1,411 meters), the range is only 7°F (2-3°C). Mean daily lows range from 36 to 56°F (2-13°C). Absolute lows below freezing are rare, but 22°F (-6°C) was recorded at San'a in December. Ta'iz, on the other hand, has never recorded a temperature below 60°F (16°C) during any Northeast Monsoon month.

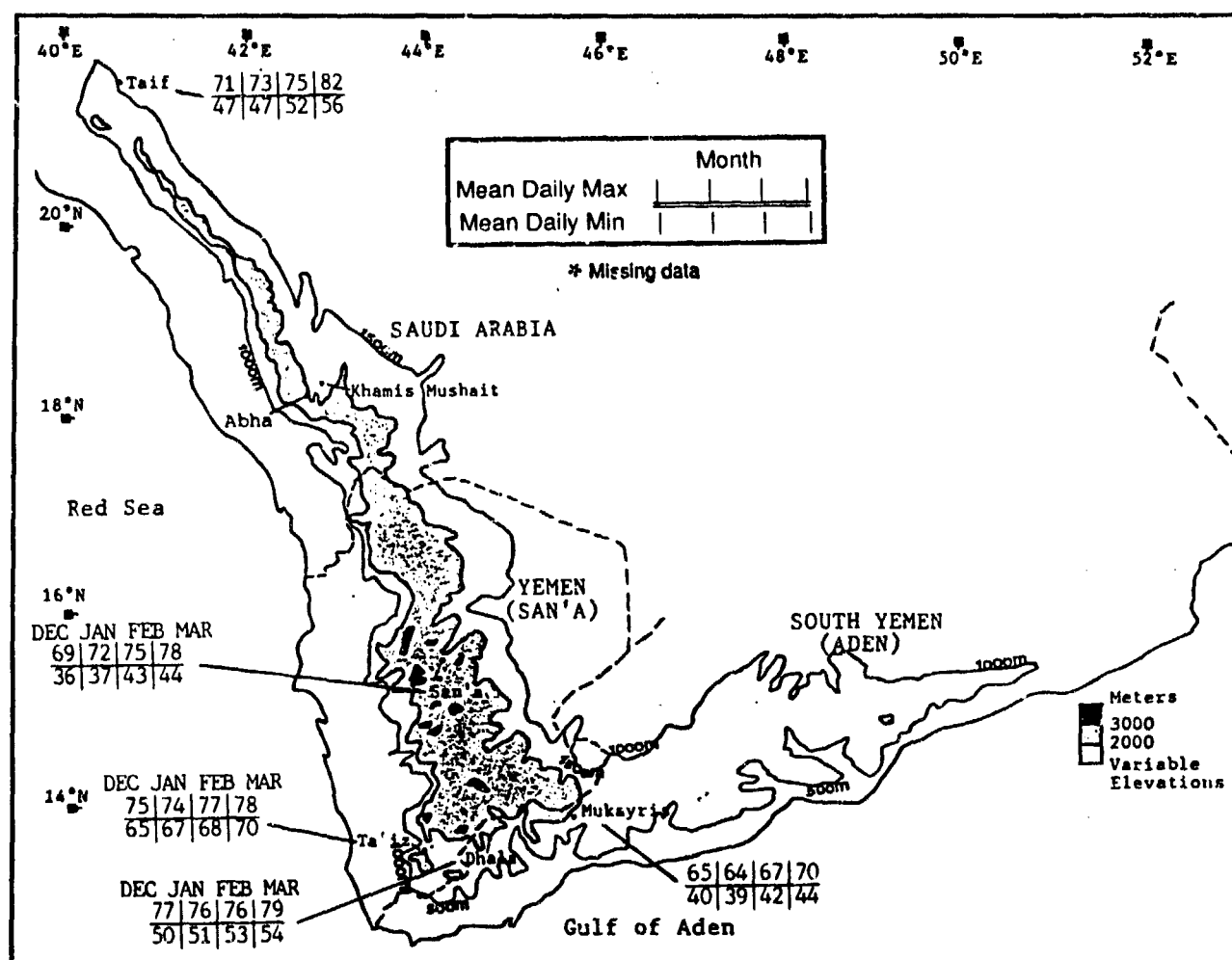


Figure 6-20. Mean Northeast Monsoon Daily Maximum/Minimum Temperature (°F), Yemen Highlands.

YEMEN HIGHLANDS **NORTHEAST-TO-SOUTHWEST MONSOON TRANSITION**

April-May

GENERAL WEATHER. Cyclonic activity, the surface Monsoon Trough, and the Red Sea Convergence Zone (RSCZ) are the most important transition weather features. By early May, the surface Monsoon Trough (with weak low-level convergence) replaces sustained northeasterly flow in the Gulf of Aden. Northeasterlies weaken rapidly in the Straits of Bab al Mandab during April. The end of the Northeast Monsoon also marks the end of the Red Sea Convergence Zone. Although the surface Monsoon Trough is inactive along the Gulf of Aden and southern Red Sea, southerly flow is established south of the Trough axis. As a result, persistent onshore low-level flow along the southern Yemen Mountains and

southern Hadhramaut Plateau intensifies the sea breeze. Light and variable winds dominate the southern and central Red Sea.

SKY COVER. Transition cloudiness frequencies (Figure 6-21) are highest (greater than 30%) in the southwestern corner of the Yemen Mountains, where elevations are below 6,000 feet (1,829 meters) MSL. Cumulus is the predominant cloud type. Over the southern Hadhramaut Plateau, the interior Yemen Mountains, and the southern Asirs, mean cloudiness is 20-30%. Mean cloudiness (mostly cirrus) in the northern Asirs is less than 20%.

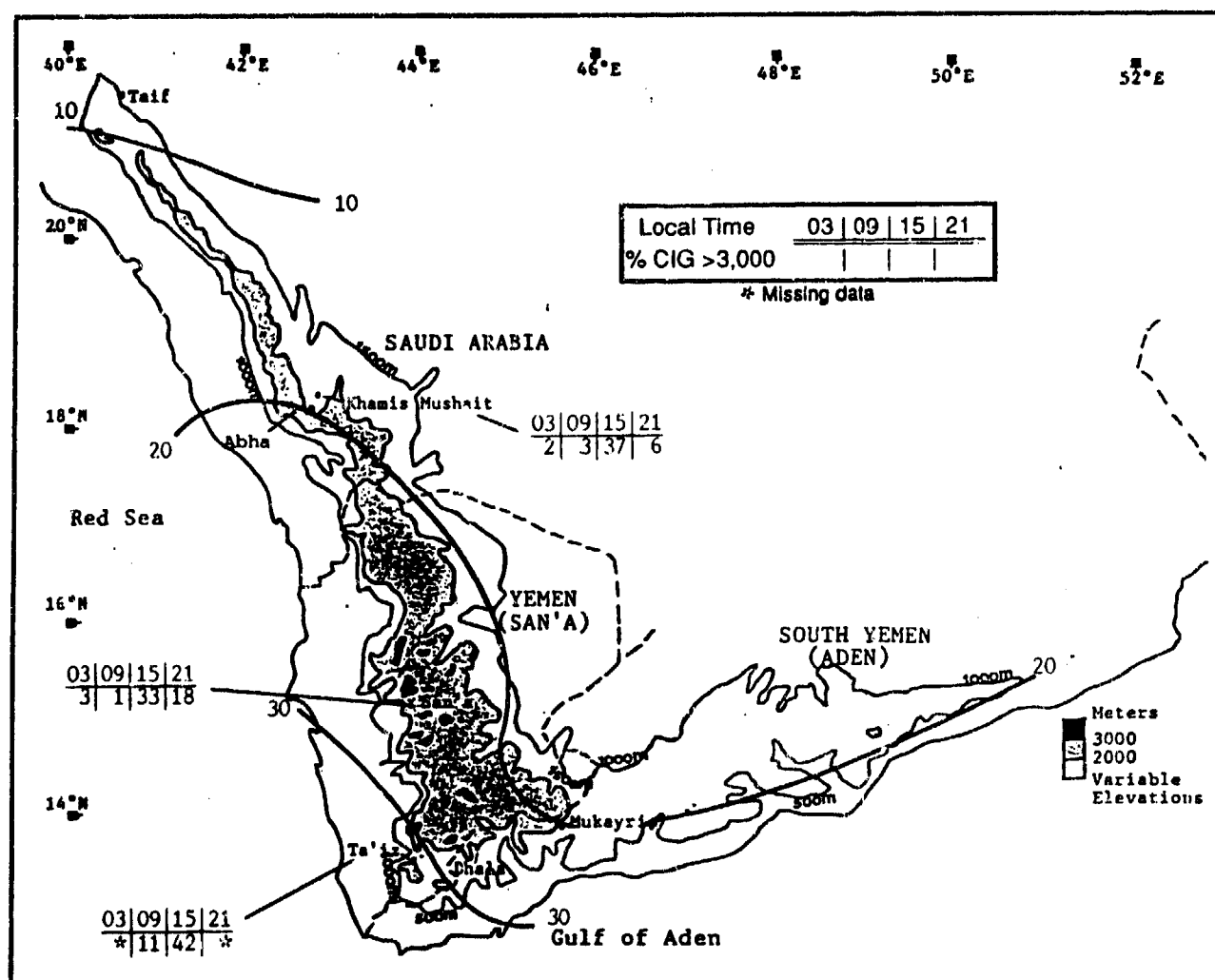


Figure 6-21. Mean NE-SW Monsoon Transition Mean Cloudiness (Isolines) and Frequencies of Ceilings Below 3,000 Feet (915 meters), Yemen Highlands. Isopleths are in 10% intervals. Mean cloudiness data was derived by calculating the grand mean for National Intelligence Summary (NIS) mean cloudiness data for specific sites in April and May.

YEMEN HIGHLANDS

NORTHEAST-TO-SOUTHWEST MONSOON TRANSITION

April-May

Stratocumulus and isolated cumulus develop along the extreme eastern edge of the RSCZ as light and variable winds along the surface Trough axis converge with local sea breezes. The resultant flow ascends the western Yemen and Asir Mountain foothills. The RSCZ's daily position along the foothills and local sea breeze orientation determines the type and extent of cloud cover and rainfall. The RSCZ disappears from the region by late April or early May.

During a typical April, RSCZ cloud cover develops north of 18° N, but convection may deviate from this mean location pattern when other synoptic features alter the low-level convergence pattern. Synoptic conditions that affect RSCZ cloud cover are migratory surface low-pressure cells and cold upper-level troughs. With either feature, isolated towering cumulus with tops to 15,000 feet (4,573 meters) MSL may extend south to 15° N.

Cyclonic activity with southerly or southwesterly flow ahead of a cold front produces more ceilings below 3,000 feet (915 meters) than any other synoptic or mesoscale weather feature. This southerly flow pattern can push sea breeze moisture to the 8,000-foot level along the western Asir and Yemen Mountains. Orographic lift produces scattered cumulus and cumulonimbus with bases at 2,000-3,000 feet (610-915 meters) and tops to 15,000 feet (4,573 meters) MSL.

In the southern Yemen Mountains and on the southern edges of the Hadhramaut Plateau, southerly flow results from a strong sea breeze reinforced by the surface Monsoon Trough in the Gulf of Aden. At San'a, ceilings are below 1,000 feet (305 meters) AGL less than 1% of the time, but between 1600-2000 LST, ceilings are between 1,000 and 3,000 feet (305-915 meters) nearly 40% of the time. Clouds are mostly cumulus and towering cumulus, but strong southerly flow may produce severe thunderstorms with tops above 40,000 feet (12,220 meters) between Aden and San'a.

YEMEN HIGHLANDS **NORTHEAST-TO-SOUTHWEST MONSOON TRANSITION**

April-May

VISIBILITY. As shown in Figure 6-22, transition visibilities are generally good. In early morning, haze is most frequently observed along the southern and western fringes of the region below 6,000 feet (1,829 meters) MSL. Blowing dust or sand occurs along the eastern

Asirs, eastern Yemen Mountains, and northern Hadhramaut Plateau in mid-afternoon. Mid-afternoon moderate to heavy rainfall in the southern Yemen Mountains results in a 1-3% frequency of lowered visibilities during that time.

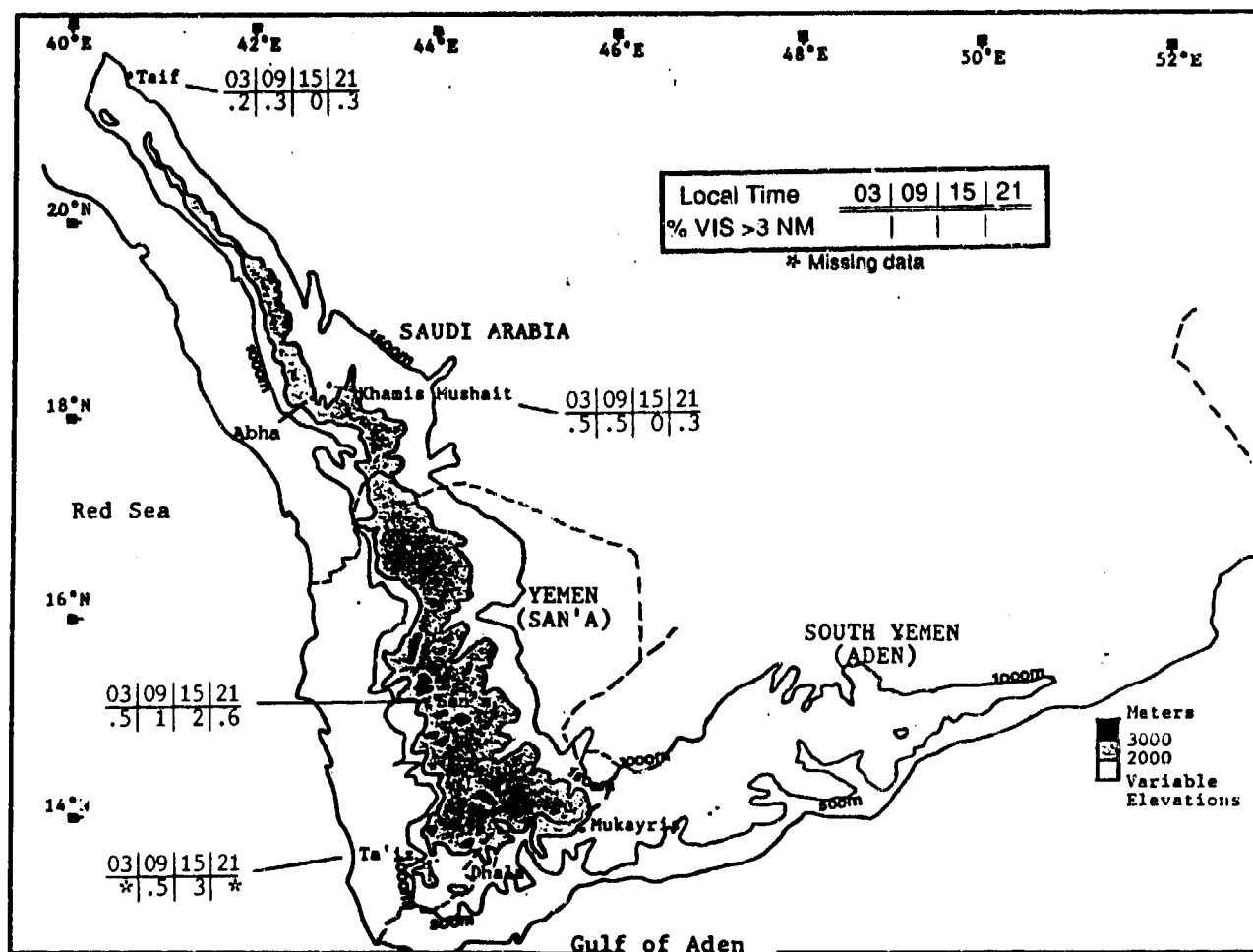


Figure 6-22. NE-SW Monsoon Transition Frequencies of Visibilities Below 3 Miles, Yemen Highlands.

WINDS. Figure 6-23 gives mean surface wind speeds and prevailing direction for Kh's Mushait (Khamis Mushait), San'a, and Ta'iz. Easterly components for

these stations reflect Northeast Monsoon low-level flow during April, and weak cyclonic outflow from the Rub al Khali in May.

	APR	MAY
S-SE		
S-ENE		
S-SE		
Kh's Mushait	7.00	5.60
San'a	5.10	6.40
Ta'iz	12.60	9.40

Figure 6-23. Mean NE-SW Monsoon Transition Wind Speed (kts) and Prevailing Direction, Yemen Highlands.

YEMEN HIGHLANDS **NORTHEAST-TO-SOUTHWEST MONSOON TRANSITION**

April-May

Upper-level (30,000-foot, 9,146-meter) MSL flow over the entire region is westerly. Mean speeds in April range from 19 knots in the south to 33 in the north. Mean May speeds range from 11 knots in the south to 23 knots in the north.

Mid-level (10,000-15,000-foot, 3,050-4,573-meter) wind direction is southwesterly at Khamis Mushait and San'a in April, but east-southeasterly over both locations in May. Speeds average 9-11 knots in April and, 11-13 knots in May. At Ta'iz, mid-level wind direction is east-northeasterly at 12 knots in April, becoming southeasterly at 8 knots in May.

Very weak (3-to 5-knot) northwesterlies may appear briefly over the eastern Hadhramaut Plateau in early May with the passage of an upper-level trough. The cold upper-level trough is reflected by a weak surface trough, but the wind shift line is negligible except in the lowest elevations of the northern Asirs and eastern Hadhramaut. Northwesterlies affect the eastern Hadhramaut Plateau for 3-12 hours. The sea breeze initiates a return to southerly flow, but easterly or northeasterly flow may replace the northwesterlies if the shift in in the evening.

The southwesterly-to-westerly flow at low levels provides moisture and induces orographic lift in the extreme southern/western Yemen Mountains and western Asirs. The southwestern Yemen Mountains (Ta'iz in particular) get the highest rainfall amounts of the year in April and May. Late afternoon convection produces extensive light to moderate rainshowers. Isolated thundershowers are common above 8,000 feet (2,439 meters) MSL.

PRECIPITATION. As shown in Figure 6-24, April rainfall is greater than May's at Taif, Mukayris, and San'a. There are several reasons for this. At Taif, wetter Aprils are the result of a higher frequency of cyclonic activity. Mean April rainfall at Mukayris is greater than May's because the prevailing low- and mid-level wind direction is southeasterly. In May, southeasterlies prevail to 10,000 feet (3,050 meters) MSL, with mean northeasterly flow at 15,000 feet (4,573 meters). Orographic convection builds along the southeast Yemen Mountains near Mukayris, but moves westward (downwind).

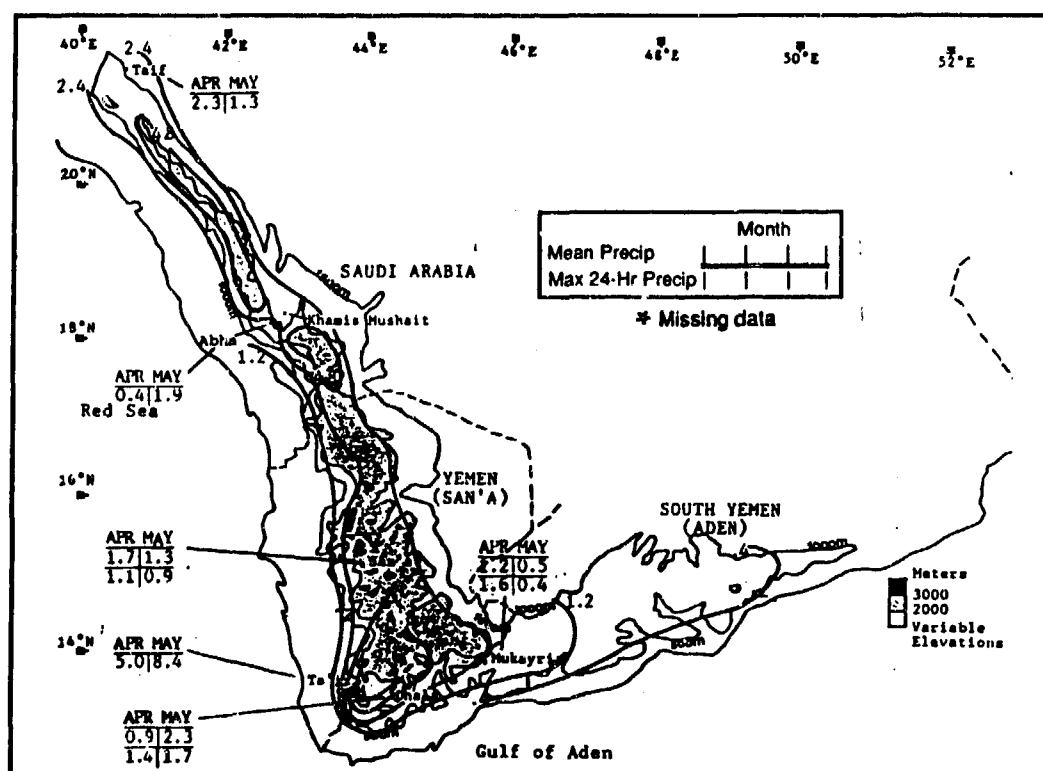


Figure 6-24. Mean NE-SW Monsoon Transition Monthly/Maximum 24-Hour Precipitation, Yemen Highlands. Maximum 24-hour rainfall not available for Ta'iz, Abha, and Taif. Isohyets represent mean seasonal rainfall totals (inches).

YEMEN HIGHLANDS **NORTHEAST-TO-SOUTHWEST MONSOON TRANSITION**

April-May

TEMPERATURE. Mean daily highs range from 72 to 91°F (22-33°C), mean daily lows from 49 to 73°F (9-23°C)--see Figure 6-25. Warm coastal waters keep nighttime temperatures pleasant, but below normal May nighttime temperatures can be expected with northeasterly flow over the Hadhramaut Plateau. Record highs include an 84°F (29°C) at Mukayris, to 100°F

(38°C) at Ta'if, both recorded in May. In unpopulated portions of the northern Hadhramaut Plateau, temperatures may exceed 100°F (38°C), and soil surface temperature may exceed 120°F (49°C). Lowest temperatures occur in April. A record low of 37°F (2°C) at San'a is in contrast to the 60°F (16°C) recorded at Ta'iz.

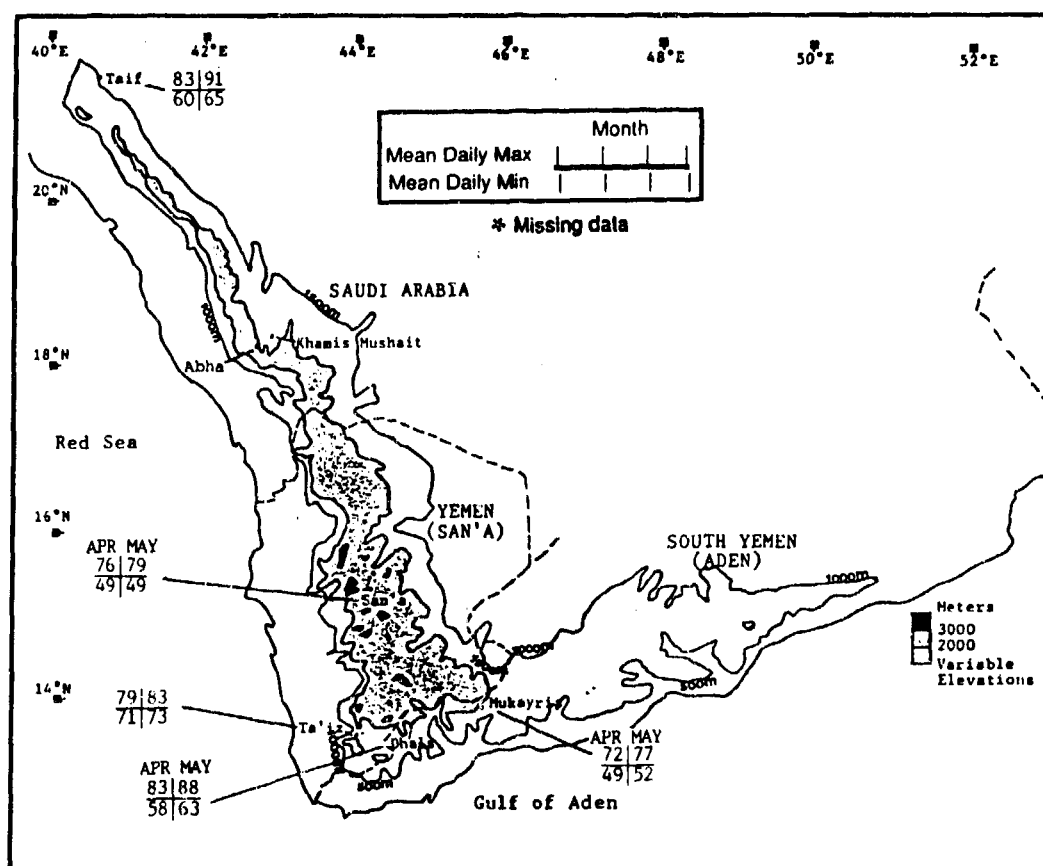


Figure 6-25. Mean NE-SW Monsoon Transition Daily Maximum/Minimum Temperatures (°F), Yemen Highlands.

BIBLIOGRAPHY

- Aden, South Yemen--A Summary of Weather Conditions, Database (POR Jan 66-Dec 76), USAF Environmental Technical Applications Center, Scott AFB, IL., date unknown.
- Africa, AWS/FM-100/001, HQ Air Weather Service, Scott AFB, IL., 1980.
- "Africa's Great Rift Valley," *National Geographic*, Vol 177, No 5, pp. 2-42, May 1990.
- Air France, *Meteorological Study of Air Route Between Jeddah and Dar-Es-Salaam*, FTD-1D(RS)T-0114-85, 1985.
- Alaka, M.A., *Aviation Aspect of Weather*, TP 26, Tech Note No. 18, Technical Division of the WMO Secretariat, WMO No 68, 1958.
- Allison, L.J., et al., *A Quasi-Global Presentation Of TIROS III Radiation Data*, NASA SP-53, 1964.
- Anderson, D.L.T., "The Low-Level Jet as a Western Boundary Current," *Monthly Weather Review*, Vol.104, pp. 907-921, 1976.
- Ardanuy, P., "On The Observed Diurnal Oscillation of the Somali Jet," *Monthly Weather Review*, Vol.107, pp. 1694-1700, 1979.
- Army Air Forces Weather Division, *Local Forecasting Studies, Asmara, Eritrea, Africa*, 1944.
- Army Air Forces Weather Division, *Local Forecasting Studies, Sheikh Othman Airfield, Aden, Yemen*, 1944.
- Atkinson, G.D., *Forecaster's Guide to Tropical Meteorology*, AWS/TR-240, HQ Air Weather Service, Scott AFB, IL., 1971.
- Atkinson, G.D. and Sadler, J.C., *Mean Cloudiness and Gradient-Level Wind Charts Over the Tropics, Volume 2, Charts*, AWSTR 215, HQ Air Weather Service, Scott AFB, IL., 1970.
- Atlee, Gizaw, *Weather and Climate at Addis Ababa, Dire Dawa, and Jimma*, Imperial Ethiopian Government Civil Aviation Administration Meteorological Service, 1965.
- Atlee, Gizaw, *Weather at Asmara*, Imperial Ethiopian Government Civil Aviation Administration Meteorological Service, 1964.
- Bannon, P.R., "On the Dynamics of the East African Jet. Part I. Simulation of Mean Conditions for July," *Journal Of Atmospheric Science*, Vol.36, pp. 2139-2152, 1979.
- Bannon, P.R., "On the Dynamics of the East African Jet. Part II. Jet Transients," *Journal Of Atmospheric Science*, Vol.36, pp. 2153-2168, 1979.
- Bannon, P.R., "On the Dynamics of the East African Jet. Part III: Arabian Sea Branch," *Journal Of Atmospheric Science*, Vol.39, pp. 2267-2278, 1982.
- Barry, R.G., *Mountain Weather and Climate*, Muethen & Co., London, 1981.
- Bruce, J.G., "The Wind Field in the Indian Ocean and the Related Ocean Circulation," *Monthly Weather Review*, Vol.111, pp. 1442-1452, 1983.

- Bryson, R.A., et al., *Normal 500mb Charts for the Northern Hemisphere*, Report No.8, AF 19 (604)-992, 1957.
- Cadet, D. and Desbois, M., "A Case Study of a Fluctuation of the Somali Jet During the Indian Summer Monsoon," *Monthly Weather Review*, Vol.109, pp. 182-187, 1981.
- Charney, J.G., "Dynamics of Deserts and Drought in the Sahel," *Quarterly Journal of the Royal Meteorological Society*, Vol 101, No. 428, pp. 193-202, 1975.
- Climate--British and Italian Somaliland*, AWS Directorate of Climatology, HQ Air Weather Service, Scott AFB, IL, December 1955.
- The Climate of Ethiopia*, AWS Technical Library, Scott AFB, IL, date unknown.
- Climatic Study--Report 4295*, USAF Climatic Center, Washington, D.C., July 1962.
- Climatic Atlas of Asia I, Maps of Mean Temperature and Precipitation*, Goscomgidromet USSR, Voeikov Main Geophysical Observatory, World Meteorological Organization, 1981.
- Climatic Study of the Red Sea South and Gulf of Aden Near Coastal Zone*, Naval Oceanography Command Detachment, Stennis Space Center, Bay St Louis, MS , 1982.
- Climatological Wind Factor Calculator-Mean Isogon-Isotach Charts*, SACM 105-2, Volume 2, Strategic Air Command, Offutt AFB, NE, 1960.
- Crutcher, H.L., *Selected Meridional Cross Sections of Height, Temperatures, and Dew Points of the Northern Hemisphere*, NCDC-NOAA, NAVAIR 50-1C-59, 1971.
- Desai, P.S., "The Summer Atmospheric Circulation Over the Arabian Sea," *Journal of Atmospheric Science*, Vol.24, pp. 216-220, 1967.
- Dubief, J., *Le Climat du Sahara--Tome II*, L'Institut de Meteorologie et de Physique du Globe de L'Algerie, Alger, 1963.
- The Easterly Jet Stream in the Tropics*, AWS/FM-100/019, HQ Air Weather Service, Scott AFB, IL, 1980.
- El-Fandy, M.G., "Barometric Lows of Cyprus," *Quarterly Journal Of The Royal Meteorological Society*, Vol.72, pp.291-306, 1946.
- El-Fandy, M.G., "The Effect of the Sudan Monsoon Low on the Development of Thundery Conditions in Egypt, Palestine and Syria," *Quarterly Journal Of The Royal Meteorological Society*, Vol.78, pp. 31-38, 1948.
- El-Fandy, M.G., "Effects of Topography and Other Factors on the Movement of Lows in the Middle East and Sudan," *Bulletin Of The American Meteorological Society*, Vol.31, Number 10, pp 375-381, 1950.
- Ethiopia (including Eritrea), Parts I and II*, Report No. 60, Investigations Division Climatological, Meteorological Office, Air Ministry, Bracknell, 1962.
- Farr, G.R., "Seasonal and Global Distribution of the Jet Stream and Its Kinetic Energies in the Northern Hemisphere," Masters Thesis, Dept of Meteorology, Univ. of Utah, 1964.
- Felt, R.W. and W.A. Bohan, *Navy Tactical Applications Guide, Volume 5, Part 1, Indian Ocean-Red Sea/Persian Gulf*, NEPRF Technical Report 83-03, NEPRF, Monterey, CA, 1983.

- Fett, R.W., *North Atlantic and Mediterranean Weather Analysis and Forecast Applications--Volume 3*, NEPRF Technical Note 80-07, NEPRF, Monterey, CA, 1980.
- Findlater, J., "Cross-Equatorial Jet Streams at Low Levels Over Kenya," *Meteorological Magazine*, Vol. 95, pp. 353-364, 1966.
- Findlater, J., "Some Further Evidence of Cross-Equatorial Jet Streams at Low Levels Over Kenya," *Meteorological Magazine*, Vol. 96, pp. 216-219, 1967.
- Findlater, J., "Interhemispheric Transport of Air in the Lower Troposphere Over the Western Indian Ocean," *Quarterly Journal of the Royal Meteorological Society*, Vol. 95, pp. 400-403, 1969.
- Findlater, J., "A Major Low-Level Air Current Near the Indian Ocean During the Northern Summer," *Quarterly Journal of the Royal Meteorological Society*, Vol. 95, pp. 362-380, 1969.
- Findlater, J., "The Strange Winds of Ras Asir," *Meteorological Magazine*, Vol. 100, pp. 46-54, 1971.
- Findlater, J., "Mean Monthly Airflow at Low Levels Over the Western Indian Ocean," *Geophysical Memoirs*, No. 115, British Meteorological Office, Vol. 16, Number 1, 1971.
- Findlater, J., "Aerial Explorations of the Low-Level Cross-Equatorial Current Over Eastern Africa," *Quarterly Journal of the Royal Meteorological Society*, Vol. 98, pp. 274-289, 1972.
- Flohn, H., *Studies on the Meteorology of Tropical Africa*, Bon Met Abhand, Heft 5, Bonn, 1965.
- Flohn, H., *Contributions to a Meteorology of the Tibetan Highlands*, Dept of Atmospheric Sciences--Colorado State Univ., Research Paper No. 130, 1968.
- Flohn, H., "Local Wind Systems," Chapter 4, *World Survey of Climatology*, Volume 2, Elsevier Publishing, Amsterdam, 1969.
- Geiger, R., *Climate Near the Ground*, 4th Ed., Harvard University Press, Cambridge, MA, 1961.
- General Circulation of the Atmosphere*, DIA LN 783-70, Portuguese Meteorological Service, 1970.
- Giles, B.D., "Extremely High Atmospheric Pressure," *Weather*, Vol. 25, pp. 19-24, 1970.
- Global Climatology for the Wet Bulb Globe Temperature (WBGT) Heat Stress Index*, U.S. Army Research Institute of Environmental Medicine, Bldg 42, Natick, MA, 1989.
- Griffiths, J.F., "Chapter 4--The Horn of Africa," *World Survey of Climatology*, Vol. 10, pp. 133-166, 1972.
- Hamilton, M.G., "Monsoons--An Introduction," *Weather*, Vol. 42, Number 6, pp. 186-193, 1987.
- Hart, J.E., et al., "Aerial Observations of the East African Low-Level Jet Stream," *Monthly Weather Review*, Vol. 106, pp. 1714-1724, 1978.
- Hastenrath, S., et al., *A Contribution to the Dynamic Climatology of Arabia*, Department of Meteorology, University of Wisconsin, Madison, Archiv fur Meteorologie Geophysik und Bioklimatologie, 1979.
- Hastenrath S., *Climate and Circulation of the Tropics*, Reidel Publ Inc., Dordrecht, 1985.

- Huzayyin, S. A., "Notes on Climatic Conditions in Southwest Arabia (Yaman and the Hadhramaut)," *Royal Meteorological Society Quarterly Journal*, Vol. 71, pp 129-140, 1945.
- Indian Ocean Atlas*, U.S. Central Intelligence Agency, 1976.
- Joshi, P.C. and P.S. Desai, "The Satellite-Determined Thermal Structure of Heat Low During Indian Southwest Monsoon Season," *Advanced Space Research*, Vol. 1, Number 6, pp. 57-60, 1985.
- Krishnamurti, T.N., et al., "Numerical Simulation of the Somali Jet," *Journal of Atmospheric Science*, Vol. 33, Number 11, pp. 2350-2362, 1976.
- Krishnamurti, T.N., et al., "On the Onset Vortex of the Summer Monsoon," *Monthly Weather Review*, Vol. 109, pp. 344-363, 1981.
- Kinuthia, J.H., and G.C. Asnani, "A Newly Found Jet in North Kenya (Turkana Channel)," *First International Conference on Southern Hemisphere Meteorology*, preprint, pp. 377-389, 1983.
- La Fontaine, C.V., et al., "Airstream Regions of North Africa and the Mediterranean," *Journal of Climate*, Vol. 3, No 3, pp. 367-372, 1990.
- Lahcy, J.F., et al., *Atlas Of 300mb Wind Characteristics for the Northern Hemisphere*, Final Report, Part 1., AF 19 (604)-2278, Univ of Wisc Press, 1960.
- Leroux, M., *The Climate of Tropical Africa-Part B*, FTD-ID(RS)T-0615-85, Foreign Technology Division translation, Wright--Patterson AFB, OH, pp. 526-566, 1983.
- Leroux, M., *The Climate of Tropical Africa--Atlas*, Volume 2, 1983.
- Marine Climatic Atlas of the World*, Vol. 9, NAVAIR 50-1C-65, Department of the Navy, 1981
- Membery, D.A., "A Unique August Cyclonic Storm Crosses Arabia," *Weather*, Vol. 40, Number 4, pp. 108-114, 1985.
- Morth, H.T., *Introduction to the Climate of Africa-Notes to Support Lectures on Regional Climatology*, East African Meteorological Service, Nairobi Kenya, date unknown.
- National Intelligence Surveys 30 & 32, Iraq/Arabian Peninsula, Section 23, Weather and Climate*, U.S. Central Intelligence Agency, May 1970.
- National Intelligence Survey 55, Ethiopia and the Somalilands, Section 23, Weather and Climate*, U.S. Central Intelligence Agency, April 1965.
- Ownbey, J.W., *Climatic Summaries For Major 7th Fleet Ports And Waters*, NWSED, NAVAIR 50-1C-62, 1973.
- Palinèn, E. and C.W. Newton, *Atmospheric Circulation Systems*, Academic Press, New York and London, 1969.
- Pant, M.C., "Some Characteristic Features of the Low-Level Jet Field Over the Arabian Sea During the Indian Summer Monsoon," *MAI/SAM*, Vol. 33, No.1, pp. 85-90, 1982.
- Pedgley, D.E., "Cyclones along the Arabian Coast," *Weather*, Vol. 24, No.11, pp. 456-468, 1969.
- Pedgley, D.E., "The Climate of Oman," *Meteorological Magazine*, Vol. 99, Number 1171, pp. 29-37, 1970.

- Pedgley, D.E., "Diurnal Incidence of Rain and Thunder at Asmara and Addis Ababa, Ethiopia," *Meteorological Magazine*, Vol. 100, pp. 67-71, 1971.
- Pruss, W.F., *Climatological Wind Factors Calculator-Charts of Vector Standard Deviation of Winds*, 3WWM 105-5, 3WW, Offutt AFB, NE, 1962.
- Rainfall in Ethiopia*, Civil Aviation Department Climatological Institute, Addis Ababa, Ethiopia, date unknown.
- Ramage, C.S., "The Subtropical Cyclone," *Journal of Geophysical Research*, Vol. 67, Number 4, pp. 1401-1411, 1962.
- Ramage, C.S., "The Summer Atmospheric Circulation Over the Arabian Sea," *Journal of Atmospheric Science*, Vol. 23, pp. 145-150, 1966.
- Ramage, C.S., *Monsoon Meteorology*, Academic Press, New York, 1971.
- Rao, G.V. and J.L. Haney, "Kinematic And Thermal Structures of Two Surges in the Northern Mozambique Channel Area," *Quarterly Journal of the Royal Meteorological Society*, Vol. 108, pp. 957-974, 1982.
- Rao, G.V., H. van de Boogaard, and W.C. Bolhofer, "Further Calculations of Sea-Level Air Trajectories Over the Equatorial Indian Ocean," *Monthly Weather Review*, Vol. 106, pp. 1465-1475, 1978.
- Red Sea And Gulf Of Aden-Oceanographical and Meteorological Data*, Number 129, Dutch Meteorological Service, Koninklijk Nederlands Meteorologisch Instituut, Amsterdam, 1949.
- Reed, R.J., "Principal Frontal Zones of the Northern Hemisphere in Winter And Summer," *Bulletin of the American Meteorological Society*, Vol. 41, Number 11, pp. 591-598, 1960.
- Riehl, H., *Jet Streams of the Atmosphere*, Tech Report No.32, Dept of Atmospheric Science, Colorado State Univ., 1962.
- Sadler, J.C., *The Mean Winds of the Upper Troposphere Over the Central and Eastern Pacific*, N62306-69 and N00188-71-M-6783, NEPRF, Monterey, CA, 1972.
- Sadler, J.C., *The Upper Tropospheric Circulation Over the Global Tropics*, UHMET 75-05, NSF Grant No. GA-36301, 1975.
- Sadler, J.C., *The Upper Tropospheric Circulation Over the Global Tropics. Part II-The Statistics*, UHMET 77-02, NSF Grant No. GA-36301, 1977.
- Saha, K., "Air and Water Vapour Transport Across The Equator in Western Indian Ocean During Northern Summer," *Tellus*, Vol. 22, Number 6, pp. 681-687, 1970.
- Sikka, D.R. and S. Gadgil, "On the Maximum Cloud Zone and the ITCZ Over Indian Longitudes During the Southwest Monsoon," *Monthly Weather Review*, Vol. 108, pp. 1840-1853, 1980.
- Singh, R. and Raj, H., "A Satellite Study of the Tropical Easterly Jet During Monsoon '77," *MAUSAM*, Vol. 33, No.1, pp. 113-120, 1982.
- Singh, R., "A Study of Sea Surface Pressure, Sea Surface Temperature and Cloudiness Patterns Over Indian Ocean Region in Some Years Of Contrasting Southwest Monsoon Rainfall: Part II," *MAUSAM*, Vol. 34, No.2, pp. 205-212, 1983.

- Solot, S.B., *The Meteorology of Central Africa*, AWSTR 105-50, HQ Air Weather Service, Scott AFB, IL, pp. 129, 1950.
- Solot, S.B., "General Circulation Over the Anglo-Egyptian Sudan and Adjacent Regions," *Bulletin Of The American Meteorological Society*, Vol. 31, Number 3, pp. 85-94, 1950.
- Steadman, R.G., "A Universal Scale of Apparent Temperature," *Journal Of Climate And Applied Meteorology*, Vol. 23, Number 12, 1984.
- Tracks Of Tropical Depressions and Cyclones in the Bay Of Bengal and Arabian Sea--1877-1960*, Indian Meteorological Department, 1964.
- Tropical East Africa*, AWS/FM-100/006, HQ Air Weather Service, Scott AFB, IL, 1980.
- Tropical Meteorology in Africa--4th Seminar*, East African Met Service, Nairobi, 1965.
- Tunnell, G.A., "World Distribution of Atmospheric Water Vapour Pressure," *Geophysical Memoirs*, British Met Office, Vol. 12, No. 100, 1958.
- van de Boogaard, H., *The Mean Circulation of the Tropical and Subtropical Atmosphere-July*, NCAR/TN-118+STR, NCAR, Boulder, CO, 1977.
- van de Boogaard, H., and G.V. Rao, "Mesoscale Structure Of The Low-Level Flow Near the Equatorial East African Coast," *Monthly Weather Review*, Vol. 113, pp. 91-107, 1984.
- Walker, J.M., "Some Ideas on Winter Atmospheric Processes Over Southwest Asia," *Meteorological Magazine*, Vol. 96, pp. 161-167, 1967.
- Walker, J.M., "The Monsoon of Southern Asia: A Review," *Weather*, Vol. 27, Number 5, pp. 178-189, 1972.
- Wallace, J., and P. Hobbs, *Atmospheric Science--An Introductory Study*, Academic Press, NYC, 1977.
- Walters, K.R., *A Descriptive Climatology for Baledogle, Somalia*, USAFETAC/TN-88/001, USAF Environmental Technical Applications Center, Scott AFB, IL, 1988.
- Weather Factors Affecting Aerial Photography in Ethiopia*, AWS Technical Library, Scott AFB, IL, date unknown.
- Weather Forecasting Affecting Aerial Photography and Operations in French Somaliland and Somali Republic*, Technical Services Office, 7 WW Climatic Services, HQ 7WW, Scott AFB, IL, January 1966.
- Weather in the Indian Ocean to Latitude 30 South and Longitude 95 East including the Red Sea and Persian Gulf, Volume I: General Information*, NAVENVPREDRSCHFAC, NEPRF, Monterey, CA, April 1980.
- Weather in the Indian Ocean to Latitude 30 South and Longitude 95 East including the Red Sea and Persian Gulf, Part II, The Gulf of Aden and West Arabian Sea to Longitude 60 East*, NAVENVPREDRSCHFAC TB 80-02, Vol. 2, NEPRF, Monterey, CA, 1980.
- Weather in the Indian Ocean to Latitude 30 South and Longitude 95 East including the Red Sea and Persian Gulf, Part IX, Coast of East Africa from the Equator to Cape Delgado*, NAVENVPREDRSCHFAC TB 80-02, Vol. 2, NEPRF, Monterey, CA, 1980.
- Western Indian Ocean*, AWS/FM-100/018, HQ Air Weather Service, Scott AFB, IL, 1980.

White, F., "Vegetation Map of Africa," *Africa: South of the Sahara*, Europa Publ. Ltd., London, 1979.

Young, J.A., et al., *Summer Monsoon Winds from Geostationary Satellite Data: Summer MONEX 1 May to 31 July, 1979*, Univ of Wisc Meteorology Dept, NSF Grant No. ATM-78-21873, 1980.

Zohdy, Hussein Mohamed, *Troughs in the Westerlies Related to Winter Rainfall Patterns in Yemen*, Thesis Paper, Cairo University, 1971.

DISTRIBUTION

OUSDA/R/AT/E/LS, Pentagon, Washington, DC 20301-3080	1
AF/XOORF, Pentagon, Washington, DC 20330-5054	1
J-34/ESD, Pentagon, Washington, DC 20318-3000	1
MAC/DOX< Scott AFB, IL 62225-5001	1
AWS/DO, Scott AFB, IL 62225-5008	1
AWS/XT, Scott AFB, IL 62225-5008	3
AWS/XTJ, Scott AFB, IL 62225008	1
AWS/XTX, Scott AFB, IL 62225008	1
AWS/PM, Scott AFB, IL 62225-5008	1
AWS/RF, Scott AFB, IL 62225-5008	1
OL A, HQ AWS, Buckley ANG Base, Aurora, CO 80011-9599	1
OL-C, HQ AWS, Chanute AFB, IL 61868-5000	1
AFOTEC/WE, Kirtland AFB, NM 87117-7001	1
CACDA, OL-E, HQ AWS, ATZL-CAW-E, Ft Leavenworth, KS 66027-5300	1
SD/CWDA, PO Box 92960, Los Angeles, CA 90009-2960	1
OL-H, HQ AWS (ATSI-CD-SW), Ft Huachuca, AZ 85613-7000	1
OL-I, HQ AWS (ATWE), Ft Monroe, VA 23651-5051	1
OL-K, HQ AWS, NEXRAD Opnl Facility, 1200 Westheimer Dr. Norman, OK 73069	1
OL-L, HQ AWS, Keesler AFB, MS 39534-5000	1
OL-M, HQ AWS, McClellan AFB, CA 95652-5609	1
Det 1, HQ AWS, Pentagon, Washington, DC 20330-6560	3
Det 2, HQ AWS, Pentagon, Washington, DC 20330-5054	2
Det 3, HQ AWS, PO Box 3430, Onizuka AFB, CA 94088-3430	1
Det 9, HQ AWS, PO Box 12297, Las Vegas, NV 89112-0297	1
1WW/DN, Hickam AFB, HI 96853-5000	3
11WS/DON, Elmendorf AFB, AK 99506-5000	1
20WS/DON, APO San Francisco 96328-5000	1
30WS/DON, APO San Francisco 96301-0420	1
2WW/DN, APO New York 09094-5000	3
7WS/DON, APO New York 09403-5000	1
28WS/DON, APO New York 09127-5000	1
31WS/DON, APO New York 09136-5000	1
3WW/DN, Offutt AFB, NE 68113-5000	3
9WS/DON, March AFB, CA 92518-5000	1
24WS/DON, Randolph AFB, TX 78150-5000	1
26WS/DON, Barksdale AFB, LA 71110-5002	1
4WW/DN, Peterson AFB, CO 80914-5000	3
2WS/DON, Andrews AFB, MD 20334-5000	20
5WW/DN, Langley AFB, VA 23665-5000	7
1WS/DON MacDill AFB, FL 33608-5000	2
3WS/DON, Shaw AFB, SC 29152-5000	15
5WS/DON, Ft McPherson, GA 30330-5000	20
25WS/DON, Bergstrom AFB, TX 78743-5000	13
AFGWC/SDSL, Offutt AFB, NE 68113-5000	6
USAFETAC, Scott AFB, IL 62225-5438	6
OL-A. USAFETAC, Federal Building, Asheville, NC 28801-2723	3
7WW/DN, Scott AFB, IL 62225-5008	3
6WS/DON Hurlburt Field, FL 32544-5000	1
15WS/DON, McGuire AFB, NJ 08641-5002	1
17WS/DON, Travis AFB, CA 94535-5986	1

3350 TECH TG/TTGU-W, Stop 62, Chanute AFB, IL 61868-5000	2
AFIT/CIR, Wright-Patterson AFB, OH 45433-6583	1
AFCSA/SAGW, Washington, DC 20330-5000	1
NAVOCEANCOMDET, Federal Building, Asheville, NC 28801-2723	1
NAVOCEANCOMDET, Patuxent River NAS, MD 20670-5103	1
NAVOCEANCOMFAC, Stennis Space Ctr, MS 39529-5002	1
COMNAVOCFANCOM, Code N312, Stennis Space Ctr, MS 39529-5000	1
NAVOCEANO, Code 9220 (Tony Ortolano), Stennis Space Ctr, MS 39529-5001	1
NAVOCEANO, Code 4601 (Ms Loomis), Stennis Space Ctr, MS 39529-5001	1
FLENUMOCEANCEN, Monterey, CA 93943-5006	1
NOARL, Monterey, CA 93943-5006	1
Naval Research Laboratory, Code 4323, Washington, DC 20375	1
Naval Postgraduate School, Chmn, Dept of Meteorology, Code 63, Monterey, CA 93943-5000	1
Naval Eastern Oceanography Ctr, 1117 McCady Bldg, NAS Norfolk, Norfolk, VA 23511-5000	1
Naval Western Oceanography Ctr, Box 113, Attn: Tech Library, Pearl Harbor, HI 96860-5000	1
Naval Oceanography Command Ctr, COMNAVMAR Box 12, FFO San Francisco, CA 96630-5000	1
Pacific Missile Test Center, Geophysics Division, Code 3253, Pt Mugu, CA 93042-5000	1
Dept of Commerce/NOAA/MASC, Library MC5 (Jean Bankhead), 325 Broadway, Boulder, CO 80303	2
Federal Coordinator for Meteorology, Suite 300, 11426 Rockville Pike, Rockville, MD 20852	1
NOAA Library-EOC4WSC4, Attn: ACQ, 6009 Executive Blvd, Rockville MD 20852	1
NOAA/NESDIS (Attn: Capt Taylor), FB #4, Rm 0308, Suitland, MD 20746	1
Armed Forces Medical Intelligence Agency, Info Sves Div., Bldg 1607, Ft Detrick, Frederick, MD 21701-5004	1
GL Library, Attn: SULLR, Stop 29, Hanscom AFB, MA 01731-5000	1
Atmospheric Sciences Laboratory, Attn: SLCAS-AT-AB, Aberdeen Proving Grounds, MD 21005-5001	1
Atmospheric Sciences Laboratory, White Sands Missile Range, NM 88002-5501	1
U.S. Army Missile Command, ATTN: AMSMI-RD-TE-T, Redstone Arsenal, AL 35898-5250	1
Technical Library, Dugway Proving Ground, Dugway, UT 84022-5000	1
NWS Training Center, 617 Hardesty, Kansas City, MO 64124	1
NCAR Library, Boulder, CO 80307-3000	1
NCDC Library (D542X2), Federal Building, Asheville, NC 28801-2723	1
NIST Pubs Production, Rm A-405, Admin Bldg, Gaithersburg, MD 20899	1
JSOC/Weather, P.O. Box 70239, Fort Bragg, NC 28307-5000	1
75th RGR ((Attn: SWO), Ft Benning GA 31905-5000	1
HQ 5th U.S. Army, AFKB-OP (SWO), Ft Sam Houston, TX 78234-7000	1
NASA-MSFC-ES44, Attn: Dale Johnson, Huntsville, AL 35812-5000	1
Dept of Atmospheric Sciences, 7127 Math Sciences, UCLA, Los Angeles, CA 90024-5000	1
Dept of Oceanography, A-008, Scripps Inst of Oceanography, Univ of Cal, La Jolla, CA 92093-5000	1
Library, USAFA (DFSEL), Colorado Springs, CO 80840-5000	1
Dept of Atmospheric Sciences, PAS Bldg, Univ of Arizona, Tucson, AZ 85721-5000	1
Dept of Atmospheric Science, Atmospheric Science Bldg, Colorado St Univ, Ft Collins, CO 80523-5000	1
Meteorology Unit/Dept of Agronomy, NYS College of Ag and Life Science, Bradford Hall, Cornell Univ, Ithaca, NY 14853-5000	1
USDAO Ndjamena, State Dept Pouch Room, Washington, DC 20521-2410	2
USDAO/AIRA Cairo, Box 9, FPO New York 09527-0061	2
USDAO Baghdad, State Dept Pouch Room, Washington, DC 20520	1
USDAO/AIRA Tel Aviv, Israel, APO New York 09672-5000	2
USDAO/AIRA Amman, APO New York 09892-5000	2
USDAO Muscat, State Dept Pouch Room, Washington, DC 20520-6220	2
USDAO/AIRA Islamabad, PSC Box 32, APO NY 09614-0006	2
USDAO/AIRA, Amembassy, APO New York, 09038-0001	2
USDAO Mogadishu, Somalia, State Dept Pouch Room, Washington, DC 20520	1
USDAO Khartoum, Box 18, Amembassy, APO New York 09668-5000	1
USDAO Damascus, State Dept Pouch Room, Washington, DC 20520	1

USDAO Sanaa, State Dept Pouch Room, Washington, DC 20521-6330	1
Aeronautical Ctr Library (AAC 64D), PO Box 25082, Oklahoma City, OK 73125-5000	1
Dept of Meteorology, Florida State Univ, Tallahassee, FL 32306-5000	1
Dept of Meteorology, Univ of Hawaii, 2525 Correa Road, Honolulu, HI 96822-5000	1
Dept of Atmospheric and Oceanic Science, Space Research Bldg, Univ of Mich, 2455 Hayward,	
Ann Arbor, MI 41809-2143	1
Dept of Meteorology and Physical Oceanography, Univ of Miami, Miami, FL 33149-1098	1
Dept of Atmospheric Science, Univ of Missouri, 701 Hitt St, Columbia, MO 65211-5000	1
Center for Agricultural Meteorology and Climatology, L.W. Chase Hall-East Campus, Univ of Nebraska-Lincoln,	
Lincoln, NE 68583-0728	1
Dept of Marine, Earth, and Atmospheric Sciences, North Carolina St Univ, Box 8208, Raleigh, NC 27695-8208	1
School of Meteorology, Univ of Oklahoma, 200 Felgar St, Norman, OK 73019-5000	1
Dept of Atmospheric Sciences, Stand Agriculture Hall, Oregon St Univ, Corvallis, OR 97331-2209	1
Dept of Meteorology, 503 Walker Bldg, Penn St Univ, University Park, PA 16802-5000	1
Dept of Marine Sciences, Univ of Puerto Rico, Mayaguez, PU 00708-5000	1
Dept of Earth and Atmospheric Sciences, Stadium Hall, Purdue Univ, West Lafayette, IN 47907-5000	1
Library, Rand Corporation, PO Box 2138, Santa Monica, CA 90406-5000	1
Dept of Earth and Atmospheric Sciences, St Louis Univ, PO Box 8099-Laclede Station, St Louis, MO	
63156-5000	1
Dept of Meteorology, Univ of St Thomas, 3812 Montrose Blvd, Houston, TX 77006-5000	1
Dept of Meteorology, San Jose St Univ, One Washington Square, San Jose, CA 95192-5000	1
Dept of Meteorology, Texas A&M Univ, College Station, TX 77843-5000	2
US Military Academy, USMA Library, West Point, NY 10996-5000	1
Dept of Oceanography, Stop 9d, US Naval Academy, Annapolis, MD 21402-5000	1
Dept of Meteorology, Univ of Utah, Salt Lake City, UT 84112-5000	1
Dept of Meteorology, Utah St Univ, UMC 4840, Logan, UT 84322-5000	1
Dept of Environmental Sciences, Clark Hall, Univ of Virginia, Charlottesville, VA 22903-5000	1
Dept of Meteorology, Univ of Wisconsin, 1225 W Dayton St, Madison, WI 53706-5000	1
DITC-FDAC, Cameron Station, Alexandria, VA 22304-6145	1
AUL/LSE, Maxwell AFB, AL 36112-5564	1
AWSTL, Scott AFB, IL 62225-5458	100